ACTA TECHNICA

ACADEMIAE SCIENTIARUM HUNGARICAE

REDIGIT: M. MAJOR

TOMUS 92
FASCICULI 1—2

AKADÉMIAI KIADÓ, BUDAPEST 1981

ACTA TECHNICA

Az *Acta Technica* angol, francia, német és orosz nyelven közöl értekezéseket a műszaki tudományok köréből.

Az *Acta Technica* változó terjedelmű füzetekben jelenik meg, több füzet alkot egy kötetet.

A közlésre szánt kéziratok a következő címre küldendők:

Acta Technica
1051 Budapest, Münnich Ferenc u. 7.

Ugyanerre a címre küldendő minden szerkesztőségi és kiadóhivatali levelezés.

Megrendelhető a belföld számára az „Akadémiai Kiadó"-nál (1363 Budapest Pf. 24. Bankszámla 215-11448), a külföld számára pedig a „Kultura" Külkereskedelmi Vállalatnál (1389 Budapest 62, P.O.B. 149 Bankszámla: 218-10990) vagy annak külföldi képviseleteinél és bizományosainál.

Die *Acta Technica* veröffentlichen Abhandlungen aus dem Bereiche der technischen Wissenschaften in deutscher, englischer, französischer und russischer Sprache.

Die *Acta Technica* erscheinen in Heften wechselnden Umfanges. Vier Hefte bilden einen Band.

Die zur Veröffentlichung bestimmten Manuskripte sind an folgende Adresse zu senden:

Acta Technica
H-1051 Budapest
Münnich Ferenc u. 7.
Ungarn

An die gleiche Anschrift ist auch jede für die Schriftleitung und den Verlag bestimmte Korrespondenz zu richten.

Bestellbar bei »Kultura« Außenhandelsunternehmen (H-1389 Budapest 62, P.O.B. 149, Bankkonto Nr. 218-10990) oder seinen Auslandsvertretungen.

ACTA TECHNICA

ACADEMIAE SCIENTIARUM HUNGARICAE

REDIGIT: M. MAJOR

TOMUS 92

AKADÉMIAI KIADÓ, BUDAPEST 1981

ACTA TECHNICA

TOMUS 92 FASC. 1—4

ACTA TECHNICA

ACADEMIAE SCIENTIARUM HUNGARICAE

REDIGIT: M. MAJOR

TOMUS 92

FASCICULI 1–2

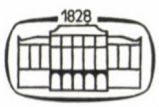

AKADÉMIAI KIADÓ, BUDAPEST 1981

Acta Technica Academiae Scientiarum Hungaricae, Tomus 92 (1—2), pp. 3—22 (1981)

A NEW METHOD FOR SOLVING ORTHOTROPIC RECTANGULAR PLATES

Dedicated to Dr.-Eng. Kázmer Szmodits
on the occasion of his 70-th anniversary

M. V. SOARE*
DOCTOR OF TECHN. SCI.

[Manuscript received: February 12, 1980]

The partial differential equation of orthotropic plates based on the smoothing of the stiffeners in two orthogonal directions is considered. It is completed with terms representing the effect of the supporting on an elastic subgrade of Winkler type, as well as the consideration of the friction between the plate and the foundation. The solution is based on the use of double series of characteristic functions and leads to the solution of a linear system with an infinity of equations and unknowns.

1. Introduction

Orthotropic plates with various supporting conditions have been dealt with in literature in an extensive manner.

Two procedures are to be distinguished for the approach and namely:

a) consideration of the discrete structure, consisting of the proper plate and the stiffeners (distributed in one or two directions) representing a regular configuration;

b) the smoothing of the stiffeners over the afferent length in order to obtain an equivalent elastic continuum [3], [10], [13].

Retaining the latter approach, the basic partial differential equation of orthotropic plates resting on an elastic foundation will be written as:

$$K_x \frac{\partial^4 w}{\partial x^4} + 2H \frac{\partial^4 w}{\partial x^2 \partial y^2} + K_y \frac{\partial^4 w}{\partial y^4} - k_x \frac{\partial^2 u}{\partial x^2} - k_y \frac{\partial^2 w}{\partial y^2} + kw = Z(x, y) \quad (1.1)$$

where w represents the deflection of the plate in a typical section (x, y),

K_x, K_y flexural rigidities of the orthotropic plate in the x and y directions, respectively,

H torsional rigidity of the orthotropic plate,

k modulus of the foundation (or Winkler type),

* Prof. Dr. Mircea V. Soare, Str. Pictor Băncilă 22, Bucureşti 5, Sector 6,R-76327, Romania.

k_x, k_y constants which introduce the friction between the plate and the foundation and include the different elastic properties (due to orthotropy) in the x and y directions,

$Z(x, y)$ normal distributed load per unit area.

Assuming that K_x, K_y, H, k, k_x, k_y are constant, the partial differential equation (1.1) has constant coefficients and solutions can be obtained, for particular supporting conditions, by using the method of variable separation.

In the case of the rectangular plan-form, the Navier type solution of double trigonometrial series is well known, if the four sides are simply supported and the Levy type solution using simple trigonometrical series with variable coefficients, when two opposite sides are simply supported and the other two sides are arbitrarily supported.

Variational and numerical solutions are also known, but it is not the purpose of the present paper to apply them.

Let us particularly mention a paper by P. LARDY [5]; the idea of the solution is quite simple and consists in the introduction of certain functions which rigorously satisfy the limit conditions on the two pairs of opposite sides of the plate. These functions called *characteristic functions* are deduced from the study of free lateral vibrations of prismatic bars (see §3).

In the manner exposed in the previously mentioned paper by P. LARDY, the characteristic functions, applied to the isotropic rectangular plate clamped on the four sides, correspond to the method of double trigonometrical series used for solving rectangular plates simply supported along the whole boundary.

The purpose of the present paper is to generalize Lardy's results and, namely:

— the four sides can be arbitrarily supported (with the restrictions mentioned in §7);

— the plate is orthotropic (the isotropic plate only represents a particular case);

— the supporting on an elastic foundation is included, characterized by two moduli of foundation (the first one considering the normal pressure of Winkler type and the second the friction between plate and foundation)*.

In the next paragraph, equation (1.1) will be reduced to a *canonical form*, underlining various particular cases met with in practice; in the 3rd paragraph will be defined the characteristic functions and some of their properties.

In paragraphs 4 and 5 the exact analytical solution and a variational approach will be presented respectively, and in the next paragraph some particular cases will be examined. Final observations conclude the paper.

* The derivation of equation (1.1) is given in *Appendix* 2.

The canonical equation of orthotropic plates

In equation (1.1) we shall divide all the terms by one of the flexural rigidities, let it be K_x

$$\frac{\partial^4 w}{\partial x^4} + 2\frac{H}{K_x}\frac{\partial^4 w}{\partial x^2 \partial y^2} + \frac{K_y}{K_x}\frac{\partial^4 w}{\partial y^4} - \frac{k_x}{K_x}\frac{\partial^2 w}{\partial x^2} - \frac{k_y}{K_x}\frac{\partial^2 w}{\partial y^2} + \frac{k}{K_x} w = \frac{Z(x, y)}{K}$$

and will carry, according to S. KRUG and P. STEIN [4] an affine change of one of the independent variables

$$y = \gamma y', \quad \frac{\partial(\cdots)}{\partial y} = \gamma \frac{(\partial \ldots)}{\partial y'}, \quad \ldots \tag{2.1}$$

The previous equation becomes

$$\frac{\partial^4 w}{\partial x^4} + 2\gamma^2 \frac{H}{K_x}\frac{\partial^4 w}{\partial x^2 \partial y'^2} + \gamma^4 \frac{K_y}{K_x}\frac{\partial^4 w}{\partial y'^4} + \frac{k_x}{K_x}\frac{\partial^2 w}{\partial x^2} - \frac{\gamma^2 k_y}{K_x}\frac{\partial^2 w}{\partial y'^2} + \frac{k}{K_x} w = \frac{Z(x, \partial y')}{K_x}. \tag{2.2}$$

The parameter γ in (2.1) can be determined in such a manner that the coefficient of $\partial^4 w/\partial y'^4$ becomes equal to unity, i.e.

$$\gamma^4 \frac{K_y}{K_x} = 1 ;$$

we deduce

$$\gamma = \sqrt[4]{\frac{K_x}{K_y}} \quad \text{and} \quad \gamma^2 = \sqrt{\frac{K_x}{K_y}}. \tag{2.3}$$

With this value, equation (2.2) is written:

$$\frac{\partial^4 w}{\partial x^4} + \frac{2H}{\sqrt{K_x K_y}}\frac{\partial^4 w}{\partial x^2 \partial y'^2} + \frac{\partial^4 w}{\partial y'^4} + \frac{k_z}{K_x}\frac{\partial^2 w}{\partial x^2} - \frac{k_y}{\sqrt{K_x K_y}}\frac{\partial^2 w}{\partial y'^2} + \frac{k}{K_x} w = \frac{Z(x, \gamma y')}{K_x}. \tag{2.4}$$

We shall denote

$$\varkappa = \frac{H}{\sqrt{K_x K_y}} \text{ the parameter of the orthotropic plate,} \tag{2.5}$$

$$k_{1x} = \frac{k_x}{K_x}, \quad k_{1y} = \frac{k_y}{\sqrt{K_x K_y}}, \quad k_1 = \frac{k}{K_x} \tag{2.6}$$

transformed moduli of foundation.

For the sake of simplicity we shall also transform the notations according to the following:

$$y' \to y, \quad K_x \to K, \quad k_{1x} \to k_x, \quad k_{1y} \to k_y, \quad k_1 \to k\,.$$

Equation (2.4) is then written in the *canonical form*

$$\frac{\partial^4 w}{\partial x^4} + 2\varkappa \frac{\partial^4 w}{\partial x^2\,\partial y^2} + \frac{\partial^4 w}{\partial y^4} - k_x \frac{\partial^2 w}{\partial x^2} - k_y \frac{\partial^2 w}{\partial y^2} + kw = \frac{Z(x,y)}{K}\,. \tag{2.7}$$

Note that in (2.7) y represents a transformed coordinate, while Z and w are functions of the *actual* coordinate x and of the *transformed* coordinate y.

For appropriate values of $\varkappa$, k, k_x and k_y equation (2.7) is reduced to classical equations; they will be examined in paragraph 6.

Characteristic functions

It is known)see for instance [2]) that the dynamic deflection of a prismatic bar undergoing free lateral vibrations is proportional to a function $X(x)$ which satisfies the ordinary differential equation:

$$\frac{d^4 X}{dx^4} - \frac{\alpha^4}{a^4} X = 0\,, \tag{3.1}$$

where a represents the span of the bar (beam), α an eigenvalue to be determined from a compatibility condition.

The general solution of equation (3.1) is

$$X(x) = C_1 \cosh \alpha \frac{x}{a} + C_2 \cos \alpha \frac{x}{a} + C_3 \sinh \alpha \frac{x}{a} + C_4 \sin \alpha \frac{x}{a}\,,$$

where C_1, C_2, C_3, C_4 represent arbitrary constants.

For various supporting conditions of the beam, one obtains a system of four linear and homogeneous equations; expressing that the main determinant of the system vanishes, there results the previously mentioned condition of compatibility which is a transcendent equations in α. There results that this equation has an infinity of roots α_m ($m = 1, 2, 3, \ldots$), therefore, there are an infinity of functions $X_m(x)$. Thus, the general solution of equation (3.1) may be considered as a series expansion of characteristic functions $X_m(x)$, each term satisfying the boundary conditions.

The trigonometric lines sin and cos are particular cases of characteristic functions, corresponding to the simply supported beam.

One of the important particularities of these functions is the property of orthogonality, i.e. the equation

$$\int_0^a X_i X_j \, dx = 0 \quad (\text{for any } i \neq j) \tag{3.2}$$

holds.

If we denote

$$\frac{dX_m}{dx} = \frac{\alpha_m}{a} X'_m, \qquad \frac{d^2 X_m}{dx^2} = \frac{\alpha_m^2}{a^2} X''_m, \ldots \tag{3.3}$$

there result the important equation

$$X''''_m = X_m \tag{3.4}$$

which expresses that by four times differentiation, the initial function is obtained.

Characteristic functions have been tabulated for various combinations of homogeneous supporting conditions (simply supported, clamped or free end); the numerical tables by D. YOUNG and R. P. FELGAR jr. [16] are to be specially mentioned, where the particular form of the characteristic functions has been chosen in such a manner that the following equation*

$$\int_0^a x_i^2 \, dx = a \tag{3.5}$$

is to be satisfied.

A synthesis of the results is given in *Appendix* 3 [12].

In what follows we shall assume that a given function $p(x)$ can be expressed in the interval $(0, a)$ by a series of characteristic functions

$$p(x) = \sum_m p_m X_m(x) \qquad (m = 1, 2, 3, \ldots) \tag{3.6a}$$

where functions $X_m(x)$ satisfy the prescribed boundary conditions and

$$p_m = \frac{1}{a} \int_0^a p(x) X_m(x) \, dx. \tag{3.6b}$$

There in particular it would be useful to expand in a series of characteristic functions the derivative of second order of such a function let X''_m:

$$X''_m = \sum_i h_{m,i} X_i, \quad (i = 1, 2, 3, \ldots) \tag{3.7a}$$

* The case of trigonometric lines is excepted, for which the second member results in a/2.

or developed

$$X_m'' = h_{mi1} X_1 + h_{m,2} X_2 + \ldots + h_{m,i} X_i + \ldots \tag{3.7b}$$

where $h_{m,i}$ $(i = 1, 2, 3, \ldots)$ are constants to be determined. The direct application of formula (3.6b) leads to

$$h_{m,i} = \frac{1}{a} \int_0^a X_m'' X_i \, dx ; \tag{3.8a}$$

the integral can be performed completely, keeping in mind the particular expressions of functions X_m and X_i. Thus one gets

— for $i \neq m$

$$h_{m,i} = \frac{1}{\alpha_i^4 - \alpha_m^4} \left| \alpha_m^2 (\alpha_i X_m X_i' - \alpha_m X_i X_m') + \alpha_i^2 (\alpha_i X_m'' X_i''' - \alpha_m X_i'' X_m''') \right|_0^a \tag{3.8b}$$

— for $i = m$

$$h_{m,m} = \frac{1}{4\alpha_m} \left| X_m X_m' + X_m'' X_m''' \right|_0^a - \frac{1}{4} (X_m'^2 - 2 X_m X_m'' + X_m'''^2)_{x=a} .$$

The particular expressions of the coefficients $h_{m,i}$ and $h_{m,m}$ for the considered supporting cases are given in *Appendix* 3.

*

For bidimensional problems the characteristic functions can be combined, corresponding to the prescribed boundary conditions, for example, an arbitrary load $Z(x, y)$ distributed per unit are will be expressed in the rectangular domain $a \cdot b$ by means of the double series

$$Z(x, y) = \sum_m \sum_n p_{mn} X_m(x) \, Y_n(y) \tag{3.9}$$

where

$$X_m(x) = C_{1m} \cosh \alpha_m \frac{x}{a} + C_{2m} \cos \alpha_m \frac{x}{a} + C_{3m} \sinh \alpha_m \frac{x}{a} + C_{4m} \sin \alpha_m \frac{x}{a} \tag{3.10a}$$

$$Y_n(y) = D_{1n} \cosh \beta_n \frac{y}{b} + D_{2n} \cos \beta_n \frac{y}{b} + D_{3n} \sinh \beta_n \frac{y}{b} + D_{4n} \sin \beta_n \frac{y}{b} \tag{3.10b}$$

and

$$p_{mn} = \frac{1}{ab} \int_0^a \int_0^b p(x, y)\, X_m(x)\, Y_n(y) dx\, dy\,. \tag{3.10c}$$

Analogously to expressions (3.3) we shall note

$$\frac{dY_n}{dy} = \frac{\beta_n}{b} Y_n^{\cdot}\,, \qquad \frac{d^2 Y_n}{dy^2} = \frac{\beta_n^2}{b^2} Y_n^{\cdot\cdot}\,, \ \ldots \tag{3.11a}$$

and obtain that by four times differentiation, function Y_n and its successive derivatives are reproduced, that is

$$Y_n^{\cdot\cdot\cdot\cdot} = Y_n\,. \tag{3.11b}$$

The second derivative of Y_n will be expressed in a similar manner to (3.7a) or (3.7b):

$$Y_n^{\cdot\cdot} = \sum_j \bar{h}_{n,j}\, Y_j\,, \quad (j = 1, 2, 3, \ldots) \tag{3.12a}$$

or developed

$$Y_n^{\cdot\cdot} = \bar{h}_{n,1}\, Y_1 + \bar{h}_{n,2}\, Y_2 + \ldots + \bar{h}_{n,j}\, Y_j + \ldots \tag{3.12b}$$

where coefficients $\bar{h}_{n,j}$ and $\bar{h}_{n,n}$ are deduced from expressions (3.8) by the substitutions

$$m \to n,\ i \to j,\ a \to b,\ \alpha_m \to \beta_n,\ \alpha_i \to \beta_j,\ X_m \to Y_n,\ X_m^1 \to Y_n^{\cdot}\ \text{a.s.o.}$$

It should be underlined that all these coefficients $h_{m,i}$ and $\bar{h}_{n,j}$ can be determined once for ever, depending on the supporting conditions and independently of the orthotropic plate parameter $\varkappa$.

Use of double series of characteristic functions

The get a solution of the partial differential equation (2.7), we shall assume that the applied load can be expressed by means of formula (3.9); there results

$$\frac{\partial^4 w}{\partial x^4} + 2\varkappa \frac{\partial^4 w}{\partial x^2 \partial y^2} + \frac{\partial^4 w}{\partial y^4} - k_x \frac{\partial^2 w}{\partial x^2} - k_y \frac{\partial^2 w}{\partial y^2} + kw = \frac{1}{K} \sum_m \sum_n p_{mn}\, X_m\, Y_n\,. \tag{4.1}$$

The form of the second member suggests for us to search for a solution having the same structure:

$$w = \sum_m \sum_n w_{mn} X_m Y_n \tag{4.2}$$

in which the dimensional coefficients w_{mn} are to be determined in the following.

Introducing equation (4.2) in (4.1), we get

$$\sum_m \sum_n \left(w_{mn} \frac{\alpha_m^4}{a^4} X_m'''' Y_n + w_{mn} \frac{\beta_n^4}{b^4} X_m Y_n'''' + k w_{mn} X_m Y_n + \right.$$
$$+ 2\varkappa \frac{\alpha_m^2 \beta_n^2}{a^2 b^2} X_m'' Y_n'' - k_x w_{mn} \frac{\alpha_m^2}{a^2} X_m'' Y_n -$$
$$\left. - k_y w_{mn} \frac{\beta_n^2}{b^2} X_m Y_n'' - \frac{1}{K} p_{mn} X_m Y_n \right) = 0 ,$$

or, keeping in mind that $X_m'''' = X_m$ and $Y_m'''' = Y_n$ and conveniently grouping the terms:

$$\sum_m \sum_n \left\{ \left[w_{mn} \left(\frac{\alpha_m^4}{a^4} + \frac{\beta_n^4}{b^4} + k \right) - \frac{p_{mn}}{K} \right] X_m Y_n + 2\varkappa w_{mn} \frac{\alpha_m^2 \beta_n^2}{a^2 b^2} X_m'' Y_n'' - \right.$$
$$\left. - w_{mn} \left(k_x \frac{\alpha_m^2}{a^2} X_m'' Y_n + k_y \frac{\beta_n^2}{b^2} Xm Y_x'' \right) \right\} = 0 . \tag{4.3}$$

One can state that in (4.3) the product $X_m Y_n$ cannot be factorized, a fact which does not allow the direct determination of w_{mn} for each range m, n.

We shall therefore express, according to P. LARDY [5] the terms X_m'' and Y_n'' by means of the expansions in series (3.7b) and (3.12b), the coefficients $h_{m,i}$, $h_{m,m}$, $\bar{h}_{n,j}$, $\bar{h}_{n,n}$ being supposed in the following, as is known.

We have, thus

$$X_m'' Y_n'' = \left(\sum_i h_{m,i} X_i \right) \left(\sum_j \bar{h}_{n,j} Y_j \right) = (h_{m,1} X_1 + h_{m,2} X_2 + \ldots$$
$$\ldots + h_{m,i} X_i + \ldots) (\bar{h}_{n,1} Y_1 + \bar{h}_{n,2} Y_2 + \ldots + \bar{h}_{n,j} Y_j + \ldots) \tag{4.4a}$$

or developed

$$X_m'' Y_n'' = h_{m,1} \bar{h}_{n,1} X_1 Y_1 +$$
$$+ h_{m,1} \bar{h}_{n,2} X_1 Y_2 + h_{m,2} \bar{h}_{n,1} X_2 Y_1 +$$
$$+ h_{m,1} \bar{h}_{n,3} X_1 Y_3 + h_{m,2} \bar{h}_{n,2} X_2 Y_2 + h_{m,3} \bar{h}_{n,1} X_3 Y_1 + \ldots \tag{4.4b}$$
$$\ldots\ldots\ldots\ldots\ldots\ldots\ldots\ldots\ldots\ldots\ldots\ldots\ldots\ldots\ldots\ldots\ldots\ldots$$

where in each line appear functions X_i and Y_j so that $i + j = \text{const.}$

In a simpler manner we have

$$X_m'' Y_n = \left(\sum_i h_{m,i} X_i\right) Y_n = h_{m,1} X_1 Y_n + h_{m,2} X_2 Y_n + \ldots + h_{m,i} X_i Y_n + \ldots \tag{4.5a}$$

$$X_m \ddot{Y}_n = \left(\sum_j \bar{h}_{n,j} Y_j\right) X_m = \bar{h}_{n,1} X_m Y_1 + \bar{h}_{n,2} X_m Y_2 + \ldots + \bar{h}_{n,j} X_m Y_j + \ldots \tag{4.5b}$$

Introducing now expressions (4.4a), (4.5a) and (4.5b) in (4.3), we get:

$$\sum_m \sum_n w_{mn} \left[\left(\frac{\alpha_m^4}{a^4} + \frac{\beta_n^4}{b^4} + k \right) X_m Y_n + 2\varkappa \frac{\alpha_m^4 \beta_n^4}{a^4 b^4} \left(\sum_i h_{m,i} X_i \right) \times \right.$$

$$\times \left(\sum_j \bar{h}_{n,j} Y_j \right) - k_x \frac{\alpha_m^2}{a^2} \left(\sum_i h_{m,i} X_i \right) Y_n - k_y \frac{\beta_n^2}{b^2} \times$$

$$\left. \times \left(\sum_j \bar{h}_{n,j} Y_j \right) X_m \right] = \frac{1}{K} \sum_m \sum_n p_{mn} X_m Y_n . \tag{4.6}$$

The terms can be raranged according to the products $X_i Y_j$. Equating to zero the coefficients of all distinct products there results an infinite linear system which determines all the unknowns w_{mn} ($m, n = 1, 2, 3, \ldots$).

In a condensed form the system can be written as follows:

$$\left(\frac{\alpha_i^4}{a^4} + \frac{\beta_j^4}{b^4} + k \right) w_{ij} + 2\varkappa \sum_m \sum_n \frac{a_m^2 \beta_k^2}{a^2 b^2} h_{m,i} \bar{h}_{n,j} w_{mn} -$$

$$- k_x \frac{\alpha_i^2}{a^2} \left(\sum_m h_{m,i} X_i \right) Y_n - k_y \frac{\beta_j^2}{b^2} X_m \left(\sum_n \bar{h}_{n,j} Y_j \right) = \frac{p_{ij}}{K} \tag{4.7}$$

where $m, n = 1, 2, 3, \ldots$ in each equation,

$i, j = 1, 2, 3, \ldots$ characterize the system equations.

The general equation (4.7) can also be written in such a manner as to evidentiate the term on the main diagonal:

$$\left(\frac{\alpha_i^4}{a^4} + \frac{\beta_j^4}{b^4} + 2\varkappa \frac{\alpha_i^2 \beta_j^2}{a^2 b^2} h_{i,i} \bar{h}_{j,j} - k_x \frac{\alpha_i^2}{a^2} h_{i,i} - k_y \frac{\beta_j^2}{b^2} \bar{h}_{j,j} \right) w_{ij} +$$

$$+ 2\varkappa \sum_m \sum_n \frac{\alpha_m^2 \beta_n^2}{a^2 b^2} h_{m,i} \bar{h}_{n,j} w_{mn} - k_x \sum_m \frac{\alpha_m^2}{a^2} h_{m,i} w_{mj} -$$

$$- k_y \sum_n \frac{\beta_n^2}{b^2} \bar{h}_{n,j} w_{in} = \frac{p_{ij}}{K} \tag{4.8}$$

(where $m \neq i$ and $n \neq j$ concomitantly).

The system of equations thus obtained has coefficients, the magnitude of which decreases rapidly. From the practical point of view, the system can

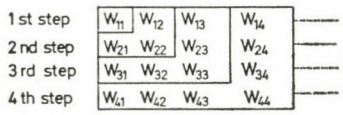

Fig. 1

be solved step by step, progressing along the main diagonal as indicated in fig. 1.

The approximation can be followed according to the desired degree of accuracy.

Since the determination of the infinite system of equations was rather lengthy, in the following paragraph we shall also examine the variational approach of the problem.

Variational approach

We shall rewrite the partial differential equation (2.7) under the form

$$\Phi(x, y, w) \equiv \frac{\partial^4 w}{\partial x^4} + 2\varkappa \frac{\partial^4 w}{\partial x^2 \partial y^2} + \frac{\partial^4 w}{\partial y^4} + \\ + k_x \frac{\partial^2 w}{\partial x^2} - k_y \frac{\partial^2 w}{\partial y^2} + kw - \frac{Z}{K} = 0; \tag{5.1}$$

assuming homogeneous boundary conditions, and shall search for an approximate solution using characteristic functions; thus the boundary conditions are fulfilled for each pair of functions $X_m Y_n$.

Let

$$w^* = \sum_m \sum_n w_{mn} X_m Y_n \tag{5.2}$$

be the proposed solution which differs from (4.2) by the initial assumption that the double sum is finite; w_{mn} represents as previously dimensional coefficients which are to be determined.

To establish their values we shall adhere to the orthogonalisation method which is a completely general method.

If w^* represented the exact solution, the operator Φ defined by (5.1) would be identically equal to zero, and this condition is equivalent to the expression Φ^* being orthogonal with respect to all the functions $(X_i Y_j)$. But since we have only a limited number of parameters $(w_{11}, w_{12}, w_{21}, \ldots, w_{mn})$ we are generally unable to satisfy more than mn conditions of orthogonality.

Setting down these conditions, we get the following system of equations

$$\int_0^a \int_0^b \Phi^* X_i Y_j \, dx dy = \int_0^a \int_0^b \Phi \left(\sum_m \sum_n w_{mn} X_m Y_n \right) X_i Y_j \, dx dy = 0 \quad (5.3)$$

$$(i, j = 1, 2, 3, \ldots)$$

which enables us to determine the coefficients w_{mn}. The differential operator being linear, the ensuing system of equation is linear too.

When applied to problems in Mechanics, the orthogonalisation method must be regarded as an approximate application of *the principle of virtual displacements*.

In this connection, note that the operator Φ, which constitutes the left hand side of the partial differential equation of the equilibrium, represents the resultant of all the external forces, as well the internal forces acting on a plate element; $X_i Y_j$ (regardless of the constant factor w_{ij}) represents the virtual displacement of this same element.

Equation (5.3) is an approximate expression for the fact that the total work done in producing the virtual displacements $X_i Y_j$ throughout the orthotropic plate is equal to zero.

*

Replacing in (5.1) — where Z is considered under the form (5.2) — we get

$$\Phi^* = \sum_m \sum_n \left\{ \left[w_{mn} \left(\frac{\alpha_m^4}{a^4} + \frac{\beta_n^4}{b^4} + k \right) - \frac{p_{mn}}{K} \right] X_m Y_n + \right.$$

$$\left. + 2\varkappa w_{mn} \frac{\alpha_m^2 \beta_n^2}{a^2 b^2} X_m'' Y_n'' - w_{mn} \left(k_x \frac{\alpha_m^2}{a^2} X_m'' Y_n + k_y \frac{\beta_n^2}{b^2} X_m Y_n'' \right) \right\}. \quad (5.4)$$

The variational conditions (5.3) are written:

$$\int_0^a \int_0^b \Phi^* X_i Y_j \, dx dy = \sum_m \sum_n \int_0^a \int_0^b \left\{ \left[w_{mn} \left(\frac{\alpha_m^4}{a^4} + \frac{\beta_n^4}{b^4} + k \right) - \right. \right.$$

$$\left. - \frac{p_{mn}}{K} \right] X_m X_i Y_n Y_j + 2\varkappa w_{mn} \frac{\alpha_m^2 \beta_n^2}{a^2 b^2} X_m'' X_i Y_n'' Y_j -$$

$$\left. - w_{mn} \left(k_x \frac{\alpha_m^2}{a^2} X_m'' X^i Y_n Y_j + k_y \frac{\beta_n^2}{b^2} X_m X_i Y_n'' Y_j \right) \right\} dx dy = 0. \quad (5.5)$$

Keeping in mind that

$$\int_0^a X_m X_i \, dx = 0 \quad \text{for} \quad m \neq i \quad \text{and} \quad \int_0^a X_i^2 \, dx = a,$$

$$\int_0^b Y_n Y_j \, dy = 0 \quad \text{for} \quad n \neq j \quad \text{and} \quad \int_0^b Y_j^2 \, dy = b,$$

equation (5.5) is reduced to the following:

$$w_{ij}\left(\frac{\alpha_i^4}{a^4}+\frac{\beta_j^4}{b^4}+k\right)-\frac{p_{ij}}{K}+2\varkappa\sum_m\sum_n\frac{\alpha_m^2\beta_n^2}{a^2b^2}\,\frac{1}{a}\int_0^a X_m''X_i\,dx\times$$

$$\times\frac{1}{b}\int_0^b Y_n''Y_j\,dy\cdot w_{mn}-\frac{k_x}{a}\sum_m w_{mn}\frac{\alpha_m^2}{a^2}\int_0^a X_m''X_i\,dx-$$

$$-\frac{k_y}{b}\sum_n w_{mn}\frac{\beta_n^2}{b^2}\int_0^b Y_n''Y_j\,dy=0\,. \tag{5.6}$$

Considering relations (3.7b) and (3.12b) which introduce the coefficients $h_{m,i}$ and $\bar{h}_{n,j}$, the results are that equation (5.6) can be written in the general form

$$\left(\frac{\alpha_i^4}{a^4}+\frac{\beta_j^4}{b^4}+k\right)w_{ij}+2\varkappa\sum_m\sum_n\frac{\alpha_m^2\beta_n^2}{a^2b^2}h_{m,i}\bar{h}_{n,j}w_{mn}-$$

$$-k_x\sum_m w_{mn}\frac{\alpha_m^2}{a^2}h_{m,i}-k_y\sum_n w_{mn}\frac{\beta_n^2}{b^2}\bar{h}_{n,j}=\frac{p_{ij}}{K} \tag{5.7}$$

which coincides with (4.7) obtained by using the exact method.

Taking $i,j=1,2,3,\ldots$ the system sought for is obtained.

If the number of approximation functions (X_iY_i) is increased indefinitely (and the double sum is transformed into a double series of characteristic functions) we can recognize that the variational solution represents the proper exact solution.

Note that the derivation of this solution is simpler and more direct.

Particular cases

In what follows we shall underline some important particular cases.

The case $k_x=k_y=0$ corresponds to the absence of friction between the plate and the foundation (Winkler type supporting on the elastic foundation). The corresponding partial differential equation is derived from (2.7) by the cancellation of k_x and k_y:

$$\frac{\partial^4w}{\partial x^4}+2\varkappa\frac{\partial^4w}{\partial x^2\,\partial y^2}+\frac{\partial^4w}{\partial y^4}+kw=\frac{Z(x,y)}{K}\,. \tag{6.1}$$

In solving the problem only the coefficients situated on the main diagonal are affected.

The case $k_x=k_y=0$ and $k=0$ corresponds to the absence of the elastic foundation. The corresponding partial differential equation is derived from (6.1) by the cancellation of k:

$$\frac{\partial^4w}{\partial x^4}+2\varkappa\frac{\partial^4w}{\partial x^2\,\partial y^2}+\frac{\partial^4w}{\partial y^4}=\frac{Z(x,y)}{K} \tag{6.2}$$

and this coincides with that which was stated by S. KRUG and P. STEIN [4].

In solving the problem only the coefficients situated on the main diagonal are affected.

With the subsequent particularisation of $\varkappa$ we get the following cases.

a) $\varkappa = 0$. This case corresponds to a zero torsional rigidity of the orthotropic plate, or to a grid of orthogonal beams (interconnected by means of hinges) or, finally, to the equivalent continuum of a double-layer parallel square mesh grid; the corresponding partial differential equation is derived from (6.2):

$$\frac{\partial^4 w}{\partial x^4} + \frac{\partial^4 w}{\partial y^4} = \frac{Z}{K} \tag{6.3}$$

and this coincides with the equations established by M. V. SOARE [8], K. SZMODITS [13] and O. ZANABONI [17].

Observing that all the secondary coefficients (not situated on the main diagonal of the system) have $\varkappa$ as a factor, vanish.

Each unknown w_{mn} directly results under the form

$$w_{mn} = \frac{p_{mn}}{K} \frac{1}{\frac{\alpha_m^4}{a^4} + \frac{\beta_n^4}{b^4}} \tag{6.4}$$

as found by P. LARDY [5] for grids and by M. V. SOARE [8] for double-layer parallel square mesh grids.

Similar results are obtained in the more general case when $k \neq 0$:

$$\frac{\partial^4 w}{\partial x^4} + \frac{\partial^4 w}{\partial y^4} + kw = \frac{Z}{K} \tag{6.5}$$

with the solution for the unknown coefficients:

$$w_{mn} = \frac{p_{mn}}{K} \frac{1}{\frac{\alpha_m^4}{a^4} + \frac{\beta_n^4}{b^4} + k} . \tag{6.6}$$

b) $\varkappa = 1$. This case corresponds to isotropic plates or to orthotropic plates for which $H^2 - K_x K_y = 0$; the governing equation is derived from (6.2):

$$\frac{\partial^4 w}{\partial x^4} + 2\frac{\partial^4 w}{\partial x^2 \partial y^2} + \frac{\partial^4 w}{\partial y^4} = \frac{Z}{K} . \tag{6.7}$$

There results only a formal simplification of the coefficients of the infinite system. Thus was studied in more detail by P. LARDY [5] for the rectangular plate built—in along the four sides. He underlined the advantage of the method which consists in reducing the solution of two inifnite systems of equations to a single one.

c) $\varkappa = 3$. This case corresponds to the equivalent continuum of a double-layer oblique square mesh grid [9]. The governing equation is derived from (6.2):

$$\frac{\partial^4 w}{\partial x^4} + 6\frac{\partial^4 w}{\partial x^2 \partial y^2} + \frac{\partial^4 w}{\partial y^4} = \frac{Z}{K} . \tag{6.8}$$

In solving the problem of the unknowns w_{mn} only the coefficients situated on the main diagonal are affected.

Concluding remarks

It is easy to see that a simply supported or clamped side implies two boundary conditions with respect to the same variable (x or y). For example, if the simply supported side $x = 0$ is concerned, the conditions $w = 0$ and $\partial^2 w/\partial x^2 = 0$ are reduced to the conditions $X = 0$ and $X'' = 0$.

Similarly for the clamped side $x = 0$, the conditions $w = 0$ and $\partial w/\partial x = 0$ lead to the conditions $X = 0$, $X' = 0$.

The various supporting cases for which the use of simple or double trigonometric series is possible and efficient have been represented in Fig. 2a; the supporting cases for which the use of characteristic functions do not present intricate problems have been represented in Fig. 2b.

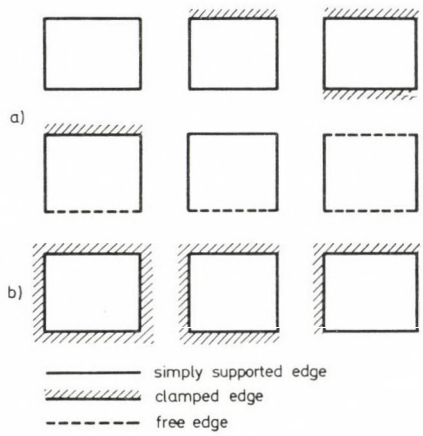

Fig. 2

A free side requires conditions of vanishing bending moment and generalized transverse shear force; in this case, the boundary conditions involve both variables x and y, i.e. a correlation between functions X, Y and their successive derivatives. Consequently from this point of view the problem remains open.

Limiting ourselves to the orthotropic plate without supporting on an elastic foundation — equation (6.2) — the use of tables and graphs of the type of influence surfaces as those published by S. KRUG and P. STEIN [4] is possible. Besides the orthotropic plate parameter $\varkappa$ a second parameter ε will intervene representing the ratio of the transformed side lengths:

$$\varepsilon = \frac{b}{a} \sqrt[4]{\frac{K_v}{K_y}} .$$

Finally the use of double series of characteristic functions may prove extremely efficient in the study of instability and large deformation of isotropic and orthotropic plates.

Notations

a, b	sides of the rectangular plate,
e_x, e_y	position of the centroidal planes in the x and y directions, with respect to the bottom plane,
f	coefficient of friction,
H	torsional rigidity of the orthotropic plate,
k	modulus of the foundation (of Winkler type),
k_x, k_y	constants which introduce the friction between the plate and the foundation,
K_x, K_y	flexural rigidities of the orthotropic plate in the x and y directions, respectively,
p	reaction of the subgrade,
p_{fx}, p_{fy}	friction between the plate and the foundation, in the x and y directions, respectively, per unit area,
w	deflection,
Z	normal distributed load per unit area,
α, β	eigenvalues of the characteristic functions,
γ	parameter of affine transformation of the coordinate y,
ε	ratio of the transformed side lengths,
$\varkappa$	parameter of the orthotropic plate.

APPENDIX 2

Derivation of the partial differential equation (1.1)

By a plate with orthotropy of material or with geometrical orthotropy, we distinguish two centroidal planes corresponding to the directions x and y. Their positions are defined by the distances e_x and e_y with respect to the bottom plane of the plate; generally $e_x \neq e_y$ if the elastic properties of the material or the stiffeners in the x and y directions are different.

The applied loads acting on a plate elements are (Fig. A.1.):

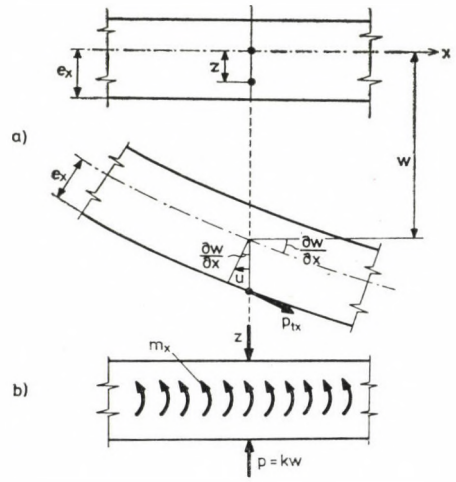

Z normal load per unit area (directed downwards),
$p = kw$ reaction of the subgrade, per unit area (directed upwards),
$P_{tx} = fu_b$ friction between the plate and the foundation, in the x direction, supposed to be proportional with the displacement u_b at the bottom,
$pt_y = fv_b$ friction between the plate and the foundation, in the y direction, supposed to be proportional with the displacement v_b at the bottom.

The geometrical equations hold

$$u_b = -e_x \frac{\partial w}{\partial y}, \quad v_b = -e_y \frac{\partial w}{\partial y}. \tag{A.1}$$

Reducing the friction forces in the centroidal planes and neglecting their in-plane effects, there result the moments

$$m_x = -p_{tx} e_x = +fe_x^2 \frac{\partial w}{\partial x},$$

$$m_y = -p_{ty} e_y = +fe_b^2 \frac{\partial w}{\partial y}; \tag{A.2}$$

introducing the new constants

$$k_x = fe_x^2, \quad k_y = fe_y^2, \tag{A.3}$$

we get

$$m_x = +k_x \frac{\partial w}{\partial x}, \quad m_y = +k_y \frac{\partial w}{\partial y}. \tag{A.4}$$

Now the equilibrium equations of the plate element can be written as follows:

$$\begin{aligned} \frac{\partial M_x}{\partial x} + \frac{\partial M_{yx}}{\partial y} - m_x &= T_x, \\ \frac{\partial M_{xy}}{\partial x} + \frac{\partial M_y}{\partial y} - m_y &= T_y, \\ \frac{\partial T_x}{\partial x} + \frac{\partial T_y}{\partial y} &= -Z + kw. \end{aligned} \tag{A.5}$$

Eliminating the transverse shear forces T_x, T_y between (A.5) we obtain (with $M_{xy} \neq M_{yx}$):

$$\frac{\partial^2 M_x}{\partial x^2} + \frac{\partial^2 M_{xy}}{\partial x\,\partial y} + \frac{\partial^2 M_{yx}}{\partial x\,\partial y} + \frac{\partial^2 M_y}{\partial y^2} - \frac{\partial m_x}{\partial x} - \frac{\partial m_y}{\partial y} - kw = -Z. \tag{A.6}$$

We can further represent the bending and twisting moments in terms of the deflections w of the plate in the form:

$$\begin{aligned} M_x &= -K_x \left(\frac{\partial^2 w}{\partial x^2} + \mu_y \frac{\partial^2 w}{\partial x^2} \right), \\ M_y &= -K_y \left(\frac{\partial^2 w}{\partial y^2} + \mu_x \frac{\partial^2 w}{\partial x^2} \right), \\ M_{xy} &= -2K_{xy} \frac{\partial^2 w}{\partial x\,\partial y}, \\ M_{yx} &= -2K_{yx} \frac{\partial^2 w}{\partial x\,\partial y}, \end{aligned} \tag{A.7}$$

where the flexural rigidities K_x, K_y, the torsional rigidities K_{xy}, K_{yx} and the Poisson's type coefficients μ_x, μ_y are to be determined separately in various specific cases.

Introducing equations (A.7) and (A.4) in (A.6) we finally get

$$\begin{aligned} K_x \frac{\partial^4 w}{\partial x^4} + (K_x \mu_y + K_y \mu_x + 2K_{xy} + 2K_{yx}) \frac{\partial^4 w}{\partial x^2\,\partial y^2} + \\ + K_y \frac{\partial^4 w}{\partial y^4} - fe_x^2 \frac{\partial^2 w}{\partial x^2} - fe_y^2 \frac{\partial^2 w}{\partial y^2} + kw = Z\,; \end{aligned} \tag{A.8}$$

introducing the notations H and k_x, k_y, equation (A.8) coincides with equation (1.1):

$$2H = K_x \mu_y + K_y \mu_x + 2K_{xy} + 2K_{yx}. \tag{A.9}$$

APPENDIX 3

Characteristic functions for three typical supporting cases

Supporting	Clamped — simply supported	Clamped — clamped	Clamped — Free
	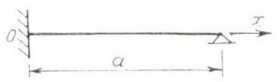	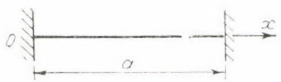	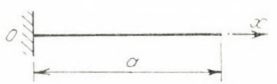
Boundary conditions	$x = 0;\ X(0) = 0;\ X'(0) = 0,$ $x = a;\ X(a) = 0;\ X''(0) = 0.$	$x = 0;\ X(0) = 0;\ X'(0) = 0,$ $x = a:\ X(a) = 0;\ X'(a) = 0.$	$x = 0;\ X\ (0) = 0;\ X'\ (0) = 0,$ $x = a:\ X''\ (a) = 0;\ X'''\ (a) = 0.$
Characteristic equation	$\tan \alpha = \tanh \alpha$	$\cos \alpha \cdot \cosh \alpha = 1$	$\cos \alpha \cdot \cosh \alpha = -1$
Roots α_m and coefficients $\varkappa_m$	$\alpha_1 = 3{,}92660 \quad \varkappa_1 = 1{,}00078$ $\alpha_2 = 7{,}06858 \quad \varkappa_2 = 1{,}00000$ $\alpha_3 = 10{,}21018 \quad \varkappa_3 = 1$ $\alpha_4 = 13{,}35177 \quad \varkappa_4 = 1$ . . . . $\alpha_m \approx \left(m + \frac{1}{4}\right)\pi \quad \varkappa_m \approx 1$	$\alpha_1 = 4{,}73004 \quad \varkappa_1 = 0{,}98250$ $\alpha_2 = 7{,}85320 \quad \varkappa_2 = 1{,}00078$ $\alpha_3 = 10{,}99561 \quad \varkappa_3 = 0{,}99997$ $\alpha_4 = 14{,}13717 \quad \varkappa_4 = 1{,}00000$ . . . . $\alpha_m \approx \left(m + \frac{1}{2}\right)\pi \quad \varkappa_m \approx 1$	$\alpha_1 = 1{,}87510 \quad \varkappa_1 = 0{,}73410$ $\alpha_2 = 4{,}69409 \quad \varkappa_2 = 1{,}01847$ $\alpha_3 = 7{,}85457 \quad \varkappa_4 = 0{,}99922$ $\alpha_4 = 10{,}99554 \quad \varkappa_, = 1_800003$ . . . . $\alpha_m \approx \left(m_m - \frac{1}{2}\right)\pi \quad \varkappa_m \approx 1$
Characteristic functions and their successive derivatives	$X_m = \cosh \alpha_m \frac{x}{a} - \cos \alpha_m \frac{x}{a} - \varkappa_m \left(\sinh \alpha_m \frac{x}{a} - \sin \alpha_m \frac{x}{a}\right),$ $\frac{a}{\alpha} \frac{dX_m}{dx} = X'_m = \sinh \alpha_m \frac{x}{a} + \sin \alpha_m \frac{x}{a} - \varkappa_m \left(\cosh \alpha_m \frac{x}{a} - \cos \alpha_m \frac{x}{a}\right),$ $\frac{a^2}{\alpha_m^2} \frac{d^2X_m}{dx^2} = X''_m = \cosh \alpha_m \frac{x}{a} + \cos \alpha_m \frac{x}{a} - \varkappa_m \left(\sinh \alpha_m \frac{x}{a} + \sin \alpha_m \frac{x}{a}\right),$ $\frac{a^3}{\alpha_m^3} \frac{d^3 X_m}{dx^3} = X'''_m = \sinh \alpha_m \frac{x}{a} - \sin \alpha_m \frac{x}{a} - \varkappa_m \left(\cosh \alpha_m \frac{x}{a} + \cos \alpha_m \frac{x}{a}\right).$		

Series expansion for a typical load

$$p(x) = \sum_m p_m X_m(x) \quad \text{where} \quad p_m = \frac{1}{a}\int_0^a p(x) X_m(x)\, dx\,.$$

Coefficients p_m for uniform load ($p = $ = const.)

$$p_m = \frac{1}{\alpha_m}\left[(X_m''')_{x=a} + 2\varkappa_m\right] p \qquad (m = 1, 2, 3, \ldots)$$

$$p_m = \frac{4\varkappa_m}{\alpha_m}\, p \qquad (m = 1, 3, 5, \ldots)$$

$$p_m = \frac{2\varkappa_m}{\alpha_m}\, p \qquad (m = 1, 2, 3, \ldots)$$

Series expansion of the second order derivative

$$X_m'' = \sum_i k_{m,i} X_i \qquad \text{where} \qquad k_{m,i} = \frac{1}{a}\int_0^a X_m'' X_l\, dx\,.$$

$k_{m,i}$ and $k_{m,m}$ coefficients

$$k_{m,m} = \frac{\varkappa_m}{\alpha_m} - \varkappa_m^2$$

$$k_{m,i} = \frac{4\alpha_m^2}{\alpha_m^4 - \alpha_l^4}(\varkappa_m\alpha_m - \varkappa_l\alpha_l) \qquad (m \neq i)$$

$$k_{m,m} = \frac{2\varkappa_m}{\alpha_m} - \varkappa_m^2$$

$$k_{m,l} = 0 \text{ for } i + m = \text{odd}$$

$$k_{m,l} = \frac{8\alpha_m^2}{\alpha_m^4 - \alpha_l^4}(\varkappa_m\alpha_m - \varkappa_i\,\alpha_i)$$

for $i + m =$ even
$(m \neq i)$

$$k_{m,m} = \frac{2\varkappa_m}{\alpha_m} - \varkappa_m^2$$

$$k_{m,l} = 4\,\frac{\varkappa_m\,\alpha_m - \varkappa_i\,\alpha_l}{\alpha_m^4 - \alpha_l^4}\,[\alpha_m^2 + (-1)^{l+m}\,\alpha_l^2] \qquad (m \neq i)$$

REFERENCES

1. BELES, A. A.—SOARE, M. V.: Elliptic and Hyperbolic Paraboloidal Shells Used in Constructions. Ed. Academiei, Bucharest 1976
2. FELGAR JR. R. P.: Formulas for Integrals Containing Characteristic Functions of a Vibrating Beam. *Bureau of Engineering Research*, Circular No. 14, The University of Texas, 1950
3. GIRKMANN, K.: Flächentragwerke, 6-te Aufl., Springer-Verlag, Wien 1963
4. KRUG, S.—STEIN, P.: Einflußfelder orthogonal anisotroper Platten. Springer-Verlag, Berlin/Göttingen/Heidelberg, 1961
5. LARDY, P.: Sur une méthode nouvelle de résolution du problème des dalles rectangulaires encastrées. Association Internationale des Ponts et Charpentes, *Mémoires*, **13,** Zürich (1953), 197—220
6. MISICU, M.: Beams and Plates on Elastic Foundation (in Romanian). *Bul. St. Acad. Republicii Populare Romane*, **3,** (1951), 361—375
7. SOARE, M. V.: A General Method for Solving Rectangular Plates (in Romanian). *St. Cerc. Mec. Apl.*, **12** (1961), 277—291
8. SOARE, M. V.: Statics and Dynamics of Double-Layer Square Mesh Grids by the Application of the Equivalent Continuum Method (in Romanian). *St. Cerc. Mec. Apl.*, **31** (1972), 673—702
9. SOARE, M. V.: On the Statics and Dynamics of Double-Layer Oblique Square Mesh Grids. *Acta Techn. Hung.* **79** (1974), 335—350
10. SOARE, M. V.: Contributions to the Analysis of Orthotropic Plates with Eccentric Stiffeners (in Romanian). *St. Cerc. Mec. Apl.*, **33** (1974), 695—710; **34** (1975), 31—44
11. SOARE, M. V.: Plates (Section No. VI of the Handbook for the Analysis of Structures) (in Romanian), 2nd Ed., Ed. Tehnica, Bucharest 1977
12. SOARE, M. V.: A General Method for Solving Orthotropic Plates (in Romanian). *St. Cerc. Mec. Apl.*, **39** (1980), 203—219
13. SZMODITS, K.: Investigation of Rectangular Plates and Gridworks on the Basis of Different Boundary Conditions. *Acta Techn. Hung.*, **48** (1964), 23—28
14. TIMOSHENKO, ST. P.—WOINOWSKY-KRIEGER, S.: Theory of Plates and Shells, 2nd Ed., McGraw-Hill Book Comp. Inc., Toronto 1959
15. WLASSOW, W. S.: Allgemeine Schalentheorie und ihre Anwendung in der Technik. Akademie-Verlag, Berlin 1958
16. YOUNG, D. H.—FELGAR JR, R. P.: Tables of Characteristic Functions Representing Normal Modes of Vibration of a Beam. *Engineering Research Bulletin* No. 4913, Bureau of Engineering Research, The University of Texas, Jul 1949
17. ZANABONI, O.: Reticoli di travi a grande numero di maglie. *Giornale del Genio Civile*, **5** (1947)

Ein neues Verfahren zur Lösung rechtwinkliger orthotroper Platten. — Es wird von der partiellen Differentialgleichung orthotroper Platten, gestützt auf die Verschmierung der Rippen in zwei orthogonalen Richtungen, ausgegangen. Diese Gleichung wird mit den Gliedern ergänzt, die die Wirkung der Lagerung auf eine elastische Winkler-Bettung und die Berücksichtigung der Reibung zwischen Platte und elastischer Bettung ausdrücken. Die auf der Anwendung doppelter Reihen von Fundamentalfunktionen beruhende Aufgabe führt zur Aufstellung und Lösung eines linearen Systems unendlich vieler Gleichungen und Unbekannten.

Acta Technica Academiae Scientiarum Hungaricae, Tomus 92 (1—2), pp. 23—32 (1981)

EFFECT OF RAPID HEAT TREATMENT ON THE MICROSTRUCTURE AND TENSILE PROPERTIES OF COLD DRAWN BORON-TREATED STEEL (ZF_7)

PART I.

M. A. ABD ELHADY*
MASTER OF TECHN. SCI.

and

J. PROHÁSZKA*
CORR. MEMBER OF THE HUNG. AC. OF SCI.

[Manuscript received: 3 March 1980]

This paper describes three methods of heat treatment for high hardenability boron-treated steel. The object of this work is to determine the change in microstructure and tensile properties due to these different heat treatment operations. The present paper is to be considered the first report on the heat treatment of cold drawn boron treated steel and will be followed by subsequent works in order to select a new technology for the heat treatment of ZF_7 steel.

1. Introduction

Boron-treated steel is one of the high hardenability steels, the effect of boron on different mechnical properties depends on the state of boron in the steel since boron appears in two states: (i) compound state, (ii) dissolved in the solid solution as interstitial element (0,87 Å radius). We assume that in ZF_7 steel boron dissolved in solid solution due to the insufficient amounts of boron and also to the small amounts of I and Ir in the steel, this beside the presence of Al in the steel.

The hardenability of boron-treated steels has long been a subject of research from both the fundamental and practical points of view [1—5]. There are several factors which affect the hardenability of boron-treated steels thermal and mechanical history, austenitizing time and temperature, chemical composition etc. Among those factors, such elements as aluminium, titanium and nitrogen play a very important role in controlling the effect of boron on the hardenability of boron-treated steels [6].

There is much controversy about the effect of boron on the brittleness of steel. Some workers [7] have suggested that boron may not have any effect on embrittling susceptibility, but others [8] report that, boron promotes

* Institute for Technology and Materials Science, Technical University Budapest.

temper brittleness. These contradictory observations can possible be reconciled with the work of BERNSTEIN [9] who found that, the degree of embrittlement is not substantially affected by the addition of boron up to 0,45% for low austenitizing temperature (850 °C), and that (ii) for higher austenitizing temperature (1200 °C) a small addition of boron (0,05%) reduces the susceptibility of steel and at higher boron contents the degree of embrittlement increases.

2. Material and experimental procedures

The material used is ZF_7 steel, MSZ 4337—71. This material was hot rolled in the form of rods having a 10 mm diameter. After that it was cold drawn from 10 mmD to 0,3 mmD at different steps, and between some steps and the others, it was annealed at 650 °C for 30 mint, and finally it was cold drawn from 3,2 to 1,46 mm diameter.

Chemical composition

Steel grade	Chemical composition %							
	C	Mn	Si	P	S	Cr	B	Al
ZF_7	0,16 0,20	1,00 1,30	0,15 0,40	0,035	0,035	1,00 1,30	0,006 0,007	0,03

3. Experimental procedures

I/A. Rapid heat treatment of cold drawn steel (time = 2 sec) with different electrical energies (KW/cm^3). The heating and cooling was done under controlled atmosphere (30% H + 70% N).

I/B. (i) Annealing of cold drawn steel (time 15 min) in a lead bath followed by cooling in air (at 650 °C ± 10).

(ii) Rapid heat treatment of the annealed steel (time 2 sec) at different electrical energies with heating and cooling atmosphere as in I/A.

I/C. This is normal annealing of cold drawn steel at different temperatures in a lead both for 15 mints. The testing methods used are metallographic and tension test to study the change in microstructure and tensil properties due to those different heat treatment methods.

4. Summary od results and discussion

I/A. experiments

Pictures 1, 2, 3, 4, 5, 6 show the change in microstructure produced due to increasing the electrical energies from 0 to 6,206 KW/cm^3.

Fig. 1 shows how the tensile properties change with the change in electrical energies.

Thus, it is clear from the microstructures and tensile properties study that:

From 0 to 2,359 KW/cm^3

The microstructures are deformed grains elongated in the direction of cold drawing (Pictures 1, 2) The effect of this range on tensile properties is not so much.

From 2,359 to 4,321 KW/cm^3

Recrystallization process takes place. This was proved from pictures 2, 3, 4 and from the tensile properties tests with values given beside each picture.

From 4,629 to 5,064 KW/cm^3

This electrical energy range, heating the samples between A_1 and A_3 are critical temperatures.

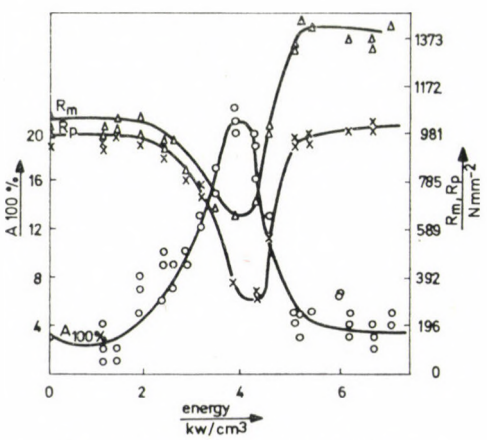

The change in tensile properties at different electrical energy during rapid heat treatment of cold drawn stell [I/A]

Fig. 1

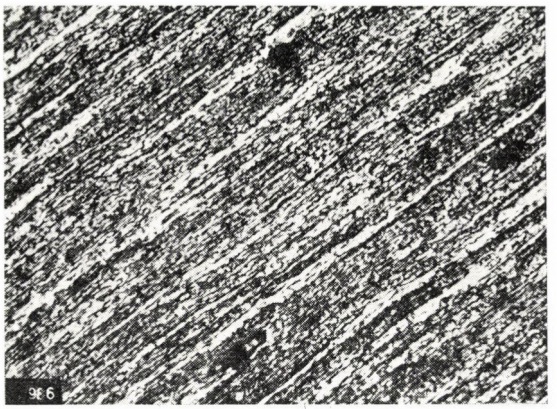

Picture 1

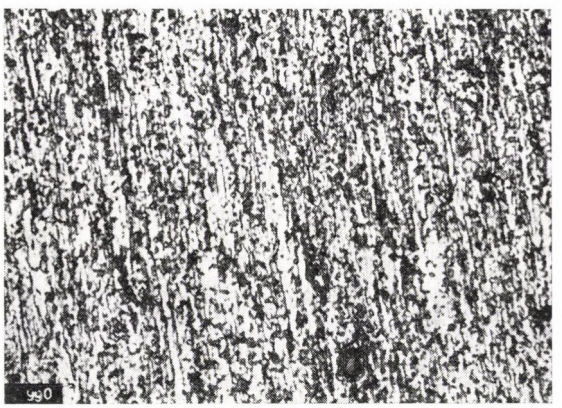

Picture 2

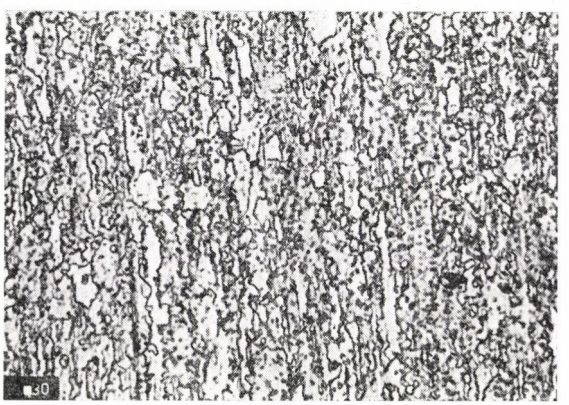

Picture 3

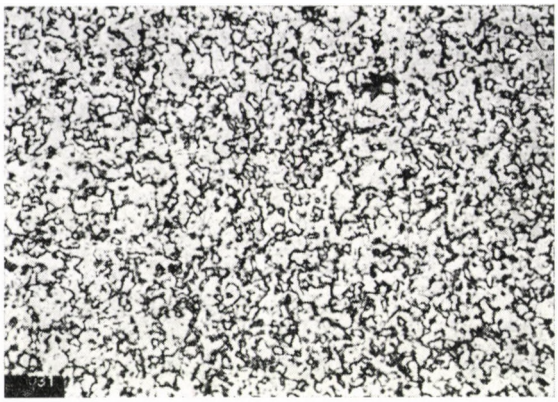

Picture 4

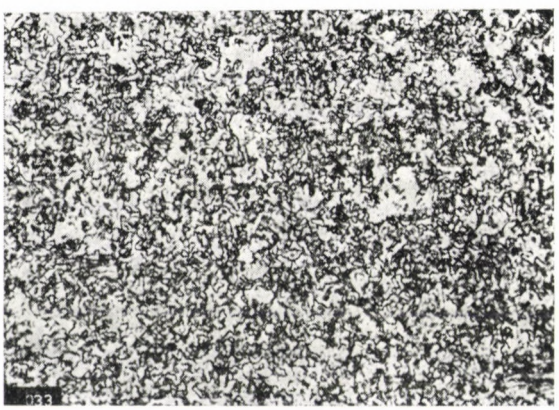

Picture 5

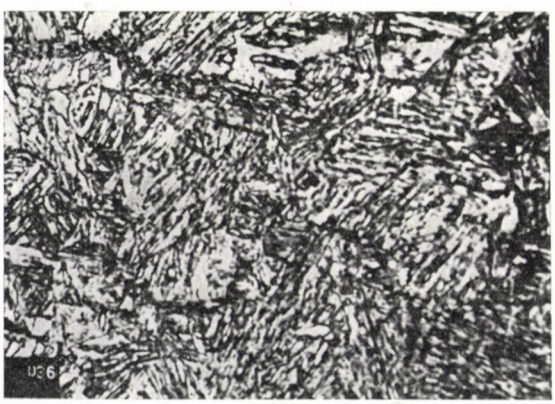

Picture 6

Thus, it is clear from Picture 5 and Fig. 1 that: The increase of electrical energy from 4,629 to 5,064 KW/cm^3 was accompanied by the increase in strength properties and decrease in plastic properties which may be due to martensitic transformation.

From 5,173 to 7.082 KW/cm^3

From picture 6 and Fig. 1 it is clear that heating the samples in this range will raise the temperature above A_3 and so martensitic transformation may be induced.

I/B. experiments

Pictures 7, 8, 9 show the change in microstructure produced due to increasing the electrical energy from 2,177 to 6,164 KW/cm^3.

Fig. 2 shows how the tensile properties varied with the electrical energy.

Thus, it is clear from the microstructure study and tensile properties study that:

From 0,920 to 4,032 KW/cm^3

In this range there is no significant difference in tensile properties (Fig. 2). The only different may be a small change in grain size.

So, this applied energy range heated the samples at temperatures below A_1.

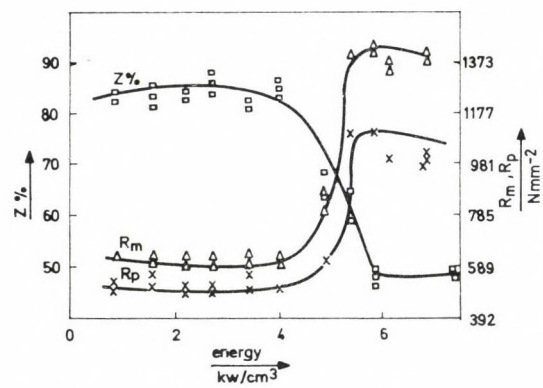

The change in tensile properties at different electrical energy during rapid heat treatment of annealed steel [I/B]

Fig. 2

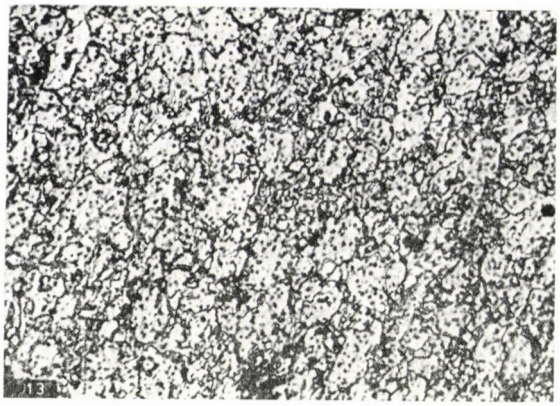

Picture 7

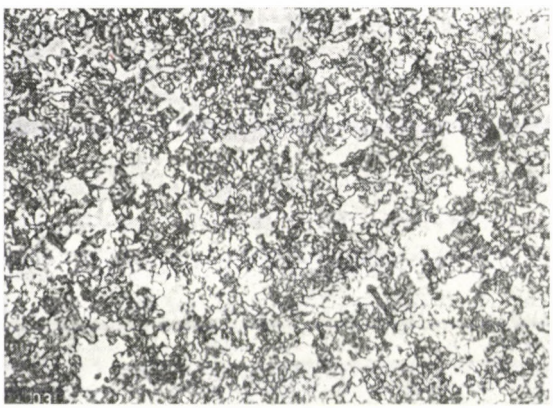

Picture 8

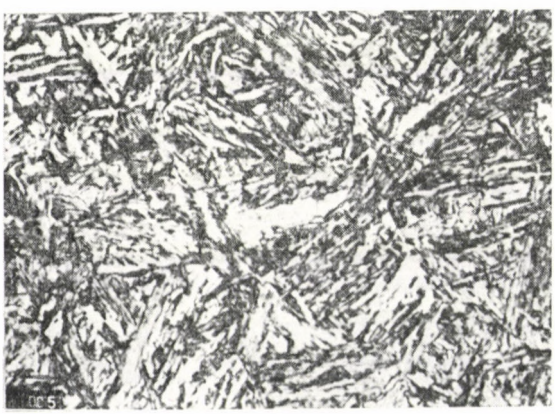

Picture 9

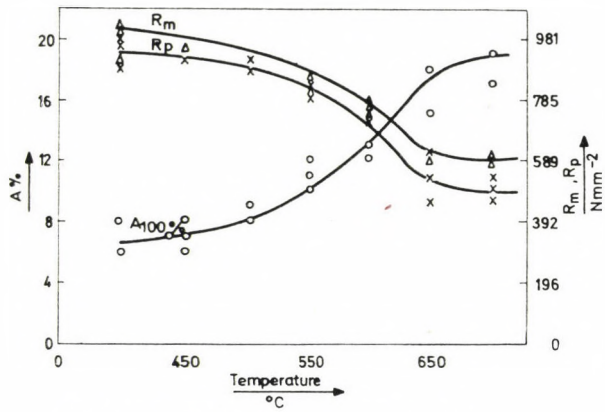

The change in tensile properties with the change in annealing temperature [I/C]

Fig. 3

From 4,921 to 5,436 KW/cm³

Considering microstructures (Picture 8) and tensile properties (Fig. 2). It is clear that the samples were heated at temperatures between A_1 and A_3.

Above 5,436 KW/cm³

The structure is martensitic and so the metal was heated above A_3.

I/C. experiments

Pictures 10, 11, 12 show how the microstructures change by increasing the annealing temperatures. Fig. 3 shows how the tensile properties varied with the annealing temperatures.

5. Conclusions

1. Annealing of a cold drawn specimen before rapid heat treatment does not produce significant effect on the tensile properties.

2. The required electrical energy for recrystallization of cold drawn steel is in the range 4,321 to 4,629 KW/cm³.

3. Heating the cold drawn steel with higher electrical energy produces martensitic transformation.

4. There is not visible difference in this work between the normal annealing of cold drawn steel and rapid heat treatment of this same steel.

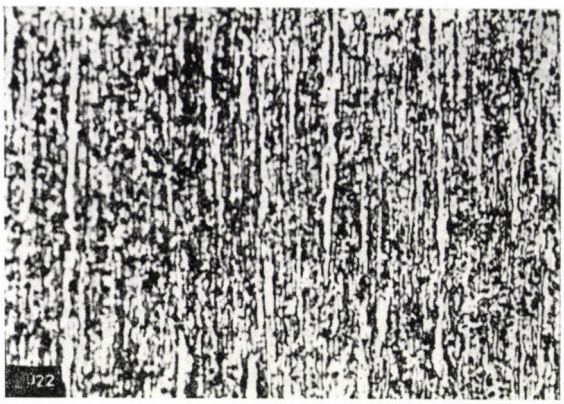

Picture 10

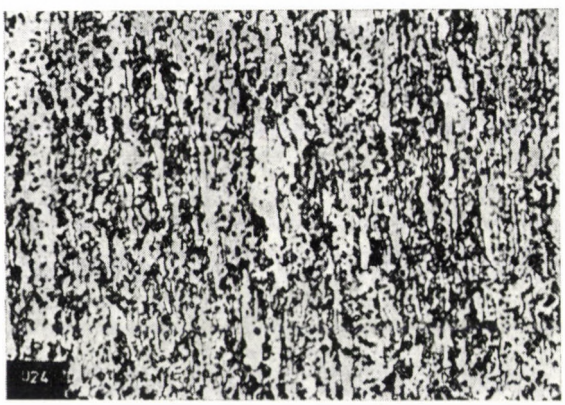

Picture 11

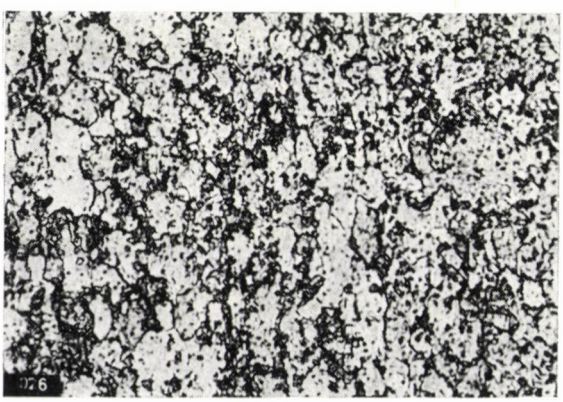

Picture 12

The only difference is the necessary time for recrystallization which is 2 sec at 4,321 KW/cm^3 rapid heat treatment and 15 mint at 650 °C in normal annealing.

REFERENCES

1. GRANGE, R. A.—GARVEY, T. M.: *Trans ASM*, **37** (1946), 136
2. OHMORI, Y.: *Trans Iron Steel Inst.* Jpn **11** (1971), 339
3. UENO, M. — INOUF, T.: *Trans Iron Steel Inst.* Jpn **13** (1973), 210
4. YAMANAKA, K.—OHMORI, Y.: *Trans Iron Steel Inst* Jpn 1974
5. NAKASATO, F.—TAKOHASHI, M.: *Metals Technology* (1979) March
6. GRANGE, R. A.: B, Ca, Cb and Zr in Iron and Steel 3—57 (1957) New York, Wiley inc
7. UDY, M. C.—ROSENTHAL, P. C.: *Trans AIME* **172** (1947), 273
8. POWERS, A. E.—CARLSON, R. F.: *Trans ASM* **45** (1954), 483
9. BENNSHTEIN, M. L.: Metallovedenici abrobotka, **2** (1956), 25, Henry Brutcher Translation No 3855
10. M. C. UDY and P, C. ROSENTHAL : *Trans AIME* (1947), **172,** 273
11. A. E. POWERS and R. F. CARLSON : *Trans ASM* (1954) **45,** 489
12. M. L. BENNSHTEIN: Metallovedenici abrobotka, (1956) **2,** 25. Henry Brutcher Translation No 3855

Einwirkung der schnellen Wärmebehandlung auf die Mikrostruktur und auf die Zugfestigkeit des kaltgezogenen Borstahls (ZF_7). I. Teil. — Es werden drei Methoden der Wärmebehandlung des borhehandelten Stahls von hoher Härte erörtert. Das Anliegen der Abhandlung ist die Ermittlung der Änderung der Mikrostruktur und der Zugfestigkeitseigenschaften infolge der verschiedenen Wärmebehandlungsmethoden. Diese Abhandlung ist als der erste Bericht über die Wärmebehandlung vom kaltgezogenen borbehandelten Stahl zu betrachten. Die Auswahl einer neuen Wärmebehandlungstechnologie des ZF_7 Stahls wird in den folgenden Berichten behandelt.

Acta Technica Academiae Scientiarum Hungaricae, Tomus 92 (1—2), pp. 33—43 (1981)

STABILITY OF A BAR ELASTICALLY BUILT-IN AT ONE OF ITS EXTREMITIES

P. CSONKA*
DOCTOR OF TECHN. SCI.

[Manuscript received 1 September, 1980]

Paper deals with the buckling caused by the dead load of a prismatic bar of vertical axis, made of elastic material. It assumes that the lover end of the bar is elastically built-in while its top end is entirely free. The critical load of the bar is determined by Timoshenko's approximate method. The deflected shape of the bar axis is approached by a third-degree polynome. In the extreme case when the foot of the bar is rigidly fixed, this assumption leads to a result hardly differing from the correct one, while in the other extreme case when the bar is absolutely rigid, it yields the exact result.

1. Introduction

The buckling of an elastic bar of vertical axis whose lower extremity is rigidly fixed, the upper end being entirely free has been treated by numerous authors, among them by TIMOSHENKO [1] in his excellent monography. The stability problem of a prismatic bar load at its extremities and supported in different ways has been treated by W. MUDRAK [2] and L. LIPTÁK [6]. Several papers also dealt with the problem how high can a column of vertical axis be built out of a given quantity of material without the danger of buckling, assuming that the column is rigidly fixed at its lower, and quite free at its upper end. Thus, J. B. KELLER [4] and then I. TADJBAKHSH and J. B. KELLER [5] studied the buckling of a column fixed at its lower end and only loaded at the top of the column. On the other end, J. B. KELLER and T. J. NIORDSON [7] investigated the most appropriate shape of a column rigidly fixed at its lower end carrying its own weight and its top end load.

Similar stability problems might occur also in the case of high, slender projects (such as chimneys and towers). Such a problem was first treated by I. MENYHÁRD, namely in connection with the construction of the 100 m high chimney of the power plant in Százhalombatta. A similar problem, i.e., the stability of constructions with a high centre of gravity has been studied by

* Prof. P. CSONKA, Bartók B. út 31. H—1114 Budapest, Hungary

E. DULÁCSKA [3], who also considered the incidental eccentricity of the vertical loads, as well as the effect of the wind load and the fact that in the deviated position of the structure the foundation might not be supported on its full surface by the elastic soil.

This paper deals with the buckling of a prismatic bar of elastic material, with the assumption that it is elastically built-in at its lower end, but being entirely free at its upper end. The bar is loaded along its axis by uniformly distributed system of vertical forces (i.e. by its dead weight). The load which causes the buckling of the bar, the so-called *critical load* is treated by Timoshenko's *method of energy* [1] currently used in the theory of structural mechanics which furnishes an upper limit of the critical load. The calculations are based on the assumption that the fixation of the bar is fully efficient also at the moment when buckling takes place.

2. Notations

In the paper, beside the designations defined in the text, the following symbols are used:

l — length of the bar
E — modulus of elasticity
I — moment of inertia
q — vertical load per unit length of bar axis
M — bending moment
M_0 — fixed end bending moment
c — moment causing unit rotation of the foundation
φ — angle of rotation of the foundation
U — bending energy at of the deflected bar axis
V — restraining energy at the fixed end
W — work performed by the applied forces during buckling

3. Fundamental relationships

By applying Timoshenko's method of energy [1] it will be assumed that the shape of the slightly deflected bar axis can be approximated by the polynome

$$y = \frac{Ax}{l} + \frac{3B}{2l^2}\left(x^2 - \frac{x^3}{3l}\right) \tag{1}$$

wherein x, y are the axes of the orthogonal system of coordinates to be seen in Fig. 1, while A and B being displacement values interpreted in Fig. 1.

According to relationship (1), at the top end of the bar, that is at $x = l$,

$$M = EI\frac{d^2y}{dx^2} = 0\,,$$

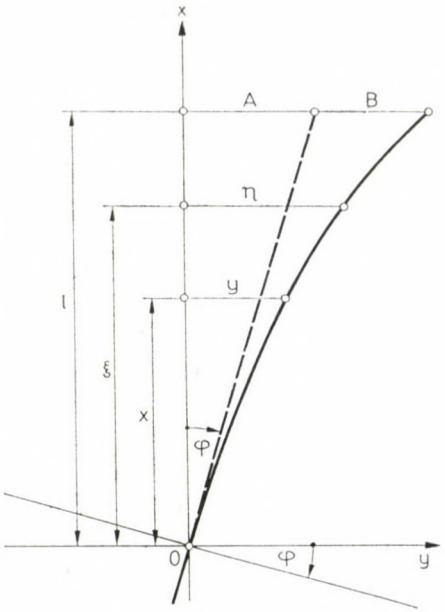

Fig. 1. Notations

which corresponds with the preliminary assumption that this end of the bar is entirely free.

The bending moment M applied to the cross section of ordinate x of the deflected bar may be expressed as follows

$$M = \int_x^l q(\eta - y)\, d\xi \,.$$

The value of y entering in the above formula can be determined by formula (1) and that of η by the relationship

$$\eta = A\frac{\xi}{l} + \frac{3B}{2l^2}\left(\xi^2 - \frac{\xi^3}{3l}\right).$$

Thus,

$$M = q\int_x^l \left[\frac{A}{l}(\xi - x) + \frac{3B}{2l^2}\left(\xi^2 - x^2 - \frac{\xi^3 - x^3}{3l}\right)\right] d\xi \,.$$

By performing the prescribed operations M may be devided into two parts:

$$M = M_1 + M_2 \,,$$

wherein

$$M_1 = A\frac{q}{l}\left(\frac{l^2}{2} - lx + \frac{x^2}{2}\right), \tag{2}$$

$$M_2 = B\frac{3q}{2l}\left(\frac{l^2}{4} - x^2 + \frac{x^3}{3l} - \frac{x^4}{4l^2}\right). \tag{3}$$

At the fixed-end i.e., at the point $x = 0$, the bending moment is

$$M_0 = A\frac{ql}{2} + B\frac{3ql}{8}. \tag{4}$$

4. Energy and work values

For applying Timoshenko's method of energy, the work accumulated in the deflected bar, further the restraining energy of the fixation, as well as the work performed by the applied forces during buckling should be determined one by one.

4.1. *The flexural energy*

This kind of energy may be calculated in the following way:

$$U = \int_0^l \frac{1}{2EI} M^2 \cdot dx = \frac{1}{2EI}\int_0^l (M_1 + M_2)^2\, dx.$$

Dividing this formula into parts, yields

$$U = \frac{1}{2EI}\left(\int_0^l M_1^2 \cdot dx + \int_0^l 2M_1 M_2 \cdot dx + \int_0^l M_2^2 \cdot dx\right). \tag{5}$$

In order to determine the values of these integral expressions, relations (2) and (3) vill be introduced. Thus, the value of the first integral becomes

$$\int_0^l M_1^2 \cdot dx = \frac{A^2 q^2}{l^2}\left[\frac{l^4 x}{4} - \frac{l^3 x^2}{2} + \frac{l^2 x^3}{2} - \frac{l x^4}{4} + \frac{x^5}{20}\right]_0^l = \frac{A^2 q^2 l^3}{20}, \tag{6a}$$

the value of the second integral expression is

$$\int_0^l 2M_1 M_2 \cdot dx = \frac{6ABq^2}{l^3}\left[\frac{l^5 x}{8} - \frac{l^4 x^2}{8} - \frac{l^3 x^3}{8} + \frac{3l^2 x^4}{8} - \right.$$

$$\left. - \frac{13\, l x^5}{40} + \frac{x^6}{8} - \frac{x^7}{56l}\right]_0^l = \frac{27\, ABq^2 l^3}{280}, \tag{6b}$$

and the value of the third integral expression will be:

$$\int_0^l M_2^2 \cdot dx = \frac{9B^2q^2}{4l^4}\left[\frac{l^6 x}{16} - \frac{l^4 x^3}{6} + \frac{l^3 x^4}{8} + \frac{7l^2 x^5}{40} - \right.$$

$$\left. - \frac{lx^6}{3} + \frac{3x^7}{14} - \frac{x^8}{16l} + \frac{x^9}{144l^2}\right]_0^l = \frac{107\,B^2q^2l^3}{2240} . \tag{6c}$$

Putting values (6a), (6b), (6c) into Eq. (5), the value of the bending energy can be expressed as follows:

$$U = \frac{q^2 l^3}{2EI}\left(\frac{A^2}{20} + \frac{27\,AB}{140} + \frac{107\,B^2}{2240}\right) . \tag{7}$$

4.2. *The restraining energy*

Under the effect of moment M_0 the clamping structure of the bar is submitted to a rotation

$$\varphi = \frac{M_0}{c} .$$

Accordingly, the restraining energy at the built-in end of the bar will be

$$V = \frac{M_0 \varphi}{2} = \frac{M_0^2}{2c} .$$

Thus, carrying out the substitution (4) and taking the relationship

$$\varphi = \frac{A}{l}$$

into account, the restraining energy can be expressed by formula

$$V = \frac{1}{2c}\left(\frac{A^2q^2l^2}{4} + \frac{3AB\,q^2l^2}{8} + \frac{9B^2q^2l^2}{64}\right)$$

which, after reduction may be written as follows:

$$V = \frac{q^2 l^2}{c}\left(\frac{A^2}{8} + \frac{3AB}{16} + \frac{9B^2}{128}\right) . \tag{8}$$

4.3. *The work of the applied forces*

During buckling of the bar axis, the elementary section dx of the bar lying between cross-sections x and $x + dx$ deviates by an angle dy/dx, and so the part of the bar of length $(l - x)$ lying above the elementary sector dx will undergo a downward displacement equal to

$$\frac{1}{2}\left(\frac{dy}{dx}\right)^2 dx \ .$$

During sinking down, the loading forces $q(l - x)$ applied on the length $(l - x)$ of the bar above the sector dx carry out the elementary work

$$dW = q(l - x) \cdot \frac{1}{2}\left(\frac{dy}{dx}\right)^2 dx \ .$$

The total work performed by the loading forces applied to the whole length l of the bar is the integral of the elementary works:

$$W = \frac{q}{2}\int_0^l (l - x)\left(\frac{dy}{dx}\right)^2 dx \ .$$

In this formula, in consequence of relationship (1)

$$\frac{dy}{dx} = \frac{A}{l} + \frac{3Bx}{l^2} - \frac{3B\,x^2}{l^3} \ ,$$

wherefrom, the work of the applied forces is

$$W = \frac{q}{2}\left[A^2\left(\frac{x}{l} - \frac{x^2}{2l^2}\right) + AB\left(\frac{3x^2}{l^2} - \frac{3x^3}{l^3} + \frac{3x^4}{4l^4}\right) + \right.$$

$$\left. + \frac{B^2}{8}\left(\frac{24\,x^3}{l^3} - \frac{35\,x^4}{l^4} + \frac{18\,x^5}{l^5} - \frac{3\,x^6}{l^6}\right)\right]_0^l \ ,$$

i.e.,

$$W = q\left(\frac{A^2}{4} + \frac{3AB}{8} + \frac{3B^2}{16}\right) . \tag{9}$$

5. The critical load

The specific value of the critical load (better to say, its upper limit) may be determined by equation

$$U + V = W$$

which expresses the equality of the deformation energy and the work of the applied forces. This equation by replacement of (7), (8), (9) becomes

$$\frac{q^2 l^2}{2EI}\left(\frac{A^2}{20}+\frac{27\,AB}{280}+\frac{107\,B^2}{2240}\right)+\frac{q^2 l^2}{c}\left(\frac{A^2}{8}+\frac{3AB}{16}+\frac{9B^2}{128}\right)=$$

$$=q\left(\frac{A^2}{4}+\frac{3\,AB}{8}+\frac{3\,B^2}{16}\right).$$

From the above equation the following formula may be deduced as the specific value of the critical load of the bar:

$$q_{cr}=\frac{\dfrac{A^2}{4}+\dfrac{3AB}{8}+\dfrac{3B^2}{16}}{\dfrac{l^3}{EI}\left(\dfrac{A^2}{40}+\dfrac{27AB}{560}+\dfrac{107\,B^2}{4480}\right)+\dfrac{l^2}{c}\left(\dfrac{A^2}{8}+\dfrac{3AB}{16}+\dfrac{9B^2}{128}\right)}. \tag{10}$$

A slight transformation of Eq. (10) yields

$$q_{cr}=\frac{EI}{l^3}\cdot\frac{1120\,A^2+1680AB+840\,B^2}{112A^2+216AB+107B^2+\dfrac{EI}{cl}(560\,A^2+840\,AB+315\,B^2)}, \tag{10a}$$

or, written in another form:

$$q_{cr}=\frac{c}{l^2}\cdot\frac{1120\,A^2+1680\,AB+840\,B^2}{\dfrac{cl}{EI}(112A^2+216AB+107B^2)+(560A^2+840AB+315\,B^2)}. \tag{10b}$$

To determine the critical load value, notations

$$\frac{B}{A}=z\,,\qquad\frac{EI}{cl}=H$$

will be introduced. Thus, formulae (10a) and (10b) may be transformed into

$$q_{cr}=\frac{280\,EI}{l^3}\cdot\frac{4+6z+3\,z^2}{(112+560H)+(216+840H)\,z+(107+315H)\,z^2} \tag{11a}$$

or

$$q_{cr}=\frac{280}{l^2}\cdot\frac{H(4+6z+3z^2)}{(112+560H)+(216+840H)z+(107+315H)\,z^2}. \tag{11b}$$

Now such a value of z is to be determined, by the use of which expressions (11) take their minimum. The preliminary condition of the desired extreme value is that

$$dq_{cr}/dz = 0 ,$$

which will be satisfied when

$$[(112 + 560H) + (216 + 840H)z + (107 + 315H)z^2](6 + 6z) - \\ -(4 + 6z + 3z)^2[(216 + 840H) + (214 + 630H)z] = 0 .$$

The above equation may be reduced to the form

$$(3 + 315H)\, z^2 + (-92 + 420H)\, z - 96 = 0 .$$

From both roots of the above second-degree equation the positive one furnishes the minimum of expressions (11). This root, i.e., the desired quotient $z = B/A$ is expressed by formula

$$z = \frac{92 - 420H + \sqrt{9616 + 43680\,H + 176400\,H^2}}{6 + 630\,H} . \qquad (12)$$

After determination of the value z, the critical load value (better to say, its upper limit) may be calculated at will by using whether formula (11a) or (11b).

In the extreme case of $H = 0$, formula (12) leads to the value $z = 31{,}676\,866$ instead of the accurate one $z = \infty$. This absurdity is the consequence of the approximate character of formula (1) , and has a reducing effect on the rigidity conditions of the bar and on the value of the force obtained as critical load. Anyhow, the approximate value of the critical load to be calculated by making use of formula (11a), hardly differs from the accurate one. Namely, formula (11a) yields, in the case of $H = 0$, the value

$$q_{cr} = 7{,}84\,822\,\frac{EI}{l^3} ,$$

while the theoretically accurate value may be expressed by the minimum positive root of the equation

$$1 - \frac{s}{1!\,4} + \frac{s^2}{2!\,4 \cdot 10} - \frac{s^3}{3!\,4 \cdot 10 \cdot 16} + \frac{s^4}{4!\,4,10 \cdot 16 \cdot 22} - + \ldots = 0 .$$

Denoting the minimum positive root by s_6, the accurate value is

$$q_{cr} = s_0 \frac{3EI}{2l^3} = 5{,}224\,898\,\frac{3EI}{2l^3} = 7{,}83735\,\frac{EI}{l^3} .$$

Table 1
Quotient z

H = EI/cl	z
0,001	28,637 188
0,003	24,014 591
0,01	15,296 876
0,03	7,417 112
0,1	2,543 347
0,3	0,833 108
1,0	0,237 840
3,0	0,077 337
10,0	0,022 964
30	0,007 631
100	0,002 287
300	0,000 762
1000	0,000 229

Table 2
Critical load

H = EI/cl	EI/l_z	c_{cr}
0,001	7,8247	0,0078
0,003	7,7779	0,0233
0,001	7,6173	0,0762
0,03	7,1830	0,2155
0,1	5,9261	0,5986
0,3	3,9267	1,1780
1,0	1,6547	1,6547
3,0	0,6244	1,8732
10	0,1961	1,9606
30	0,0662	1,9867
100	0,0200	1,9960
300	0,0067	1,9987
1000	0,0020	1,9996

Table 3
Ratio l_0/l

H = EI/cl	l_0/l
0,001	1,123
0,003	1,126
0,01	1,138
0,03	1,172
0,01	1,129
0,3	1,585
1,0	2,442
3,0	3,976
10,0	7,094
30	12,210
100	22,214
300	38,381
1000	70,248

The approximate value to be calculated by using formula (11b) is only by 0,14 per cent higher than the above one.

In the extreme case of $H = \infty$, the critical load value calculated by making use of formula (11b) is

$$q_{cr} = \frac{2c}{l^2},$$

which precisely agrees with the theoretically accurate value.

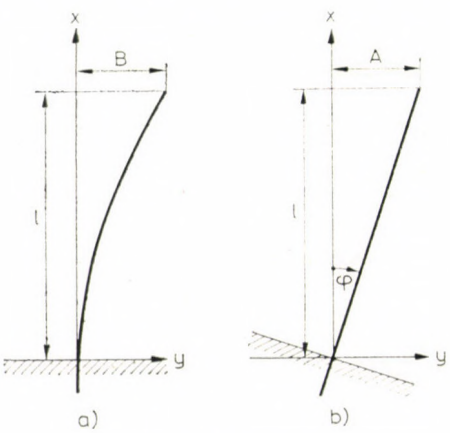

Fig. 2. Extreme cases

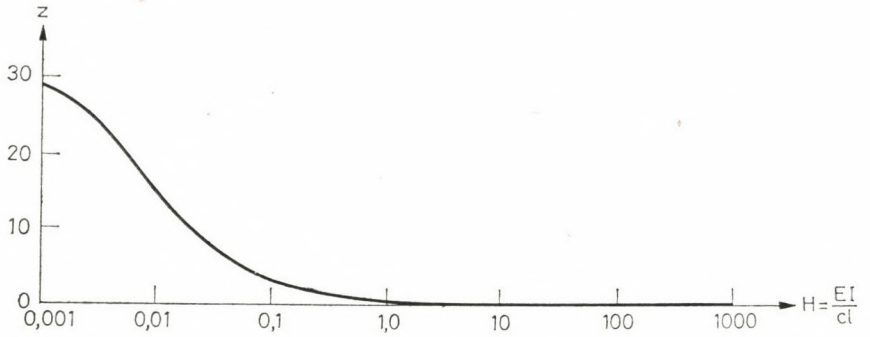

Fig. 3. The quotient z

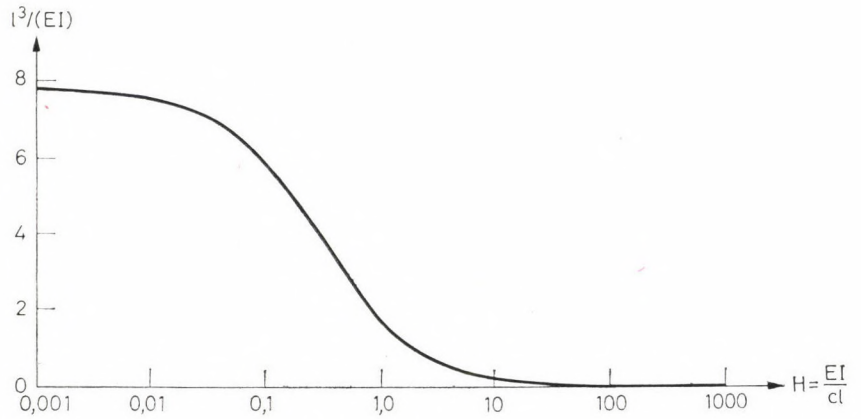

Fig. 4. Diagram of the critical load

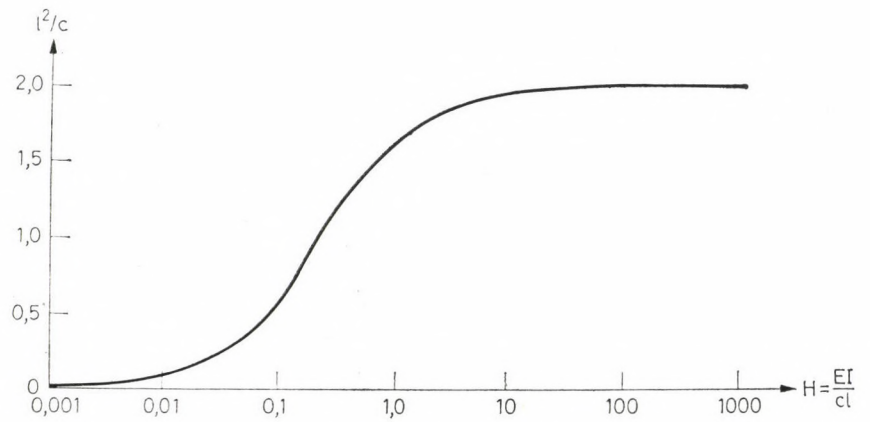

Fig. 5. Diagram of the critical load

The values of the quotient z for different conditions of rigidity are presented in Table 1. The corresponding diagram is depicted in Fig. 3.

The values of the critical load for different values of ratio H are summarized in Table 2. These values are plotted in Figs 4 and 5 respectively.

Finally, Table 3 gives answer to the question, what length should have a bar hinged at both ends, if it is desired that its critical load should be the same as that of the bar treated above. This bar length l_6 may be calculated from relationship

$$q_{cr}\, l = \frac{\pi^2 EI}{l}$$

expressing the equality of the two critical laods.

Acknowledgements

The publication of Table 3 has been proposed by E. DULÁCSKA who also calculated the values of the table. Wherefore the writer is deeply indepted.

REFERENCES

1. TIMOSHENKO, S.: Theory of Elastic Stability. McGraw-Hill Book Ccmpany, Inc., New York and London 1936
2. MUDRAK, W.: Die Knickbedingungen für den geraden Stab. *Der Bauingenieur* (1941), 153
3. DULÁCSKA, E.: Die Stabilität der Bauwerke mit hochliegendem Schwerpunkt. *Acta Techn. Hung.* **53** (1966), 439—444
4. KELLER, J. B.: The Shape of the Strongest Column. *Archiv. Rat. Mech. and Anal.*, **5** (1960), 275—285
5. LIPTÁK, L.: Elastic buckling of a prismatic bar of straight axis in case of any kind of clamping conditions (In Hungarian). *Építés- és Közlekedéstudományi Közlemények* **4** (1960), 621—626
6. TADJBAKHSH, I.—KELLER, J. B.: Strongest Columns and Isoperimetric Inequalities for Eigenvalues. *J. Appl. Mech.* **29** E. (1962), 159—164
7. KELLER, J. B.—NIORDSON, F. I.: The Tallest Column. *J. of Math. and Mech.* **16** (1966), 433—446

Stabilität des an einem Ende elastisch eingespannten Stabes. — Der Aufsatz beschäftigt sich mit der Knickung eines vertikalen prismatischen Stabes, dessen unteres Ende elastisch eingespannt, während sein oberes Ende ganz frei ist. Die Belastung ist ein längs der Stabachse gleichmäßig verteiltes, vertikales Kraftsystem. Der kritische Wert der Belastung wird mit Timoshenkos Energiemethode bestimmt. Die Form der ausgeknickten Stabachse wird mit einem Polygon dritten Grades approximiert. In dem Sonderfall, wo das untere Ende des Stabes fest eingespannt ist, liefert die angegebene Methode ein fast korrektes Resultat. In dem anderen Sonderfall, wo der Stab vollkommen steif ist, ergibt sich ein absolut exaktes Ergebnis.

Acta Technica Academiae Scientiarum Hungaricae, Tomus 92 (1—2), pp. 45—65 (1981)

REMARKS AND CONTRIBUTIONS TO THE VARIATIONAL PRINCIPLES OF THE LINEARIZED THEORY OF ELASTICITY IN TERMS OF THE STRESS FUNCTIONS

I. KOZÁK*
DR. OF TECHN. SCI.

[Manuscript received: 3 March 1980]

The paper gives a definition of such functionals in which the stress function tensor has only three (suitably selected) non-zero coordinates, and which makes the detailed investigation of the boundary conditions possible. From the introduced dual functionals, by the variation of the stress function tensor, three compatibility field equations and the compatibility boundary conditions are obtained, as the sufficient and necessary conditions of the compatibility of the strain field.

1. Introductions, Remarks

1.1 The stress fields, determined from stress functions, satisfy the equilibrium equation of the continuummechanics

$$t^{kl}_{\cdot\cdot;k} + q^l = 0\,. \tag{1.1}$$

t^{kl} the stress tensor, q^l the body force vector, the semicolon is the notation of the covariant differentiation.

The coordinate system x^1, x^2, x^3 is assumed to be arbitrary and curvilinear. All three coordinates are denoted by x.

Let the body bounded by a single closed surface and let $\overset{*}{t}{}^{kl}$ be a particular solution of (1.1). In such a case an arbitrary stress field, which satisfies the equation (1.1) can be determined by the stress function tensor f_{rs}, as was pointed out by FINZI B. [1] and BLOH, V. I. [2]:

$$t^{kl} - \overset{*}{t}{}^{kl} = \varepsilon^{krm}\,\varepsilon^{lsp}\,f_{rs;mp}\,. \tag{1.2}$$

(ε^{krm} is the permutation tensor.) BLOH has also pointed out the fact, that it is sufficient — without violation of the universality — that among the six independent coordinates of f_{rs}, there should be only three suitably selected non-

* Prof. Dr. I. KOZÁK, Dózsa Gy. u. 14. H-3525 Miskolc, Hungary

zero coordinates. Let us denote them, as stress functions $f_{RS} = f_{SR}$, and let $f_{AB} = f_{BA}$ be the zero coordinates of the stress function tensor. (In those index pairs, which are denoted by capital letters, the indices take up — from the usual values 1, 2, 3 — only selected values). The index pairs of the coordinates f_{AB} can be such, that by changing from the all possible variations of the index pairs rs, on which the equation

$$\beta_{(A;\,B)} = \frac{1}{2}(\beta_{A;\,B} + \beta_{B;\,A}) = \alpha_{AB}(x) \tag{1.3}$$

has a solution on the vector field $\beta_k(x)$, in the case of arbitrary functions $\alpha_{AB}(x)$. (Indices in spherical parenthesis denote the symmetric part of the tensor i.e. they denote the coordinates of the symmetric part.) After, the index pairs RS should be chosen in such a way, that the index pairs AB, BA and RS, SR give all the possible index pairs of f_{rs}. For instance, in the case of MAXWELL stress functions:

$$f_{RS} = f_{11}, f_{22}, f_{33} \quad \text{and} \quad f_{AB} = f_{12} = f_{23} = f_{31} = 0\ ,$$

while in the case of MORERA stress functions:

$$f_{RS} = f_{12}, f_{23}, f_{31} \quad \text{and} \quad f_{AB} = f_{11} = f_{22} = f_{33} = 0$$

is the structure of the tensor f_{rs}.

It can be shown, that there are maximum 21 ways of selections of three non zero independent coordinates in the stress function tensor, which can be stress functions, according to formula (1.2).

1.2 As it is known, from the kind of variational principles of the linearized theory of elastostatics, — which has stress functions in their functionals — we can determine the compatibility conditions of the strain field by the variation of the stress functions.

We call the strain field, $a_{kl}(x)$ as compatible, if to the given rigid body motion and to the single valued, at least two times differentiable field $a_{kl}(x)$ of the body, the formula *Cesaro* determines a single valued displacement field $u_k(x)$ of the body.

For the sake of the following let us introduce the symmetric incompatible (dislocation) tensor field $e^{ab}(x)$ which is formed from the strain field $a_{kl}(x)$:

$$e^{ab} = \varepsilon^{akm}\,\varepsilon^{blp}\,a_{kl;\,mp}\ . \tag{1.4}$$

The equations $e^{ab} = 0$ give the previously introduced compatibility conditions of the strain field, i.e. the six Saint-Venant compatibility equations.

For the determination of the compatibility equations from the variational principle — concretely from the principle of minimum complementary

energy — stress functions were applied first by SOUTHWELL, R. V. [3]. It was found that in this way, with the Maxwell stress functions, only three compatibility equations, $e^{11} = e^{22} = e^{33} = 0$ can be obtained, and the other three compatibility equations $e^{12} = e^{23} = e^{31} = 0$ can be obtained by the Morera stress functions. In this way came into being the "Southwell-paradox" due to which the six Saint-Venant compatibility field equations can be obtained from the principle of minimum complementary energy only in such a manner, if both the Maxwell and the Morera stress functions are considered, however, arbitrary stress field can be formed either separately by the Maxwell, or separately by the Morera stress functions.

The above formulated "Southwell-paradox" can be generalized in such a way, that by selecting any kind of three stress functions we obtain only three Saint-Venant compatibility field equations from the principle of minimum complementary energy.

Meanwhile further variational principles have also been formulated in the terms of stress functions in the linearized elasticity, for example by TONTI, E. [4], ODEN, J. T.—REDDY, J. N. [5] and ABOVSKIJ, N. P. —ANDREEV, N. P.—DERUGA, A. P. [6]. These variational principles have the common feature — to avoid the "Southwell-paradox" — that all of the six independent coordinates of the stress function tensor are taken to be non-zero and varied. Actually, due to the meaning of paragraph 1.1, in the case of well formulated variational principles, three stress functions should be sufficient to prove the compatibility of the strain field, by considering all of the possible variations of the stress functions.

1.3 Actually, on completion of the partial solution of WASHIZU, K. [7], by making use of the Bianchi's identity, it was shown by the author [8] that, if

$$e^{RS} = e^{SR} = 0; \quad x \in V \tag{1.5}_1$$

also, altogether three suitably selected Saint-Venant compatibility field equations and further,

$$n_b \, e^{ab} = 0; \quad x \in S \,, \tag{1.5}_2$$

the so-called compatibility boundary conditions are valid, then the remaining three Saint-Venant compatibility equations are also valid:

$$e^{AB} = e^{BA} = 0; \quad x \in V \,.$$

V is the volume region of the body, S is its single connected boundary and n_b is its outer normal.

In $(1.5)_1$ the three RS index pairs can be chosen in the same way, as those three non-zero coordinates of the stress function tensor which can be taken to be stress functions.

$(1.5)_1$ and $(1.5)_2$ are together the sufficient and necessary conditions of the compatibility of the strain field. By the stipulation that among the only three Saint-Venant compatibility equations should be necessary, the "Southwell's paradox" has been solved, but only for the reason that also the fulfilment of the compatibility boundary conditions $(1.5)_2$ must be assured. It was shown by the author [9], that in the case of fulfilment of the principle of minimum complementary energy as variational principle, not only the compatibility field equations $(1.5)_1$ but the comptaibility boundary conditions $(1.5)_2$ are fulfilled.

Also, it follows that the principle of minimum complementary energy is a correctly formulated variational principle.

1.4 Summerizing, what has been said above, for the investigation of the compatibility of the strain field by variational principle, two requirements should be set up.

I. These kind of stress function tensor should be applied, which has only three (suitably selected) non zero coordinates.

II. Conditions of the body boundary should be analysed particularly.

The variational principles of the papers [4], [5], [6], including stress functions do not satisfy either the first, or the second requirement. The same kind of variational principles of the text [7] satisfy only the second requirement.

1.5 The present paper gives contributions — which has been noted in the title — in respects of the above mentioned requirements, to the dual system of equations involving stress functions and to the variational principles, being ordered to them, as it was written in the paper of ODEN and REDDY [5]. For this reason in the following first we summarize briefly the most important conclusions of [5].

On the base of TONTI, E.'s work [10], ODEN and REDDY made general statements on the variables of physical problems, on the primal and dual systems of equations and on the functionals of variational principles which can be ordered to them. The linear (classical) elasticity occurs as an example.

Owing to the latest, by the displacement vector u_k — as by configuration variable — by the strain tensor a_{kl} and stress tensor t^{kl} — as by a pair of intermediate variables — and by the body force vector q^l — as by the source variable — *the primal system of equations* of the linear elasticity can be formulated in the following form

$$\frac{1}{2}(u_{k;t} + u_{l;k}) = a_{kl}\,, \tag{1.6}_1$$

$$u_k = \tilde{u}_k\,, \quad x \in Su\,, \tag{1.6}_2$$

$$b^{klpq}\, a_{pq} = t^{kl}\,, \tag{1.7}$$

$$t^{kl}_{..;k} + q^l = 0 \ , \tag{1.8}_1$$

$$n_k t^{kl} = \tilde{t}^l \ , \quad x \in St \ , \tag{1.8}_2$$

where $(1.6)_1$ is the kinematical equation, (1.6_2) is the displacement boundary condition, (1.7) is the constitutive equation, $(1.8)_1$ is the equilibrium equation (balance equation), $(1.8)_2$ is the stress boundary condition, b^{klpq} is the tensor involving the material constants, $\tilde{u}_k$ is the given displacements on the boundary part Su and $\tilde{t}^l$ is the given traction of the boundary part St.

To the primal system (1.6)—(1.8) is attached — as primal variational principles and functionals — the Hu-Washizu principle and its functional, the Hellinger—Reissner principle and its functional, the Lagrange principle and its functional (the total potential energy), and the Castigliano principle and its functional (the total complementary energy).

The configuration variable of the *dual system* of equations is the stress function tensor, f_{rs} its pair of intermediate variables are the tensors a_{kl} and t^{kl} and the source variable is the incompatibility (dislocation) tensor e^{ab}.

As in the case of a primal system the quantity q^l characterizes the measure of the unbalance of the field $t^{kl}(x)$, likely in the case of a dual system, the quantity e^{ab} can be considered to be a variable characterizing the incompatibility of the field $a_{kl}(x)$. Due to further analogy $n_k t^{kl} = t^l; x \in S$ are the surface forces on the boundary; while $n_a e^{ba} = e^b; x \in S$ is the surface incompatibility field on the boundary. When the strain field is compatible, then $e^{ab} = 0$. The dual system of equations itself, due to ODEN and REDDY:

$$\varepsilon^{krm} \varepsilon^{lsp} f_{rs;mp} = t^{kl} \ , \tag{1.9}$$

$$c_{klpq} t^{pq} = a_{kl} \ , \tag{1.10}$$

$$\varepsilon^{akm} \varepsilon^{blp} a_{kl;mp} = e^{ab} \ , \tag{1.11}$$

c_{klpk} is the inverse of the tensor b^{klpq}.

It is to be noted that the dual equations (1.9)—(1.11) do not involve boundary conditions in comparison with the equations (1.6)—(1.8), which do. Due to this fact there are no surface integrals in the dual functionals — being formulated to the equations (1.9)—(1.11) — either. All of these suggest, that the dual system of equations and the dual variational principles of ODEN and REDDY do not make the investigation of the compatibility of the strain field in the sense of paragraph 1.4 possible.

1.6 The paragraph 2. of this paper modifies the dual system of equations (1.9)—(1.11) in such a way, that they assure the compatibility of the strain field also in that case, when the stress function tensor has the structure: $f_{RS} \neq 0, f_{AB} = 0$. For this purpose, the number of the scalar equations (1.11) should be reduced from six to three, and by the contribution of suitable bound-

ary conditions to the system of equations (1.9)—(1.10) the fulfilment of the compatibility boundary conditions both on the boundary part St and Su had to be assured.

Paragraph 3. introduces dual functionals having variations resulting the modified and contributed dual system of equations as was written in paragraph 2. For the variation due to the stress functions, the invention is fundamental, that the stress function tensor, which fulfils the stress boundary condition can also be varied on the boundary part St.

2. The modified and contributed dual system of equations of the linearized elasticity

2.1 Let in the arbitrary curvilinear coordinate system x^1, x^2, x^3 be the equation of the boundary surface S as $x^k = x^k(\xi^1, \xi^2)$, (ξ^1, ξ^2 are surface parameters), and let us introduce on the boundary S and in its neighbourhood V_S the coordinate system ξ^1, ξ^2, ξ^3, in which ξ^3 is the directed distance along the outer normal of S and on S $\xi^3 = 0$. Further, let us denote the coordinate system x^1, x^2, x^3 by (x) and the coordinate system (ξ^1, ξ^2, ξ^3) by (ξ). This last is called coordinate system bounded to the boundary.

In the following, the quantities and their derivatives, being understood in the region V_S and on the boundary S, are given and written in the coordinate system (ξ), without drawing special attention. For instance, the coordinates of the outer normal of S: $n_\alpha = 0$ and $n_3 = 1$; or $n_k t^{kl} = n_3 t^{3l} = t^{3l}$.

We shall introduce, that in the coordinate system (ξ) the Greek letter indices can take up only the values 1, 2.

Let the transformation formula between the tensors written in the two coordinate system as

$$c_e^{\cdot d}(\xi) = \tau_e^{\cdot k} \underset{-1}{\tau}{}_l^{\cdot d} c_d^{\cdot l}(x) , \tag{2.1}_1$$

where

$$\det \tau_e^{\cdot k} \neq 0 ; \quad \tau_e^{\cdot k} \underset{-1}{\tau}{}_k^{\cdot d} = \delta_e^d , \tag{2.1}_2$$

and $c_k^{\cdot l}(x)$ is an arbitrary tensor written in the coordinate system (x) and δ_e^p is the Kronecker symbol.

2.2 On the stress function tensor f_{rs}, the transformation formula due to (2.1) is the following:

$$f_{ed}(\xi) = \tau_e^{\cdot r} \tau_d^{\cdot s} f_{rs}(x) . \tag{2.2}$$

Because during the transformation, the structure of the stress function tensor changes (its zero and non zero coordinates) and because the structure of the stress function tensor in the region V_S need not be the same as the

structure of $f_{rs}(x)$, in the following we denote the stress function tensors — being understood in the region V_S — by another letter, this being $h_{ed}(\xi)$.

It is practical to choose $h_{ed}(\xi)$ in such a way, that its coordinates h_{e3} should be zero, but $h_{\eta\vartheta}(\xi) \neq 0$. Between the tensors $h_{ed}(\xi)$ and $f_{rs}(x)$ — in the case of any possible structure of $f_{rs}(x)$ — with the aid of $(2.1)_1$ the following equations can be written:

$$h_{\eta\vartheta}(\xi) = \tau_{\eta}^{\cdot r}\, \tau_{\vartheta}^{\cdot s}\, f_{rs}(x) + \beta_{(\eta;\,\vartheta)}(\xi)\,, \qquad (2.3)_1$$

$$h_{e3}(\xi) = \tau_{e}^{\cdot r}\, \tau_{3}^{\cdot s}\, f_{rs}(x) + \beta_{(e;\,3)}(\xi) = 0\,, \qquad (2.3)_2$$

The vector field $\beta_e(\xi)$ should be chosen, so that the equation $(2.3)_2$ is valid. This last problem can always be solved. Of course, the structure $h_{ed}(\xi)$ can be chosen in another way as well.

The equation $(2.3)_1$ can also be considered in such a way, as a *mutual* and after the determination of $\beta_e(\xi)$ a *unique relation* between the three non zero stress functions $h_{\eta\vartheta}(\xi)$ in the coordinate system (ξ) and also the three non zero stress functions $f_{RS}(x)$ in the coordinate system (x).

The addition of the term $\beta_{(e;\,d)}(\xi)$ to the tensor $f_{ed}(\xi)$ — which was obtained by the transformation (2.2) — does not change the tensor field $t^{kl}(\xi)$, because

$$\varepsilon^{kem}\, \varepsilon^{ldp}\, \beta_{(e;\,p);\,mp} = \frac{1}{2}\, \varepsilon^{kcm}\, \varepsilon^{ldp}\, (\beta_{e;\,dmp} + \beta_{d;\,emp}) = 0\,.$$

2.3 The dual system of equations of the boundary problem (1.6)—(1.8) which give the primal system of equations, will be formulated by the next *basic assumption and requirement.*

Basic assumption:

— Due to paragraph 1.1,the coordinates $f_{RS} = f_{SR}$ of the stress function tensor $f_{rs}(x)$ are different from zero, but its coordinates $f_{AB} = f_{BA}$ are zero;

— the coordinates $h_{\eta\vartheta}$ of the stress function tensor $h_{ed}(\xi)$ which was introduced in paragraph 2.2, are different from zero, but the coordinates h_{e3} are zero.

Basic requirement:

— the strain field $a_{kl}(x)$ should be compatible.

According to the above assumptions and requirement the dual equation system can be written in the following way:

$$\varepsilon^{krm}\, \varepsilon^{lsp}\, f_{rs;\,mp} = t^{kl} - \overset{*}{t}{}^{kl}\,, \qquad (2.4)_1$$

$$h_{\eta\vartheta} = \tilde{h}_{\eta\vartheta} \quad \text{és} \quad h_{\eta\vartheta;\,3} = \tilde{h}_{\eta\vartheta;\,3}\,, \qquad \xi \in St\,, \qquad (2.4)_2$$

$$c_{klpq}\, t^{pq} = a_{kl}\,, \tag{2.5}$$

$$\varepsilon^{Rkm}\, \varepsilon^{Slp}\, a_{kl;\,mp} = e^{RS} = e^{SR} = 0\,, \tag{2.6}_1$$

$$\varepsilon^{3\eta\mu}\, \varepsilon^{bdp}\, a_{\eta d;\,p\mu} = e^{3b} = e^{b3} = 0\,, \qquad \xi \in St\,, \tag{2.6}_2$$

$$a_{\eta\vartheta} = \tilde{u}_{(\eta;\,\vartheta)}\,, \qquad \xi \in Su\,, \tag{2.6}_3$$

$$a_{\eta\vartheta;3} - a_{\eta 3;\,\vartheta} - a_{3\vartheta;\,\eta 3} = \tilde{u}_{3;\,\eta\vartheta}\,, \qquad \xi \in Su\,. \tag{2,6}_4$$

Beside the notations, which were previously introduced, the functions $\tilde{h}_{\eta\vartheta}(\xi^1, \xi^2)$, $\tilde{h}_{\eta\vartheta;3}(\xi^1, \xi^2)$, $\tilde{h}_{e3}(\xi^1, \xi^2) = \tilde{h}_{e3;\,3}(\xi^1, \xi^2) = 0$ satisfy the following equation on boundary part St which can be written on the base of $(1.8)_2$:

$$t^{3l} - \dot{t}^{3l} = \varepsilon^{3\eta\mu}\, \varepsilon^{ldp}\, h_{\eta d;\,p\mu} = \tilde{t}^{l} - \dot{t}^{3l}\,; \quad \xi \in St\,. \tag{2.7}$$

In the case of a compatible strain field, for which the equation system (2.4)—(2.6) concerns due to the basic requirement, $e^{RS} = 0$, $x \in V$ and $e^{3b} = 0$ $\xi \in S$.

In the dual system of equations, due to $(2.4)_2$ and (2.7) the stress boundary conditions are fulfilled. (2.5) is the constitutive equation.

Due to paragraph 1.3 the equations (2.6) assure the compatibility of the strain field a_{kl}. That is, because $(2.6)_1$ is equal to $(1.5)_2$, $(2.6)_2$ is equal to $(1.5)_2$ on the boundary part St, while $(2.6)_{3,4}$ equivalent to $(1.5)_2$ on the boundary part Su, where $u_e = \tilde{u}_e$ is the prescribed displacement. This last should be proved.

Due to the (1.4) interpretation of the incompatibility tensor it is valid on the whole boundary S:

$$e^{33} = \varepsilon^{3\eta\mu}\, \varepsilon^{3\vartheta\pi}\, a_{\eta\vartheta;\,\mu\pi}\,, \tag{2.8}_1$$

and

$$e^{3\beta} = \varepsilon^{3\eta\mu}\, \varepsilon^{\beta\vartheta 3}\, (a_{\eta\vartheta;3\mu} - a_{\eta 3;\,\vartheta\mu})\,. \tag{2.8}_2$$

By the substitution of $(2.6)_3$ into $(2.8)_1$ and $(2.6)_4$ into $(2.8)_2$, we really obtain, that $(1.5)_2$ is also fulfilled on the boundary part Su:

$$e^{33} = \frac{1}{2}\, \varepsilon^{3\eta\mu}\, \varepsilon^{3\vartheta\pi} (\tilde{u}_{\eta;\,\vartheta} + \tilde{u}_{\vartheta;\,\eta})_{;\mu\pi} \equiv 0\,, \tag{2.9}_1$$

$$e^{3\beta} = \varepsilon^{3\eta\mu}\, \varepsilon^{\beta\vartheta 3} (\tilde{u}_{3;\,\eta\vartheta} + a_{3\vartheta;\,\eta})_{;\mu} \equiv 0\,. \tag{2.9}_2$$

The formula Cesaro determines a unique valued displacement field to the strain field $a_{kl}(x)$ of the dual system (2.4)—(2.6) and to the given rigid body motion of the body.

2.4 We get the basic system of equations, in terms of stresses $t^{kl}(x)$, from the equations system (2.4)—(2.6), if we write the equilibrium equation

instead of $(2.4)_1$ and the stress boundary condition instead of $(2.4)_2$:

$$(t^{kl} - \overset{\cdot}{t}^{kl})_{;k} = 0\,, \qquad (2.10)_1$$

$$t^{3l} = \tilde{t}^{l} \qquad \xi \in St\,, \qquad (2.10)$$

and the equations (2.5)—(2.6) are allowed to be unaltered [9]. In this way to the determination of the six independent coordinates of the stress tensor, we have $(2.10)_1$ and $(2.6)_1$, also six scalar field equations altogether.

3. The contributed dual variational principles of the linearized elastostatics

3.1 Formulating the Euler equations and the boundary conditions of the dual functionals the relation

$$\int_{(V)} \varepsilon^{krm}\, \varepsilon^{lsp}\, a_{kl}\, \delta f_{rs;\,mp}\, dV =$$

$$= \int_{(V)} \varepsilon^{krm}\, \varepsilon^{lsp}\, a_{kl;\,mp}\, \delta f_{rs}\, dV +$$

$$+ \int_{(S)} \varepsilon^{\varkappa\eta 3}\, \varepsilon^{ldp}\, (a_{\varkappa l}\, \delta h_{\eta d;\,p} - a_{\varkappa l;\,p}\, \delta h_{\eta d})\, dS \qquad (3.1)$$

— which can be written by making use of the identity

$$\varepsilon^{krm}\, \varepsilon^{lsp}\, a_{kl}\, \delta f_{rs;\,mp} =$$

$$= \varepsilon^{krm}\, \varepsilon^{lsp}\, a_{kl;\,mp}\, \delta f_{rs} - (a_{kl;\,p}\, \delta f_{rs})_{;\,m} +$$

$$+ (a_{kl}\, \delta f_{rs;\,p})_{;\,m}$$

the Gauss—Ostrogradski-theorem and the transformation formula (2.1) — has a basic importance (δ denotes variation).

3.2 To the transformation of the surface integrals the Stokes' theorem will also be needed. For this purpose, let the surface of the body be divided into parts denoted by S^A and S^B, and let q be the common curve of S^A and S^B

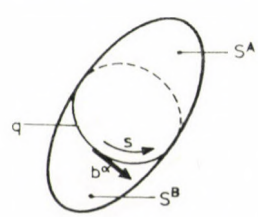

Fig. 1

(Figure 1.). Let s be the length along the curve q in the drawn direction and let b^α be the suitable unit vector. Due to Stokes' theorem, on the vector field $c_a(\xi^1, \xi^2)$ — which is arbitrary on S^A, or on S^B or on both S^A and S^B — the following equations are valid:

$$\int_{(S^A)} \varepsilon^{\alpha\beta 3} c_{\alpha;\beta}\, dS = -\oint_{(q)} (b^\alpha c_\alpha)^A\, ds\,, \tag{3.2}_1$$

$$\int_{(S^B)} \varepsilon^{\alpha\beta 3} c_{\alpha;\beta}\, dS = \oint_{(q)} (b^\alpha c_\alpha)^B\, ds\,. \tag{3.2}_2$$

The notations A and B emphasize in the line integrals, that the integrands are thought of on the boundary part S^A or S^B.

3.3 The dual functionals will be formulated by complete stress function tensors $f_{rs}(x)$ and $h_{ed}(\xi)$, and the variations of the functionals will be formed in the same way. The basic assumptions and the basic requirement concerning the strain tensor — which was introduced at the beginning of paragraph 2.3 — will only be considered after forming of the variations.

And now, let us formulate — to the dual system of equations of the boundary problems (1.6)—(1.8) of the linearized elasticity — the following dual functionals.

I. If previously there is no prescription to the fulfilment of any equation:

$$L(f_{rs}, t^{kl}, a_{pq}) = L^V + L^T + L^U + L^Q\,, \tag{3.3}_1$$

where

$$L^V = \int_{(V)} \frac{1}{2} t^{kl} c_{klpq} t^{pq}\, dV - \int_{(V)} e^{rs} f_{rs}\, dV -$$

$$- \int_{(V)} a_{kl} (t^{kl} - \dot{t}^{kl} - \varepsilon^{krm} \varepsilon^{lsp} f_{rs;mp})\, dV\,; \tag{3.3}_2$$

$$L^T = \int_{(St)} \varepsilon^{\varkappa\eta 3} \varepsilon^{ldp} \left[-(h_{\eta d;p} - \tilde{h}_{\eta d;p})\, a_{\varkappa l} + \right.$$

$$\left. + (h_{\eta d} - \bar{h}_{\eta d})\, a_{\varkappa l;p}\right] dS\,; \tag{3.3}_3$$

$$L^U = \int_{(Su)} \tilde{u}_l (\varepsilon^{\varkappa\eta 3} \varepsilon^{ldp} h_{\eta d;p} - \dot{t}^{3l})\, dS =$$

$$= -\int_{(Su)} t^{3l} \tilde{u}_l\, dS\,; \tag{3.3}_4$$

$$L^Q = \oint_{(q)} \{b^\eta (\tilde{u}_l)^U \varepsilon^{ldp} (h_{\eta d;p} - \tilde{h}_{\eta d;p}) +$$

$$+ b^\vartheta \varepsilon^{\varkappa\eta 3}]\,[\tilde{u}_{3;\varkappa} - a_{3\varkappa})^U (h_{\eta\delta} - \tilde{h}_{\eta\vartheta}) -$$

$$- (\tilde{u}_{[\vartheta;\varkappa]})^U (h_{\eta 3} - \tilde{h}_{\eta 3})]\}\, ds\,. \tag{3.3}_5$$

The functions $\tilde{h}_{ed}(\xi^1, \xi^2)$, $\tilde{h}_{ed;3}(\xi^1, \xi^2)$, being in $(3.3)_{3,5}$ satisfy the stress boundary condition (2.7), but they are not fixed, so can be varied. (See formula (3.15)). The function $\tilde{u}_l(\xi^1, \xi^2)$ in the integral $(3.3)_4$ is the prescribed displacement on the boundary part Su. The line integral should be taken along the common curve q. St agrees with S^A and S^B agrees with Su. (In the integrand of the line integral U or T denote — later on, too — that the given quantity should be taken either on the boundary part Su or on the boundary part St and, of course, on the curve q.) The indices in the square parenthesis denote in the formula $(3.3)_5$ according to the relation

$$\tilde{u}_{\vartheta;\varkappa} = \tilde{u}_{(\vartheta,\varkappa)} + \tilde{u}_{[\vartheta;\varkappa]}$$

the skew symmetric part of the given tensor.

II. If the constitutive equation (1.7) *is valid*:

$$M(f_{rs}\,; a_{pq}) = M^V + M^T + M^U + M^Q, \tag{3.4}_1$$

where

$$M^V = -\int_{(V)} \frac{1}{2}\, a_{kl}\, b^{klpq}\, a_{pq}\, dV - \int_{(V)} e^{rs} f_{rs}\, dV + \\ + \int_{(V)} a_{kl}\, (\dot{t}_{kl} + \varepsilon^{krm}\, \varepsilon^{lsp}\, f_{rs;mp})\, dV; \tag{3.4}_2$$

$$M^T = L^T;\ M^U = L^U \text{ und } M^Q = L^Q, \tag{3.4}_{3,4,5}$$

or by the substitution of $a_{kl} = c_{klpq}\, t^{pq}$:

$$M^*(f_{rs}\,; t^{pq}) = \ldots . \tag{3.5}$$

III. If the constitutive equation, the equation $(2.4)_1$ *and the stress boundary condition* $(2.4)_2$ *are valid*, i.e. the equation

$$\varepsilon^{3\eta\mu}\, \varepsilon^{ldp}\, (h_{\eta d;\, p\mu} - \tilde{h}_{\eta d;\, p\mu}) = 0;\ \ \xi \in St \tag{3.6}_1$$

is true (here the functions, denoted by wavy lines are fixed):

$$K(f_{rs}) = K^V + K^U, \tag{3.6}_2$$

where

$$K^V = \int_{(V)} \frac{1}{2}\, \overset{t}{\underset{f}{t}}{}^{pq}\, c_{pqkl}\, \overset{t}{\underset{f}{t}}{}^{kl}\, dV - \int_{(V)} e^{rs}\, f_{rs}\, dV, \tag{3.6}_3$$

$$K^U = L^U, \tag{3.6}_4$$

and

$$\underset{f}{t^{kl}} = \overset{\circ}{t}{}^{kl} + \varepsilon^{krm}\,\varepsilon^{lsp}\,f_{rs;\,mp}\,. \tag{3.6}_5$$

The volume parts of the functionals (3.3), (3.4) and (3.6) agree in order with the functionals (4.20), (4.21) and (4.19) of the paper [5] written by ODEN and REDDY.

3.4 The functionals (3.3), (3.4) and (3.6) satisfy the purpose of paragraph 1.6 according to which, the variations of the functionals — together with those equations, previously prescribed as subsidiary conditions — give the modified and contributed dual system of equations. To prove this, let form firstly the different variations of the functional (3.3). Next to the mark of the variation a small letter denotes the variable, to which the variation is to be formed:

$$\delta_t\,L(f_{rs},\,t^{kl},\,a_{pq}) = \delta_t\,L^V = \int_{(V)} \delta t^{kl}\,(c_{klpq}\,t^{pq} - a_{kl})\,dV, \tag{3.7}$$

$$\begin{aligned}\delta_a L(f_{rs},\,t^{kl},\,a_{pq}) &= \delta_a L^V + \delta_a L^T + \delta_a L^Q = \\ &= -\int_{(V)} \delta a_{kl}\,(t^{kl} - \dot{t}^{kl} - \varepsilon^{krm}\,\varepsilon^{lsp}\,f_{rs;\,mp})\,dV + \\ &+ \int_{(St)} \varepsilon^{\varkappa\eta 3}\,\varepsilon^{ldp}\,[-(h_{\eta d;\,p} - \tilde{h}_{\eta d;\,p})\,\delta a_{\varkappa l} + \\ &+ (h_{\eta d} - \tilde{h}_{\eta d})\,\delta a_{\varkappa l}]\,dS + \\ &+ \oint_{(q)} b^{\vartheta}\,\varepsilon^{\varkappa\eta 3}\,[-(\delta a_{3\varkappa})^U (h_{\eta\vartheta} - \tilde{h}_{\eta\vartheta})]\,ds\,;\end{aligned} \tag{3.8}$$

$$\delta_f\,L\,(f_{rs},\,t^{kl},\,a_{pq}) = \delta_f\,L_0^V + \delta_f\,L_0^T + \delta_f\,L_0^U + \delta_f L_0^Q\,, \tag{3.9}_1$$

where

$$\delta_f L_0^V = \int_{(V)} (a_{kl}\,\varepsilon^{krm}\,\varepsilon^{lsp}\,\delta f_{rs;\,mp} - e^{rs}\,\delta f_{rs})\,dV, \tag{3.9}_2$$

$$\begin{aligned}\delta_f\,L^T &= \delta_h L_0^T + \boldsymbol{d}_{\tilde{h}} L_0^T = \\ &= \int_{(St)} \varepsilon^{\varkappa\eta 3}\,\varepsilon^{ldp}\,[-a_{\varkappa l}\,(\delta h_{\eta d;\,p} - \delta\tilde{h}_{\eta d;\,p}) + \\ &+ a_{\varkappa l;\,p}\,(\delta h_{\eta d} - \delta\tilde{h}_{\eta d})]\,dS\,,\end{aligned} \tag{3.9}_3$$

$$\delta_f L_0^U = \delta_h L_0^U = \int_{(Su)} \varepsilon^{\varkappa\eta 3}\,\varepsilon^{ldp}\,\tilde{u}_l\,\delta h_{\eta d;\,p\varkappa}\,\boldsymbol{dS}\,, \tag{3.9}_4$$

$$\delta_f L_0^Q = \delta_h L_0^Q + \delta_{\tilde{h}} L_0^Q =$$

$$= \oint_{(q)} \{ b^\eta (\tilde{u}_l)^U \varepsilon^{ldp} (\delta h_{\eta d;\, p} - \delta \tilde{h}_{\eta d;\, p}) +$$

$$+ b^\vartheta \varepsilon^{\varkappa\eta 3} [(\tilde{u}_{3;\varkappa} - a_{3\varkappa})^U (\delta h_{\eta\vartheta} - \delta \tilde{h}_{\beta\vartheta}) -$$

$$+ (\tilde{u}_{[\vartheta;\varkappa]}) (\delta h_{\eta 3} - \delta \tilde{h}_{\eta 3})] \} \, ds \, . \qquad (3.9)_5$$

Next to the mark of the variation, the index $\tilde{h}$ or h denotes, whether the variable $h_{ed}(\xi)$ or $\tilde{h}_{ed}(\xi)$ is varied in the concerning integral.

3.5 From the dual variational principle

$$\delta_t L (f_{rs}, t^{kl}, a_{pq}) = 0 \qquad (3.10)$$

formed by (3.7) — considering, that δt^{kl} can be arbitrary on the region V — follows the constitutive equation (2.5) of the dual system.

3.6 From the dual variational principle

$$\delta_a L (f_{rs}, t^{kl}, a_{pq}) = 0 \qquad (3.11)$$

formed by (3.8), considering that δa_{kl} on V, and $\delta a_{\varkappa\lambda}$ and $\delta a_{\varkappa\lambda;3}$ on St can be arbitrary, follow the next equations of the dual system: the equation $(2.4)_1$, the stress boundary conditions

$$h_{\eta\vartheta} = \tilde{h}_{\eta\vartheta}; \; h_{\eta\vartheta;3} = \tilde{h}_{\eta\vartheta;3}; \; h_{e3} = \tilde{h}_{e3}; \qquad \xi \in St, \qquad (3.12)^1$$

which agree with $(2.4)_2$ and the condition along the curve q

$$h_{\eta\vartheta} = \tilde{h}_{\eta\vartheta}; \quad \xi \in q \, . \qquad (3.12)_2$$

3.7 The integrals of the dual variational principle

$$\delta_f L (f_{rs}, t^{kl}, a_{pq}) = 0 \qquad (3.13)$$

formed by (3.9), need further transformations.

The volume part $\delta_f L_0^V$ can be transformed into the following form with the aid of (3.1)

$$\delta_f L_0^V = \delta_f L_1^V + \delta_f L_{V0}^{TU} \, , \qquad (3.14)_1$$

where

$$\delta_f L_1^V = \int_{(V)} (\varepsilon^{krm} \varepsilon^{lsp} a_{kl;\, mp} - e^{rs}) \, \delta f_{rs} \, dV \, , \qquad (3.14)_2$$

$$\delta_f L_{V0}^{UT} = \delta_h L_{V0}^T + \delta_h L_{V0}^U =$$

$$= \int_{(S)} \varepsilon^{\varkappa\eta 3} \varepsilon^{ldp} (a_{\varkappa l} \, \delta h_{\eta d;\, p} - a_{\varkappa l;\, p} \, \delta h_{\eta d}) \, dS \, . \qquad (3.14)_3$$

The index TU denotes, that the integral should be taken on the whole boundary $S = St + Su$.

Varying the functional $L(f_{rs}, t_{pq}, a_{pq})$ due to the stress function tensor, it should also be considered, that due to (2.7) the stress boundary condition does not determine the tensor $\tilde{h}_{ed}$ and its derivatives, i.e. $\tilde{h}_{ed}$ can also be varied there. The variations $\tilde{h}_{ed}(\xi)$ formed on St due to (2.7) must fulfil the following equation:

$$\varepsilon^{\varkappa\eta 3}\, \varepsilon^{ldp}\, \delta\tilde{h}_{\eta d;\, p\varkappa} = 0\,; \quad \xi \in St\,. \tag{3.15}$$

The general solution of (3.15) is given by the symmetric part of the gradient of an arbitrary vector field $\delta v_e(\xi)$:

$$\delta\tilde{h}_{ed} = \delta v_{(e,\,d)} = \frac{1}{2}(\delta v_{e;\,d} + \delta v_{d;\,e})\,. \tag{3.16}$$

Introducing the notation

$$\delta w^l = \delta w^l(\xi) = -\frac{1}{2}\,\varepsilon^{ldp}\,\delta v_{d;\,p} \tag{3.17}$$

the correctness of the formulas

$$\delta\tilde{h}_{\eta d} = \delta v_{d;\,\eta} + \varepsilon_{d\eta n}\,\delta w^n\,, \tag{3.18}_1$$

$$\varepsilon^{ldp}\,\delta\tilde{h}_{\eta d;\,p} = -\delta w^l_{;\,\eta} \tag{3.18}_2$$

can be seen, too.

The formulas (3.18) remain valid, if $\tilde{h}_{e3} = 0$ is assumed to be valid. In this case, due to (3.16), the equations

$$\delta v_{\eta;3} = -\delta v_{3;\,\eta} \quad \text{and} \quad \delta v_{3;3} = 0 \quad \xi \in St$$

should be valid, however, the function $\delta v_e(\xi^1, \xi^2)$, or $\delta w^l(\xi^1, \xi^2)$ in this case remain arbitrary, as well as on the boundary part St.

The second term of the formula $(3.9)_3$ can be transformed into a new form on the base of the above, by the relations (3.18) and the Stokes' theorem $(3.2)_1$:

$$\delta_{\tilde{h}} L_0^T = \delta_{\tilde{h}} L_1^T + \delta_{\tilde{h}} L_T^Q\,, \tag{3.19}_1$$

where

$$\delta_{\tilde{h}}\, L_1^T = \int_{(St)} \varepsilon^{\varkappa\eta 3}\, \varepsilon^{ldp}\, a_{\varkappa l;\, p\eta}\, \delta v_d\, dS\,, \tag{3.19}_2$$

$$\delta_{\tilde{h}}\, L_T^Q = \oint_{(q)} (b^\vartheta\, a_{\vartheta l}\, w^l)^T + (b^\vartheta\, \varepsilon^{ldp}\, a_{\vartheta l;\, p}\, \delta v_d)^T]\, ds\,.$$

To the transformations of the formulas $(3.9)_4$ the Stokes' theorem $(3.2)_2$ is repeatedly applied:

$$\delta_h L_0^U = \delta_h L_{V1}^U + \delta_h L_{VU}^Q , \tag{3.20}_1$$

where

$$\delta_h L_1^U = \int_{(Su)} \varepsilon^{\varkappa\eta 3}\, \varepsilon^{\lambda\vartheta 3} \left[-\tilde{u}_{3;\varkappa\lambda}\, \delta h_{\eta\vartheta} - \tilde{u}_{(\lambda;\varkappa)}\, \delta h_{\eta\vartheta;3} + \right.$$
$$\left. + \tilde{u}_{(\lambda;\varkappa)}\, \delta h_{\eta 3;\vartheta} - \tilde{u}_{[\lambda;\varkappa[;\vartheta}\, \delta h_{\eta 3} \right] dS , \tag{3.20}_2$$

$$\delta_h L_U^Q = \oint_{(q)} \left\{ -b^\eta\, \tilde{u}_l\, \varepsilon^{ldp}\, \delta h_{\eta d;} - \right.$$
$$\left. - b^\vartheta\, \varepsilon^{\varkappa\eta 3} \left[\tilde{u}_{3;\varkappa}\, \delta h_{\eta\vartheta} - \tilde{u}_{[\vartheta;\varkappa]}\, \delta h_{\eta 3} \right] \right\}^U ds . \tag{3.20}_3$$

The term $\delta_f L_{V0}^U$ in $(3.14)_3$ can further be transformed by the Stokes theorem $(3.2)_2$

$$\delta_h L_{V0}^U = \delta_h L_{V1}^U + \delta_h L_{VU}^Q , \tag{3.21}_1$$

where

$$\delta_h L_{V1}^U = \int_{(Su)} \varepsilon^{\varkappa\eta 3}\, \varepsilon^{\lambda\vartheta 3} \left[(a_{3\varkappa;\lambda} + a_{3\varkappa;\lambda} - a_{\varkappa 3;\lambda} - {}_{\varkappa\lambda;3})\, \delta h_{\eta\vartheta} + \right.$$
$$\left. + a_{\lambda\varkappa}\, \delta h_{\eta\vartheta;3} - a_{\varkappa\lambda}\, \delta h_{\eta 3;\vartheta} + a_{\varkappa\lambda}\, \delta h_{\eta 3} \right] dS ; \tag{3.21}_2$$

$$\delta_h L_{VU}^Q = \oint_{(q)} \left[b^\vartheta\, \varepsilon^{\varkappa\eta 3}\, a_{3\varkappa}\, \delta h_{\eta\vartheta} \right]^U ds . \tag{3.21}_3$$

And now after the transformations, going back to the variational principle (3.13), which was formed by (3.9):

$$\delta_f L(f_{rs}, t^{kl}, a_{pq}) = \delta_f L^V + \delta_h L^T + \delta_{\tilde{h}} L^T + \delta_h L^U +$$
$$+ \delta_h L^Q + \delta_{\tilde{h}} L^Q = 0 , \tag{3.22}_1$$

where

$$\delta_f L^V = \delta_f L_1^V , \tag{3.22}_2$$
$$\delta_h L^T = \delta_h L_0^T + \delta_h L_{V0}^T ; \quad \delta_{\tilde{h}} L^T = \delta_{\tilde{h}} L_1^T , \tag{3.22}_{3,4}$$
$$\delta_h L^U = \delta_h L_1^U + \delta_h L_{V1}^U , \tag{3.22}_5$$
$$\delta_h L^Q = \delta_h L_0^Q + \delta_h L_{VU}^Q + \delta_h L_U^Q , \tag{3.22}_6$$
$$\delta_{\tilde{h}} L^Q = \delta_{\tilde{h}} L_0^Q + \delta_{\tilde{h}} L_T^Q . \tag{3.22}_7$$

The integrands in the integrals of equation $(3.22)_1$ consist of such sums of products in which one of the factors can be freely varied. It follows, that the fulfilment of the equation $(3.22)_1$ can be true in the case if the integrals

in $(3.22)_1$ are separately equal to zero. Making order in the separate integrals and making valid the basic assumption of paragraph 2.4 on the structure of the stress function tensor, and considering, that the tensors $f_{rs}(x)$ and $h_{ed}(\xi)$ are transformed due to formula (2.3), we can make the following statements:

a) Due to equation $\delta_f L^V = 0$, which can be written on the base of $(3.22)_2$, $(3.14)_2$, because $\delta f_{RS}(x)$ can be arbitrary:

$$\varepsilon^{Rkm}\,\varepsilon^{Slp}\,a_{kl;\,mp} = e^{RS}\,, \quad x \in V\,. \tag{3.23}$$

b) The equation $\delta_h L^T = 0$ — which can be written on the base of $(3.22)_3$, $(3.9)_3$ and $(3.14)_4$ — is identically true.

c) Due to equation $\delta_{\tilde{h}} L^T = 0$, which can be written on the basis of $(3.22)_4$ and $(3.19)_2$, because $\delta v_d(\xi)$ can be arbitrary on the boundary part St:

$$\varepsilon^{3\varkappa\lambda}\,\varepsilon^{dlp}\,a_{kl;\,p\eta} = e^{3d} = 0\,; \quad \xi \in St\,. \tag{3.24}$$

d) Due to the equation $\delta_h L^U = 0$, which can be written on the base of $(3.22)_5$, $(3.20)_2$ and $(3.21)_2$, exist the following equations

$$a_{\lambda\varkappa} = \tilde{u}_{(\lambda,\,\varkappa)} = \frac{1}{2}\,(\tilde{u}_{\lambda;\varkappa} + \tilde{u}_{\varkappa,\lambda})\,; \quad \xi \in Su\,, \tag{3.25}_1$$

$$a_{3\varkappa;\lambda} - a_{\varkappa\lambda;3} = \tilde{u}_{3;\varkappa\lambda} - a_{3\lambda;\varkappa}\,; \qquad \xi \in Su\,, \tag{3.25}_2$$

$$\varepsilon^{\lambda\vartheta 3}\,a_{\varkappa\lambda;\,\vartheta} = \frac{1}{2}\,\varepsilon^{\lambda\vartheta 3}\,(\tilde{u}_{\,\lambda;\varkappa} - \tilde{u}_{\varkappa;\lambda})_{;\vartheta}\,, \tag{3.25}_3$$

because on Su δt^{3l}, following in the same place

$$\varepsilon^{\varkappa\eta 3}\,\varepsilon^{\lambda\vartheta 3}\,\delta h_{\eta\vartheta} \quad \text{and} \quad \varepsilon^{\varkappa\eta 3}\,\varepsilon^{\lambda\vartheta 3}\,\delta h_{\vartheta\vartheta;3}$$

can be arbitrary.

The equation $(3.25)_3$, following from the coefficient of the coordinate $\delta h_{\eta 3}$, is identically true if $(3.25)_1$, is valid. So really, we do not lose a valuable equation, if the case $h_{\eta 3} = 0$ is chosen in accordance with the basic assumption.

e) The equation $\delta_h L^Q = 0$, which can be written on the base of $(3.22)_6$, $(3.9)_5$, $(3.21)_3$, and $(3.20)_3$ is identically true.

f) On the base of formulas $(3.22)_7$, $(3.9)_5$ and $(3.19)_3$ considering (3.18) the following equation can be written:

$$\begin{aligned}\delta_{\tilde{h}} L^Q = \oint_{(q)} [&(b^\vartheta\,a_{\vartheta l}\,\delta w^l)^T + (b^\vartheta\,\varepsilon^{ldp}\,a_{\vartheta l;\,p}\,\delta v_d)^T + \\ &+ b^\eta(\tilde{u}_l)^U(\delta w^l_{;\eta})^T - b^\eta(\tilde{u}_{3;\varkappa} - a_{3\varkappa})^U\,\varepsilon^{\varkappa\eta 3}(\delta v_{\eta;\vartheta} + \varepsilon_{\eta\vartheta 3}\,\delta w^3)^T + \\ &+ b^\vartheta\,(\tilde{u}_{[\vartheta;\lambda]})^U\,\varepsilon^{\varkappa\eta 3}(\delta v_{3;\eta} + \varepsilon_{3\eta\nu}\,\delta w^\nu)^T]\,ds = 0\,.\end{aligned} \tag{3.26}$$

During the further transformation of equation (3.26) we can take the next identity into consideration:

$$\tilde{u}_{[\vartheta;\varkappa]} = \frac{1}{2}(\tilde{u}_{\vartheta;\varkappa} - \tilde{u}_{\varkappa;\vartheta}) = \frac{1}{2}\,\varepsilon_{\vartheta\varkappa 3}\,\varepsilon^{\alpha\beta 3}\,\tilde{u}_{\alpha;\beta}\,. \tag{3.27}$$

After the integrations along the curve q and transformations the following is obtained:

$$\begin{aligned}\delta_{\tilde{h}} L^{Q} = \oint_{(q)} \Bigg[\Bigg\{ &\{(b^{\vartheta}\, a_{\vartheta\lambda})^{T} - [\tilde{u}_{(\lambda;\vartheta)}\, b^{\vartheta}]^{U}\}\, \delta w^{\lambda} + \\ &+ \{(b^{\vartheta}\, a_{\vartheta 3})^{T} - (b^{\vartheta}\, a_{3\vartheta})^{U}\}\, \delta w^{3} + \\ &+ \{[\varepsilon^{\varkappa\eta 3}\, b^{\vartheta}\,(a_{\vartheta\varkappa;3} - a_{\vartheta 3;\varkappa})^{T} - [\,\varepsilon^{\varkappa\eta 3}\, b^{\vartheta}\,(a_{3\varkappa;\vartheta} - \tilde{u}_{3;\varkappa\vartheta})]^{U}\}\, \delta v_{\eta} + \\ &+ \Bigg\{ - [\varepsilon^{\varkappa\eta 3}\, b^{\vartheta}\, a_{\vartheta\varkappa;\eta}]^{T} + \left[\frac{1}{2}\,\varepsilon^{\varkappa\eta 3}\,\tilde{u}_{\varkappa;\vartheta\eta}\, b^{\vartheta}\right]^{U} \Bigg\}\, \delta v_{3} \Bigg\} \Bigg]\, ds = 0\,. \end{aligned} \tag{3.28}$$

Due to equation (3.28) — because δw^{l} and δv_{e} on the curve q can be arbitrary — the next equations are true:

$$(b^{\vartheta}\, a_{\vartheta\lambda})^{T} = [b^{\vartheta}\,\tilde{u}_{(\lambda;\vartheta)}]\,; \qquad \xi \in q\,, \tag{3.29}_1$$

$$(b^{\vartheta}\, a_{\vartheta 3})^{T} = (b^{\vartheta}\, a_{3\vartheta})^{U}\,; \qquad \xi \in q\,, \tag{3.29}_2$$

$$[b^{\vartheta}\,\varepsilon^{\varkappa\eta 3}\,(a_{\vartheta\varkappa;3} - a_{\vartheta 3;\varkappa})]^{T} = [b^{\vartheta}\,\varepsilon^{\varkappa\eta 3}(a_{3\varkappa;\vartheta} - \tilde{u}_{3;\varkappa\vartheta})]^{U}\,; \qquad \xi \in q, \tag{3.29}_3$$

$$[b^{\vartheta}\,\varepsilon^{\varkappa\eta 3}\, a_{\vartheta\varkappa;\eta}]^{T} = \frac{1}{2}\,[\varepsilon^{\varkappa\eta 3}\,\tilde{u}_{\varkappa;\vartheta\eta}\, b^{\vartheta}]^{U}\,; \qquad \xi \in q\,. \tag{3.29}_4$$

If in the functional (3.3) and in the variational principle (3.13) we put the substitution $e^{RS} = 0$, the equations determined from the variational principle (3.13) get the following meanings:

— the equation (3.23) agrees with the compatibility field equation $(2.6)_1$ of the dual system:

— the equation (3.24) agrees with the compatibility boundary condition $(2.6)_2$ of the dual system on the boundary part St:

— the equations (3.25) agree with the displacement boundary conditions $(2.6)_{3,4}$ on the boundary part Su. From these last it follows that due to (2.8) and (2.9) the compatibility boundary condition will be true on the boundary part Su, as well.

On the base of results of paragraph 3.7 we can conclude, that from the variations of the dual functional (3.3) follows the total dual system of equations (2.4)—(2.6.)

The equations (3.29) express — by taking (3.25) also into consideration — that the displacement field and the derivative of the rotation field along the curve q, i.e. the displacement field and the rotation field themselves along the curve q, are the same either looking from the boundary part Su, or from the boundary part St.

3.8 From the dual variational principles

$$\delta_a M(f_{rs}, a_{pq}) = 0\,, \tag{3.30}$$

$$\delta_f M(f_{rs}, a_{pq}) = 0 \tag{3.31}$$

being formed by the dual functional (3.4), the total dual equation system can be obtained, except the constitutive equation, if we repeat the chain of ideas of paragraphs 3.6—3.7. No details are given here.

3.9 To the dual functional $(3.6)_2$ involving the fulfilment of the constitutive equation and equations $(2.4)_{1,2}$, the dual variational principle relates:

$$\delta_f K(f_{rs}) = 0\,. \tag{3.32}$$

By substitution of $e^{rs} = 0$, $K(f_{rs})$ gives the total complementary energy, and (3.32) is the Castigliano's variational principle (principle of minimum complementary energy). Further $e^{rs} = 0$.

Leaving the distinct notation f, on the base of $(3.6)_2$ the equation

$$\delta K(f_{rs}) = \delta K_0^V + \delta K_0^U = 0 \tag{3.33}_1$$

can be written, where due to $(3.6)_{3.5}$ and (3.1)

$$\delta K_0^V = \delta K^V + \delta K_{V0}^T + \delta K_{V0}^U\,, \tag{3.33}_2$$

$$\delta K^V = \int_{(V)} \varepsilon^{krm}\, \varepsilon^{lsp}\, a_{kl;\,mp}\, \delta f_{rs}\, dV\,, \tag{3.33}_3$$

$$\delta K_{V0}^T = \int_{(St)} \varepsilon^{\varkappa\eta 3}\, \varepsilon^{ldp}\, (a_{\varkappa l}\, \delta h_{\eta d;\,p} - a_{\varkappa l;\,p}\, \delta h_{\eta d})\, dS\,, \tag{3.33}_5$$

$$\delta K_{V0}^U = \int_{(Su)} \varepsilon^{\varkappa\eta 3}\, \varepsilon^{ldp}\, (a_{\varkappa l}\, \delta h_{\eta d;\,p} - a_{\varkappa l;\,p}\, \delta h_{\eta d})\, dS\,, \tag{3.33}_5$$

and further due to $(3.6)_4$, $(3.3)_4$, $(3.9)_4$ and (3.20)

$$\delta K_0^U = \delta_h L_0^U = \delta_h L_1^U + \delta_h L_U^Q\,. \tag{3.33}_6$$

In the present case the functions $h_{ed}(\xi^1, \xi^2)$ and $h_{\eta\vartheta;\,3}(\xi^1, \xi^2)$ are fixed, also the variations $\delta h_{ed}(\xi)$ should satisfy the following equation, which comes from $(3.6)_1$:

$$\varepsilon^{\varkappa\eta 3}\, \varepsilon^{ldp}\, \delta h_{\eta d;\, p\varkappa} = 0\,.$$

Comparing this latest equation with (3.15), we can realize, that the transformation of the expression $(3.33)_4$ can be carried out in the same way as that of the second term of the expression $(3.9)_3$. Taking (3.19) also into consideration, the following equation can be written:

$$\delta K^T_{V\,0} = \delta_h K^T_1 + \delta_h K^Q_T\,, \qquad (3.34)_1$$

where

$$\delta_h K^T_1 = \delta_{\tilde{h}} L^T_1 \quad \text{and} \quad \delta_h K^Q_T = \delta_{\tilde{h}} L^Q_T\,. \qquad (3.34)_{2,3}$$

Comparing $(3.33)_5$ and $(3.14)_3$ we obtain likewise — taking into consideration (3.21) as well — that,

$$\delta K^U_{V0} = \delta_h L^U_{V0} = \delta_h L^U_{V1} + \delta_h L^Q_{VU}\,. \qquad (3.34)_4$$

As a result of the transformations the variational principle (3.32) can be written in the following manner:

$$\delta K(f_{rs}) = \delta K^V + \delta_h K^T + \delta_h L^U_{V1} + \delta_h L^U_1 + \\ + \delta_h K^Q_T + \delta_h L^Q_U + \delta_h L^Q_{VU} = 0\,. \qquad (3.35)$$

Because the integrals, concerning the regions V, St, Su and q can be taken separately to be equal zero, and taking the basic assumptions of the beginning of paragraph 2.3 on the structure of the stress function tensor to be valid again, and also the transformation formula (2.3), we can find the next statements:

a) Due to equation $\delta K^V = 0$, which can be written on the base of $(3.33)_3$, because $\delta f_{RS}(x)$ can be artbitrary:

$$\varepsilon^{Rkm}\, \varepsilon^{Sdp}\, a_{\varkappa l;\, mp} = 0\,; \qquad x \in V\,. \qquad (3.36)$$

b) Due to equations $\delta_h K^T = \delta_h K^T_1 = \delta_{\tilde{h}} L^T_1 = 0$, which can be written on the base of the formulas (3.34) and $(3.19)_2$, because $\delta v_d(\xi)$ can be arbitrary on the surface part St:

$$\varepsilon^{3\varkappa\eta}\, \varepsilon^{ldp}\, a_{\varkappa l;\, p\eta} = 0\,; \qquad \xi \in St\,. \qquad (3.37)$$

c) Due to equation $\delta K^U = \delta_h L^U = \delta_h L^U_{V1} + \delta_h L^U_1 = 0$, which can be written on the base of the formulas $(3.21)_2$, $(3.20)_2$ and $(3.22)_5$, the formulas (3.25) are valid on the boundary part Su.

d) On the base of the formulas $(3.34)_3$, $(3.19)_3$, $(3.20)_3$ and $(3.21)_3$ the following equation can be written:

$$\begin{aligned}\delta K^Q = \delta_h K^Q_T + \delta_h L^Q_U + \delta_h L^Q_{VU} = \\ = \oint_{(q)} \{(b^\vartheta a_{\vartheta l} \delta w^l)^T + (b^\vartheta \varepsilon^{ldp} a_{\vartheta l;p} \delta v_d)^T - \\ - (b^\eta \tilde{u}_l \varepsilon^{ldp} \delta h_{\eta d;p}) - \\ - [b^\vartheta \varepsilon^{\varkappa\eta 3} (\tilde{u}_{3;\varkappa} - a_{3\varkappa}) \delta h_{\eta\vartheta}]^U + \\ + [b^\vartheta \varepsilon^{\varkappa\eta 3} \tilde{u}_{[\vartheta;\varkappa]} \delta h_{\eta 3}]^U\} ds = 0 . \end{aligned} \tag{3.38}$$

Assuming later that along the curve q

$$(\varepsilon^{ldp} \delta h_{\eta d;p})^U = (\varepsilon^{ldp} \delta h_{\eta d;p})^T , \qquad \xi \in q , \tag{3.39}_1$$

$$(\delta h_{\eta d})^U = (\delta h_{\eta d})^T , \qquad \xi \in q , \tag{3.39}_2$$

and taking into consideration the formulas (3.18), the identity of equations (3.38) and (3.26) turns out to be at once. So, following from equation (3.38), the equations (3.29) are also valid along the curve q.

On the base of the result of paragraph 3.9 we can summerize, that from the dual variational principle $\delta K = 0$ being formed by the functional due to (3.6) — the compatibility conditions of the dual system, i.e. the compatibility conditions of the strain field

$$a_{pq} = c_{pqkl} (\varepsilon^{krm} \varepsilon^{lsp} f_{rs:mp} + \overset{\cdot}{t}{}^{kl})$$

are derived. They are: compatibility field equations (3.36), compatibility boundary condition (3.37) on the boundary part St, and the displacement boundary condition (3.25) on the boundary part Su, which satisfy at the same place the compatibility boundary conditions.

REFERENCES

1. FINZI, B.: Integrazione delle equazioni indefinite della meccanica dei sistemi continui. *Rend. Lincei*, Ser. 6., **19** (1934), pp 578—584; 620—623
2. БЛОХ, В. И.: Функций напряжений в теории упругости. *Прикл. Мат. Мех.*, **14** (1950), 415—422
3. SOUTHWELL, R. V.: Castigliano's Principle of Minimum Strain-Energy and the Conditions of Compatibility for Strain. S. Timoshenko 60th Anniversary Volume. The MacMillan Co., 1938

4. Tonti, E.: Variational Principles in Elastostatics. *Meccanica*, **2** (1967), pp 201—208
5. Oden, J. T.—Reddy, J. N.: On Dual-Complementary Variational Principles in Mathematical Physics. *Int. J. Engng. Sci.*, **12** (1974), pp 1—29
6. АБОВСКИЙ, Н. П.—АНДРЕЕВ, Н. П.—ДЕРУГА, А. П.: Вариационные принципи теории упругости и теории оболочек. Изд. «Наука», Москва, 1978
7. Washizu, K.: A Note on the Conditions of Compatibility. *Journal of Mathematics and Physics*, **36** (1957), pp 406—312
8. Kozák, I.: Notes on the Field Equations with Stresses and on the Boundary Conditions in the Linearized Theory of Elastostatics. *Acta Techn. Hung.*, **90** (1980), 221—245
9. Kozák, I.: Determination of Compatibility Boundary Conditions in Linear Elastostatics with the Aid of the Principle of Minimum Complementary Energy. *Publ. Techn. Univ. Heavy Industry*, Ser. D. Natural Sciences **34** (1980), 83—98
10. Tonti, E.: A Mathematical Model for Physical Theories. *Rend. Accad. Lincei*, **52** (1972), pp 175—181; 350—356

Bemerkungen und Beitrag zu den Variationsprinzipien der linearisierten Theorie der Elastizität ausgedrückt mit Hilfe von Spannungsfunktionen. — Die Abhandlung gibt eine Definition von Funktionalen, in welchen der Tensor der Spannungsfunktion nur drei nicht verschwindende (zweckmäßig ausgewählte) Koordinaten besitzt, und eine ausführliche Untersuchung der Randbedingungen ermöglicht. Von den eingeführten Dualfunktionalen können durch die Variation des Spannungsfunktionstensors drei Kompabilitätsgleichungen und die Kompatibilitätsrandbedingungen, als notwendige und hinreichende Kompatibilitätsbedingungen abgeleitet werden.

Acta Technica Academiae Scientiarum Hungaricae, Tomus 92 (1–2), pp. 67–88 (1981)

EXISTENCE AND UNIQUENESS CRITERIA OF THE MEMBRANE STATE OF SHELLS

II. PARABOLIC SHELLS

T. TARNAI*

[Manuscript received 1 June, 1977]

Criteria of support will be considered, needed or allowed to be specified in the edges of a shell under vertical loads of arbitrary distribution in order to have the shell in a statically determinate membrane state. Part I of this paper published earlier considered criteria of existence and uniqueness of the solution of the membrane shell equation in connection with hyperbolic shells. This Part II extends the analysis to parabolic shells.

1. Introduction

The equilibrium of membrane shells is described in the orthogonal coordinate system xyz by

$$\mathfrak{L}F = \frac{\partial^2 z}{\partial y^2}\frac{\partial^2 F}{\partial x^2} - 2\frac{\partial^2 z}{\partial x\,\partial y}\frac{\partial^2 F}{\partial x\,\partial y} + \frac{\partial^2 z}{\partial x^2}\frac{\partial^2 F}{\partial y^2} = -g \tag{1}$$

where $z = z(x, y)$ is the equation of the middle surface of the shell,

$$\mathfrak{L} = \frac{\partial^2 z}{\partial y^2}\frac{\partial^2}{\partial x^2} - 2\frac{\partial^2 z}{\partial x\,\partial y}\frac{\partial^2}{\partial x\,\partial y} + \frac{\partial^2 z}{\partial x^2}\frac{\partial^2}{\partial y^2}$$

is the Pucher operator, $g = g(x, y)$ is the intensity function of an external load parallel to the z-axis (vertical), and $F(x, y)$ the unknown stress function yielding the reduced internal forces as follows:

$$n_x = \frac{\partial^2 F}{\partial y^2}\,,\quad n_{xy} = n_{yx} = -\frac{\partial^2 F}{\partial x\,\partial y}\,,\quad n_y = \frac{\partial^2 F}{\partial x^2}\,.$$

The first part of this paper [9] published earlier examined the criteria of existence and uniqueness of the solution of Eq. (1) of membrane shells

* Dr. T. Tarnai, Kolostor u. 17. H–1037 Budapest, Hungary

hyperbolic at all points of the domain of definition, and subjected to vertical loads. This part will consider the criteria at which there exists a unique solution of Eq. (1) for a shell parabolic at all points of its ground plan configuration, i.e., discriminant

$$D = \frac{\partial^2 z}{\partial x^2} \frac{\partial^2 z}{\partial y^2} - \left(\frac{\partial^2 z}{\partial x \partial y} \right)^2$$

is throughout zero.

The mathematical literature almost never concerns itself in examining the solvability of the parabolic differential equation in the case where first derivatives of the unknown function do not occur in the equation. For instance, monography [5], rather detailed about parabolic equations, does not mention this equation, probably because of its rather simple built-up.

General solution of a parabolic equation in the canonical form

$$\frac{\partial^2 u}{\partial x^2} = f(x, y) \tag{2}$$

may be produced by twice integrating with respect to x, to yield:

$$u(x, y) = \int \left[\int f(x, y)\, dx \right] dx + C_1(y)\, x + C_2(y)$$

where $C_1(y)$ and $C_2(y)$ are functions of integration.

Solutions twice continuously differentiable are sought for, requiring function $f(x, y)$ to be continuous at any point (x, y) of the given domain, and twice continuously differentiable with respect to variable y. Also functions $C_1(y)$ and $C_2(y)$ have to be twice continuously differentiable.

Assuming function $f(x, y)$ to be continuous with respect to variable x, and piece-wise twice continuously differentiable with respect to variable y, while functions $C_1(y)$ and $C_2(y)$ to be piece-wise twice continuously differentiable then $\partial^2 u/\partial x^2$ and $\partial^2 u/(\partial x \partial y)$ will be continuous, while partial derivative $\partial^2 u/\partial y^2$ will have discontinuities. For $u \equiv F$ and $f \equiv -g$, Eq. (2) describes the equilibrium of the vault shell of equation $z = y^2/2$. With the above assumptions, this shell is in membrane state, since n_y and n_{xy} are continuous, while n_x may be discontinuous along a finite number of straight lines described by $y = const.$ Such discontinuities do not affect the equilibrium of internal forces.

In this discussion, a boundary will be understood as a projection on the ground plan xy of the real edge line of the shell. Real edge line of the shell will be denoted by $\bar{S}$, its projection on the ground plan by S.

2. Initial-value problem in the parabolic case (Cauchy problem)

As an introduction let us mention that, in the literature, Cauchy problem of a parabolic equation is generally understood other (p. 344 in [7]) than that of quasilinear equations (p. 134 in [3]) or of hyperbolic equations. In this paper, the term "Cauchy problem" will be applied for parabolic equation with the same meaning as for e.g. hyperbolic equations.

Let us first consider the simplest of initial value problems. Be J an interval with end points a_1, a_2 along the y-axis. Let us find a twice continuously differentiable solution $u(x, y)$ of Eq. (2) where:

$$u(0, y) = \varphi_1(y), \qquad a_1 \leqq y \leqq a_2\,,$$

$$\frac{\partial u(0, y)}{\partial x} = \varphi_2(y), \qquad a_1 \leqq y \leqq a_2\,, \tag{3}$$

φ_1 and φ_2 being given, twice continuously differentiable functions. Also $f(x, y)$ in Eq. (2) is stipulated to be continuous and twice continuously differentiable with respect to y.

Now, Eq. (2) has a solution under conditions (3). Namely, integrating (2) twice with respect to variable x:

$$\int_0^x \int_0^\tau \frac{\partial^2 u(\xi, y)}{\partial x^2}\, d\xi\, d\tau = \int_0^x \int_0^\tau f(\xi, y) d\xi d\tau$$

leads to

$$u(x, y) = u(0, y) + x \frac{\partial u(0, y)}{\partial x} + \int_0^x \int_0^\tau f(\xi, y) d\xi d\tau\,.$$

Substituting there conditions (3) yield the solution:

$$u(x, y) = \varphi_1(y) + x\varphi_2(y) + \int_0^x \int_0^\tau f(\xi, y) d\,\xi d\tau \tag{4}$$

defined in the infinite strip between straight lines $y = a_1$ and $y = a_2$.

This solution is unique. Namely, if functions u_1 and u_2 satisfying Eq. (2) and meeting conditions (3) would exist, they ought to take the form (4). Subtracting forms (4) written for u_1 and u_2 from each other, yields $u_1 - u_2 = 0$, hence $u_1 = u_2$.

The solution is continuously dependent on the initial conditions. Namely, for fixed y, Eq. (2) is an ordinary linear differential equation that can be reduced

to a system of linear differential equations (p. 139 in [8]) continuously dependent on the initial values (p. 182 in [8]). Thus, the problem is properly posed.

Let us generalize this problem. Rather than in the interval J on the y-axis, with end points a_1 and a_2, initial-values will be given along a curve with end points on straight lines $y = a_1$ and $y = a_2$, single-valued in y. The curve has to be indicated so that the new initial-value problem can be reduced to the original one, that is, if the function indicated on the curve is twice continuously differentiable with respect to the arc length, then this function has also to be twice continuously differentiable with respect to variable y. Be s the arc length parameter. Be the equation of the boundary curve $h = h(y)$, and be given a function $\varphi(s)$ twice continuously differentiable with respect to s on this curve. $\varphi(s(y))$ is wanted to be twice continuously differentiable with respect to y. The arc length is given by the well-known formula

$$s = \int_{a_1}^{y} \sqrt{1 + h'^2(\eta)}\, d\eta$$

where supersript comma denotes derivation with respect to y. Let us now differentiate $\varphi(s(y))$ twice with respect to y, to obtain:

$$\varphi'' = (1 + h'^2)\frac{d^2 f}{ds^2} + \frac{h' h''}{\sqrt{1 + h'^2}} \cdot \frac{df}{ds}.$$

This relationship also includes h' and h''. Thus, in order that φ be twice continuously differentiable also in respect to variable y it is necessary that also $h(y)$ be twice continuosly differentiable. Now, also h' has to be finite, i.e., curve $h = h(y)$ must not have points where the tangent is parallel to the x-axis. Otherwise, curve $h = h(y)$ cannot have a tangent parallel to the x-axis since by giving the u value on the curve, also the $\partial u/\partial x$ value has been unambiguously given at the contact point. Thus, here no arbitrary value of derivative $\partial u/\partial x$ can be prescribed.

If function $z = z(x, y)$ of the middle surface is four times continuously differentiable, then a transformation twice continuously differentiable bringing Eq. (1) to canonical form is known to exist (p. 64 in [7]). If a function is twice continuously differentiable then it remains so even after canonical transformation.

According to the above, the generalized Cauchy problem for Eq. (1) can be formulated in the parabolic case.

Be S a shell edge part bounded by points A and B in ground plan projection (in the plane xy) and be it given a direction i (unit vector) at every point of the boundary curve S. Let stress function F on boundary S assume values defined by a given function φ and let its derivative in direction i have values

defined by a given function ψ. Now, the Cauchy problem

$$\left.\begin{aligned} \mathfrak{L}F &= -g\,, && \text{(5a)} \\ F|_S = \varphi\,,\ \left.\frac{\partial F}{\partial i}\right|_S &= \psi && \text{(5b)} \end{aligned}\right\}$$

has a twice continuously differentiable solution uniquely determined in the infinite strip bounded by characteristics passing through points A and B (Fig. 1a) if the following conditions are satisfied:

a) the boundary curve S lies in the domain of definition of Eq. (5a);

b) each characteristic intersects the boundary curve S at most at one point;

c) not one characteristic is tangent to the boundary curve S;

d) S is twice continuously differentiable;

e) in every point of the boundary curve S the direction i is tangent to the characteristic passing through the point;

f) $g(x, y)$ is continuous and twice continuously differentiable normally to the characteristics;

g) φ and ψ are twice continuously differentiable;

h) $z(x, y)$ is four times continuously differentiable.

Now, other boundary sections of the shell have to be in the half strip between characteristics passing through points A and B, either to the right

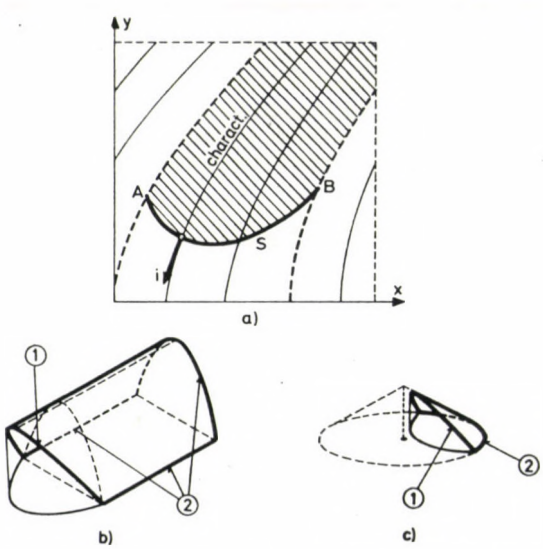

Fig. 1. a) Domain of solution of the initial-value problem; *b)* Vault shell of parabolic directrix with a free edge part; *c)* Apse-like shell formed from a cone surface; ① free edge part; ② fully supported edge part

or to the left of S. No condition can be specified on these boundary sections. Here the supports have to carry both internal forces transmitted by the shell.

In this problem, derivative in direction i on the boundary may be replaced by that in the normal n. The two data are, however, not fully equivalent. Namely, since F can be differentiated continuously twice on the boundary, derivative $\partial F/\partial t$ in the direction of the tangent can but once be continuously differentiated. According to conditions c), d) and e), the normal derivative $\partial F/\partial n$ may be expressed in terms of derivatives $\partial F/\partial t$ and $\partial F/\partial i$ but since $\partial F/\partial t$ is but once continuously differentiable, so will be $\partial F/\partial n$. Conditions $F|_S$, $\partial F/\partial i|_S$ and $F|_S$, $\partial F/\partial n|_S$ will be equivalent if F is three times continuously differentiable on the boundary.

In problem (5a, b) the edge may be specified as being free, namely, then $F|_S = 0$, $\partial F/\partial x|_S = 0$, $\partial F/\partial y|_S = 0$ hence $\partial F/\partial i|_S = 0$. Thus, in condition (5b) edge freedom can be specified by substituting $\varphi \equiv 0$, $\psi \equiv 0$. A parabolic vault shell and an apse-like cone shell with such a free edge part can be seen in Figs (1b) and (1c).

If boundary S is straight, then also normal and tangential internal forces can be given there [9]. These have to be continuously differentiable. In either case, the shell is in a uniquely determined membrane state. Boundary conditions for internal forces uniquely determine the internal forces of the shell.

The shell remains in a membrane state if functions in conditions d), f) and g) are required piece-wise twice continuous differentiability rather than twice continuous differentiability. (Also in this case, functions have to be once continuously differentiable.) Now, normal forces in the direction of the characteristics will be discontinuous along characteristics passing through points where second derivatives of the mentioned functions are discontinuous. In case of lower requirements for any of the mentioned functions (e.g. piece-wise once continuous differentiability), the shell cannot be in a membrane state any longer, as a rule.

These statements will be illustrated on a simple example. Be the middle surface of the shell the parabolic vault of function $z = (1/2)y^2$. Let the shell

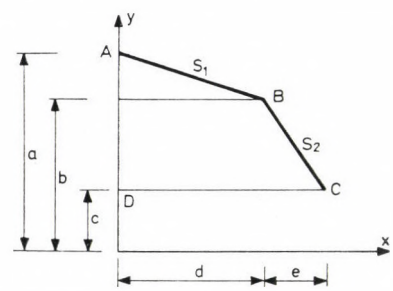

Fig. 2. Ground plan of the vault shell with a free edge part. Ground plan projection of the free edge part consists of straight parts S_1 and S_2

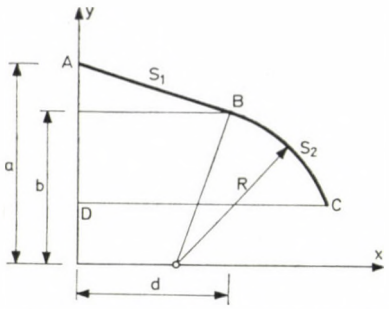

Fig. 3. Ground plan of the vault shell with a free edge part. Ground plan projection of the free edge part consists of straight line S_1 and circular arc S_2

be subjected to a uniform load $g = const.$ Be its edge S free. Let edge S consist of two adjacent curve parts S_1 and S_2. Let us find the solution for the Cauchy problem

$$\frac{\partial^2 F}{\partial x^2} = -g\,, \tag{6a}$$

$$F|_S = 0, \frac{\partial F}{\partial x}\bigg|_S = 0\,. \tag{6b}$$

(Shell edge parts AD and DC outside S (Figs 2 and 3) are fully supported.)

2.1. First let boundary $S = S_1 \cup S_2$ be piece-wise once continuously differentiable.

Let connection point B of curves S_1 and S_2 be a knee point. For the sake of simplicity, let boundary sections S_1 and S_2 be straight (Fig. 2).

$$\text{Equation of } S_1\text{: } x = -\frac{d}{a-b}(y-a)\,,$$

$$\text{while equation of } S_2\text{: } x = -\frac{e}{b-c}(y-b) + d\,.$$

Solution of problem (6a, b) will be produced according to [2]. Accordingly, in the strip between characteristics of equations $y = a$ and $y = b$ passing through end points A and B of boundary section S_1, the stress function has an equation:

$$F_1 = \frac{g}{2}\left[\frac{d}{a-b}(y-a) + x\right]^2$$

and in the strip between characteristics of equations $y = b$ and $y = c$ passing through the end points B and C of boundary section S_2:

$$F_2 = -\frac{g}{2}\left[\frac{e}{b-c}(y-b) - d + x\right]^2.$$

Reduced internal forces in the strip containing boundary section S_1 are:

$$n_x^{(1)} = \frac{\partial^2 F_1}{\partial y^2} = -g\left(\frac{d}{a-b}\right)^2$$

$$n_{xy}^{(1)} = -\frac{\partial^2 F_1}{\partial x\,\partial y} = g\frac{d}{a-b},$$

$$n_y^{(1)} = \frac{\partial^2 F_1}{\partial x^2} = -g$$

and in that containing S_2:

$$n_x^{(2)} = \frac{\partial^2 F_2}{\partial y^2} = -g\left(\frac{e}{b-c}\right)^2,$$

$$n_{xy}^{(2)} = -\frac{\partial^2 F_2}{\partial x\,\partial y} = g\frac{e}{b-c},$$

$$n_y^{(2)} = \frac{\partial^2 F_2}{\partial x^2} = -g\,.$$

Apparently, forces n_x and n_{xy} are discontinuous along the line $y = b$. Because of the discontinuity of n_{xy}, the internal forces cannot be in equilibrium, hence the shell itself cannot be in a membrane state.

It is worth mentioning that a similar analysis of a hyperbolic shell of free edge with a knee demonstrated the shell to be in a membrane state in spite of the knee of its edge curve [9].

2.2. Be boundary $S = S_1 \cup S_2$ piece-wise twice continuously differentiable.

It is known to require a once continuous differentiability of the boundary curve. Now let boundary section S_2 join tangentially, without knee, edge S_1 expressed by:

$$x = -\frac{d}{a-b}(y-a)\,.$$

Be boundary section S_2 e.g. a circular arc with centre on the x-axis, and joining S_1 at B (Fig. 3) expressed by:

$$x = \sqrt{b^2 + \frac{b^2}{d^2}(a-b)^2 - y^2} + d - \frac{b}{d}(a-b).$$

In the strip containing boundary section S_1, the stress function is the same as function F_1 under 2.1. In the strip between characteristics passing through end points B and C of the circular arc S_2, the stress function becomes:

$$F_2 = -\frac{g}{2}\left[\sqrt{b^2 + \frac{b^2}{d^2}(a-b)^2 - y^2} + d - \frac{b}{d}(a-b) - x\right]^2.$$

Because of the complexity of F_2, the reduced internal forces will not be written in the strip containing boundary section S_2 but only along the connection line $y = b$ such as:

$$n_x^{(2)}|_{y=b} = -g\left[\frac{d^2}{(a-b)^2} + (x-d)\,d\,\frac{(a-b)^2 + d^2}{b(a-b)^3}\right],$$

$$n_{xy}^{(2)}|_{y=b} = g\frac{d}{a-b},$$

$$n_y^{(2)}|_{y=b} = -g\,.$$

Among the reduced internal forces, only n_x is seen to be discontinuous along the characteristic $y = b$, but it is also continuous at $x = d$, i.e. the joining point of boundary curves S_1 and S_2. In spite of the discontinuity of n_x, internal forces are in equilibrium, hence the shell is in a membrane state.

2.3. Be boundary $S = S_1 \cup S_2$ twice continuously differentiable.

This is the case e.g. where boundary S_1 is also now considered to be a straight line tangentially joined at B by a third or higher degree algebraic curve such as curve S_2. Now, stipulations made in the general formulation of the Cauchy problem are satisfied, and all internal forces will be continuous. It could be demonstrated by a simple calculation similar to the above one.

Notice that, similar to hyperbolic shells (7.2. in [9]), initial conditions for edge S of parabolic shells can be given so that the shell has several not overlapping free edge parts on edge S. If the shell has several edge parts not fitting a piece-wise twice continuously differentiable curve satisfying conditions b) and c) then the shell cannot be in a membrane state. Though, if there is such a curve but only boundary values rather than smoothly joining initial values or nothing are specified for curve parts between free edge parts, then the shell is in — though not unique — membrane state.

3. Boundary-value problems in the parabolic case

Let us again consider Eq. (2) in a canonical form. This partial differential equation becomes an ordinary differential equation for any fixed x, solved in the form:

$$u(x) = k(x) + C_1 x + C_2\,.$$

This equation is known to yield unique constants C_1 and C_2 from the boundary conditions if the system of linear equations written according to the conditions for unknowns C_1 and C_2 has a unique solution, a case occurring if the system has a non-zero determinant. If there is a unique solution, it continuously depends on the boundary values, since solution of boundary-value problems can be composed from the linear combination of the solutions of two, linearly independent initial-value problems. Though, the solution of initial-value problems — in conformity with the statement in Chapter 2 — is a continuous function of the initial values. Now the problems are properly posed ones.

Let us enumerate the major possibilities.

(i) Let the $u(x)$ value be given at two different points $x = a$ and $x = b$. Now, the equation system has a non-zero determinant:

$$\begin{vmatrix} a & 1 \\ b & 1 \end{vmatrix} = a - b.$$

Thus, this boundary value problem has a unique solution.

(ii) Let the $u(x)$ value be given at point $x = a$ and that of du/dx at $x = b$. Now, determinant of the equation system is:

$$\begin{vmatrix} a & 1 \\ 1 & 0 \end{vmatrix} = -1 .$$

Also this boundary-value problem has a unique solution.

(iii) Let the du/dx value be given in two different points $x = a$ and $x = b$. Now, determinant of the equation system is:

$$\begin{vmatrix} 1 & 0 \\ 1 & 0 \end{vmatrix} = 0 .$$

Thus, this problem has no unique solution.

(iv) Let values of linear combinations $\alpha_1(du/dx) + \beta_1 u$ and $\alpha_2(du/dx) + \beta_2 u$ be given at $x = a$ and $x = b$, respectively. Now, determinant of the equation system is:

$$\begin{vmatrix} \alpha_1 + a\beta_1 & \beta_1 \\ \alpha_2 + b\beta_2 & \beta_2 \end{vmatrix} = (a - b)\beta_1 \beta_2 + \alpha_1 \beta_2 - \alpha_2 \beta_1 .$$

Thus, this problem has a unique solution only for

$$(a - b)\beta_1 \beta_2 + \alpha_1 \beta_2 - \alpha_2 \beta_1 \neq 0.$$

In case (i), (ii) and to a degree, (iv) constants C_1 and C_2 can be determined for any fixed y, permitting the solution of the problem — twice continuously differentiable with respect to x if $f(x, y)$ is continuous.

Let us consider sections of straight lines $x = a$ and $x = b$ between $y = a_1$ and $y = a_2$. Be function $f(x, y)$ in (2) continuous and twice continuously differentiable with respect to variable y.

Obviously, indicating the value of the sought function $u(x, y)$ in (2) for fixed $x = a$ and $x = b$, so that it is twice continuously differentiable with respect to variable y, then also functions $C_1(y)$ and $C_2(y)$ will be twice continuously differentiable.

Thus, specifying the value of function $u(x, y)$ along lines $x = a$ and $x = b$ in the interval $[y = a_1, y = a_2]$ so that it is twice continuously differentiable with respect to variable y, then Eq. (2) has a unique solution having the given values in the interval $[y = a_1, y = a_2]$ of lines $x = a$ and $x = b$.

The same refers to the case of giving the function value in one interval, and the partial derivative with respect to variable x of the function in the other one (or the linear combination $\alpha(\partial u/\partial x) + \beta u$) both so that they are twice continuously differentiable with respect to variable y.

Similar to the initial-value problem, these two (or three) problems can be generalized in the meaning that the boundary values are specified for curves rather than for straight sections. On this basis, generalized boundary-value problems for Eq. (1) can be formulated.

3.1. First boundary-value problem for the parabolic Pucher differential equation

Let edge S (in ground plan projection) consist of two curved parts S^1 and S_2 with no common point. Let stress function assume values φ and ψ on boundary sections S_1 and S_2, respectively. Let us now solve the boundary-value problem

$$\mathfrak{L}\, F = -g\,, \tag{7a}$$

$$F|_{S_1} = \varphi\,, \quad F|_{S_2} = \psi\,. \tag{7b}$$

Problem (7a, b) has a unique, twice continuously differentiable solution in the "quadrangle" $ABCD$ defined by the end points of the boundary curves (Fig. 4a), provided the following conditions are satisfied:

a) boundary curves S_1 and S_2 are in the domain of definition of Eq. (7a);

b) characteristics intersect boundary curves S_1 and S_2 in at the most one point each;

c) no characteristic is tangent to curves S_1 and S_2;

d) S_1 and S_2 are twice continuously differentiable;

e) corresponding end points of curves S_1 and S_2 (A, D and B, C) are on the same characteristic (Fig. 4a);

f) $g(x, y)$ is continuous, and twice continuously differentiable normally to the characteristics;

g) φ and ψ are twice continuously differentiable;

h) $z(x, y)$ is four times continuously differentiable.

Condition h) provides for the canonical transformation of Eq. (7a). During canonical transformation, the quoted functions keep properties settled under the conditions. Now, transforming the boundary curves according to p. 870 in [4], the problem in a canonical form can be interpreted in a rectangular domain. This problem — as is shown in item (i) introducing Chapter 3 — has a unique solution twice continuously differentiable in conformity with the conditions.

Obviously, no condition can be specified on edge parts of the shell connecting points A and D, B and C, lying on characteristics.

Value of stress function F on boundaries S_1 and S_2 may be given so as to make it a plane curve. It is known to physically mean that edge beams along edges S_1 and S_2 are vertically supported. In shell edge parts $\widehat{AD}$ and $\widehat{BC}$, edge beams have to carry any force transmitted by the shell. A shell supported in this way may be exemplified by the conical shell of parabolic directrix seen in Fig. 4b. If boundary sections S_1 and S_2 are straight lines then also the value of the normal forces on the edge can be specified, that may be zero in a particular case keeping edges S_1 and S_2 exempt from lateral pressure. The membrane state of the shell is, however, not unique in either case. Boundary conditions fail to uniquely determine internal forces of the shell. Namely — although the boundary-value problem (7a, b) has a unique solution for any fixed boundary value, — the boundary conditions still include free constants of arbitrary value, leading to an infinity of solutions. Cases where curves S_1 and S_2 have a common point, where F is continuous, are exceptions.

It should be stressed — as for the Cauchy problem — that a parabolic shell may be in a membrane state even if the function of the normal force

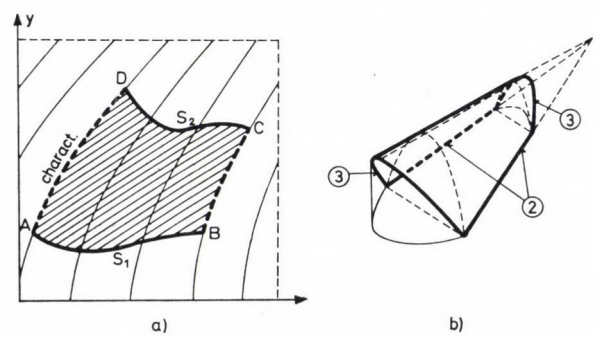

Fig. 4. a) Domain of solution of boundary-value problems; *b)* cone shell of parabolic directrix with arched edge parts in ground plan; ② fully supported edge part, ③ edge part with vertically supported edge beam

in the direction of the characteristics has discontinuities along a finite number of characteristics. This is why a mere piece-wise twice continuous differentiability of functions under conditions d), f) and g) may be admitted on the self-intended condition to be once continuously differentiable.

3.2. *Second boundary-value problem for the parabolic Pucher differential equation*

This problem where derivatives of stress function F in the direction of characteristics on boundaries S_1 and S_2 are given (Fig. 4a) has, in general, none or no unique solution. The truth of this statement after canonical transformation follows from item (iii) in Chapter 3.

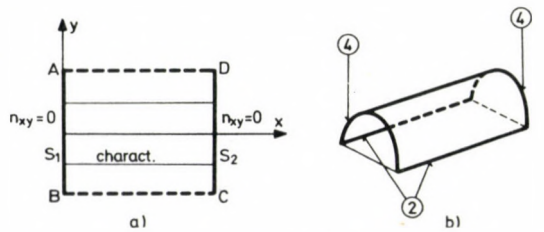

Fig. 5. Cylindrical shell over rectangular ground plan *a)* ground plane; *b)* axonometric view, ② fully supported edge part, ④ edge part free from shear forces

Otherwise, also structural considerations point to that, this problem is an ill-posed one. Let us consider a cylindrical shell concluded by straight boundaries S_1 and S_2 normal to the generatrices (Fig. 5).

Let us specify the derivatives of the stress function in direction x on boundaries S_1 and S_2. Be

$$\left.\frac{\partial F}{\partial x}\right|_{S_1} = \left.\frac{\partial F}{\partial n}\right|_{S_1} = 0\,, \quad \left.\frac{\partial F}{\partial x}\right|_{S_2} = \left.\frac{\partial F}{\partial n}\right|_{S_2} = 0\,.$$

These conditions are known to mean no shear forces in edges S_1 and S_2. Thus, external loads can only raise normal forces in the edges S_1 and S_2. Such a support permits displacement of shell edge points along y, hence inextensional deformation of the shell [6]. In general, however, a shell able to inextensional deformation cannot be in a membrane state.

3.3 *Third boundary-value problem for the parabolic Pucher differential equation*

This problem will not be considered, in general, since there is only a single curve known where the third boundary condition of the form $\alpha(\partial F/\partial n) + \beta F$ can be interpreted. This curve is a circular arc of radius R where the

shear force value can be given by a function χ. This condition may be formulated as in [9]:

$$-\frac{\partial F}{\partial n}+\frac{1}{R}F=\int \chi ds+c$$

where s is the arc length parameter of the circular arc, and c is a constant. The exemptness of the circular arc edge from shear is expressed by:

$$-\frac{\partial F}{\partial n}+\frac{1}{R}F=c\,.$$

Let us consider a case where normals of the circular arc point are in the direction of the characteristics. Taking a cone (not absolutely a right circular cone) with its vertex on the z-axis and with a part the projection of which on the plane xy is an annular sector confined by circular arcs of radii R_1 and R_2 and by radii (characteristics) passing through their end points (Fig. 6a). Be these circular arc edges exempt from e.g. shear, a case illustrated in Fig. 6b on a right circular cone shell for the sake of simplicity.

Now, let us find a solution of the problem

$$\left.\begin{aligned} \mathfrak{L}F &= -g, \\ \left(-\frac{\partial F}{\partial n}+\frac{1}{R_1}F\right)\Big|_{S_1} &= c_1\,, \\ \left(-\frac{\partial F}{\partial n}+\frac{1}{R_2}F\right)\Big|_{S_2} &= c_2 \end{aligned}\right\}$$

to be determined by proceeding from characteristic to characteristic — without canonical transformation of the equation. Let us now consider the existence of the solution to this problem. Taking the characteristic as coincident with the x-axis — involving $y=0$ hence zero coefficient of $\partial^2F/\partial y^2$ and $\partial^2F/(\partial x\partial y)$ in Eq. (1) in conformity with item (iv) in Chapter 3, the problem has a unique solution if

$$(a-b)\beta_1\beta_2+\alpha_1\beta_2-\alpha_2\beta_1\neq 0\,.$$

In our case $\alpha_1=\alpha_2=-1$,

$$\beta_1=1/R_1\,,\quad \beta_2=1/R_2\,,\quad a=R_1\,,\quad b=R_2\,.$$

Substitution of these values leads to uncompliance with the quoted condition, the value of the indicated expression being zero. Thus, there is no solution along the examined characteristic. Similar outcomes result for the

other characteristics, since, by rotating the coordinate system about its z-axis, the tested characteristic can be made to coincide with the x-axis. In a final account, the third boundary-value problem stated above can be said not to have a unique solution, the shell cannot be in a unique membrane state. There is either none or no unique membrane state.

If the normals to the circular arcs are not parallel to the characteristics, then the determination of the unknown functions of integration from the third boundary conditions will, in a general case, be by solving a system of linear inhomogeneous differential equations, the solvability of which the solvability of the boundary-value problem depends on, a problem not to be considered here.

3.4. Mixed boundary-value problem for the parabolic Pucher differential equation

Take an edge S consisting (in ground plan projection) of two boundary sections S_1 and S_2 with no common point. Assign a direction i (unit vector) to each point of curve S_2. Let the value of stress function F be given by a function φ on boundary S_1, while the value of the derivative of stress function F in direction i be given by a function ψ on boundary S_2. Solution of boundary-value problem

$$\left.\begin{aligned} &\mathfrak{L}\, F = -g\,, \\ &F|_{S_1} = \varphi\,, \quad \left.\frac{\partial F}{\partial i}\right|_{S_2} = \psi \end{aligned}\right\} \qquad \begin{aligned} &\text{(8a)} \\ &\text{(8b)} \end{aligned}$$

has to be found.

Problem (8a, b) has a unique twice continuously differentiable solution in the "quadrangle" $ABCD$ defined by the end points of the boundary curves (Fig. 4a) if conditions a) to h) under 3.1 are satisfied, and if direction i is tangent to the characteristic at every point of boundary curve S_2.

Namely, according to condition h), Eq. (8a) can be brought to a canonical form. After this transformation, direction i will be parallel to the x-axis. The resulting problem has a unique solution in conformity with item (ii) in Chapter 3. The solution is twice continuously differentiable, since canonical transformation does not affect differentiability of functions involved in the conditions.

No condition can be prescribed on the boundary sections connecting points A and D, B and C, lying on characteristics. These edge parts have to be fully supported.

Considering again the example of a cylindrical shell under 3.2 (Fig. 5), under boundary conditions

$$F|_{S_1} = 0\,, \quad \partial F/\partial x|_{S_2} = \partial F/\partial n|_{S_2} = 0$$

edges S_1 and S_2 of the cylindrical shell are free from normal forces, and shears, respectively. The boundaries being straight lines, even non-zero normal and shear force values may be specified for edges S_1 and S_2, resp. These boundary conditions uniquely determine the internal forces of the shell. Thus, the shell is uniquely in a membrane state.

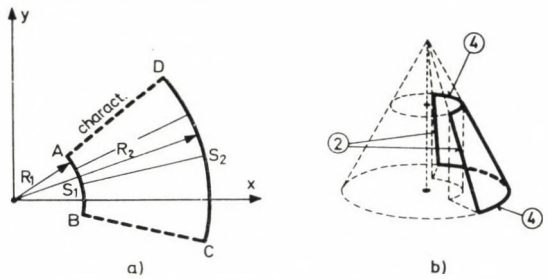

Fig. 6. a) Cone shell ground plan; *b)* shell surface cut out from a right circular cone; ② fully supported edge part; ④ edge part free from shear forces

The cone shell problem under 3.3 (Fig. 6) becomes a properly posed problem by indicating the first rather than the third boundary value on boundary S_1, leading to a mixed boundary-value problem. Under conditions

$$F|_{S_1} = a_1\sqrt{R_1^2 - y^2} + b_1 y + c_1\,,$$

$$\left(-\frac{\partial F}{\partial n} + \frac{1}{R_2}F\right)\Big|_{S_2} = c_2$$

differential equation of the cone shell has unique solutions for any fixed constant a_1, b_1, c_1, c_2. Now, edge beam of edge S_1 will be vertically supported, and edge S_2 will be free from shear forces Remember that even non-zero shear forces on circular arc S_2 may be specified. This problem may have a solution since boundary conditions satisfy condition (iv) in Chapter 3 for any characteristic. Namely, now:

$$\alpha_1 = 0\,,\quad \alpha_2 = -1\,,\quad \beta_1 = 1\,,\quad \beta_2 = \frac{1}{R_2}\,,$$

$$a = R_1,\ b = R_2$$

thus

$$(a-b)\beta_1\beta_2 + \alpha_1\beta_2 - \alpha_2\beta_1 = (R_1 - R_2)\frac{1}{R_2} + 1 = \frac{R_1}{R_2}\,.$$

Apart from the case of rotational symmetry, the problem can be solved for any load except for $R_1 = 0$, that is, if also the cone vertex belongs to the domain of definition. Notice that in this problem curve S_1 may be other than a circular arc.

In this problem, for $R_1 \neq 0$, the cone may always be in a membrane state but boundary conditions fail to uniquely determine the internal forces. The shell is not in unique membrane state.

Admitting the normal force pointing in the direction of the characteristics to be discontinuous along a finite number of characteristics, then curves S_1, S_2, functions φ and ψ as well as load function g may only be required piecewise twice continuously differentiable rather than twice continuously differentiable.

4. Problem of a closed edge curve

Similar to hyperbolic shells, conditions prescribed on the closed edge curve often leads to overdeterminacy in parabolic shell problems. In certain cases, however, a solution exists even for closed edge curves.

Among non-self-intersecting, twice continuously differentiable, closed curves in the middle surface of the shell, let us consider those intersected in a minimum of points by asymptotic lines (their projections on the xy plane are the characteristics). These curves may be fundamentally of two kinds. One type of curves is not intersected by any asymptotic line of the surface, but if one does, then at two points, apart from the contact points. Curves of the other type are intersected by any asymptotic line at exactly one point. This type only occurs for cylinders and cones of closed directrix.

4.1. Initial-value problem for a closed boundary curve

Be boundary S the ground plan projection of a closed curve of the first type, then — conditions b) and c) in Chapter 2 not being satisfied — initial-value problem (5a, b) has no solution. This is why no cylindrical or cone shell with a free-edged opening can be in a membrane state.

Be boundary S the ground plan projection of a curve of the second type and also be conditions e) to h) in Chapter 2 satisfied, then initial-value problem (5a, b) has a unique solution. For instance, a closed cone shell (Fig. 7a) with

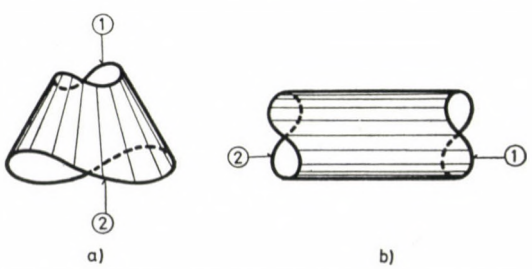

Fig. 7. a) Cone shell with closed directrix; *b)* cylindrical shell with closed directrix; ① free edge; ② fully supported edge

a free spatial curve edge at one end satisfying conditions in Chapter 2 may be in unique membrane state. Of course, no conditions may be prescribed on the other shell edge. Here the edge beam has to carry any internal force. In Fig. 7a, the upper edge is quite free, and the lower one is fully supported, but it may also be reversed: the upper edge fully supported and the lower one free. For a two-valued middle surface function (such as for a horizontal cylinder or cone), conditions b) and c) in Chapter 2 do not seem to be satisfied. The edge curve (in projection) is intersected at two points by the characteristics, and is tangent to those on the contour. Condition b) may be satisfied by separately handling lower and upper points of the surface. Now, boundary curve parts belonging to the lower and upper surface part, will each be intersected by the characteristics at a single point. Condition c) will be replaced by the requirement that no asymptotic line may be tangent to the real edge curve $\bar{S}$ (on the middle surface) of the shell. These conditions are, however, not yet sufficient for the shell to be in membrane state. The shell will be in a membrane state under loads (actually, of two-valued function) such that shear forces and annular normal forces along the junction line (characteristic) of the lower and upper shell part are in equilibrium. This condition is always satisfied for e.g. cylindrical shells (Fig. 7b) if along the junction characteristic, load function g with its first derivatives is bounded. In case of unbounded loads (e.g. self weight) the Pucher equation is unifit to ascertain the existence of the membrane state. Now reduced internal forces are advisably replaced by real ones and the problem examined in a natural coordinate system [10], is not to be considered here.

4.2. Boundary-value problems for closed boundary curves

4.2.1. For the first boundary-value problem, no common point of boundary curves S_1 and S_2, the conditions were specified for, was stipulated, in order that boundary values can be given separately for boundary curves S_1 and S_2. Namely, if they have a common point, it will be common even after canonical transformation. Thus, along the characteristic passing through this point determinant under (i) in Chapter 3 is zero, hence at this point and along the characteristic passing through it, there is either none or no unique solution. This consideration would involve that points A and D, B and C in the solution domain in Fig. 4a may be infinitely close but not coincident. A further stipulation for the sake of solvability, was to have no characteristic tangent to the boundary curves. Accordingly, if the boundary is ground plan projection of a closed curve type 1, then value of stress function F can be prescribed on the curve, save at contact points (Fig. 8a).

This is not quite true for practical problems. The stress function is required to be continuous also along the boundary, thus, in the common point

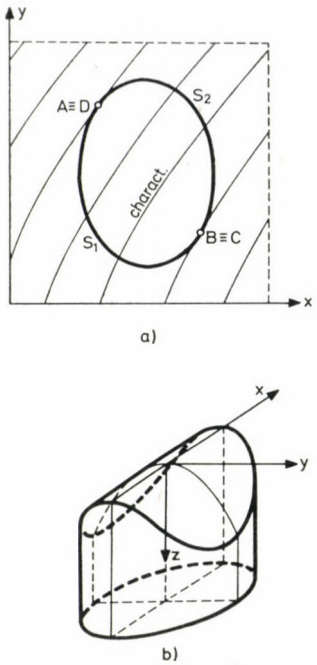

Fig. 8. a) Closed edge curve of the first type; *b)* Parabolic cylinder over elliptic ground plan

of S_1 and S_2, the boundary values have to be identical. Thus, there exists a solution along the characteristic passing through the common boundary point, but outside it the solution will not be unique, irrelevant to our problem where the solution is sought for in the bounded domain surrounded by the boundary curves, and its behaviour outside this domain is unimportant. Thus the existence of a characteristic along which the solution is not unique but only at one point is irrelevant. Also boundary curves S_1 and S_2 may be permitted to be tangent to a characteristic at the common point. Now, based on the continuous differentiability of stress function F, merely identity of derivatives of boundary value functions given on S_1 and S_2 at the common contact point has to be required. For the sake of a twice continuously differentiable solution, identity of both first and second derivatives of the quoted functions at the common contact point has to be required.

Now, a horizontal parabolic shell over an elliptic ground plan subjected to a vertical load is in unique membrane state if condition $F|_S = 0$ is specified all around the boundary (Fig. 8b) [1].

The shell edge may also consist of two closed curves of type 2, with no common part. Provided conditions under 3.1 are satisfied — with completions under *4.1* for edge curves — then the shell may be in membrane state even for closed edge curves. For instance, cylindrical and cone shells in Fig. 7 are in

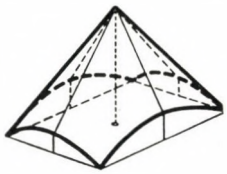

Fig. 9. Cone shell over rectangular ground plan

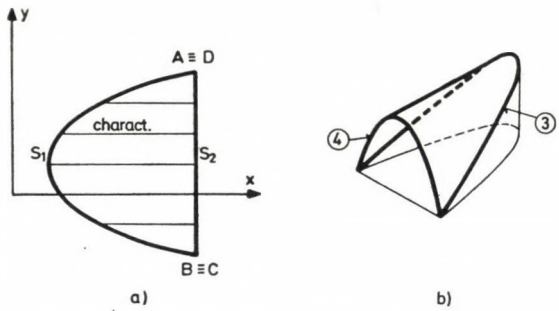

Fig. 10. Cylindrical shell; *a)* ground plan; *b)* axonometric view; ③ edge part with fully supported edge beam; ④ edge part free from shear forces

membrane state if their edges ① and ② are bordered by an annular closed edge beam vertically supported. Now, stress function values on the boundaries have to be specified so as to result in separate plane curves. Cone has, in fact, its lower edge supported, but some vertical forces have also to be applied on the top edge so that the top edge ring be a funicular curve of the applied forces. In an extreme case, the top edge ring may shrink to a point, the cone vertex, provided for by the non-zero determinant under (i) in Chapter 3. For instance, even a cone with a vertical axis over a polygonal ground plan (Fig. 9) may be in membrane state if polygon corners are rounded off, and the closed edge beam is vertically supported. Membrane state of these shells is, in general, not unique, since the boundary conditions involve free constants.

4.2.2. The second boundary-value problem, and the case we studied of *the third boundary-value problem* have no unique solution for closed boundary curves.

4.2.3. Mixed boundary-value problems, in general, have a solution even for closed boundary curves. Let us consider the ground plan of the cylinder in Fig. 5a. Be boundary S_2 fixed, and boundary S_1 assumed to have its end points common with those of S_2 (Fig. 10a), intersected at most once by each characteristic, and be it twice continuously differentiable. Let us prescribe the value of stress function F on curve S_1, and the value of normal derivative $\partial F/\partial x$ on straight line S_2. This problem has a unique solution, since determinant under (ii) of Chapter 3 will be non-zero for any characteristic. Thereby edge S_1 may

be required to have a vertically supported edge beam, edge S_2 to be free from shear forces, and the shell will be in membrane state (Fig. 10b). The membrane state is, however, not unique because of the free constant in the boundary conditions. Uniqueness is only possible if S_1 and S_2 normally join at one of the end points. Otherwise, a non-zero shear force value may be specified on edge S_2.

A similar problem may be stated for a cone shell. Let us consider the cone ground plan in Fig. 6a. Be edge S_2 fixed, and assume edge S_1 to be as before, leading to the ground plan in Fig. 11a. Let us specify the F value on curve S_1, and the value of the linear combination

$$-\frac{\partial F}{\partial n}+\frac{1}{R_2}F$$

on circular arc S_2. Also this problem has a unique solution, determinant under (iv) of Chapter 3 being non-zero for any characteristic, namely now:

$$\alpha_1 = 0\,, \quad \alpha_2 = -1\,, \quad \beta_1 = 1\,, \quad \beta_2 = \frac{1}{R_2}\,, \quad a = a\,, \quad b = R_2$$

and

$$(a-b)\beta_1\beta_2 + \alpha_1\beta_2 - \alpha_2\beta_1 = \frac{a}{R_2}\,.$$

Quotient a/R_2 will be, however, non-zero for any possible a value, hence also for $a = R_2$. Also in this problem, edge beam of S_1 may be required to be vertically supported, and edge S_2 to be free from shear forces (Fig. 11b). Also non-zero shear forces may be specified for edge S_2. Free constant involved in the boundary condition causes as a rule non-uniqueness of the membrane state. Uniqueness is only possible if S_1 and S_2 normally join at one of the end points.

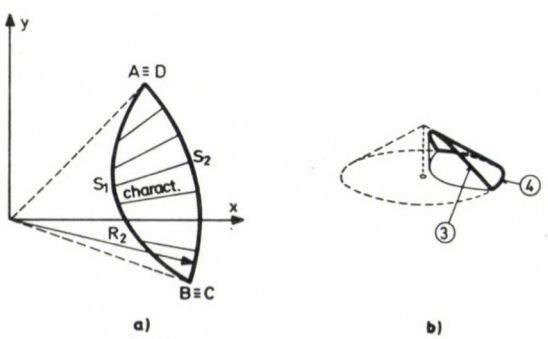

Fig. 11. Cone shell; *a)* ground plan; *b)* axonometric view; ③ edge part with vertically supported edge beam; ④ edge part with no shear forces

Mixed boundary-value problem under 3.4 can be extended to cylinders or cones of closed directrix. Now, actual shell edges $\bar{S}_1$ and $\bar{S}_2$ (curves S_1 and S_2 being projections on the plane xy) have to be twice continuously differentiable closed curves intersected by any asymptotical line at a single point and non tangent to any asymptotical line.

Supplementing the cone ground plan in Fig. 6a to a full circular ring, according to the above and to those under 3.4, cone edge S_1 may be required to be vertically supported, and edge S_2 to be free from shear forces. Namely, determinant under (iv) in Chapter 3 will be R_1/R_2 hence non-zero for any characteristic. It will only be zero for $R_1 = 0$ hence a full rather than a truncated cone. Thus, a full cone over circular ground plan with a vertex having a projection on the ground plan coincident with the centre of the circle and exposed to vertical loads, cannot be kept in equilibrium by normal forces (of generatrix direction) acting on the edge. Equilibrium is known to be possible in that exceptional case if resultant from outer forces passes through the vertex. In this case, however, the problem becomes a statically indeterminate one, the state of equilibrium, i.e. the membrane state of the shell is not a unique one. Unique solution is only possible if both the cone and the outer load, hence also the stress function are rotational symmetric.

REFERENCES

1. CSONKA, P.: Membranschalen. Bauingenieur-Praxis, Heft 16. W. Ernst u. Sohn, Berlin—München 1966
2. CSONKA, P.: Cross Vault Shaped Sectorial Shells with Cantilever-like Overhanging Free Boundary. *Acta Techn. Hung.* **50** (1965), pp. 43—52
3. CZÁCH, L.—SIMON L.: Partial Differential Equations I. Notebook of the Eötvös Loránd University. Tankönyvkiadó, Budapest 1969 (In Hungarian)
4. FRANK, PH.—VON MISES, R.: Die Differential- und Integralgleichungen der Mechanik und Physik. Bd. I. 2. Aufl. Vieweg u. Sohn, Braunschweig 1930
5. FRIEDMAN, A.: Partial Differential Equations of Parabolic Type. Prentice-Hall, INC. Englewood Cliffs., N. J. 1964
6. KOLLÁR, L.: Die dehnunglosen Formänderungen von Schalen. *Konstruktiver Ingenieurbau Berichte.* Ruhr-Universität Bochum. Heft **20** (1974), S., 35—51
7. ПЕТРОВСКИЙ, И. Г.: Лекции об уравнениях с частными производными. Гос. Изд. Физико—Мат. Лит. Москва, 1961 (PETROVSKII, I. G.: Lectures on Partial Differential Equations. Interscience, New York, 1955)
8. ПОНТРЯГИН, Л. С.: Обыкновенные дифференциальные уравнения. Изд. Наука, Москва, 1970.
9. TARNAI, T.: Existence and Uniqueness Criteria of the Membrane State of Shells. I. Hyperbolic Shells. *Acta Techn. Hung.* **91** (1980), pp. 81—110
10. ГОЛЬДЕНВЕЙЗЕР, А. Л.: Теория упругих тонких оболочек. Изд. второе. Изд. Наука, Москва 1976.

Über die Existenz- und Eindeutigkeitsbedingungen des Membranzustandes der Schalen. II. Parabolische Schalen. — In diesem Aufsatz wird die Frage behandelt, welche Stützbedingungen an Rändern einer Schale unter lotrechten Lasten von beliebiger Verteilung vorgeschrieben werden sollen oder dürfen, damit die Schale in statisch bestimmten Membranzustand sei. Der früher erschienene erste Teil dieses Aufsatzes untersuchte die Existenz- und Eindeutigkeitsbedingungen der Lösung der Membranschalengleichung für hyperbolische Schalen. Dieser zweite Teil ist eine Fortsetzung der Untersuchungen an parabolischen Schalen.

Acta Technica Academiae Scientiarum Hungaricae, Tomus 92 (1—2), pp. 89—120 (1981)

NON-TECTONIC SYSTEMS

AN ILLUSTRATED REPORT OF THE LIGHTWEIGHT SILICATE-BASED HEAT STORING BUILDING SYSTEMS*

M. PÁRKÁNYI**
DOCTOR OF TECHN. SCI.

[Manuscript received 1 October, 1978]

Prefatory note

General problems of building in developing countries

Before expounding our proposition for a building technology for mass-housing in subtropical or arid tropical areas it seems important to concentrate here as a preliminary on one topic, that is *the problem of building in developing countries*. This theme has been dealt with many times at different international congresses and symposia. Almost fifteen years ago at a congress in Copenhagen Gunnar MYRDAL in his opening address, entitled "Needs Versus Capacity", wrote as follows: "We need more and better shelter. This is the challenge of humanity to building research and the industry." Then, later he continued: "All this now adds up to an enormous demand for construction, a demand that is constantly rising and tends to overwhelm any rise in building capacity".

These are clear words and nothing can be added to them. As we all know the situation so far in many developing countries has even grown worse and one cannot help feeling a sort of uneasiness, that we may easily witness again to a new decade of frustration.

We think it is an important task of integrated technological, economic and social research to reanalyse in its really complex interdependence the fundamental inner contradiction of building in developing countries, which is very often and misleadingly simplified by the cliché "capital-intensiveness versus labour-intensiveness".

We all know that, considered from the social and economic point of view, the type and extent of building necessary in the developing areas creates a fundamentally new technological problem, a problem really unprecedented

* This report was compiled by the Institute for Building Constructions, Faculty of Architecture, Technical University Budapest on the invitation of the Industrial Operations Division UNIDO Vienna. The theme was elaborated by Mihály PÁRKÁNYI D. Sci. and his co-workers: Dr. L. HAJDU, J. BARCZA, Ms. R. KÖVESDI and L. RAJK. Consultants were Prof. L. GÁBOR academician, A. ZÖLD C. Sc., L. GARAY C. Sci.

**Dr. M. PÁRKÁNYI, Kandó K. u. 6., H—1027 Budapest, Hungary

in history of mankind, the solution of which cannot be directly derived from the experience of developed nations. The recognition of this fact, however, can by no means be equivalent to our accepting the view that traditional methods can show us a way out, it is also not equivalent to accepting the view that technology despite its predominant role in the world of today, is not appropriate to the needs of developing countries. It is our firm conviction that the major breakthrough in mass-production of housing will come from the technological field.

We completely know that research in itself, is not a solution to these problems, and that there is no solution in transplantation of research and technology and existing ready-made solutions from one group of countries to the other, but we definitely doubt the view — proclaimed by so many today — that the adequate housing situation can only and exclusively be solved by an *economic revolution*, firstly because it may transplant the search for a solution into an unknown, perhaps distant future and may tend, as a result of our subsequent frustrations, to a loss of faith in engineering ingenuity, and secondly because we think that the *technological possibilities* in this particular field have not yet been exploited by a long way.

Considerations: Analysis of requirements

The reason why the situation in the field of construction has grown so much worse in course of these years, why the challenge ever since remained an almost insoluble problem, becomes immediately evident if we try to analyse at least the most important requirements to be satisfied by a building technology if it is really supposed to be applicable to conditions in developing areas, both from technological and from social, economic points of view.

From the *technological* point of view, it is extremely important that the technology to be applied, on the one hand, be industrialized to be able to cope with problems of mass-construction; on the other hand, build on the existing foundations; be based on the use of local materials; be adaptable to variable architectural and functional requirements including housing, schools, community centres, industrial workshops etc. in urban and rural areas as well; be applicable to variable geographic and climatic conditions ranging from earthquake safeness up to advantageous building physical properties; in one word: be as open as possible, that is to establish an open system industrialization.

From the *social* point of view, when introducing the technology it is equally important that due attention be paid to the use of relatively unskilled labor, that only a few engineers and technicians be needed; to help the worker to leave the backward world of traditional building thus making new hands get used to machines and acquire the reflexes and mentality, which help them

to enter into the modern world; to stimulate growth of centres other than cities; to create fields where self-help can be applied as one of the means of solving problems of mass-housing on the spot; etc. etc.

From the *economic* point of view, it is almost a precondition that the technology should not be bound to a built out infrastructure, in other words: to avoid requiring huge planted factories; to eliminate the use of heavy transportation facilities, trailers, cranes and other sophisticated equipments; to promote an easy transition from present traditional methods to future mechanization; to stimulate new methods other than concentration for the organization of building activity in developing countries; and, last but not least, to achieve an extremely significant reduction of costs in each individual field starting from investment costs up to the very cost of building, etc.

Conclusion: Outline of problem-solving

To postulate requirements of a building technology is always a relatively "simpler" task, the basic difficulty in technology spells problem-solving, that is to reply the question of how to reach the aim requested, what we have to do to call into being at least the preconditions of the applicability of a building technology. Bearing in mind, that the adaptability of a building technology to developing countries can only be scaled by the degree with which it satisfies the manifold and often contrasting demands enumerated above, we set out from a thorough analysis of the contemporary building technologies. This lead us to interesting results. The analysis of the existing industrialized technologies, namely, clearly proved that there is none among them, which could in itself meet at least the majority of the demands, and this was the reason that called our attention many years ago to looking for *basically new* building methods for solving problems of mass-housing in these areas.

Now, in order to establish a fundamentally new building technology capable of meeting all the requirements, we started out from a fundamental law in technology according to which establishing a real revolutionary, that is qualitative change in technology is always equivalent to creating an *axiomatic change*, which in turn, is characterized by carrying out the principle of doing "*the same thing in a different way*". Thus we knew from the very beginning, that it was not the further development but the transformation of the old, that would characterize the axiomatic change. The Gutenberg typography, the printing from movable types is no more a further development of handwriting as a gun is a further development of the arrow, and — accordingly — the solution we elaborated, *the non-tectonic system*, that is the fundamentally new building method *is not a further development but a transformation of industrialization of building*, as will be expounded and illustrated on the forthcoming pages.

First we introduce in very broad lines the theoretical and scientific foundations of the system (Section 1), this is followed by a brief report on the tests carried out and the results achieved (Section 2), the final section is a summary of the advantages and inherent possibilities of the non-tectonic systems.

Section 1

NON-TECTONIC SYSTEMS

Breaking with Tectonics

TECTONIC STRUCTURES

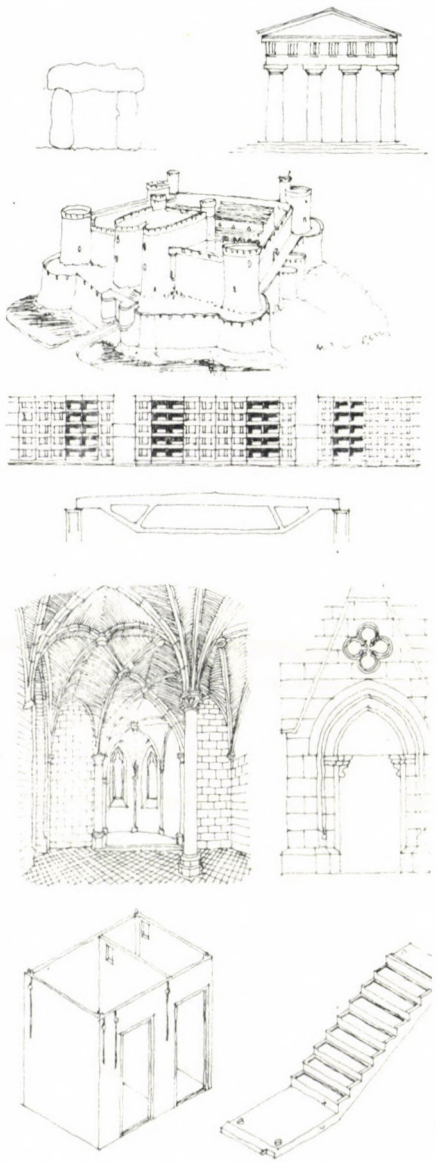

THE PRINCIPLE OF TECTONICS: BUILDING WITH LOADBEARING STRUCTURAL ELEMENTS

As we all know, both traditional and industrialized building as a process is based on the *axiom of tectonics*. This simply means that you first put down an element (i.e. a piece of stone, a manufactured large panel) strong enough to support a load and then you place on it another element (a beam, a manufactured floor slab, etc.) to be supported.

The principle of building with load-bearing structural elements, in other words: the simple principle of putting load-bearing — i.e. *tectonic* — *structural* elements on one another (according to a certain order, of course), this is the essence of every *tectonic* structure, be it traditional or industrialized.

In *traditional tectonic* structures emphasis is on the load-bearing elements and irrespective whether they are finally shaped in form and size (i.e. bricks) or not finally shaped (i.e. pieces of stone) they are always individually workable and have an immediate *load-bearing* capacity, therefore, architectural variability is just boundless (as proven by history of traditional building) because it is created through additivity of individually *workable* tectonic elements.

Manufactured tectonic systems put the emphasis on the usual manufacture of the components of the *load-bearing* structure (such as beams, panels, box-units, etc.) and since all these elements are finally shaped in form and size,

NON-TECTONIC STRUCTURES

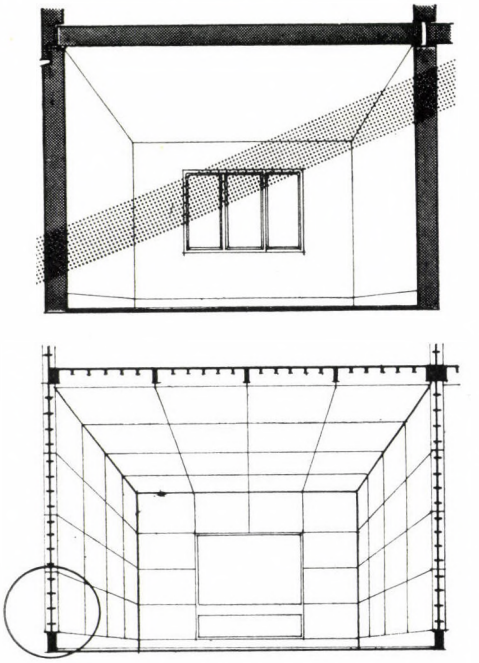

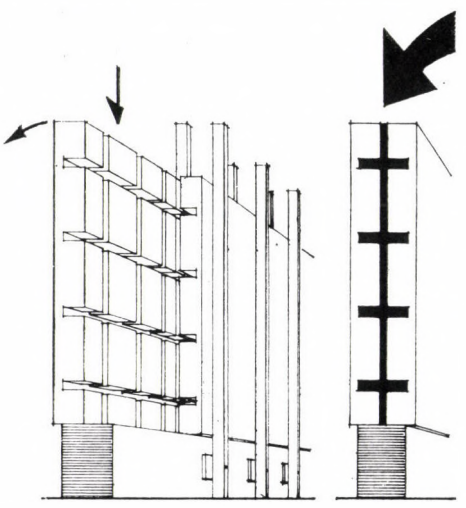

THE PRINCIPLE OF SURFACE:
BUILDING WITH NON-LOADBEARING
SURFACE ELEMENTS

therefore architectural variability is very limited (as proven by practice) because it can only be based on the additivity of individually *unworkable* tectonic building components.

The *non-tectonic* systems break with the axiom of tectonics and substitute it for the *principle of surface*. This simply means that instead of working with structural elements, they work with surface elements.

*

The surface elements of the loadbearing structure are of low specific gravity (they are mostly made of gypsum) consequently they have *no carrying capacity*; they are very thin, after all they are skin construction consequently they have *no immediate stability* either. In brief: they are non-loadbearing, *non-tectonic* elements to be kept in position by simple regainable *auxiliary* structures during concreting.

As a consequence of the moisture absorbing capacity of the gypsum, the concrete — poured into the very thin cavities and channels arising between the surface elements — becomes stabilized almost immediately: if *freezes* on the gypsum.

The new — *non-tectonic* — construction arising as a result of this process is a *light-weight, silicate-based, rigid, monolithic r.c. structure* and as such it is really unique in the industrialized building.

*

The principle of building with non-loadbearing surface elements, in other words: the simple principle of vertical and horizontal alignment of non-loadbearing — i.e. *non-tectonic* — *surface* elements next to one another (according to a certain order, of course) and uniting them into a monolithic structure (through pouring concrete into the cavities and channels arising between, within or on top of these surface elements) — this is the essence of every *non-tectonic* structure, be it done by handicraft forms of production or by any higher level of industrialization.

Changing the principles of design, manufacture and construction

The change-over from the present tectonic structures to non-tectonic systems is a real axiomatic change, which completely transforms each individual principle of design, manufacture and construction, and thereby — as we shall see — it transforms at the same time the very structure of building industry as well.

1. Principles of Design

a. *Some architectural aspects*:
— *the aesthetic neutrality*

THE AESTHETIC NEUTRALITY

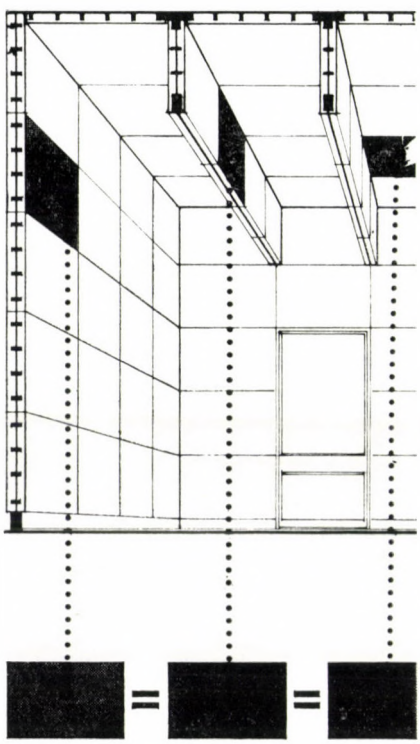

THE NEUTRALITY OF THE SURFACE

The principle of building with non-loadbearing surface elements changes first of all the *architectural* aspect of industrialization of building. The elements of the finished surface, namely are absolutely *neutral* from an aesthetic, architectural point of view. The non-tectonic elements with their glass-smooth surface on their final visible side never "betray" what they are the surface of. You never can tell from this surface, whether it will become a surface of a dwelling, or that of an industrial hall, whether it will become a surface of a wall, or that of a floor, the *surface being the same* in all these cases.

This fact is very important because this kind of *aesthetic* neutrality is extremely favourable from point of view of architectural *design*. The neutrality of the elements, namely, almost "calls" for calling into being real *open systems of construction* and this in turn, is a fundamental *architectural* precondition of *planning for change*.

We have thus seen that in the non-tectonic systems the surface elements are *semantically meaningless* since they are not bound to any particular location in any particular building. This however means that the non-tectonic building method actually transplants the well known *Gutenberg-principle* to the industrialized building.

THE „TYPES"
THE LETTERS OF THE ALPHABET

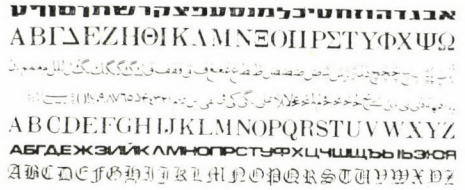

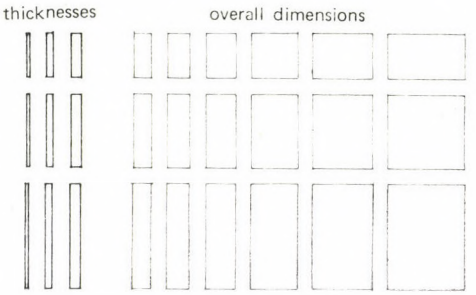

THE NON-TECTONIC BRICKS:
LETTERS OF A STRUCTURAL SYSTEM

— the Gutenberg-principle

Similarly to the *letters* of the phonetic alphabet, or more accurately: similarly to the types of the printed alphabet, which in themselves have no meaning yet allow any kind of texts to be printed;

the surface elements of the non-tectonic system — the so-called non-tectonic bricks — are no structures themselves yet they permit to assemble any kind of buildings.

The *non-tectonic bricks* are actually nothing else but letters of a structural system and, as such, they can equally be used for housing, schools, communal buildings, industrial halls, etc;

REPETITION OF BUILDINGS

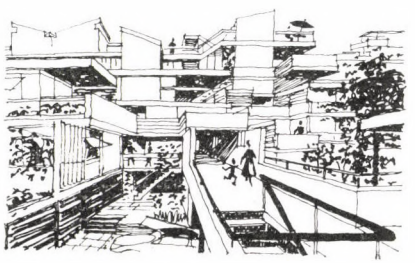

PLANNING FOR CHANGE

— variability versus repetition of buildings

This explains why in the Gutenberg-principled building there is finally no reason for typification of any kind, since instead of aiming at the repetition of *typified* buildings, the non-tectonic systems aim at establishing a real *variability* of final products.

The non-tectonic surface elements with their most variable overall dimensions, forms, thicknesses, etc., which can be used for the most variable kinds of buildings, actually create every architectural precondition of *planning for change.*

b. *Planning for Change*

— *open, light-weight systems versus closed, heavy-weight systems*

Mechanization based building — as it is known — starts out immediately from a definite final product, the building, and breaks it up into large sized, heavy-weight, loadbearing — i.e. *tectonic* — structural elements: the large panels.

MECHANIZATION BASED BUILDING...

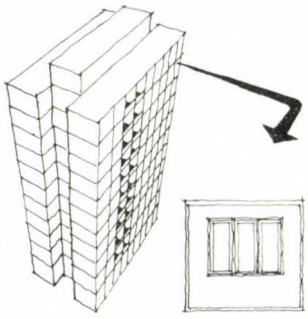

The elementary part — *the large panel* — is actually nothing else than a large sized *manufactured tectonic brick* but as such, it is *not neutral* from an architectural point of view. On the contrary, it is *semantically meaningful* since — as opposed to the traditional brick — it is not only a part of a building, but a *determined part of a determined building*, consequently it definitely influences the final shape of the building.

Systems of tectonic bricks inevitably create *closed, heavy-weight* systems, since the large size *structural* elements they work with, are definitely bound to determined location in determined buildings.

This, however, does not apply to the Gutenberg-principled building.

Gutenberg-principled building starts out from an undetermined final product, more accurately: it starts out from the surface of undetermined buildings and breaks up this surface into medium size, light-weight, non-loadbearing — i.e. *non-tectonic* — elements. The Gutenberg-principled building conceives the surface as a mould, that is the negative of the final loadbearing structure.

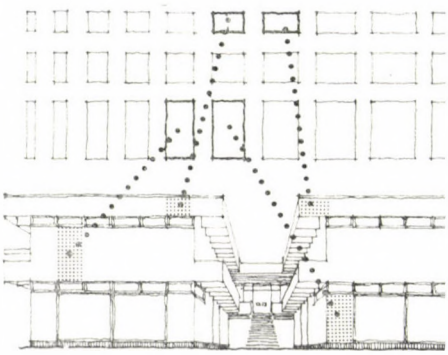

...GUTENBERG-PRINCIPLED BUILDING

The elementary part — *the surface element* — is a simple skin construction a lost casing element in gypsum. It is actually nothing else than a *manufactured non-tectonic brick* and as such it is really *neutral* from an architectural point of view, since — similarly to the traditional brick — it is *semantically meaningless*. It is really only a part of a building, more accurately: it is only an *undetermined part of an undetermined building*, consequently it does not influence the final shape of the building.

Systems of non-tectonic bricks inevitably call into being *open, light-weight* systems since the medium size *surface* elements they work with, are definitely not bound to any determined location in any determined building.

Gutenberg-principled building aims at *planning for change.*

MECHANIZATION BASED BUILDING:
THE HOUSING FACTORIES
„SEE" THE FINAL PRODUCT

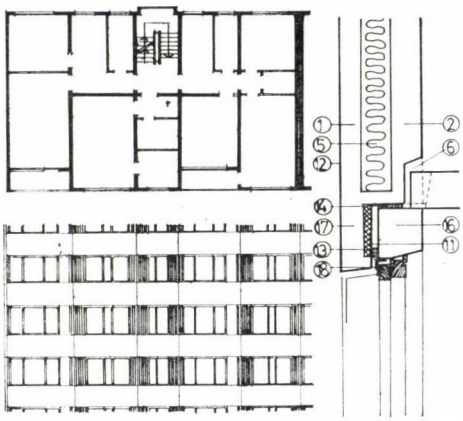

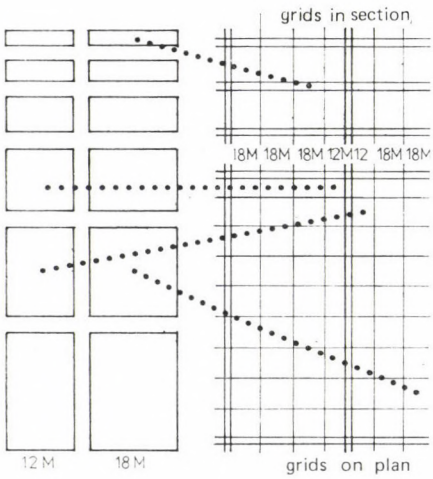

GUTENBERG-PRINCIPLED BUILDING:
THE FACTORIES DO NOT SEE THE FINAL
PRODUCT, THE MANUFACTURE IS BLIND

2. Principles of Manufacture

a. "*Blind manufacture*"

— *an approach to producing light-weight, silicate-based open systems*

Breaking with the axiom of tectonics and substituting it for the principle of surface, completely changes the principle of manufacture as well.

Mechanization based building — as we have seen — operates with closed systems of heavy *tectonic* bricks. You can not start, however, the *manufacture* of these large elements unless you *see* the completed whole, that is the building to be erected, know the ground plans, sections with all their least details. The housing factories have to see the final product, since otherwise the large size tectonic elements (these determined *structural* elements to determined locations in determined buildings) wouldn't match and so they could not fit into the building. As opposed to this:

The Gutenberg-principled building operates with open systems of light-weight *non-tectonic* bricks. Here the building is undetermined and so the knowledge of the final product is not a precondition of *manufacture*. All you have to know is the system of grids on plan and in section, since the non-tectonic elements (these undetermined *surface* elements to undetermined locations in undetermined buildings) will fit into that grid system anyway. The factories do not have to see the final product.

This type of manufacture, however, is of a completely different character. It is *blind manufacture*.

MANUFACTURE OF LOADBEARING ELEMENTS...

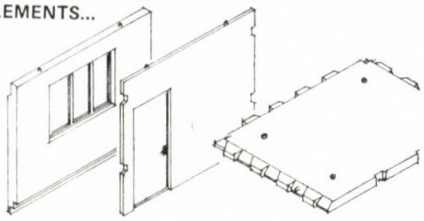

...VERSUS...

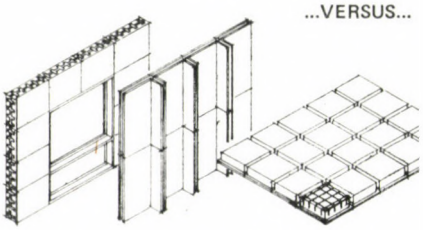

...MANUFACTURE OF SURFACE

Blind manufacture is a fundamentally new approach to mass-producing light-weight, silicate-based, open systems of construction.

As opposed to any other manufactured *tectonic* system, in which the emphasis is always put on the manufacture of the components of the *load-bearing structure*;

the *non-tectonic* system puts the emphasis of manufacture on the surface, that is on the manufacture of the non-loadbearing surface elements and instead of manufacturing heavy, load-bearing, tectonic beams, wall or floor elements, etc. light, *non-loadbearing* non-tectonic *surfaces* of beams, walls, floors etc. are mass-produced.

— *a technological aspect:*
the neutrality of the machine

THE TECHNOLOGICAL NEUTRALITY

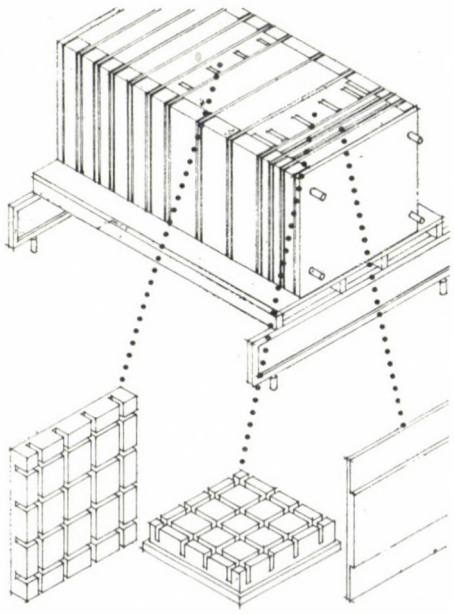

THE NEUTRALITY OF THE MACHINE

The principle of building with non-loadbearing surface of beam, wall or floor elements completely changes the *technological* aspect of industrialization as well. These elements, namely, are absolutely *neutral* from a technological point of view: they do not require specific apparatuses for beams, walls, floors, they can be produced by the same convertible machine, the final visible *surface being the same* in all the cases.

This fact is very important because this kind of *technological* neutrality, the neutrality of the machine is very favourable from point of view of *mass-production* of surface elements, it almost calls for *open system industrialization* which in turn, is the technological precondition of *producing for change.*

ARCHITECTURAL VARIABILITY
IN MECHANIZATION BASED BUILDING:
REPETITION OF THE FINAL PRODUCT

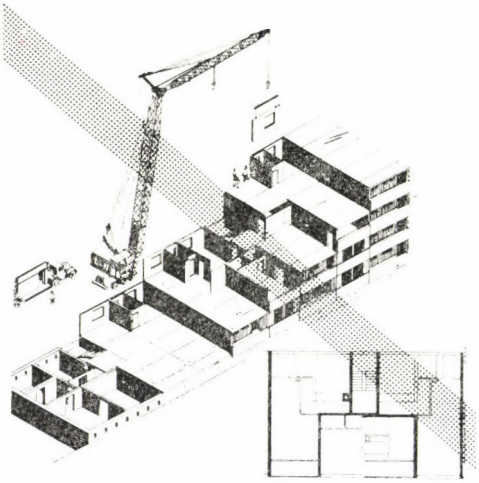

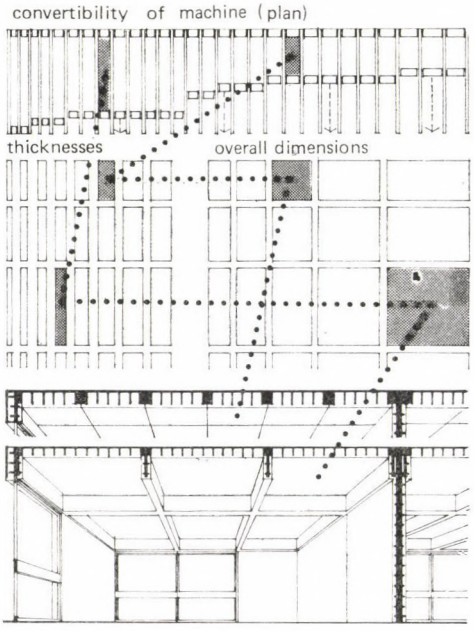

ARCHITECTURAL VARIABILITY IN
GUTENBERG-PRINCIPLED BUILDING:
PRODUCING FOR CHANGE

b. *Producing for Change*
— *workability of structure and convertibility of machine*

Now, in order to be able to make the non-tectonic surface elements fit into the modular grid system of any undetermined building at all events — blind manufacture combines the shaping of the building, or rather, the workability of the structure (which is a precondition of planning for change) with the convertibility of the machine (which, in turn, is a precondition of producing for change).

Whereas in any mechanization based tectonic system, the shaping of the building, that is, the architectural variability is necessarily limited since it can only be based on the additivity of heavy, tectonic structural elements finally shaped in form and size, as shown by figure above;

the Gutenberg-principled building offers practically unrivalled possibilities to increase architectural variability.

In the non-tectonic systems the shaping of the building, that is, architectural variability is practically unlimited, first: because it is based on the additivity of light-weight non-tectonic surface elements, second: because in the non-tectonic systems the surface elements themselves become variable: in blind manufacture the variability of the elements is based on the convertibility of the machines, and thereby the sizes and forms selectable for the elements may reach a maximum.

Architectural variability in the non-tectonic systems is founded on a simultaneous workability of the structure and convertibility of the machine.

— *transplantable workshops versus planted factories; decentralization versus concentration of building industry*

Blind manufacture, this new approach to open system industrialization completely transforms finally the very structure of building industry both from technological and from socio-economic points of view.

MECHANIZATION BASED BUILDING MANUFACTURES IN PLANTED FACTORIES AND TENDS TOWARDS CONCENTRATION OF INDUSTRY

GUTENBERG-PRINCIPLED BUILDING MANUFACTURES IN TRANSPLANTABLE WORKSHOPS AND TENDS TOWARDS DECENTRALIZATION OF INDUSTRY

As opposed to *mechanization based building* in which the mechanized production of heavy structural elements requires huge *planted factories* established at enormous costs and which therefore, aims at the *concentration* of building industry mainly around urban areas;

the *Gutenberg-principled building* aims at *decentralization.* The blind manufacture of the light-weight surface elements, namely is founded on a system of *transplantable workshops.* These elementary factories can be scattered throughout the country, require low investment costs, work with cheap, small, convertible, transportable and transplantable manufacturing apparatuses which can be operated even by unskilled workers.

3, Principles of Construction

„BEAM LONGER THAN SPAN"

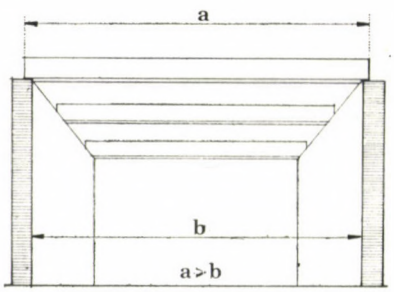

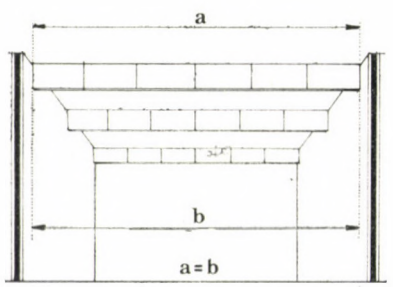

„SPAN EQUALS BEAMLENGTH"

a. *Unique features of non-tectonic structures*

The simple fact that in the non-tectonic systems the vertically and horizontally aligned surface elements (which have no carrying capacity and no immediate stability) are always put next to one another (and not on top of each other) renders the non-tectonic structures quite a series of unique features. Here are some:

— "*span equals beamlength*"

As opposed to tectonic structures, where the length of the horizontal structural element — i.e. the length of a beam — is always longer than the span (otherwise it could not be supported),

in the non-tectonic structures "span equals beamlength" since we work with the surface of the loadbearing structure;

TECTONIC JUNCTION

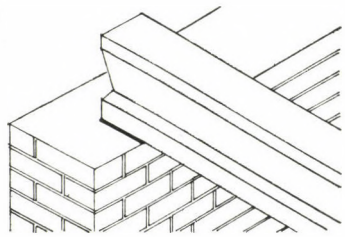

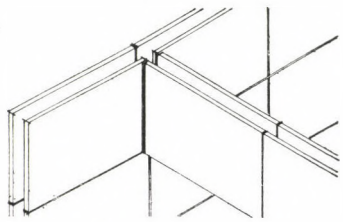

NON-TECTONIC JUNCTION

— *non-tectonic junctions*

Tectonic junctions spell vertical ("on top of") connection between superimposed loadbearing structural elements. This kind of "load-supporting-load-transferring" junction can not arise in the non-tectonic systems, where we work with the surface of the structure.

Non-tectonic junctions spell horizontal ("next to") connection between the vertically aligned and horizontally aligned surface elements, as schematically shown by figure.

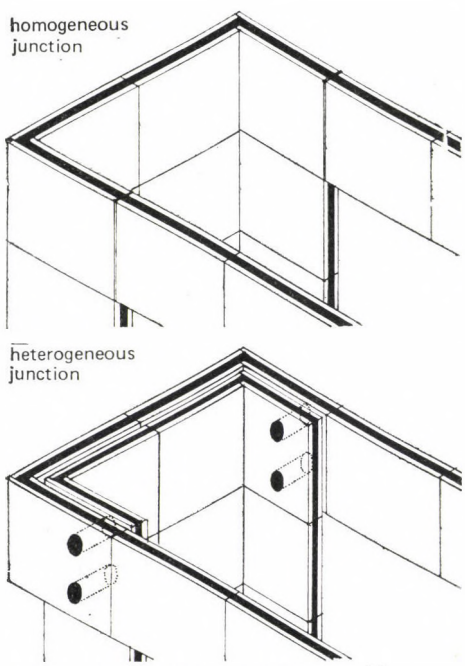

TWO BASIC TYPES OF NON-TECTONIC JUNCTIONS

— *two basic types of non-tectonic junctions*

Homogeneous junction: that is a monolithic reinforced concrete junction created by pouring concrete into the cavities or channels arising between the aligned surface elements.

Heterogeneous junction created by steel jointing points used for creating structural connection between the adjacent vertical and horizontal monolithic reinforced concrete structures, as schematically shown by figure.

CREATING MONOLITHIC STRUCTURE THROUGH THE ADDITIVITY OF SURFACE ELEMENTS

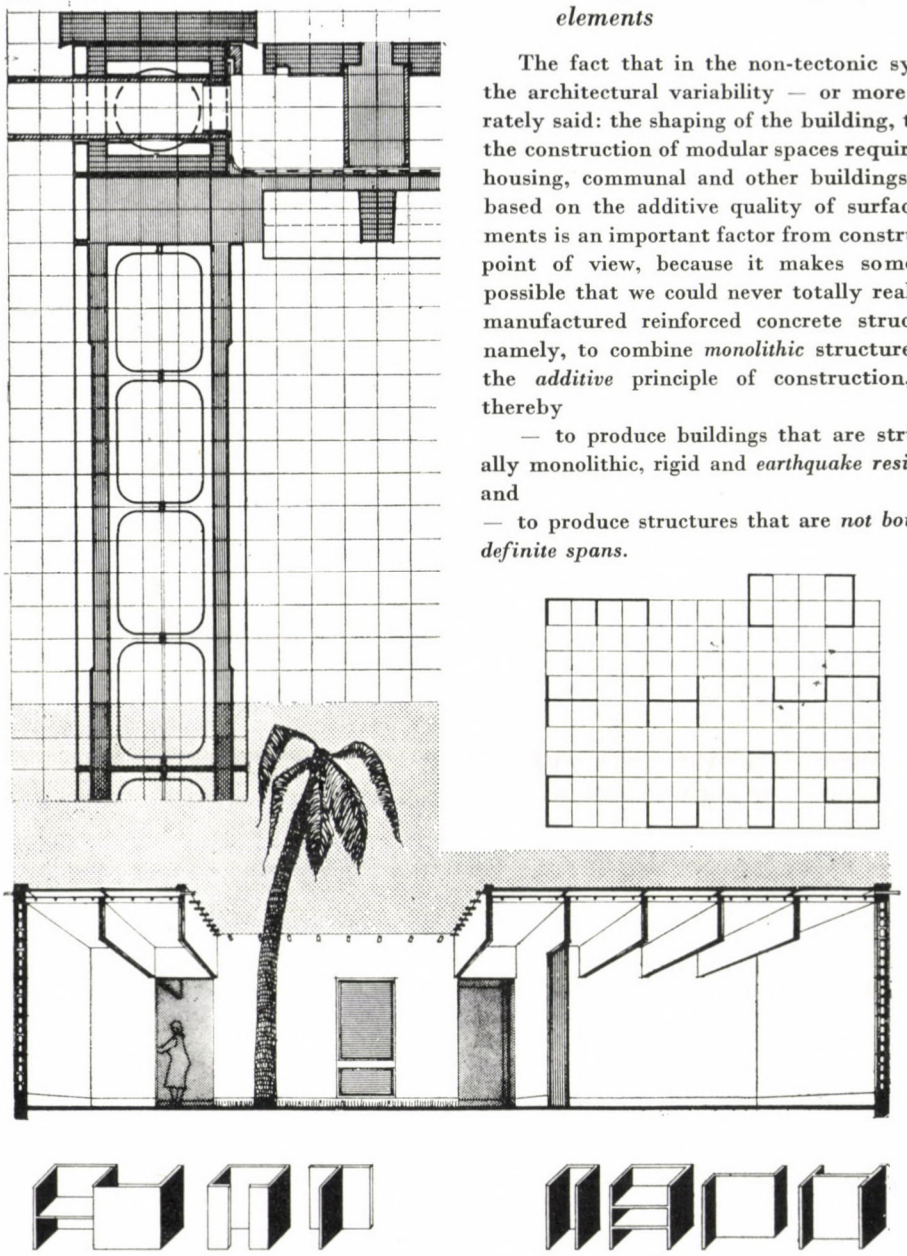

— *creating monolithic structure through the additivity of surface elements*

The fact that in the non-tectonic systems the architectural variability — or more accurately said: the shaping of the building, that is the construction of modular spaces required for housing, communal and other buildings — is based on the additive quality of surface elements is an important factor from construction point of view, because it makes something possible that we could never totally realize in manufactured reinforced concrete structures, namely, to combine *monolithic* structure with the *additive* principle of construction, and thereby

— to produce buildings that are structurally monolithic, rigid and *earthquake resistant;* and

— to produce structures that are *not bound to definite spans.*

MANUFACTURED TECTONIC STRUCTURES ARE BOUND TO DEFINITE SPANS

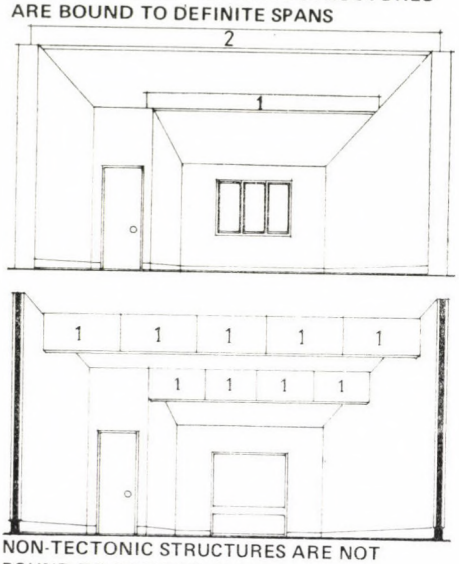

NON-TECTONIC STRUCTURES ARE NOT BOUND TO DEFINITE SPANS: „SPAN-INDIFFERENT" STRUCTURES

— *"span-indifferent" structures*

Whereas in the tectonic systems the manufactured horizontal, loadbearing reinforced concrete structural elements are unambiguously bound to determined spans;

the non-tectonic structures are "span-indifferent"; by keeping the surface elements of the horizontal loadbearing structure below parameter size, the non-tectonic systems make the span relatively independent of the structure, the span, namely, is not a question of manufacture but of the additivity of surface elements. Instead of manufacturing one large beam, or floorslab, the non-tectonic systems achieve the same by the alignment of mediumsize surface elements.

TRADITIONAL FORMWORK RESISTS HYDROSTATIC PRESSURE

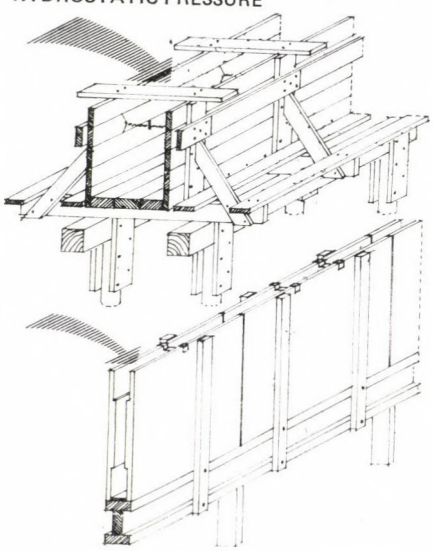

GYPSUM ELEMENTS ELIMINATE HYDROSTATIC PRESSURE: FROZEN REINFORCED CONCRETE STRUCTURES

— *frozen reinforced concrete structures*

As opposed to traditional r.c. structures where the formwork has to resist enormous side pressure, in the non-tectonic system the hydrostatic pressure of the concrete can be totally eliminated if properly chosen concrete is poured in between properly formed gypsum layers.

Gypsum by its pourability, porosity, low specific gravity, cheapness and availability has really unrivalled endowments.

The arising new constructions, the *frozen r.c. structures* are very thin membranes, they combine the highest structural qualities with an utmost reduction of weight of structure thro' reduction in material. Their application for mass-housing is seemingly very promising.

CREATING REFERENCE BETWEEN STRUCTURAL THICKNESSES AND PARAMETERS

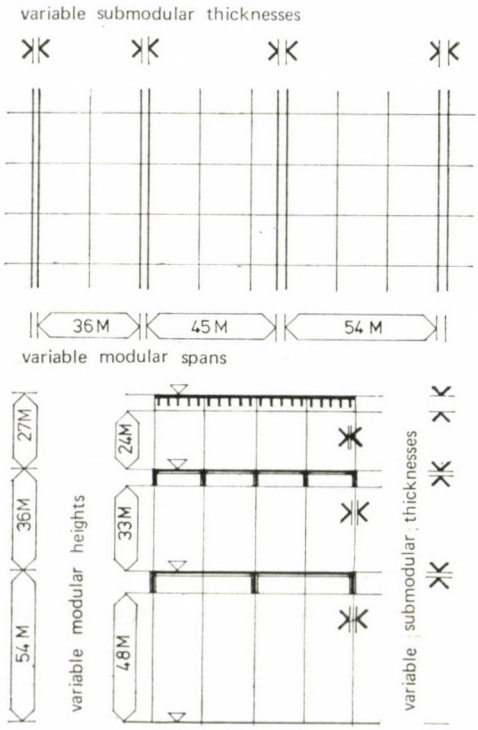

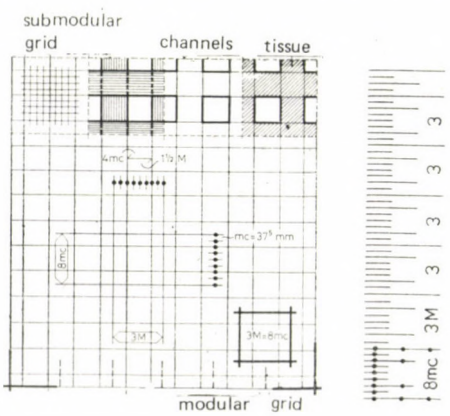

DOUBLE CO-ORDINATED STRUCTURES

— *creating reference between submodular structural thicknesses and modular structural parameters*

Now, in order to be able to combine workability of structure (a precondition of planning for change) with the convertibility of machine (in turn, a precondition of producing for change) the non-tectonic systems relate the variable *modular parameters* (spans, heights etc.) to the variable *submodular thicknesses* (structural thicknesses, thicknesses of elements, etc.) and thereby the non-tectonic systems establish

on the one hand a *modular* reference between the *elements* and the *modular (parameter) grids* on the building site, and

on the other hand a *submodular* reference between the *thicknesses* and the *submodular (micro) grid* built into the manufacturing apparatus.

The ratio of modular to submodular grids can be expressed in a simple mathematical form. This *formula of double-coordination* in our case is 3 M = 8 mc as symbolically illustrated by the figure. This formula means that 3 basic module grid units (M = module = 10 cm) within the structural system correspond to 8 micro grid units (mc = microcell = 37,5 mm) within the manufacturing apparatus.

Through this unique double-reference system, which cannot be realized in silicate-based manufactured, closed, tectonic systems, we realize an *optimum structural engineering performance* in which the variable loads and all the variable modular and submodular dimensions of the loadbearing, frozen reinforced concrete structure are strictly related to one another.

THERMAL STABILIZATION AND HEAT CONTROL OF BUILDINGS

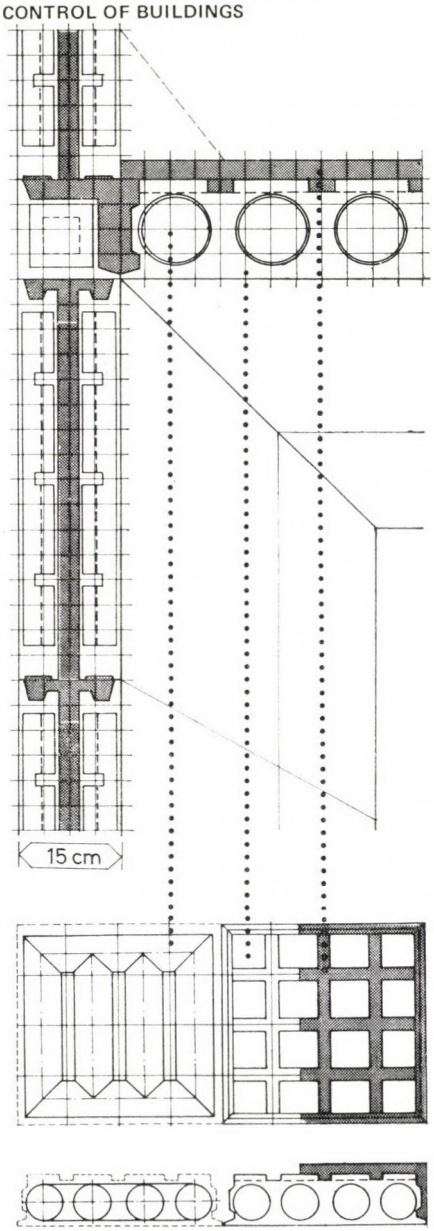

LIGHT-WEIGHT, SILICATE-BASED HEAT-STORING STRUCTURES

— *light-weight, silicate-based, heat-storing prefabrication systems*

Last but not least: if the buildings require thermal stabilization, then the non-tectonic systems may incorporate proper equipments, that is: sealed registers containing a phase change material (PCM) into the surface elements themselves and thereby they call into being heat-storing prefabrication systems without giving up any principle of design, manufacture and construction.

By increasing the heat-storing capacity of the light-weight construction practically without increasing its weight it becomes possible to decrease the heating and/or cooling load and thereby to reduce prime, energy and running costs.

The media for heat-storage are phase-change materials (PCMs). The temperature level at which heat can and has to be stored can be chosen according to actual conditions.

The PCMs have a high specific heat capacity and low vapour pressure. They are non-corrosive, non-toxic, inflammable, chemically inert and stable, there is no danger of fracturing their container.

The built-in, sealed registers are plastic tubes or specific reservoirs made by polimerization.

By the use of the heat-stabilizing equipment built into the structure and operated on a physico-chemical method, the light-weight, silicate-based constructions can be rendered almost equivalent to heavy-weight constructions from point of view of building physics by storing solar heat gain in the phase change material.

TRANSLATION OF THE LANGUAGE OF STEEL STRUCTURES TO THE LANGUAGE OF REINFORCED CONCRETE STRUCTURES

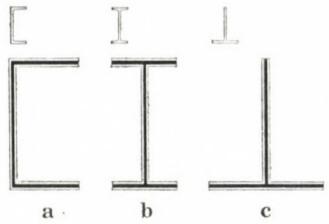

— *the translation of the language of steel structures to the language of reinforced concrete structures*

According to the general theory of technology, each technology can be conceived as a particular *language* which can be translated to the language of other technologies. The non-tectonic building method was conceived as a translation of the language of steel structures to the language of reinforced concrete structures.

Starting out from this consideration the non-tectonic systems transform the traditional reinforced concrete structures in such a way, that

firstly: they translate the well-known *forms* (profiles, sections etc.) so well proved in steel structures into the language of reinforced concrete structures by switching over from the traditional r.c. structures to the r.c. *folded shell* constructions (as schematically shown by figures a, b, c and further expounded on page to follow);

secondly: they translate the well-known methods of *jointing* so well proved in steel structures (d. riveting; e. welding) into the language of the reinforced concrete *tissue* (f.).

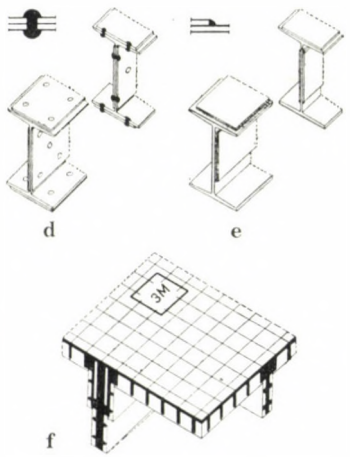

SWITCHING OVER FROM THE TRADITIONAL REINFORCED CONCRETE STRUCTURES TO THE MODERN FOLDED SHELL AND TISSUE CONSTRUCTIONS

This translation, this transformation of the traditional reinforced concrete technology — this is finally the characteristic feature of the frozen reinforced concrete constructions.

TRADITIONAL R.C. STRUCTURES

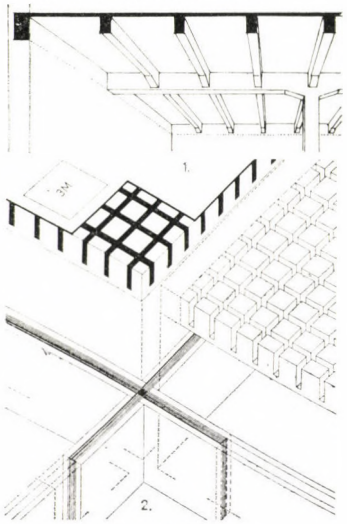

FROZEN R.C. STRUCTURES

b. *Two basic types of frozen reinforced concrete structures — the folded shell and the tissue*

As opposed to *traditional* r.c. structures representing the homogeneous, isotropic, monolithic constructions, the *frozen* r.c. constructions created by the non-tectonic systems are inhomogeneous, anisotropic, monolithic constructions. They are

inhomogeneous, in so far as the final structure is composed mostly of two materials (reinforced concrete stabilized between, within or on top of surface elements of low specific gravity);

anisotropic, since the physical property of the final r.c. structure varies with the direction in the body;

monolithic, because the additivity of surface elements leads to creating continuous structures.

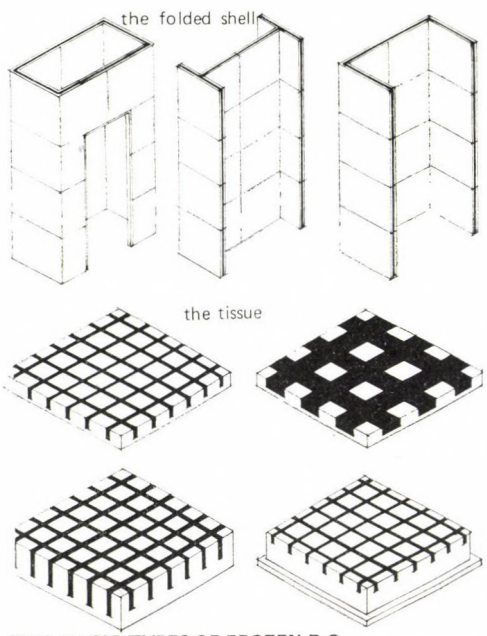

TWO BASIC TYPES OF FROZEN R.C. STRUCTURES

Frozen reinforced concrete structures have two basic types:

The *folded shell*: the reinforced concrete visible *primary structure* — or, rather, cellular structure — stabilized between the surface elements. Its form is that of a closed or open steel section (I; T; U-profiles) or, rather, of a cardboard carton with reinforcement led around the corners. The frozen shell is, namely, a thin folded r.c. membrane.

The *tissue*: the hidden reinforced concrete *microstructure* — or, rather, microcellular structure — stabilized within the two-way channel system of the surface elements always appearing in the form of a r.c. grid reminding on the form of tissue of a woven cloth. Hence its name.

TECTONIC STRUCTURES

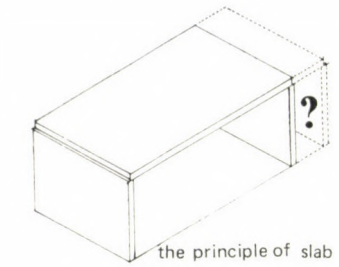

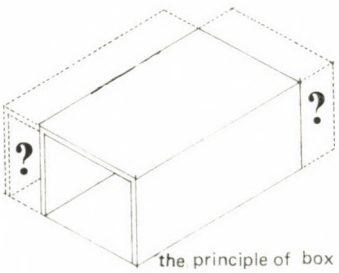

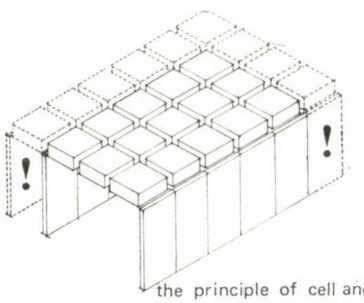

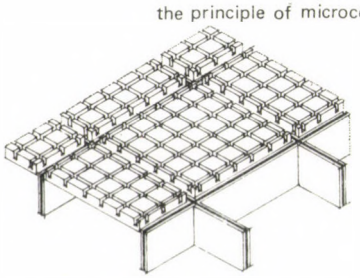

TWO BASIC PRINCIPLES OF FROZEN REINFORCED CONCRETE STRUCTURES

c. *Two basic principles of frozen reinforced concrete structures — the principle of cell and the principle of microcell*

In order to be able to satisfy all possible (architectural, functional, technological, socio-economic etc.) demands the non-tectonic systems definitely aim at enormously increasing the number of variations not only on plan and in section but in the very form of construction as well.

Since the analysis of the large panel systems clearly shows, that the inevitable tendency towards increasing the span is incompatible with maintaining the *slab* as principle of construction; and

since the analysis of heavy, space-unit building method clearly shows, that the tendency towards increasing the sizes of the parameters runs counter the *box* as principle of construction.

Therefore: the non-tectonic systems give up the idea of working either with the slab, or with the box as principles of construction and as opposed to these characteristic principles of contemporary, manufactured, silicate-based, heavy, closed systems, they introduce

first: working with the *cell* as principle of construction for the frozen, reinforced concrete *primary structure* (which means the use of many different forms of the *folded shells)*;

then: working with the *microcell* as principle of construction for the frozen reinforced concrete *microstructure* (which, in turn, means the use of many different forms of *tissue-structures*).

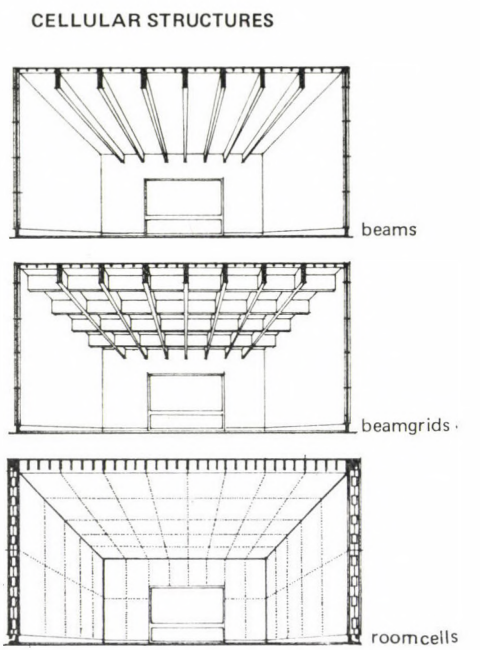

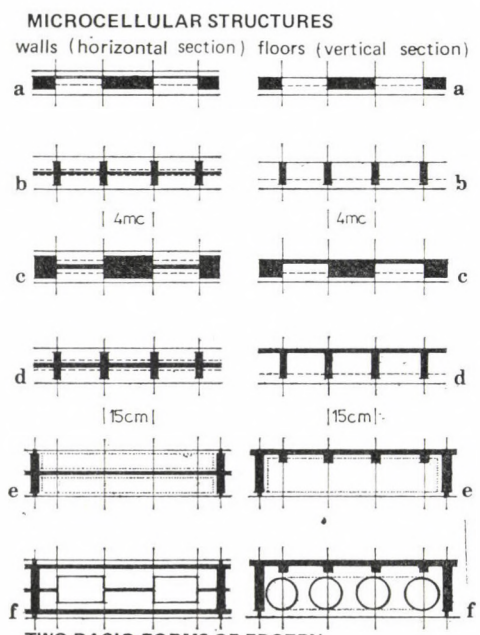

TWO BASIC FORMS OF FROZEN REINFORCED CONCRETE STRUCTURES

d. *Two basic forms of frozen reinforced concrete structures — the cellular and the microcellular systems*

The two basic forms of frozen reinforced concrete structures — the cellular and microcellular systems — which mostly arise as a combination of some form of r.c. folded shell and r.c. tissue, offer a very wide range for satisfying different requirements by rendering it possible to select quite a series of different structural solutions for the same plans, functional arrangements, etc.

Cellular systems may operate with beams, beamgrids, or with the room units (room-cells) themselves. These forms represent the visible forms of non-tectonic structures.

The thin and delicate *microcellular* structures — irrespective whether they are used for walls or floors, or whether they are made of r.c. tissue, or of a combination of r.c. tissue and r.c. shell always remain hidden behind the surface.

In case of *walls* e.g. we may use tissue exclusively, the tissue can be "loose" or "dense" (*a*, *b*), or combinations of tissue and shell (*c*, *d*) combinations of ribs, hidden beams or beamgrids with shell (e), or combinations of ribs and double shell (f) etc.

In case of *floors* e.g. if the cellular system works with beams or beamgrids we may again use r.c. tissue (a, b), combinations of tissue and shell (c, d), if room-cells are applied then we may again use e.g. combinations of ribs, tissue and shell (e,.f), the heat-stabilizing equipments in this case may be hidden within the surface elements (f), etc. etc.

„LIFTING" METHODS

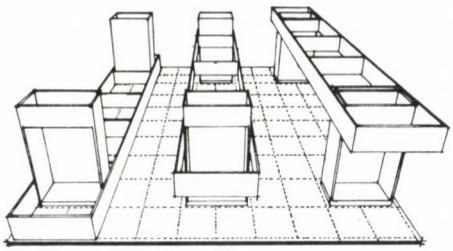

„lift-grid"

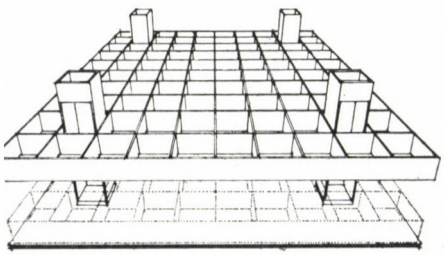

„lift-field"

„IN-SITU" METHODS

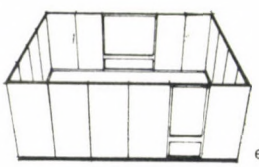

erection of walls

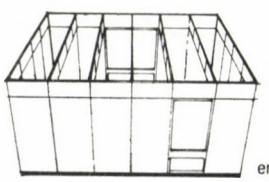

erection of beams

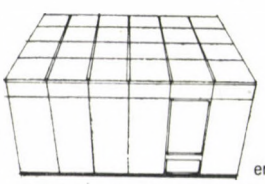

erection of floors

TWO BASIC METHODS OF NON-TECTONIC BUILDING

e. *Two basic methods of non-tectonic building*
— *the lifting and the in-situ building methods*

Non-tectonic systems may apply two basic types of building methods.

In case of the so-called *lifting methods* the horizontal load-bearing structure — e.g. the beam-grid — is built exactly underneath the final "in-situ" position and it can be lifted into final position even by hand, through mechanical transmission. No cranes are used. The lifting apparatuses integrated with the vertical load-bearing structure are always mounted on top of the folded shell walls or pillars.

If the horizontal load-bearing structure is built and lifted in parts, then the method is called "*lift-grid*", if it is built and lifted at one go, the method is called "*lift-field*".

In case of the "*in-situ*" building methods the chronological and logical order of the building process itself corresponds to that of mechanization based tectonic building, in so far as the building is erected "from below upwards", each structure is built in its final position, floors following the erection of walls and the process is repetitive.

The individual technological cycles of the non-tectonic building process, however, are completely different, the sequence of operations, the junctions and consequently all the details follow the non-tectonic principle as we shall see. Heavy, sophisticated equipments of transportation and hoisting are completely eliminated, heavy scaffolding is not used either.

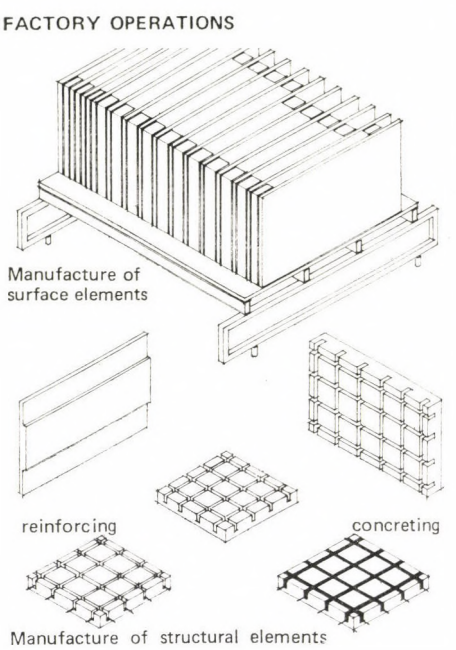

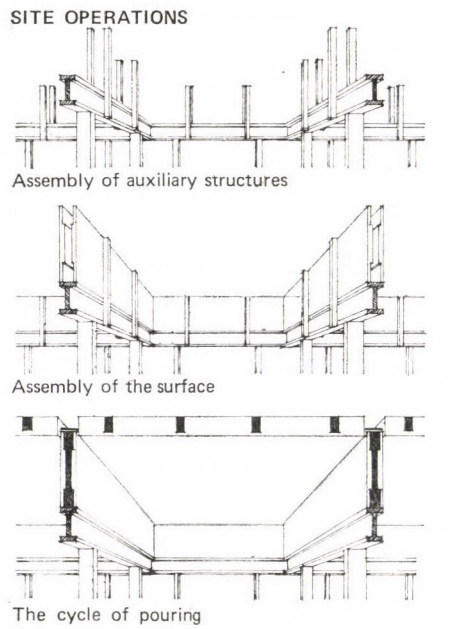

THE PROCESS OF NON-TECTONIC BUILDING

f. *The process of non-tectonic building — establishment of a complementary building method*

In non-tectonic systems, building is a complementary process that is a process combining the *factory* production of surface elements with an *in-situ* technology of pouring. In very broad lines:

In the factory there are two basic operations:

Manufacture of surface elements; whereby we actually produce the total system of non-tectonic bricks.

Manufacture of structural elements; in this operation reinforcement is located with in the channels of the surface elements and then the channels are poured out to create the microstructure, that is the structural tissue within the elements.

On the site there are three basic operations:

Assembly of auxiliary structures; to keep the surface elements (which in themselves have no carrying capacity and no stability) in position during concreting.

Assembly of the surface; whereby we actually create the negative of the load-bearing structure through the vertical and horizontal alignment of the non-tectonic surface elements, and finally:

The cycle of pouring; whereby we actually unite the aligned surface elements by the reinforced concrete primary structure poured in between, within, or top of the surface elements.

Section 2.

EXPERIMENTAL STRUCTURAL UNIT

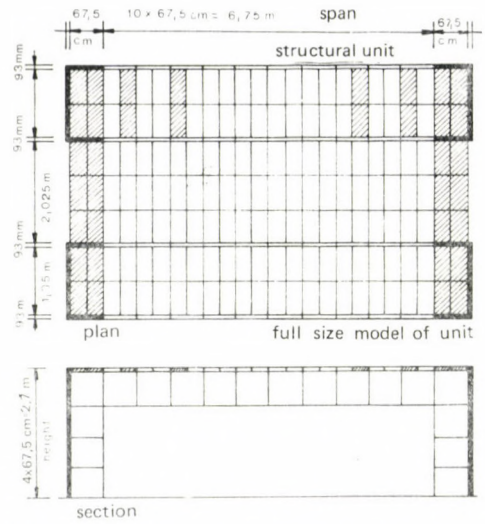

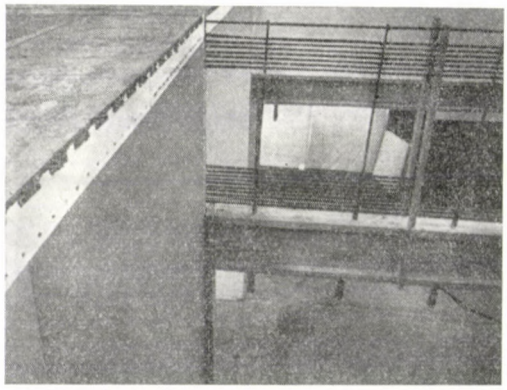

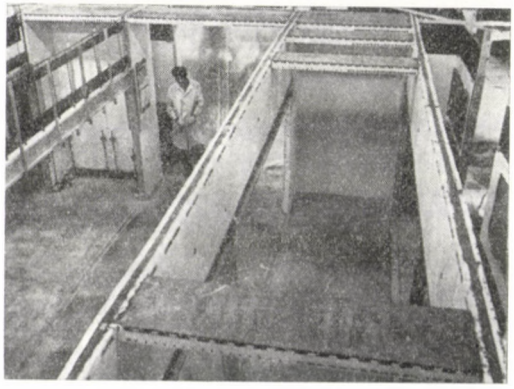

THE TEST-UNITS AND BUILDINGS

In course of our research work five experimental programs have been completed. This section gives a very condensed report on the tests carried out and the results achieved.

1. Experimental structural unit

The first test, an experimental structural unit realized on laboratory level is first of all destined to give a clear indication of how non-tectonic systems can be conceived. The emphasis of the experiments therefore was laid on showing the principles of design, manufacture and assembly.

In order to show both the structural system and the process of construction the test-unit is divided in two parts the one is the very system, the second part is built in a full size model directly exhibiting the interior structure as shown by the figures and photos.

The structural unit itself is composed of very thin U-shaped reinforced concrete folded shell wall-pillars, r.c. shell beams and tissue structural floors.

The best succeeded in proving that the non-tectonic systems may reduce the weight of structure extremely significantly and that today they represent the *lightest weight structures which can be realized on the silicate basis.*

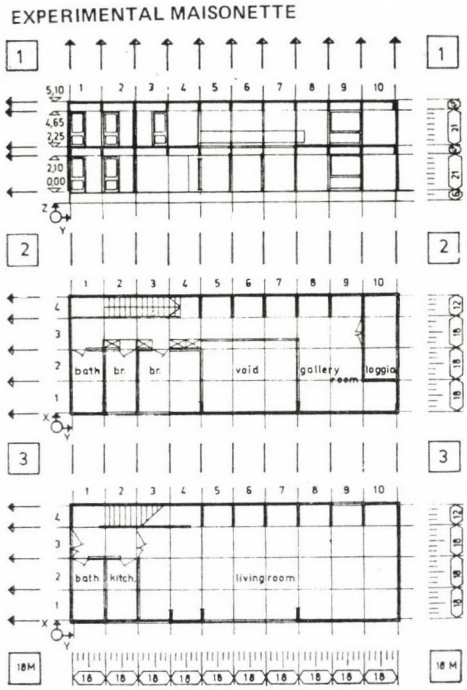

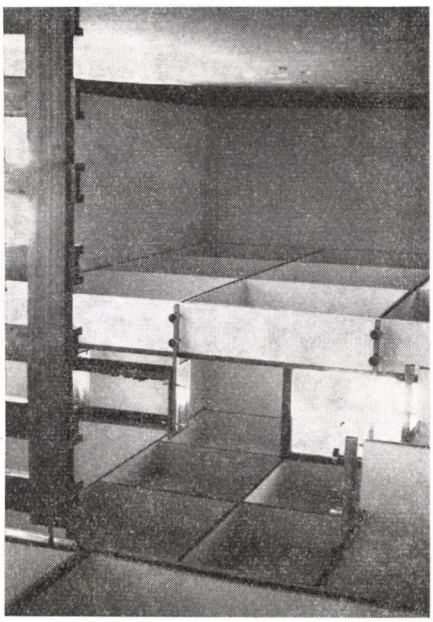

2. Experimental non-tectonic maisonette

The test building is a one family house, an experimental maisonette in non-tectonic construction having a total area of 219,68 m^2 and a total volume of 605,88 m^3.

The test building was first of all destined to give a proof of the universality of the open, non-tectonic structural system, so we elaborated an architectural and technological variation on a system of non-tectonic bricks. The product — the experimental maisonette — goes far beyond illustrating a structural principle since it clearly proves that the non-tectonic structures may open a possible way towards open-system industrialization in building.

In order to prove simultaneously the openness and universality of the structure and the architectural and technological efficiency of the non-tectonic systems, the test building — that is the maisonette containing one two-level dwelling — was designed to include at least one example for every essential structural detail occurring in a residential unit. According to this, simple and composed spaces, stiffened and unstiffened walls, intermediate and top floors, smaller and longer spans beam-grids and beam-walls, profile principled walls and slab principled walls, smaller and bigger heights, cantilever and loggia structures can equally be found in the building.

The test succeeded in proving, that the non-tectonic system is an *open system* in which function, formation of buildings can be freely chosen since all characteristic dimensions including spans, heights, thicknesses can be absolutely variable.

„LIFT-FIELD" EXPERIMENTAL HALL

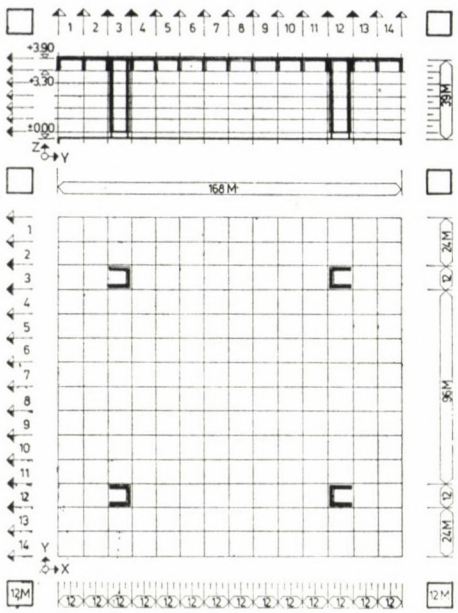

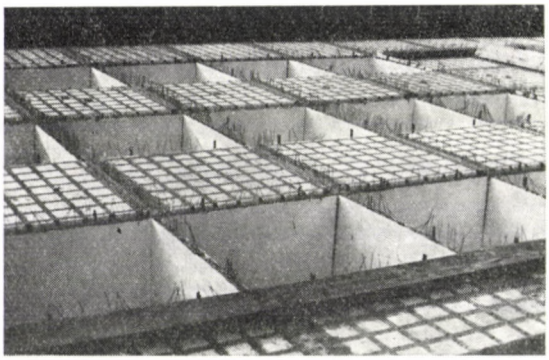

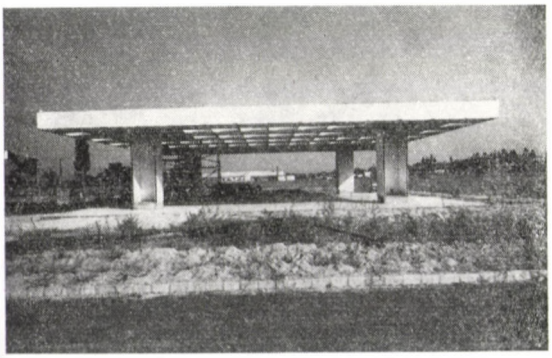

3. *"Lift-field" experimental non-tectonic hall*

The test building — the "lift-field" experimental hall — is an undivided large space, a self-contained structural unit, a non-tectonic cellular construction of a total area of 284 m² and a total volume of 1108 m³.

The project was primarily intended to give a simultaneous proof of the relative span-indifference in two directions of cellular systems, and of the feasibility of the "lift-field"-method.

By creating a beam grid structure with large spans and cantilevers in two directions it has been proven that cellular systems built underneath final position can be lifted into final position even by hand, through mechanical transmission.

The structural and technological concept was embodied in a single-storey structure an undivided large space realized on semi-workshop level. The vertical load-bearing structure consists of four U-shaped r.c. folded shell pillars built in situ, whereas the horizontal one of a single, large-size r.c. frozen shell beam-grid with large span and cantilevers in two direction built underneath final position, lifted gradually by hand with lifting mechanisms mounted on top of pillars and fixed in final position by heterogeneous junctions.

The test finally practically proved the adaptability of non-tectonic structures to communal and industrial buildings and revealed inherent possibilities of the *relative span-indifference.*

EXPERIMENTAL TWIN COTTAGE

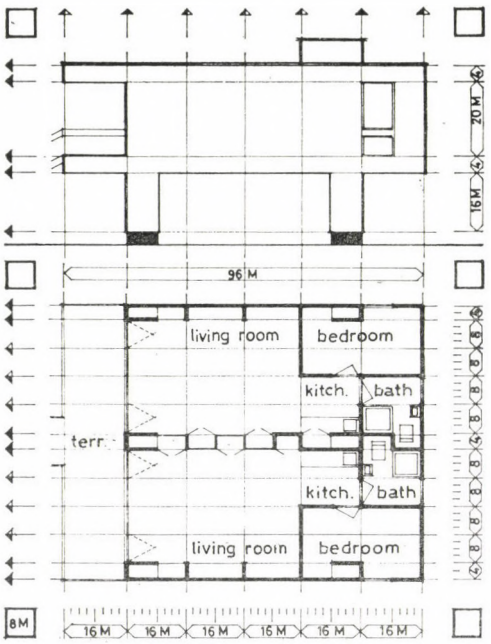

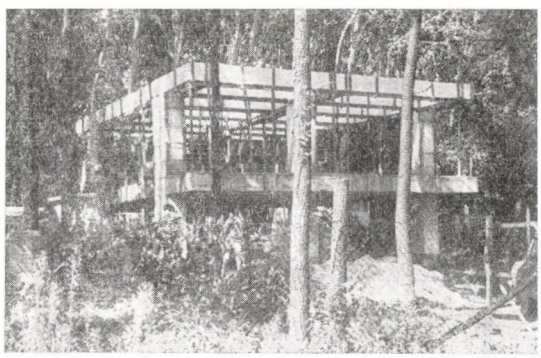

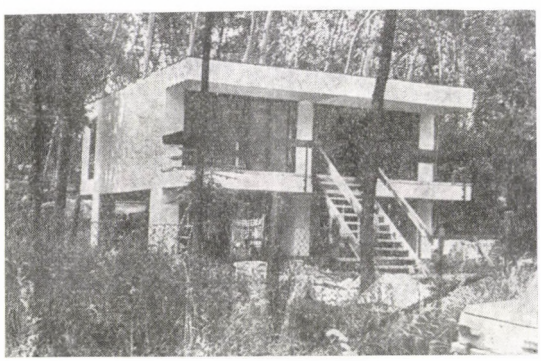

5. *Experimental twin cottage*

The test building is a two level arrangement, an experimental twin cottage having a total area of 146 m^2 and a total volume of 358 m^3.

The test building erected in a remote wood exemplifies an adaptation of the "do it yourself" method to the non-tectonic systems. It was first of all destined to give an unambiguous proof of the *economicalness* of the non-tectonic building method.

For this purpose an utmost reduction of weight was achieved through reductions in material, the manufacturing apparatuses were designed to last only as long as the building was completed so as to be as cheap as possible, the timber auxiliary structures were later transformed into doors, windows, cupboards, frames railing and stairs.

In order to prove the adaptability of the building technology to rural areas in developing countries, exclusively unskilled labor was used.

The test building itself is composed of six r.c. folded shell pillars (structural thickness: 25 mm), the horizontal load-bearing structure is a r.c. frozen shell beam-grid built in-situ, the floors are tissue-structural.

The test unit finally succeeded in reducing the cost of building extremely significantly. The total cost was approximately four times less, as if it had been built with traditional building methods.

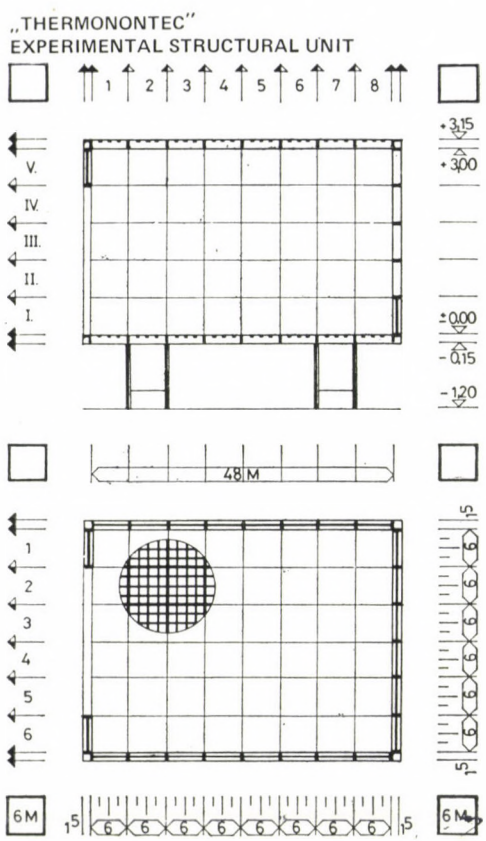

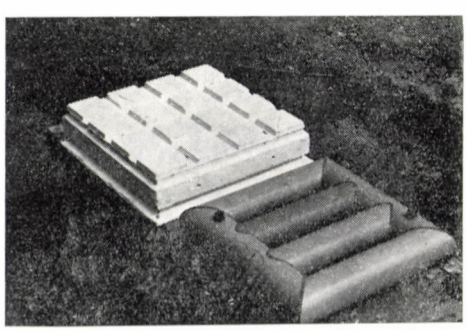

6. *"Thermonontec" experimental structural unit*

The heat storage offers the possibility of rational heating and cooling. The thermal capacity of light weight constructions is low, consequently heating or cooling systems of a big maximum capacity are required to provide a fix indoor temperature.

The "Thermonontec" experimental structural unit, a simple room-cell unit composed of four very thin r.c. shell pillars tissue structural floors with the built-in heat stabilizing equipments containing the phase change material (PCM), the media for heat storage, and walls constructed of a combination of ribs and r.c. shells was destined to offer a relatively unexpensive and simple method for storing the incident excess energy and for activizing the heat accumulated in the non-tectonic structure.

By incorporating a small quantity (appr. 20—30 kg/m^2) of the PCM the thermal inertia of the light weight construction increases to the tenfold, therefore the passive phase change process (PCP) in itself provides for the thermal comfort without a mechanical air-conditioning system.

The "Thermonontec" test successfully proved firstly, that the non-tectonic systems may easily integrate the heat-stabilizing equipments into the very structure without giving up any principle of design, manufacture and construction, and secondly, that thereby they can render the light weight constructions almost equivalent to heavy weight constructions from point of view of building physics.

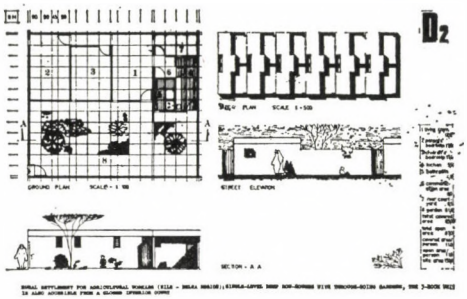

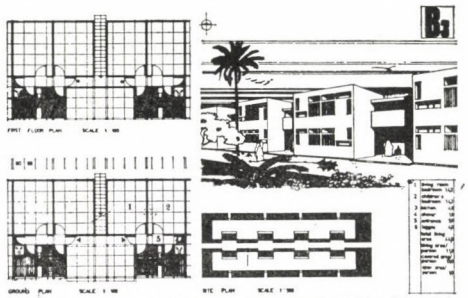

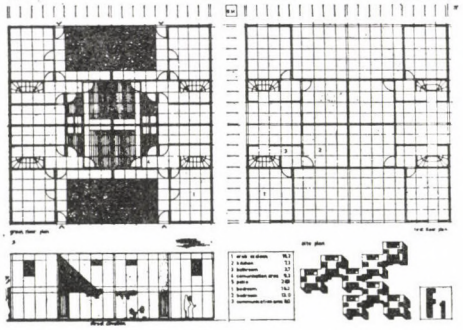

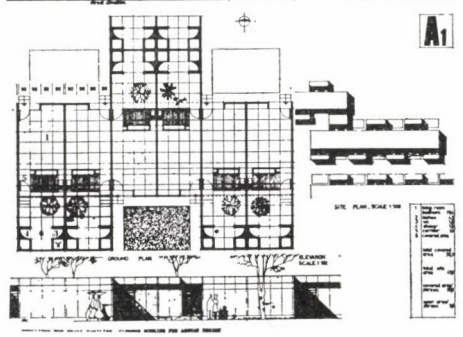

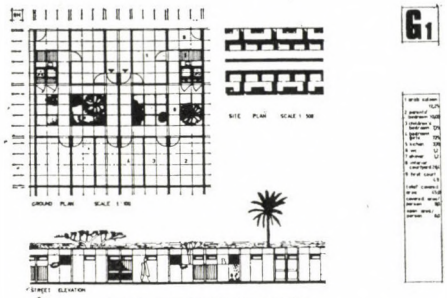

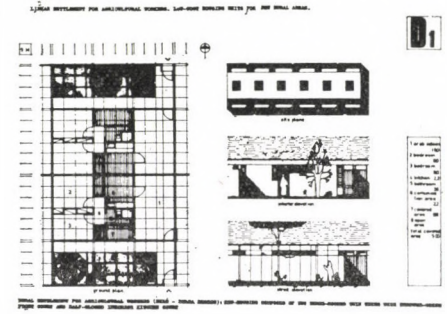

Let us mention finally that together with the experimentations in Hungary, quite a series of preliminary studies and detailed plans have been elaborated for different countries in hot arid tropical and subtropical areas. This work included among others ten settlement studies for Egypt, low-cost housing units and school-units for Mogadiscio (Somalia), a residential estate composed of four level apartment houses for Bagdad (Iraq), variations on bachelor-houses for Dubai (U.A.E.), sample houses for Abu Dhabi (U.A.E.), industrial hall for Chalis (Iraq).

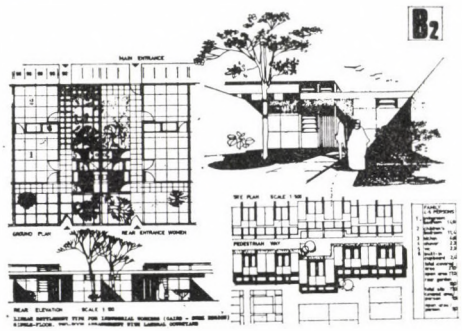

Section 3.

SUMMARY

The advantages and inherent possibilities of the non-tectonic building methods in developing countries

Considering the results achieved hitherto, the system seems to be very promising for use in hot arid countries (where gypsum is available) for low-cost housing, community centres, industrial workshops rural health centres for many reasons:

1. because the system which calls into being the light-weight, silicate-based constructions is an open system, it is equally applicable to various types of buildings: the ground-plans, arrangements, functions, formation of the buildings, namely, can be freely chosen since all characteristic dimensions (including: spans, heights, structural thicknesses, overall dimensions of the elements, thicknesses of elements, etc.) can be variable without giving up any principle of design, manufacture and construction;

2. because the materials applied are traditional hydraulic silicate materials which can be found in abundance in these areas;

3. because the very significant reduction in weight of buildings through reductions in material absolutely eliminates heavy transportation and lifting equipments; non-tectonic systems are not bound to a built out infrastructure;

4. because instead of requiring huge factories, the investment costs of which are large, the structure of the building industry can be founded on a system of transplantable elementary factories, the simple devices of which can be operated even by unskilled workers and because, last but not least, site work does not require the use of skilled labor either;

5. because by the use of the heat stabilizing equipment built into the structure and operated on a physical-chemical method the light weight constructions can be rendered almost equivalent to heavy weight constructions from point of view of building physics by storing solar heat gain in the phase change material.

REFERENCES

The publications enumerated below are only those immediately related to the subject matter.

1. PÁRKÁNYI, M.: The Inherent Contradictions of the Closed Systems of Prefabrication and the Future. Trends of Evolution. Contribution at the third CIB Congress. Published in "Towards Industrialized Building". Elsevier Publishing Company Amsterdam 1965.
2. PÁRKÁNYI, M.: Prefabrication with Gypsum. Meeting on Prefabrication in Africa and the Middle East. 17—29 April 1972 Budapest, Hungary; Bucharest, Roumania, ID/WG 122/20 March 1972 pp 5
3. PÁRKÁNYI, M.: Non-tectonic Systems. *Periodica Politechnica. Architecture.* Vol. **17** No. 4. 1973. pp 122—165
4. PÁRKÁNYI, M.: Experimental Non-tectonic Maisonette. *Per. Pol Arch.* Vol. **18** No. 3—4. pp 189—214

5. GARAY, L., PÁRKÁNYI, M.: Trends Towards Synthesis in Structural Engineering. CIB 6th Congress, Budapest, 1974. Subject Theme II/3 pp 453—463
6. PÁRKÁNYI, M.: Final Report of the Expert on Manufacture of Prefabricated Gypsum Wall Panels. Somalia, February 1974. Manuscript. Prepared for UNIDO 70 pp. Restricted.
7. PÁRKÁNYI, M.: "Lift-field" Experimental Non-tectonic Hall. *Per. Pol. Arch.* Vol. 22. No. 1 1978. pp 21—48
8. PÁRKÁNYI, M.: Proposition for a Building Technology for Mass Housing in Subtropical or Arid Tropical Areas. CIB 6th Congress, 1974 Budapest, Subject Theme VI/2. Discussion. pp 406—407. Elsevier Publishing Company. Amsterdam 1976
9. Non-tectonic System developed. *UNIDO Newsletter*, **132** (1979) April pp 2—3. Vienna, Austria

Nicht-tektonische Systeme. Ein illustrierter Bericht über die silikatbasischen Wärmespeichernden Bausysteme. — Die Abhandlung ist eine kurzgefasste Zusammenfassung einer technologischen Versuchsforschungsarbeit, durchgeführt im Bauinstitut der Technischen Universität in Budapest seit dem Jahre 1971 auf dem Gebiet der silikat-basischen, nicht tektonischen Baumethode, d.h., einer Baumethode, worin das Endprodukt (das Gebäude) durch ein spezifisches Verfahren hergestellt wird. Dieses Verfahren besteht darin, daß die Additivität (d.h., das axiomatische Bauprinzip) auf die Nicht-Tragfähigkeit und auf die zugleich vorübergehende Instabilität der nicht-tragenden (nicht-tektonischen), schemantisch unbedeutenden (dem Gutenberg-Prinzip folgenden) Flächenelemente realisiert wird. Deshalb ist das unmittelbare Ziel der Fertigung in diesem Bauverfahren nicht eine tragfähige Konstruktion, sondern die Oberfläche derselben. Folglich wird die Fluchtführung der waagerechten und der senkrechten Elemente der Konstruktionen nicht zu unmittelbaren tragfähigen lastübertragenden (tektonischen) Verbindungen zwischen den Oberflächen Elementen führen.

Acta Technica Academiae Scientiarum Hungaricae, Tomus 92 (1—2), pp. 121—137 (1981)

ОСЕСИММЕТРИЧНАЯ КОНТАКТНАЯ ЗАДАЧА В ЛИНЕЙНОЙ МОМЕНТНОЙ ТЕОРИИ УПРУГОСТИ

Г. СЕЙДЛ*

Поступила: 21. 2. 1979.

В работе рассматривается задача о вдавливании круглого жесткого штампа в полупространство с учетом влияния моментных напряжений. Решение полученной смешанной граничной задачи, аналогично классическому случаю, приводится к парным интегральным уравнениям. В работе доказывается, что для двух предельных значений упругой постоянной l^2 ($l^2 = 0$ и $l^2 \to \infty$) дается классическое распределение нормальных напряжений под основанием плоского штампа. Другое решение основано на принципе минимума дополнительной работы. Минимизация дополнительной энергии проводится по методу *Ритца*. Численный пример относится к плоскому штампу. На показанных диаграммах хорошо видны отличия от классического случая.

1. Введенне

Насколько известно автору, решению контактных задач в линейной моментной теории упругости до сих пор посвящена только работа [1]. В работе [1] дается решение для напряженного состояния в упругой полуплоскости, создаваемого прижатым к ее границе жестким гладким штампом. Однако, решение — в отличие от классического случая — не ведет к замкнутому виду.

В настоящей работе, с учетом влияния моментных напряжений, рассматривается статическая осесимметричная контактная задача о вдавливании кругового жестого штампа в упругое полупространство. Трение между штампом и полупространством не учитывается. При решении приняты основные предположения линейной моментной теории упругости. Численное решение основано на принципе дополнительной работы в силу механической наглядности этой теоремы. В связи с этим коротко покажем возможности применения принципа минимума дополнительной работы для тех смешанных граничных задач в линейной моментной теории упругости, которые по характеру совпадают с указанной контактной задачей.

Аналогичные задачи классической теории упругости и их решения подробно изложены в монографиях по теории упругости, например, в книге СНЕДДОНА [13].

* Dr. Gy. Szeidl, Rácz Á. u. 2., H—3532 Miskolc

2. Приведение контактной задачи к парным интегральным уравнениям

В случае рассматриваемой граничной задачи целесообразно записывать уравнения в цилиндрической системе координат r, v, z (рис. 1.). Пусть плоскость $z = 0$ является плоскостью, ограничивающей полупространство. Во введенной цилиндрической системе координат u_r, 0, u_v — обозначают компоненты вектора перемещений; σ_{rr}, σ_{vv}, σ_{zz}, τ_{zr}, τ_{rz} — не нулевые составляющие тензора напряжений; μ_{zv}, μ_{vz} μ_{rv}, μ_{vr} — составляющие тензора моментных напряжений, которые не равны тождественно нулю. Граничные условия на плоскости, ограничивающей полупространство, имеют следующий вид:

$$\left.\begin{aligned} u_z(0, r) = \dot{u}_z = \delta - w_0(r); \quad & 0 \leq r < a \\ \sigma_{zz}(0, r) = 0; \quad & a < r \end{aligned}\right\} \tag{2.1-1,2}$$

$$\tau_{zr}(0, r) = \mu_{z\vartheta}(0, r) = 0; \quad 0 \leq r \tag{2.1-3,4}$$

Здесь $\delta = \text{const}$, a — радиус штампа, а $w_0(r)$ — гладкая функция, определяющая форму поверхности основания штампа.

Предполагается, что перемещения и напряжения в случае $r \to \infty$ и $z \to \infty$ исчезают.

В работе [4] построено решение осесимметричной граничной задачи линейной моментной теории упругости для полупространства, когда на плоскости $z = 0$ действует известная распределенная нагрузка. Граничные условия, соответствующие задаче рассмотренной в работе [4] отличаются от выше указанных только тем, что на месте зависимостей (2.1—1,2) стоит уравнение

$$\sigma_{zz}(0, r) = p(r) \tag{2.2}$$

где $p(r)$ является заданной функцией.

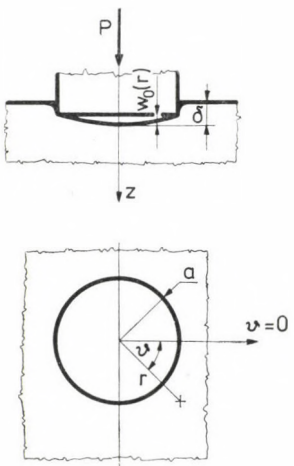

Рис. 1.

Отсюда следует, что можно применять все формулы для перемещений u_r, u_z, напряжений σ_{rr}, σ_{vv}, σ_{zz}, τ_{rz}, τ_{zr} и моментных напряжений μ_{zv}, μ_{vr} из [4] и в настоящем случае, если известно распределение нормальных напряжений, $p(r)$ под штампом. Для определения последнего — то есть $p(r)$ — на основании формул (4.10—2,6) из [4] с использованием неудовлетворительных граничных условий (2.1—1,2) получаем следующие парные интегральные уравнения:

$$\delta - w_0(r) = -\int_0^\infty \frac{\lambda + 2\mu}{2\mu(\lambda + \mu)} \frac{\bar{p}(k)}{1 + \frac{\lambda + 2\mu}{\lambda + \mu} 2l^2k^2\left(1 - \frac{k}{n}\right)} J_0(kr)\, dk\,;$$

$$0 \leq r < a \qquad (2.3\text{-}1)$$

$$\sigma_{zz}(0, r) = 0 = \int_0^\infty k\bar{p}(k)\, J_0(kr)\, dk; \qquad a < r \qquad (2.3\text{-}2)$$

Здесь приняты следующие обозначения: $J_0(kr)$ — функция Бесселя нулевого порядка, λ, μ, l^2 — постоянные, характеризующие упругие свойства материала, $p(k)$ — преобразование Ханкеля нулевого порядка функции $p(r)$, $n^2 = k^2 + 1/l^2$.

Преобразование Ханкеля функции $p(r)$ и его обращение определяются формулами

$$\bar{p}(k) = \int_0^a rp(r)\, J_0(kr)\, dr\,, \quad p(r) = \int_0^\infty k\bar{p}(k)\, J_0(kr)\, dk \qquad (2.4)$$

где учтено и (2.1—2).

Если в (2.3), (2.4) произвести замены переменных и ввести обозначения по формулам

$$r/a = \varrho; \quad ak = \xi; \quad L^2 = l^2/a^2; \quad N^2 = \xi^2L^2 + 1;$$

то эти уравнения примут вид

$$-(\Delta - W_0(\varrho)) = \int_0^\infty \bar{p}(\xi)\,[1 + G(\xi L)]\, J_0(\xi\varrho)\, d\xi; \quad 0 \leq \varrho < 1 \qquad (2.5\text{-}1)$$

$$a^2\sigma_{zz}(\varrho) = \int_0^\infty \xi\bar{p}(\xi)\, J_0(\xi\varrho)\, d\xi) = 0; \qquad 1 < \varrho \qquad (2.5\text{-}2)$$

где

$$G(\xi L) = \alpha \frac{1 - 2L^2\,\xi^2(1 - \xi L/N)}{1 + 2\alpha L^2\xi^2(1 - \xi L/N)} \qquad (2.6\text{-}1)$$

$$W_0(\varrho) = a\beta w_0(\varrho); \quad \Delta = a\beta\delta$$

и

$$\alpha = \frac{\lambda + 2\mu}{\lambda + \mu} = 2(1 - \nu); \quad \beta = 2\mu \frac{2\lambda + 3\mu}{\lambda + 2\mu} = E \frac{3 - 2\nu}{2(1 - \nu)}$$

(E — модуль Юнга, ν — коэффициент Пуссона).
Нетрудно видеть, что $\lim_{u \to \infty} G(u) = 0$, $u = \xi L$.

Впервые задача о парных интегральных уравнениях вида (2.5—1,2) изучена ТРАНТЕРОМ [5]. В работе КУКА предложен метод сведения парных интегральных уравнений к интегральному уравнению Фредгольма второго рода.

В настоящей работе метод решения парных интегральных уравнений излагается на основании [7, 9]. Отметим однако, что методы, найденные в [6, 7] являются эквивалентными. Теория парных интегральных уравнений подробно изложена в монографии СНЕДДОНА [14].

3. Решение парных интегральных уравнений

Решение парных уравнений (2.5—1,2) будем искать в виде:

$$\bar{p}(\xi) = \int_0^1 \varphi(\eta) \cos \xi\eta \, d\eta \tag{3.1}$$

где $\varphi(\eta)$ является новой неизвестной функцией. Представление решения $\bar{p}(\xi)$ по этой форме тождественно удовлетворяет уравнению (2.5—2). Чтобы убедиться в этом, подставим (3.1) в (3.2) и проинтегрируем по частям с учетом равенства ([15], 6.671—1):

$$\int_0^\infty \sin \xi\eta \, J_0(\xi\varrho) \, d\xi = \begin{cases} (\eta^2 - \varrho^2)^{-\frac{1}{2}} & \varrho < \eta \\ 0 & \varrho > \eta \end{cases} \tag{a}$$

Для определения $\varphi(\eta)$, после подстановки (3.1) в (2.5—1) с использованием формулы ([15], 6.671—1):

$$\int_0^\infty \cos \xi\eta \, J_0(\xi\varrho) \, d\xi = \begin{cases} 0 & \varrho > \eta \\ (\varrho^2 - \eta^2)^{-\frac{1}{2}} & \varrho < \eta \end{cases} \tag{b}$$

найдем, что

$$\int_0^\varrho \frac{\varphi(\eta)}{\varrho^2 - \eta^2} \, d\eta + \int_0^1 \varphi(\eta) \int_0^\infty G(\xi L) \cos \xi\eta \, J_0(\xi\varrho) \, d\xi \, d\eta =$$
$$= W_0(\varrho) - \Delta; \qquad 0 \leq \varrho < 1$$

Если в первом интеграле правой части на основании соотношения $\eta = \varrho \sin \psi$ перейдем к новой переменной, а во втором подставим известное представление функции Бесселя ([15], 8.411—2):

$$J_0(\xi\varrho) = \frac{2}{\pi} \int_0^{\pi/2} \cos\,(\varrho\xi \sin \psi)\, d\psi$$

то приходим к уравнению

$$\int_0^{\pi/2} \left[\varphi(\varrho \sin \psi) + \frac{2}{\pi} \int_0^1 \varphi(\eta) \int_0^\infty G(\xi L) \cos\, \xi\eta \cos\,(\xi\varrho \sin \psi)\, d\xi d\eta \right] d\psi = \\ = W_0(\varrho) - \Delta \tag{3.2-1}$$

которое является интегральным уравнением ШЛЕМИЛЬХА [7, 16]:

$$\int_0^{\pi/2} F(\varrho \sin \psi)\, d\psi = W(\varrho) = W_0(\varrho) - \Delta \tag{3.2-2}$$

Подставляя в решение уравнения

$$F(\varrho) = \frac{2}{\pi} \left[W(0) + \varrho \int_0^{\pi/2} W'(\varrho \sin \psi)\, d\psi \right] = \hat{W}(\varrho) \tag{3.3}$$

значение $F(\varrho)$ на основании (3.2—1) приходим к интегральному уравнению Фредгольма второго рода с симметричным ядром относительно новой неизвестной функции $\varphi(\varrho)$:

где

$$\left.\begin{aligned} &\varphi(\varrho) \frac{1}{\pi} \int_0^1 \varphi(\eta)\, K(\eta, \varrho)\, d\eta = \hat{W}(\varrho) \\ &K(\eta, \varrho) = \hat{G}(\eta + \varrho) + \hat{G}(\eta - \varrho) \\ &\hat{G}(\eta) = \int_0^\infty G(\xi L) \cos\, \xi\eta\, d\xi\,. \end{aligned}\right\} \tag{3.4}$$

Исходя из (2.3—2), (3.1) можем проверить, с учетом (*a*), что распределение нормальных напряжений под штампом и осевая сила, вдавливающая штамп в полупространство имеют следующий вид:

$$a^2 \sigma_{zz}(\varrho) = \frac{\varphi(1)}{\sqrt{1 - \varrho^2}} - \int_{\eta=\varrho}^1 \frac{\varphi'(\eta)}{\sqrt{\eta^2 - \varrho^2}}\, d\eta \tag{3.5}$$

$$P = -2\pi \int_0^1 \varphi(\varrho)\, d\varrho \tag{3.6}$$

В случае неполного погружения штампа с неплоским основанием нормальное напряжение σ_{zz} является непрерывным на плоскости $z = 0$. Из этого вытекает, что

$$\varphi(1) = 0 \tag{3.7}$$

Если известна вдавливающая сила P, на основании (3.6) и (3.7) можно определить погружение штампа δ и радиус контактной площадки штампа a.

4. Сравнение с классическим решением и вопрос разрешимости

Пусть штамп имеет плоское основание ($w_0(r) = 0$). Покажем, что решение интегрального уравнения (3.4) в случае $L \to 0$ $L \to \infty$ ведет к классическому решению.

1) Если $L \to 0$, исходя из (3.4) получим, что

$$\varphi^0(\varrho) + \frac{1}{\pi}\int_0^1 \varphi^0(\eta)\, K^0(\eta, \varrho)\, d\eta = -\frac{2}{\pi}\Delta \tag{4.1}$$

где предел обозначается символом «o», стоящим справа вверху.

Известно — ([15], 3.741—2) — что

$$\int_0^\infty \frac{1}{\xi}\cos\xi\eta \sin\xi\varrho\, d\xi = \left\{\begin{array}{ll} \pi/2 & \eta < \varrho \\ \pi/4 & \eta = \varrho \\ 0 & \eta > \varrho \end{array}\right\} = \frac{\pi}{2} H(\varrho - \eta) \tag{4.2}$$

где H функция Хевисайда.

Нетрудно видеть, с использованием (4.2) и (3.4—2,3), что функционал [17]

$$F_L(\eta, \varrho) = \int_1^\infty \frac{1}{\xi} G(\xi L)\cos\xi\eta \sin\xi\varrho\, d\xi \tag{4.3}$$

удовлетворяет равенствам

$$\left.\begin{aligned} F_L^0(\eta, \varrho) &= \frac{\pi}{2} G(0)\, H(\varrho - \eta) \\ K^0(\eta, \varrho) &= \lim_{L\to 0} \frac{d}{d\varrho} F_L(\eta, \varrho) = \frac{\pi}{2} G(0)\, \delta(\varrho - \eta) \end{aligned}\right\} \tag{4.4}$$

где δ является функцией Дирака. Искомый предел $\varphi(\varrho)$ получается после подстановки (4.4—2) в (4.4—1)

$$\varphi^0(\varrho) = -2\Delta/\pi(1 + G(0)) \tag{4.5}$$

с использованием чего в силу (3.6) и (3.5) определяются вдавливающая сила:

$$P = 4\Delta/(1 + G(0)) \tag{4.6}$$

и неизвестное распределение нормальных напряжений:

$$\lim_{L\to 0} \sigma_{zz}(r, 0) = -\frac{P}{2\pi a^2} \frac{1}{(1-(r/a)^2)^{1/2}}; \quad 0 \leq r < a \tag{4.7}$$

2) В случае $L \to \infty$ предел ядра $K(\eta, \varrho)$ равен нулю и поэтому из (3.4) следует, что

$$\lim_{L\to\infty} \varphi(\varrho) = -2\Delta/\pi \tag{4.8}$$

С использованием этого из (3.6) и (3.5) получим вдавливающую силу

$$P = 4\Delta \tag{4.9}$$

и распределение напряжений

$$\lim_{L\to\infty} \sigma_{zz}(r, 0) = -\frac{P}{2\pi a^2} \frac{1}{(1-(r/a)^2)^{1/2}}; \quad 0 \leq r < a \tag{4.10}$$

Соотношения (4.8) и (4.10) действительно совпадают с соотношением для классического распределения нормальных напряжений под штампом.

В дальнейшем рассматривается вопрос о разрешимости контактной задачи.

Запишем обычный вид интегрального уравнения Фредгольма второго рода с симметричным ядром (3.4):

$$\varphi(\varrho) - \lambda \int_0^1 \varphi(\eta)\, \tilde{K}(\eta, \varrho)\, d\eta = \hat{W}(\varrho) \tag{4.11}$$

где

$$\lambda = 1, \quad \tilde{K}(\eta, \varrho) = -\frac{1}{\pi} K(\eta, \varrho) \tag{4.12}$$

В соответствии с теоремой Фредгольма об альтернативе [18a], неоднородное интегральное уравнение (4.11) имеет одно и только одно решение [18*b*], если $\lambda = 1$ не является собственным числом однородного сопряженного уравнения. Вследствие непрерывности ядра в промежутке $[0, 1]\times[0,1]$ условие теоремы

выполнено, если на множестве кусочно-гладких функций ψ в промежутке [0, 1] справедливо неравенство

$$I_b(\psi) = \int_\delta^1 \int_\delta^1 \widetilde{K}(\eta, \varrho)\, \psi(\eta)\, \psi(\varrho)\, d\eta\, d\varrho =$$

$$= -\frac{2}{\pi} \int_\delta^1 \int_\delta^1 \int_0^\infty G(\xi L) \cos \xi\eta \cos \xi\varrho d\xi \psi(\eta) \psi(\varrho)\, d\eta\, d\varrho < 0;\ \delta \in (0, 1) \quad (4.13)$$

то есть ядро является отрицательно определенным.

В промежутках $\eta \in [\delta, 1]$, $\varrho \in [\delta, 1]$ интеграл

$$I(\eta, \varrho) = \int_0^\infty G(\xi L) \cos\, \xi\eta \cos\, \xi\varrho\, d\xi$$

сходится равномерно, так как $\lim\limits_{u \to \infty} G(u) = C/u^2$. ($C$ — постоянная.) Поэтому в (4.13) можно изменить порядок интегрирования. Это приводит к неравенству

$$I\delta(\psi) = -\frac{2}{\pi} \int_0^\infty G(\xi L) \left\{ \int_0^1 \psi(\varrho) \cos\, \xi\varrho\, d\varrho \right\}^2 d\xi < 0$$

что и требовалось доказать. При этом учтено то, что $G(\xi L) < 0$ $0 < \xi < \infty$; $L \geq 0$ и $-\infty < v \leq 0{,}5$.

5. Приближенное решение

Разложим искомое решение уравнения Фредгольма (3.4) в ряд по четным полиномам Лежандра:

$$\varphi(\varrho) = \sum_{k=0}^{\infty} (-1)^k a_k g_k P_{2k}(\varrho)$$

$$g_0 = 1;\quad g_k = (2k-1)!!/2k!!\quad k = 1, 2, \ldots \quad (5.1)$$

Для вычисления неизвестных коэффициентов a_k исходя из (3.4) по методу ортогональных многочленов [9] можно построить бесконечную систему линейных уравнений.

Сведение к этой системе здесь не будет показано, ограничимся только определением характера распределения нормальных напряжений под штампом.

Учитывая интеграл[1]

$$\int_0^1 P_{2k}(\eta)\, \cos\, \xi\eta\, d\eta = (-1)^k \sqrt{\frac{\pi}{2\xi}}\, J_{2k+1/2}(\xi)$$

[1] Нетрудно убедиться в его справедливости.

для преобразования Ханкеля распределения нормальных напряжений под штампом на основании (3.1) и (3.2) будем иметь выражение:

$$\bar{p}(\xi) = \sum_{k=0}^{\infty} a_k g_k \sqrt{\frac{\pi}{2\xi}} J_{2k+1/2}(\xi) \tag{5.2}$$

Можно показать, используя последовательно формулы (29) **7.7.4,** (1) **2.9,** (21) **10.9,** (21) и (24) **10.10** из [18], что

$$\int_0^{\infty} \sqrt{\xi} J_{2k+1/2}(\xi) J_0(\xi\varrho)\, d\xi = \sqrt{\frac{2}{\pi}} \frac{1}{g_k} (1-\varrho^2)^{-1/2} P_{2k}\left(\sqrt{1-\varrho^2}\right) \tag{5.3}$$

если $\varrho \in [0,1)$. Подставим (5.2) в (2.3—2), с учетом (5.3), находим искомое распределение напряжений:

$$p(\varrho) = \frac{1}{a^2} \sum_{k=0}^{\infty} a_k (1-\varrho^2)^{-1/2} P_{2k}\left(\sqrt{1-\varrho^2}\right) \tag{5.4}$$

В работе АЛЕКСАНДРОВА [11] другим путем, строго математически получено решение исходной метематической задачи (2.4), (2.5—1,2) и форме (5.4).

С использованием принципа минимума дополнительной работы также можно построить приближенное решение рассматриваемой контактной задачи. В классическом случае применение принципа минимума дополнительной работы показано в работе КАЛКЕРА [10]. Эта возможность в линейной моментной теории упругости рассматривается в «Приложении» к настоящей работе. В дальнейшем излагается применение этой возможности к рассматриваемой контактной задачи.

В соответствии с формулой (7.10) «Приложения» в осесимметричном случае будем искать минимальное значение функционала

$$\Phi(p) = \int_0^a p(r)\,(u_z - 2\mathring{u}_z)\, r dr \tag{5.5}$$

где u_z является решением, принадлежащим к неизвестному $p(r)$, а $\mathring{u}_z$ заданное перемещение. Пользуясь соотношениями (2.1—1) и (2.1—2) — второе из них дает решение для $u_z(r, 0)$ — с учетом преобразований, выполненных при получении (2.5—1), из (5.5) следует, что;

$$J(p) = -\frac{2\beta}{a} \int_0^1 \left(\delta - w_0(\sigma)\right) \varrho p(\varrho)\, d\varrho - \int_0^{\infty} [1 + G(\xi L)]\, T^2(\xi)\, d\xi \tag{5.6}$$

Здесь

$$J(p) = \beta\Phi(p)/a^3$$

и

$$T(\xi) = \int_0^1 \eta p(\eta)\, J_0(\xi\eta)\, d\eta \qquad (5.7)$$

Отметим, что вариационный метод, предлагаемый НОБЛОМ для решения интегрального уравнения (3.4), ведет к одному и тому же функционалу [12, 14].

Минимальное значение функционала $J(p)$ будем искать по методу Ритца. Выбирая $p(\varrho)$ в соответствии с (5.4), необходимые условия минимума

$$\frac{\partial J(p)}{\partial a_k} = 0, \quad k = 0, 1, 2, \ldots \qquad (5.8)$$

приводят к бесконечной системе линейных уравнений для определения неизвестных коэффициентов a_k.

При следующих преобразованиях целесообразно учитывать ортогональносль многочленов Лежанбра:

$$\int_0^1 P_{2i}\left(\sqrt{1-\varrho^2}\right) P_{2j}\left(\sqrt{1-\varrho^2}\right) \varrho(1-\varrho^2)^{-1/2}\, d\varrho = \begin{cases} 0 & i \neq j \\ (4i+1)^{-1} & i = j, \end{cases}$$

выражение:

$$\int_0^1 J_0(\xi\eta)\, P_{2k}\left(\sqrt{1-\eta^2}\right) \eta(1-\eta^2)^{-1/2}\, d\eta = \sqrt{\frac{\pi}{2\xi}}\, g_i\, J_{2i+1/2}(\xi)$$

полученное обратным преобразованием (5.3), которое считается преобразованием Ханкеля нулевого порядка, и ряд

$$\delta - w_0(\varrho) = \sum_{k=0}^{\infty} b_k\, P_{2k}\left(\sqrt{1-\varrho^2}\right)$$

где

$$b_k = (4k+1)\int_0^1 \varrho\big(\delta - w_0(\varrho)\big)(1-\varrho^2)^{-1/2}\, P_{2k}\left(\sqrt{1-\varrho^2}\right) d\varrho$$

Не останавливаясь на выкладках, приходим к следующей системе линейных уравнений для a_k:

$$\sum_k A_{ik}\, a_k = B_i; \quad i, k = 0, 1, \ldots \qquad (5.9)$$

где матрица коэффициентов и правая часть имеют вид:

$$A_{ik} = g_i g_k [\delta_{ik}/(4k+1) + I_{ik}]; \quad B_k = -\frac{2}{\pi} \frac{\beta a b_k}{4k+1}$$

$$I_{ik} = \int_0^\infty \frac{1}{\xi} G(\xi L) J_{2i+1/2}(\xi) J_{2k+1/2}(\xi) d\xi; \quad \delta_{ik} = \begin{cases} 0 & i \neq k \\ 1 & i = k \end{cases} \tag{5.10}$$

если принять во внимание и интеграл ([5], 6.538—2):

$$\int_0^\infty \frac{1}{\eta} J_{2i+1/2}(\eta) J_{2j+1/2}(\eta) d\eta = \begin{cases} 0 & i \neq \\ (4j+2)^{-1} & i = j \end{cases}.$$

Условие (3.7) выражается уравнением

$$\sum_{k=0}^{\infty} a_k = 0 \tag{5.11}$$

Значение вдавливающей силы:

$$P = -2\pi a_0 \tag{5.12}$$

Можно доказать, следуя работе [9], что метод ортогональных многочленов для интегрального уравнения (3.4) тоже приводит к линейной системе уравнений (5.9—10). Предложенный в настоящей работе способ получения линейной системы уравнений (5.9—10) вызван своей механической наглядностью.

Приближенное решение — конечное число уравнений — получается с использованием частной суммы ряда (5.4).

6. Пример

Численный пример относится к штампу с плоским основанием. Принимая во внимание, что в этом случае

$$B_0 = \frac{2}{\pi} \beta a \delta; \quad B_k = 0 \quad k \neq 0$$

и

$$A_{00} = 1 + I_{00}$$

с учетом (5.12) находим следующее первое приближение:

$$\sigma_{zz}(r, 0) = -\frac{P}{2\pi a^2} \frac{1}{(1-(r/a)^2)^{1/2}}; \quad P = 4\beta a\delta/(1 + I_{00})$$

Отсюда — в соответствии с (5.10—3) I_{00} является функцией от L — при $L \to 0$ и $L \to \infty$ получим соотношения (4.6, 7) и (4.9, 10).

Численные результаты для $\nu = 0, 0{,}5$, $E = 1{,}86 \cdot 10^5\ \mathrm{N/mm^2}$ $\delta = 0{,}025\ \mathrm{mm}$, показаны на рис. 2., 3. Характер отдельных кривых совпадает с характером кривых, полученных при решении аналогичной плоской задачи [1].

Хорошо видно, что $\lim_{L\to\infty} \sigma_{zz}/\mathring{\sigma}_{zz} \to 1$.

Для $L \to 0$ предел тоже равен 1. В начале кривой с параметром $L = 0{,}1$ это явление также чувствуется из сравнения кривых для $L = 0{,}2, 0{,}4$. Напряжение σ_{zz} по направлению к границе штампа быстрее возрастает, чем в классическом случае, что совпадает с характером изменения, полученным в [1].

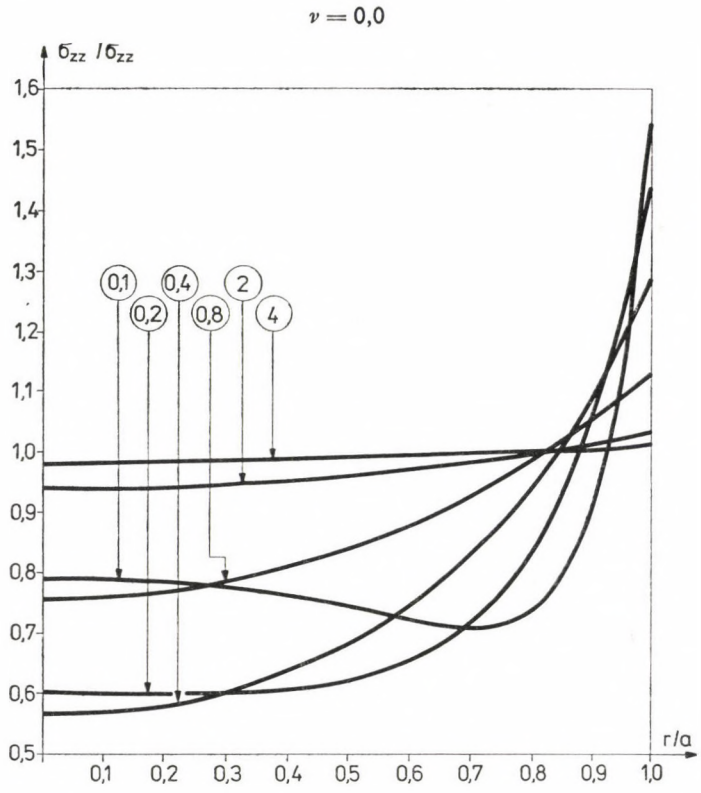

Рис. 2. Соотношение между напряжением σ_{zz} и решением для классического случая $\mathring{\sigma}_{zz}$, если давливающая сила одна и та же при $\nu = 0$

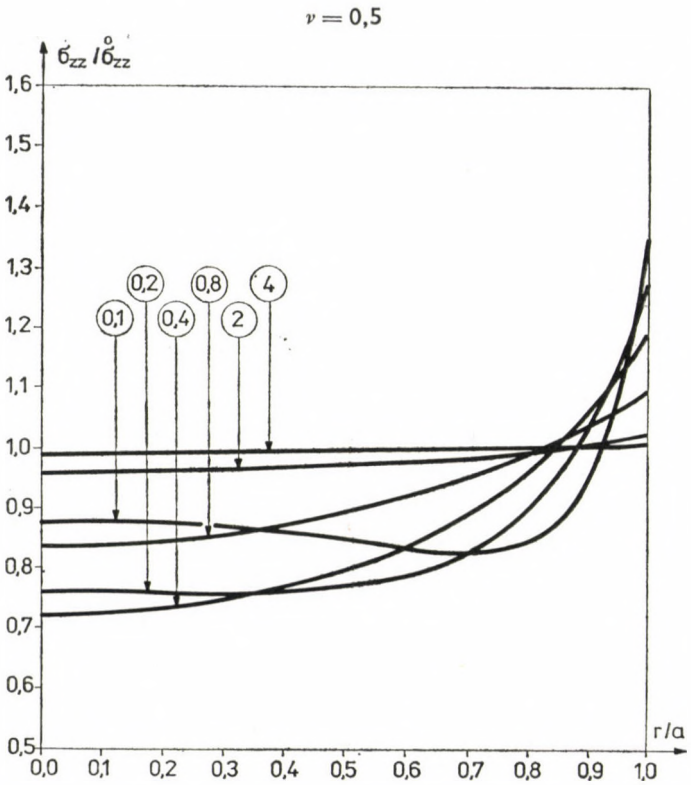

Рис. 3. Соотношение между напряжением σ_{zz} и решением для классического случая $\dot{\sigma}_{zz}$, если давливающая сила одна и та же при $\nu = 0{,}5$

7. Приложение

В дальнейшем рассматривается возможность применения принципа минимума дополнительной работы для смешанных граничных задач контактного типа в линейной моментной теории упругости. Осесимметричная контактная задача для полупространства является специальным случаем рассматриваемой здесь граничной задачи.

В декартовой системе координат (x_1, x_2, x_3) приняты обычные обозначения: δ_{qs} — символ Кронекера, ε_{pqs} — антисимметричный тензор Леви—Чивиты, соглашение о суммировании. Произвольный индекс, следующий за запятой, указывает, что берется частная производная по координате, принадлежащей к индексу.

Объемные силы и моменты не будут учтены.

Уравнения поля линейной моментной теории упругости составляются из кинематических уравнений, связывающих вектор поворота φ_p, тензор де-

формации ε_{pq}, и тензор изгиба-кручения $\varkappa_{pq}$ с перемещением u_p:

$$\varphi_q = \frac{1}{2}\,\varepsilon_{qvr}\,u_{r,v}$$

$$\varepsilon_{pq} = \frac{1}{2}(u_{p,q} + u_{q,p}), \quad \varkappa_{pq} = \varphi_{q,p} \tag{7.1}$$

закона Гука для центрально-симметричного материала:

$$\varepsilon_{pq} = \underset{-1}{C}_{pqrs}\,\sigma_{(rs)}; \quad \varkappa_{qp} = \underset{-1}{A}_{pqrs}\,\overset{D}{\mu}_{rs} \tag{7.2}$$

в котором приняты следующие обозначения: $\underset{-1}{C}_{pqrs}$, $\underset{-1}{A}_{pqrs}$ — тензоры механических постоянных материала, $\sigma_{pq} = \sigma_{(pq)} + \sigma_{[pq]}$ (символы ( ) и [ ] означают симметричную и антисимметричную части), $\overset{D}{\mu}_{pq}$ — девиатор тензора μ_{pq}; уравнений равновесия

$$\sigma_{pq,p} = 0\,, \qquad \mu_{pq,p} + \varepsilon_{qrs}\,\sigma_{rs} = 0 \tag{7.3}$$

Рассмотрим тело (рис. 4), имеющее объем V, ограниченное для простоты гладкой поверхностью A. Задаются следующие граничные условия:

$$u_s = 0, \quad \varphi_p(\delta_{ps} - n_p n_s) = 0; \qquad x_k \in A_u \tag{7.4}$$

$$P_s = n_q\left[\sigma_{(qr)} + \frac{1}{2}\,\varepsilon_{qrs}\,(\overset{D}{\mu}_{rk,k} - \underset{(n)}{\mu}_{,r})\right] = 0\,; \qquad x_k \in A_p \tag{7.5}$$

$$n_p\,\overset{D}{\mu}_{pq}(\delta_{qs} - n_q n_s) = 0\,; \quad x_k \in A_p \cup A_c$$

$$u_q n_q n_s = \mathring{u}_s, \quad P_q(\delta_{qs} - n_q n_s) = 0 \quad x_k \in A_c \tag{7.6}$$

где $\underset{(n)}{\overset{D}{\mu}} = n_p\,\overset{D}{\mu}_{pq}\,n_q$ и $\mathring{u}_s$ является заданной гладкой функцией на A_c.

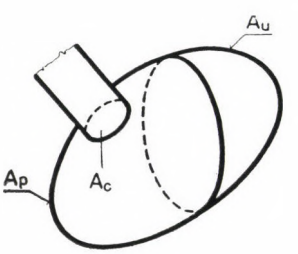

Рис. 4.

В случае записанных граничных условий только нормальная нагрузка имеет место на поверхности A_c, которая представляет собой контактную область.

Поля σ^*_{rs}, μ^*_{rs} по определению статически возможны, если удовлетворяют уравнениям поля (7.3) и динамическим граничным условиям (7.5), (7.7—2).

Выражение для дополнительной работы имеет следующий вид:

$$\pi_c(\sigma^*_{rs}, \mu^*_{rs}) = \frac{1}{2}\int_V \left(\underset{-1}{C}_{pqrs}\,\sigma_{pq}\,\sigma_{rs} + \underset{-1}{A}_{pqrs}\,\overset{D}{\mu}_{pq}\,\overset{D}{\mu}_{rs}\right) dV - \int_{A_c} P_q\,n_q\,n_s\,\mathring{u}_s\,dA \qquad (7.7)$$

В соответствии с принципом минимума дополнительной работы при точном решении для σ_{rs}, μ_{rs} (7.7) имеет строгий минимум.

Рассмотрим теперь другую краевую задачу, отличающуюся от предыдущей — определенной уравнениями поля (7.1,2,3) и граничными условиями (7.4), (7.5) и (7.6) — всего лишь граничным условием на A_c.

Пусть новое граничное условие имеет вид:

$$P_q\,n_q\,n_s = p^*_s \quad x_k \in A_c \qquad (7.8)$$

где p^*_s заданная нормальная нагрузка. Предполагаем, что известно решение новой граничной задачи определенной уравнениями поля (7.1,2,3) и граничными условиями (7.4), (7.5), (7.6—2) и (7.8). Это решение представляет собой статистически возможные перемещения, вектор поворота, тензоры деформации, изгиба-кручения и тензоры напряжений, моментных напряжений для предыдущей граничной задачи (7.1, 2,3), (7.4, 5,6).

Подставляя эти решения в (7.7) с учетом (7.1, 2) объемный интеграл, стоящий в (7.7) можно привести к поверхному интегралу. В этих преобразованиях применялись соотношение

$$\sigma_{[pq]} = \frac{1}{2}\,\varepsilon_{pqr}\,\mu_{rk;\,k}$$

полученное из (7.3), теорема Гаусса-Остроградского, и интеграл

$$\int_A n_q\,\underset{(n)}{\varepsilon_{qrs}}\,(\mu\,u_s)_{,\,r}\,dA = 0$$

который следует из гладкости поверхности тела. Применяя вышеуказанные преобразования, найдем:

$$\int_V \left(\underset{-1}{C}_{pqrs}\,\sigma^*_{(pq)}\,\sigma^*_{(rs)} + \underset{-1}{A}_{pqrs}\,\overset{D}{\mu}{}^*_{pq}\,\overset{D}{\mu}{}^*_{rs}\right) dV =$$

$$= \int_A \left(n_p\,\sigma^*_{pq}\,u^*_p + n_p\,\overset{D}{\mu}{}^*_{pq}\,\varphi^*_q\right) dA =$$

$$= \int_A \left[P^*_p\,u^*_s + n_p\,\overset{D}{\mu}{}^*_{pr}\,(\delta_{rq} - n_r\,n_q)\,\varphi^*_q\right] dA$$

с использованием чего и граничных условий (7.4), (7.5), (7.6—2) и (7.8) из (7.7) получим, что

$$\pi_c(\sigma_{rs}^*, \mu_{rs}^*) = \int_{A_c} p_s^* \left(\frac{1}{2} u_s^* - \mathring{u}_s \right) dA \tag{7.9}$$

В случае рассматриваемой осесимметричной граничной задачи A_c — круговая область под штампом, радиусом a, A_p — часть плоскости, ограничивающей полупространство вне A_c, A_u — бесконечно удаленная плоскость (здесь, как перемещения, так и напряжения исчезают), $p^* - p(r)$, $u^* - u_z$ (z не является индексом). Итак, решение этой задачи приводит к отысканию минимума функции

$$\Phi(p) = \int_0^a p(r)(u_z - 2\mathring{u}_z)\, rdr \tag{7.10}$$

то есть, к определению минимизирующего $p(r)$.

ЛИТЕРАТУРА

1. Muki, R.—Sternberg, E.: The Influence of Couple-Stresses on Singular Stress Concentrations in Elastic Solids, *ZAMP*, **16** (1965), 611—648
2. Mindlin, E. D.—Tiersten, H. F.: Effects of Couple-Stresses in Linear Elasticity, *Archives for Rational Mechanics and Analysis*. **11** (1962), 415—448
3. Koiter, W. T.: Couple Stresses in the Theory of Elasticity, *Proceedings Koninklijke Nedelandske Akademie van Wetenshappen*, **B67** (1964) 17—29, 30—44
4. СЕЙДЛ Д.: Осесимметричная граничная задача в линейной моментной теории упругости. *Publications of Technical University for Heavy Industry, Series-D Natural Sciences*, **34** (1979), 27—41.
5. Tranter, C. J.: On Some Dual Integral Equations Occuring in Potential Problems with Axial Symmetry, *Quart. J. Mech. and Applied Math.*, **3** (1950), 411—419
6. Cooke, J. C.: A Solution of Tranter's Dual Integral Equations Problem, *Quart, J. Mech. and Applied Math.* **9** (1956), 103—110
7. ЛЕБЕДЕВ, П. Н.—УФЛЯНД, Я. С.: Осесимметричная контактная задача для упругого слоя, *ПММ* 22 (1958), 321—324
8. Schlömlich, O.—Witzschel, B.: Ueber die Besselsche Funktion, *Zeitschrift für Mathematik und Physik* II., (1857), 138—165
9. Szefer, G.—Gaszynski, J.: Axisymmetric Punch Problem under Condition of Consolidation, *Archives of Mechanics* **27** (1975), 497—515
10. Kalker, J. J.: Variational Principles of Contact Elastostatics, *J. Inst. Maths. Applics* **20** (1977), 199—219
11. АЛЕКСАНДРОВ, В. М.: О приближенном решении некоторых интегральных уравнений теории упругости и математической физики, *ПММ*, Вып. **6.** (1967), 1117—1131
12. Noble, B.: The Approximate Solution of Dual Integral Equations by Variational Methods, *Proc. Edinburgh Mathem. Soc.* **11** (1958), 115—126
13. Sneddon, I. N.: Fourier Transforms, McGraw-Hill, New York—Toronto—London 1951
14. Sneddon, I. N.: Mixed Boundary Value Problems in Potential Theory, North-Holland, Amsterdam 1966
15. ГРАДШТЕЙН, И. С.—РЫЖИК, И. М.: Таблицы интегралов сумм, рядов и произведений, Физматгиз, Москва 1963
16. Whittaker, E. T.—Watson, G. N.: A Course of Modern Analysis, University Press, Cambridge 1952, 229

17. LIGHTHILL, M. J.: Introduction to Fourier Analysis and Generalised Functions, University Press, Cambridge, 1959
18. PETROWSKY, I. G.: Lectures on the Theory of Integral Equations, Mir Publishers, Moscow, 1971, *a* 19, *b* 101
19. ERDÉLYI, A. BATEMAN, H.: Higher Transcendental Functions, McGraw-Hill Book Company, New York—Toronto—London 1955

An Axisymmetrical Punch Problem in the Linear Couple-stress Theory of Elasticity. — The case of the elastic half space under a cylindrical rigid punch is investigated by taking the effect of the couple-stresses into account. The solution of the resulting mixed boundary-problem leads, similarly to the classic case, to dual integral equations. It is pointed out that to the case of the two extreme values ($l^2 = 0$ and $l^2 \to \infty$) of the material property l^2 for the flat-end cylindrical punch, the classic stress distribution is obtained. For another solution the principle of minimum complementary energy might be suggested. Minimizing of the functional of the complementary energy is carried out by using Ritz's method. A numerical example relates to the flat-end punch. The diagrams plotted suggest the deviations from the classic case.

Ein achsialsymmetrisches Kontaktproblem in der linearen Momentenspannungs-Elastizitätstheorie. — Untersucht wird der Fall des auf den elastischen Halbraum wirkenden, starren Zylinderstempels unter Berücksichtigung der Wirkung der Momentenspannung. Die Lösung der sich daraus ergebenden gemischten Randwertaufgabe führt, wie im klassischen Fall, zu dualen Integralgleichungen. Es wird demonstriert, daß sich für die zwei Randwerte ($l^2 = 0$ und $l^2 \to \infty$) des Stoffwerts l^2 im Fall eines durch eine ebene Fläche abgeschlossenen Stempels die klassische Spannungsverteilung ergibt. Als eine andere Lösung der Aufgabe kann das Prinzip des Minimums der Komplementärenenergie benutzt werden. Die Minimalisierung des Komplementärenenergiefunktionals wird mit Hilfe der Ritzschen Methode durchgeführt. Ein numerisches Beispiel behandelt einen durch eine Fläche abgeschlossenen Stempel. Die vorgeführte Diagramme zeigen die Abweichungen vom klassischen Fall.

Acta Technica Academiae Scientiarum Hungaricae, Tomus 92 (1—2), pp. 139—152 (1981)

SWITCHING SURGE BREAKDOWN CHARACTERISTICS OF LARGE CONDUCTOR—TOWER AIR GAPS

I. L. KRÓMER*
CAND. OF. TECHN. SCI.

[Manuscript received 3 March 1980]

A comprehensive series of impulse tests on a variety of simulated transmission tower insulation is described. The influence of the waveshape on positive polarity switching surge strength of large tower configurations was investigated by applying different waves with times-to-crest between 35 and 1200 μs. The test results overlap and extend beyond existing data, making available a generalized flashover voltage-wavefront characteristics. Special tests were designed to provide additional experimental information for developing a model of large air gap flashover. The parameters affecting the corona to leader transition and the leader propagation have also been evaluated. The comparison of the experimental results with theoretical predictions indicates that the simulation of the discharge phenomena is advanced.

1. Introduction

The insulation design of high voltage transmission lines requires very expensive and time consuming experimental testing. Moreover, the problem of designing insulation for switching surges is complicated by the great variety of parameters influencing the dielectric strength of the air gaps. Consequently considerable interest is being shown in developing suitable methods for predicting the switching surge flashover parameters of practical air gaps.

The shape of switching surges significantly affects the flashover of the air insulation. Considerable amount of the existing experimental data is related to the critical waveshape, which gives the results of the minimum value of the switching impulse strength. Nevertheless, the importance of a comprehensive analysis of the effect of the positive switching impulse shape on the dielectric strength of air insulation is shown by the fact that it may lead to an important reduction of the insulation clearances and better criteria for the choice of the impulse shapes used in laboratory tests. Accordingly, part of this paper deals with the influence of the front duration on the positive polarity switching impulse flashover voltage of the transmission line insulation.

* Dr. I. L. KRÓMER, Sasadi út 14., H—1118 Budapest, Hungary

Substantial progress has recently been made in understanding of the switching surge breakdown of long air gaps and in the generation of several physical models for predicting the switching surge flashover characteristics [1—3]. However, at the present time, none of the models is sufficient to predetermine the flashover voltage for all possible conditions influencing the dielectric strength. The incompleteness of existing physical characteristics demonstrates the need for additional detailed experimental data in a variety of gap configurations. So far most of the considerable amount of experimental data have been obtained for rod-plane gaps. Because of the importance of the matter, it is therefore considered worthwhile to carry out special tests in practical conductor-tower air gaps and to apply the acquired data to the refinement of existing calculation methods.

2. Test setup and test procedures

The simulated tower insulation tests were performed at the VEIKI (Institut for Electrical Power Research) outdoor high voltage laboratory in Budapest. The switching impulses were supplied by an all-weather 4 MV, 320 kJ impulse generator, which covered front times of 35 to 1200 μs. Its automatic control system allows for a long series of tests with a reliable control of electric parameters. Voltage measurements were made by a digital crest voltmeter through a general use capacitive voltage divider. The test tower is a steel structure with a 32 meter high and 16 meter wide window. A horizontal truss of 1,1 meter cross-section and movable pseudo-legs permit great flexibility in tower and conductor arrangements. Wire mesh screens 1,1 and 3 m in width and 25 m in length were used to simulate the tower leg. The conductor models were $16 \div 24$ m in length.

The conductor models used for the special predischarge tests were arranged in such a way so that physical measurements were possible. Special precautions were taken to insure, that the phenomena being measured, were predominantly due to the conductors themselves. The test arrangement is shown schematically in Fig. 1.

In order to measure the predischarge current and charge in conductor-tower leg configurations a central section was insulated from the rest of the conductor model. Predischarge current and charge were recorded automatically in a HV Faraday cage connected between the insulated section of the conductor and the impulse generator. This arrangement allowed a shunt connected by means of an insulated measuring cable in series with the central conductor section to measure predischarge current from this region, while excluding current from corona activity in the other parts of the conductor and the thin wire used to connect the HV electrode to the generator. Charge measurements were made with the aid of a series capacitor.

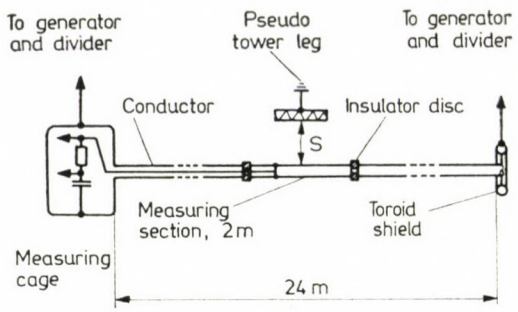

Fig. 1

In order to determine the 50% flashover voltage and standard deviation 200 shots were applied at a four voltage level in the voltage range of $U_{50\%} \pm \pm 2\sigma$. No correction for relative air density or humidity have been considered, because the lack of precise information on these corrections for the tested configurations.

3. Test results

To attack the influence of waveform, four conductor-tower models of different sizes were tested. Minimum clearances were in the range of 2,5 to 6,2 meters.

Table 1 gives the 50% flashover voltage ($U_{50\%}$) and the standard deviation as functions of the waveform. The impulse shapes in the table are determined by their real time-to-crest (T_{cr}) and their time to half value.

It can be seen that $U_{50\%}$ depends significantly on the shape of the switching impulse. There exists a critical time-to-crest for which the insulation breaks down under a minimum voltage. For times-to-crest above or below the critical, the conductor-tower air gaps show higher breakdown voltages. It can also be seen that the critical time-to-crest depends on the clearance of the gap and increases as the clearance increases. The critical time-to-crest is plotted against the gap spacing in Fig. 2. The empirical formula relating to the critical time-to-crest and the gap spacing (S) is:

$$T_{cr} = 45 \times S \tag{1}$$

where T_{cr} — critical time-to-crest in μs,

S — gap spacing in meters.

By analyzing the 50% flashover test results a similarity has been found between the U-shaped flashover characteristics, which can lead to a general expression for determining the switching impulse strength of any conductor-

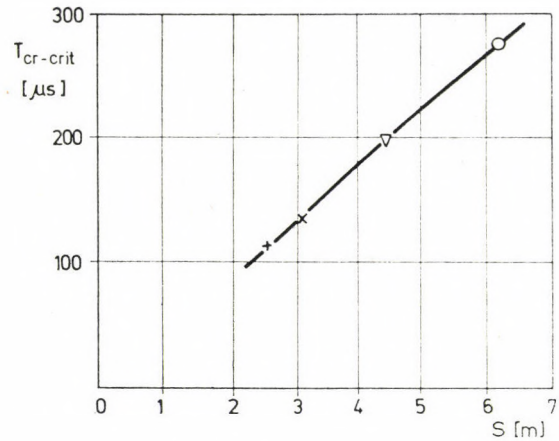

Fig. 2

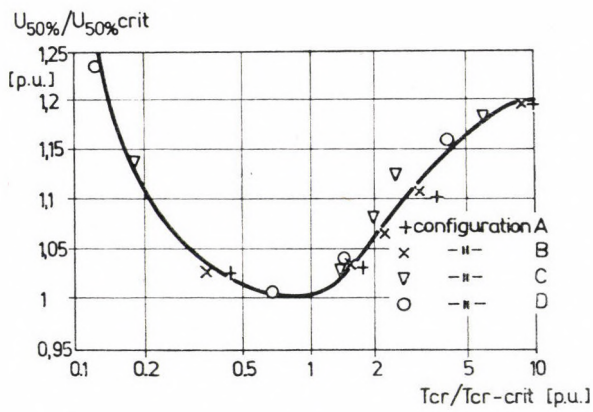

Fig. 3

tower air gap as a function of the time-to-crest. For this purpose the values of $U_{50\%}$ and T_{cr} were reduced to the corresponding critical values. In Fig. 3 the generalized flashover voltage-wavefront characteristics is presented. It can be seen that the deviations from the average curve are in the range of the estimated measurements accuracy.

For numerical purposes a simple expression can be proposed for time-to-crest value $T_{cr} > T_{cr-\text{crit}}$:

$$U_{50\%}(T_{cr}) = U_{50\%-\text{crit}}\left[1{,}255 - 0{,}51\,\frac{T_{cr-\text{crit}}}{T_{cr}} + 0{,}255\left(\frac{T_{cr-\text{crit}}}{T_{cr}}\right)^2\right] \qquad (2)$$

where $U_{50\%-\text{crit}}$ and $T_{cr-\text{crit}}$ are, respectively, the critical flashover voltage and the critical time-to-crest, $U_{50\%}(T_{cr})$ is the flashover voltage corresponding to

time-to-crest $T_{cr} > T_{cr-crit}$. It is interesting to note that the variation of the standard deviation with time-to-crest also shows an U-shaped curve which reaches a minimum value close to the minimum 50% flashover voltage.

The fact, that the generalized flashover voltage-wavefront characteristics is consistent with previous data for rod-plane gaps [4] suggests its applicability to all the gaps whose positively charged electrode has equivalent radius smaller than or equal to the critical radius in the actual configuration [1]. The critical radius is defined as the radius below which the breakdown voltage remains constant. The generalized flashover voltage-wavefront characteristics not only enables an accurate assessment of the switching surge strength of various transmission line configurations for the all ranges of the internal transient voltage stresses, but also an important saving of money by means of reducing the direct laboratory tests.

Table 1

Switching impulse test results: influence of waveshape

Clearance	Waveshape $\mu s/\mu s$	$U_{50\%}$ kV	σ %
2,5	50/1000	943	4,8
	200/1800	950	4,4
	430/2500	1010	6,0
	1150/9900	1100	7,5
3,1	50/1000	1121	4,8
	200/1800	1095	4,7
	300/2200	1160	5,4
	430/2500	1205	6,6
	1150/9900	1305	8,0
4,5	35/1000	1785	8,6
	200/2200	1572	4,7
	280/2300	1622	5,0
	400/2500	1703	5,8
	500/6000	1770	6,4
	1200/10500	1860	7,2
6,2	35/2000	2195	9,8
	190/2270	1783	4,2
	280/2300	1778	3,6
	400/2500	1840	5,5
	1200/10500	2054	6,2

Table 2

Flashover test results

Clearance m	Conductor number	Tower width m	T_{cr} μs	50% CFOV kV
2	1	1,1	175	840
2	2	1,1	175	835
2	1	3	175	820
2	2	3	175	825
2,8	1	1,1	175	1097
2,8	2	1,1	175	1100
3,0	1	3	175	1090
3,0	2	3	175	1100
4,2	2	1,1	200	1480
4,2	2	3,0	200	1380
6,1	4	1,1	300	1900

Since the scope of the special tests was to establish the effect of the gap geometry on the discharge parameters, different conductor-tower leg configurations were selected. The conductor itself was either a single conductor or a bundle of subconductors typical on EHV transmission lines. The 2 and 4-conductor boundles have spacings of 0,4 and 0,6 m, respectively. The results of the flashover test for different configurations are given in Table 2. The values for the critical flashover voltages are consistent with previous data [5].

The breakdown mechanism of long air gaps submitted to positive polarity switching surges includes various stages as first corona, leader inception and leader propagation. The following picture of the breakdown process emerges from physical measurements [6]. As the voltage increases from zero, after the field strength at the high voltage electrode has reached a certain value, the onset of corona is detected by the appearance of short pulses of current. Once corona is formed, due to the effect of the positive space charge left near the high voltage electrode, a streamer initiates. Under the action of the total field the positive space charge moves step by step from the high voltage electrode into the gap. The streamer is able to propagate far into the gap, where the preexisting electrostatic field has values well below the one necessary for collisional ionization. When the streamers have reached a certain size required for the streamer-to-leader transition, the leader development is initiated. The leader channel is preceded by the leader-streamers, emanating from its tip and extending more and more as the leader advances. During the first stage the leader elongates with almost constant velocity and the current flowing through the leader stem is also constant. When the leader-streamers

reach the opposite electrode the final jump starts during which the leader crosses the last part of the gap at increasing velocity. During this stage the leader never stops.

The corona and leader inception times reported in this paper were found from oscillograms of the conductor current. The preparation of the data is based on the principal results of simultaneous optical and current measurements, detailed in the reference [6]. Nevertheless, it should be noted that the interpretation of the records for the conductor-tower leg gap is more difficult than in simpler geometries.

Statistical analysis of the corona and leader inception data has been performed as a function of the applied voltage. It can be stated that the first corona and the continuous leader inception parameters, such as the inception voltage and the charge injected into the gap, are all practically independent of the flashover probability, whilst the total charge, which is injected into the gap during the discharge process, is a function of the applied crest voltage. This observation is representative of all the analysed cases and leads to the conclusion that for practical purposes the experimental investigation of the discharge characteristics can be carried out at the 50% flashover voltage.

In order to record the predischarge phenomena for different configurations a test program with 40 shots per test series was utilized. Corona and leader inception data at the 50% flashover voltage are shown in Table 3. The mean values are listed with their 95% confidence intervals. Fig. 4 shows the variation of the continuous leader inception voltage (U_{1c}) with the gap spacing for various tower width. It can be seen that the dependence of U_{1c} on the gap

Table 3

Corona and leader inception parameters

Clearance m	Conductor No	Tower width	U_i kV	T_i μs	Q_i μs	U_{1c} kV	T_{1c} μs	Q_{1c} μC	T_B μs	Q_B or total μC
2	1	1,1	350±17	22±1	7,2±0,2	744±45	78±5	30,8±1,5	113±13	38,8±2,2
2	2	1,1	380±19	25±1	10,6±0,7	725±64	73±7	32,4±3,3	118±14	38,2±2,5
2	1	3	330±13	22±1	6,9±0,2	680±30	72±3	30,9±1,6	117±10	44,1±2,6
2	2	3	358±18	23±1	10,1±1,4	698±44	70±4	32,1±2,8	120±11	42,8±4,1
2,8	1	1,1	395±21	19±1	7,0±1,3	977±58	82±5	34,9±2,1	130±8	52,4±4,7
2,8	2	1,1	432±18	21±1	10,4±0,6	951±62	81±6	35,4±2,7	145±15	48,9±3,4
3	1	3	378±20	18±1	7,0±0,3	911±48	72±4	36,1±3,8	140±13	51,9±5,2
3	2	3	415±20	21±1	11,0±1,1	957±63	80±6	38,5±4,6	157±19	58,3±5,7
4,2	2	1,1	462±19	18±1	11,2±1,3	1265±70	85±6	42,2±4,1	199±10	75,2±5,2
4,2	2	3	438±21	18±1	10,8±1,5	1175±65	80±5	42,6±4,7	198±11	77,6±6,2
6,1	4	1,1	827±40	39±2	—	1580±85	117±6	—	298±8	—

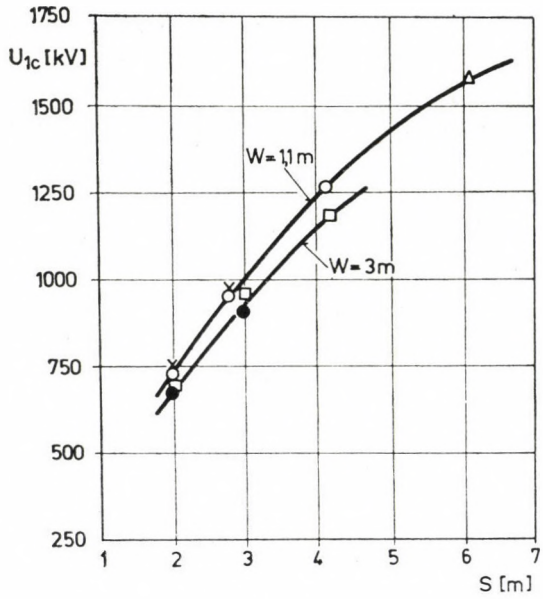

Fig. 4

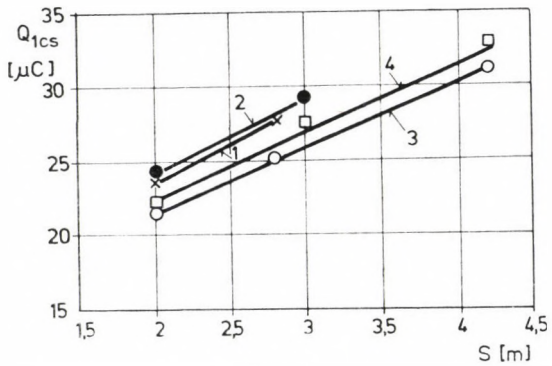

Fig. 5

geometry shows trends which are in agreement with the dependence of $U_{50\%}$ on gap spacing and tower width.

The charge injected into the gap, due to the discharge alone, is obtained by subtracting the magnitude of the charge just before the first corona inception. As the charge measured before the corona inception is purely capacitive, the magnitude of the conductor capacitance can be evaluated. Furthermore, the capacitance was calculated by means of a charge simulation technique. The calculated and the measured values agree to within the 10% estimated accuracy. The results of Table 3 concerning the instantaneous space charge

(Q_{1cs}) when continuous leader propagation begins are summarized in Fig. 5. Note that Q_{1cs} increases with the gap spacing and decreasing the field inhomogeneity at the conductor, a decrease in the value of Q_{1cs} may be observed.

Fig. 6 shows the dependence of the space charge injected during the leader development upon the leader propagation time. The charge injected during the continuous leader propagation grows linearly with the propagation time. If a constant velocity is assumed for the leader propagation ($v = 1{,}5$ cm/μs) the average value of the charge injected per unit for the leader length at the HV electrode during the continuous leader propagation is about 20 μC/m.

On the base of the experimental data listed in Table 3 the continuous leader propagation time has been computed, assuming that the leader tip potential is constant during the continuous propagation stage. The following values of the leader velocity (v_l) and streamer gradient (E_s) were considered in the calculation: $v_l = 1{,}5$ cm/μs, $E_s = 5$ kV/cm. A fair accordance of measured and computed values of continuous propagation time can be observed. Consequently, it may be noted that in the case of critical impulse shape the leader tip potential remains constant. This result is consistent with some conclusions of theoretical approaches [7].

Considerable interest is being shown in the electric gradient of the leader channel due to its importance in predicting the switching surge strength of

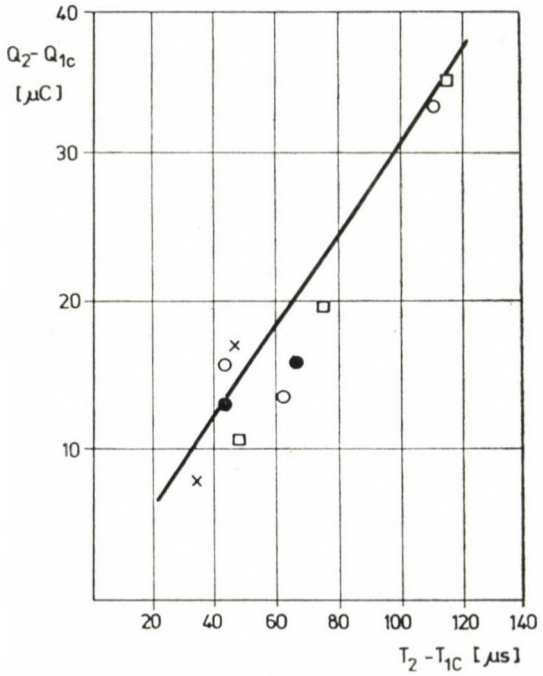

Fig. 6

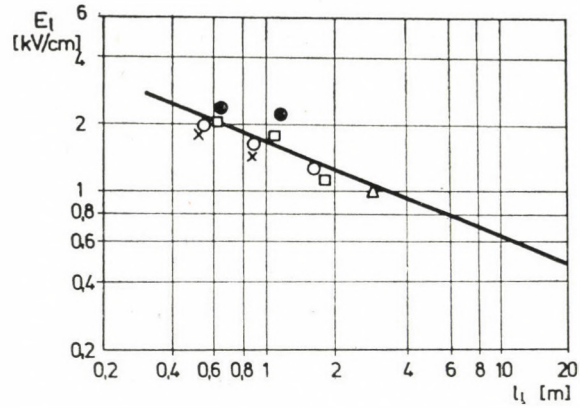

Fig. 7

extra long air gaps. Fig. 7 shows the average leader gradient in function of the leader length (l). To evaluate the leader length, it is assumed that the leader propagates straightforward along the minimum clearance and the leader tip potential remains nearly constant during the propagation. Thus

$$l = S - U_1/E_s \tag{3}$$

Where S the gap spacing E_s — the mean gradient along the streamer filaments ahead of the leader tip at the moment of the final jump. A regression analysis of the measured values leads to an approximate expression:

$$E_l = 1{,}65 \cdot l^{-0{,}42} \tag{4}$$

where E_l in kV/cm, l in meters. This evolution of the average leader gradient is due to the ageing of the channel behind the tip.

4. Approach towards an improved calculation method

The wide range of parameters, such as geometry, waveshape, etc. to which a general model must apply, seems to preclude the success of a physical model by the fact that knowledge of the basic physics involved cannot be inferred from the existing data without the aid of assumptions, Nevertheless, the implication of the outlined experimental results for predicting the switching surge breakdown voltage may lead to a more general applicability of the existing calculation methods.

The experimentally observed constancy of the leader tip potential during the continuous propagation permits the determination of the 50% breakdown voltage as the sum of two voltage components:

— the continuous leader inception voltage U_{1c};

— the voltage increase during the leader propagation, ΔU_l.

The tests results, outlined in this paper, have shown that any modification in the geometry which changes the electric field distribution in the vicinity of the high voltage electrode calls forth a change in the leader inception voltage. The present study stipulates some plausible conditions which govern the streamer to leader transition. For the numerical analysis of the streamer length the following assumption was used. The leader streamers cease to grow when the electric field at the front envelope of the streamers become less than a certain threshold. On the base of optical observations it may be reasonably assumed, that the critical electric field has an average value of 2,1 kV/cm. The existence of such a field value has been experimentally demonstrated [8]. Thus the streamer length can be found by electric field calculations.

To introduce a parameter of equivalence of the gap geometry let us consider the charge injected into the gap before the continuous leader inception, in function of the field divergences. In Fig. 8 the space charge Q_{1c} is reduced to the unit streamer length and plotted as a function of the field divergence. The space charge is assumed to be distributed in such a way that the electric field in the leader streamers tends to become uniform and constant. The choice of the geometrical parameters for the field divergence evaluation is based on the following observations and assumptions. The first value ($x_1 = 0{,}15$ m) is approximately the limit of variation of the critical radius for positively charged conductors [1], the second ($x_2 = 1$ m) is in the range of the critical

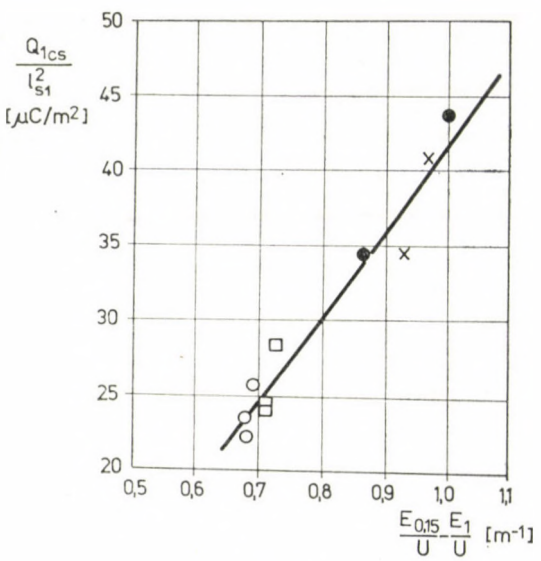

Fig. 8

streamer length needed for the continuous leader propagation. Obviously, the choice of the geometrical parameters is rather arbitrary, but fortunately the results are not too sensitive within given limits of the choice. Note, that the reduced critical space charge linearly grows with the field divergence. This statement provides valuable information concerning the interaction of the electric field with the space charge accumulation.

Assuming that the continuous streamer-leader transition begins, due to a critical amount of the current produced, by the movement of the positive space charge in the applied electric field, in reference to the relationship presented in Fig. 8 the following parameter of equivalence can be proposed for numerical purposes:

$$\mathrm{K} = E_1/U\,(E_{0,15}/U - E_1/U)\,, \tag{5}$$

where $E_{0,15}$ and E_1 — respectively, the field strength at distances 0,15 m and 1 m from the conductor, U — applied voltage across the gap. Fig. 9 shows the computed critical streamer length as a function of the parameter of equivalence in the investigated conductor-tower leg air gaps. A regression analysis of experimental results gives an expression:

$$l_{s1} = 1{,}6 - 3{,}6\,\mathrm{K}\,, \tag{6}$$

where l_{s1} in meters, K in m^{-2}.

The linearity of the obtained relationship $l_{s1} = f(\mathrm{K})$ gives evidence of the applicability of the taken assumptions. This empirical relation can be applied to the numerical evaluation of the critical streamer length of conductor-tower air gaps. Once the critical streamer length has been computed, the leader inception voltage can be found by a simple electric field calculation. On the other hand the voltage increase during the leader propagation can be evaluated with the aid of the leader length, l at the moment of the final jump.

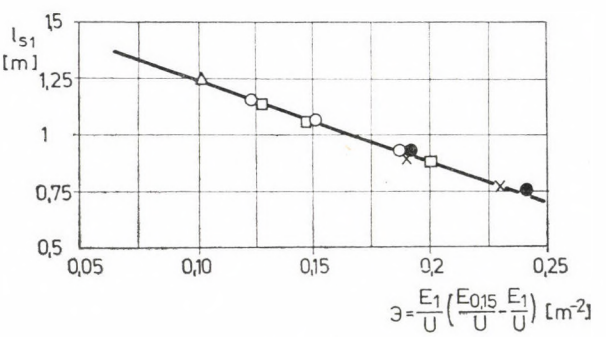

Fig. 9

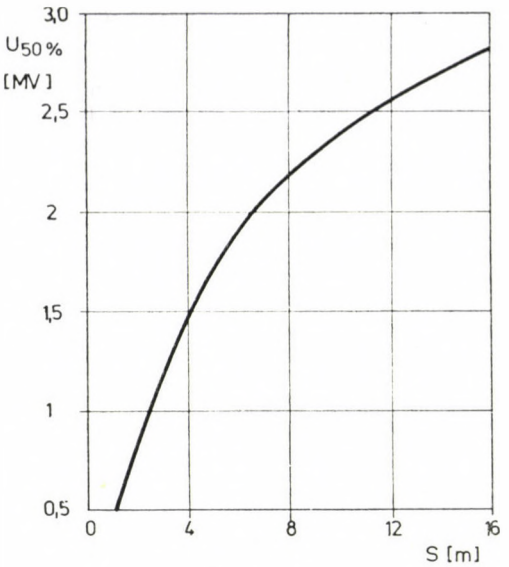

Fig. 10

In order to analyse the possibilities of the proposed model for conductor-tower leg configurations of practical interest, the influence of the field distribution was studied in a wide range of geometrical parameters. Among the promising results for transmission line insulation design, it is interesting to note the computed values of the critical flashover voltage of extra long boundle conductor-tower air gaps. The critical positive switching surge flashover voltages for a wide range of gap distances are shown in Fig. 10. Due to the slight increase of the continuous leader inception voltage at a very long gap distance the increase of the flashover voltage must be mainly attributed to the increase of the leader length. The computed evolution of the flashover voltage as a function of the gap distance is in accordance with new test results [9].

5. Conclusions

1. A generalized 50% flashover voltage-time-to-crest characteristics of transmission line insulation has been established, which enables an accurate assessment of switching surge strength in the whole range of impulse shapes.

2. The space charge needed for the continuous streamer-leader transition is a function of the electric field distribution.

3. In the case of the critical impulse shape the leader tip potential is almost constant during the continuous propagation stage.

4. The average leader gradient decreases with the leader length.

5. An improved model for the prediction of the switching surge strength can be based on the interaction of the critical conditions of streamer-leader transition with the field distribution in the large air gaps.

Acknowledgements

The author would like to acknowledge the helpful support of Dr. B. CSIKÓS (Hungarian Overhead Line Co.) and Dr. K. KARSAI (Institute for Electrical Power Research).

REFERENCES

1. CARRARA, G.—THIONE, L.: Switching Surge Strength of Large Air Gaps: A Physical Approach, *IEEE Transactions on PAS*, **95** (1975), 512—524
2. ALEXANDROV, G. N.: Switching Surge Breakdown Peculiarities of Long Air Gaps, *Elektrichestvo* (1975) № **6**, pp. 15—18
3. LOS, E. J.—SCHNEIDER, H. M.: Switching Surge Breakdown Development in Large Conductor — Tower Air Gaps, *IEEE Transactions on PAS*, **97** (1978), 866—874
4. AIHARA, Y.—HARADA, T.—AOSHIMA, Y.—ITO, Y.: Impulse Flashover Characteristics of Long Air Gaps and Atmospheric Correction, *IEEE Transactions on PAS*, **97** (1978), 342—348
5. GALLET, G.—LEROY, G.—LACEY, R.—KRÓMER, I. L.: General Expression for Positive Switching Impulse Strength Valid up to Extra Long Air Gaps, *IEEE Transactions on PAS*, **94** (1975), 1989—1993
6. *Renardières Group:* Positive Discharge in Long Air Gaps at les Renardières — 1975 Results and Conclusions, N- **53** *Electra* (1977), 31—153
7. BALDO, G.—CORTINA, R.—THIONE, L.: The Dielectric Strength of Large Air Insulation in the Light of the Physics of Discharge, *WELC* № 2—17, Moscow 1977
8. GALLIMBERTI, I.: A Computer Model for Streamer Propagation, *J. Phys. D: Appl. Phys.*, **5** (1972), 2179—2189
9. PIGINI, A.—RIZZI, G.—BRAMBILLA, R.—GARBAGNATI, E.: Switching Impulse Strength of Very Large Air Gaps, *Third International Symposium on High Voltage Engineering* № **52**, 15, Milan 1979

Charakteristiken des Luftfunkenstrecken-Durchschlags infolge von Schaltüberspannungen an Hochspannungsmasten. — Eine Reihe von umfassenden Impulsversuchen an zahlreichen Modellen von Hochspannungsmasten wird beschrieben. Der Einfluß der Wellenform auf die positive Schaltdurchschlagspannung an Hochspannungsmasten wurde durch Anwendung verschiedener Wellen zwischen Zeitdauern von 35 bis 1200 μs bis zum Wellenscheitelwert untersucht. Die Versuchsergebnisse überlappen und überschreiten die zur Verfügung stehenden Daten, wodurch verallgemeinerte flash-over Charakteristiken für die Spannungswellenfront beigestellt wurden. Spezialversuche wurden vorgesehen um weitere Informationen für die Entwicklung eines Modells für flash-over Luftspalte zu erhalten. Auch die Parameter, die den Übergang von der Korona zum Leader und Leaderentwicklung beeinflußen, wurden berechnet. Eine Gegeneinanderstellung der Versuchsergebnisse und der theoretischen Berechnungsresultate bringt den Beweis herbei, daß die Simulation der Entladungserscheinung damit befördert wurde.

Acta Technica Academiae Scientiarum Hungaricae, Tomus 92 (1—2), pp. 153—166 (1981)

CALCULATION METHOD FOR DETERMINING LOAD FREQUENCY CONSTANT

M. FÜREDI*
CANDIDATE OF TECHN. SCI.

and

T. TERSZTYÁNSZKY**
CANDIDATE OF TECHN. SCI.

[Manuscript received 15 August, 1980]

Following a review of several publications the paper describes a new calculation method which can be used for determining long term load frequency constant and frequency exponent by computation based on the consumers' structure and the electrical characteristics of the system. With the use of available information, in the data base of energy economy, the paper presents cases for application. As a main result of calculation it has been found, in the period of 1970—78, that the yearly average resulting load frequency constant for Hungarian consumers was varying between 1,04—1,08 expressed in a non-dimensional value.

1. Introduction

Frequency, i.e. one of the most important quality characteristics of electrical energy, cannot always be guaranteed at its rated value or at a value within a tolerance limit for various reasons in practice.

All calculations carried out so far at home and abroad at system level or at the level of interconnected systems have invariably confirmed that frequency deviation may unfavourably affect the cooperation of electric power systems.

These problems were already the subjects for intensive discussion a few decades ago (when national energy systems were established) in order to create safety for a parallel operation. The reason why interest and research has repeatedly been focussed on these questions at present is that large (both geographically and technically) pools of electric energy systems have been established, which have, in fact, several technical-economic advantages (e.g. keeping frequency more constant), but operate at a frequency, extending over a number of countries, which cannot on their own be changed by the participating systems. Frequency changes would unfavourably influence consumers' operation, and could result in large-scale power flow or even disintegration of an interconnected system [1].

* Prof. Dr. M. FÜREDI, Vahot u. 3. H—1119 Budapest, Hungary
** Dr. T. TERSZTYÁNSZKY, Tomori köz 4, H—1138 Budapest, Hungary

Within this broad field of problems the present paper intends to discuss the calculation method for the reaction of consumer load to frequency changes, and wants to describe a method (using Hungarian consumers as an example) for determining by calculation the frequency characteristics of electricity consumers.

2. Foreign and Hungarian background

Comprehensive inquiries for determining consumers' load frequency constant in various power systems and pools of such systems were carried out in the period following World War II.

Effects of reduced frequencies on active and reactive power input of consumers in the USSR were studied between 1949—1952 both for partial and entire systems [2].

Inquiries made in the USA referred to the period between 1944—1955 when shortages in generating capacities were practically everyday events. Between 1955—1976 system frequency rarely differed from the band of 59,96—60,04 Hz, and, therefore, no further inquiries followed. System breakdowns and their consequences in recent years have again drawn attention to the importance of frequency constant and of determining its value [3].

Calculations for establishing the dependence of active consumers' load on frequency and voltage changes in Switzerland were made from 1950 onwards both in laboratories and for partial networks [4, 5, 6].

In Great Britain, strikes in mining in 1973—74 caused in many cases [3] frequency drops below rated value. Based on experiences from system operation the value of active power response to frequency (n_p) was determined for CEGB ranging from 1 to 3 [7].

The main aim in the Interconnected System of the CMEA countries, within the framework of Section 4 of the Permanent Commission on Electrical Energy, CMEA, beginning from the early 1960's, was to determine the resulting frequency factor for each sytem, but inquiries made in respect of partial networks in the GDR also led to the determination of the value of consumers' frequency factor at a system level [8, 9, 10].

In Hungary's energy system the first investigations made in 1953—54 were to determine the value of the load frequency constant both for partial networks and the national interconnected energy system [11]. Measurement results were used for drawing resulting characteristic curves for a single day and night in each case. These curves were considered to characterize the dependence of system load on frequency.

An inquiry made in 1963 used recordings of the frequency of power exchanges to evaluate the resulting frequency constant of the system [12].

Table 1

Load frequency constant at system level in different countries (published data)

Origin	Date	K_F^*	Description	Remarks
USSR	1949–1952	1,7	day; 60 MW system	1.
USSR	1949–1952	0,9	day; 65 MW system	1.
		1,82	day; system of a capacity of unknown size	2.
		2,0	day; system of a capacity of unknown size	2.
		1,91	day; system of a capacity of unknown size	2.
		3,0	day; 20 MW system	3.
	1942	1,2	unknown circumstances	
	1949	2,6	day; 5000 MW system	2.
USA		1,87	235 MW system	4.
	1978	1,2	333, 300 MW system	4.
		1,32÷1,44	333, 300 MW system	4.
	1974	1,0	unknown circumstances	
Great Britain	1978	1,0÷3,0		4.; 2.
	1964	1,25÷1,43		
CMEA	1965	1,5÷2,0	power system of the GDR	
	1966	1,5÷2,5		
	1978	2,0		2.
	1967	1,5÷2,0		
Other publications	1971	1,0÷3,0		
	1974	2,0		
	1978	1,0÷2,4		
Hungary	1954	1,7	day; 1% frequency drop with 0.8% voltage drop	1.
		2,0	average of nightly measurements; 1% frequency drop with 0,8% voltage drop	1.

Remarks: 1. Automatic voltage regulation is provided; voltage falling parallel with frequency.
2. Voltage falling parallel with frequency.
3. No automatic voltage regulation; voltage dropping parallel with frequency.
4. U = const.

Value of the consumers' frequency constant adopted and used in the Interconnected System of the CMEA is $K_F^* = 2$ [13, 14, 15].

Published calculation results on the value of load frequency constant are contained in Table 1.

Based on these investigations and related results the following important statements can be made:

— in a power pool the area frequency response characteristics of each system is determined either directly by experimental measurements, or from measurement results by using mathematical-statistical method for computation. The use of frequency recordings made from power exchanges is equally suitable but only for determining the resulting frequency factor. Frequency based constant of a system implicitly contains the consumers' load frequency constant, but its value cannot be determined at all from the resultant but can only be estimated;

— load frequency constant is equally determined from experimental measurements;

— values of load frequency determined for each system and published in literature can be compared and adapted with difficulty because the detailed characteristics of each system and of the actual investigations, including the consumers' structure itself, are not known;

— in spite of these factors of uncertainty it can be generally said that the load frequency constant of an energy system is between 0,9—3,0.

The calculation method, based on an analysis of loads and consumption, as described in the following, can be used for determining the load frequency constant for each consumer category and also for the system.

3. Information used for the calculation and available as a data base

Elaboration of the calculation method based on the analysis of the consumption structure, loads and consumption requires a knowledge of the character of the information system used in the country's energy economy and the relative data base. Part of the available data can be directly used, and another part in an indirect way, by applying methodological criteria.

Direct information is obtained from measurement results of monthly measured days. These measurements disclose, inter alia, maximum loads of consumer groups and their relative times. Information given by the electric power system contains the size and date of the national consumers' peak load, as well as frequency values for characteristic dates and periods.

Not contained in the country's data base are consumers' loads are broken down to types of use (e.g. for motors, thermal purposes).

Indirect information is contained in the data base for electric power consumption. From this data base one can learn the data of the annual power consumption by sectors of the big industry, and consumption broken down by uses. The data also contain the annual power consumption by sectors other than big industry, and, within these, electric power consumption by subscribers (broken down by types of uses) who are obliged to making a balance and accounting. This indirect information can be converted into a direct one

generally with the formula:

$$P_{cs} = \frac{W}{t_{cs}}$$

where:

P_{cs} : peak load of the period under review, MW (in this study: a year)
W : power consumption of the period under review, MWh (in this study: year)
t_{bs} : peak utilization hours

4. Description of the calculation method

The system of conditions for the method consists of the following limitations:

— subject of the present paper is the effect of frequency changes on active power input;

— in determining the dependence of consumers' active load on frequency, the related values of peak time in big industry should be considered as a basis;

— annual peak load of each sector takes place at the time of annual peak load of big industry (in good agreement with practical experiences);

— system voltage is unchanged during frequency changes (U = const).

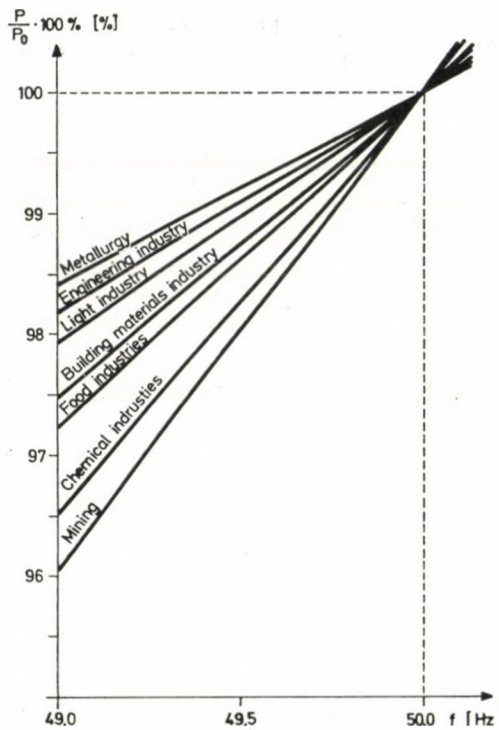

Fig. 1. Percentage variations of active power demand for big industry sectors in function of frequency variations in Hungary in 1978 (U = const.)

For the calculation the indigeneous consumers will be arranged in two groups:

— consumers of big industry (in the following, industrial sectors being marked with index A)

— consumers other than of big industry (total of other consumer groups marked with index E).

Resulting consumers' frequency constant at system level will be obtained (as a non-dimensional value) from frequency constant, summed up, of these two groups:

$$K_F^* = K_{FA}^* + K_{FE}^* = \sum_{i=1}^{m} K_{Fi} + K_{FE}^* \tag{1}$$

where

m: stands for the description of each sector (e.g. mining, metallurgy).

A detailed discussion of the calculation method is given in the Appendix.

4.1. *Determination of frequency characteristics for big industry consumers' load*

Load frequency constant within each sector (see Appendix):

$$k_{Fi} = b_i \cdot \frac{P_i}{f} = \frac{(P_1 + 3P_3)_i}{f} \text{ [MW/Hz]} \tag{2a}$$

which has the following non-dimensional value at system level:

$$K_{Fi} = k_{Fi} \cdot \frac{f_0}{\bar{P}_R} = \frac{(P_1 + 3P_3)_i}{\bar{P}_R} \cdot \frac{f_0}{f} \tag{2b}$$

where

P_1 and P_3 : within the load of each sector, the load depending on f^1 and f^3
$\bar{P}_R$: average annual load of the power system
f : system frequency related to P_i.
f_0 : system related frequency

The expression (2b) can be used for practical computation: in time of annual peak load of big industry, it takes the following form for the i-th sector:

$$K_{Fi} = \frac{\dfrac{W_i + 3W_{3i}}{W_i} \cdot P_{csi}}{\bar{P}_R} \cdot \frac{f_0}{f_{cs}} \tag{2c}$$

where

W_{1i} : electrical energy used in the i-th sector for driving machines and for other mechanical purposes of stationary character [MWh]
W_{3i} : electrical energy used in the i-th sector for compression and ventilation [MWh]*

* It will be noted that the load requirement of compressors changes in accordance with the first power of frequency. The data base in Hungary, however, contains the electrical energy used for compression and ventilation as a single data, and so the share of energy used for compression cannot be singled out from the whole.

W_i : total annual electrical energy use in the i-th sector (MWh]
P_{csi} : sectoral load taking place at the time of maximum annual load (P_{cs}) of measurement days in the big industry
f_{cs} : system frequency valid for the time of P_{cs}.

Resulting sectoral consumers' frequency constant at system level (according to Hungary's data base the number of big industry sectors, $m = 7$):

$$K_{FA}^{*} = \sum_{i=1}^{7} K_{Fi} \,. \tag{3}$$

The value of frequency exponent can be evaluated for each sector by using the relationship

$$b_i = \frac{W_i + 3W_{3i}}{W_i} \,. \tag{4}$$

Load frequency characteristics evaluated for some consumer groups in Hungary are shown in Table 2.

Table 2

Load frequency characteristics evaluated for consumer groups and at system level in 1970, 1975 and 1978

Sectors and resulting values		1970	1975	1978
Mining	b	1,88	1,99	2,01
	K_F	0,1547	0,1362	0,1182
Metallurgy	b	0,64	0,73	0,8
	K_F	0,124	0,117	0,108
Engineering industry	b	0,83	0,86	0,89
	K_F	0,103	0,0918	0,092
Building materials industry	b	1,22	1,2	1,26
	K_F	0,05072	0,052	0,0546
Chemical industry	b	1,89	1,87	1,76
	K_F	0,2431	0,233	0,208
Light industries	b	0,94	0,97	1,03
	K_F	0,0722	0,0704	0,0722
Food industry	b	1,46	1,48	1,4
	K_F	0,0607	0,0599	0,0545
Freq. const. big ind.	$K_{FA}^{*} = \Sigma K_{Fi} K_{Fi}^{*}$	0,808	0,7603	0,7075
Freq. const. other than big ind.	K_{FE}^{*}	0,2654	0,2824	0,3654
Resulting load freq. const.	K_F^{*} $U = \text{const}$	1,073	1,043	1,073

4.2. *Determination of frequency constant for consumers other than big industry*

In section 4.1. we have determined, based on an additional analysis within the category of big industry consumers, also the frequency constant for each sector at system level.

In the category of other than big industry consumers no additional analysis is required since, in their load (consumption), the share of energy used for motors is considerably lower than in the load of the category of big industry (e.g. 28,3% as against 67,5% in big industry in 1978); also their effect on the value of K_F^* is, therefore, smaller.

Based on the Appendix and section 4.1. the resulting load frequency constant of other than big industry consumers is evaluated in the following way:

$$K_{FE}^* = \frac{\frac{W_{1E} + 3W_{3E}}{W_E} \cdot P_E}{\bar{P}_R} \cdot \frac{f_0}{f_{cs}} \tag{5}$$

where

W_E : annual electric power consumption by other than big industry category [MWh],
P_E' : load of other than big industry taking place at the time of P_{cs} [MW].

For determining the value of W_{1E} and of W_{3E} it had to be assumed that the breakdown (in percentage) by types of uses, which can be evaluated from consumption data of consumers being obliged to prepare balance and accounting of other than big industry category, is applicable to the total annual consumption by the category other than big industry.

4.3. *Determination of resulting load frequency constant at system level*

Resulting load frequency constant, as being the sum of frequency constant for consumers of the categories big industry and other than big industry, can be evaluated according to equation (1) in the following way:

$$K_F^* = \frac{f_0}{f_{cs}} \cdot \frac{1}{\bar{P}_R} \left(\sum_{i=1}^{7} \frac{W_{1i} + 3W_{3i}}{W_i} \cdot P_{csi} + \frac{W_{iE} + 3W_{3E}}{W_E} \cdot P_E \right). \tag{6}$$

From relationships contained in Section 4 it can be seen that the exponent of consumers' frequency (b) and the frequency constant (K_F^*) include consumption structure and the character of energy system, as well. If evaluation is carried out with annual data for load and consumption, it will also be possible to follow time (annual) changes of the frequency-dependent characteristics.

5. Applications

5.1. *Evaluation of consumers' load changes in the energy system*

Load frequency constant non-dimensional case at system level is expressed in precentage, according to definition, as follows:

$$K_F^* = \frac{\Delta P_R\,\%}{\Delta f\,\%} \tag{7}$$

where

$$\Delta P_R\% = \frac{P_{R0} - P_R}{P_R} \cdot 100.$$

P_R : consumers' load of energy system related to the actual frequency value,
Δf : frequency deviation,

Frequency-dependent power change, therefore, be:

$$\Delta P_R\,\% = K_F^* \cdot \Delta f\,\%.$$

If we intend to convert consumers' load taking place at $f < f_0$ to f_0, then consumers' load related to f_0 (e.g. annual peak load) can be evaluated, since $\Delta P_R\%$ is known:

$$P_{R_0} = P_R \cdot \frac{1}{1 - \frac{\Delta P_R\,\%}{100}}\ [\mathrm{MW}] \tag{8}$$

By means of Table 2 it can, therefore, be said that, if voltage is assumed to be constant, to a change of 1% in frequency a change of nearly 1,1% in consumers' load at system level can be related.

5.2. *Calculation of active load changes of sectors*

Changes in relative power demand in function of frequency changes can be described, in a general form, by the following equation (see Appendix):

$$\frac{\Delta P}{P} = b \cdot \frac{\Delta f}{f}. \tag{9}$$

By arranging Eq. (9) the active load change of sectors can be evaluated:

$$\frac{P_i}{P_{0i}} \cdot 100 = \frac{100}{1 + b_i \cdot \frac{\Delta f}{f}}\ \% \tag{10}$$

where

P_{0i} : power demand, related to f_0, of the sector in question.

Calculation results within frequency range between 49 and 50 Hz are shown in Fig. 1.

5.3. *Consideration of simultaneous voltage changes*

The calculation method described will yield the load frequency constant for consumer categories and for consumers at system level on the assumption that $U =$ constant. In practical operation, however, some voltage change would inevitably take place, simultaneously with frequency change. Simultaneous voltage change would result in a value above that of load frequency constant determined for $U =$ const [1, 11, 13]

In the light of the empirical data obtained from large power systems, in case of $U < U_{\text{const.}}$ and at system level, $10 \div 20\%$ higher load frequency constant can be expected [3]. Accordingly, for purposes of system operation K_F^* would be usefully taken into consideration with a value of 1,2-times as high. It means that values 1,04—1,073 in Table 2 could be 1,25—1,29.

5.4. *Further possible applications*

Within the system of conditions mentioned the calculation method described, will, in addition, make possible to carry out the following:

— analysis from consumption side of the value of area frequency response characteristics (obtained as an average from experimental measurements and calculations carried out in interconnected systems) and its inner structure while considering the growth of power system and the structural changes in power demand;

— determination of size and character of changes in frequency-dependent production by industrial consumers;

— determination of frequency sensitivity (expected at present and in future) of consumers' power demand.

All of them are relevant for advenced system control.

6. Conclusion

Following a review of available publications the present paper describes a new calculation method which can be used for determining load frequency constant and frequency exponent by computation, based on the consumers' structure and the electrical characteristics of the energy system. With the use of information available in the data base of energy economy the paper presents cases for application in practice. As a main result of evaluations it has been found that, in the period of 1970—1978, the yearly load frequency constant for Hungarian consumers was varying between 1,04—1,08 expressed in non-dimensional value.

APPENDIX

A.1. Functional relationships between consumers' active load and frequency

A.1.1. Determination of frequency exponent (b)

Dependence of active loads of a consumer (consumer group) on system frequency is in a general form [13]:

$$P(f) = P = a_0 + a_1 \cdot f + a_2 \cdot f^2 + \ldots + a_n \cdot f^n = \\ = P_a + P_1 + P_2 + P_3 + \ldots + P_n . \qquad (1.1.1)$$

From an analysis of electrical energy used by consumers, classified according to its uses, and also from the character of consumer installations it follows that the active consumers' load consists in practice and in majority of the following three components:

$$P = P(f) = P_a + P_1 + P_3 \qquad (1.1.2)$$

where

P_a : that (constant) part of the load, which is independent of frequency, e.g. electric lighting, electric resistance furnaces

P_1 : the part of load, depending on first power of frequency; e.g. machine tools, mills, compressors

P_3 : the part of load, depending on third power of frequency; e.g. fans, centrifuges, centrifugal pumps.

Consumers' load can also be written as a direct function of frequency [5]:

$$P = c \cdot f^b \qquad (1.1.3)$$

where

c: proportion factor,
P and f: related values for power and frequency respectively.

The frequency exponent b, found by producing the differential of equations (1.1.2) and (1.1.3), can be expressed as:

$$b = \frac{P_1 + 3P_3}{P} . \qquad (1.1.4)$$

A.1.2. Determination of consumers load frequency' constant

In accordance with definition:

$$k_F = \frac{\Delta P}{\Delta f} \, [\mathrm{MW/Hz}] ,$$

while at system level, in non-dimensional value:

$$K_F = k_F \cdot \frac{f_0}{P} \tag{1.2.1}$$

where

f_0 : rated frequency [Hz],
P_r : characteristic load of the power system, usefully chosen, as a basis for reference [MW].

By producing the differential of equation (1.1.3) we obtain (by abandoning the residual term):

$$\frac{\Delta P}{\Delta f} = b \cdot \frac{P}{f} = k_F \quad [\mathrm{MW/Hz}] . \tag{1.2.2}$$

By using (1.1.4) and (1.2.2) we obtain, from equation (1.2.1) the general form of load frequency constant wanted at system level (in non-demensional form):

$$K_F = \frac{P_1 + 3P_3}{\bar{P}_R} \cdot \frac{f_0}{f}$$

where

$\bar{P}_R$: annual average load of electric power system.

A.2. Structural analysis of load and consumption

The information system of energy economy does not contain the classified loads according to planned uses; it does contain, however, the yearly consumption of electrical energy as broken down to types of uses.

It is, therefore, necessary to convert indirect information (on consumption) to direct information (on loads).

A.2.1. Big industry consumers

It will be assumed that each sector has its maximum load (as measured on the day fixed for this purpose during the year) at the time when daily peak load of big industry is measured during the year. (This assumption is in good agreement with cases in practice.)

Equation (1.1.2) is also valid for sectoral loads, including, therefore, the i-th sector:

$$P_{cs_i} = P_{cs_{ai}} + P_{cs_{1i}} + P_{cs_{3i}} . \tag{2.1.1}$$

Using the annual electric power consumption and also the data of breakdown to types of uses, we obtain for:

— peak utilization hours:

$$t_{cs_i} = \frac{E_i}{P_{cs_i}}; \tag{2.1.2}$$

— part of load, depending on first power of frequency:

$$P_{cs_{1i}} = \frac{W_{1i}}{W_i} \cdot P_{cs_i};$$

— part of load, depending on third power of frequency:

$$P_{cs_{3i}} = \frac{W_{3i}}{W_i} \cdot P_{cs_i}. \tag{2.1.3}$$

A.2.2. Consumers' category of other than big industry

Is marked by P_E. It includes the load of other than big industry taking place at the time of annual peak load of big industry (P_{cs}). Equation (1.1.2) is equally valid in this case:

$$P_E = P_{o_E} + P_{1E} + P_{3E} \tag{2.2.1}$$

By using α, i.e. the factor for the share in peak load, and also the peak utilization hours for the consumers of other than big industry, the equation (2.2.1) will appear in a new form from which the parts of loads dependent on frequency will be obtained:

$$\alpha = \frac{P_E}{P_{cs_E}}; \quad t_{cs\ E} = \frac{W_E}{P_{cs_E}}$$

where

P_{csE} : annual maximum load of consmers other than big industry [MW],
W_E : annual electric power consumption by consumers other than big industry [MW].

Therefore:

$$P_E = \alpha \frac{W_{aE} + W_{1E} + W_{3E}}{t_{cs_E}} = \alpha \cdot P_{cs_E} \cdot \frac{W_{oE} + W_{1E} + W_{3E}}{W_E}, \tag{2.2.2}$$

from which:

$$P_{1E} = \frac{W_{1E}}{W_E} \cdot P_E \tag{2.2.3}$$

and

$$P_{3E} = \frac{W_{3E}}{W_E} \cdot P_E. \tag{2.2.4}$$

REFERENCES

1. ASAL—LUDER—WONG—GOLDSCHMIDT: Disturbances in West-European Network. *Bull. SEV.* **49** (1980) No. 13. (in German)
2. MOSHALEV, A. G.: Frequency Characteristics of Power Supply Systems (in Russian). *Electrichestvo* (1952) No. 9
3. SCHLEIF FERBER R.: Interconnected Power Systems Operation at Below Normal Frequency. *Final Report EPRI*, EL-976, TPS 78—784 1979
4. LAIBLE, TH.: Das Verhalten der Synchronmaschinen, Induktionsmaschinen und Netze bei periodisch schwankender Spannung und Frequenz. *Scientia Electrica* (1954) No. 4
5. JUILLARD, E.: Influence des variations de tension et de fréquence sur la charge absorbée par les consommateurs *Bull. SEV*, **49** (1958) No. 13
6. GADEN, G.: Raport existant entre les variations de la charge consommée par le clientele d'un réseau et les variations de fréquence qui en resultent *Bull. ASE* (1958), No 10.
7. SHACKSHAFT—ASHMOLE: The Influence of Load Characteristics on Power Supply Performance. *CIGRÉ Report* 31—02 (1978)
8. *Permanent Commision on Electric Energy, CMEA.* Analysis of Load Frequency Characteristics. Report of Section **4** (1965) (Russian)
9. VITEK, V.—JOSEFUS, J.: Problems Connected with Automatic Control of Frequency and Power Exchanges. *Publications of Permanent Comm. on Electric Energy, CMEA* (1972), No. **1** (Russian)
10. VITEK, V.—GERTL, V.: Experimental Measurement of Parameters of the Unified Electric Power System of CMEA Countries, using Statistical Methods. *Ibid.*, (1978), No. **12** (Russian)
11. RONKAY, F.—BRAUN, P.: Time Constants and Frequency Factors of Co-operating Power Systems on the Basis of Frequency Recordings of Power Exchanges *VILLENKI Report* (1963) (Hungarian)
12. RONKAY, F.: Regulation of Co-operating Systems. University notes BME-MTKI, 1965 (Hungarian)
13. BENDES, T.: Automatic Load Control and Automatic Devices Used in International Systems "20 Years of Hungary's Electric Power System" (1971), (Hungarian)
14. RONKAY, F.: Technical Conditions for International Co-operation. *6th National Conference on Power Stations*, 1974 (Hungarian)

Eine Berechnungsmethode zur Ermittlung der Konstanten der Belastungsfrequenz. — Nach einer Übersicht von einigen Publikationen wird eine auf die Stromabnehmerkonstruktion und auf die Kennwerte des Systems basierende Berechnungsmethode zur Ermittlung der Konstanten der Belastungsfrequenz und des Frequenzexponents behandelt. Durch die Benutzung der vorhandenen Informationsbasis für die Energiewirtschaft führt die Abhandlung Einzelfälle der praktischen Anwendung vor. Als ein Hauptergebnis der Berechnung wurde in den Jahren 1970 bis 1978 ermittelt, daß sich das Jahresmittel der dimensionslosen Belastungsfrequenzkonstanten der ungarischen Verbraucher zwischen 1,04 und 1,08 befand.

Acta Technica Academiae Scientiarum Hungaricae, Tomus 92 (1—2), pp. 167—187 (1981)

OVERALL BUCKLING OF HYPERBOLIC SHELLS OF REVOLUTION WITH UNMOVABLE LOWER EDGE

E. DULÁCSKA,
CAND. OF TECHN. SCI.*

J. NAGY**—I. BÓDI***

[Manuscript received 12 May, 1980]

The paper treats the general buckling of hyperbolic shells of revolution (i.e. of shells with negative Gaussian curvature), using the linear theory. For the derivation of the critical load the shell of revolution is substituted by a hyperbolic paraboloid having the same curvatures. The numerical values of the critical load are determined for geometric ratios of the shell occurring in the practice, and are presented in a table. Finally, a numerical example shows the application of the method.

1. Introduction

Modern cooling towers are generally built of shells of revolution having a negative Gaussian curvature ("hyperbolic" surfaces). The elevation of such a tower is shown in Fig. 1. Among the hyperbolic shells of revolution the most simple one is the hyperboloid of revolution. This surface can be generated by rotating a pair of hyperbolas around their axis of symmetry not intersecting them. However, they can also be generated by rotating e.g. a parabola or any other curve around the axis.

The dimensions of the cooling towers built of hyperbolic shells of revolution was steadily increasing for years without their stability problem being thoroughly investigated. After the collapse of three cooling towers in Ferrybridge (United Kingdom), 1965 [6], [13], the research in stability of hyperbolic shells of revolution begun. Due to the comparatively short time elapsed since then and to the intricateness of the problem, no exhaustive and easy-to-survey treatment of the subject is to be found, so that there is some uncertainty in the determination of the critical loads of such shells. E.g., due to difficulties in the investigations, the results of the researches are exactly valid only for certain simplified boundary conditions only. There are hardly any results to be found for an elastically supported bottom edge.

* Dr. E. DULÁCSKA
** J. NAGY
*** I. BÓDI
Town Planning Office BVTV
H 1052 Budapest, V.
Városház u. 9—11.

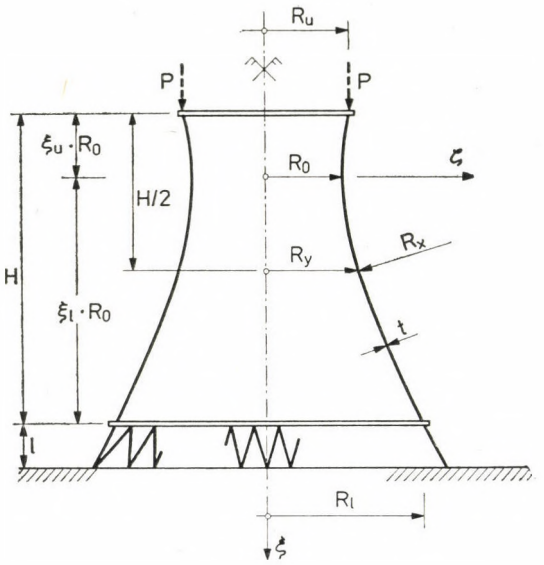

Fig. 1

It is well known that the hyperbolic surfaces with certain geometric ratios and support conditions are able to develop inextensionally [8], [9]. [12], E.g. if we equip both edges of a hyperboloid of revolution by hinge-like diaphragms rigid only in their own planes, the inextensional deformation of the shell will pratically never be prevented.

The shell supported in this way is capable of inextensional deformation in the case of every geometric ratio when, starting from an edge point and proceeding along straight generatrices, we can come back after a finite number of steps into the starting position. The inextensional deformation has a sine shape in both directions, some of which are shown in Fig. 2. Here m denotes the half wave length in the meridional direction and n the full wave length in the ring direction.

If we return to the initial position in a finite number of steps, after going round the circumference once, then the inextensional deformation has only one half wave in the meridional direction ($m = 1$). From this condition the throat radius R_0 of that shell which is capable to such an inextensional deformation can be computed by formula

$$R_{0,\,\text{inextensional}\ (m=1)} = \sqrt{\frac{R_l^2 R_u^2 \left(1 - \cos^2 \frac{\pi}{2n}\right)}{R_l^2 + R_u^2 - 2R_l R_u \cos \frac{\pi}{2n}}} \,. \tag{1}$$

Here n denotes the full wave number in the circumferential direction ($n \geq 2$), while the other notations are explained in Fig. 1.

However, if we prevent the vertical displacement along one of the edges in addition to the hinged diaphragms described above, the inextensional deformation will be excluded. Indeed, there is no possibility of inextensional deformation if we support only one of the edges, but here we prevent two displacement components (e.g. the radial and the vertical ones).

The possibility of the inextensional deformation has a great influence on the buckling of the shell, since in shells having geometric proportions close to those compatible with the inextensional deformation, only insignificant membrane forces arise during buckling, and, due to this circumstance, a low critical load results.

Several older papers on model tests did not mention the support conditions applied in the experiments. Their results often considerably differ from each other. It seems thus probable that the discrepancy could be explained by the difference in the kinds of support. An other possible explanation is that, when investigating experimentally the compression in the meridian direction, the results concerning the general buckling (extending over the whole surface) and the local buckling (see in Sec. 2) were not separated, so that these results could have appeared mixed.

In the last years, however, computer calculations were developed which took the actual boundary conditions of the models into account [14], [15]. The critical loads determined by these computer calculations were in a rather good agreement with the experimental values [15]. These investigations included several loading cases and different boundary conditions. For the

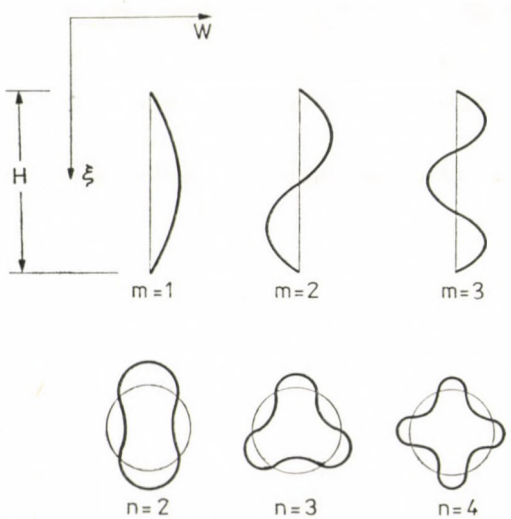

Fig. 2

ratio of the experimental to the calculated critical load the following mean values and variational coefficients were obtained:

— vertical load:	0,96	(0,10)
— lateral pressure:	1,04	(0,12)

Unfortunately, not every engineer has access to the aforementioned computer calculations. Moreover, it will take a long time before, on the basis of numerical examples calculated by the exact computer programs, practical recommendations can be set up. Hence it seems necessary to present some less accurate but easy-to-use results and methods obtained by simpler means.

2. Boundary conditions, assumptions and approximations

The boundary conditions to be taken into consideration in the stability analysis of hyperbolic shells of revolution used as cooling towers depend on their structural solution and are as follows:

At the *upper edge* mostly a stiffening ring is applied, due to which the following boundary conditions apply for the buckling of the shell:

$$w = \partial^2 w_1/\partial x^2 = v = n = 0 .$$

(The definitions of the internal forces and displacements are to be found in Fig. 5.)

At the *lower edge* a stiffening ring is applied in every case, sometimes realized by the thickening of the shell wall. The ring at the lower edge is mostly supported by a truss resting on the soil, through which the cooling air can stream into the tower. The compression of this truss and the subsidence of the foundation act as an elastic support on the shell. However, we cannot take this kind of support into consideration yet. Hence we consider the lower shell edge in the vertical direction either free to displace (soft foundation) or unmovable (rigid foundation), otherwise the edge is supposed to be hinged. The actual stiffness values of the foundation mostly lie close to the rigid ones [17].

In the case of a soft foundation the boundary conditions of the lower edge are, with respect to the buckling deformation and internal forces, as follows:

$$w = \frac{\partial^2 w}{\partial x^2} = v = n_x = 0 .$$

The rigid foundation can be characterized by the boundary conditions:

$$w = \frac{\partial^2 w}{\partial x^2} = v = u = 0 .$$

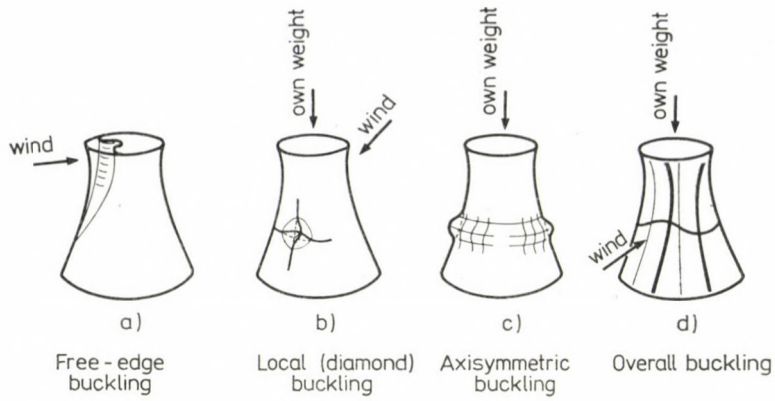

Fig. 3

The hyperbolic shells have four characteristic *buckling modes.*

In the case of a free upper edge, the wind pressure may cause a buckling pattern shown in Fig. 3a [4], which we shall call *free edge buckling.*

The meridional directed forces may cause *local buckling* in a diamond-shaped pattern show in Fig. 3b. This phenomenon is similar to the buckling of cylinders under axial compression. The boundary conditions do not influence this buckling mode, since usually in the vicinity of the upper edge ring the meridian directed forces are small, so that they cause no local buckling here, while near the lower edge the usual thickening of the shell wall prevents the local buckling.

In this paper we do not treat these two buckling modes.

The meridional directed forces may also cause an *axisymmetric buckling* shown in Fig. 3c. We will not deal with this mode separately, however, because, on the one hand, it yields a higher critical load than the other modes [16], on the other hand, it represents a special case of the overall buckling, to be treated next.

The reticulated buckling pattern, extending to the entire surface (Fig. 3d), is called *overall buckling.* This buckling mode is markedly influenced by the boundary conditions, and can be caused not only by the meridional directed but also by the hoop forces.

In the following we will treat the overall buckling mode.

The classical (linear) critical value of the meridional directed force, which causes overall buckling extending to the entire surface, is usually described by the following formula:

$$n_{x,\,cr} = \lambda \frac{Et^2}{R_y}, \tag{2}$$

where E is the modulus of elasticity, while t and R- are shown in Fig. 1.

For the factor λ, various researchers obtained different results from the evaluation of model tests:

[1] KRÄTZIG (1968):	$\lambda = 0{,}079$
[3] ROSEMEIER:	$\lambda = 0{,}07 \sim 0{,}10$
[4] DER and FIDLER:	$\lambda = 0{,}18$
[7] WIANECZKI:	$\lambda = 0{,}12$
[5] MATEJA:	$\lambda = 0{,}21 \sim 0{,}27$

The lowest value among the above results is only one fourth of the highest one.

As possible reasons for this discrepancies we may mention the different geometric ratios and boundary conditions, occurring in the model tests of the various authors.

The next step was made by KRÄTZIG [2] who calculated numerical tables, from which we can set up the following expression for λ:

$$\lambda = (1{,}13 \sim 1{,}85) \sqrt[3]{\frac{t}{4R_0}} .$$

His tables make possible to compute the values of $n_{x,cr}^{\text{lin},0}$ and $n_{y,cr}^{\text{lin},0}$ separately, as functions of the ratio of throat to lower radii R_0/R and of the dimensionless height factor ξ_l. Here $n_{x,cr}^0$ and $n_{y,cr}^0$ are critical forces in the cases $n_y = 0$ and $n_x = 0$ respectively. From these two values the actual critical force, valid for a given case, can be computed from a Dunkerley-type relation.

Unfortunately, these tables do not allow to take the influence of the dimensions of the upper part of the tower (above the throat) and of the ratio R_y/t properly into account. The critical loads computed by these tables give results that are by $30 \sim 50\%$ higher than those obtained by exact computations confirmed by model tests [15].

It should be mentioned that there is a proposal [10] to take the critical load of the shell considered capable of inextensional deformation as the actual one. This method certainly yields a safe but far too low value, not confirmed by the practice. Due to all these circumstances we developed a method by which the influence of the geometric parameters and the boundary conditions can be taken into account.

In the analysis we stipulate that the material of the shell is linearly elastic. The shell is stiffened along its lower and upper edge by rings which can be regarded as rigid in their planes, so that the radial displacements of these edges are equal to zero. As far as the lower vertical support of the shell is concerned, we stipulate either that it is free to move in the meridional direction (soft foundation), or that no meridional displacement can come about at all (rigid foundation).

We determine the critical load on the basis of the linear buckling theory of the shallow shells approximately, since we substitute a hyperbolic paraboloid for the hyperboloid of revolution and compute the critical load of this former one. The width of the hyperbolic paraboloid equals the buckling wavelength in the circumferential direction of the original shell, see Fig. 4.

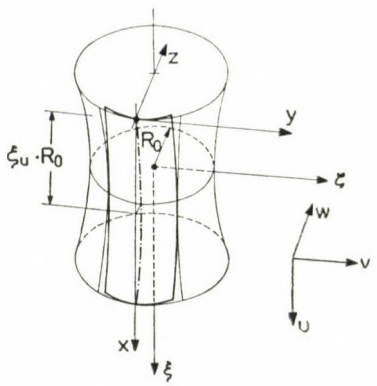

Fig. 4

Since the hyperbolic paraboloid is a translational surface and, therefore, has no twist, it is less rigid than the hyperbolic shell of revolution, and has a somewhat lower critical load, which is, however, much more easy to determine.

The radius of curvature in the y direction, R_y, of the substituting hypar is assumed to be equal to the horizontal radius R_y of the shell of revolution at its half way height. For the other radius of the hypar, R_x, we choose, in the halfway height of the tower, the radius of curvature of the flat parabola arc which lies in common plane with the axis of revolution and passes through the end points of R_u, R_y and R_l (Fig. 1), i.e.:

$$R_x = \frac{H^2}{8\left(\frac{R_u + R_l}{2} - R_y\right)} . \tag{3}$$

By using these data, we can write the equation of the substituting hypar surface (Fig. 4) as follows:

$$z = -\frac{x^2}{2R_x} + \frac{y^2}{2R_y} + \frac{\xi_u R_0 x}{2R_x} . \tag{4}$$

The definitions of the internal forces and displacements are shown in Fig. 5.

3. The equations of buckling

The condition of the neutral equilibrium state of the shell structure can be expressed by the theorem of the minimum potential energy [11], according to which the second variation of the potential energy Π has to be equal to zero:

$$\delta^2 \Pi = 0 \,. \tag{5}$$

Assuming zero value for Poisson's ratio, the above condition can be established for shallow shells, using the notations of Fig. 5,

$$\delta^2 \Pi = \int_{(T)} (n_{x0}\, w'^2 + 2n_{xy0}\, w' \dot{w} + n_{y0}\, \dot{w}^2)\, dT +$$

$$+ B \int_{(T)} (w''^2 + 2w'^2 + \ddot{w}^2)\, dT + \frac{1}{D} \int_{(T)} (F''^2 + 2F'^2 + \ddot{F}^2)\, dT = 0, \tag{6}$$

where T denotes the area of the buckle.

In addition, we have to use the compatibility equation:

$$F'^{\vee} + 2F''^{\cdot\cdot} + \ddot{F}^{\cdot\cdot} = -D(\ddot{z}\, w'' - 2\dot{z}' w' + z'' \ddot{w}). \tag{7}$$

In these two equations prime and not denote differentiation with respect to x and y respectively, the subscripts zero of the internal forces refer to their initial values, i.e. to the pre-buckling stress state, w is the z-directed buckling displacement, F is the pertaining stress function, $B = Et^3/12$ and $D = Et$ are the bending and tensile stiffnesses, respectively. The internal forces that arise during buckling are to be computed from the stress function F according to the formulas:

$$n_x = \ddot{F}; \; n_{xy} = -F'; \; n_y = EF'' \,. \tag{8}$$

The procedure of the determination of the critical force begins with assuming the deformation w which satisfies the boundary conditions. This will be introduced into the compatibility equation (7) and the stress function F will be expressed herefrom. After the determination of the necessary derivatives of F and w, the x-directed critical force $n_{x,cr}$ is to be computed from the rearranged Eq. (6), with the assumptions $n_{y,0}/n_{x,0} = \text{const.}$ and $n_{xy,0} = 0$:

$$n_{x,cr} = \frac{B \int_{(T)} (w''^2 + 2w'^2 + \ddot{w}^2)\, dT + \frac{1}{D} \int_{(T)} (F''^2 + 2F'^2 + \ddot{F}^2)\, dT}{\int_{(T)} \left(1 - \eta \frac{x}{H}\right) \left(w'^2 + \frac{n_{y,0}}{n_{x,0}} \dot{w}^2\right) dT} \,. \tag{9}$$

The value of the factor η depends on the character of the vertical load. In the case of a line load P acting uniformly distributed along the upper edge of the shell (i.e. a "concentrated" load on top of the structure), $\eta = 0$. In the case of a surface load uniformly distributed along the vertical x direction with the intensity q per unit height (that approximately corresponds to the own weight of the hyperbolic shell), $\eta = 1$. Hence the factor η can be expressed as follows:

$$\eta = \frac{1}{1 + \dfrac{P}{qH}} .$$

4. Determination of the critical force

We assume for the buckled shape the function

$$w = \sin \frac{n\pi}{R_y} \sum_{(m)} A_m \sin \frac{m\pi}{H} x , \tag{10}$$

which satisfies the boundary conditions $w = 0$ and $w^{||} = 0$ along the edges of the substituting hyperbolic paraboloid. Here m and A_m denote the number and the corresponding amplitude of the half buckling waves in the x direction, respectively.

To this w pertains the stress function

$$F = D \sin \frac{n\pi}{R_y} \sum_{(m)} A_m F_m \sin \frac{m\pi}{H} x . \tag{11}$$

The values of w, $w^{''}$ and $F^{||}$ are equal to zero along the edges $x = 0$ and $x = H$. Hence there is no change either in curvature or in normal force across these boundaries, moreover the condition $v = 0$ is also satisfied along the upper and lower edges.

Introducing Eqs (10) and (11) for w and F into the compatibility equation (7), the coefficient F_m can be written in the form:

$$F_m = \frac{-\beta/R_x + m^2\alpha/R_y}{(\beta + m^2\alpha)^2} , \tag{12}$$

where

$$\alpha = \frac{\pi^2}{H^2} ; \qquad \beta = \frac{n^2}{R_y^2} . \tag{13a,b}$$

Performing the integrations in Eq. (9) we arrive at the following expression for the critical force:

$$n_{x,cr} = D \frac{\sum\limits_{(m)} (\beta + m^2 \alpha)^2 \left(\frac{B}{D} + F_m^2 \right) A_m^2}{\left(1 - \frac{\eta}{2}\right) \sum\limits_{(m)} \left[(\beta\gamma + m^2 \alpha) A_m^2 \right] + \Delta} \tag{14}$$

with

$$\gamma = n_{y,0}/n_{x,0}$$

and

$$\Delta = -\eta \int_0^H \frac{y}{H} \cdot \frac{\pi R_x}{2n} \left\{ \left[\sum_{(m)} A_m \frac{m\pi}{H} \cdot \cos \frac{m\pi}{H} y \right]^2 + \right.$$

$$\left. + \gamma \frac{n^2}{R_x^2} \left[\sum_{(m)} A_m \sin \frac{m\pi}{H} y \right]^2 \right\} dy .$$

The term Δ, as it is to be seen, depends on the geometric parameters of the shell, on η and on the value and sign of $A_m \cdot \eta = 0$ yields $\Delta = 0$.

Since the computation of the term Δ is — due to the necessary integrals — rather cumbersome, we investigated whether it can be neglected in Eq. (14). We found that when neglecting Δ, the critical (total) value of the load uniformly distributed along the height becomes twice as much as that of the line load acting along the upper edge. This ratio corresponds to that valid for compressed straight bars.

A more thorough analysis of Δ showed that taking Δ into account always reduces the critical load of compressed bars obtained by the approximation $\Delta = 0$ by 6 per cent, but in the cases of hyperbolic shells of revolution it may either increase or reduce the critical load obtained by the approximation $\Delta = 0$, depending on the buckling shape. Visually it can be said that if the buckling shape bulges in the lower section (two-hinged bar loaded by its own weight), than taking Δ into account always reduces while in the opposite case it increases the critical load.

As it will be shown later, the shell with unmovable lower edge always buckles in a shape that bulges in its lower section. Thus, taking Δ into account always increases the critical load obtained by the approximation $\Delta = 0$.

However, this increase is significant only in the case of the buckling wave characterized by $m = 1$. According to our detailed calculations, in the case of hyperbolic shells of revolution with completely restrained lower-edge displacements, we commit only a slight error, always to the benefit of safety.

Now we have to choose the characteristic parameters (A_m; $n = 2, 3, 4, \ldots$; $m = 1, 2, 3, \ldots$) in such a way as to fulfill the unmovability condition of the lower edge in the vertical direction, furthermore to produce the minimum critical force.

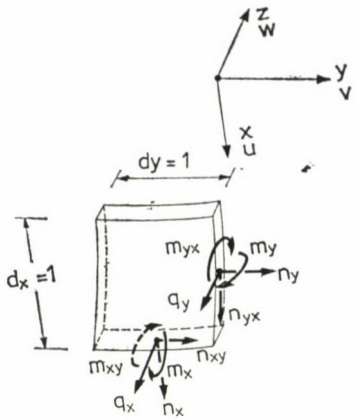

Fig. 5

Using the approximations of the shallow shell equations and those of the linear buckling theory, the vertical displacement of the lower edge can be written as follows:

$$u' = \frac{w}{R_x} + F'' \,. \tag{15}$$

Substituting for w and F their expressions (10) and (11) and performing the integration we arrive at the relation

$$u = \sum_{(m)} \frac{A_m}{m\sqrt{\alpha}} \left(\frac{1}{R_x} + \beta F_m \right) \tag{16}$$

which is easy to compute. If $u = 0$ is prescribed, Eq. (16) turns over into a relation between the coefficients A_m.

If we try to solve the problem by taking one single term for w with m_j ($j = 1, 2, 3, \ldots$) half waves, we obtain meridional directed displacements along the lower edge. Among these buckling shapes that one furnishes the lowest critical load which lies closest to the inextensional deformation shape.

If we prevent the vertical displacements of the lower edge, the buckling shape consists of the sum of several w terms with various m values. Namely, each term furnishes a meridional displacement, so that at least two terms are needed to cancel each other's effect.

We investigated: how many terms in w are necessary to obtain the minimum critical load (fulfilling the boundary condition $u = 0$)? We have found that they are always two term that yield the minimum critical load. This is visually shown in Fig. 6. The variation along the circumference of the

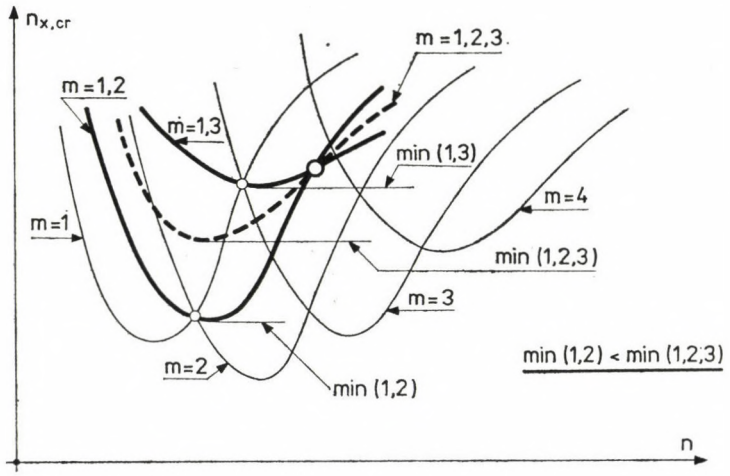

Fig. 6

critical forces pertaining to the individual terms m_j $(j = 1, 2, 3, \ldots)$ are shown with thin full lines as functions of the wave number n in circumferential direction (considering n as a continous variable).

When two waves with different m-values (e.g. $m_1 = 1$ and $m_2 = 2$) combine, the critical force pertaining to the combined wave (m_1, m_2) falls between those corresponding to the individual waves m_1 and m_2. Hence the curve representing the critical force of the combined wave (heavy full line in Fig. 6) passes through the intersection point of the curves pertaining to m_1 and m_2. If three waves combine (e.g. m_1, and m_3), the corresponding critical force dashed line in Fig. 6) falls between those pertaining to (m_1, m_2) and (m_2, m_3).

The curves clearly show that the minimum value of the critical force is given in any case by the combination of two individual waves.

Hence, in the formulas, the symbol Σ always denote the sum of *two* values. Be these values $m_1 = i$ and $m_2 = k$, so we obtain from Eqs (14) and (16) for the expressions of the critical force and for the boundary condition (neglecting Δ) the following:

$$n_{x,\,cr} = D \frac{(\beta + m_i^2 \alpha)^2 \left(\frac{B}{D} + F_i^2\right) A_i^2 + (\beta + m_k^2 \alpha)^2 \left(\frac{B}{D} + F_k^2\right) A_k^2}{\left(1 - \frac{\eta}{2}\right) \left[(\beta\gamma + m_i^2 \alpha) A_i^2 + (\beta\gamma + m_k^2 \alpha) A_k^2\right]}; \quad (17)$$

$$u = 0 = \frac{A_i}{i\sqrt{\alpha}} \left(\frac{1}{R_x} + \beta F_i\right) + \frac{A_k}{k\sqrt{\alpha}} \left(\frac{1}{R_x} + \beta F_k\right). \quad (18)$$

Eq. (18) furnishes the relation between A_i and A_k.

In a given case we can determine the critical force numerically. This will be shown at the end of the paper in the numerical example.

5. The values of the critical force

According to our assumptions, the buckling of the shell depends on the meridian directed force n_x and the hoop force n_y. The interaction curve is a straight line if we restrict ourselves to a unique buckling shape (with given n, $m_1 = i$ and $m_2 = k$). This relation is depicted in the co-ordinate system n_x, n_y in Fig. 7.

In the following $\bar{n}_{x,cr}$ and $\bar{n}_{y,cr}$ denote the critical values of the internal forces n_x and n_y respectively, that cause buckling alone (the other force having zero value) with a given buckling shape. Both corresponding loading cases are shown in Fig. 8. As a matter of fact, to the two minimum critical values

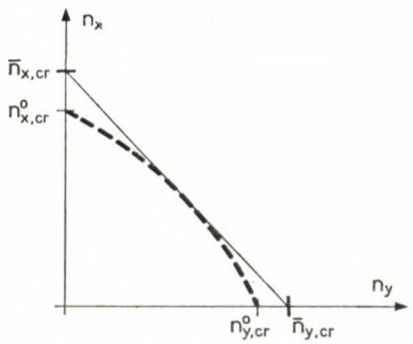

Fig. 7

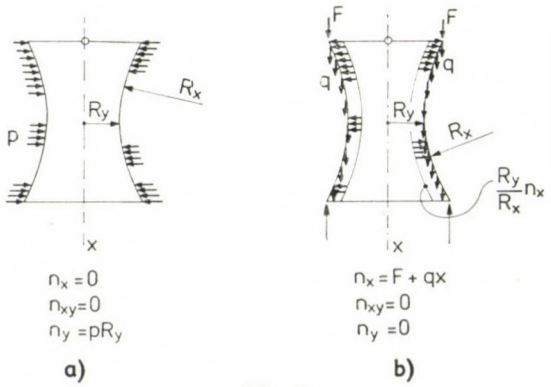

Fig. 8

Table 1

Values of λ_x^0

$$n_{x,cr}^0 = \lambda_x^0 \frac{Et^2}{R_y}$$

R_y/t	100										
H/R_y	1	2	3	4	5	6	7	8	1	2	3
$R_x/R_y =$ 1	0,256	0,182	—	—	—	—	—	—	0,221	0,131	—
2	0,345	0,224	0,164	0,137	—	—	—	—	0,255	0,180	0,142
3	0,354	0,246	0,198	0,183	0,152	0,128	—	—	0,311	0,212	0,169
4	0,387	0,289	0,227	0,188	0,179	0,183	0,132	—	0,356	0,240	0,178
5	0,413	0,316	0,256	0,241	0,202	0,166	0,170	0,142	0,370	0,252	0,215
6	0,431	0,344	0,287	0,255	0,204	0,192	0,186	0,153	0,387	0,276	0,231
7	0,448	0,370	0,298	0,258	0,226	0,237	0,176	0,192	0,407	0,305	0,253
8	0,462	0,392	0,314	0,264	0,240	0,238	0,192	0,199	0,427	0,333	0,265
9	0,474	0,410	0,332	0,277	0,261	0,244	0,217	0,192	0,443	0,349	0,272
10	0,485	0,424	0,349	0,294	0,288	0,246	0,247	0,199	0,454	0,364	0,284

Table 2

Values of λ_y^0

$$n_{y,cr}^0 = \lambda_y^0 \frac{Et^2}{R_y}$$

R_y/t	100										
H/R_y	1	2	3	4	5	6	7	8	1	2	3
$R_x/R_y =$ 1	0,297	0,181	—	—	—	—	—	—	0,239	0,138	—
2	0,183	0,115	0,091	0,070	—	—	—	—	0,151	0,087	0,069
3	0,142	0,091	0,075	0,057	0,049	0,045	—	—	0,119	0,075	0,059
4	0,134	0,092	0,062	0,055	0,050	0,040	0,034	—	0,094	0,060	0,049
5	0,134	0,070	0,054	0,049	0,039	0,034	0,037	0,028	0,087	0,058	0,045
6	0,136	0,062	0,053	0,040	0,037	0,036	0,028	0,030	0,084	0,057	0,040
7	0,137	0,058	0,051	0,038	0,034	0,032	0,027	0,027	0,084	0,050	0,036
8	0,139	0,057	0,044	0,039	0,034	0,029	0,029	0,023	0,084	0,044	0,035
9	0,140	0,057	0,040	0,040	0,031	0,026	0,029	0,022	0,086	0,041	0,036
10	0,141	0,057	0,037	0,035	0,030	0,025	0,025	0,023	0,087	0,040	0,036

200					300							
4	5	6	7	8	1	2	3	4	5	6	7	8
—	—	—	—	—	0,184	0,127	—	—	—	—	—	—
0,133	—	—	—	—	0,232	0,157	0,114	0,160	—	—	—	—
0,130	0,114	0,105	—	—	0,267	0,176	0,137	0,124	0,099	0,093	—	—
0,159	0,152	0,155	0,110	—	0,312	0,209	0,166	0,133	0,120	0,174	0,101	—
0,169	0,147	0,136	0,135	0,122	0,346	0,235	0,179	0,164	0,135	0,125	0,121	0,115
0,193	0,176	0,170	0,136	0,159	0,374	0,249	0,198	0,172	0,152	0,146	0,115	0,197
0,218	0,200	0,164	0,144	0,162	0,386	0,264	0,228	0,177	0,157	0,137	0,135	0,140
0,228	0,194	0,170	0,177	0,146	0,403	0,286	0,234	0,192	0,168	0,161	0,160	0,130
0,245	0,203	0,183	0,191	0,151	0,420	0,309	0,244	0,218	0,183	0,179	0,148	0,138
0,257	0,220	0,208	0,186	0,170	0,430	0,329	0,262	0,234	0,208	0,183	0,155	0,165

200					300							
4	5	6	7	8	1	2	3	4	5	6	7	8
—	—	—	—	—	0,195	0,121	—	—	—	—	—	—
0,067	—	—	—	—	0,123	0,080	0,060	0,081	—	—	—	—
0,046	0,038	0,035	—	—	0,109	0,063	0,048	0,043	0,034	0,030	—	—
0,040	0,035	0,034	0,041	—	0,088	0,056	0,045	0,034	0,029	0,038	0,024	—
0,035	0,032	0,030	0,029	0,023	0,073	0,047	0,037	0,032	0,030	0,028	0,026	0,021
0,034	0,032	0,026	0,027	0,031	0,069	0,046	0,037	0,028	0,025	0,022	0,019	0,035
0,033	0,026	0,023	0,023	0,021	0,066	0,044	0,032	0,027	00,23	0,021	0,022	0,018
0,029	0,025	0,022	0,022	0,018	0,065	0,045	0,031	0,026	0,022	0,021	0,018	0,016
0,027	0,025	0,023	0,020	0,019	0,065	0,039	0,029	0,025	0,022	0,020	0,017	0,017
0,026	0,022	0,022	0,018	0,021	0,066	0,035	0,028	0,024	0,020	0,018	0,016	0,016

Table 3

Values of λ_x

R_y/t	100										
H/R_y	1	2	3	4	5	6	7	8	1	2	3
$R_x/R_y = 1$	0,143	0,096	—	—	—	—	—	—	0,115	0,067	—
2	0,188	0,121	0,086	0,069	—	—	—	—	0,145	0,089	0,072
3	0,207	0,140	0,105	0,089	0,075	0,066	—	—	0,193	0,113	0,086
4	0,235	0,162	0,119	0,103	0,100	0,086	0,067	—	0,193	0,124	0,093
5	0,267	0,194	0,141	0,124	0,098	0,084	0,094	0,070	0,213	0,137	0,114
6	0,297	0,203	0,151	0,127	0,109	0,106	0,089	0,082	0,230	0,163	0,122
7	0,323	0,207	0,168	0,131	0,118	0,116	0,090	0,103	0,251	0,180	0,131
8	0,346	0,217	0,187	0,143	0,130	0,122	0,105	0,095	0,271	0,199	0,137
9	0,365	0,230	0,207	0,158	0,149	0,121	0,125	0,098	0,290	0,199	0,149
10	0,382	0,244	0,207	0,175	0,156	0,123	0,141	0,106	0,309	0,203	0,163

$\bar{n}_{x,cr} = n^0_{x,cr}$ and $\bar{n}_{y,cr} = n^0_{y,cr}$, different buckling shapes belong. Consequently the straight line starting from $n^0_{x,cr}$ representing the linear interdependence, intersects the n_x axis at a value n_y higher than $n^0_{y,cr}$. The same statement holds for the other axis as well. We thus obtain two tangents which the slightly bulged curve, characterizing the interaction between the critical values of n_x and n_y, has to osculate. This curve can be approximated to the benefit of safety by the Dunkerley-type streight line (Fig. 9):

$$\frac{n_y}{n^0_{y,cr}} + \frac{n_x}{n^0_{x,cr}} = 1\,. \tag{19}$$

The values of the critical forces $n^0_{y,cr}$ and $n^0_{x,cr}$ can be expressed as follows:

$$n^0_{y,cr} = \lambda^0_y \frac{Et^2}{R_y}\,, \tag{20}$$

$$n^0_{x,cr} = \lambda^0_x \frac{Et^2}{R_y}\,. \tag{21}$$

We here determined the values λ^0_y and λ^0_x, referring to a lower edge unmovable in the meridional direction, according to the method described above, and compiled them in Tables 1 and 2. (The values are given only for possible geometric ratios).

To assess the outwards bulging of the interaction curve we computed the value of one of its mid-points which corresponds to a shell loaded at the

200					300							
4	5	6	7	8	1	2	3	4	5	6	7	8
—	—	—	—	—	0,095	0,062	—	—	—	—	—	—
0,067	—	—	—	—	0,120	0,079	0,058	0,081	—	—	—	—
0,067	0,057	0,053	—	—	0,153	0,094	0,070	0,066	0,050	0,046	—	—
0,080	0,075	0,073	0,054	—	0,189	0,115	0,087	0,067	0,059	0,081	0,049	—
0,086	0,077	0,071	0,073	0,059	0,093	0,123	0,091	0,081	0,071	0,067	0,065	0,056
0,107	0,094	0,081	0,067	0,085	0,206	0,131	0,110	0,090	0,075	0,070	0,058	0,106
0,112	0,096	0,085	0,076	0,078	0,219	0,149	0,116	0,091	0,084	0,071	0,073	0,066
0,125	0,099	0,087	0,094	0,073	0,236	0,166	0,121	0,105	0,086	0,087	0,076	0,065
0,126	0,110	0,099	0,094	0,079	0,253	0,181	0,133	0,116	0,099	0,089	0,074	0,072
0,129	0,117	0,113	0,091	0,094	0,270	0,197	0,140	0,117	0,104	0,092	0,081	0,087

top by meridional directed forces. In this case, besides n_y also a hoop force

$$n_y = n_x \frac{R_y}{R_x} \tag{22}$$

arises, and the critical force can be described by the expression

$$n_{x,cr} = \lambda_x \frac{E_t^2}{R_y} . \tag{23}$$

The computed values of λ_x are to be found in Table 3.

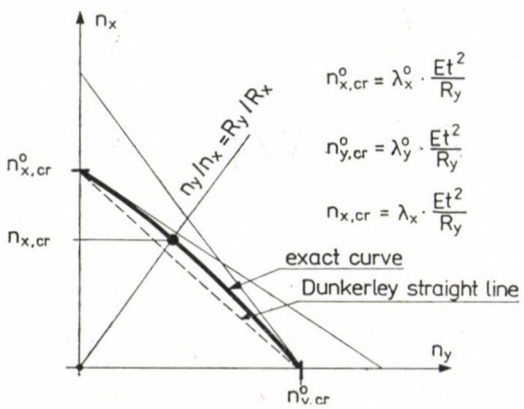

Fig. 9

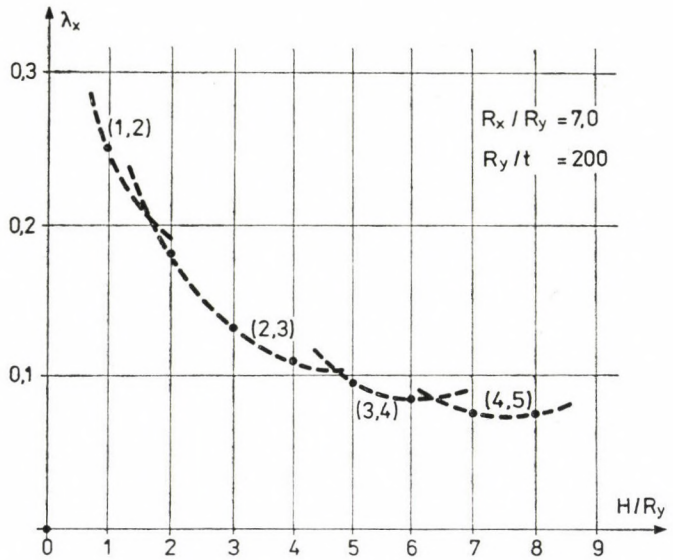

Fig. 10

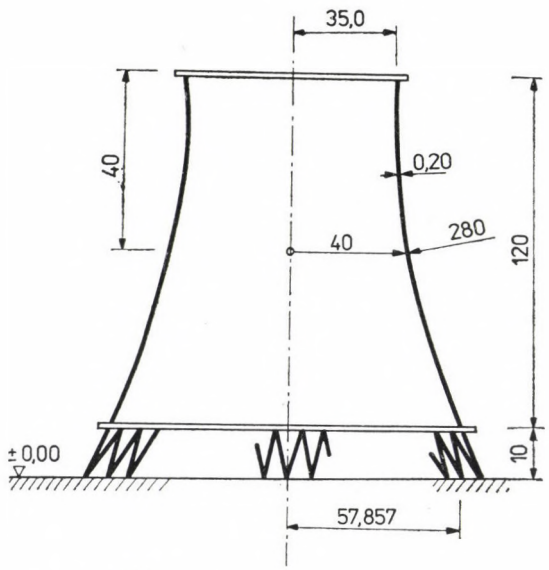

$$H/R_y = \frac{120}{40} = 3$$

$$R_y/R_x = \frac{40}{280} = \frac{1}{7}$$

$$R_y/t = \frac{40}{0{,}20} = 200$$

$$R_x = \frac{120^2}{8\left|\frac{35+57{,}857}{2} - 40\right|} = 280$$

Fig. 11

With the aid of the tables the critical combination of forces for a given shell can be readily determined.

It should be mentioned that the values of the tables furnish festoon curves with individual "slings" bulging downwards. Such a sling is to be seen in Fig. 10. Consequently, by linear interpolation we would commit an error to the detriment of safety, so that we recommend a more exact interpolation between the values of the tables, e.g. to plot the section of the festoon curve in the vicinity of the value sought for and to read it off from the curve.

We compared our results with those of [15] and found a very close agreement. Thus we can consider our method sufficiently accurate.

6. Numerical example

Let us analyse a cooling tower shell shown in Fig. 11 with the following data:

$$R_u = 35{,}00 \text{ m},$$
$$R_l = 57{,}86 \text{ m},$$
$$R_0 = 34{,}92 \text{ m},$$

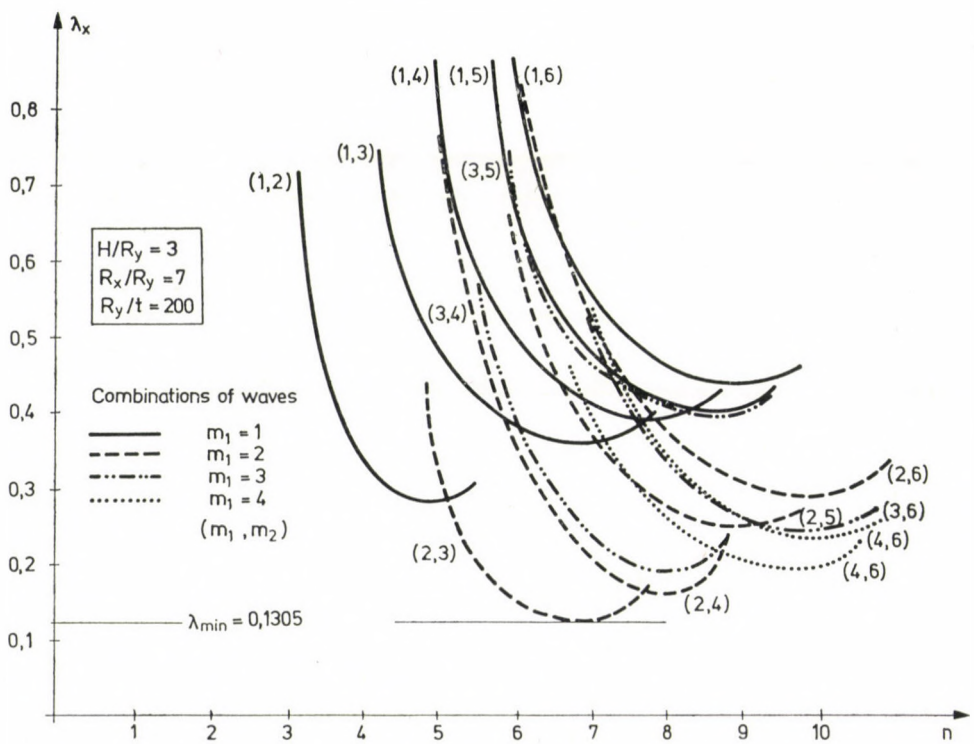

Fig. 12

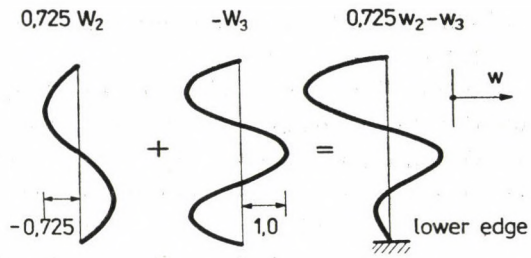

Fig. 13

$$R_y = 40{,}00 \text{ m},$$
$$R_x = 280{,}00 \text{ m},$$
$$t = 0{,}20 \text{ m},$$
$$H = 120{,}00 \text{ m}.$$

Hence, the characteristic parameters of the shell become:

$$H/R_y = \frac{120}{40} = 3{,}0,$$

$$R_y/R_x = \frac{280}{40} = 7{,}0,$$

$$R_y/t = \frac{40}{0{,}20} = 200.$$

Be the shell subjected to a load P uniformly distributed along the upper edge. We computed the parameter λ_x of the critical force and plotted the festoon curve against n in Fig. 12. The lowest ordinate of the festoon curve is $\lambda_x^{\min} = 0{,}131$, which, of course, coincides with the corresponding value of Table 3. The meridional section of the buckling shape pertaining to the minimum critical load is shown in Fig. 13.

If we want to determine the approximate critical load from Eq. (19), we may take the values $\lambda_{x,0} = 0{,}253$ and $\lambda_{y,0} = 0{,}036$ from Tables 1 and 2. Introducing these into (19) and taking (22) into account yields:

$$\frac{\lambda_x}{\lambda_{x,0}} + \frac{R_y}{R_x}\,\frac{\lambda_x}{\lambda_{y,0}} = \frac{\lambda_x}{0{,}253} + \frac{1}{7}\cdot\frac{\lambda_x}{0{,}036} = 1.$$

From this equation we obtain $\lambda_x = 0{,}126$ which is by 3 per cent less than the exact value.

The critical meridional directed force becomes (with a modulus of elasticity $E = 15\times10^6$ kN/m²):

$$n_{x,cr} = \lambda_x \frac{Et^2}{R_y} = 0{,}131 \cdot \frac{15\times10^6\times0{,}2^2}{40} = 1965 \text{ kN/m}.$$

REFERENCES

1. KRÄTZIG, W.: Statische und dynamische Stabilität der Kühlturmschale. Naturzug-Kühltürme. Ihre Festigkeitsberechnung und Konstruktion. Tagung vom 19. April 1968. Vulkan-Verlag, Dr. W. CLASSEN, Essen.
2. KRÄTZIG, W. B.: Große Naturzug-Kühltürme aus Stahlbeton. *VGB Kraftwerkstechnik* **55** (1975), 191—197

3. ROSEMEIER, G.: Zur Stabilität von Hypar- und Hyperboloidschalen. *Bauingenieur.* **48** (1973), 437—444
4. DER, T. J.—FIDLER, R.: A Model Study of the Buckling Behaviour of Hyperbolic Shells. *Proc. of the Institute of Civil Engineers, London.* **41** (1968), Sept. 105—118
5. MATEJA, O.: O badaniach nod statecznoscia hiperboloidalnych chlodni wiezowcyh. *Inzynierie i budownictwo.* **23** (1966), 428—431
6. HAMPE, E.: Kühltürme. VEB Verl. Bauwesen, Berlin 1975
7. WIANECZKI, J.: Stabilité d'une coque en form d'hyperboloïde de révolution sous des charges uniformément réparties sur les bords et symétriques par rapport à son axe. *Cahiers de la Recherche*, nr **19**. Eyrolles, Paris 1965
8. VLASZOV, V. Z.— GARAI, T.: Nyomatékmentes forgáshéjak kinematikai határozatlanságának feltétele. (The condition for the kinematic indeterminacy of momentless shells of revolution) *MTA. VI. Műsz. Oszt. Közl.* **14** (1956), 211—223
9. KOLLÁR, L.: Héjak nyúlásmentes alakváltozásai. (Inextensional Deformations of Shells). *Építés-Építészettudomány* (1971), 19—38
10. WITTEK, U.: Überblick und theoretische Einführung in das Stabilitätsverhalten von Kühlturm-Schalen. Kühlturm-Symposium (1977) Bochum. Konstruktiver Ingenieurbau Berichte, Heft 29/30.
11. BÜRGERMEISTER, G.—STEUP, H.—KRETZSMAR, H.: Stabilitätstheorie. Akademie-Verlag Berlin 1966
12. RABICH, R.: Die Membrantheorie der einschalig hyperbolischen Rotationsschalen. *Bauplanung-Bautechnik* **7** (1953), 310—318
13. "Report of the Committee of Inquiry into Collapse of Cooling Towers at Ferrybridge". Central Electricity Generating Board, London, England, Nov. 1965
14. LEHMKÄMPER, O.: Versteifte Kühlturmschalen aus Stahlbeton. Institut für Konstruktiven Ingenieurbau. Ruhr-Universität Bochum. Nr. 78—6. *Technical Reports* (1978)
15. VERONDA, D. R.—WEINGARTEN, V. J.: Stability of Hyperboloidal Shells: An Experimental and Analytical Investigation. USCCE 009, School of Eingineering, University of Southern California Los Angeles, Calif. Mar. 1973
16. KOHLI, J.: Beitrag zum axialsymmetrischen Ausbeulen einer einschaligen Hyperboloidschale. Dissertation (1968), Karlsruhe
17. COLE, P. P.—ABEL, J. F.—BILLINGTON, D. P.: Buckling of Cooling-Tower Shells. *Journ. Struct. Div. ASCE.* **101,** No. ST6, June 1975. 1185—1222

Allgemeine Beulung von hyperbolisch-parabolischen Rotationsschalen mit unbeweglichen unteren Rändern. — Behandelt wird die allgemeine Beulung der hyperbolischen Rotationsflächentragwerke aufgrund der linearen Beulungstheorie. Die Methode der Ermittlung der kritischen Belastung durch Ersetzung des Rotationsflächentragwerkes mit einer hyperbolischen Paraboloidschale von identischer Krümmung wird vorgeführt. Für Flächentragwerke von in der Praxis vorkommenden Dimensionen werden die kritischen Belastungswerte ermittelt und in einer Tabelle zusammengefasst. Schließlich wird die Anwendung des Verfahrens durch ein Beispiel demonstriert.

Acta Technica Academiae Scientiarum Hungaricae, Tomus 92 (1—2), pp. 189—214 (1981)

COMBINED TORSIONAL AND FLEXURAL BUCKLING OF A CANTILEVER WITH UNSYMMETRIC CROSS SECTION SUBJECTED TO DISTRIBUTED NORMAL LOADS

K. ZALKA*

[Manuscript received April 1, 1980]

This paper deals with the combined torsional and flexural buckling of a bar with a built-in lower and a free upper end subjected to uniformly distributed normal loads. The critical load is given for bars with mono-symmetric and with unsymmetric cross section. The eigenvalue problem of the system of the third-order differential equations of variable coefficients is traced back to a simple algebraic problem by generalizing the power series method. The algebraic problem is solved by trial and error. The eigenvalues needed for the calculation of the critical load are given in tables. A numerical example is presented to show how to use the formulas derived.

1. Introduction

Axially compressed thin-walled bars with initially straight axis and with open cross section often lose their stability by combined torsional and flexural buckling. There is a simple way given by TIMOSHENKO [6] for the calculation of the critical load of bars with arbitrary cross section subjected to a vertical load on top: The value of the critical load equals the smallest root of a cubic algebraical equation. As far as we know, however, the spatial stability problem of bars with arbitrary cross section subjected to distributed normal load has not been solved. AKESSON [1] has analyzed the spatial stability of rack structures, his results, however, are valid only for special bars with no torsional rigidity.

The simultaneous differential equations of combined torsional and flexural buckling of a bar with a built-in lower and a free upper end subjected uniformly distributed normal load are as follows [7, 8]:

$$u''' + \frac{qz}{EI_y}(u' + y_0\varphi') = 0\,, \tag{1.1}$$

$$v''' + \frac{qz}{EI_x}(v' - x_0\varphi') = 0\,, \tag{1.2}$$

* ZALKA K., Nyár u. 19. I/4, H—1043 Budapest, Hungary

$$\varphi''' - \left(\frac{GI_t}{EI_\omega} - \frac{qzI_0}{EI_\omega A}\right)\varphi' - \frac{qz}{EI_\omega}(x_0 v' - y_0 u') = 0\,. \tag{1.3}$$

The boundary conditions for the differential equations are:

$$u(0) = v(0) = \varphi(0) = 0\,, \tag{1.4}$$

$$u'(H) = v'(H) = \varphi'(H) = 0\,, \tag{1.5}$$

$$u''(0) = v''(0) = \varphi''(0) = 0\,. \tag{1.6}$$

In the equations the following notations are used (Fig. 1):

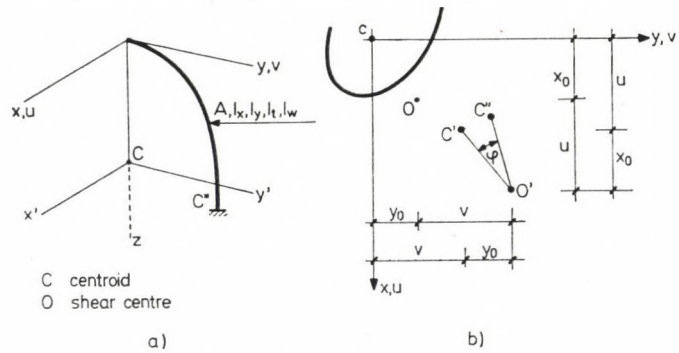

Fig. 1

u and v	deflections of the shear center O in the directions of x and y,
x and y	principal axes of inertia
φ	angle of rotation,
x_0 and y_0	coordinates of the shear center,
A	cross-sectional area,
EI_x and EI_y	bending rigidities with respect to the axes x and y,
GI_t	torsional rigidity,
EI_ω	warping rigidity,
$I_0 = I_x + I_y + A(x_0^2 + y_0^2)$	polar moment of inertia of the cross section with regard to shear centre,
H	height of the bar,
q	intensity of the critical load, i.e. the eigenvalue of the problem.

In a previous paper [8] we dealt with the special case of a bar with double-symmetric cross section in detail, and we presented a table and a set of diagrams for the exact calculation of the critical load of pure torsional buckling. On the basis of Föppl's theorem [3] we presented closed formulas for the approximate calculation of the critical load of a bar with mono-symmetric and with unsymmetric cross sections.

The aim of this paper is to present the exact solution of the simultaneous differential equations set up for the spatial buckling of cantelivers with mono-symmetric and with unsymmetric cross sections subjected to distributed nor-

mal loads. To obtain the solution, the modified version of the power series method, efficient especially for eigenvalue problems, will be generalized. The problem has several independent variables, so that the exact value of the critical load can be calculated using tables or sets of diagrams.

2. Bars with mono-symmetric cross section

In the case of a mono-symmetric cross section the shear centre lies on the axis of symmetry. Let us assume that the axis x is an axis of symmetry. In this case we have

$$y_0 = 0 ,$$

and the differential equations of the problem become

$$u''' + \frac{qz}{EI_y} u' = 0 , \tag{2.1}$$

$$v''' + \frac{qz}{EI_x} (v' - x_0 \varphi') = 0 , \tag{2.2}$$

$$\varphi''' - \left(\frac{GI_t}{EI_\omega} - \frac{qzI_0}{EI_\omega A} \right) \varphi' - \frac{qz}{EI_\omega} x_0 v' = 0 . \tag{2.3}$$

The boundary conditions are still expressed by Eqs (1.4) to (1.6). The first equation does not contain the angle of rotation φ and shows that the buckling in the plane of symmetry is independent of that by pure torsion. In that case the value of the critical load of buckling in the plane of symmetry is given by the formula

$$N_{cr,x} = \frac{7{,}84\, EI_y}{H^2} . \tag{2.4}$$

In the case of buckling perpendicular to the plane of symmetry buckling occurs by a combination of bending of the axis of the bar in the plane yz and twist of the cross sections about the shear centre axis which results in buckling by torsion and flexure. The value of the critical load for torsional-flexural buckling can be obtained by solving the simultaneous differential equations (2.2) and (2.3). This procedure will now be presented.

Let us introduce the following notations so that we can work with non-dimensional quantities:

$$\alpha = \frac{qH^3 i_p^2}{7{,}84\, EI_\omega} = \frac{N_{cr}}{N^\omega_{cr,\varphi}} , \tag{2.5}$$

$$\beta = \frac{GI_t H^2}{7{,}84\, EI_\omega} = \frac{N^t_{cr,\varphi}}{N^\omega_{cr,\varphi}}, \tag{2.6}$$

$$\gamma = \frac{EI_\omega}{EI_x i_p^2} = \frac{N^\omega_{cr,\varphi}}{N_{cr,y}}, \tag{2.7}$$

$$\tau = \frac{x_0}{i_p} = \sqrt{\frac{I_0 - I_x - I_y}{I_0}}, \tag{2.8}$$

where

$N_{cr} = q_{cr} H$ critical load for combined torsional and flexural buckling,

$N_{cr,y} = \dfrac{7{,}84 EI_x}{H^2}$ critical load for flexural buckling in direction y,

$N^\omega_{cr,\varphi} = \dfrac{7{,}84 EI_\omega}{i_p^2 H^2}$ critical load associated with the warping rigidity,

$N^t_{cr,\varphi} = \dfrac{GI_t}{i_p^2}$ critical load associated with the torsional rigidity,

$I_0 = I_x + I_y + Ax_0^2$ polar moment of inertia referred to the shear centre,

$i = \sqrt{\dfrac{I_0}{A}}$ polar radius of inertia.

With these notations the simultaneous differential equations of the eigenvalue problem are as follows:

$$v''' + \alpha\gamma \frac{7{,}84}{H^3} z\,(v' - i_p \tau\varphi') = 0, \tag{2.9}$$

$$\varphi''' - \left(\beta \frac{7{,}84}{H^2} - \alpha \frac{7{,}84}{H^3} z\right)\varphi' - \alpha \frac{7{,}84\,\tau}{H^3 i_p} z v' = 0, \tag{2.10}$$

where α is the parameter of the eigenvalue. The boundary conditions for the differential equations are:

$$v(0) = \varphi(0) = 0, \tag{2.11}$$

$$v'(H) = \varphi'(H) = 0, \tag{2.12}$$

$$v''(0) = \varphi''(0) = 0. \tag{2.13}$$

In Eqs (2.9) and (2.10) there is only one coefficient, the polar radius of inertia i_p, which is not a non-dimensional one. Its presence follows from the fact that the displacement v and the rotation φ — or rather their differential coefficients — in the same equation are not of the same dimension. So there must be a factor there, in our case the polar radius of inertia, that "equalizes" this difference in dimension. Later on, however, this coefficient will drop out of

the expressions so that the equations for the calculation of the critical load will be non-dimensional ones.

The simultaneous differential equations (2.9) and (2.10) have no solution of closed form. Let us try to find the solution in the form of the following infinite power series:

$$v = b_0 + \sum_{k=1}^{\infty} b_k z^k , \tag{2.14}$$

$$\varphi = c_0 + \sum_{k=1}^{\infty} c_k z^k , \tag{2.15}$$

where b_k and c_k are the set of coefficients for the solution-series yet unknown. Having substituted the necessary derivatives

$$v' = \sum_{k=1}^{\infty} k b_k z^{k-1} , \tag{2.16}$$

$$v'' = \sum_{k=2}^{\infty} k(k-1) b_k z^{k-2} , \tag{2.17}$$

$$v''' = \sum_{k=3}^{\infty} k(k-1)(k-2) b_k z^{k-3} , \tag{2.18}$$

$$\varphi' = \sum_{k=1}^{\infty} k c_k z^{k-1} , \tag{2.19}$$

$$\varphi'' = \sum_{k=2}^{\infty} k(k-1)\, c_k z^{k-2} , \tag{2.20}$$

$$\varphi''' = \sum_{k=3}^{\infty} k(k-1)(k-2)\, c_k z^{k-3} \tag{2.21}$$

into the simultaneous differential equations (2.9) and (2.10) we have to ensure that the equations are equal to zero. It follows that the coefficients of each power z have to be equal to zero, or — framing this conditions in an other way — that the following set of "equalization" conditions must be fulfilled:

$$\left.\frac{dV}{dz}\right|_{z=0} \equiv 0 , \quad \left.\frac{d^2 V}{dz^2}\right|_{z=0} \equiv 0, \ldots \left.\frac{d^i V}{dz^i}\right|_{z=0} \equiv 0 , \tag{2.22}$$

and

$$\left.\frac{d\psi}{dz}\right|_{z=0} \equiv 0 , \quad \left.\frac{d^2 \psi}{dz^2}\right|_{z=0} \equiv 0, \quad \ldots \left.\frac{d^i \psi}{dz^i}\right|_{z=0} \equiv 0 , \tag{2.23}$$

where V and ψ denote the polynomials resulting from Eqs (2.9) and (2.10), and where

$$i = 1, 2 \ldots .$$

On the basis of these conditions the following formulae can be generated for the successive determination of the unknown coefficients b_k and c_k:

$$b_k = -\frac{7{,}84\alpha\gamma(k-3)}{(k-2)(k-1)kH^3} b_{k-3} + \frac{7{,}84\alpha\gamma\tau i_p (k-3)}{(k-2)(k-1)kH^3} c_{k-3}, \tag{2.24}$$

$$c_k = \frac{7{,}84\beta}{(k-1)kH^2} c_{k-2} - \frac{7{,}84\alpha(k-3)}{(k-2)(k-1)kH^3} c_{k-3} + \\ + \frac{7{,}84\alpha\tau(k-3)}{(k-2)(k-1)ki_p H^3} b_{k-3}, \tag{2.25}$$

where $k \geqq 3$.

The initial values needed for the calculations are obtained by making use of the boundary conditions (2.11), (2.13) and of the power series (2.14), (2.15) and their derivatives (2.17), (2.20).

Thus:

$$b_0 = c_0 = 0, \tag{2.26}$$

$$b_1 = c_2 = 0. \tag{2.27}$$

The formulae for the successive determination of the unknown coefficients (2.24), (2.25) show that the coefficients b_k and c_k can be expressed as a function of b_1 and c_1, respectively:

$$b_k = A_{k,11} b_1 + i_p A_{k,12} c_1, \quad k \geqq 3 \tag{2.28}$$

$$c_k = \frac{1}{i_p} A_{k,21} b_1 + A_{k,22} c_1, \quad k \geqq 3 \tag{2.29}$$

where

$$A_{k,ij} = f(\alpha, \beta, \gamma, \tau, k) \qquad i, j = 1, 2 \tag{2.30}$$

By making use of the last boundary conditions (2.12) the following system of "conditional" equations can be set up:

$$b_1 + \sum_{k=3}^{\infty} k b_k H^{k-1} = 0, \tag{2.31}$$

$$c_1 + \sum_{k=3}^{\infty} k c_k H^{k-1} = 0. \tag{2.32}$$

Eqs (2.28) and (2.9) show that this system of "conditional" equations can be considered a linear combination of b_0 and c_1:

$$A_{1\,1} b_1 + i_p A_{12} c_1 = 0\,, \tag{2.33}$$

$$\frac{1}{i_p} A_{21} b_1 + A_{22} c_1 = 0\,. \tag{2.34}$$

The coefficients b_1 and c_1 are equal to zero only in the case of the trivial solution and in every other case they are different from zero. It follows therefore that from the homogeneous, linear equation

$$\mathbf{A}\mathbf{x} = 0 \tag{2.35}$$

the

$$|\mathbf{A}| = 0 \tag{2.36}$$

expression yields the nontrivial solution, where

$$\mathbf{A} = \begin{bmatrix} A_{11} & i_p A_{12} \\ \dfrac{1}{i_p} A_{12} & A_{22} \end{bmatrix}, \qquad \mathbf{x} = \begin{bmatrix} b_1 \\ c_1 \end{bmatrix}. \tag{2.37}$$

Every element of the matrix **A** results from an infinite summation but we will take only n terms into consideration. To decide the necessary value of n we set the error limit to be 10^{-8} when calculating the terms. Setting the determinant of the matrix **A** equal to zero we obtain an algebraical equation of the n-th degree in α. The roots of the function are the eigenvalues of the problem (Fig. 2). The determination of the critical load is easy because we know the shape of the n-th degree algebraical function. It is also helpful that we need only find the smallest root because only the smallest eigenvalue is of interest.

The eigenvalue problem of the system of the differential equations of variable coefficients for combined torsional and flexural buckling has thus

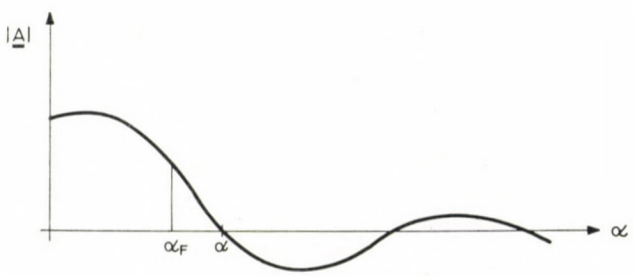

Fig. 2

been simplified: The value of the critical load can be calculated from an n-th degree algebraical function by trial and error.

When carrying out the successive approximation we used initial values (α_F, Fig. 2) calculated with the aid of Föppl's theorem [3]. We took into consideration the fact that these values are lower bounds for the critical load, i.e.:

$$\alpha_F \leq \alpha. \tag{2.38}$$

The Eq. (2.36) has been solved for different ratios of rigidity. The error limit was 10^{-8}. The eigenvalues needed for the calculation of the critical load are given by Table 1 and Fig. 3.

It is worth analysing the two extreme values of the parameter τ in detail. $\tau = 0$ corresponds to the case of $x_0 = 0$, that is, we have a double-symmetric cross section. Failure may occur by torsional *or* flexural buckling as is shown by the two intersecting lines. While the critical load for the pure torsional buckling is smaller than the critical load for flexural buckling the combined critical load equals the former one, and when the critical load for the flexural buckling is smaller than the critical load for the pure torsional buckling, the combined critical load equals the latter one.

$\tau = 1{,}0$ corresponds to the case when the shear centre is at infinity. In that case the warping rigidity predominates over the torsional rigidity. It follows that the deflection curve is characterized by the deflection associated with the warping rigidity and this deflection curve and that of the flexural buckling are of the same type. In the case of two deflection curves of the same type Föppl's theorem yields the exact solution [2]. Actually, the

Table 1

τ \ $\frac{N_{cr,\varphi}}{N_{cr,y}}$	0,5	1,0	2,0	3,0	4,0	5,0
0,0	0,500	1,000	1,000	1,000	1,000	1,000
0,1	0,496	0,910	0,986	0,992	0,998	1,000
0,2	0,483	0,834	0,962	0,980	0,992	0,993
0,3	0,464	0,770	0,926	0,956	0,977	0,981
0,4	0,443	0,715	0,882	0,925	0,962	0,966
0,5	0,424	0,667	0,841	0,895	0,936	0,947
0,6	0,403	0,626	0,800	0,862	0,913	0,927
0,7	0,384	0,589	0,765	0,832	0,885	0,905
0,8	0,365	0,556	0,728	0,802	0,853	0,881
0,9	0,349	0,527	0,699	0,775	0,826	0,858
1,0	0,333	0,500	0,667	0,750	0,800	0,833

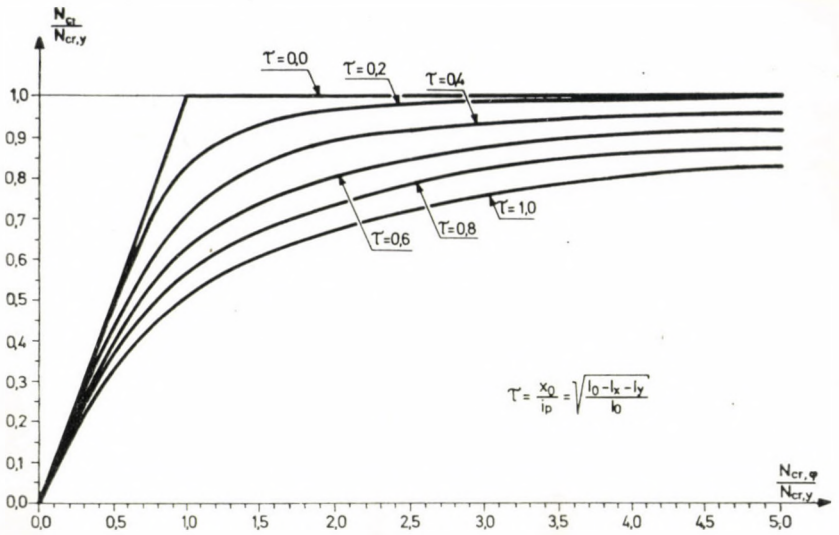

Fig. 3

lowest curve on Fig. 3 corresponds to the values calculated by Föppl's theorem. These values were used as initial values for the successive approximations.

The critical load for torsional-flexural buckling can be calculated as follows.

The critical load for the Euler-type buckling perpendicular to the plane of symmetry is given by the formula

$$N_{cr,y} = \frac{7{,}84\, EI_x}{H^2} \,. \tag{2.39}$$

This Euler-type buckling combines with the pure torsional buckling The critical load for pure torsional buckling $N_{cr,\varphi}$ can be calculated by making use of [8]. Having calculated $N_{cr,y}$ and $N_{cr,\varphi}$ — taking into account the rigidity ratio τ — we can get the combined critical load N_{cr} from the formula

$$N_{cr} = \varepsilon N_{cr,y}, \tag{2.40}$$

where values for the parameter ε are given in Table 1 and Fig. 3.

In the plane of symmetry the Euler type buckling does not combine with the pure torsional buckling. The critical load $N_{cr,x}$ is given by formula (2.4).

Only the lowest of the critical loads N_{cr} and $N_{cr,x}$ is of interest in practical applications.

3. Bars with unsymmetric cross section

The combined torsional and flexural buckling of a cantilever subjected to uniformly distributed normal load is characterized by the system of equations (1.1), (1.2), (1.3) and the boundary conditions (1.4), (1.5), (1.6).

Let us introduce the following non-dimensional quantities:

$$\alpha = \frac{qH^3 i_p^2}{7{,}84\, EI_\omega} = \frac{N_{cr}}{N^\omega_{cr,\varphi}}, \tag{3.1}$$

$$\beta = \frac{GI_t\, H^2}{7{,}84\, EI_\omega} = \frac{N^t_{cr,\varphi}}{N^\omega_{cr,\varphi}}, \tag{3.2}$$

$$\delta = \frac{EI_\omega}{EI_y\, i_p^2} = \frac{N^\omega_{cr,\varphi}}{N_{cr,x}}, \tag{3.3}$$

$$\gamma = \frac{EI_\omega}{EI_x\, i_p^2} = \frac{N^\omega_{cr,\varphi}}{N_{cr,y}}, \tag{3.4}$$

$$\tau_x = \frac{x_0}{i_p} = \sqrt{\frac{I_0 - I_x - I_y - y_0^2 A}{I_6}}, \tag{3.5}$$

$$\tau_y = \frac{y}{i_p} = \sqrt{\frac{I_0 - I_x - I_y - x_0^2 A}{I_0}}, \tag{3.6}$$

where

$$i_p^2 = \frac{I_0}{A} = \frac{I_x + I_y + x_0^2 A + y_0^2 A}{A}. \tag{3.7}$$

With these notations the system of the above-mentioned differential equations becomes

$$u''' = \alpha\delta \frac{7{,}84}{H^3} z\,(u' + i_p\, \tau_y\, \psi') = 0, \tag{3.8}$$

$$v''' + \alpha\gamma \frac{7{,}84}{H^3} z\,(v' - i_p\, \tau_x\, \varphi') = 0, \tag{3.9}$$

$$\varphi''' - \left(\beta \frac{7{,}84}{H^2} - \alpha \frac{7{,}84}{H^3} z\right)\varphi' - \alpha \frac{7{,}84\, \tau_x}{H^3 i_p} zv' + \alpha \frac{7{,}84\, \tau_y}{H^3 i_p} zu' = 0. \tag{3.10}$$

The boundary conditions are still expressed by Eqs (1.4) to (1.6). The angle of rotation φ appears in all three equations showing that in the general case the Euler-type buckling in both xz and yz planes combines with the pure torsional buckling.

We can apply the same method shown in detail in the previous Section on bars with monosymmetric cross section in the case of bars with unsymmetric cross section. The solution again can be found by means of infinite power series:

$$u = a_0 + \sum_{k=1}^{\infty} a_k \, z^k \,, \tag{3.11}$$

$$v = b_0 + \sum_{k=1}^{\infty} b_k \, z^k \,, \tag{3.12}$$

$$\varphi = c_0 + \sum_{k=1}^{\infty} c_k \, z^k \,. \tag{3.13}$$

Using the "equalization" conditions (See Eqs (2.22), (2.23)) and the boundary conditions, a system of three "conditional" equations can now be set up. These equations are formed by a linear combination of the coefficients a_1, b_1 and c_1. Proceeding in this way the eigenvalue problem of the system of differential equations can be traced back again to a simple algebraic problem and from the equation

$$\mathbf{Ax} = 0 \tag{3.14}$$

the expression

$$|\mathbf{A}| = 0 \tag{3.15}$$

yields the eigenvalues of the problem from which, using formula (3.1), the smallest one gives the value of the critical load. The elements of the matrix A have the form

$$\mathbf{A}_{i,j} = f(\alpha, \beta, \gamma, \delta, \tau_x, \tau_y), \qquad i, j = 1, 2, 3. \tag{3.16}$$

The necessary computation has been carried out for different ratios of rigidity with an error limit of $\Delta = 10^{-8}$. The load factors needed for the calculation of the critical load are given in Tables 2...11.

Using the Tables 2...11 the critical load can be calculated as follows.

The value of τ_x shows which Table is to be used. As a function of the ratios

$$\frac{N_{cr,\varphi}}{N_{cr,x}}, \quad \frac{N_{cr,\varphi}}{N_{cr,y}}$$

and the quantity τ_y, the load factor

$$\lambda = \frac{N_{cr}}{N_{cr,\varphi}}$$

Table 2

$\tau_x = 0{,}1$

$\frac{N_{cr,\varphi}}{N_{cr,y}}$ \ $\frac{N_{cr,\varphi}}{N_{cr,x}}$	0,2	0,4	0,6	0,8	1,0	2,0	3,0	4,0	5,0	τ_y
	1,000	1,000	1,000	1,000	1,000	0,500	0,333	0,250	0,200	0,0
	0,991	0,976	0,950	0,905	0,843	0,481	0,326	0,247	0,198	0,2
	0,964	0,916	0,857	0,787	0,715	0,443	0,311	0,238	0,192	0,4
0,2	0,926	0,846	0,767	0,692	0,626	0,402	0,290	0,226	0,184	0,6
	0,881	0,777	0,690	0,617	0,556	0,365	0,269	0,212	0,176	0,8
	0,835	0,716	0,626	0,557	0,501	0,333	0,250	0,201	0,167	1,0
	0,996	0,996	0,996	0,996	0,996	0,500	0,333	0,250	0,200	0,0
	0,987	0,972	0,947	0,904	0,833	0,481	0,326	0,247	0,198	0,2
	0,960	0,914	0,854	0,786	0,714	0,443	0,310	0,238	0,192	0,4
0,4	0,922	0,844	0,765	0,691	0,625	0,402	0,290	0,226	0,184	0,6
	0,878	0,776	0,689	0,616	0,556	0,365	0,269	0,212	0,176	0,8
	0,883	0,715	0,626	0,557	0,501	0,333	0,250	0,201	0,167	1,0
	0,988	0,988	0,988	0,988	0,988	0,500	0,333	0,250	0,200	0,0
	0,980	0,965	0,942	0,900	0,831	0,481	0,326	0,247	0,198	0,2
	0,954	0,909	0,852	0,785	0,713	0,443	0,310	0,238	0,192	0,4
0,6	0,918	0,841	0,764	0,691	0,625	0,402	0,290	0,226	0,184	0,6
	0,874	0,774	0,688	0,616	0,555	0,365	0,269	0,212	0,176	0,9
	0,830	0,714	0,626	0,556	0,501	0,333	0,250	0,201	0,167	1,0
	0,970	0,970	0,970	0,970	0,970	0,449	0,333	0,250	0,200	0,0
	0,962	0,950	0,929	0,891	0,827	0,481	0,326	0,247	0,198	0,2
	0,939	0,899	0,846	0,781	0,712	0,443	0,311	0,238	0,192	0,4
0,8	0,907	0,835	0,760	0,689	0,624	0,402	0,290	0,226	0,184	0,6
	0,867	0,770	0,687	0,615	0,555	0,365	0,269	0,212	0,176	0,8
	0,825	0,712	0,624	0,556	0,501	0,334	0,250	0,201	0,167	1,0
	0,910	0,910	0,910	0,190	0,910	0,499	0,333	0,250	0,200	0,0
	0,906	0,901	0,890	0,867	0,818	0,481	0,326	0,247	0,198	0,2
	0,895	0,870	0,830	0,774	0,708	0,443	0,311	0,238	0,192	0,4
1,0	0,874	0,821	0,755	0,687	0,622	0,402	0,290	0,226	0,184	0,6
	0,846	0,764	0,684	0,614	0,554	0,365	0,269	0,212	0,175	0,8
	0,812	0,708	0,622	0,555	0,500	0,334	0,250	0,201	0,167	1,0
	0,495	0,495	0,495	0,495	0,495	0,495	0,333	0,250	0,200	0,0
	0,495	0,495	0,495	0,495	0,495	0,478	0,326	0,247	0,198	0,2
	0,495	0,495	0,495	0,494	0,494	0,440	0,310	0,238	0,192	0,4
2,0	0,495	0,494	0,494	0,493	0,492	0,401	0,290	0,226	0,184	0,6
	0,495	0,494	0,493	0,491	0,488	0,364	0,269	0,212	0,175	0,8
	0,494	0,493	0,491	0,488	0,477	0,333	0,250	0,201	0,167	1,0
	0,331	0,331	0,331	0,331	0,331	0,331	0,331	0,250	0,200	0,0
	0,331	0,331	0,331	0,331	0,331	0,331	0,325	0,247	0,198	0,2
	0,331	0,331	0,331	0,331	0,331	0,330	0,309	0,238	0,192	0,4
3,0	0,331	0,331	0,331	0,331	0,331	0,329	0,289	0,226	0,184	0,6
	0,331	0,331	0,331	0,331	0,331	0,325	0,269	0,212	0,175	0,8
	0,331	0,331	0,331	0,331	0,331	0,316	0,250	0,200	0,167	1,0
	0,249	0,249	0,249	0,249	0,249	0,249	0,249	0,249	0,200	0,0
	0,249	0,249	0,249	0,249	0,249	0,249	0,249	0,246	0,198	0,2
	0,249	0,249	0,249	0,249	0,249	0,249	0,249	0,237	0,192	0,4
4,0	0,249	0,249	0,249	0,249	0,249	0,249	0,249	0,248	0,226	0,184	0,6
	0,249	0,249	0,249	0,249	0,249	0,249	0,247	0,212	0,175	0,8
	0,249	0,249	0,249	0,249	0,249	0,248	0,244	0,200	0,167	1,0
	0,199	0,199	0,199	0,199	0,199	0,199	0,199	0,199	0,199	0,0
	0,199	0,199	0,199	0,199	0,199	0,199	0,199	0,199	0,197	0,2
	0,199	0,199	0,199	0,199	0,199	0,199	0,199	0,199	0,191	0,4
5,0	0,199	0,199	0,199	0,199	0,199	0,199	0,199	0,198	0,184	0,6
	0,199	0,199	0,199	0,199	0,199	0,199	0,199	0,198	0,175	0,8
	0,199	0,199	0,199	0,199	0,199	0,199	0,198	0,196	0,167	1,0

Table 3

$\tau_x = 0{,}2$

$\frac{N_{cr,\varphi}}{N_{cr,y}}$ \ $\frac{N_{cr,\varphi}}{N_{cr,x}}$	0,2	0,4	0,6	0,8	1,0	2,0	3,0	4,0	5,0	τ_y
	0,993	0,993	0,993	0,993	0,993	0,500	0,333	0,250	0,200	0,0
	0,984	0,969	0,945	0,902	0,832	0,481	0,326	0,247	0,198	0,2
	0,957	0,912	0,853	0,785	0,713	0,443	0,311	0,238	0,192	0,4
0,2	0,920	0,842	0,764	0,691	0,625	0,402	0,290	0,226	0,184	0,6
	0,876	0,774	0,688	0,616	0,555	0,365	0,269	0,212	0,176	0,8
	0,832	0,714	0,626	0,556	0,501	0,333	0,250	0,201	0,167	1,0
	0,978	0,978	0,978	0,978	0,978	0,500	0,333	0,250	0,200	0,0
	0,969	0,956	0,933	0,894	0,827	0,481	0,326	0,247	0,198	0,2
	0,945	0,902	0,846	0,781	0,711	0,443	0,310	0,238	0,192	0,4
0,4	0,909	0,836	0,760	0,688	0,623	0,402	0,290	0,226	0,184	0,6
	0,868	0,770	0,685	0,614	0,554	0,365	0,269	0,212	0,176	0,8
	0,825	0,711	0,623	0,555	0,500	0,333	0,250	0,201	0,167	1,0
	0,952	0,952	0,952	0,952	0,952	0,500	0,333	0,250	0,200	0,0
	0,945	0,933	0,914	0,880	0,820	0,481	0,326	0,247	0,198	0,2
	0,923	0,885	0,935	0,774	0,708	0,443	0,310	0,238	0,192	0,4
0,6	0,892	0,825	0,753	0,685	0,621	0,402	0,290	0,226	0,184	0,6
	0,854	0,763	0,681	0,612	0,553	0,365	0,269	0,212	0,175	0,8
	0,815	0,706	0,621	0,553	0,499	0,333	0,250	0,201	0,167	1,0
	0,907	0,907	0,907	0,907	0,907	0,500	0,333	0,250	0,200	0,0
	0,902	0,894	0,890	0,855	0,808	0,481	0,326	0,247	0,198	0,2
	0,886	0,856	0,816	0,763	0,702	0,443	0,310	0,238	0,192	0,4
0,8	0,862	0,806	0,743	0,679	0,618	0,402	0,290	0,226	0,184	0,6
	0,831	0,751	0,676	0,609	0,551	0,364	0,269	0,212	0,175	0,8
	0,797	0,698	0,617	0,552	0,498	0,333	0,250	0,201	0,167	1,0
	0,834	0,834	0,834	0,834	0,834	0,500	0,333	0,250	0,200	0,0
	0,832	0,827	0,820	0,808	0,781	0,481	0,326	0,247	0,198	0,2
	0,823	0,806	0,781	0,743	0,691	0,442	0,310	0,238	0,192	0,4
1,0	0,809	0,773	0,725	0,670	0,613	0,402	0,290	0,226	0,184	0,6
	0,789	0,730	0,666	0,604	0,549	0,364	0,269	0,212	0,175	0,8
	0,766	0,685	0,611	0,549	0,496	0,333	0,250	0,201	0,167	1,0
	0,481	0,481	0,481	0,481	0,481	0,481	0,333	0,250	0,200	0,0
	0,481	0,481	0,481	0,481	0,481	0,467	0,326	0,247	0,198	0,2
	0,481	0,481	0,481	0,480	0,479	0,433	0,310	0,237	0,192	0,4
2,0	0,481	0,480	0,479	0,478	0,475	0,396	0,289	0,226	0,184	0,6
	0,481	0,479	0,477	0,474	0,467	0,361	0,269	0,212	0,175	0,8
	0,480	0,478	0,473	0,466	0,453	0,331	0,250	0,200	0,167	1,0
	0,326	0,326	0,326	0,326	0,326	0,326	0,326	0,250	0,200	0,0
	0,326	0,326	0,326	0,326	0,326	0,326	0,321	0,247	0,198	0,2
	0,326	0,326	0,326	0,326	0,326	0,326	0,306	0,237	0,192	0,4
3,0	0,326	0,326	0,326	0,326	0,326	0,324	0,287	0,226	0,184	0,6
	0,326	0,326	0,326	0,326	0,326	0,320	0,267	0,212	0,175	0,8
	0,326	0,326	0,326	0,326	0,325	0,311	0,249	0,200	0,167	1,0
	0,247	0,247	0,247	0,247	0,247	0,247	0,247	0,247	0,200	0,0
	0,247	0,247	0,247	0,247	0,247	0,247	0,247	0,243	0,198	0,2
	0,247	0,247	0,247	0,247	0,247	0,247	0,246	0,235	0,192	0,4
4,0	0,247	0,247	0,247	0,247	0,247	0,246	0,245	0,224	0,184	0,6
	0,247	0,247	0,247	0,247	0,246	0,246	0,243	0,211	0,175	0,8
	0,247	0,247	0,247	0,246	0,246	0,245	0,238	0,199	0,167	1,0
	0,198	0,198	0,198	0,198	0,198	0,198	0,198	0,198	0,198	0,0
	0,198	0,198	0,198	0,198	0,198	0,198	0,198	0,198	0,195	0,2
	0,198	0,198	0,198	0,198	0,198	0,198	0,198	0,197	0,191	0,4
5,0	0,198	0,198	0,198	0,198	0,198	0,198	0,198	0,197	0,183	0,6
	0,198	0,198	0,198	0,198	0,198	0,198	0,197	0,195	0,174	0,8
	0,198	0,198	0,198	0,198	0,198	0,197	0,197	0,192	0,166	1,0

Table 4

$\tau_x = 0{,}3$

$\frac{N_{cr,\varphi}}{N_{cr,y}}$ \ $\frac{N_{cr,\varphi}}{N_{cr,x}}$	0,2	0,4	0,6	0,8	1,0	2,0	3,0	4,0	5,0	τ_y
	0,981	0,981	0,981	0,981	0,981	0,500	0,333	0,250	0,200	0,0
	0,973	0,959	0,936	0,895	0,828	0,481	0,326	0,247	0,198	0,2
	0,947	0,903	0,847	0,781	0,712	0,443	0,311	0,238	0,192	0,4
0,2	0,911	0,836	0,760	0,688	0,623	0,402	0,290	0,226	0,184	0,6
	0.870	0.771	0.686	0.615	0.554	0.365	0.269	0.212	0.176	0.8
	0.826	0.711	0.623	0.555	0.500	0.333	0.250	0.201	0.167	1.0
	0.950	0.950	0.950	0.950	0.950	0.500	0.333	0.250	0.200	0.0
	0.943	0.931	0.912	0.878	0.819	0.481	0.326	0.247	0.198	0.2
	0.922	0.883	0.833	0.772	0.706	0.443	0.310	0.238	0.192	0.4
0,4	0,889	0,822	0,751	0,683	0,620	0,402	0,290	0,226	0,184	0,6
	0,851	0,760	0,680	0,611	0,552	0,365	0,269	0,212	0,176	0,8
	0,812	0,704	0,619	0,553	0,498	0,333	0,250	0,201	0,167	1,0
	0,906	0,906	0,906	0,906	0,906	0,500	0,333	0,250	0,200	0,0
	0,900	0,891	0,877	0,850	0,804	0,481	0,326	0,247	0,198	0,2
	0,883	0,852	0,811	0,758	0,698	0,442	0,310	0,238	0,192	0,4
0,6	0,857	0,801	0,739	0,675	0,616	0,401	0,290	0,226	0,184	0,6
	0,826	0,746	0,671	0,606	0,550	0,365	0,269	0,212	0,175	0,8
	0,791	0,694	0,614	0,550	0,496	0,333	0,250	0,200	0,167	1,0
	0,844	0,844	0,844	0,844	0,844	0,499	0,333	0,250	0,200	0,0
	0,840	0,835	0,826	0,809	0,778	0,481	0,326	0,247	0,198	0,2
	0,829	0,808	0,778	0,737	0,687	0,442	0,310	0,238	0,192	0,4
0,8	0,811	0,769	0,719	0,663	0,609	0,401	0,290	0,226	0,184	0,6
	0,788	0,724	0,660	0,599	0,546	0,363	0,269	0,212	0,175	0,8
	0,761	0,679	0,606	0,545	0,494	0,333	0,250	0,200	0,167	1,0
	0,770	0,770	0,770	0,770	0,770	0,499	0,333	0,250	0,200	0,0
	0,768	0,775	0,760	0,752	0,736	0,481	0,326	0,247	0,198	0,2
	0,761	0,750	0,732	0,705	0,667	0,441	0,310	0,237	0,192	0,4
1,0	0,751	0,725	0,689	0,646	0,599	0,400	0,290	0,226	0,184	0,6
	0,736	0,692	0,642	0,589	0,540	0,363	0,269	0,212	0,175	0,8
	0,718	0,657	0,595	0,539	0,491	0,332	0,250	0,200	0,167	1,0
	0,464	0,464	0,464	0,464	0,464	0,464	0,333	0,250	0,200	0,0
	0,464	0,464	0,463	0,463	0,463	0,451	0,326	0,247	0,198	0,2
	0,463	0,463	0,462	0,461	0,460	0,422	0,309	0,237	0,192	0,4
2,0	0,463	0,462	0,460	0,457	0,454	0,388	0,288	0,226	0,184	0,6
	0,462	0,460	0,457	0,452	0,445	0,356	0,267	0,212	0,185	0,8
	0,460	0,457	0,451	0,443	0,432	0,328	0,249	0,200	0,167	1,0
	0,319	0,319	0,319	0,319	0,319	0,319	0,319	0,250	0,200	0,0
	0,319	0,319	0,319	0,319	0,319	0,319	0,314	0,246	0,198	0,2
	0,319	0,319	0,319	0,319	0,319	0,318	0,301	0,237	0,192	0,4
3,0	0,319	0,319	0,319	0,319	0,319	0,316	0,283	0,225	0,184	0,6
	0,319	0,319	0,319	0,318	0,318	0,309	0,264	0,212	0,175	0,8
	0,319	0,319	0,318	0,318	0,316	0,300	0,247	0,199	0,167	1,0
	0,243	0,243	0,243	0,243	0,243	0,243	0,243	0,243	0,200	0,0
	0,243	0,243	0,243	0,243	0,243	0,243	0,243	0,240	0,198	0,2
	0,243	0,243	0,243	0,243	0,243	0,242	0,242	0,232	0,191	0,4
4,0	0,243	0,243	0,243	0,243	0,242	0,242	0,240	0,221	0,184	0,6
	0,243	0,243	0,243	0,242	0,242	0,241	0,236	0,209	0,174	0,8
	0,243	0,243	0,242	0,242	0,242	0,240	0,231	0,198	0,167	1,0
	0,195	0,195	0,195	0,195	0,195	0,195	0,195	0,195	0,195	0,0
	0,195	0,195	0,195	0,195	0,195	0,195	0,195	0,195	0,194	0,2
	0,195	0,195	0,195	0,195	0,195	0,195	0,195	0,195	0,188	0,4
5,0	0,195	0,195	0,195	0,195	0,195	0,195	0,195	0,194	0,181	0,6
	0,195	0,195	0,195	0,195	0,195	0,194	0,194	0,191	0,173	0,8
	0,195	0,195	0,195	0,195	0,195	0,194	0,193	0,188	0,165	1,0

Table 5

$\tau_x = 0{,}4$

$\frac{N_{cr,\varphi}}{N_{cr,y}}$ \ $\frac{N_{cr,\varphi}}{N_{cr,x}}$	0,2	0,4	0,6	0,8	1,0	2,0	3,0	4,0	5,0	τ_y
	0,966	0,966	0,966	0,966	0,966	0,500	0,333	0,250	0,200	0,0
	0,957	0,945	0,923	0,886	0,823	0,481	0,326	0,247	0,198	0,2
	0,934	0,893	0,840	0,776	0,708	0,443	0,310	0,238	0,192	0,4
0,2	0,900	0,829	0,756	0,685	0,621	0,402	0,290	0,226	0,184	0,6
	0,860	0,765	0,682	0,612	0,553	0,365	0,269	0,212	0,175	0,8
	0,819	0,707	0,621	0,553	0,499	0,333	0,250	0,201	0,167	1,0
	0,918	0,918	0,918	0,918	0,918	0,500	0,333	0,250	0,200	0,0
	0,912	0,902	0,885	0,857	0,806	0,481	0,326	0,247	0,198	0,2
	0,893	0,859	0,815	0,760	0,699	0,442	0,310	0,238	0,192	0,4
0,4	0,864	0,805	0,740	0,676	0,616	0,401	0,290	0,226	0,184	0,6
	0,831	0,747	0,672	0,606	0,549	0,364	0,269	0,212	0,175	0,8
	0,795	0,695	0,614	0,550	0,496	0,333	0,250	0,201	0,167	1,0
	0,857	0,857	0,857	0,857	0,857	0,500	0,333	0,250	0,200	0,0
	0,853	0,846	0,835	0,816	0,781	0,481	0,326	0,247	0,198	0,2
	0,840	0,815	0,781	0,738	0,686	0,441	0,310	0,237	0,192	0,4
0,6	0,819	0,772	0,719	0,663	0,608	0,400	0,290	0,226	0,184	0,6
	0,792	0,725	0,658	0,598	0,544	0,364	0,269	0,212	0,175	0,8
	0,764	0,678	0,605	0,544	0,493	0,332	0,250	0,200	0,167	1,0
	0,788	0,788	0,788	0,788	0,788	0,499	0,333	0,250	0,200	0,0
	0,784	0,781	0,774	0,763	0,743	0,480	0,326	0,247	0,198	0,2
	0,776	0,760	0,738	0,708	0,667	0,440	0,310	0,237	0,192	0,4
0,8	0,763	0,730	0,691	0,645	0,597	0,399	0,290	0,226	0,184	0,6
	0,744	0,694	0,639	0,587	0,537	0,363	0,269	0,212	0,175	0,8
	0,723	0,656	0,592	0,536	0,488	0,332	0,250	0,200	0,167	1,0
	0,715	0,715	0,715	0,715	0,715	0,499	0,333	0,250	0,200	0,0
	0,713	0,711	0,708	0,701	0,691	0,479	0,326	0,247	0,198	0,2
	0,708	0,699	0,686	0,667	0,640	0,439	0,310	0,237	0,192	0,4
1,0	0,700	0,680	0,653	0,620	0,581	0,398	0,289	0,226	0,184	0,6
	0,688	0,655	0,615	0,571	0,529	0,362	0,268	0,212	0,175	0,8
	0,674	0,626	0,576	0,527	0,482	0,331	0,250	0,200	0,167	1,0
	0,443	0,443	0,443	0,443	0,443	0,443	0,333	0,250	0,200	0,0
	0,443	0,443	0,443	0,443	0,442	0,433	0,326	0,247	0,198	0,2
	0,443	0,442	0,441	0,440	0,439	0,409	0,308	0,237	0,192	0,4
2,0	0,442	0,441	0,439	0,436	0,433	0,379	0,288	0,225	0,184	0,6
	0,441	0,439	0,435	0,430	0,424	0,350	0,267	0,212	0,175	0,8
	0,440	0,435	0,429	0,422	0,412	0,323	0,248	0,200	0,167	0,0
	0,311	0,311	0,311	0,311	0,311	0,311	0,311	0,250	0,200	0,0
	0,311	0,310	0,310	0,310	0,310	0,310	0,306	0,246	0,198	0,2
	0,310	0,310	0,310	0,310	0,310	0,308	0,294	0,236	0,192	0,6
3,0	0,310	0,310	0,310	0,309	0,309	0,305	0,278	0,224	0,184	0,6
	0,310	0,310	0,309	0,309	0,308	0,298	0,260	0,211	0,175	0,8
	0,310	0,309	0,309	0,308	0,306	0,290	0,243	0,198	0,167	1,0
	0,238	0,238	0,238	0,238	0,238	0,238	0,238	0,238	0,200	0,0
	0,238	0,238	0,238	0,238	0,238	0,237	0,237	0,235	0,197	0,2
	0,238	0,238	0,237	0,237	0,237	0,237	0,236	0,228	0,191	0,4
4,0	0,238	0,237	0,237	0,237	0,237	0,236	0,234	0,218	0,183	0,6
	0,237	0,237	0,237	0,237	0,237	0,236	0,230	0,206	0,174	0,8
	0,237	0,237	0,237	0,237	0,236	0,234	0,225	0,195	0,166	1,0
	0,192	0,192	0,192	0,192	0,192	0,192	0,192	0,192	0,192	0,0
	0,192	0,192	0,192	0,192	0,192	0,192	0,192	0,192	0,191	0,2
	0,192	0,192	0,192	0,192	0,192	0,192	0,192	0,191	0,186	0,4
5,0	0,192	0,192	0,192	0,192	0,192	0,191	0,191	0,190	0,179	0,6
	0,192	0,192	0,192	0,192	0,192	0,191	0,191	0,187	0,171	0,8
	0,192	0,192	0,192	0,192	0,191	0,191	0,189	0,184	0,164	1,0

Table 6

$\tau_x = 0{,}5$

$\frac{N_{cr,\varphi}}{N_{cr,y}}$ \ $\frac{N_{cr,\varphi}}{N_{cr,x}}$	0,2	0,4	0,6	0,8	1,0	2,0	3,0	4,0	5,0	τ_y
	0,947	0,947	0,947	0,947	0,947	0,500	0,333	0,250	0,200	0,0
	0,940	0,928	0,909	0,875	0,817	0,481	0,326	0,247	0,198	0,2
	0,919	0,880	0,830	0,770	0,705	0,443	0,310	0,238	0,192	0,4
0,2	0,887	0,819	0,750	0,681	0,619	0,402	0,290	0,226	0,184	0,6
	0,849	0,758	0,678	0,609	0,551	0,365	0,269	0,212	0,175	0,8
	0,809	0,702	0,618	0,552	0,498	0,333	0,250	0,201	0,167	0,1
	0,883	0,883	0,883	0,883	0,883	0,500	0,333	0,250	0,200	0,0
	0,877	0,869	0,856	0,833	0,791	0,481	0,326	0,247	0,198	0,2
	0,861	0,833	0,795	0,747	0,690	0,442	0,310	0,238	0,192	0,4
0,4	0,837	0,785	0,726	0,667	0,610	0,401	0,290	0,226	0,184	0,6
	0,807	0,733	0,663	0,600	0,545	0,364	0,269	0,212	0,175	0,8
	0,775	0,683	0,608	0,545	0,494	0,332	0,250	0,201	0,167	0,1
	0,811	0,811	0,811	0,811	0,811	0,500	0,333	0,250	0,200	0,0
	0,807	0,802	0,794	0,780	0,754	0,480	0,326	0,247	0,198	0,2
	0,796	0,777	0,750	0,716	0,671	0,440	0,310	0,237	0,192	0,4
0,6	0,780	0,742	0,697	0,648	0,598	0,399	0,290	0,226	0,184	0,6
	0,758	0,701	0,643	0,588	0,538	0,363	0,269	0,212	0,175	0,8
	0,734	0,660	0,594	0,537	0,488	0,331	0,250	0,200	0,167	1,0
	0,737	0,737	0,737	0,737	0,737	0,499	0,333	0,250	0,200	0,0
	0,735	0,732	0,727	0,719	0,706	0,479	0,326	0,247	0,198	0,2
	0,729	0,716	0,699	0,676	0,644	0,439	0,310	0,237	0,192	0,4
0,8	0,718	0,692	0,661	0,623	0,582	0,398	0,289	0,226	0,184	0,6
	0,703	0,663	0,618	0,572	0,528	0,361	0,268	0,212	0,175	0,8
	0,686	0,631	0,577	0,526	0,481	0,331	0,250	0,200	0,167	1,0
	0,667	0,667	0,667	0,676	0,667	0,499	0,333	0,250	0,200	0,0
	0,666	0,664	0,661	0,657	0,650	0,477	0,426	0,247	0,198	0,2
	0,662	0,655	0,645	0,630	0,610	0,436	0,309	0,237	0,192	0,4
1,0	0,655	0,639	0,619	0,593	0,562	0,395	0,289	0,226	0,184	0,6
	0,646	0,619	0,588	0,552	0,515	0,360	0,268	0,212	0,175	0,8
	0,635	0,597	0,555	0,513	0,474	0,329	0,250	0,200	0,167	1,0
	0,422	0,422	0,422	0,422	0,422	0,422	0,333	0,250	0,200	0,0
	0,422	0,422	0,422	0,422	0,422	0,415	0,325	0,246	0,198	0,2
	0,422	0,421	0,420	0,419	0,418	0,395	0,307	0,237	0,192	0,4
2,0	0,421	0,420	0,418	0,416	0,412	0,369	0,285	0,225	0,184	0,6
	0,420	0,418	0,414	0,409	0,403	0,342	0,265	0,212	0,175	0,8
	0,419	0,415	0,409	0,402	0,393	0,317	0,247	0,199	0,167	1,0
	0,301	0,301	0,301	0,301	0,301	0,301	0,301	0,250	0,200	0,0
	0,301	0,301	0,301	0,301	0,301	0,300	0,297	0,246	0,198	0,2
	0,301	0,300	0,300	0,300	0,300	0,298	0,286	0,236	0,191	0,4
3,0	0,300	0,300	0,300	0,300	0,299	0,293	0,271	0,222	0,184	0,6
	0,300	0,300	0,299	0,299	0,298	0,287	0,255	0,209	0,174	0,8
	0,300	0,299	0,298	0,297	0,295	0,280	0,240	0,198	0,166	1,0
	0,232	0,232	0,232	0,232	0,232	0,232	0,232	0,232	0,200	0,0
	0,232	0,232	0,232	0,232	0,232	0,232	0,232	0,229	0,197	0,2
	0,232	0,232	0,232	0,232	0,232	0,231	0,230	0,223	0,191	0,4
4,0	0,232	0,232	0,232	0,232	0,232	0,230	0,228	0,214	0,182	0,6
	0,232	0,232	0,232	0,231	0,231	0,229	0,224	0,203	0,173	0,8
	0,232	0,232	0,231	0,231	0,230	0,227	0,219	0,193	0,165	1,0
	0,188	0,188	0,188	0,188	0,188	0,188	0,188	0,188	0,188	0,0
	0,188	0,188	0,188	0,188	0,188	0,188	0,188	0,188	0,187	0,2
	0,188	0,188	0 188	0,188	0,188	0,188	0,188	0,188	0,183	0,4
5,0	0,188	0 188	0,188	0,188	0,188	0,188	0,188	0,185	0,177	0,6
	0,188	0,188	0,188	0,188	0,188	0,187	0,186	0,183	0,169	0,8
	0,188	0,188	0 188	0,188	0,188	0,187	0,185	0,179	0,162	1,0

Table 7

$\tau_x = 0{,}6$

$\frac{N_{cr,\varphi}}{N_{cr,y}}$ \ $\frac{N_{cr,\varphi}}{N_{cr,x}}$	0,2	0,4	0,6	0,8	1,0	2,0	3,0	4,0	5,0	τ_y
	0,927	0,927	0,997	0,927	0,927	0,500	0,333	0,250	0,200	0,2
	0,920	0,909	0,892	0,862	0,809	0,481	0,326	0,247	0,198	0,0
	0,900	0,864	0,819	0,763	0,700	0,442	0,310	0,238	0,192	0,4
0,2	0,871	0,808	0,742	0,677	0,616	0,401	0,290	0,226	0,184	0,6
	0,836	0,750	0 673	0,606	0,550	0,364	0,269	0,212	0,175	0,8
	0,798	0,695	0,614	0,550	0,496	0,333	0,250	0,200	0,167	1,0
	0,847	0,847	0,847	0,847	0,847	0,500	0,333	0,250	0,200	0,0
	0,842	0,836	0,825	0,806	0,773	0,480	0,326	0,247	0,198	0,2
	0,829	0,805	0,772	0,730	0,680	0,441	0,310	0,238	0,192	0,4
0,4	0,808	0,762	0,711	0,657	0,603	0,400	0,290	0,226	0,184	0,6
	0,782	0,716	0,652	0,593	0,541	0,363	0,269	0,212	0,175	0,8
	0,753	0,671	0,599	0,540	0,490	0,331	0,249	0,200	0,167	1,0
	0,767	0,767	0,767	0,767	0,767	0,500	0,333	0,250	0,200	0,0
	0,764	0,760	0,753	0,743	0,725	0,479	0,326	0,247	0,198	0,2
	0,756	0,740	0,719	0,691	0,653	0,439	0,310	0,237	0,192	0,4
0,6	0,742	0,711	0,674	0,632	0,587	0,398	0,289	0,226	0,184	0,6
	0,724	0,676	0,626	0,577	0,530	0,361	0,268	0,212	0,175	0,8
	0,704	0,640	0,581	0,529	0,483	0,330	0,249	0,200	0,167	1,0
	0,692	0,692	0 692	0,692	0,692	0,499	0,333	0,250	0,200	0,0
	0,691	0,688	0,684	0,679	0,670	0,477	0,326	0,247	0,198	0,2
	0,685	0,676	0,663	0,645	0,620	0,436	0,309	0,237	0,192	0,4
0,8	0,677	0,656	0,632	0,601	0,567	0,395	0,289	0,226	0,184	0,6
	0,665	0,632	0,595	0,556	0,517	0,360	0,268	0,212	0,175	0,8
	0,651	0,605	0,559	0,515	0,474	0,329	0,249	0,200	0,167	1,0
	0 626	0,626	0,626	0,626	0,626	0,499	0,333	0,250	0,200	0,0
	0,625	0,623	0,621	0,618	0,613	0,475	0,326	0,247	0,198	0,2
	0,621	0,615	0,608	0,597	0,581	0,432	0,309	0,237	0,192	0,4
1,0	0,616	0,603	0,587	0,567	0,542	0,392	0,288	0,226	0,184	0,6
	0,609	0,587	0,561	0,532	0,501	0,357	0,267	0,212	0,175	0,8
	0,601	0,568	0,533	0,498	0,463	0,327	0,249	0,200	0,167	1,0
	0,402	0,402	0,402	0,402	0,402	0,402	0,333	0,250	0,200	0,0
	0,402	0,402	0,402	0,402	0,402	0,396	0,324	0,246	0,198	0,2
	0,402	0,401	0,400	0,399	0,398	0,379	0,305	0,236	0,191	0,4
2,0	0,401	0,400	0,398	0,395	0,392	0,357	0,284	0,224	0,184	0,6
	0,400	0,398	0,394	0,390	0,384	0,333	0,263	0,211	0,175	0,8
	0,398	0,395	0,389	0,383	0,375	0,311	0,245	0,198	0,166	1,0
	0,290	0,290	0,290	0,290	0,290	0,290	0,290	0,250	0,209	0,0
	0,290	0,290	0,290	0,290	0,290	0,289	0,287	0,245	0,197	0,2
	0,290	0,290	0,290	0,290	0,289	0,288	0,278	0,234	0,191	0,4
3,0	0,290	0,290	0,289	0,289	0,288	0,284	0,264	0,221	0,183	0,6
	0,290	0,289	0,288	0,288	0,287	0,278	0,250	0,208	0,174	0,8
	0,289	0,288	0,288	0,286	0,284	0,270	0,236	0,196	0,165	1,0
	0,226	0,226	0,226	0,226	0,226	0,226	0,226	0,226	0,200	0,0
	0,226	0,226	0,226	0,226	0,266	0,226	0,226	0,224	0,197	0,2
	0,226	0,226	0,226	0,226	0,226	0,225	0,224	0,218	0,190	0,4
4,0	0,226	0,226	0,226	0,226	0,226	0,224	0,221	0,209	0,181	0,6
	0,226	0,226	0,226	0,225	0,225	0,222	0,217	0,200	0,172	0,8
	0,226	0,226	0,225	0,225	0,225	0,221	0,212	0,190	0,164	1,0
	0,184	0,184	0,184	0,184	0,184	0,184	0,184	0,184	0,184	0,0
	0,184	0,184	0,184	0,184	0,184	0,184	0,184	0,184	0,183	0,2
	0,184	0,184	0,184	0,184	0,184	0,184	0,184	0,183	0,179	0,4
5,0	0,184	0,184	0,184	0,184	0,184	0,184	0,183	0,181	0,174	0,6
	0,184	0,184	0,184	0,184	0,184	0,184	0,182	0,178	0,167	0,8
	0,184	0,184	0,184	0,184	0,184	0,183	0,181	0,174	0,160	1,0

Table 8

$\tau_x = 0{,}7$

$\frac{N_{cr,y}}{N_{cr,x}}$ \ $\frac{N_{cr,\varphi}}{N_{cr,x}}$	0,2	0,4	0,6	0,8	1,0	2,0	3,0	4,0	5,0	τ_y
	0,905	0,905	0,905	0,905	0,905	0,500	0,333	0,250	0,200	0,0
	0,898	0,889	0,874	0,847	0,800	0,481	0,326	0,247	0,198	0,2
	0,881	0,848	0,806	0,753	0,694	0,441	0,310	0,238	0,192	0,4
0,2	0,853	0,795	0,733	0,671	0,612	0,400	0,290	0,226	0,184	0,6
	0,821	0,740	0,667	0,602	0,547	0,364	0,269	0,212	0,175	0,8
	0,786	0,688	0,610	0,547	0,495	0,333	0,250	0,200	0,167	1,0
	0,812	0,812	0,812	0,812	0,812	0,500	0,333	0,250	0,200	0,0
	0,808	0,802	0,793	0,779	0,753	0,480	0,326	0,247	0,198	0,2
	0,796	0,776	0,748	0,712	0,668	0,440	0,310	0,238	0,192	0,4
0,4	0,778	0,739	0,694	0,645	0,595	0,399	0,290	0,226	0,184	0,6
	0,756	0,698	0,640	0,585	0,536	0,362	0,260	0,212	0,175	0,8
	0,731	0,657	0,591	0,534	0,487	0,330	0,249	0,200	0,167	1,0
	0,727	0,727	0,727	0,727	0,727	0,500	0,333	0,250	0,200	0,0
	0,725	0,721	0,716	0,709	0,695	0,478	0,326	0,247	0,198	0,2
	0,718	0,705	0,688	0,665	0,635	0,438	0,310	0,237	0,192	0,4
0,6	0,706	0,681	0,650	0,614	0,574	0,396	0,289	0,226	0,184	0,6
	0,691	0,651	0,608	0,564	0,522	0,360	0,268	0,212	0,175	0,8
	0,674	0,620	0,567	0,519	0,477	0,329	0,249	0,200	0,167	1,0
	0,653	0,653	0,653	0,653	0,653	0,499	0,333	0,250	0,200	0,0
	0,651	0,650	0,646	0,643	0,636	0,476	0,326	0,247	0,198	0,2
	0,647	0,639	0,629	0,615	0,596	0,433	0,309	0,237	0,192	0,4
0,8	0,639	0,623	0,603	0,578	0,550	0,393	0,288	0,226	0,184	0,6
	0,630	0,603	0,573	0,539	0,505	0,357	0,267	0,212	0,175	0,8
	0,619	0,581	0,541	0,501	0,465	0,328	0,249	0,200	0,167	1,0
	0,589	0,589	0,589	0,589	0,589	0,499	0,333	0,250	0,200	0,0
	0,588	0,587	0,585	0,583	0,579	0,472	0,326	0,247	0,198	0,2
	0,585	0,581	0,574	0,566	0,554	0,429	0,308	0,237	0,192	0,4
1,0	0,581	0,570	0,557	0,541	0,521	0,389	0,288	0,225	0,184	0,6
	0,574	0,557	0,536	0,512	0,485	0,354	0,267	0,212	0,175	0,8
	0,567	0,542	0,512	0,482	0,451	0,325	0,248	0,199	0,167	1,0
	0,383	0,383	0,383	0,383	0,383	0,383	0,333	0,250	0,200	0,0
	0,383	0,383	0,383	0,382	0,382	0,378	0,322	0,246	0,198	0,2
	0,383	0,382	0,381	0,381	0,379	0,364	0,302	0,236	0,191	0,4
2,0	0,382	0,381	0,379	0,377	0,374	0,345	0,281	0,223	0,184	0,6
	0,381	0,379	0,375	0,371	0,367	0,324	0,260	0,210	0,174	0,8
	0,380	0,376	0,371	0,365	0,359	0,304	0,243	0,198	0,166	1,0
	0,280	0,280	0,280	0,280	0,280	0,280	0,280	0,250	0,200	0,0
	0,280	0,280	0,280	0,280	0,280	0,279	0,277	0,244	0,197	0,2
	0,280	0,279	0,279	0,279	0,279	0,277	0,269	0,233	0,191	0,4
3,0	0,279	0,279	0,278	0,278	0,278	0,274	0,257	0,219	0,183	0,6
	0,279	0,278	0,278	0,277	0,276	0,268	0,244	0,206	0,174	0,8
	0,279	0,278	0,277	0,276	0,274	0,260	0,231	0,195	0,165	1,0
	0,219	0,219	0,219	0,219	0,219	0,219	0,219	0,219	0,200	0,0
	0,219	0,219	0,219	0,219	0,219	0,219	0,219	0,218	0,196	0,2
	0,219	0,219	0,219	0,219	0,219	0,219	0,217	0,212	0,188	0,4
4,0	0,219	0,219	0,219	0,219	0,219	0,218	0,215	0,205	0,180	0,6
	0,219	0,219	0,219	0,219	0,218	0,216	0,211	0,195	0,171	0,8
	0,219	0,219	0,219	0,218	0,218	0,214	0,206	0,187	0,163	1,0
	0,180	0,180	0,180	0,180	0,180	0,180	0,180	0,180	0,180	0,0
	0,180	0,180	0,180	0,180	0,180	0,180	0,180	0,180	0,179	0,2
	0,180	0,180	0,180	0,180	0,180	0,180	0,180	0,178	0,175	0,4
5,0	0,180	0,180	0,180	0,180	0,180	0,180	0,178	0,177	0,170	0,6
	0,180	0,180	0,180	0,180	0,180	0,180	0,178	0,174	0,164	0,8
	0,180	0,180	0,180	,0180	0,179	0,179	0,176	0,171	0,157	1,0

Table 9

$\tau_x = 0{,}8$

$\frac{N_{cr,\varphi}}{N_{cr,y}}$ \ $\frac{N_{cr,\varphi}}{N_{cr,x}}$	0,2	0,4	0,6	0,8	1,0	2,0	3,0	4,0	5,0	τ_y
	0,882	0,882	0,882	0,882	0,882	0,500	0,333	0,250	0,200	0,0
	0,876	0,868	0,854	0,831	0,789	0,481	0,326	0,247	0,198	0,2
	0,860	0,831	0,792	0,744	0,688	0,441	0,310	0,237	0,192	0,4
0,2	0,836	0,782	0,724	0,665	0,609	0,400	0,290	0,226	0,184	0,6
	0,805	0,730	0,660	0,598	0,544	0,364	0,269	0,212	0,175	0,8
	0,773	0,681	0,605	0,543	0,492	0,332	0,250	0,200	0,167	1,0
	0,778	0,778	0,778	0,778	0,778	0,500	0,333	0,250	0,200	0,0
	0,774	0,770	0,763	0,751	0,730	0,479	0,326	0,247	0,198	0,2
	0,765	0,747	0,725	0,694	0,655	0,439	0,310	0,237	0,192	0,4
0,4	0,750	0,716	0,676	0,633	0,587	0,398	0,289	0,226	0,184	0,6
	0,730	0,679	0,626	0,576	0,529	0,361	0,268	0,212	0,175	0,8
	0,709	0,641	0,581	0,528	0,482	0,329	0,249	0,200	0.167	1,0
	0,690	0,690	0,690	0,690	0,690	0,500	0,333	0,250	0,200	0,0
	0,688	0,685	0,681	0,646	0,666	0,477	0,326	0,246	0,198	0,2
	0,682	0,672	0,658	0,640	0,615	0,435	0,309	0,237	0,192	0,4
0,6	0,673	0,652	0,626	0,595	0,561	0,394	0,288	0,226	0,184	0,6
	0,660	0,626	0,589	0,550	0,512	0,358	0,267	0,212	0,175	0,8
	0,647	0,600	0,553	0,510	0,470	0,327	0,248	0,199	0,167	1,0
	0,617	0,617	0,617	0,617	0,617	0,499	0,333	0,250	0,200	0,0
	0,616	0,614	0,612	0,609	0,604	0,474	0,326	0,246	0,198	0,2
	0,612	0,606	0,598	0,587	0,571	0,430	0,309	0,237	0,192	0,4
0,8	0,606	0,593	0,577	0,556	0,532	0,390	0,288	0,225	0,184	0,6
	0,598	0,576	0,550	0,522	0,492	0,355	0,267	0,212	0,175	0,8
	0,588	0,557	0,523	0,489	0,456	0,325	0,248	0,199	0,167	1,0
	0,556	0,556	0,556	0,556	0,556	0,499	0,333	0,250	0,200	0,0
	0,555	0,554	0,553	0,551	0,549	0,467	0,326	0,246	0,198	0,2
	0,553	0,549	0,544	0,537	0,529	0,424	0,308	0,237	0,192	0,4
1,0	0,550	0,541	0,530	0,517	0,501	0,384	0,287	0,225	0,184	0,6
	0,544	0,529	0,512	0,492	0,470	0,351	0,266	0,212	0,175	0,8
	0,537	0,517	0,492	0,467	0,440	0,322	0,247	0,199	0,167	1,0
	0,365	0,365	0,365	0,365	0,365	0,365	0,333	0,250	0,200	0,0
	0,365	0,365	0,365	0,364	0,364	0,361	0,320	0,246	0,198	0,2
	0,365	0,364	0,364	0,363	0,362	0,350	0,298	0,236	0,191	0,4
2,0	0,354	0,363	0,361	0,360	0,357	0,333	0,278	0,222	0,184	0,6
	0,364	0,361	0,358	0,355	0,351	0,315	0,258	0,209	0,174	0,8
	0,362	0,358	0,354	0,349	0,343	0,297	0,240	0,197	0,166	1,0
	0,270	0,270	0,270	0,270	0,270	0,270	0,270	0,250	0,200	0,0
	0,269	0,269	0,269	0,269	0,269	0,269	0,267	0,243	0,197	0,2
	0,269	0,269	0,269	0,269	0,268	0,267	0,260	0,230	0,191	0,4
3,0	0,269	0,269	0,268	0,268	0,267	0,263	0,250	0,217	0,182	0,6
	0,269	0,268	0,267	0,267	0,266	0,258	0,238	0,204	0,173	0,8
	0,268	0,267	0,267	0,265	0,264	0,251	0,226	0,193	0,164	1,0
	0,212	0,212	0,212	0,212	0,212	0,212	0,212	0,212	0,200	0,0
	0,212	0,212	0,212	0,212	0,212	0,212	0,212	0,211	0,195	0,2
	0,212	0,212	0,212	0,212	0,212	0,212	0,211	0,206	0,187	0,4
4,0	0,212	0,212	0,212	0,212	0,212	0,211	0,208	0,200	0,178	0,6
	0,212	0,212	0,212	0,212	0,212	0,209	0,204	0,191	0,169	0,8
	0,212	0,212	0,212	0,212	0,211	0,207	0,200	0,184	0,161	1,0
	0,176	0,176	0,176	0,176	0,176	0,176	0,176	0,176	0,176	0,0
	0,176	0,176	0,175	0,175	0,175	0,175	0,175	0,175	0,174	0,2
	0,175	0,175	0,175	0,175	0,175	0,175	0,175	0,174	0,171	0,4
5,0	0,175	0,175	0,175	0,175	0,175	0,175	0,174	0,172	0,167	0,6
	0,175	0,175	0,175	0,175	0,175	0,174	0,173	0,169	0,160	0,8
	0,175	0,175	0,175	0,175	0,174	0,174	0,171	0,166	0,154	1,0

Table 10

$\tau_x = 0{,}9$

$\frac{N_{cr,\varphi}}{N_{cr,y}}$ \ $\frac{N_{cr,\varphi}}{N_{cr,x}}$	0,2	0,4	0,6	0,8	1,0	2,0	3,0	4,0	5,0	τ_y
	0,859	0,859	0,859	0,859	0,859	0,500	0,333	0,250	0,200	0,0
	0,853	0,846	0,834	0,814	0,778	0,480	0,326	0,247	0,198	0,2
	0,839	0,812	0,778	0,733	0,681	0,440	0,310	0,237	0,192	0,4
0,2	0,816	0,767	0,714	0,658	0,604	0,399	0,290	0,226	0,184	0,6
	0,788	0,719	0,653	0,594	0,541	0,363	0,269	0,212	0,175	0,8
	0,759	0,672	0,600	0,540	0,490	0,332	0,250	0,200	0,167	1,0
	0,746	0,746	0,746	0,746	0,746	0,500	0,333	0,250	0,200	0,0
	0,743	0,739	0,733	0,724	0,708	0,478	0,326	0,247	0,198	0,2
	0,735	0,720	0,701	0,674	0,641	0,437	0,309	0,237	0,192	0,4
0,4	0,722	0,692	0,658	0,619	0,578	0,396	0,288	0,226	0,184	0,6
	0,705	0,660	0,613	0,567	0,523	0,359	0,267	0,212	0,175	0,8
	0,685	0,626	0,571	0,521	0,478	0,328	0,249	0,199	0,167	1,0
	0,657	0,657	0,657	0,657	0,657	0,500	0,333	0,250	0,200	0,0
	0,655	0,653	0,650	0,645	0,638	0,475	0,326	0,246	0,198	0,2
	0,650	0,642	0,630	0,616	0,595	0,431	0,309	0,237	0,192	0,4
0,6	0,643	0,625	0,603	0,577	0,547	0,391	0,288	0,226	0,184	0,6
	0,632	0,603	0,571	0,537	0,502	0,355	0,267	0,212	0,175	0,8
	0,619	0,580	0,539	0,499	0,463	0,325	0,247	0,199	0,167	1,0
	0,585	0,585	0,585	0,585	0,585	0,499	0,333	0,250	0,200	0,0
	0,584	0,583	0,581	0,578	0,574	0,470	0,326	0,246	0,198	0,2
	0,581	0,576	0,569	0,560	0,548	0,426	0,308	0,237	0,192	0,4
0,8	0,576	0,565	0,551	0,535	0,515	0,386	0,287	0,225	0,184	0,6
	0,570	0,551	0,529	0,505	0,479	0,352	0,266	0,212	0,175	0,8
	0,561	0,535	0,506	0,476	0,446	0,323	0,247	0,199	0,167	1,0
	0,527	0,527	0,527	0,527	0,527	0,499	0,333	0,250	0,200	0,0
	0,526	0,525	0,524	0,522	0,521	0,461	0,325	0,246	0,198	0,2
	0,524	0,521	0,517	0,512	0,504	0,418	0,307	0,236	0,192	0,4
1,0	0,521	0,514	0,505	0,495	0,481	0,380	0,286	0,225	0,184	0,6
	0,516	0,505	0,490	0,473	0,454	0,347	0,265	0,211	0,175	0,8
	0,511	0,494	0,473	0,451	0,427	0,319	0,246	0,199	0,167	1,0
	0,349	0,349	0,349	0,349	0,349	0,349	0,333	0,250	0,200	0,0
	0,349	0,349	0,348	0,348	0,348	0,345	0,316	0,245	0,198	0,2
	0,348	0,348	0,347	0,347	0,346	0,336	0,295	0,235	0,191	0,4
2,0	0,347	0,346	0,345	0,343	0,341	0,322	0,274	0,222	0,183	0,6
	0,347	0,344	0,342	0,340	0,336	0,305	0,255	0,209	0,174	0,8
	0,346	0,343	0,339	0,334	0,329	0,289	0,238	0,196	0,165	1,0
	0,260	0,260	0,260	0,260	0,260	0,260	0,260	0,250	0,200	0,0
	0,260	0,260	0,259	0,259	0,259	0,259	0,257	0,240	0,197	0,2
	0,259	0,259	0,259	0,259	0,258	0,258	0,251	0,227	0,190	0,4
3,0	0,259	0,259	0,258	0,258	0,257	0,255	0,243	0,215	0,181	0,6
	0,259	0,258	0,257	0,257	0,256	0,251	0,232	0,202	0,172	0,8
	0,259	0,257	0,257	0,256	0,253	0,244	0,221	0,191	0,164	1,0
	0,206	0,206	0,206	0,206	0,206	0,206	0,206	0,206	0,200	0,0
	0,206	0,206	0,206	0,206	0,206	0,206	0,205	0,205	0,194	0,2
	0,206	0,206	0,206	0,206	0,206	0,205	0,204	0,201	0,185	0,4
4,0	0,206	0,206	0,205	0,205	0,205	0,204	0,202	0,195	0,176	0,6
	0,206	0,205	0,205	0,205	0,205	0,202	0,198	0,187	0,167	0,8
	0,206	0,205	0,205	0,205	0,205	0,201	0,194	0,180	0,160	1,0
	0,171	0,171	0,171	0,171	0,171	0,171	0,171	0,171	0,171	0,0
	0,171	0,171	0,171	0,171	0,171	0,171	0,171	0,171	0,170	0,2
	0,171	0,171	0,171	0,171	0,171	0,171	0,171	0,170	0,167	0,4
5,0	0,171	0,171	0,171	0,171	0,171	0,170	0,169	0,167	0,163	0,6
	0,171	0,171	0,171	0,171	0,171	0,170	0,168	0,164	0,157	0,8
	0,171	0,171	0,171	0,171	0,170	0,169	0,167	0,162	0,152	1,0

Table 11

$\tau_x = 1{,}0$

$\frac{N_{cr,\varphi}}{N_{cr,y}}$ \ $\frac{N_{cr,\varphi}}{N_{cr,x}}$	0,2	0,4	0,6	0,8	1,0	2,0	3,0	4,0	5,0	τ_y
	0,836	0,836	0,836	0,836	0,836	0,500	0,333	0,250	0,200	0,0
	0,831	0,824	0,814	0,796	0,765	0,480	0,326	0,247	0,198	0,2
	0,818	0,794	0,763	0,722	0,674	0,440	0,310	0,237	0,192	0,4
0,2	0,797	0,753	0,703	0,650	0,599	0,398	0,289	0,226	0,184	0,6
	0,772	0,708	0,646	0,588	0,537	0,362	0,268	0,212	0,175	0,8
	0,743	0,663	0,594	0,536	0,487	0,331	0,249	0,199	0,166	1,0
	0,716	0,716	0,716	0,716	0,716	0,500	0,333	0,250	0,200	0,0
	0,713	0,710	0,705	0,698	0,685	0,478	0,326	0,247	0,198	0,2
	0,706	0,694	0,677	0,655	0,626	0,435	0,309	0,237	0,192	0,4
0,4	0,695	0,670	0,640	0,605	0,567	0,395	0,288	0,226	0,184	0,6
	0,680	0,640	0,599	0,557	0,516	0,358	0,267	0,212	0,175	0,8
	0,663	0,609	0,559	0,513	0,471	0,327	0,248	0,199	0,166	1,0
	0,626	0,626	0,626	0,626	0,626	0,500	0,333	0,205	0,200	0,0
	0,625	0,622	0,620	0,616	0,611	0,473	0,326	0,246	0,198	0,2
	0,620	0,613	0,604	0,591	0,575	0,429	0,309	0,237	0,192	0,4
0,6	0,614	0,598	0,581	0,558	0,533	0,389	0,288	0,226	0,184	0,6
	0,605	0,581	0,553	0,522	0,491	0,354	0,267	0,212	0,175	0,8
	0,594	0,559	0,524	0,488	0,454	0,324	0,247	0,198	0,166	1,0
	0,557	0,557	0,557	0,557	0,557	0,499	0,333	0,250	0,200	0,0
	0,555	0,554	0,553	0,551	0,548	0,466	0,326	0,246	0,198	0,2
	0,553	0,549	0,543	0,536	0,526	0,422	0,308	0,237	0,192	0,4
0,8	0,549	0,539	0,528	0,514	0,497	0,382	0,286	0,225	0,184	0,6
	0,543	0,527	0,509	0,488	0,466	0,349	0,265	0,212	0,175	0,8
	0,536	0,513	0,488	0,461	0,435	0,320	0,246	0,198	0,166	1,0
	0,500	0,500	0,500	0,500	0,500	0,499	0,333	0,250	0,200	0,0
	0,500	0,499	0,498	0,497	0,495	0,453	0,325	0,246	0,198	0,2
	0,498	0,495	0,492	0,488	0,482	0,411	0,306	0,236	0,191	0,4
1,0	0,495	0,489	0,482	0,473	0,462	0,374	0,284	0,224	0,184	0,6
	0,491	0,481	0,469	0,455	0,439	0,343	0,263	0,211	0,174	0,8
	0,487	0,471	0,454	0,435	0,415	0,315	0,244	0,198	0,165	1,0
	0,333	0,333	0,333	0,333	0,333	0,333	0,333	0,250	0,200	0,0
	0,333	0,333	0,333	0,333	0,333	0,330	0,311	0,245	0,197	0,2
	0,333	0,333	0,332	0,331	0,330	0,322	0,290	0,234	0,191	0,4
2,0	0,333	0,331	0,330	0,329	0,326	0,310	0,270	0,221	0,183	0,6
	0,332	0,329	0,327	0,325	0,322	0,296	0,251	0,207	0,174	0,8
	0,331	0,327	0,324	0,320	0,316	0,281	0,234	0,195	0,164	1,0
	0,250	0,250	0,250	0,250	0,250	0,250	0,250	0,250	0,200	0,0
	0,250	0,250	0,250	0,250	0,250	0,250	0,248	0,237	0,197	0,2
	0,250	0,250	0,250	0,250	0,249	0,248	0,243	0,224	0,189	0,4
3,0	0,250	0,249	0,249	0,249	0,248	0,245	0,235	0,212	0,181	0,6
	0,250	0,249	0,248	0,248	0,247	0,240	0,226	0,199	0,171	0,8
	0,249	0,248	0,247	0,246	0,244	0,234	0,215	0,188	0,161	1,0
	0,200	0,200	0,200	0,200	0,200	0,200	0,200	0,200	0,200	0,0
	0,200	0,200	0,200	0,200	0,199	0,199	0,199	0,198	0,191	0,2
	0,200	0,199	0,199	0,199	0,199	0,199	0,198	0,195	0,183	0,4
4,0	0,199	0,199	0,199	0,199	0,199	0,198	0,195	0,189	0,174	0,6
	0,199	0,199	0,199	0,198	0,198	0,196	0,192	0,183	0,165	0,8
	0,199	0,199	0,198	0,198	0,198	0,195	0,188	0,175	0,157	1,0
	0,167	0,167	0,167	0,167	0,167	0,167	0,167	0,167	0,167	0,0
	0,167	0,167	0,167	0,167	0,167	0,167	0,166	0,166	0,165	0,2
	0,167	0,167	0,167	0,167	0,166	0,166	0,166	0,165	0,163	0,4
5,0	0,167	0,167	0,167	0,167	0,166	0,166	0,164	0,163	0,159	0,6
	0,166	0,166	0,166	0,166	0,166	0,166	0,164	0,160	0,153	0,8
	0,166	0,166	0,166	0,166	0,165	0,165	0,161	0,157	0,148	1,0

can be found in one of the Tables. The value of $N_{cr.\varphi}$ can be calculated by making use of [8], the other two quantities are given by formulae

$$N_{cr,x} = \frac{7{,}84\, EI_y}{H^2}, \tag{3.17}$$

$$N_{cr,y} = \frac{7{,}84 EI_x}{H^2}. \tag{3.18}$$

In knowledge of the loading parameter λ the following formula gives the value of the critical load:

$$N_{cr} = \lambda N_{cr,\varphi}. \tag{3.19}$$

To make the calculation of the load factor reasonably simple we have given the values for τ_x between 0,1 and 1,0 in increments of 0,1 and the values for τ_y between 0,0 and 1,0 in increments of 0,2. In this way we have got ten tables and in each table there are values of τ_y in increments of 0,2 in successive lines so that interpolation is fairly simple. The tables contain quite a large number of values for the load factor so that linear interpolation is considered accurate enough for practical application.

Let us analyse the two extreme cases.

$\tau_y = 0$ corresponds to tha case of a bar with monosymmetric cross section. In that case buckling in the plane of symmetry xz does not combine with the torsional-flexural buckling perpendicular to the plane of symmetry. Values in the tables always give the lowest critical load factor, that is, for example if

$$\frac{N_{cr,\varphi}}{N_{cr,y}} = 0{,}8,$$

and $\tau_x = 1{,}0$ then we get 0,557 for the value of

$$\frac{N_{cr}}{N_{cr,\varphi}}$$

independently of the value of

$$\frac{N_{cr,\varphi}}{N_{cr,x}}$$

(because bending in the plane xz is independent of torsional-flexural bending in the plane yz) until we reach the value of

$$\frac{N_{cr,\varphi}}{N_{cr,x}} = 1.$$

After exceeding this value, the values of the critical load factor for buckling in the plane of symmetry become lower than those of the torsional-flexural ones, so the tables give these lower values.

$\tau_x = \tau_y = 1$ corresponds to the case when both coordinates of the shear centre are at infinity. It is in that case that the approximate formula

$$\frac{1}{N_{cr}} < \frac{1}{N_{cr,x}} + \frac{1}{N_{cr,y}} + \frac{1}{N_{cr,\varphi}}, \tag{3.20}$$

based on Föppl's theorem, gives the best approximate value for the critical load. However, in this unsymmetrical case, there are no geometrical and rigidity ratios when the Föppl's formula gives the exact critical load, contrary to the case of the monosymmetrical cross section. This discrepancy can clearly be proved when the column is subjected to a concentrated load on top [5].

The values in the tables indicate certain symmetry properties. Let us take $\tau_x = \tau_y$. In that case the elements on the right and on the left sides of the diagonal of a table are symmetric. The reason for this symmetry is that buckling in the plane xz or in the plane yz is the same physical phenomenon. The governing differential equations for buckling (1.1), (1.2) also show this fact.

4. Practical application

The given formulae, tables and diagrams are applicable not only for the stability analysis of thin-walled bars which are applied as individual elements in different kinds of structures, but for the stability analysis of the bracing system of tall buildings as well.

A building subjected to vertical loads — as other "column" structures — can develop three kinds of deformations: buckling in the two principal planes of inertia and pure torsional buckling. In general the bracing system of a building has no axes of symmetry (or it has only one), so that the pure torsional buckling combines with flexural bucklings in the two principal planes of inertia (or in one of the principal planes of inertia). The critical load of the pure torsional buckling can be considerably smaller than that of the planar buckling and in this case the critical load of the building is small as well [4].

If there is only one core bracing the building subjected to vertical loads on each floor, then by distributing the loads along the height of the building we get a cantilever subjected to distributed normal loads. For the stability analysis we need the bending, torsional and warping rigidities. These rigidities have to be calculated by making use of the rigidity and geometrical characteris-

tics of the core. On the other hand, the polar radius of inertia has to be calculated from the ground plan dimensions of the building. This follows from the derivation of the differential equation of the pure torsional buckling (Eq. (1.3) in [8]). The derivation of the equation is based on the analysis of the behaviour of the longitudinal fibres of the cross section during buckling. The external loads act along these fibres and cause torsion. The bar balances this effect by means of its torsional and warping rigidities. In our case (in the case of a tall building) the external loads act on the floors and they are transmitted by columns and walls (longitudinal fibres). It follows therefore that the larger the ground plan of a building, the smaller the value of the critical load for pure torsional buckling, because in these cases the arm of the forces which cause torsion becomes longer and so the value of the external torque becomes greater as well.

In the general case when there are several cores or perpendicular shear walls bracing the building we can use a substitute cantilever with the following rigidities: The torsional rigidity is the sum of the torsional rigidities of the elements while the warping rigidity is a weighted sum [5].

5. Design example

Using the given formulae, diagrams and tables let us determine the critical load of the cantilever with a thin-walled open cross section shown in Fig. 4 subjected to uniformly distributed normal load along its height. The data are given in Fig. 4. The values needed for the calculation are as follows.

The polar moment of inertia:

$$I_0 = I_x + I_y + Ax_0^2 = 329{,}6 \text{ cm}^4 .$$

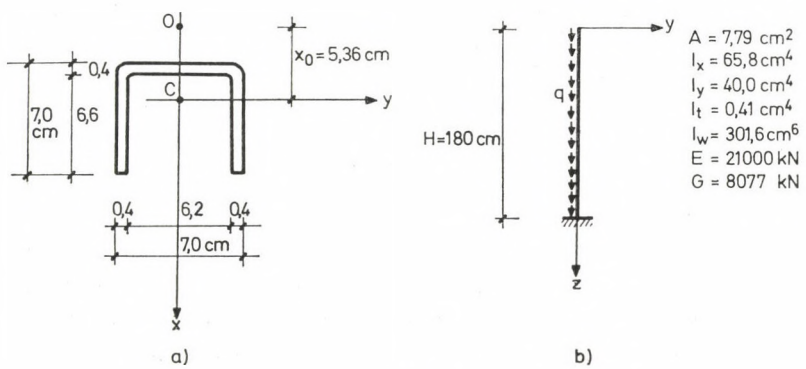

Fig. 4

The polar radius of inertia:

$$i = \sqrt{\frac{I_0}{A}} = 6{,}5 \text{ cm}.$$

The factor τ (2.8) which characterizes the torsion (warping, twist):

$$\tau = \frac{x_0}{i_p} = \sqrt{\frac{I_0 - I_x - I_y}{I_0}} = 0{,}82\,.$$

The critical load for buckling in the plane of symmetry (2.4):

$$N_{cr,x} = \frac{7{,}84 E I_y}{H^2} = 203{,}3 \text{ kN}\,. \tag{5.1}$$

The critical load for buckling perpendicular to the plane of symmetry (2.39):

$$N_{cr,y} = \frac{7{,}84 E I_x}{H^2} = 334{,}4 \text{ kN}\,. \tag{5.2}$$

This Euler-type buckling combines with the pure torsional buckling. For the calculation of the critical load for pure torsional buckling we need the following quantities [8]:

The critical load associated with the torsional rigidity:

$$N^t_{cr,\varphi} = \frac{G I_t}{i_p^2} = 78{,}3 \text{ kN}\,.$$

The critical load associated with the warping rigidity:

$$N^{\omega}_{cr,\varphi} = \frac{7{,}84 E I_{\omega}}{H^2 i_p^2} = 36{,}2 \text{ kN}\,.$$

The ratio of the above two "partial" critical loads (2.6):

$$\beta = \frac{N^t_{cr,\varphi}}{N^{\varphi}_{cr,\varphi}} = 2{,}16\,.$$

As a function of β the diagram in Fig. 7 in [8] gives the following ratio:

$$\frac{N_{cr,\varphi}}{N^{\omega}_{cr,\varphi}} = 5{,}82\,,$$

so the critical load for pure torsional buckling is as follows:

$$N_{cr,\varphi} = 5{,}82\, N^{\omega}_{cr,\varphi} = 210{,}7 \text{ kN}. \tag{5.3}$$

By making use of the ratios

$$\frac{N_{cr,\varphi}}{N_{cr,y}} = 0{,}63$$

and

$$\tau = 0{,}82,$$

Fig. 3 gives

$$\varepsilon = 0{,}465,$$

so the value for the "combined" critical load can be calculated from the formula (2.40):

$$N_{cr} = \varepsilon N_{cr,y} = 155{,}5 \text{ kN}. \tag{5.4}$$

This value is smaller than the critical load for buckling in the plane of symmetry (5.2), so this is of practical interest.

We also have calculated the critical load of the cantilever by making use of Föppl's approximate formula [8] and it has given a value by 16 per cent less than the exact one.

We have made calculations for cantilevers with different ratios of rigidity by making use of the approximate formula published in [8] and the exact one given in this paper. The evalution of the figures shows that the error made by using the approximate formula is up to 50 per cent in the case of monosymmetric cross sections and is up to 66,7 per cent in the case of unsymmetric cross sections. The nearer the ratio of the critical loads, which are to be combined, to unity and the values of τ or $\tau_x$and τ_y to zero, the larger the error.

Although the approximate formulae yield the critical load always on the safe side, the deviation may be as much as 66,7 per cent, so it seems to be reasonable to use the exact formulae derived in this paper if we want to design economic structures.

REFERENCES

1. Akesson, B.: Overall Buckling in Bending and Torsion of Rack Structures. Thin Walled Structures. Ed. J. Rhodes and A. C. Walker, pp 127—144, 1980
2. Éliás, E.: On One of Föppl's Theorems.* Budapest, 1977, Manuscript.
3. Föppl, L.: Über das Ausknicken von Gittermasten, insbesondere von hohen Funktürmen. *Zeitschrift fur Angewandte Mathematik und Mechanik* **13** (1933), 1—10
4. Kollár, L.: Stiffening of Buildings against Torsional Buckling. Proceedings of the Regional Colloquium on Stability of Steel Structures. pp 411—422 Balatonfüred—Budapest 1977, Hungary
5. Szmodits, K.: Structural Analysis for Prefabricated Buildings.* *Publication of the Building Research Institute.* Budapest 1975
6. Timoshenko, S.—Gere, J.: Theory of Elastic Stability. McGraw-Hill, New York 1961
7. Vlasov, V. Z.: Thin-walled Elastic Beams. (Translated from Russian) Israel Program for Scientific Translations, Jerusalem, 1961
8. Zalka, K.: Torsional Buckling of a Cantilever Subjected to Distributed Normal Loads. *Acta Tech. Hung.* **90** (1980) 91—108

Torsions- und Biegeknickung eines Kragträgers mit asymmetrischem Querschnitt unter gleichförmig verteilter Normalbelastung. — Die zusammengesetzte Torsions- und Biegeknickung eines am unteren Ende eingespannten und am oberen Ende freibleibenden, durch gleichförmig verteilte Normalkräfte belasteten Stabes wird behandelt. Die kritische Belastung ist für Stäbe mit monosymmetrischen und mit asymmetrischem Querschnitt angegeben. Die Eigenwertsaufgabe des Differentialgleichungssystems dritter Ordnung mit veränderlichen Koeffizienten wird durch Verallgemeinerung der Potenzreihenmethode zu einer einfachen algebraischen Aufgabe zurückgeführt Die algebraische Aufgabe wird mit Hilfe des Annäherungsverfahrens gelöst. Die zur Berechnung erforderlichen Eigenwerte der kritischen Belastung sind tabellarisch zusammengafasst. Durch ein numerisches Beispiel wird die Anwendung der abgeleiteten Formeln demonstriert.

* In Hungarian

Acta Technica Academiae Scientiarum Hungaricae, Tomus 92 (1—2), pp. 215—223 (1981)

DESCRIPTION OF THE GAS CONSUMPTION PROCESS BY MEANS OF PROBABILITY CALCULATION

M. VIDA*
CAND. OF TECHN. SCI.
and
L. GARBAI**

[Manuscript received 9. September, 1980]

In their presentation the authors deal with some points concerning the random gas consumption of energetic nature of individual major gas consumer groups. It is determined that the characteristics of random gas consumption (quantity, intensity, simultaneity, etc.) are probability variables in mathematical sense. In scheduling gas consumption, the chances of the realization of the characteristics and the probability distribution of same, also have to be determined. The authors relate the determination of scheduled values to the extent of assumption of risk. In their study, the authors present new methods based on the theory of stochastic processes for describing the process of gas consumption and for determining the probability distribution of consumption values.

1. Introduction

It is a well-known fact that the gas consumption of a residential area or urban sector, moreover of any major group of industrial consumers is generally not uniform, however, it shows very great fluctuations within a day and the consumption levels per days, weeks and months are different as well. Generally, the nature of consumption within a day shows substantial fluctuation, including a.m. and p.m. peak periods, low consumption level between these periods and modulations superimposed on the peaks and valleys.

The actual causes of consumption fluctuations by parts of the day and week in the domestic sector are well known and are to be searched for in the hygienic habits and organization of work and living conditions of the population.

The possible fluctuations of industrial consumption are in connection with the fluctuations of the industrial productions process and these may also include random effects.

The pattern of consumption fluctuation may follow certain constancy and regularity but the superimposed modulations are entirely of random character and cannot be predicted with accuracy.

* Dr. M. VIDA, Baranyai út 24, H—1117 Budapest, Hungary.
** Dr. L. GARBAI, Tamási Áron u. 4., H—1124 Budapest, Hungary.

Finally, the case is that the consumers will generally be involved in the gas consumption at random times and will consume gas with varying intensity and for random periods. Therefore, both the resulting consumption intensity and its volume show random variations.

For this reason, when designing and operating gas supplying installation, the random character of gas consumption cannot be neglected. At the same time it should be pointed out that up to the present, no comprehensive theoretical study of this subject has been carried out.

2. Rudiments

The following should be studied in the course of selecting and designing the operation of gas producing and gas supplying equipment:

— the consumption at a certain period (peak period), consumption per hour, consumption per minute or the total volume of the daily consumption,

— the whole daily pattern of the consumption intensity,

— certain derived characteristics, the tendencies of the ununiformity and simultaneity factors, etc.

The process of gas consumption as a phenomenon, will be described by means of the above characteristics.

Theoretical limitations and maximums can be assigned to every characteristic. But generally, the actual values of gas consumption are more or less under these values, while the realisation of maximum is neither a case of zero probability. The gas consumption characteristics are probability variables.

Taking into consideration the probability variable nature of the above characteristics, the following reasonable questions arise: what value of the above characteristics should be considered as a basis for designing and in the course of operation management, at any time what demands have we to be prepared to meet by means of production and storage?

When carrying out the comprehensive theoretical study of this subject, the process of gas supply and consumption should be based on exact probability calculations. Probability measures, distributions should be assigned to the various characteristics of gas consumption and the chances of realizations should be given. Thereafter, excluding the realizations with low probability and undertaking risks which can be computed accurately, the values which serve for a basis of designing, operative service and operation management, can be specified.

Some of the specific aspects of the above subject will be treated in our paper.

The probability calculation models, which are suitable for the mathematical description of the random gas consumption process in case of randomly consuming group of gas consumers, will be presented.

3. Probability calculation models of the gas consumption process

The description of the gas consumption process by means of probability calculation may be carried out in two ways, i.e. the following may be studied:

— the process nature of the gas consumption on the basis of the theory of stochastic processes in the sense of which the following distribution is searched for

$$P(Q(\tau)); \qquad P(\dot{Q}(\tau)); \tag{1}$$

— the state character of the gas consumption based on "static" models as well as the probability distribution of gas consumption in a finite period or the distribution of the simultaneity of consumption. Therefore, in this case the following relationships should be disclosed.

$$P(Q(\tau_0, \tau_1)) \tag{2}$$

and

$$P(\dot{Q}(\tau_i)) \,. \tag{3}$$

The most up-to-date inspection method which provides the most information and which is at the same time the most complicated one, is based on the theory of the stochastic processes. The probability distribution of gas consumption as a stochastic process, is a function of time and includes some explicitly. The consumption fluctuations by parts of of the day can be described only on the basis of this conception. In the sense of probability the model will give information concerning the gas consumption process at any time.

The static models are not suitable for the above purposes. The main difference between the static models and the stochastic process models is that a distribution below

$$P(Q(\tau_0; \tau_1))$$

discloses nothing on the process behaviour beyond the particular period, moreover the behaviour within this period can only be described in the case of a process which is homogeneous in time with the use of the conclusions to be drawn from the static model.

In course of the description of gas consumption by means of probability calculation, the theory of stochastic processes will be taken as a basis in our paper and the random gas consumption will be treated as a process. The employment of the static models is an established field which generally covers the application of well-known statistic means.

3.1. *The analysis of gas consumption process based on the theory of stochastic processes in the case of consumers consuming at random times and have identical consumption intensities and can be characterized by "0—1" connection state*

3.1.1. *Probability distribution of the gas volume consumed at any period*

The process of random gas consumption is a so-called secondary stochastic process. In the process of gas consumption in any time interval the consumers will enter into consumption independently of each other.

The probability of the events of entering into consumption is described by the Poisson process as follows, on the basis of the principle of independence

$$P(k, t) = \frac{\Lambda(t)^k}{k!} e^{-\Lambda(t)} \tag{4}$$

where

$$\Lambda(t) = \int_0^t \lambda(u)\, du \tag{5}$$

is the expected value of the connections occurring within the $(0, t)$time interval Therefore, the density of consumption (density of events) is generally a function of time.

Within the $(0, t)$ time interval the consumers enter into consumption at random t_k times having uniform distribution. All the consumers entering into consumption at t_k times, will consume for random χ_k periods. The distribution of the χ_k period of connection is

$$H(x) = P(\chi_k \leq x)\,. \tag{6}$$

As a probability variable, the consumption of a consumer until t time entering into consumption at any time $(0 \leq t_i \leq t)$, is

$$f(t - t_k, \chi_k) \tag{7}$$

and its distribution function is

$$P(f(t - t_k, \chi_k) \leq x) = h(t, x)\,. \tag{7-1}$$

If in the $(0, t)$ time interval k number of consumer enterings occurred, the value of consumption, i.e. the volume of gas consumption within the $(0, t)$ period at time t will obviously be

$$Q(t) = \sum_k f(t - t_k, \chi_k)\,. \tag{8}$$

It is our objective to formulate the distribution function

$$P(Q(t) \leq x) = G(t, x). \tag{8-1}$$

One way of formulating the distribution function (8—1) is to examine the characteristic functions.

Under the condition that the connection of the consumer into the gas supply occurred at u time ($0 \leq u \leq t$), according to Takács's theorem (1), the characteristic function of the distribution function (7—1) is as follows:

$$\varphi(t - u, \omega) = \int_{-\infty}^{\infty} e^{i\omega f(t-u, x)}\, dH(x)\ . \tag{9}$$

As the distribution function of u is $\Lambda(u)/\Lambda(t)$, therefore, utilizing the theorem for the hypothetical expected values, the characteristic function of the consumption which started at random time and measured at t time, is

$$\psi_t(\omega) = \frac{1}{\Lambda(t)} \cdot \int_0^t \varphi(t - u, \omega)\, d\Lambda(u)\ . \tag{10}$$

If in the time interval $(0, t)$ the number of connections into the gas supply was "k", the sum of the consumption values would be the sum of "k" number of independent probability variables, the characteristic function of which is (1)

$$(\psi_t(\omega))^k\ ,$$

and finally the characteristic function of the searched for distribution function (8—1) is

$$\Phi(t, \omega) = \sum_{n=0}^{\infty} e^{-\Lambda(t)} \frac{(\Lambda(t))^n}{n!} (\psi_t(\omega))^n\ . \tag{11}$$

From the complex range the characteristic function (1)) can be transformed back into the real range by using of the so-called inversion integral. Through the inversion of the characteristic function (11) the probability distribution (8—1) of the gas consumption process (8) will be obtained.

As is known, the inversion integral is (5)

$$G(t, x) - G(t, y) =$$

$$= \frac{1}{2\pi} \int_{-\infty}^{\infty} \left(\Phi(t, \omega) \right) \frac{e^{-i\omega y} - e^{-i\omega x}}{2i\omega} - \Phi(t, -\omega) \frac{e^{i\omega y} - e^{i\omega x}}{2i\omega} \Bigg) d\omega\ . \tag{12}$$

The time function of the gas consumption of a consumer (7) may be written more simply as follows;

$$f(t - u, \chi) = \begin{cases} \dot{q} \cdot \chi & 0 \leq \chi \leq t - u \\ \dot{q}(t - u) & \chi \geq t - u \end{cases}\ . \tag{13}$$

It is a reasonable assumption, concerning the probability distribution of the connection period χ that

$$H(\chi) = P(\chi \leq x) = \begin{cases} 1 - e^{-\mu x} & 0 \leq x\,, \\ 0 & x < 0\,. \end{cases} \tag{14}$$

Based on the above formulas, the conditional characteristic function (10) is

$$\varphi(t-u,\,\omega) = \frac{i \cdot \omega \cdot \dot{q}}{i \cdot \omega \cdot \dot{q} - \mu}\, e^{(i\omega\dot{q}-\mu)(t-u)} - \frac{\mu}{i\omega\dot{q} - \mu}\,. \tag{15}$$

When examining the case where the connections into gas supply occur as a process homogeneous in time, the characteristic function (10) is

$$\lambda(u) \equiv \lambda\,;$$

$$\psi_t(\omega) = \frac{1}{t}\,\frac{i\omega \cdot \dot{q}}{(i\omega\dot{q} - \mu)^2}\,(e^{(i\omega q - \mu)\,t} - 1) - \frac{\mu}{i\omega\dot{q} - \mu}\,. \tag{16}$$

The characteristic function of the searched for distribution function (8—1) will be obtained by substituting formula (16) into formula (11).

It is a disadvantage to form the distribution function (8—1) with the help of the characteristic function, is that, the inversion of the characteristic function will not lead to an explicite formula.

The distribution function (8—1) can be formed directly by means of set and probability algebraical means.

If the examination of the process of gas consumption is started at a time τ_0 when

$$\dot{Q}(\tau_0) = 0;$$

the probability distribution of the gas consumption process can be written reasonably as follows:

$$G(t,\,x) = P(Q(t) \leq x) = P(0,\,t) + P(1;\,t) \cdot P\left(\bar{\chi}_1 \leq \frac{x}{1 \cdot \dot{q}}\right) +$$

$$+ P(2;\,t) \cdot P\left(\bar{\chi}_2 \leq \frac{x}{2 \cdot \dot{q}}\right) + \ldots + P(k;\,t) \cdot P\left(\bar{\chi}_k \leq \right.$$

$$\left. \leq \frac{x}{k \cdot \dot{q}}\right) + \ldots + \,. \tag{17}$$

As has already been mentioned the connections to the gas supply occur as a Poisson process. When this is taken into consideration, the formula can be

written in more details as follows:

$$G(t, x) = P\big(Q(t) \leq x\big) = e^{-\Lambda(t)} + \frac{\Lambda^{(t)}}{1!} e^{-\Lambda(t)} \cdot$$

$$\cdot P\left(\bar{\chi}_1 \leq \frac{x}{1 \cdot \dot{q}}\right) + \frac{\Lambda(t)^2}{2!} e^{-\Lambda(t)} \cdot P\left(\bar{\chi}_2 \leq \frac{x}{2 \cdot \dot{q}}\right) + \ldots +$$

$$+ \frac{\Lambda(t)^k}{k!} e^{-\Lambda(t)} \cdot P\left(\bar{\chi}_k \leq \frac{x}{k \cdot \dot{q}}\right) + \ldots \infty . \tag{18}$$

As a probability variable, the average connection period of the consumers is

$$\bar{\chi}_k = \frac{\chi_{k,1} + \chi_{k,2} + \ldots + \chi_{k,k}}{k} . \tag{19}$$

The density function [5] of the average connection period, as a probability variable, is

$$g_k(y) = \frac{\mu^k \cdot y^{k-1}}{(k-1)!} e^{-\mu y} \cdot \frac{1}{k} . \tag{20}$$

And its distribution function is

$$F_k\left(\bar{\chi} \leq \frac{x}{k \cdot \dot{q}}\right) = \frac{1}{k} \int_0^{x/k \cdot \dot{q}} \frac{\mu^k \cdot y^{k-1}}{(k-1)!} e^{-\mu y} \, dy . \tag{21}$$

By means of the distribution function, the expected value of the average connection period can be computed:

$$M(\bar{\chi}_k) = \frac{1}{\mu} . \tag{22}$$

By transforming same for gas consumption

$$\frac{1}{\mu} \cdot \dot{q} . \tag{23}$$

The expected value of distribution (18) is

$$M(Q(t)) = \Lambda(t) \cdot \dot{q} \cdot \frac{1}{\mu} . \tag{24}$$

As concerning the actual consumption, there is a physical upper limit of consumption, i.e. this is the case where all of the consumers consume gas

continuously within the inspected period, the following relationship is valid:

$$P(Q(t) \leq Q_{\max}) = 1 . \tag{25}$$

Therefore, by curtailing formula (18) the real distribution function is

$$G^x(x) = \begin{cases} \dfrac{G(x)}{G(Q_{\max})} & ; \ x \leq Q_{\max} , \\ 1 & ; \ x > Q_{\max} . \end{cases} \tag{26}$$

The expected value of consumption on the basis of curtailed distribution is

$$M^x(Q(t)) = \Lambda(t) \cdot \dot{q} \cdot \frac{1}{\mu} \cdot \frac{1}{G(Q_{\max})} . \tag{27}$$

3.1.2. *The probability distribution of gas consumption intensity in case of consumption having a connection with density homogeneous in time*

In this case the tendency of consumption intensity of a consumer is expressed by the function $f(t - u, \chi)$

$$f(t - u, \chi) = \begin{cases} \dot{q} & ; \ \chi \geq t - u , \\ 0 & ; \ \chi < t - u . \end{cases} \tag{28}$$

With the use of the function $f(t - u, \chi)$ and by using the $\lambda(u) = \lambda$ conditional characteristic function of the consumption intensity of a consumer:

$$\varphi_{(t-u,\,\omega)} = \int_0^{t-u} dH(x) + \int_{t-u}^{\infty} e^{i\omega\dot{q}}\, dH(x) = 1 - e^{-\mu(t-u)}\,(1 - e^{i\omega\cdot\dot{q}}) . \tag{29}$$

With the use of formula (29), the characteristic function of the consumption intensity of a consumer is

$$\psi_t(\omega) = \frac{1}{t}\int_0^t \left(1 - e^{-\mu(t-u)}\,(1 - e^{i\omega\dot{q}})\right) du =$$

$$= 1 - (1 - e^{i\mu\dot{q}})\,\frac{1 - e^{-\mu t}}{\mu t} . \tag{30}$$

The characteristic function of the totalled consumption can be obtained by substituting formula (30) into relationship (11).

Symbols

$P(\ )$	Probability distribution function,
τ, t	Time, as a mathematical variable,
$Q(\tau_0; \tau_1)$	Consumed gas volume in the time interval $(\tau_0; \tau_1)$
$\dot{Q}(\tau)$	Gas consumption intensity at the moment,
$Q(\tau)$	Consumed gas volume, as a function of time,
$\dot{Q}(\tau)$	Gas consumption intensity, as a function of time,
$\dot{q}$	The consumption intensity of a consumer.

REFERENCES

1. TAKÁCS, L.: Poisson folyamatok által származtatott másodlagos folyamatokról és azok fizikai alkalmazásáról. (Secondary processes derived by means of Poisson process and their physical application), MTA III. O. K. **4** (1954), 473—504
2. TAKÁCS, L.: Bizonyos fizikai regisztráló berendezésekkel kapcsolatos sztochasztikus folyamatokról. (Stochastic processes associated with some physical recording devices) MTA III. O.K. **4** (1954), 471—584
3. TAKÁCS, L.: Elektroncsövek anódáram ingadozásának valószínűségszámítási tárgyalásáról (Description of the probability calculation of electronic tube anode current fluctuations) MTA III. O.K. **6** (1956), 27—51
4. Műszaki matematikai gyakorlatok. Valószínűségszámítás. (Technical mathematical practices. Probability calculation), Editors: Dr. MEDGYESSY P., Dr. TAKÁCS L.: Tankönyvkiadó, Budapest 1966
5. PRÉKOPA, A.: Valószínűségelmélet. (Probability theory) Műszaki Könyvkiadó, Budapest 1972

Beschreibung der Gasverbrauchsprozesses durch die Wahrscheinlichkeitstheorie. — Die Probleme der energetikbezweckten zufallbestimmten Gasverbrauch einiger größeren Verbrauchergruppen werden behandelt. Es wird festgesetzt daß die Kennwerte (Größe, Intensität, Gleichzeitigkeit, usw.) des zufallbestimmten Gasverbrauchs im mathematischen Sinne Zufallsveränderlichen sind. Im Laufe des Voranschlags des Gasverbrauchs sollten auch die Realisationswahrscheinlichkeiten und die wahrscheinliche Verteilung der Kennwerte ermittelt werden. Die Ermittlung der Entwurfswerte sind mit dem Maße der Risikoübernahme verbunden. Aufgrund der Theorie der stochastischen Prozesse sind neue Methoden zur Beschreibung des Gasverbrauchsprozesses und zur Ermittlung der Wahrscheinlichkeitsverteilung der Verbrauchswerte entwickelt worden.

INDEX

PRINTED IN HUNGARY
Akadémiai Nyomda, Budapest

Acta Techn. Hung. **92** (1981) pp. 3—22

SOARE, M. V.: *A New Method for Solving Orthotropic Rectangular Plates*

The partial differential equation of orthotropic plates based on the smoothing of the stiffeners in two orthogonal directions is considered. It is completed with terms representing the effect of the supporting on an elastic subgrade of Winkler type, as well as the consideration of the friction between the plate and the foundation. The solution is based on the use of double series of characteristic functions and leads to the solution of a linear system with an infinity of equations and unknowns.

Acta Techn. Hung. **92** (1981) pp. 33—43

CSONKA, P.: *Stability of a Bar Elastically Built-in at one of its Extremities*

Paper deals with the buckling caused by dead load of a prismatic bar of vertical axis made of elastic material. It assumes that the lower end of the bar is elastically built-in while its top end is entirely free. The critical load of the bar is determined by Timoshenko's approximate method. The deflected shape of the bar axis is approached by a third-degree polynome. In the extreme case when the foot of the bar is rigidly fixed, this assumption leads to a result hardly differing from the correct one, while in the other extreme case when the bar is absolutely rigid, it yields the exact result.

Acta Techn. Hung. **92** (1981) pp. 23—32

ABD ELHADY, M. A.—PROHÁSZKA, J.: *Effect of Rapid Heat Treatment on the Microstructure and Tensile Properties of Cold Drawn Boron-Treated Steel (ZF).*

This paper describes three methods of heat treatment for high hardenability boron-treated steel. The object of this work is to determine the change in microstructure and tensile properties due to these different heat treatment operations. The present paper is to be considered the first report on the heat treatment of cold drawn boron treated steel and will be followed by subsequent works in order to select a new technology for the heat treatment of ZF_7 steel.

Acta Techn. Hung. **92** (1981) pp. 45—65

KOZÁK, I.: *Remarks and Contributions to the Variational Principles of the Linearized Theory of Elasticity in Terms of the Stress Functions*

The paper gives a definition of such functionals in which the stress function tensor has only three (suitably selected) non-zero coordinates, and which makes the detailed investigation of the boundary conditions possible. From the introduced dual functionals, by the variation of the stress function tensor, three compatibility field equations and the compatibility boundary conditions are obtained, as the sufficient and necessary conditions of the compatibility of the strain field.

Acta Techn. Hung. **92** (1981) pp. 67—88

TARNAI, T.: *Existence and Uniqueness Criteria of the Membrane State of Shells, Part. II.*

Criteria of support will be considered, needed, or allowed to be specified in the edges of a shell under vertical loads of arbitrary distribution in order to have the shell in a statically determinate membrane state. Part I of this paper published earlier considered criteria of existence and uniqueness of the solution of the membrane shell equation in connection with hyperbolic shells. This Part II extends the analysis to parabolic shells.

Acta Techn. Hung. **92** (1981) pp. 121—137

SEIDL, GY.: *An Axisymmetrical Punch Problem in the Linear Couple-stress Theory of Elasticity*

The case of the elastic half space under a cylindrical rigid punch is investigated by taking the effect of the couple-stress into account. The solution of the resulting mixed boundary-problem leads, similarly to the classic case, to dual integral equations. It is pointed out that to the case of the two extreme values ($l^2 = 0$ and $l^2 \to \infty$) of the material property l^2 for the flat-end cylindrical punch, the classic stress distribution is obtained. For another solution the principle of minimum complementary energy might be suggested. Minimizing of the functional of the complementary energy is carried out by using Ritz's method. A numerical example relates to the flat-end punch. The diagrams plotted suggest the deviations from the classic case.

Acta Techn. Hung. **92** (1981) pp. 139—152

KRÓMER, I. J.: *Switching Surge Breakdown Characteristics of Large Conductor — Tower Air Gaps*

A comprehensive series of impulse tests on a variety of simulated transmission tower insulation is destribed. The influence of the waveshape on positive polarity switching surge strength of large tower configurations was by applying different waves with times-to-crest between 35 and 1200 μs. The test results overlap and extend beyond existing data, making available a generalized flashover voltage-wavefront characteristics. Special tests were designed to provide additional experimental information for developing a model of large air gap flashover. The parameters affecting the corona to leader transition and the leader propagation have also been evaluated. The comparison of the experimental results with theoretical predictions indicates that the simulation of the discharge phenomena is advanced.

Acta Techn. Hung. **92** (1981) pp. 153—166

FÜREDI, M.—TERSZTYÁNSZKY, T.: *Calculation Method for Determining Load Frequency Constant*

Following a review of several publications the paper describes a new calculation method which can be used for determining long term load frequency constant and frequency exponent by computation based on the consumers' structure and the electrical characteristics of the system. With the use of available information, in the data base of energy economy, the paper presents cases for application. As a main result of calculation it has been found, in the period of 1970—78, that the yearly average resulting load frequency constant for Hungarian consumers was varying between 1,04—1,08 expressed in a non-dimensional value.

Acta Techn. Hung. **92** (1981) pp. 167—187

DULÁCSKA, E.—NAGY, J.—BÓDI, L.: *Overall Buckling of Hyperbolic Shells of Revolution with Unmovable Lower Edge*

The paper treats the general buckling of hyperbolic shells of revolution (i.e. of shells with negative Gaussian curvature), using the linear theory. For the derivation of the critical load the shell of revolution is substituted by a hyperbolic paraboloid having the same curvatures. The numerical values of the critical load are determined for geometric ratios of the shell occurring in the practice, and are presented in a table. Finally, a numerical example shows the application of the method.

Acta Techn. Hung. **92** (1981) pp. 189—214

ZALKA, K.: *Combined Torsional and Flexural Buckling of a Cantilever with Unsymmetric Cross Section Subjected to Distributed Normal Loads*

This paper deals with the combined torsional and flexural buckling of a bar with a built-in lower and a free upper end subjected to uniformly distributed normal loads. The critical load is given for bars with mono-symmetric and with unsymmetric cross section. The eigenvalue problem of the third-order differential equations of variable coefficients is traced back to a simple algebraic problem by generalizing the power series method. The algebraic problem is solved by trial and error. The eigenvalues needed for the calculation of the critical load are given in tables. A numerical example is presented to show how to use the formulas derived.

Acta Techn. Hung. **92** (1981) pp. 215—223

VIDA, M.—GARBAI, L.: *Description of the Gas Consumption Process by Means of Probability Calculation*

In their presentation the authors deal with some points concerning the random gas consumption of energetic nature of individual major gas consumer groups. It is determined that the characteristics of random gas consumption (quantity, intensity, simultaneity. etc.) are probability variables in mathematical sense. In scheduling gas consumption, the chances of the realization of the characteristics and the probability distribution of same, also have to be determined. The authors relate the determination of scheduled values to the extent of assumption of risk. In their study, the authors present new methods based on the theory of stochastic processes for describing the process of gas consumption and for determining the probability distribution of consumption values.

The *Acta Technica* publish papers on technical subjects in English, French, German and Russian.

The *Acta Technica* appear in parts of varying size, making up one volume.

Manuscripts should be addressed to

Acta Technica
H-1051 Budapest
Münnich Ferenc u. 7.
Hungary

Correspondence with the editors and publishers should be sent to the same address.

Orders may be placed with "Kultura" Foreign Trading Company (H-1389 Budapest 62, P.O.B. 149. Account No. 218-10990) or its representatives abroad.

Les *Acta Technica* paraissent en français, allemand, anglais et russe et publient des travaux du domaine des sciences techniques.

Les *Acta Technica* sont publiés sous forme de fascicules qui seront réunis en volumes.

On est prié d'envoyer les manuscrits destinés à la rédaction à l'adresse suivante:

Acta Technica
H-1051 Budapest
Münnich Ferenc u. 7.
Hongrie

Toute correspondance doit être envoyée à cette même adresse.

On peut s'abonner à l'Entreprise du Commerce Extérieur «Kultura» (H-1389 Budapest 62, P.O.B. 149. Compte courant No. 218-10990) ou chez représentants à l'étranger.

«*Acta Technica*» публикуют трактаты из области технических наук на русском-немецком, английском и французском языках.

«*Acta Technica*» выходят отдельными выпусками разного объема. Несколько выпусков составляют один том.

Предназначенные для публикации рукописи следует направлять по адресу:

Acta Technica
H-1051 Budapest
Münnich Ferenc u. 7.
Венгрия

По этому же адресу направлять всякую корреспонденцию для редакции и администрации.

Заказы принимает предприятие по внешней торговле «Kultura» (H-1389 Budapest 62, P.O.B. 149. Текущий счет № 218-10990) или его заграничные представительства и уполномоченные.

Reviews of the Hungarian Academy of Sciences are obtainable at the following addresses:

AUSTRALIA
C.B.D. LIBRARY AND SUBSCRIPTION SERVICE
Box 4886, G.P.O. *Sydney N.S.W. 2001*
COSMOS BOOKSHOP, 145 Ackland Street
St. Kilda (Melbourne), Victoria 3182

AUSTRIA
GLOBUS, Höchstädtplatz *3, 1206 Wien XX*

BELGIUM
OFFICE INTERNATIONAL DE LIBRAIRIE
30 Avenue Marnix, *1050 Bruxelles*
LIBRAIRIE DU MONDE ENTIER
162 rue du Midi, *1000 Bruxelles*

BULGARIA
HEMUS, Bulvar Ruszki 6, *Sofia*

CANADA
PANNONIA BOOKS, P.O. Box 1017
Postal Station "B", *Toronto, Ontario M5T 2T8*

CHINA
CNPICOR, Periodical Department, P.O. Box 50
Peking

CZECHOSLOVAKIA
MAD'ARSKÁ KULTURA, Národni třida 22
115 66 Praha
PNS DOVOZ TISKU, Vinohradská 46, *Praha 2*
PNS DOVOZ TLAČE, *Bratislava 2*

DENMARK
EJNAR MUNKSGAARD, Norregade 6
1165 Copenhagen K

FEDERAL REPUBLIC OF GERMANY
KUNST UND WISSEN ERICH BIEBER
Postfach 46, *7000 Stuttgart 1*

FINLAND
AKATEEMINEN KIRJAKAUPPA, P.O. Box 128
SF-00101 Helsinki 10

FRANCE
DAWSON-FRANCE S.A., B. P. 40, *91121 Palaiseau*
EUROPÉRIODIQUES S.A., 31 Avenue de Versailles, *78170 La Celle St. Cloud*
OFFICE INTERNATIONAL DE DOCUMENTATION ET LIBRAIRIE, 48 rue Gay-Lussac
75240 Paris Cedex 05

GERMAN DEMOCRATIC REPUBLIC
HAUS DER UNGARISCHEN KULTUR
Karl Liebknecht-Straße, 9, *DDR-102 Berlin*
DEUTSCHE POST ZEITUNGSVERTRIEBSAMT
Straße der Pariser Kommüne 3-4, *DDR-104 Berlin*

GREAT BRITAIN
BLACKWELL'S PERIODICALS DIVISION
Hythe Bridge Street, *Oxford OX1 2ET*
BUMPUS, HALDANE AND MAXWELL LTD.
Cowper Works, *Olney, Bucks MK46 4BN*
COLLET'S HOLDINGS LTD., Denington Estate
Wellingborough, Northants NN8 2QT
WM. DAWSON AND SONS LTD., Cannon House
Folkestone, Kent CT19 5EE
H. K. LEWIS AND CO., 136 Gower Street
London WC1E 6BS

GREECE
KOSTARAKIS BROTHERS INTERNATIONAL BOOKSELLERS, 2 Hippokratous Street, *Athens-143*

HOLLAND
MEULENHOFF-BRUNA B.V., Beulingstraat 2
Amsterdam
MARTINUS NIJHOFF B.V.
Lange Voorhout 9-11, *Den Haag*
SWETS SUBSCRIPTION SERVICE
347b Heereweg, *Lisse*

INDIA
ALLIED PUBLISHING PRIVATE LTD., 13/14
Asaf Ali Road, *New Delhi 110001*
150 B-6 Mount Road, *Madras 600002*
INTERNATIONAL BOOK HOUSE PVT. LTD.
Madame Cama Road, *Bombay 400039*
THE STATE TRADING CORPORATION OF INDIA LTD., Books Import Division, Chandralok
36 Janpath, *New Delhi 110001*

ITALY
INTERSCIENTIA, Via Mazzé 28, *10149 Torino*
LIBRERIA COMMISSIONARIA SANSONI, Via Lamarmora 45, *50121 Firenze*
SANTO VANASIA, Via M. Macchi 58
20124 Milano
D. E. A., Via Lima 28, *00198 Roma*

JAPAN
KINOKUNIYA BOOK-STORE CO. LTD.
17-7 Shinjuku 3 chome, Shinjuku-ku, *Tokyo 160-91*
MARUZEN COMPANY LTD., Book Department, P.O. Box 5050 Tokyo International, *Tokyo 100-31*
NAUKA LTD. IMPORT DEPARTMENT
2-30-19 Minami Ikebukuro, Toshima-ku, *Tokyo 171*

KOREA
CHULPANMUL, *Phenjan*

NORWAY
TANUM-TIDSKRIFT-SENTRALEN A.S., Karl Johansgatan 41-43, *1000 Oslo*

POLAND
WĘGIERSKI INSTYTUT KULTURY, Marszałkowska 80, *00-517 Warszawa*
CKP I W, ul. Towarowa 28, *00-958 Warszawa*

ROUMANIA
D. E. P., *Bucureşti*
ILEXIM, Calea Grivitei 64-66, *Bucureşti*

SOVIET UNION
SOJUZPECHAT—IMPORT, *Moscow*
and the post offices in each town
MEZHDUNARODNAYA KNIGA, *Moscow G-200*

SPAIN
DIAZ DE SANTOS, Lagasca 95, *Madrid 6*

SWEDEN
ALMQVIST AND WIKSELL, Gamla Brogatan 26
101 20 Stockholm
GUMPERTS UNIVERSITETSBOKHANDEL AB
Box 346, *401 25 Göteborg 1*

SWITZERLAND
KARGER LIBRI AG, Petersgraben 31, *4011 Basel*

USA
EBSCO SUBSCRIPTION SERVICES
P.O. Box 1943, *Birmingham, Alabama 35201*
F. W. FAXON COMPANY, INC.
15 Southwest Park, *Westwood, Mass. 02090*
THE MOORE-COTTRELL SUBSCRIPTION AGENCIES, *North Cohocton, N. Y. 14868*
READ-MORE PUBLICATIONS, INC.
140 Cedar Street, *New York, N. Y. 10006*
STECHERT-MACMILLAN, INC.
7250 Westfield Avenue, *Pennsauken N. J. 08110*

YUGOSLAVIA
JUGOSLOVENSKA KNJIGA, Terazije 27, *Beograd*
FORUM, Vojvode Mišića 1, *21000 Novi Sad*

HU ISSN 0001—7035 Index: 26.025

ACTA TECHNICA

ACADEMIAE SCIENTIARUM HUNGARICAE

REDIGIT: M. MAJOR

TOMUS 92
FASCICULI 3—4

AKADÉMIAI KIADÓ, BUDAPEST 1981

ACTA TECHNICA

Az *Acta Technica* angol, francia, német és orosz nyelven közöl értekezéseket a műszaki tudományok köréből.

Az *Acta Technica* változó terjedelmű füzetekben jelenik meg, több füzet alkot egy kötetet.

A közlésre szánt kéziratok a következő címre küldendők:

Acta Technica
1051 Budapest, Münnich Ferenc u. 7.

Ugyanerre a címre küldendő minden szerkesztőségi és kiadóhivatali levelezés.

Megrendelhető a belföld számára az „Akadémiai Kiadó"-nál (1363 Budapest Pf. 24. Bankszámla 215-11448), a külföld számára pedig a „Kultura" Külkereskedelmi Vállalatnál (1389 Budapest 62, P.O.B. 149 Bankszámla: 218-10990) vagy annak külföldi képviseleteinél és bizományosainál.

Die *Acta Technica* veröffentlichen Abhandlungen aus dem Bereiche der technischen Wissenschaften in deutscher, englischer, französischer und russischer Sprache.

Die *Acta Technica* erscheinen in Heften wechselnden Umfanges. Vier Hefte bilden einen Band.

Die zur Veröffentlichung bestimmten Manuskripte sind an folgende Adresse zu senden:

Acta Technica
H-1051 Budapest
Münnich Ferenc u. 7.
Ungarn

An die gleiche Anschrift ist auch jede für die Schriftleitung und den Verlag bestimmte Korrespondenz zu richten.

Bestellbar bei »Kultura« Außenhandelsunternehmen (H-1389 Budapest 62, P.O.B. 149, Bankkonto Nr. 218-10990) oder seinen Auslandsvertretungen.

Acta Technica Academiae Scientiarum Hungaricae, Tomus 92 (3–4), pp. 225–243 (1981)

APPLICATION OF THE BENEDICT, WEBB AND RUBIN EQUATION OF STATE TO THE EVALUATION OF THE VOLUMETRIC AND THERMODYNAMIC PROPERTIES OF THE CH_4—CO_2 SYSTEM

PART I

MUHAMMAD A. I. BUKHARI*

[Manuscript received March 14, 1978]

Part I of this paper outlines the development and the evolution of the BWR equation of state. The equation, in its new form, using the pure component parameters and the newly proposed mixing rules of BISHNOI and ROBINSON is tested at low temperature and high pressures, using the data of ARAI, KAMINISHI and SAITO. The equation has proved super adaptability for correlating P-V-T-x relationships, particularly at high pressures and lower temperatures where binary interaction comes into play more and more.

A_0, B_0, C_0,
a, b, c, α, ν = parameter of the BWR equation of state
BWR_I = the Benedict, Webb and Rubin equation state using Cullen and Kobe constants for CO_2 and Benedict, Webb and Rubin constants for CH_4
BWR_{II} = the Benedict, Webb and Rubin equation of state using Bishnoi and Robinson constants
BWR_{III} = Benedict, Webb and Rubin equation of state using the mixing rules and pure component parameters of Bishnoi and Robinson
P = pressure
R = universal gas constant
T = temperature
T_{cij} = characteristic critical temperature, characteristic of i-j molecular interaction
V = molal volume
V_{cij} = interaction critical volume
Z = compressibility factor
d = density
k_{12} = parameter characterising deviation from the geometric mean assumption for characteristic temperature
X = mole fraction, liquid-phase
y = mole fraction, vapour-phase

Subscripts

c = Critical point
i, j = general indices, components

Application of the Benedict, Webb and Rubin equation of state to the evaluation of volumetric and thermodynamic properties of CH_4—CO_2 mixtures

Increasing demand for natural gas has necessitated the utilization of sources previously considered to be uneconomical. Direct experimental determinations of usually unavailable wide scopes of thermodynamic properties

* Present address: M. A. I. BUKHARI, P.O. Box 2408 Khartoum, Sudan

of systems such as the CH_4-CO_2 system, if not impossible are, by all means, inconceivable from the point of view of required costs, human efforts and time. To facilitate engineering design work associated with gaseous mixtures in industrial operations, an accurate method of predicting the pressure-volume-temperature behaviour and properties of the gas being processed, is essential. The most accurate P-V-T-X relationships are obtained by the use of an equation of state which can also be utilized for the evaluation of other thermodynamic properties. The Benedict, Webb and Rubin equation of state [1—5] was originally developed primarily to permit the description of the phase behaviour of multicomponent hydrocarbon mixtures of relatively low molecular weight, is traditionally associated with these compounds, and is considered to be the best, presently available for hydrocarbon systems. The equation has been extensively and successfully used by its authors and others for correlating volumetric and thermodynamic properties of fluids and has appeared to researchers to be the most promising method for obtaining precise thermal data on mixtures. Pure component constants for the equation have been evaluated for paraffin hydrocarbons, unsaturated hydrocarbons and various non-hydrocarbon fluids, and a technique was developed for combining pure component parameters of the BWR equation for the prediction of mixture properties. Some of the largest reservoirs of natural gas contain appreciable concentrations of CO_2 and therefore, attempts have been made to evaluate a set of BWR equation constants for CO_2 that would permit prediction of the effect of CO_2 on the P-V-T behaviour of hydrocarbon mixtures. However, earlier workers have reported difficulties in the prediction of properties of hydrocarbon mixtures containing non-hydrocarbons [6—10]. However, recent improvements of the pure component BWR parameters, and modifications of the mixing rules by the introduction of corrections for binary molecular interaction have, beyond no doubt, rendered the BWR equation of state highly suitable for the correlation of the volumetric and thermodynamic properties of the CH_4-CO_2 system over wide ranges of pressures and low temperatures.

The BWR equation

The BWR equation of state is

$$P = RTd + \left(B_0 RT - A_0 - \frac{C_0}{T^2}\right) \cdot d^2 + (bRT - a)d^3 + \\ + a\alpha d^6 + \frac{cd^3(1 + \gamma d^2) \cdot \exp(-\gamma d^2)}{T^2} . \tag{1}$$

Benedict, Webb and Rubin have shown that their proposed 8-parameter equation can be correctly used to represent P-V-T properties of the gas phase

up to about twice the critical density. However, according to the authors, owing primarily to limitations in the parameter A_0, the errors at higher densities become much higher, and have suggested that better agreement at higher densities could not have been obtained without the use of several more parameters. The same equation of state holds for mixtures provided they do not react chemically, and the authors have made use of the results of the statistico-mechanical treatment of J. E. MAYER (1939), [11], to formulate mixing rules for their equation of state. For a binary mixture these are:

$$B_0 = x_1 B_{01} + x_2 B_{02} \quad \text{(linear combination)} \tag{2}$$

$$A_0 = x_1^2 A_{01} + x_2^2 A_{02} + 2x_1 x_2 (A_{01} A_{02})^{1/2} \tag{3}$$

$$C_0 = x_1^2 C_{01} + x_2^2 C_{02} + 2x_1 x_2 (C_{01} C_{02})^{1/2} \tag{4}$$

$$b = [x_1 b_1^{1/3} + x_2 b_2^{1/3}]^3 \tag{5}$$

$$a = [x_1 a_1^{1/3} + x_2 a_2^{1/3}]^3 \tag{6}$$

$$c = [x_1 c_1^{1/3} + x_2 c_2^{1/3}]^3 \tag{7}$$

$$\alpha = [x_1 \alpha_1^{1/3} + x_2 \alpha_2^{1/3}]^3 \tag{8}$$

$$\nu = [x_1 \nu_1^{1/2} + x_2 \nu_2^{1/2}]^2. \tag{9}$$

Interaction parameters: In these equations, constants with suffixes refer to the pure components, and those in the form $(A_{01}A_{02})^{1/2}$ are a property of the mixture arising from interactions between unlike molecules. These are termed by the authors as *interaction constants* of the mixture.

Numerical values of the parameters

BENEDICT, WEBB and RUBIN have determined and listed numerical values of the 8-parameters for 12 hydrocarbons, including methane, estimated from data comprising P-V-T and critical properties and vapour pressures above one atmosphere. CULLEN and KOBE (1955) [8] have used P-V-T and vapour pressure data to determine two sets of pure component constants for carbon dioxide, each applicable to a particular temperature range. EAKON and ELLINGTON (1959) [6] have suggested the use of two sets of CO_2 constants recommended over different composition ranges.

Modified parameters

BONO and STARLING (1970) [12] and BISHNOI and ROBINSON (1971) [13] have concluded in their studies that the BWR parameters obtained by choosing specific volume as the dependent variable give a more satisfactory cor-

relation of the volumetric behaviour than that given by the parameters obtained by choosing pressure (or compressibility factor) as the dependent variable. STARLING (1970) [16] has reported BWR parameters for CO_2, CH_4 and C_3H_8 estimated by using volumetric and vapour pressure data simultaneously, since the P-V-T data are available for these substances in both the gaseous and liquid regions. Likewise, BISHNOI and ROBINSON [14, 15] have estimated parameters for methane, propane, n-butane, carbon-dioxide and hydrogen sulfide by minimizing the sum of relative error squares in specific volume using a non-linear least squares technique. The parameters thus determined, are useful to correlate the volumetric properties and to calculate the fugacities of the liquid and gas phases at the saturation points.

The mixing rules

The prediction of the properties of mixtures of hydrocarbons using the previously mentioned mixing rules was found satisfactory in many cases. However, various workers have reported difficulties in predicting the properties of hydrocarbon mixtures containing non-hydrocarbons [6—10]. CULLEN and KOBE [8] have attributed this lack of success of the BWR equation in certain cases to the increased interaction of the molecules of the components in the liquid phase. Deviations have then been believed to be due to the method of expressing the dependence of the parameters of the equation on composition. When one or more of the components is dissimilar in chemical character from the others, added interactions which are not accounted for by the present method, come into play.

Low temperature applications

As early as 1951, BENEDICT et al. have suggested that one of the parameters in their equation of state be made a function of temperature in order to treat systems at very low temperatures. For temperatures below the normal boiling point, use of the original BWR coefficients understimates vapour pressures and overestimates enthalpies of pure components. BENEDICT et al. have thus recommended that the parameter C_0 be determined to fit the vapour pressure curve, while the other seven coefficients be kept constant.

Experience with the A_0 mixing rule in its present form, has shown that when it is applied to mixtures, inaccuracies may still be encountered even though the pure components have been well described. This failure is ascribed to failure of the mixing rules to account for solution non-ideality, especially in the liquid-phase. STOTLER and BENEDICT (1953) [7] in their evaluation

of a BWR equation for CH_4-N_2 vapour-liquid equilibria at low temperatures, have found that they could not correlate the equilibria using the original method. Accordingly, at first they resorted to adjusting the value of C_0 for pure CH_4 and pure N_2 to exactly agree with vapour pressures of the pure components at each temperature of interest. Then, for the mixture, they have suggested an adjustment of the rule for determining the parameter A_0, Equation 3, by introducing a factor into the geometric mean interaction constant, and have reported an improvement:

$$A_0 = x_1^2 A_{01} + x_2^2 A_0^2 + 2x_1 x_2 \, m(A_{01} A_{02})^{1/2}. \tag{10}$$

The factor m has been found to be almost independent of temperature and pressure, but depends on the specific binary system.

KAMISHI, ARAI, SAITO and MAEDA (1968) [10] have investigated vapour-liquid equilibria in systems containing CO_2 with the purpose of obtaining fundamental data that nay be useful for the separation of CO_2 by liquefaction.

From observed data they have examined the usefulness of the BWR equation of state for the prediction of vapour-liquid equilibria, and have reported large discrepancies between calculated and experimental results by applying the original BWR equation. By introducing the modification of A_0, proposed by STOTLER and BENEDICT, Equation 10, KAMINISHI et al. have shown that the modification improves the degree of agreement, except in the critical region.

BARNER and ADLER (1968) [9] while reviewing the BWR equation at low temperatures, have concluded that the resolution of the deficiencies of the BWR equation for mixtures depends on improving the combining rules.

ORYE (1969) [17] has suggested pure component coefficients for the BWR equation to extend its range to low temperatures which are now becoming more common in natural gas processing. However, he pointed out that considerable attention must be given to the mixing rules used in the equation. To account for solution non-ideality he has followed the suggestion of STOTLER and BENEDICT in modifying the rule for A_0. Furthermore, for low temperature applications, ORYE has recommended the desirability to obtain C_0 as a smoothly varying function of temperature, so that the equation becomes more easily adaptable to computer programs.

GUN (1958) [18] has studied the volumetric properties of non-polar gaseous mixtures, and concluded that an equation of state, regardless of the number of parameters involved, cannot calculate accurately the thermodynamic properties of mixtures unless the parameters for the mixtures reflect the true nature of the forces of interaction between unlike, as well as like, molecules. He has been able to improve predictions of second virial coefficients for binary mixtures using the BWR equation of state by introducing a cor-

rection to characteristic critical temperature, ΔT_{cij}, characteristic of the *i-j* molecular interaction. This constant has been defined as follows:

$$T_{cij} = (T_{ci}\, T_{cj})^{1/2} - \Delta T_{cij}\,. \tag{11}$$

Later, CHEUH and PRAUSNITZ (1967) [19] have formulated mixing rules for the Redlich—Kwong equation of state by defining an interaction critical temperature as follows:

$$T_{cij} = (T_{ci}\, T_{cj})^{1/2}(1 - k_{ij})\,. \tag{12}$$

The binary constant k_{ij} represents a deviation from the geometric mean for T_{cij}. They utilized the values of k_{ij} estimated from the experimental information on second virial coefficients for binary mixtures in formulating a method for calculating the generalized third virial coefficients of gaseous mixtures.

The most recent, and perhaps the most significant contribution so far, in the evolution process of developing the BWR equation of state, is that afforded by BISHNOI and ROBINSON [13—15]. The two authors have assimilated the observations and findings of previous workers to formulate new mixing rules for the BWR parameters. In their development of the mixing rules, they have followed a system of logic similar to that used by the latter mentioned authors [18, 19]. The rules contain a binary interaction parameter readily obtainable from information on binary interactions, or other data available in the literature, namely from experimental values of the second virial cross-coefficients. They have tested the validity of their improved mixing rules, and newly proposed pure component BWR parameters by using them to predict the volumetric behaviour of binary mixtures of CO_2 with methane, ethane and propane at elevated pressures. They have then compared the predicted densities with experimental values, and for any of the three mixtures, the standard error of the predictions was approximately equal to or less than the sum of the standard errors of fit of the pure components.

These newly proposed mixing rules, when applied to a binary mixture take the form:

$$B_0 = x_1^2 B_{01} + x_2^2 B_{02} + 2x_1 x_2 (B_{01} B_{02})^{1/2} \cdot \gamma_{12}\,, \tag{13}$$

$$A_0 = x_1^2 A_{01} + x_2^2 A_{02} + 2x_1 x_2 (A_{01} A_{02})^{1/2} \cdot (1 - k_{12}) \cdot \gamma_{12}, \tag{14}$$

$$C_0 = x_1^2 C_{01} + x_2^2 C_{02} + 2x_1 x_2 (C_{01} C_{02})^{1/2} \cdot (1 - k_{22})^3 \cdot \gamma_{12}, \tag{15}$$

$$b = x_1^3 b_1 + x_2^3 b_2 + 3x_1 x_2 (x_1 b_1^{1/3} + x_2 b_2^{1/3}) \cdot b_1^{1/3} b_2^{1/3} \cdot \gamma_{12}, \tag{16}$$

$$a = x_1^3 a_1 + x_2^3 a_2 + 3x_1 x_2 (x_1 a_1^{1/3} + x_2 a_2^{1/3}) \cdot \cdot (1 - k_{12})^{2/3} \cdot a_1^{1/3} a_2^{1/3} \cdot \gamma_{12}\,, \tag{17}$$

$$c = x_1^3 c_1 + x_2^3 c_2 + 3x_1 x_2 (x_1 c_1^{1/3} + x_2 c_2^{1/3}) \cdot \cdot (1 - k_{12})^2 \cdot c_1^{1/3} c_2^{1/3} \cdot \gamma_{12}\,, \tag{18}$$

$$\alpha = x_1^3 \alpha_1 + x_2^3 \alpha_2 + 3x_1 x_2(x_1 \alpha_1^{1/3} x_2 \alpha_2^{1/3}) \alpha_1^{1/3} \alpha_2^{1/3} \cdot \gamma_{12}, \tag{19}$$

$$v = [x_1 v_1^{1/2} + x_2 v_2^{1/2}]^2 . \tag{20}$$

In all cases

$$\gamma_{ij} = V_{cij}/(V_{ci} V_{cj})^{1/2}. \tag{21}$$

The assumption made by BISHNOI and ROBINSON for the interaction critical volume is different from that made by other workers [18, 19], who have used the relationship:

$$V_{cij} = \frac{1}{2}(V_{ci}^{1/3} + V_{cj}^{1/3})^{1/3}. \tag{22}$$

BISHNOI and ROBINSON preferred the geometric average, where $\gamma_{ij} = 1$, because it helps in obtaining a simplified form of the mixing rules, and because they have felt that the effect of this assumption on the calculated results will be relatively small if V_{ci} and V_{cj} did not differ appreciably. For mixtures where molecules of greatly different sizes are involved, this assumption may not be adequate and the authors have recommended that Eq. (22) be used. It may be observed that when k_{ij} is taken as zero and γ_{ij} as unity, the new rules reduced to the original BWR rules, except for the parameter B_0 now given by:

$$B_0 = [x_1 B_{01}^{1/2} + x_2 B_{02}^{1/2}]^2 \tag{23}$$

for which the geometric mean combining rule, rather than the Lorentz, or Linear rule, is used because of reported considerable advantages.

The parameters obtained by BISHNOI and ROBINSON for CH_4 and CO_2 are given in Table (I).

Table I

Modified parameters of the BWR equation of state

Parameter	CH_4	CO_2
$B_0 \times 10^2$	4,3203053	3,2014927
A_0	1,8712416	1,8367101
$C_0 \times 10^{-5}$	0,23500139	1,7602805
$b \times 10^3$	3,9787382	6,2536078
a	0,069197996	0,24204855
$c \times 10^{-4}$	0,30179295	1,9008120
$\alpha \times 10^5$	9,6835765	4,8784066
$\nu \times 10^3$	5,7118125	4,2808218

Units: Atmospheres, °K, lit/gmole.

Application of the new parameters and new mixing rules to CH_4—CO_2 mixtures

The new parameters

LEE and MATHER (1972) [20] have recently measured the excess enthalpies (heats of mixing) of methane and carbon dioxide in a flow calorimeter, over the complete composition range, for six isotherms between 10 °C and 80 °C, at pressures up to 100 atmospheres. All measurements are for the mixing of two gas phases. The authors have compared their experimental results with various methods of prediction with the objective of testing the reliability of prediction methods of various kinds in predicting the enthalpies of mixtures. The methods of prediction chosen are all computer-oriented and include:

(a) Use of the BWR equation of state with the constants of CULLEN and KOBE for CO_2 and the constants of BENEDICT, WEBB and RUBIN for CH_4 in one set — and the constant of BISHNOI and ROBINSON in the other set.

(b) The principle of corresponding states with the use of Z_c as the third parameter was used to predict enthalpy departures by LYDERSEN, GREENKORN and HOUGEN [21]. YEN and ALEXANDER (1965) [22] have modified their correlation by the incorporation of recent experimental data and put it in a form suitable for computer calculations.

(c) The method developed by ORENTLICHER and PRAUSNITZ (1967) [23] for the calculation of the enthalpies of mixtures from the statistical theory of dense fluids. They used a simple potential which is qualitatively correct, and adjusted three parameters to obtain a fit with pure component data.

LEE and MATHER have observed that the second and third methods poorly agree with measured values at higher pressures, and that the BWR equation is the most satisfactory method for quantitative prediction of excess enthalpies.

Figures 1, 2 and 3 compare these experimental values with values calculated by the BWR equation of state. Here

BWR_I = Equation using CULLEN and KOBE constants for CO_2 and BENEDICT, WEBB and RUBIN constants for CH_4.
BWR_{II} = Equation using BISHNOI and ROBINSON constants.

It is to be observed that, while both sets of coefficients are in reasonable agreement, BWR_{II} predicts values closer to the experimental results than BWR_I.

BISHNOI and ROBINSON (1971) [24] have carried out experiments to determine the heat capacities of carbon dioxide-methane mixtures, with data collected on two binary mixtures containing 14,49 and 42,30 mole % methane at temperatures of about 40°, 60° and 90 °C and pressures up to about 155 atmospheres. Because of the unavailability of experimental heat capacities in

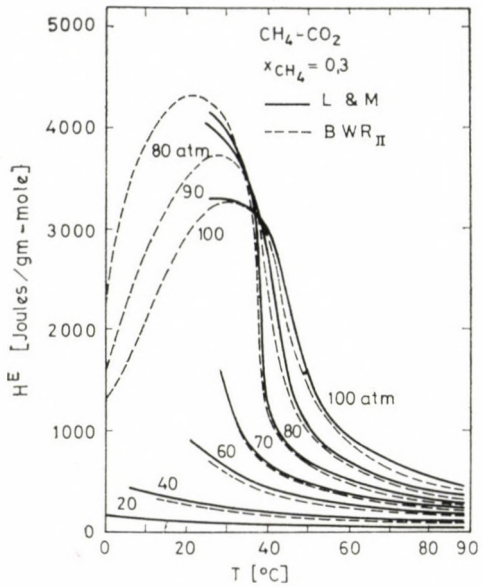

Fig. 1 Comparison of experimental data for CH_4—CO_2 with values calculated using BWR_{II}

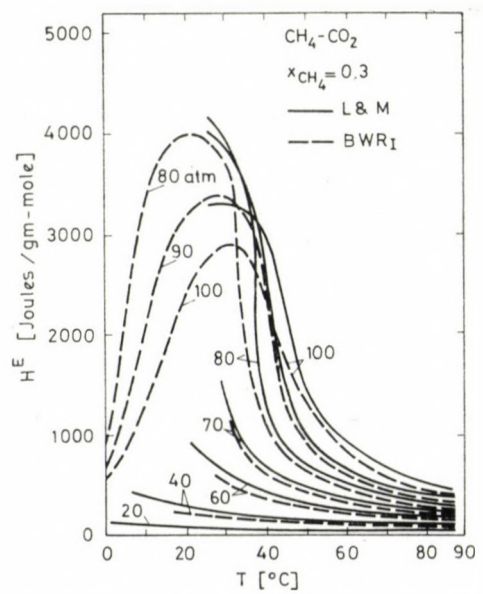

Fig. 2 Comparison of experimental data for CH_4—CO_2 with values calculated using BWR_I.

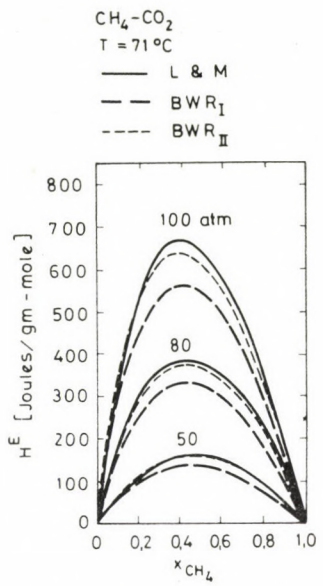

Fig. 3 Comparison of experimental data for CH_4—CO_2 at 71 °C with values calculated using BWR_I and BWR_{II}.

the literature, the authors have compared their experimental results with values calculated by several of the commonly used methods. These include the BWR equation of state, the generalized correlations of YEN and ALEXANDER [22] and CURL and PITZER (1958) [25] and the method of ORENTLICHER and PRAUSNITZ [23].

Use of the BWR equation has been performed by using the original BWR mixing rules. In one set, the parameters of CO_2 and CH_4 reported by CULLEN and KOBE and DOUSLIN et al. (1964) [26] respectively have been utilized. In another set, the newly proposed Bishnoi and Robinson parameters have also been used. The calculations have revealed that the values are best predicted by the BWR equation using the recently reported coefficients of BISHNOI and ROBINSON. The largest deviation of these predictions from the experimental values is found to be about 11,6% as compared to 51,33% when CULLEN and KOBE and DOUSLIN et al. coefficients are used for the BWR equation, 31% by the ORENTLICHER and PRAUSNITZ method, 25% by the CURL and PITZER correlation, and 14% by the YEN and ALEXANDER correlation.

The new mixing rules

BISHNOI and ROBINSON [14] have tested the applicability of the new mixing rules developed by them by using them to predict densities of the binary mixtures of carbon dioxide with methane, ethane and propane, utilizing

the pure component parameters reported by them. The values of the parameter k_{12} for these binaries have been taken from the work of CHUEH and PRAUSNITZ [19] who have reported the k_{12} value for the carbon dioxide-methane system as $0{,}05 \pm 0{,}02$, but BISHNOI and ROBINSON have utilized the lower limit of this value, 0,03. The densities have been calculated by using the Benedict, Webb and Rubin rules, referred to as BWR_{II}, and the new mixing rules, referred to as BWR_{III}, and the results have been compared separately with experimental data. For the CH_4-CO_2 system the authors have used the experimental data of REAMER, OLDS, SAGE and LACEY (1944) [27], who studied the volumetric behaviour of four mixtures of methane and carbon dioxide at seven temperatures ranging from 100° to 460 °F and throughout the pressure interval from 100 to 10 000 pounds per square inch. BISHNOI and ROBINSON have found the ability of their proposed rules in predicting mixture densities undoubtedly better than that of the original BWR equation in the case of $CO_2-C_2H_6$ and $CO_2-C_3H_8$ mixtures.

However, for the CO_2-CH_4 system, both rules make errors of the same order of magnitude. The authors attribute this to the probability that the k_{12} value chosen for this system is very small and hence does not have an appreciable effect at the temperatures where the data are predicted.

In another assessment of their new mixing rules, BISHNOI and ROBINSON [15] have used them to predict the densities of several binary mixtures of hydrogen sulphide with methane and ethane, and the phase behaviour of the carbon dioxide-propane, hydrogen sulphide-methane, hydrogen sulphide-propane and hydrogen sulphide-carbon dioxide binary systems. The predictions have confirmed the effectiveness of the new rules for predicting the densities of hydrocarbon—non-hydrocarbon binaries, and they have showed that acceptable accuracy can be obtained in predicting the phase behaviour of difficult binary systems even when no phase behaviour data are used for evaluating the parameters in the equation of state. For making the predictions on the systems they have studied, the authors have taken the parameter r_{ij} as a unity. This is done because it has already been shown by the authors [14], that the use of the geometric mean value for V_{cij} gives good predictions of the densities of mixtures of carbon dioxide and propane, and this system has the largest difference in critical volumes of all the binaries studied.

In this work, the new mixing rules are further tested for the CH_4-CO_2 system, around the phase boundaries, using the data of ARAI, KAMINISHI and SAITO (1971) [28], who have recently measured the P-V-T-X relations around the phase boundaries for the CO_2-N_2 and the CO_2-CH_4 systems. The measurements were for three isotherms: 15 °C, 0 °C and −20 °C, and various compositions in the vapour region, liquid region and the saturated region. The pressure range covered is from 20 to 150 atmospheres. A 9100 B Hewlett –

Packard calculator-printer is used for this purpose. Volumes are calculated using the Benedict et al. rules and the new mixing rules proposed by BISHNOI and ROBINSON whose newly proposed sets of constants for the pure components are used in either case. The parameter r_{ij} is likewise taken as a unity, but since use of the lower limit (0,03) of the parameter k_{ij} reported by BISHNOI and ROBINSON to produce errors of the same order, an elaborate trial-and-error procedure has been adopted here using various values of the k_{ij} factor ranging between the lower and the upper limits. It was found that the average value of the two limits (0,05) produces the best general fit over the whole range of data available. This corresponds to a characteristic critical temperature T_{c12} of 229 °K defined by Eq. (12). The characteristic critical volume of the system, V_{c12}, is accordingly 96,4 cm^3/gm-mole defined by Eq. (21). Results of these comparisons are tabularly presented in [31]. Percent deviations are calculated as:

$$\% \text{ Dev.} = \frac{V_{\text{exp.}} - V_{\text{cal.}}}{V_{\text{exp.}}} V \times 100. \tag{24}$$

Average percent deviations are calculated as the averages of the absolute values. Since the BWR equation is implicit in density, an iterative procedure of calculations is used. Iterations are continued until when the calculated pressures are within 0,0001 atmospheres of the measured ones.

Gas and liquid regions

For the 15 °C isotherm, both rules predict volumetric data with very good and acceptable engineering precision using the Bishnoi and Robinson pure component constants, both in the gas and in the liquid region, though the original rules (BWR_{II}) predict values closer to the measured ones than the new mixing rules (BWR_{III}). Over the various compositions, BWR_{II} gives average deviations varying in magnitude between 0,322% and 2,539%, while BWR_{III} gives errors ranging between 0,295% and 5,084%.

For the 0 °C isotherm, BWR_{II} starts to predict values with deviations flinging higher with increasing pressures, reaching a maximum of 13,348%, though the average percent deviations are much lower. However, with the new mixing rules, BWR_{III}, % deviations in predicted values remain very low along all the range, reaching a maximum of 2,969%. Here average deviations over the various compositions vary between 0,524% and 2,879%, compared to values ranging between 0,584% and 6,489% with BWR_{II}.

The saturated region

In the saturated liquid-vapour region, the ability of the new mixing rules in predicting mixture volumes, Table (II), is clearly observed to be super-

Table II

$P-V-T-X$ relations of the CH_4-CO_2 system at saturated dew and bubble points

P	X	$T = 15$ °C V cm³/gm-mol			Dew point		d gm-mol/lit
		Exp.	BWR_{II}	%Dev.	BWR_{III}	%Dev.	BWR_{III}
53,8	,043	248	248,208	— ,084	250,609	—1,052	3,990
58,7	,091	218	216,076	,883	221,440	—1,578	4,516
61,8	,116	203	197,203	2,856	204,429	— ,704	4,892
66,2	,146	185	172,058	6,996	182,105	1,565	5,491
69,7	,167	162	154,112	4,869	166,392	—2,711	6,010
73,0	,182	145	137,032	5,495	151,455	—4,452	6,603
80,1	,182*	99,2	90,206	9,067	105,297	— 6,146	9,497
				4,321		2,601	
		$T = 15$ °C			Bubble point		
61,7	,043	55,6	55,074	— ,853	56,657	—1,901	17,650
72,0	,091	61,2	60,526	1,101	62,631	—2,338	15,967
76,5	,116	66,5	63,760	4,120	67,483	—1,478	14,819
80,0	,146	77.4	70,115	9,412	77,519	— ,154	12,900
80,4	,167**	87,2	79,503	8,827	91,527	—4,962	10,926
				4,863		2,167	

* Retrograde condensation point
** Critical opalescence was clearly observed

mounting compared to the original mixing rules, and especially as temperatures go lower and mole fractions and pressures higher, the magnitudes of errors in BWR_{II} predicted values increase, while those predicted by BWR_{III} remain very small and fairly unchanged throughout the range. Average deviations in values calculated by BWR_{II} are in the order of 4,321% to 8,910%, with a maximum deviation of 15,456%. Those calculated by BWR_{III} are in the order of 0,500% to 2,601%, with a maximum deviation of 6,146%. It may be noteworthy to observe that, though BISHNOI and ROBINSON have recommended the applicability of their constants for pure CO_2 to a lowest temperature of 0 °C, for the —20 °C isotherm BWR_{III} predicts volumes with very precise accuracy over compositions ranging between 0,204 to 0,551 mole fraction CH_4. Also noteworthy is that it predicts volumes with similar accuracy at points of retrograde condensation, while BWR_{II} shows maximum deviations at these points. It is quite apparent that it is here that the effect of the correction for binary interactions comes into play, as molecular interaction increases with decreasing temperatures and rising pressures.

Table II (contd)

P	X	$T = 0$ °C V Exp.	V BWR_{II}	%Dev.	Dew point BWR_{III}	%Dev.	d BWR_{III}
41,5	,129	362	357,709	1,185	362,338	— ,093	2,760
49,8	,220	287	278,091	3,104	286,123	,306	3,495
56,4	,276	242	230,886	4,593	241,288	,294	4,144
64,2	,321	197	183,943	6,628	197,302	— ,153	5,068
84,1	,321*	93,4	79,741	14,624	92,553	,907	10,805
68,9	,340	174	159,028	8,605	174,317	,182	5,737
82,7	,340*	105	90,294	14,006	105,857	— ,816	9,447
73,3	,349	154	135,543	11,985	152,869	,734	6,542
81,7	,349*	115	97,226	15,456	113,830	1,017	8,785
				8,910		,500	
		$T = 0$ °C			Bubble point		
65,4	0,129	53,0	52,992	,015	53,944	—1,781	18,538
80,2	0,220	62,6	59,112	5,572	62,201	,637	16,077
84,1	0,276	75,0	66,677	11,097	73,831	1,559	13,544
				5,561		1,326	

Table II (contd)

P	X	$T = -20$ °C V Exp.	V BWR_{II}	%Dev.	Dew point BWR_{III}	%Dev.	d BWR_{III}
26,0	,204	606	611,807	— ,958	617,551	—1,906	1,619
31,0	,302	496	498,791	— ,563	506,577	—2,133	1,974
43,2	,444	326	327,719	— ,527	338,268	—2,763	2,956
52,6	,499	254	244,190	3,862	256,836	—1,117	3,894
81,8	,499*	91,8	77,231	15,870	91,019	,851	10,987
67,8	,551	168	152,259	9,370	169,277	— ,760	5,907
74,9	,551*	134	116,321	13,193	135,159	— ,865	7,399
				6,283		1,628	
		$T = -20$ °C			Bubble point		
61,5	,204	47,7	48,819	—2,346	49,579	—3,939	20,170
73,2	,302	53.9	52,860	1,930	54,604	—1,306	18,314
81,8	,444	71,6	64,899	9,359	72,771	—1,636	13,771
				4,545		2,294	

The critical region

Table III shows a comparison between predicted critical volumes and those reported by ARAI et al. for the three isotherms. BWR_{II} predicts critical volumes for the 15 °C, 0 °C and −20 °C isotherms with relative deviations

Table III

Critical point P—V—T—X data

T °C	X_c	P_c atm.	V_c cm³/gm-mol						
			Exp.	BWR_{II}	%Dev.	BWR_{III}	%Dev.	BWR_{III} Interp.	%Dev.
15	0,166	80,5	85,5	78,707	7,945	90,361	−5,685	89,29	−4,430
0	0,300	84,4	81,9	72,460	11,526	82,546	− ,789	81,63	0,330
−20	0,475	82,4	79,8	70,465	11,698	81,340	−1,930	78,43	1,590

Table IV

Critical compressibility data

T °C	X_c	P_c atm.	Z_c					
			Exp.	BWR_{II}	%Dev.	BWR_{III}	%Dev.	BWR_{III} Interp.
15	0,166	80,5	0,2911	0,2680		0,3076		0,3040
0	0,300	84,4	0,3084	0,2729		0,3105		0,3074
−20	0,475	82,4	0,3166	0,2795		0,3227		0,3111

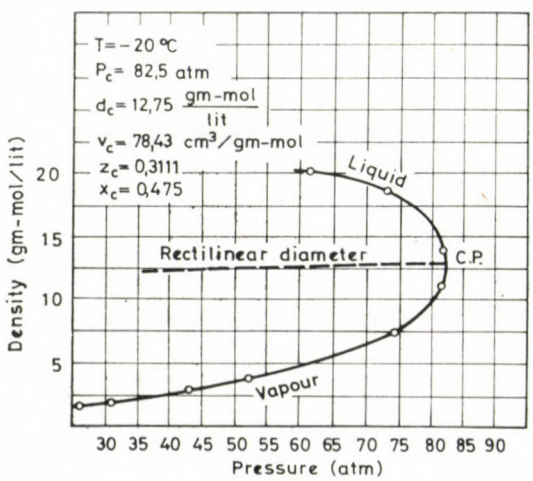

Fig. 4

of 7,945%, 11,526% and 11,698% respectively, compared to corresponding errors of −5,685%, −0,789% and −1,930% when BWR_{III} is used. Still better values are obtained graphically, using BWR_{III}, as shown, when the densities of the coexisting liquid and vapour phases are plotted, and the rectilinear diameter is drawn using the Cailletet and Mathias rule, Figs 4 through 8. For the −40 °C isotherm the vapour-liquid equilibria data of KAMINISHI et al. [10]

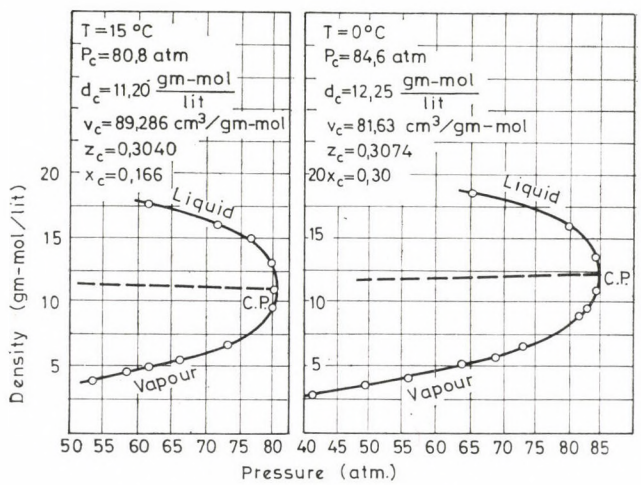

Fig. 5 *Fig. 6*

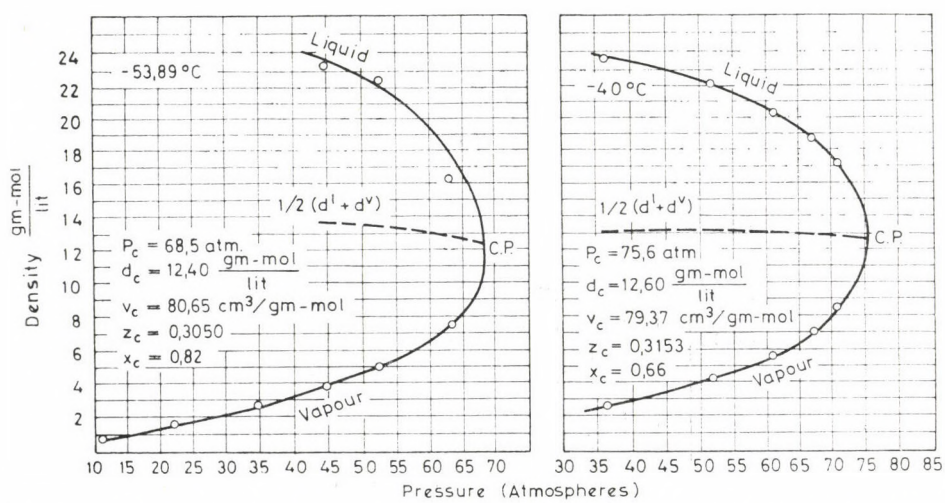

Fig. 7 and 8. BWR_{III} Calculated saturation densities of CH_4—CO_2 system AT—53.89 °C & −40 °C

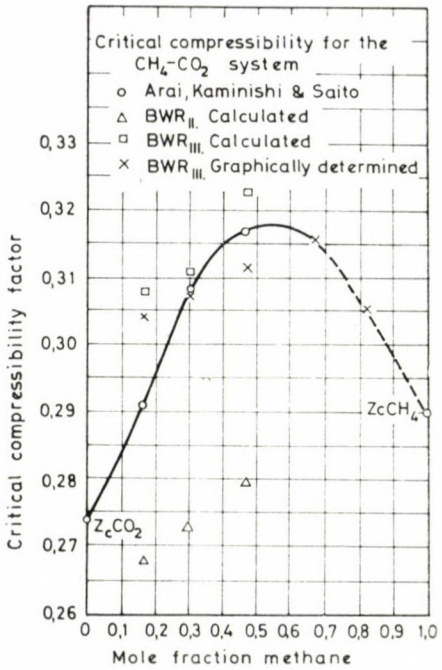
Critical compressibility for the
CH4-CO2 system
o Arai, Kaminishi & Saito
Δ BWRII Calculated
□ BWRIII Calculated
× BWRIII Graphically determined
Critical compressibility factor
0,33
0,32
0,31
0,30
0,29
0,28
0,27
0,26
ZcCH4
ZcCO2
0 0,1 0,2 0,3 0,4 0,5 0,6 0,7 0,8 0,9 1,0
Mole fraction methane

Fig. 9

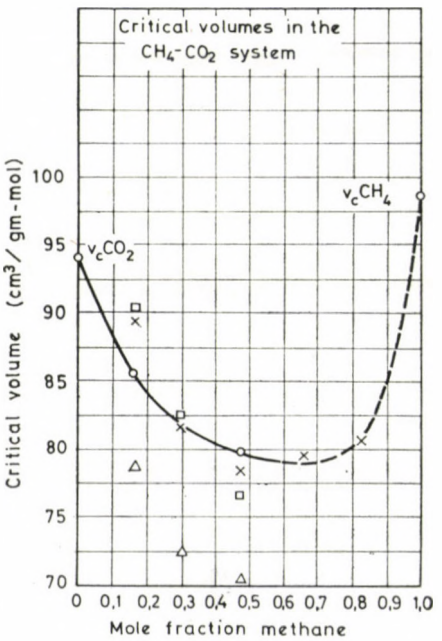
Critical volumes in the
CH4-CO2 system
Critical volume (cm3/gm-mol)
100
95
90
85
80
75
70
vcCH4
vcCO2
0 0,1 0,2 0,3 0,4 0,5 0,6 0,7 0,8 0,9 1,0
Mole fraction methane

Fig. 10

is used, and for the −53,89 °C isotherm the data of DONELLY and KATZ [29] is used Table V. Diagrams for the critical compressibility factors and the critical volumes in the CH_4—CO_2 system, respectively, are drawn in Figs 9 and 10.

Table V

BWR_{III} calculated saturated phases $P-V-T-X$ data

T °C	P atm.	Bubble point			Dew point		
		X M.F. CH_4	d gm-mol/lit	V cm³/gm-mol	y	d	V
	10,96	...			0,477	0,679	1472
	22,25	...			0,717	1,477	677,0
−53,89	35,18	...			0,789	2,616	382,2
	44,84	0,261	23,139	43,22	0,813	3,727	268,3
	52,60	0,344	22,134	45,18	0,815	4,996	200,2
	...	0,350	...	...	0,820	...	...
	52,25	...	...	...	0,822	4,878	205,0
	63,42	0,661	16,274	61,45	0,836	7,447	134,3
	...	0,664	...	...	0,830	...	...
	36,5	0,130	23,361	42,81	0,657	2,534	394,7
−40	52 0	0,250	21,851	45,76	0,717	4,190	238,7
	61,2	0,360	20,238	49,41	0,727	5,629	177,7
	67,2	0,450	18,626	53,69	0,720	7,046	141,9
	71,0	0,519	17,044	57,67	0,703	8,517	117,4

REFERENCES

1. BENEDICT, M., WEBB, G. B., RUBIN, L. C.: *J. Chem. Phys.* **8,** No. 4, (1940) 334.
2. BENEDICT, WEBB, RUBIN: Ibid. **10,** (1942) 747.
3. BENEDICT, WEBB, RUBIN: *Chem. Eng. Progress* **47,** No. 9, (1951) 449.
4. BENEDICT, WEBB, RUBIN: Ibid. **47,** No. 11 (1951) 571.
5. BENEDICT, WEBB, RUBIN: Ibid. **47,** No. 12, (1951) 609.
6. EAKON, B. E., ELLINGTON, R. T.: Thermodynamics and Transport Properties of Gases, Liquids and Solids. (Symposium on Thermodynamic Properties.) Am. Soc. of Mech. Eng. N. Y. Mc. Graw-Hill Book Co. Inc. Feb. (1959).
7. STOTLER, H. H., BENEDICT, M.: *Chem. Eng. Prog. Symp. Ser.* **49,** No. 6, (1953) 25.
8. CULLEN, E. J., KOBE, K. A.: *A. I. Ch. E. J.* **1,** No. 4, (1955) 452.
9. BARNER, H. E., ADLER, S. B.: *Hydrocarbon Process.* **47,** No. 10, (1968) 150.
10. KAMINISHI, G. I., ARAI, Y., MAEDA, S.: *J. Chem. Eng. Japan,* **1,** No. 2, (1968) 109.
11. MAYER, J. E.: *J. Phys. Chem.* **43,** (1939) 71.
12. BONO, J. L., STARLING, K. E.: *Can. J. Chem. Eng.* **48,** (1970) 468.
13. BISHNOI, P. R., ROBINSON, D. B.: Ibid. **49,** (1971) 642.
14. BISHNOI, P. R., ROBINSON, D. B.: Ibid. **50,** (1972) 101.
15. BISHNOI, P. R., ROBINSON, D. B.: Ibid. **50,** (1972) 506.
16. STARLING, K. E.: *Proceedings of the 49th Annual Meeting Natural Gas Processing Assoc.* **49,** (1970) 9.

17. ORYE, R. V.: *Ind. & Eng. Chem. Process. Design and Dev.* **8,** No. 4, (1969) 579.
18. GUN, R. D.: M. Sc. Thesis, Chem. Eng. Dept. Univ. of California (1958).
19. CHUEH, P. L., PRAUSNITZ, J. M.: *Ind. Eng. Chem. Fund.* **6,** No. 4, (1967) 492.
20. LEE, J. I., MATHER, A. E.: *Can. J. Chem. Eng.* **50,** (1972) 95.
21. LYDERSEN, A. L., GREENKORN, R. A., HOUGEN, O. A.: Wisconsin Univ. Eng. Exp. Sta. Rept. No. **4,** Oct (1955).
22. YEN, L. C., ALEXANDER, R. E.: *Al. Ch. E. J.* **11,** No. 2, (1965) 334.
23. ORENTLICHER, M., PRAUSNITZ, J. M.: *Can. J. Chem. Eng.* **45,** (1967) 78.
24. BISHNOI, P. R., ROBINSON, D. B.: Ibid. **49,** (1971) 657.
25. CURL, R. F. Jr., PITZER, K. S.: *Ind. & Eng. Chem.* **50,** No. 2, (1958) 265.
26. DOUSLIN, D. R., HARRISON, R. H., MOORE, R. T., MC CULLOUGH, J. P.: *J. Chem. Eng. Data* **9,** (1964) 3, 358.
27. REAMER, H. H., OLDS, R. H., SAGE, B. H., LACEY, W. N.: *Ind. Eng. Chem.* **36,** No. 1, (1944) 88.
28. ARAI, Y., KAMINISHI, G., SAITO, S.: *J. Chem. Eng. Japan.* **4,** No. 2, (1971) 113.
29. DONELLY, G. H., KATZ, D. L.: *Ind. Eng. Chem.* **46,** No. 3, (1954) 511.
30. DIN, F.: Thermodynamic Functions of Gases. Vol. I (1956), Vol. **3** (1961). Butterworths Scientific Publications, London.
31. BUKHARI, M. A. I.: Enthalpy-Composition Diagrams for the Methane-Carbondioxide System and Correlations of Volumetric and Thermodynamic Properties. A Candidate of Science Dissertation, Technical University of Budapest; Department of Energetics (1974).

Anwendung der Zustandsgleichung zur Ermittlung der volumetrischen und thermodynamischen Kennwerte des CH_4—CO_2 Systems. — I. Teil. Infolge des zunehmenden Energiebedarfs wurde die Benützung der eher für unwirtschaftlich abgeschätzten, mit CO_2 verunreinigten Erdgasvorräte erforderlich geworden. Hinsichtlich dessen, daß das verunreinigte Erdgas größtenteils eine Mischung der Gase CH_4 und CO_2 bildet und andere Komponenten nur in Spuren enthält, kann bei den Untersuchungen das verunreinigte Erdgas als ein Zweikomponentensystem von CO_2—CH_4 betrachtet werden. Zur Durchführung der mit der Behandlung (Separation) der verunreinigten Gase zusammenhängenden Berechnungen ist die Kenntnis der thermodynamischen Angaben des Zweikomponentensystems erforderlich im breiten P-V-T-X Bereich. Außer der unmittelbaren Ermittlung müssen die thermodynamischen Kennwerte auch theoretisch ermittelt werden. Die Zustandsgleichung BWR dient mit der korrigierten Mischungsregel und mit den revidierten Komponentenparametern zu diesem Zweck. In beiden Teilen dieser Abhandlung sind die Ergebnisse derartiger Berechnungen in Tabellen und durch Diagramme vorgeführt. Diese Berechnungen umfassen einen Temperaturbereich von —120 °C bis +30 °C und einen Druckbereich von 10 bis 80 at, und bedecken das Gasbereich, den Flüssigkeit und Dampf Gleichgewichtsbereich, den Flüssigkeitsbereich und schließlich den Festzustand — Flüssigkeit — Dampfbereich.

Acta Technica Academiae Scientiarum Hungaricae, Tomus 92 (3—4), pp. 245—255 (1981)

ERSTELLUNGSMETHODEN DER STATISTIKEN VON SPITZENBELASTUNGEN

E. JÁNOSDEÁK*

KANDIDAT DER TECHNISCHEN WISSENSCHAFTEN

[Eingegangen am 3. November, 1980]

Die Statistik von Spitzenbelastungen, d. h. von während der Lebensdauer von stochastisch beanspruchten Strukturen auftretenden höchsten Belastungen, ist in der Literatur bisher teils auf Grund der statistischen Theorie der Extremen zur Deutung von Messergebnissen, teils auf Grund der Theorie der kontinuierlichen stochastischen Signale insbesondere auf den Fall von Gaussschen Signalen angewendet worden. Es wird gezeigt, daß auf Grund dieser letzteren Theorie auch eine allgemeingültigere, die bisherigen Ergebnisse in sich integrierende Behandlung des Problemkreises möglich ist, was eine wichtige Voraussetzung dafür geschaffen hat, daß — unter Einbeziehung der Rechenmethoden für das dynamische Verhalten von Strukturen — die Statistik der Spitzenbelastungen schon im Entwurfsstadium bestimmt werden kann.

1. Problemstellung, gegenwärtiger Entwicklungsstand

Angesichts des dynamischen Bruches von stochastisch beanspruchten Strukturen ist die Kenntnis jener Beanspruchungsgrenze, welche mit gewählter Wahrscheinlichkeit von den Spitzenbelastungen nicht überschritten wird, von höchstem Interesse. Unter Spitzenbelastung wird jene höchste Belastung verstanden, welche in einem gewissen Betriebszeitintervall (z. B. Lebensdauer) auftritt. Diese Frage wurde zuerst unter Einbeziehung von Lastkollektivmessungen und der statistischen Theorie der Extremen und der folgenden Annahmen beantwortet:

— Stationärität und Ergodizität des Belastungsgeschehens;

— Zerlegung in diskrete »Ereignisse« der sich kontinuierlich ändernden Belastung (z. B. Berücksichtigung von Spannungsspitzen);

— Verteilung exponentiellen Typs der Ereignisse, was in vielen praktischen Fällen zutrifft.

Im Anhang haben wir für die Charakterisierung dieses Entwicklungsstandes — grundsätzlich den Gedankengang von O. BUXBAUM und O. SWENSON [1] folgend — die Ableitung mitgeteilt dafür, daß wenn der betrachtete Zeitintervall in Z Segmente unterteilt wird, die Anzahl der irgendwie definierten diskreten Ereignisse mit r, die Grenze der Belastungen y^* mit y, die Wahrschein-

* Dr. E. JÁNOSDEÁK, Komszomol sétány 28, H-1105 Budapest, Ungarn

lichkeit, womit y in dem betrachteten Zeitintervall nicht überschritten wird, mit $p(0)$ bezeichnen, bei einer exponentiellen Verteilung $F(y^*) = 1 - e^{-\alpha y^*}$ der y^* Werte der Zusammenhang

$$y = \frac{1}{\alpha} \ln \frac{r}{\ln\left(1/p(0)\right)} + \frac{1}{\alpha} \ln Z \tag{1}$$

bestehen muß. Die Formel ergibt wegen während der Ableitung eingeleiteten mathematischen Näherungen nur für $p(0)$ Werte nahe 1,0 eine akzeptable Näherung, was aber nur eine Folge von Transformationen ist, welche von uns zwecks Vergleichbarkeit mit späteren Zusammenhängen durchgeführt worden sind. Der Parameter α muß für jedes untersuchte Belastungssignal experimentell ermittelt werden, während r von der gewählten, mehr oder weniger zutreffenden Art der Diskretisierung abhängt und somit eine gewisse Unsicherheit in der Anwendung darstellt.

T. DAHLBERG [4, pp. 246, Formel 14] gibt für den Fall von stationären Gaussschen Signalen folgende Lösung:

$$y = \sigma_y \left[2 \ln \left(\sigma_y T / 2\pi\sigma_{\dot{y}} P_1\right)\right]^{1/2}. \tag{2}$$

σ_y und $\sigma_{\dot{y}}$ bezeichnen hier die Streuung der Belastung y^* bzw. der Belastungsgeschwindigkeit $\dot{y}^*$, P_1 ist die Wahrscheinlichkeit dafür, daß der Pegel y (mindestens einmal) innerhalb des Zeitintervalles T überschritten wird.

2. Die Berechnung der Statistik von Spitzenspannungen auf Grund der Theorie der kontinuierlichen stochastischen Signale

Wir werden zeigen, daß auf Grund der Theorie der kontinuierlichen stochastischen Signale und in völligem Einklang mit (1) und (2) als spezielle Fälle, eine Beantwortung von allgemeinerer Gültigkeit des umrissenen Problems möglich ist, was — abgesehen vom theoretischen Interesse — auch der Erhöhung der Zuverlässigkeit der Bemessung zugute kommt.

Wir gehen von der sehr plausiblen Annahme aus, daß die auf technischen Objekten messbaren Signale auf langen (mit der Lebensdauer vergleichbaren) Zeitintervallen bezogen als stationär und ergodisch zu betrachten sind, das heißt, daß auf eine Menge von Objekten in bestimmten Zeitpunkten gebildete Statistiken (z. B. Effektivwerte, Momente verschiedener Ordnung) einander, und hinsichtlich der einzelnen Objekte (Signalrealisationen) nach der Zeit gebildeten ähnlichen Statistiken gleich sind. Es spricht nichts gegen die Gültigkeit dieser Annahme auch bei solchen technischen Objekten, deren Betrieb nach der Umgangssprache als ausgesprochen »instationär« ist (z. B. die meisten

Fahrzeuggattungen), vorausgesetzt, daß die Betriebsart während der Lebensdauer und hinsichtlich der betrachteten Objektmenge sich nicht ändert. Wir wollen nun beweisen, daß die Durchschreitungszahl irgendeines Signalpegels (Belastungsniveaus) innerhalb des Zeitintervalles T, vorausgesetzt, daß T viel größer ist, als jene Zeitverschiebung τ, welche durch das Verschwinden der Autokorrelation bedingt wird, eine Poissonsche Verteilung aufweist. Es seien

u und v	Zeitpunkte, wofür $0 \leq u \leq v < T$ gilt,
y_1 und y_2	Signalpegel in u und v,
β und δ	Signalgeschwindigkeiten in u und v,
y	der Signalpegel im allgemeinen,
$f_{uv}(y_1, \beta, y_2, \delta)$	eine Verteilungsdichtefunktion,
$\overline{N_y}$, $\overline{N_y(T)}$	die Durchschreitungszahl von y in einer (positiven) Richtung in der Zeiteinheit, bzw. in T.

Bestimmen wir nun den quadratischen Mittelwert $\overline{N_y^2(T)}$. Das Produkt der Überschreitungszahlen in den elementaren Zeitintervallen du, dv und in den elementaren Bereichen $(dy_1, d\beta)$ und $(dy_2, d\delta)$ ist

$$\frac{f_{uv}(y_1, \beta, y_2, \delta)\, dy_1\, dy_2\, d\beta\, d\delta\, du\, dv}{\frac{dy_1}{|\beta|} \cdot \frac{dy_2}{|\delta|}} = |\beta| \cdot |\delta| \cdot f_{uv}(y_1, \beta, y_2, \delta)\, d\beta\, d\delta\, du\, dv \tag{3}$$

Uns auf Pegelüberschreitungen in nur positiver Richtung beschränkend, können wir auf die Absolutwerte verzichten. Danach erhalten wir für $y_1 = y_2 = y$:

$$\overline{N_y^2(T)} = \int_0^\infty \int_0^\infty \int_0^T \int_0^T \beta\delta f_{uv}(y, \beta, y, \delta)\, du\, dv\, d\beta\, d\delta. \tag{4}$$

Wir führen nun durch Umkehrung der Integrationsfolge die Bezeichnung

$$S(u, v) = \int_0^\infty \int_0^\infty \beta\delta f_{uv}(y, \beta, y, \delta)\, d\beta\, d\delta \tag{5}$$

ein. Damit ergibt sich

$$\overline{N_y^2(T)} = \int_0^T \int_0^T S(u, v)\, du\, dv\,. \tag{6}$$

Nach Einführung der Zeitverschiebung

$$\tau = v - u \tag{7}$$

besteht offensichtlich, daß

$$S(u, v) = S(v - u) = S(u - v) = S(\tau) = S(-\tau), \tag{8}$$

womit wir statt (6)

$$\overline{N_y^2(T)} = \int_0^T \int_v^{v-T} S(\tau)\,(-d\tau)\, dv \tag{9}$$

erhalten.

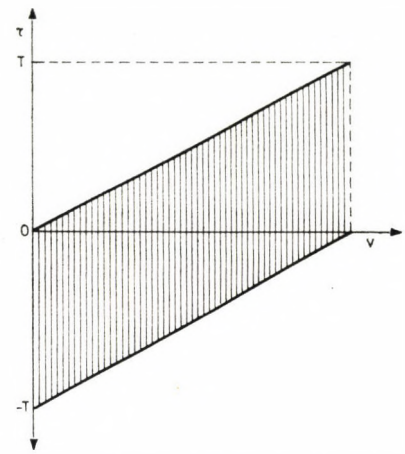

Bild 1. Deutung des Integrationsbereiches anhand der Formeln (9) und (10)

Anhand des Bildes 1. zur Deutung der Integrationsgrenzen führen wir weitere Umformungen durch:

$$\overline{N_y^2(T)} = \int_0^T \int_0^{v-T} S(\tau)(-d\tau)dv = \int_0^T \int_{v-T}^{v} S(\tau)\, d\tau\, dv =$$

$$= \int_0^{-T} \int_0^{T+\tau} S(\tau)\, dv\, d\tau + \int_0^T \int_\tau^T S(\tau)\, dv\, d\tau =$$

$$= \int_0^T \int_0^{T-\tau} S(\tau)\, dv\, d\tau + \int_0^T \int_\tau^T S(\tau)\, dv\, d\tau =$$

$$= 2\int_0^T (T - \tau)\, S(\tau)\, d\tau\,. \tag{10}$$

Zerlegen wir (10) in die Summe von zwei Integralen so daß $\varepsilon \ll T$:

$$\overline{N_y^2(T)} = \underbrace{2\int_0^{\varepsilon} (T - \tau)\, S(\tau)\, d\tau}_{I_1} + \underbrace{2\int_{\varepsilon}^{T} (T - \tau)\, (S(\tau)\, d\tau}_{I_2}. \tag{11}$$

Bestimmen wir I_1.

In einem genügend kurzen Zeitintervall ε entsteht mit zu berücksichtigender Wahrscheinlichkeit keine, oder nur eine einzige Signalpegelüberschreitung, deshalb gilt mit äußerst guter Näherung

$$\overline{N_y^2(\varepsilon)} = \overline{N_y(\varepsilon)}. \tag{12}$$

Nach Substitution von $\overline{N^2(\varepsilon)}$ nach (10) erhalten wir

$$\overline{N_y^2(\varepsilon)} = 2\int_0^{\varepsilon} (\varepsilon - \tau)\, S(\tau)\, d\tau = \overline{N_y(\varepsilon)}. \tag{13}$$

Da im Falle eines stationären Signals laut [2, Zusammenhang 3—153], wenn mit $f(y, \beta)$ eine Dichtefunktion ohne Zeitparameter bezeichnet wird,

$$\overline{N}_y = \int_0^\infty \beta f(y, \beta)\, d\beta, \tag{14}$$

besteht offensichtlich

$$\overline{N_y(\varepsilon)} = \overline{N}_y \varepsilon\,. \tag{15}$$

Nach Substitution in (13) und Differentiation der beiden Seiten nach ε:

$$\overline{N}_y = 2\frac{d}{d\varepsilon}\int_0^\varepsilon (\varepsilon - \tau) S(\tau)\, d\tau = 2\left[\int_0^\varepsilon S(\tau)\, d\tau + (\varepsilon - \tau) S(\tau)|_{\tau=\varepsilon}\right] =$$

$$= 2\int_0^\varepsilon S(\tau)\, d\tau\,. \tag{16}$$

Aus (16) folgt, daß wenn ε sich an Null nähert, $S(\tau)$ muß sich an $\overline{N}_y \cdot \delta(\tau)$ nähern, wenn mit $\delta(\tau)$ die Diracsche Impulsfunktion bezeichnet wird. Unter Berücksichtigung dieses Zusammenhanges erhalten wir für I_1 laut (11):

$$I_1 = 2\int_0^\varepsilon (T - \tau)\, \overline{N}_y \cdot \delta(\tau)\, d\tau = \overline{N}_y \cdot T. \tag{17}$$

Bestimmen wir nun I_2 in (11). Wenn ε so gewählt wird, daß für $\tau < \varepsilon$ der Wert der Autokorrelation Null wird, die Dichtefunktion $f_{uv}(y_1, \beta, y_2, \delta)$ für $y_1 = y_2$ zerfällt für τ Werte, die diese Bedingung erfüllen, in das Produkt von zwei identischen Dichtefunktionen:

$$f_{uv}(y, \beta, y, \delta) = f(y, \beta) f(y, \delta), \tag{18}$$

womit (5) in Form von

$$S(u, v) = S(\tau) = \left[\int_0^\infty \beta f(y, \beta)\, d\beta\right]\left[\int_0^\infty \delta\, f(y, \delta)\, d\delta\right] \tag{19}$$

geschrieben werden kann.

Unter Berücksichtigung von (14) erhalten wir:

$$S(\tau) = (\overline{N}_y)^2\,. \tag{20}$$

Nach Substitution in I_2 in (11) erhalten wir

$$I_2 = 2 \cdot \int_{\varepsilon \cong 0}^{T} (T - \tau)\, (\overline{N}_y)^2\, d\tau = (\overline{N}_y)^2 \cdot T^2\,. \tag{21}$$

Nach weiterer Substitution von (17) und (21) in (11):

$$\overline{N_y^2(T)} = I_1 + I_2 = \overline{N}_y T + (\overline{N}_y)^2 T^2, \tag{22}$$

bzw. da in an (15) ähnlicher Weise $\overline{N_y(T)} = \bar{N}_y \cdot T$, nach Umformung

$$\overline{N_y^2(T)} - \left(\overline{N_y(T)}\right)^2 = \overline{N_y(T)} \,. \tag{23}$$

Da die Differenz des quadratischen Mittelwertes und des Quadrates des Erwartungswertes der Varianz gleich ist, (23) drückt die Gleichheit der Varianz mit dem Erwartungswert, was bei der Poissonschen Verteilung erfüllt wird. Die Verteilungsdichte der Anzahl x der Überschreitungen des Pegels y in einer einzigen Richtung im Zeitintervall T ist danach

$$p(x) = \frac{(\bar{N}_y T)^x}{x!} \cdot e^{-\bar{N}_y \cdot T} \,. \tag{24}$$

Durch die Substitution $x = 0$ erhalten wir die Wahrscheinlichkeit dafür, daß der Signalpegel (Belastungsniveau) y in dem Zeitintervall T nicht überschritten wird:

$$p(0) = e^{-\bar{N}_y T}. \tag{25}$$

Bei praktischen Anwendungen können wir oft mit einer exponentiellen oder einer Gaussschen Verteilung der Pegeldurchschreitungszahlen rechnen:

$$\bar{N}_y = \bar{N}_0 \, e^{-\alpha y} \,, \tag{26}$$

oder

$$\bar{N}_y = \bar{N}_0 \, e^{-\frac{y^2}{2\sigma^2}} \,, \tag{27}$$

wo $\bar{N}_0$ der Mittelwert der Durchschreitungszahlen des Nullpegels in der Zeiteinheit, α ein konstanter Parameter und σ den Effektivwert des Gaussschen Signals bedeutet.

Nach Einsetzen von (26) bzw. (27) in (25) erhalten wir nach Umformungen

$$y = \frac{1}{\alpha} \ln \frac{\bar{N}_0}{\ln\left(1/p(0)\right)} + \frac{1}{\alpha} \ln T \,, \tag{28}$$

bzw. nach Einführung von $P_1 = 1 - p(0)$

$$y = \sigma_y \left[2 \ln \left(\bar{N}_0 T / P_1\right)\right]^{1/2}, \tag{29}$$

was mit der Formel von DAHLBERG laut (2) identisch ist, wenn wir berücksichtigen, daß entsprechend der Formel von RICE [laut 2, pp. 127, Formel 3—162 und 3—164] $\bar{N}_0 = \sigma_y / 2\pi\sigma_{\dot{y}}$ ist. Die Übereinstimmung mit dieser letzten Formel in dem speziellen Fall der Gaussschen Signalen ist eine Folge des

gemeinsamen theoretischen Hintergrundes. Im Falle der Formeln (1) bzw. (28) kann man nur von einer vollkommenen Analogie sprechen. In gewissen Fällen aber, bei entsprechender Wahl des Begriffes des diskreten Ereignisses, ist auch eine vollkommene Übereinstimmung der zwei Formeln zu erreichen. Es ist auch zu erwähnen, daß laut der Ableitung die quantitative Zuverlässigkeit der Formel (28) auch bei $p(0) \ll 1{,}0$ gesichert werden kann, insofern die Erfüllung der anfänglichen Voraussetzungen bei der Ableitung gesichert ist.

Da $p(0)$ in Anbetracht der Definition auch als die Wahrscheinlichkeit dafür gedeutet werden kann, daß keine Signalspitzen den Pegel y überschreiten, kann sie auch als Verteilungsfunktion der Spitzenbelastungen aufgefaßt werden. Für den Fall einer exponentiellen Pegelüberschreitungsverteilung ergibt sich die Verteilungsdichtefunktion der Spitzenbelastungen als die erste Ableitung von $p(0)$ nach y:

$$g_c(y) = \overline{N}_0 T\alpha \, e^{-\overline{N}_0 T e^{-\alpha y} - \alpha y}. \tag{30}$$

Als Anwendungsbeispiel dafür, daß die bisherigen Ergebnisse welche Möglichkeiten der Interpretation von Versuchsergebnissen darbieten, zeigen wir auf Bild 2. die zu verschiedenen Parametern $p(0)$ gehörigen Grenzen ϱ der Spitzenspannung in dem hinteren Dachpfosten eines Omnibusses in Abhängigkeit von der Betriebszeit T, während auf Bild 3. die Verteilungsdichte $g_c(\varrho)$ derselben

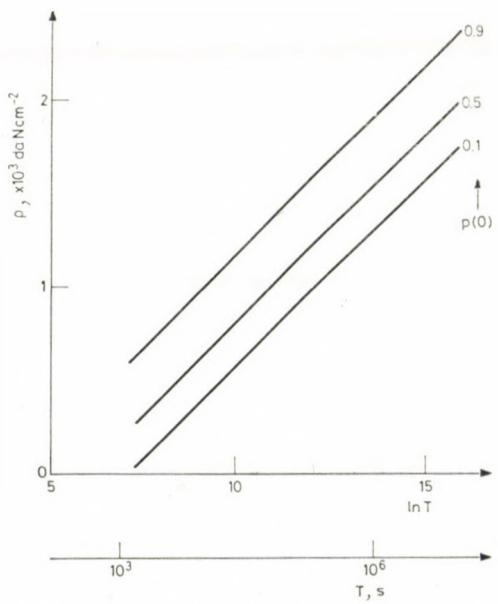

Bild 2. Zeitabhängigkeit der mit verschiedenen Wahrscheinlichkeiten nicht überschrittenen Spannungspegeln im hinteren Dachpfosten eines Omnibusses

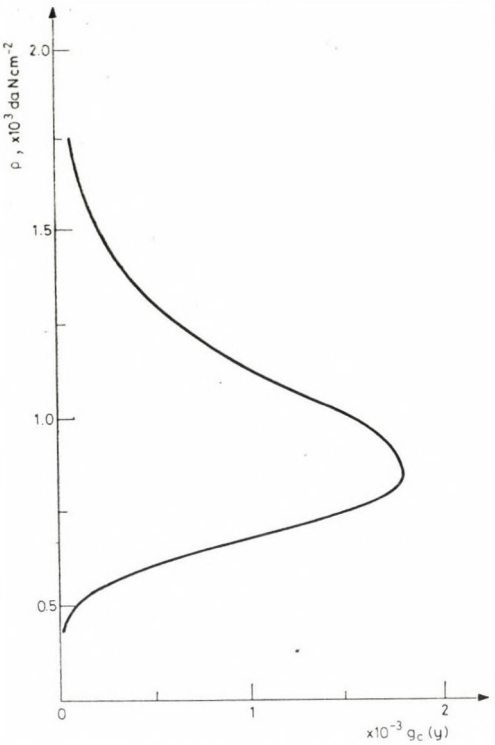

Bild 3. Verteilungsdichte der im hinteren Dachpfosten eines Omnibusses auftretenden Spitzenspannungen innerhalb einer Betriebszeit von $4 \cdot 10^4$ s (anhand einer Menge von Realisationen der Betriebszeit gedeutet)

Spitzenspannung nach einer Betriebszeit von $T = 4 \cdot 10^4$ s veranschaulicht. Die versuchsweise, anhand einer Pegelüberschreitungsmessung auf einer Zeitbasis von $1{,}44 \cdot 10^3$ s ermittelten Parameterwerte sind dabei $\overline{N}_0 = 1{,}895 \cdot 10^{-3}\ s^{-1}$ und $\alpha = 5{,}0 \cdot 10^{-3}\ cm^2$ da N^{-1} gewesen. Es sei noch bemerkt, daß diese Werte als reine Erfahrungswerte zu betrachten sind in jenem besonderen Fall, wo die exponentielle Näherung nach (26) nur bei sehr hohen Pegeln möglich ist. In solchen Umständen verliert natürlich $\overline{N}_0$ seine physikalische Bedeutung als Nullpegeldurchschreitungszahl.

3. Möglichkeit der Erstellung von Statistiken von Spitzenbelastungen durch Vorausberechnung in bezug auf technische Objekte im Entwurfstadium

Wir wollen noch zeigen, daß die von uns abgeleiteten Zusammenhänge einen wesentlichen Schritt in Richtung der Vorausberechnung von Spitzenbelastungen von Objekten im Entwurfsstadium darstellen.

Insbesondere die auf Fahrzeugen oft messbaren exponentiellen Pegeldurchschreitungszahlverteilungen nach [5] und [6] entstehen dadurch, daß der Effektivwert von Gaussschen Signalen mit Pegeldurchschreitungszahlverteilungen laut (27) sich bei nahezu konstantem spektralen Charakter in der Zeit quasistationär, widerum einer Gaussschen Verteilungsdichte

$$g(\sigma) = 2 \frac{1}{(1/\alpha)\sqrt{2\pi}} e^{-y^2/2(1/\alpha)^2} \tag{31}$$

folgend verändert. Der Parameter α erweist sich da als der Kehrwert der Streuung der Effektivwerte, der im Falle von auf Radaufstandspunkten auftretenden Eingangssignalen von Straßenfahrzeugen, z. B. in Anbetracht der Straßendecken- und Geschwindigkeitsverhältnisse, sich auch als Erfahrungswert annehmen läßt. Bei gegebenem spektralen Charakter der Eingangssignale lassen sich — das Fahrzeug als gegebenes lineares System betrachtend — auch die Effektivwerte und die spektrale Verteilung der Ausgangssignale (z. B. Spannungen) durch bekannte Input-Output Zusammenhänge bestimmen, wodurch nochmals anhand der schon erwähnten RICEschen Formel und Formel (31) auch die nur vom spektralen Charakter abhängige und je nach Signal etwa konstante $\bar{N}_0$ und die α Werte der Ausgangsignale für die Anwendung der Formel (28) bestimmt werden können.

Die Anwendung der Formel (29) bzw. (2) in dem in der Praxis sehr selten vorkommenden Grenzfall von Gaussschen Signalen mit konstantem Effektivwert (der Fall eines Ackerschleppers z. B.) benötigt keine weitere Erläuterung.

In der Praxis können von (26) und (27) verschiedene Pegelüberschreitungsverteilungen auftreten. Die Anwendung der Formel (24) von allgemeinerer Gültigkeit bereitet auch in solchen Fällen keine Schwierigkeiten.

Auf Grund der hier dargestellten Zusammenhänge wird es offenbar, daß die Bestimmung in dem Entwurfsstadium von technischen Objekten von Pegelgrenzen, die mit gewünschter Wahrscheinlichkeit während der Lebensdauer nicht überschritten werden, in Zukunft von der Möglichkeit der immer besseren Vorausberechnung von Pegelüberschreitungsverteilungen abhängt. [5] und [6] stellen einen diesbezüglichen Versuch dar für Fälle, wo nach (26) oder (27) getroffene Annahmen nicht befriedigen können.

Zum Schluß möchten wir noch darauf verweisen, daß die Berücksichtigung der erörterten Zusammenhänge — trotz ihrer relativen Einfachheit — in der Vorausberechnung der Spitzenbelastungsgrenzen eine ebenso nicht entbehrliche Voraussetzung darstellt, wie das Vorhandensein von hochentwickelten Finite Element-Programmsystemen, die die dynamische und festigkeitsgemäße Erfassung des Verhaltens von komplexen Strukturen im Falle von gegebenen Eingangssignalen ermöglichen.

SCHRIFTTUM

1. BUXBAUM, O.—SWENSON, O.: Extreme Value Analysis of Flight Load Measurements. Aircraft fatigue design, operational and economic aspects. *Proceedings of the Symposium held in Melbourne* 22—24 *May* 1967. Edited by J. J. MANN and J. S. MILLIGAN. Pergamon Press, Australia 1971.
2. BENDAT, J. S.: Principles and Applications of Random Noise Theory. John Wiley and Sons, Inc. New York 1958.
3. GUMBEL, E. J.: Statistics of Extremes. Columbia University Press, New York 1958.
4. DAHLBERG, T.: Optimization Criteria for Vehicles Travelling on a Randomly Profiled Road — A Survey. *Vehicle System Dynamics* **8,** (1979), 239—252.
5. JÁNOSDEÁK, E.—KERESZTES, A.—MICHELBERGER, P.: Allgemeine Gesetzmäßigkeiten der Statistiken von Fahrzeugbeanspruchungen und deren Vorausberechnung während der Entwicklungsphase. *FISITA XVIII. Internationaler Kongress* 5—8 *Mai* 1980. Hamburg, Vortrag Nr. **80,** 1. 4. 2.
6. JÁNOSDEÁK, E.: Ein Nachweis der statistischen Merkmale von Signalen, die durch das Straßenprofil oder Bewegungsmedium ausgelöst in Fahrzeugsystemen wirken. *Acta Techn. Hung.* **89** (1979), 145—158.

ANHANG

Es sei $F(y)$ die Verteilungsfunktion einer in der Zeit diskreten stochastischen Variablen y^* (Belastung). Jenen Zeitintervall, in bezug auf welchem wir die Statistik der Spitzenwerte (höchste im betrachteten Zeitintervall, z. B. Fahrzeuglebensdauer, je nach Realisation erreichte Werte) erstellen wollen, teilen wir in Z Segmente auf; jeder Segment enthalte r diskrete Ereignisse betreffend y^*. Die Wahrscheinlichkeit dafür, daß jeder von diesen innerhalb der Grenzen y verbleibt, ist offensichtlich

$$P_A = F^r(y), \tag{1*}$$

während die Wahrscheinlichkeit dafür, daß eine Überschreitung auftritt

$$P_E = 1 - P_A \tag{2*}$$

ist. Wenn die Verteilung der Ereignisse dem exponentiellen Gesetz folgt, lautet die Verteilungsfunktion

$$F(y) = 1 - e^{-\alpha y}. \tag{3*}$$

Logarithmierend (1*), dann die so erhaltene logarithmische Funktion in eine Taylorsche Reihe entwickelnd nach $F(y)$ um den Wert 1,0, nur die ersten zwei Glieder erhaltend bekommen wir

$$\ln P_A \cong r[F(y) - 1], \tag{4*}$$

wonach

$$P_A \cong e^{r[F(y)-1]}. \tag{5*}$$

Nach Substitution von (3*):

$$P_A \cong 1 - e^{-re-\alpha y}. \tag{6*}$$

Jene Anzahl Z von Segmenten, welche dazu notwendig ist, daß die Überschreitung des Pegels y durchschnittlich einmal vorkommen soll, ist gleich $1/P_e$; demnach jene Anzahl Z, welche zur erwähnten Überschreitung nach wiederholten Versuchen von der Dauer von Z Segmenten mit einer relativen Häufigkeit bzw. Wahrscheinlichkeit P_1 führt,

$$Z = \frac{P_1}{P_E} \cong \frac{P_1}{1 - e^{-re-\alpha y}} \tag{7*}$$

ist.

Während in [1] dieser Zusammenhang angewendet wird, führen wir zum Zwecke der Vergleichbarkeit mit unseren Zusammenhängen noch weitere Umformungen durch. Das exponentielle Glied nach $+e^{-\alpha y}$ in Reihe entwickelnd und nur die erste zwei Glieder erhaltend bekommen wir

$$Z = \frac{P_1}{r} e^{\alpha y}, \tag{8*}$$

oder nach weiterer Umformung

$$y \cong -\frac{1}{\alpha} \ln \frac{P_1}{r} + \frac{1}{\alpha} \ln Z . \tag{9*}$$

Nach Einführung von

$$p(0) = 1 - P_1 \cong e^{-P_1} , \tag{10*}$$

das ist

$$P_1 \cong \ln \frac{1}{p(0)} , \tag{11*}$$

nach Substitution in (9*) erhalten wir

$$y \cong \frac{1}{\alpha} \ln \frac{r}{\ln (1/p(0))} + \frac{1}{\alpha} \ln Z . \tag{12*}$$

Methods for the Statistical Treatment of Peak Loads. — The statistics of peak loads, that is, the highest loads occurring in the lifetime of structures submitted to stochastic loadings, is applied by the literature to the subject, up till now partly on the basis of the theory of statistics of extreme values for the evaluation of measurement results, partly on the basis of the theory of continuous stochastic signals, particularly for the case of the Gaussian signals. It is pointed out that on the basis of this latter theory also a treatment of the problem of general validity involving the results found so far, is possible. This created, by making use of the calculation methods for estimating the dynamic behaviour of structures, a significant precondition for the establishment of the statistics of peak loads, already in the phase of designing.

Acta Technica Academiae Scientiarum Hungaricae, Tomus 92 (3—4), pp. 257—265 (1981)

A STATE ESTIMATION METHOD FOR NONLINEAR DISTRIBUTION NETS

D. SINGER*

DOCTOR OF ENG. SCI.

[Manuscript received November 13, 1980]

The paper gives an estimation method for the non-measured state variables of non-linear nets (gas and water nets, etc.). The state estimation occurs in two steps. In the first a pre-estimation of the node loads are calculated founded on long-time statistical data of the total network load and on some hypotheses concerning the structure of the load distribution. In the second step the node load data are refined by an LS-estimation. The quality index of the estimation has a minimum if the calculated node potentials and the measured ones differ minimally. According to the non-linear character of the system, the estimation is executed as a *recursive* process of linear estimation steps.

Introduction

The importance of practical state estimation methods for distribution nets is evident considering that their instrumentation is generally poor. Some relevant papers on the topic are in the bibliography under [1], [2], [3]. In the following a new state estimation method is given, applicable also for non-linear nets, as gas oil, water nets, etc. We assume that the computer data management systems of the net contain all data on the topology, on physical characteristics of the branches, on the locations of the individual consumers, and on their integral consumes registered manually for accounting.

Our considerations are founded on the following:

a) The net is in stationary state.

b) On the nodes a great number of consumers are connected. (The consumptions of individual consumers can vary in the limits of some hundred percents.)

c) The source flows and the consumption of large consumers are continually registered.

d) The state variables: the electric node potentials, the node pressures, etc. are continually registered in n_M nodes, where $n_M \geq 0{,}1\ n$; n is the total number of nodes.

* Dr. D. SINGER II. Nyéki u. 9., 1021 Budapest, Hungary

The estimation method consists from two steps: *a)* the pre-estimation of the node loads, *b)* the refining of the node load estimation with a method applicable also for non-linear systems, *c)* calculating the best estimate of the state variables (node potentials).

Pre-estimation of node loads

The mass balance of the net can be given in the following form

$$\sum_{i=1}^{n} W_{Ai}(t) + \sum_{i=1}^{n} \sum_{j=1}^{b_i} W_{Bij}(t) - \sum_{i=1}^{n} W_{si}(t) = 0 . \tag{1}$$

W_{si} is the source flow of the i-th node, W_{Ai} is the total consumption of consumers with no instantaneous flow metering at the i-th node, W_{Bi} is the total consumption of consumers with flow metering (large consumers) at the i-th node, b_i is its number.

As a first gess we assume that, the time dependence of the node loads differs approximately only in a multiplication factor c_i from that of the *total* net load $W^*(t)$, originating from the node consumptions $W_{Ai}(t)$

$$W_{Ai}(t) = c_i W^*(t), \quad i = 1, 2, \ldots, n \tag{2}$$

According to (1)

$$W^*(t) = \sum_{i=1}^{n} W_{si}(t) - \sum_{i=1}^{n} \sum_{j=1}^{b_i} W_{Bij}(t) . \tag{3}$$

For the determination of c_i we use the plausible assumption that (2) holds also for the year-middles, therefore

$$c_i = \frac{W_{Ai}(t)}{W^*(t)} . \tag{4}$$

The pre-estimates of the node load computables from the available data, are, in vectorial form

$$W_e(t) = W_A(t) + W_B(t) . \tag{5}$$

Refining of the node-load estimates

We refine the node-load estimates defining the estimation quality index R in the following manner: R will be minimal if the node potentials, calculated according to the best estimates of the node loads, differ minimally from the directly measured node potentials. R has the form

$$R = E\{(e_M - \tilde{e}_M)\, \Theta (e_M - \tilde{e}_M)\} . \tag{6}$$

e_M and $\tilde{e}_M$ are the calculated and measured potentials, Θ is a weighting (diagonal) matrix; e_M can be calculated from W using the network equation

$$e(t) = F[W(t)]. \tag{7}$$

Partitioning (7) according to the nodes with measured and unmeasured potentials, e_M and e_U respectively, $e = [e_M e_U]$ one obtains

$$e_M(t) = F_1[W(t)] \tag{8}$$

$$e_U(t) = F_2[W(t)]. \tag{9}$$

The optimal estimate of $W(t)$, $\hat{W}(t)$ is according to the condition $R \to \min$,

$$W(t) = F_1^{-1}[\hat{e}_M(t)] \tag{10}$$

where F_1^{-1} is the inverse function of F_1 and $\hat{e}_M(t)$ is the optimal value of $e_M(t)$. For the non-measured potentials we obtain from (9) and (10)

$$e_U(t) = F_2\{F_1^{-1}[e_M(t)]\} \tag{11}$$

The explicit formulation of the network equations

The estimation of $W(t)$ will be a multistep recurcive linear process. We therefore formulate the network equations in a linear recursive form. According to the method of companion models, the solution of a non-linear network can be replaced by a recursive series of linear networks of the same topology [4]. The branch equation of such a model can be obtained in the following manner (Fig. 1).

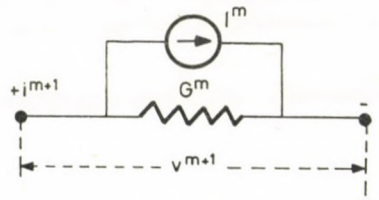

Fig. 1

Expanding the branch equation $i = f(v)$ in a truncated Taylor series, one obtains

$$i^{m+1} = i^m + \left(\frac{\partial i}{\partial v}\right)_{v=v^m} (v^{m+1} - v^m), \tag{12}$$

or

$$i^{m+1} = G^m v^{m+1} + (i^m - G^m v^m) \tag{13}$$

where $G^m = \partial i/\partial v|_{v=v^m}$. The expression in parentheses in (13) can be considered as a source flow I^m. The companion model of the whole network can be synthesized from the one of the single branch in Fig. 1. The resulting model is a network consisting from linear resistors (conductances), virtual and real flow sources, resp. The companion model of a simple gas net consisting from 3 tubes is shown in Fig. 2. The nodal equation of the linear network is

$$e = -[\mathbf{AGA}^T]^{-1}[W_a - \mathbf{AGV}]\,. \tag{14}$$

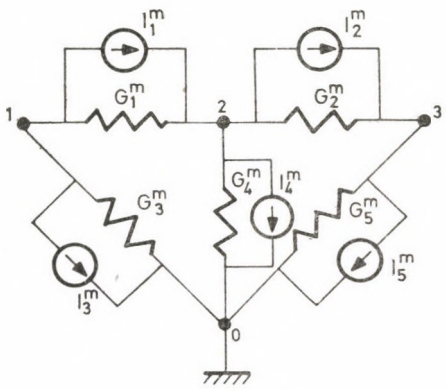

Fig. 2

A is the node branch incidence matrix, **G** the conductance matrix, W_a and **V** are the nodal source load and the branch source potential vectors, respectively: Eq. (14) can be applied directly to the linear companion network

$$e^{m+1} = -[\mathbf{AG}^m\mathbf{A}^T]^{-1}[W_e^m + W_c^m] \tag{15}$$

where $W_e^m = W_a - \mathbf{AG}^m\mathbf{V}$; $W_c^m = \mathbf{AI}^m$; W^m is the *effective*, W_c^m the *virtual* node load originating from the non-linearities of the network. With the notation $\mathbf{AG}^m\mathbf{A} = \mathbf{Y}^m$; $W_e + W_c^m = W^m$ (15) becomes

$$e^{m+1} = [\mathbf{Y}^m]^{-1}W^m; \quad m = 0, 1, 2, \ldots \tag{16}$$

For decomposing (16) according to (8) and (9), we decompose W_e to $[W_M^m W_U]$ and $\mathbf{Y}^m$ to

$$\mathbf{Y}^m = \begin{bmatrix} \mathbf{Y}_{11}^m & \mathbf{Y}_{12}^m \\ \mathbf{Y}_{21}^m & \mathbf{Y}_{22}^m \end{bmatrix}. \tag{17}$$

The submatrices $\mathbf{Y}_{k1}$ are defined as follows:

$$\mathbf{Y}_{11}^m = \mathbf{A}_{11}\mathbf{G}_{11}^m\mathbf{A}_{11}^T + \mathbf{A}_{12}\mathbf{G}_{22}^m\mathbf{A}_{21}^T; \quad \mathbf{Y}_{12}^m = \mathbf{A}_{11}\mathbf{G}_{11}^m\mathbf{A}_{21}^T + \mathbf{A}_{12}\mathbf{G}_{22}^m\mathbf{A}_{22}^T$$
$$\mathbf{Y}_{21}^m = \mathbf{A}_{21}\mathbf{G}_{11}^m\mathbf{A}_{11}^T + \mathbf{A}_{22}\mathbf{G}_{22}^m\mathbf{A}_{21}^T; \quad \mathbf{Y}_{22}^m = \mathbf{A}_{21}\mathbf{G}_{11}^m\mathbf{A}_{21}^T + \mathbf{A}_{22}\mathbf{G}_{22}^m\mathbf{A}_{22}^T \tag{18}$$

where A_{ij}, $\mathbf{G}_{11}^m$ and $\mathbf{G}_{22}^m$ are the appropriate submatrices of $\mathbf{A}$ and $\mathbf{G}^m$.

The inversion of $\mathbf{Y}^m$ can be accomplished according to the rules for inversion of composite matrices

$$[\mathbf{Y}^m]^{-1} = \begin{bmatrix} \mathbf{S}_{11}^m & \mathbf{S}_{12}^n \\ \mathbf{S}_{21}^n & \mathbf{S}_{22}^m \end{bmatrix}. \tag{19}$$

The S_{k1}^m denotes the following matrix expressions:

$$\mathbf{S}_{11}^m[n_M \times n_M] = \mathbf{Y}_1^m + (\mathbf{Y}_{11}^m)^{-1}\mathbf{Y}_{12}^m[\mathbf{Y}_{22}^m - \mathbf{Y}_{21}^m\mathbf{Y}_{11}^m\mathbf{Y}_{12}^m]^{-1}\mathbf{Y}_{21}^m\mathbf{Y}_{11}^m,$$
$$\mathbf{S}_{12}^m[n_M \times n_U] = -\mathbf{Y}_{11}^m\mathbf{Y}_{12}[\mathbf{Y}_{22}^m - \mathbf{Y}_{21}^m\mathbf{Y}_{11}^m\mathbf{Y}_{12}^m]^{-1},$$
$$\mathbf{S}_{12}^m[n_U \times n_M] = -[\mathbf{Y}_{22}^m - \mathbf{Y}_{21}^m\mathbf{Y}_{11}^m\mathbf{Y}_{12}^m]^{-1}\mathbf{Y}_{21}^m\mathbf{Y}_{11}^m, \tag{20}$$
$$\mathbf{S}_{22}^m[n_U \times n_U] = \mathbf{Y}_{22}^m - \mathbf{Y}_{21}^m\mathbf{Y}_{11}^m\mathbf{Y}_{12}^m,$$

(16) can be now written as

$$\begin{bmatrix} e_M^{m+1} \\ e_U^{m+1} \end{bmatrix} = \begin{bmatrix} \mathbf{S}_{11}^m & \mathbf{S}_{12}^m \\ \mathbf{S}_{21}^m & \mathbf{S}_{22}^m \end{bmatrix} \begin{bmatrix} W_M^m \\ W_U^m \end{bmatrix}, \tag{21}$$

or in a more explicit form

$$e_M^{m+1} = \mathbf{S}_{11}^m W_M^m + \mathbf{S}_{12}^m W_U^m, \tag{22}$$

$$e_U^{m+1} = \mathbf{S}_{21}^m W_M^m + \mathbf{S}_{22}^m W_U^m. \tag{23}$$

Formulation of the best estimate of the node loads and node potentials

In (6) a global quality index of the estimation was formulated. We refine this now asking that all load values obtained by optimal estimation in LS-sense should be as near as possible to the pre-estimated values. Thus beside (6), also

$$E\{(W^n - W_p)^T\Psi(W^m - W_p)\} \to \min \tag{24}$$

should be valid. We write here W_p instead of W for the vector of pre-estimated load values. Using the sum of (6) and (24) as quality index, we obtain with (22)

$$R^m = E\{(W^m)^T\,\Theta(S_1)^T\,S_1^m\,W^m - \tilde{e}_M^T\,\Theta\,S_1 W^m -$$
$$- (W^m)^T\,(S_1^m)^T\,\Theta\,\tilde{e}_M + \tilde{e}_M^T\,\Theta\,\tilde{e}_M +$$
$$+ (W_m)^T\,\Psi\,W^m - (W_p^m)^T\,\Psi\,W^m - (W^m)^T\,\Psi\,W_p + W_p\,\Psi\,W_p \qquad (25)$$

where $S_1^m = [S_{11}^m\,S_{12}^m]$; $\tilde{e}_M$ is the vector of measured node potential values, Θ and Ψ are weighing matrices.

As in the scalar case, the minimum of R^m is characterized by the roots of the equation $dR^m/dW^m = 0$. Concerning linear estimation methods, see e.g. [7], [8]. We use the following rules for the derivation of a matrix by a vector,

$$\frac{\mathrm{d}(c^T\mathbf{F}c)}{\mathrm{d}c} = 2c^T\mathbf{F}\,; \qquad \frac{\mathrm{d}(a^T c)}{\mathrm{d}c} = a^T \qquad (26)$$

where a and c are arbitrary column vectors, $\mathbf{F}$ is an arbitrary matrix. Applying (26) to (25), one gets

$$(W^m)^T\,(S_1^m)^T\,\Theta\,S_1^m - \tilde{e}_M^T\,\Theta\,S_1^m + (W^m)^T\,\Psi - W_p^T\,\Psi = 0\,. \qquad (27)$$

By rearranging and solving, one obtains

$$W^m = [(S_1^m)^T\,\Theta\,S_1^m + \Psi]^{-1}\,[(S_1^m)^T\,\Theta\,\tilde{e}_M - W_p]\,. \qquad (28)$$

W^m is the best estimate of the node loads in the m-th recursion cycle.

Substituting the numerical values of (28) in Eq. (21), one obtains a $(m+1)$-th value for the best estimate of the node potential vector. The recursion process can be continued calculating new values for $\mathbf{G}^m$ and $\mathbf{J}^m$ and according to these, also new values for the matrices $\mathbf{Y}_{k1}^m$ and $\mathbf{S}_{k1}^m$ can be obtained. Using these in (28), one obtains better values for W^m, etc. The recursion is continued until $|\hat{W}^{m+1} - \hat{W}^m| \leq \varepsilon$ where ε is a given small vector. Using the last value $\hat{W}^m$, one can determine with (21) the best estimates of the node potential.

As a short reference how to use the method, we give a short example concerning the high pressure gas network. The constitutive relations of the branches here are

$$p_1^2 - p_2^2 = kq^2\,. \qquad (29)$$

p_1 and p_2 are the pressures on both ends of the branch, q is the flow, k a constant. To transform (29) into the form $i = f(v)$, we define new potentials Π_j according to $\Pi_j = p_j^2$.

$$q = \left(\frac{1}{k}\right)^{1/2}(\Pi_1 - \Pi_2)^{1/2} = K v^{1/2} \qquad (30)$$

where $v = \Pi_1 - \Pi_2$, $K = \left(\frac{1}{k}\right)^{1/2}$.

From (13) and (30) we get for $\mathbf{G}_j^m$ and $\mathbf{J}_j^m$

$$\mathbf{G}_j^m = \frac{1}{2} K_j v_j^{-1/2}|_{v_j = v_j^m}; \quad \mathbf{J}_j^m = -\frac{1}{2} K_j v_j^{1/2}|_{v_j = v_j^m}. \tag{31}$$

For the conductance matrix $\mathbf{G}^m$ and the vector of the virtual branch source

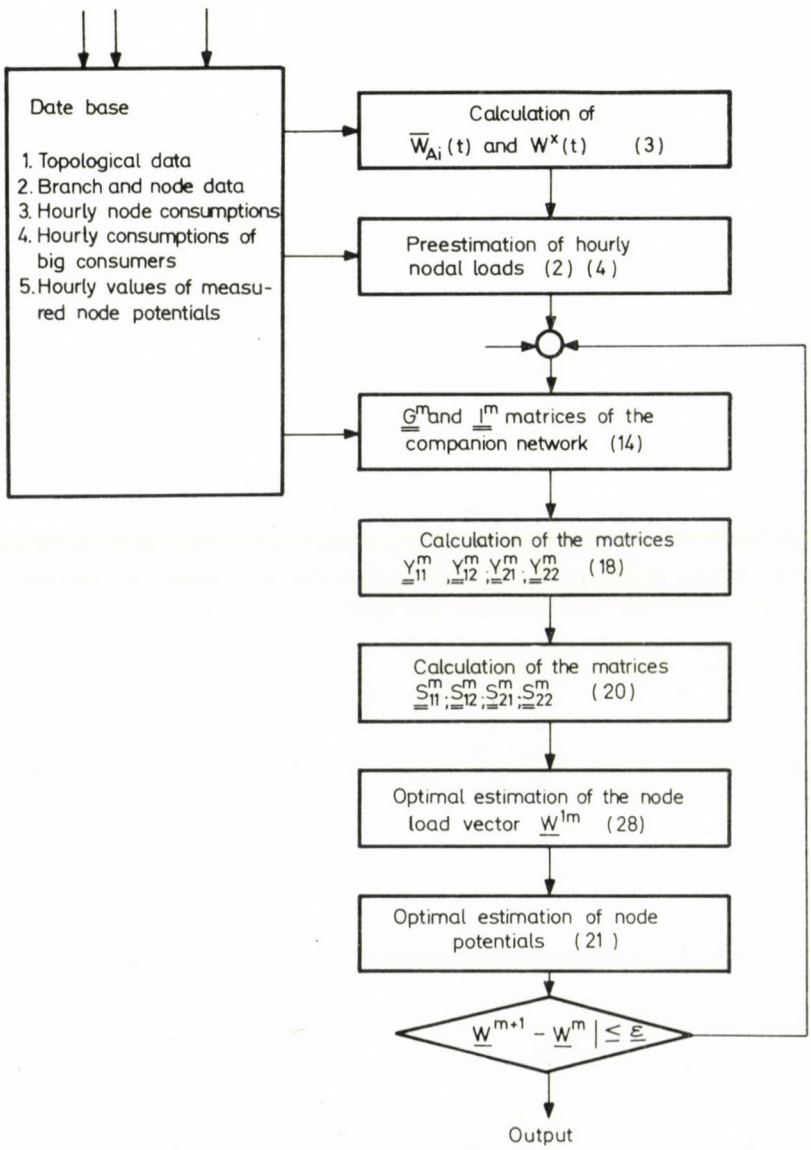

Fig. 3

flow $\mathbf{J}^m$ and $\mathbf{AJ}^m = W_c^m$, we obtain — using the node-to-base pressure vector e, instead of the branch vector $v = \Pi_i - \Pi_j = p_i^2 - p_j^2$ — according to the relation $v = \mathbf{A}^T e$

$$\mathbf{G}^m = \frac{1}{2} K \{\text{diag}\,[\mathbf{A}^T(e^{-1/2})]\}|_{e=e^m}, \tag{32}$$

$$W_c^m = -\frac{1}{2}\mathbf{AK}[\mathbf{A}^T(e^{1/2})]_{e=e^m} \tag{33}$$

diag $[\mathbf{A}^T(e^{-1/2})]$ is the matrix obtained by the diagonalization of the vector $[\mathbf{A}^T(e^{-1/2})]$.

The flow sheet of the algorithm is on Fig. 3.

Some remarks

Our short remarks concern the quality, stability and time demand of the method.

The quality of the estimation depends mainly on two factors:

a) the ratio of nodes with measured and unmeasured potentials;

b) on the distribution uniformity of the measured node in the net.

On the convergence, one can say the followings: As iterative methods generally, also the given algorithm is not absolutely convergent. It is impossible to give sufficient conditions for the convergency. The danger of inconvergency can be reduced by chosing appropriate starting values for $\mathbf{A}^m$ and $\mathbf{J}^m$. For this purpose it is useful to calculate the node potentials for the dre-estimated values of node potentials with a fast standard analysis program for non-linear network [9].

The time consumption depends on the computer hardware and the quality of the matrix-operation software. According to the sparsity of the network incidence matrix, a matrix inversion software utilizing the sparsity of the node branch incidence matrix is in all circumstances on place. The second factor influencing computer time is the "strength" of the non-linearities. For a linear network, the estimation needs only one iteration step.

REFERENCES

1. Schweppe, F. G.—Wildes, J.: Power System Static State Estimation. Exact Model. *Trans IEEE* PAS-89, 1 (1970), 120—125; ibid. 125—130; ibid. 130—135.
2. Larson, R. E.—Tinney, W. F.—Peschon, J.: State Estimation in Power Systems, Part I. *IEEE Trans.* PAS-89, 1970, 345—352; ibid., Part II. (1970), 353—363.
3. Galliana, F. D.—Handschin, E.—Fichter, A. R.: Identification of Stochastic Electric Load Models from Physical Data. *IEEE Trans.* AC-19, (1974), 887—893.
4. Katzenelson, J.—Seitelmann, L. H.: An Iterative Method for Solution of Nonlinear Resistors. *Trans. IEEE*, CR-13 (1966), 317—322.

5. GÉHER, K.: Lineáris hálózatok (Linear Networks). 4. ed. Műszaki Könyvkiadó, Budapest 1979.
6. VÁGÓ, I.: A gráfelmélet alkalmazása villamoshálózatok számítására (Use of Graph-theory for Computation of Electric Networks). Műszaki Könyvkiadó, Budapest 1976.
7. BÁNYÁSZ, Cs.—KEVICZKY, L.: Discrete-time Identification of Linear Dynamic Processes. *MTA SZTAKI-Studies*, No. 94, Budapest, 1978.
8. SINGER, D.—ELEK, J.: Softwarefragen der Analyse, Projektierung und Steuerung von Gasnetzen. *Acta Techn. Hung.*, **87**, (1978) 391—406.

Eine Estimationsmethode für Nichtlineare Verteilungsnetze. — Die Arbeit beschreibt eine Estimationsmethode für Zustandsvariablen von nicht linearen Netzen (Gas- und Wassernetzen usw.). Die Estimation verlauft in zwei Schritten. Im ersten Schritt wird eine vorläufige Vorhersage der Knotenpunktsbelastungen auf Grund statistischen Überlegungen gegeben. Im zweiten Schritt werden diese Daten auf Grund einer LS-Estimation verfeinert. Der Qualitätsindex der Estimation weist ein Minimum auf, wenn die Abweichungen der gemessenen und berechneten Knotenpunktdrücke eine minimale Abweichung aufweisen. Wegen des nichtlinearen Charakters der Problematik stellt die Methode ein Rekursivverfahren dar.

Acta Technica Academiae Scientiarum Hungaricae, Tomus 92 (3—4), pp. 267—290 (1981)

CYLINDER-SYMMETRICAL AND PLANE PROBLEMS

G. LÁMER*

[Manuscript received March 12, 1980]

In this paper the cylinder-symmetrical and plane problems are systematized and analysed. A review is given on the literature for the subject dealing with the definition of the problems and pointing out the discrepancies in them. By considering the diverging definitions as different problems, new types of states have been defined both in the case of the existence of cylindrical-symmetry and plane problems. Uniform definitions of the newly introduced states, equations determining them, and the function classes of the solutions valid for the displacement components are presented. In the process of the analysis it has been pointed out that the uniformly defined states differ from each other by a stress component each, and only in this conception is it possible to trace back the plane stress pattern to the plane deformation state by the transformation of the moduli of elasticity.

Symbols

$\mathbf{i}, \mathbf{j}, \mathbf{k}$	— unit vectors in a system of orthogonal coordinates
x_i	— orthogonal coordinates
x, y, z	— Cartesian coordinates
r, φ, z	— cylindrical coordinates
$\mathbf{u}$	— displacement vector
u_i	— displacement component
u, v, w	— displacement components in a system of Cartesian coordinates
u_r, u_φ, u_z	— displacement components in a system of cylindrical coordinates
$\mathbf{T}_\varepsilon$	— deformation tensor; its components being $t_{ij}(\varepsilon) = \frac{1}{2}\left(\frac{\partial u_i}{\partial x_j} + \frac{\partial u_j}{\partial x_i}\right)$; in the text the more generally adopted notation $\varepsilon_x, \ldots, \gamma_{xy}, \ldots$ are used.
ε	— volumetric change, $\varepsilon = t_{ii}(\varepsilon)$
$\mathbf{T}_\sigma$	— stress tensor, its components being $t_{ij}(\sigma) = \lambda\delta_{ij}\varepsilon + 2Gt_{ij}(\varepsilon)$; in the text the more generally adopted notation $\sigma_x, \ldots, \tau_{xy}, \ldots$ are used
δ_{ij}	— Kronecker's symbol
λ, G	— Lamé's coefficients of elasticity
μ	— coefficient of transverse contraction, $\mu = \lambda/2(\lambda + G)$
$\mathbf{E}(\zeta)$	— *translation* by vector ζ directed to unit vector $\mathbf{k}$
$\mathbf{T}(S_k)$	— *mirror image* to plane S_k of normal $\mathbf{k}$
u_0, v_0, w_0	— displacement components independent of z
$u_r^0, u_\varphi^0, u_z^0$	— displacement components independent of φ
$\nabla_0^2 = \frac{\partial^2}{\partial x^2} + \frac{\partial^2}{\partial y^2}$	— two-dimensional Laplacian operator

* LÁMER, G. Dipl. Eng. Vas u. 15/B, H-1088 Budapest, Hungary

1. Introduction

In determining the stress pattern of a structure, models of different types (bar, plate, shell) are used according to the geometrical conditions. In the case of a more complex geometric configuration the governing equations of the theory of elasticity should be applied. Also these equations might be reduced, thus for example, in calculating solids of revolution with cylinder-symmetrical load or in solving inplane problems. In that way, the three-dimensional problem will be reduced to a two-dimensional one. (Or, expressed more precisely, the mechanical state characteristics are the functions of only two, but not of three variables; the solid to be investigated is in both cases of three dimensions.) This reveals the fact that these problems are thoroughly elaborated chapters of the theory of elasticity.

1.1 The theory and calculation of the solids of revolution is extensively elaborated, particularly the theory of the circular symmetrical plates and shells where the two free arguments can be divided (which is the case of plates) or, analytic relationships can be established for their definition (the case of shells of revolution). These problems are dealt with by the monographs [21] and [36]. One of the most completed studies [15] written about the theory of the three-dimensional solids of revolution (i.e., thick-walled shells of revolution) treats, beside the problems of the theory of elasticity, also that of the thermal stresses and non-elastic behaviour, not only in the case of cylinder-symmetrical loads but also in the case of loads of optional pattern. Almost in all theoretical and practical works, a few chapters are assigned to the theory of the solids of revolutions [2, 3, 6, 10, 18, 19, 26, 31, 34], and in the finite element method, as an applied scheme of solution, also the ring shaped elements needed for the calculation of the solids of revolution appeared [5, 16, 23, 25, 27, 37, 38].

1.2 Quoting the words of LURJE: "*The plane problem constitutes the chapter of the theory of elasticity being elaborated generally and in the most detailed way.*" (See [19], p. 462.) The justification of this statement is to be found in the ease which is assured by the solution of partial differential equations of two variables in comparison to that of the partial differential equations of three variables. The evolution of plane problems, as one of the chapters of the theory of elasticity, took place after the adoption of the complex variables [14], [11, 12, 19, 22, 34], also a great number of solutions by the application of non-complex functions also occurred (theory of bending, elastic plane, half-plane and wedge) [7, 8, 10, 11, 17, 19, 24, 32, 33, 34, 35].

2. Survey on the literature on the subject

2.1 *Cylindric-symmetrical state*

The technical literature relates to the cylinder-symmetrical problems, to geometric configurations of cylinder-symmetry, i.e., to solids of revolution [2, 3, 6, 18, 19, 31, 32, 33]. In the state of cylinder-symmetry, beside the deformation and stress fields, also the displacement field is considered as cylinder-symmetric. In that case, both the equilibrium and geometric equations fall into two groups (Table 1). Such an arrangement of the cylinder-symmetrical problem may be found in the pertinent literature [6, 19, 26, 33], while several authors [2, 3, 10, 18, 31, 32], in the case of axi-symmetrical loading of the solids of revolution, in investigating the displacement field, i.e., the deformation and stress fields, consider the axisymmetry to be at the same time a cylindrical symmetry and axisymmetry, add to the independence on φ, also the conditions $u_\varphi = 0$ and $\tau_{r\varphi} = \tau_{\varphi z} = 0$. This way of proceeding does not lead, in practice, to an error, because by the requirement of axisymmetry the torsion is separated from the general cylinder-symmetrical state. In turn, the axisymmetry in itself also permits non-cylinder-symmetrical loading (for example, in the case of pure bending). Therefore, it is convenient to emphasize

Table 1

	Cylindric-symmetrical state	
	Evenly cylindric-symmetrical state	Torsion
Equilibrium equations	$\frac{\partial \sigma_r}{\partial r} + \frac{\partial \tau_{rz}}{\partial z} + \frac{\sigma_r - \sigma_z}{r} = 0$ $\frac{\partial \tau_{rz}}{\partial r} + \frac{\partial \sigma_z}{\partial z} + \frac{\tau_{rz}}{r} = 0$	$\frac{\partial \tau_{r\varphi}}{\partial r} + \frac{\partial \tau_{\varphi z}}{\partial z} + \frac{2\tau_{r\varphi}}{r} = 0$
Geometrical equations	$\varepsilon_r = \frac{\partial u_r}{\partial r}, \quad \varepsilon_z = \frac{\partial u_z}{\partial z}$ $\varepsilon_\varphi = \frac{u_r}{r}, \quad \gamma_{rz} = \frac{1}{2}\left(\frac{\partial u_r}{\partial z} + \frac{\partial u_z}{\partial r}\right)$	$\gamma_{r\varphi} = \frac{1}{2}\left(\frac{\partial u_\varphi}{\partial r} - \frac{u_\varphi}{r}\right)$ $\gamma_{\varphi z} = \frac{1}{2}\frac{\partial u_\varphi}{\partial z}$

that the cylinder-symmetry and axisymmetry should exist *at the same time.* Considering the denomination and interpretation of the symmetries [9, 20] a uniform definition might be suggested which helps in separating, also the definition from each other, the cylindric-symmetrical states containing or not containing torsion. To this latter, author suggests the designation *evenly* cylinder-symmetrical. Namely, in this state $u_\varphi = 0$, $\gamma_{r\varphi} = \gamma_{\varphi z} = 0$, $\tau_{r\varphi} = \tau_{\varphi z} = 0$. The other state characteristics are *even functions* of the radius in any plane containing the axis of revolution. Therefore, by analogy of the even function used in the theory of functions, the term evenly cylinder-symmetrical might be suggested.

2.2 *Plane problems*

It is usual to divide the plane problems into the states of plane deformation and stress and generalized plane stress.

The preferred plane is designated by XOY.

2.2.1 The definition of the plane deformation state is mostly uniform. The most generally adopted formulation is as follows [3, 7, 11, 17, 18, 22, 31]: in the case of plane deformation the components (u, v) of the displacement in the preferred plane are the functions of the variables (x, y) lying in the direction of the coordinates defining the plane; while the displacement component (w) normal to the plane, is equal to zero:

$$\begin{aligned} u &= u(x, y) , \\ v &= v(x, y) , \\ w &= 0 . \end{aligned} \tag{1}$$

An equivalent formulation with the previous one is: in the case of plane deformation, the displacements taking place in the plane, are parallel to a given plane (XOY) [2, 8, 32]. BEZUHOV [2] changes over to the investigation of the deformation and stress tensors. A. FÖPPL and L. FÖPPL [8] as well as TIMOSHENKO [32] do not take w to be equal to zero:

$$\begin{aligned} u &= u(x, y) , \\ v &= v(x, y) , \\ w &= c_1 z + c_0 . \end{aligned} \tag{2}$$

LURJE [19] and NOWACKI [24] introduce the state of plane deformation by reducing the three dimensional problem to a two-dimensional one. While LURJE uses the relationships (2), NOWACKI considers the expressions

$$\begin{aligned} \varepsilon_z &= 0 , \\ \gamma_{yz} &= 0 , \\ \gamma_{zx} &= 0 \end{aligned} \tag{3}$$

as basic conditions; he does not carry out their integration, but considers the relationships (2) as the consequences of (3) with the condition $c_1 = 0$.

A solution also widely used for defining the state is the investigation of an example. This method is built on the suggestiveness, although considering the example as having verifying force: The infinitely long *prismatic* bar (structure) is in the state of plane deformation which is submitted to a load of invariable intensity in the direction **k** [6, 10, 12, 26, 33, 34]. It is to be noted

that by [6, 33, 34] practical instances are investigated by making use of the formulae (1); in [10] using the formulae (2), in [26] formulae (1) and in [12] by making use of the complex theory of functions, the problem is dealt with theorically which refer only to the basic problem. LURJE, A. FÖPPL and L. FÖPPL after the definition mention uses as the field of application the example mentioned above.

Practically, three definitions may be sharply separated. The first definition accentuates the property of the displacement that it is parallel to plane XOY. The second one applied only by NOWACKI, characterizes the deformation as being parallel to the XOY plane. The third definition is not to be considered as a definition but as a consequence, i.e., by taking into account some negligible quantities, (Saint-Venant's effect), as a field of application.

2.2.2 Some of the authors [6, 7, 12, 32] do not treat the plane stress pattern. The most generally adopted is the definition [8, 11, 17, 18, 19, 33, 34] that, in the solid, the planes being parallel to the plane XOY are unstressed:

$$\begin{aligned} \sigma_z &= 0 , \\ \tau_{yz} &= 0 , \\ \tau_{zx} &= 0 . \end{aligned} \tag{4}$$

Some of the authors prefer the illustrative definition. They consider a thin disc whose faces are unstressed and is, along its edge (i.e., mantle) subjected to a system of forces parallel to its faces [2, 3, 22, 31]. By neglecting the thickness of the disc [2, 3, 10, 22, 31], and assuming the load to be symmetrical, with respect to the bisecting plane of the disc [22, 26], they apply integral (which in case of MUSZHELISVILI [22] is already equivalent to the definition of generalized plane stress pattern), change over to the mean value of stress. In that case, if there are no loadings at the basic faces, the relationships (4) are valid in the whole disc to the mean stress-values. Further, some of the authors refer to the problem as already not being two dimensional, because the displacement components u and v are already also the functions of z and w, x, y. Therefore, also the deformation and stress tensors are the functions of z. In analysing the problem, the authors of the works [11, 17] neglect this fact. LOVE [18] points out that by the application of the function of *translation*, and LURJE by that of the *stress* function, the role of the coordinate z. After introducing the stress mean value, LOVE discusses the generalized plane stress pattern. LURJE assumes the loading to be symmetrical with respect to the bisecting plane of the disc and traces the problem back by the integration to the plane deformation state, thus, eliminating the coordinate z and the displacement component.

NOWACKI considers the independence of the stresses of z as definite, and points out that the plane stress state also contains the torsion about the axis z.

In neither of the definitions, excepting NOWACKI's one, are to be found definite contrasts. The first definition states that the planes XOY are unstressed. Further, by referring to the example, he mentions that the other stress components are independent of z. None of the authors makes such a statement definitely but LURJE. The second definition which is applied only by NOWACKI, considers the independence of the stresses of z as basic relation. In the third definition, the thickness of the disc investigated has a significant role because the extension in the other two directions is much larger, wherefore, the stresses acting at the surfaces of the planes of normal **k** are negligible. This is already a transition into the plane stress state.

It is to be noted that most of the authors traces back the plane stress pattern to the plane deformation state by introducing the moduli of elasticity $\lambda' = 2\,\lambda G/(\lambda + 2\,G)$ and $G' = G$. This similitude is true only to the stress components; in the case of the displacement components a certain degree of approximation should be applied.

2.2.3 Some authors define the generalized plane stress pattern by neglecting the thickness of the disc investigated [3, 6, 12]. In the studies [17, 18, 19, 32] the stress mean values are introduced by integration. Then, Saint-Venant's principle is applied and refers to the fact that the Eqs (4) are valid. As a matter of course, also in this case the independence or dependence on z of the other stress components might be considered.

As it must be separately decided for every actual instance that types of the plane problems could be applied without approximation or not, in the following the generalized plane problems will not be discussed.

2.2.4 The plane problems can also be defined in the systems of coordinates of principal strain and principal stresses [4, 28]. In doing this, the state defined for one point should carefully be generalized for the whole solid. For this reason, in practice, a definition defined in an external global system of coordinates, which is coaxial with the preferred direction, has been widely accepted.

3. Definitions

In this paper it is assumed that the solids investigated are of homogeneous, isotropic, elastic material. For the characterization of them both the moduli of elasticity λ and G introduced by LAMÉ and the coefficient of transverse contraction μ are equally used.

The states to be investigated will be interpreted to solids of special geometry: in the state of cylindrical symmetry to the solids of revolution, and in the plane state to straight* prismatic solids. A common property of these

* The base faces are perpendicular to the generatrices of the prismatic solid. In the following, the attribute *straight* will be omitted but the prismatic solid mentioned in the paper will always be considered as straight.

geometric solids is that they satisfy the invariance properties of the states, i.e., the symmetry of the revolution and translation.

At the states in question, the boundary conditions, both the supports and loadings, should satisfy the conditions defining the states, i.e., the invariances. This will only be clearly fulfilled in the case where the investigated solid itself also satisfies the conditions of the invariance. If this is not the case, nothing else could be said, than that the deformation and/or stress state satisfies the equations defining the state.

3.1 *Symmetry*

3.1.1 The invariance of the state displayed against the revolution by an angle φ has been considered as the definition of the cylinder-symmetric state. Therefore, the partial derivative of both the displacement field and the deformation and stress field with respect to φ is equal to zero.

From the existence of the cylindric-symmetrical displacement field ($\partial \mathbf{u}/\partial\varphi = 0$) follows that both the deformation and the stress field is cylinder-symmetrical. On the contrary, the problem is defined as cylindric-symmetrical deformation and stress states (in the case of actual problems it is the stress which is of significance from the viewpoint of the user), therefore it is to be proved that the validity of $\partial \mathbf{T}_\varepsilon/\partial\varphi = 0$ and/or $\partial \mathbf{T}_\sigma/\partial\varphi = 0$, in case of a cylinder-symmetrical solid also involves the truth of the identity $\partial \mathbf{u}/\partial\varphi = 0$.

N o t e: For an isotropic elastic material, from the linear relationship of the deformation and stress tensors it follows that in any arbitrary system of orthogonal coordinates x_1, x_2, x_3 the systems of equations $\partial \mathbf{T}_\varepsilon/\partial x_3 = 0$ and $\partial \mathbf{T}_\sigma/\partial x_3 = 0$ are equivalent with each other.

n the analysis it is shown that from equation $\partial \mathbf{T}_\varepsilon/\partial\varphi = 0$ follows the relationship $\partial \mathbf{u}/\partial\varphi = 0$. Thus, it is sufficient to speak about a cylindric-symmetrical state because the cylindric-symmetry of a field involves that of the other two.

3.1.2 In case of plane problems, similarly to those of cylindrical symmetry, we try to consider the state as an invariant in respect to some kind of transformation. It is convenient for an invariance against a translation ζ arbitrarily be selected, as a primary symmetry. By this symmetry it is demanded that the partial derivative with respect to z of the fields characterizing the state should be equal to zero:

$$\partial \mathbf{T}_\varepsilon/\partial z = 0\,, \quad \partial \mathbf{T}_\sigma/\partial z = 0\,. \tag{5, 6}$$

Beside the invariance displayed against the translation, also the invariance shown against mirroring on the plane of $\mathbf{k}$ normal $T(S_\mathbf{k})$ might be investigated. This condition implies that the specific angle torsions and shear stresses characterizing the plane XOY are equal to zero:

$$\gamma_{yz} = \gamma_{zx} = 0\,, \tag{7, 8}$$

$$\tau_{yz} = \tau_{zx} = 0\,. \tag{9, 10}$$

Besides, two zero-conditions of z-direction are needed for the formulation of the problem.

In the case of plane deformation, i.e., plane stress pattern the solid is not submitted to deformation in the z-direction:

$$\varepsilon_z = 0\,, \tag{3a}$$

i.e., no normal stress is induced in it:

$$\sigma_z = 0\,. \tag{4a}$$

3.1.3 Generalization

The plane deformation and plane stress patterns may be generalized in such a way that one does not consider the invariances, but maintains the plane property characteristic to the condition, i.e., the planes of $\mathbf{k}$ normal do not alter their plain form and remain unstressed.

3.2 *Definitions*

In the following, by considering the above symmetry definitions, those of the different states will be given.

3.2.1 Definitions of the cylindrical symmetry

a) By the term *cylindric-symmetrical state* the state of the solid of revolution is designated wherein the state characteristics of the solid are invariant against a revolution of angle φ:

$$\frac{\partial \mathbf{T}_\varepsilon}{\partial \varphi} = 0\,, \quad \frac{\partial \mathbf{T}_\sigma}{\partial \varphi} = 0\,, \quad \frac{\partial \mathbf{u}}{\partial \varphi} = 0\,. \tag{11, 12, 13}$$

b) By the term *evenly cylinder-symmetrical state*, such a state is designated where the state characteristics of the solid are invariant against the revolution of angle φ and against mirroring to any plane containing the axis of revolution: See relations (11, 12, 13) and

$$\gamma_{r\varphi} = \gamma_{\varphi z} = 0\,, \quad \tau_{r\varphi} = \tau_{\varphi r} = 0\,, \quad u_\varphi = 0\,. \tag{14, 15, 16, 17, 18}$$

3.2.2 Definitions of the plane state

One is faced with an inplane problem in the case where the solid is found in one of the states defined as follows.

a) An *inplane problem* is the state of a prismatic solid wherein both the invariants of the deformation field and that of the stress field against the translation $\mathbf{E}(\zeta)$ are the relationships (5) and (6).

b) The *symmetrical inplane problem* is the state of the prismatic solid where the invariants of both the deformation field and the stress field against the translation $\mathbf{E}(\zeta)$ and the mirroring $\mathbf{T}(S_k)$ are the relationships (5 to 10).

c) A *plane deformation state* is the state of a prismatic solid where the solid is not submitted to any deformation in the z-direction; the deformation tensor is invariant against the translation $\mathbf{E}(\zeta)$ and the mirroring $\mathbf{T}(S_k)$: relationships (5, 7, 8 and 3a).

d) Plain stress state is the designation of the state of a prismatic solid wherein the stress tensor is invariant both against the translation $\mathbf{E}(\zeta)$ and mirroring $\mathbf{T}(S_k)$, and no normal stress is induced in the solid in the z-direction: see the relationships (6, 9, 10, 4a).

e) General plane deformation state is called the state of a prismatic solid wherein only in the planes S_k do deformations occur, i.e., the planes S_k do not alter their plain form and are not displaced in comparison to each other. Thus, only the fulfilment of the relationships (7, 8, 3a) is required.

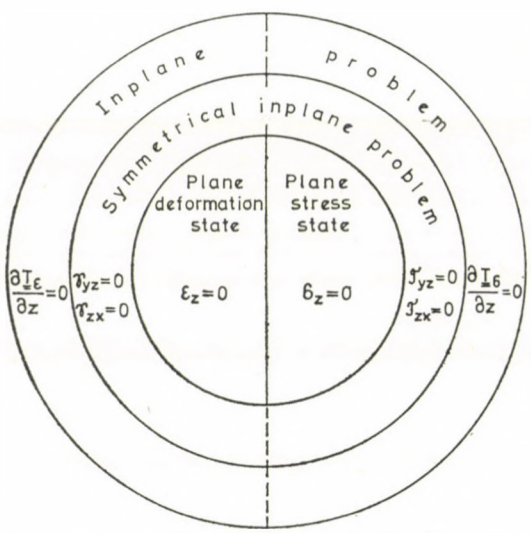

General plane deformation state	General plane stress state
$\varepsilon_z = 0$	$\sigma_z = 0$
$\gamma_{yz} = 0$	$\tau_{yz} = 0$
$\gamma_{zx} = 0$	$\tau_{zx} = 0$

Fig. 1 — Interconnection between the plane problems

f) General plane stress state is the state of a prismatic solid wherein the surface of the planes S_k is unstressed. Therefore, only the satisfaction of the relationships (9, 10, 4a) is needed.

N o t e: In the case where in advance it is known that the conditions characterizing the plane state, do not exist in all of the planes or in the whole plane, but the effect of the accidental exactitudes may be negligible, we are facing *generalized* plane problems.

The connection between each state is depicted in Fig. 1.

4. Analysis of the cylindric-symmetrical states

In consequence of the equivalence of Eqs (11) and (12) it is enough to analyse the following system of equations:

$$\frac{\partial}{\partial\varphi}\frac{\partial u_r}{\partial r}=0\,,\quad \frac{\partial}{\partial\varphi}\left(\frac{1}{r}\frac{\partial u_\varphi}{\partial\varphi}+\frac{u_r}{r}\right)=0\,,\quad \frac{\partial}{\partial\varphi}\frac{\partial u_z}{\partial z}=0\,, \qquad (19,20,21)$$

$$\frac{\partial}{\partial\varphi}\left(\frac{\partial u_\varphi}{\partial r}-\frac{u_\varphi}{r}+\frac{1}{r}\frac{\partial u_r}{\partial\varphi}\right)=0\,,\quad \frac{\partial}{\partial\varphi}\left(\frac{\partial u_\varphi}{\partial z}+\frac{1}{r}\frac{\partial u_z}{\partial\varphi}\right)=0\,,$$

$$\frac{\partial}{\partial\varphi}\left(\frac{\partial u_z}{\partial r}+\frac{\partial u_r}{\partial z}\right)=0\,. \qquad (22,23,24)$$

Let us integrate Eqs (19 to 21):

$$u_r=u_r^0(r,z)+u_r^1(\varphi,z)\,, \qquad (25)$$

$$u_\varphi=u_\varphi^0(r,z)+u_\varphi^1(r,z)\,\varphi-u_r^0(r,z)\,\varphi-\int u_r^1(\varphi,z)\,d\varphi\,, \qquad (26)$$

$$u_z=u_z^0(r,z)+u_z^1(r,\varphi)\,, \qquad (27)$$

and replace them into Eqs (22 to 24):

$$\frac{1}{r}\frac{\partial^2 u_z^1(r,\varphi)}{\partial\varphi^2}+\frac{\partial u_\varphi^1(r,z)}{\partial z}-\frac{\partial u_r^0(r,z)}{\partial z}-\frac{\partial u_r^1(\varphi,z)}{\partial z}=0\,, \qquad (28)$$

$$r\frac{\partial}{\partial r}\frac{u_\varphi^0(r,z)}{r}-r\frac{\partial}{\partial r}\frac{u_r^0(r,z)}{r}+\frac{u_r^1(\varphi,z)}{r}+\frac{1}{r}\frac{\partial^2 u_r^1(\varphi,z)}{\partial\varphi^2}=0\,, \qquad (29)$$

$$\frac{\partial^2 u_z^1(r,\varphi)}{\partial r\,\partial\varphi}+\frac{\partial^2 u_r^1(\varphi,z)}{\partial\varphi\,\partial z}=0\,. \qquad (30)$$

The most general integral of Eq. (30) is:

$$u_z^1(r, \varphi) = r f_{rz}(\varphi) + f_z(\varphi) + f_z(r)\,, \tag{30a}$$

$$u_r^1(\varphi, z) = -r f_{rz}(\varphi) + f_r(\varphi) + f_r(z)\,, \tag{30b}$$

replacement of Eqs (30a) and (30b) into Eq. (28) yields

$$\frac{\partial^2 f_{rz}(\varphi)}{\partial \varphi^2} + \frac{1}{r}\frac{\partial^2 f_z(\varphi)}{\partial \varphi^2} + \frac{\partial u_\varphi^1(r, z)}{\partial z} - \frac{\partial u_r^0(r, z)}{\partial z} + \\ + f_{rz}(\varphi) - \frac{\partial f_r(z)}{\partial z} = 0\,. \tag{28'}$$

In this equation the expression $\partial^2 f_{rz}/\partial \varphi^2 + f_{rz}(\varphi)$ depends only on φ, wherefore,

$$f_{rz}(\varphi) = A \sin \varphi + B \cos \varphi \tag{28a}$$

the expression $\partial^2 f_z(\varphi)/r\partial \varphi^2$ depends only on φ and r, wherefore

$$f_z(\varphi) = a\varphi + b \tag{28b}$$

similarly, the expression

$$\frac{\partial u_\varphi^1(r, z)}{\partial z} + \frac{\partial u_r^0(r, z)}{\partial z}$$

is only the function of r and z, wherefore,

$$u_\varphi^1(r, z) = u_r^0(r, z) + f_\varphi^1(r)\,. \tag{28c}$$

Let us replace the expressions (28a) and (28b) into Eq. (29)

$$r\frac{\partial}{\partial r}\frac{f_\varphi^1(r)}{r} + \frac{f_r(\varphi)}{r} + \frac{f_r(z)}{r} + \frac{1}{r}\frac{\partial^2 f_r(\varphi)}{\partial \varphi^2} = 0 \tag{29'}$$

which yields

$$f_r(z) = 0, \tag{29a}$$

$$f_r(\varphi) = C \sin \varphi + D \cos \varphi\,, \tag{29b}$$

$$f_\varphi^1(r) = cr\,. \tag{29c}$$

The displacement components take the following form:

$$u_r = u_r^0(r, z) - z(A \sin \varphi + B \cos \varphi) + (C \sin \varphi + D \cos \varphi), \tag{31}$$

$$u_\varphi = u_\varphi^0(r, z) + z(-A \cos \varphi + B \sin \varphi) - (-C \cos \varphi + \\ + D \sin \varphi) + cr\varphi\,, \tag{32}$$

$$u_z = u_z^0(r, z) + r(A \sin \varphi + B \cos \varphi) + a\varphi + b. \tag{33}$$

Acta Technica Academiae Scientiarum Hungaricae 92, 1981

Table 2

	Cylindric-symmetrical state	
	Evenly cylindric-symmetrical state	Cylindric-symmetrical torsion
Displacement components	$u_r = u_r^0 - z\,(A \sin\varphi + B\cos\varphi) + (\mathrm{C}\sin\varphi + D\cos\varphi)$ $u_z = u_z^0 + r(A\sin\varphi - B\cos\varphi)$	$u_\varphi = u_\varphi^0 - z\,(A\cos\varphi - B\sin\varphi) +$ $+ (C\cos\varphi - D\sin\varphi)$
Reduced Lamé-equations	$(\lambda+G)\dfrac{\partial}{\partial r}\left(\dfrac{\partial u_r^0}{\partial r} + \dfrac{u_r^0}{r} + \dfrac{\partial u_z^0}{\partial z}\right) + G\left(\dfrac{\partial^2 u_r^0}{\partial r^2} + \dfrac{\partial}{\partial r}\dfrac{u_r^0}{r} + \dfrac{\partial^2 u_r^0}{\partial z^2}\right) = 0$ $(\lambda+G)\dfrac{\partial}{\partial z}\left(\dfrac{\partial u_r^0}{\partial r} + \dfrac{u_r^0}{r} + \dfrac{\partial u_z^0}{\partial z}\right) + G\left(\dfrac{\partial^2 u_z^0}{\partial r^2} + \dfrac{1}{r}\dfrac{\partial u_z^0}{\partial r} + \dfrac{\partial^2 u_z^0}{\partial z^2}\right) = 0$	$\dfrac{\partial^2 u_\varphi^0}{\partial r^2} + \dfrac{\partial}{\partial r}\dfrac{u_\varphi^0}{r} + \dfrac{\partial^2 u_\varphi^0}{\partial z^2} = 0$
Deformation tensor components	$\varepsilon_r = \varepsilon_r^0, \quad \varepsilon_\varphi = \varepsilon_\varphi^0, \quad \varepsilon_z = \varepsilon_z^0, \quad \gamma_{rz} = \gamma_{rz}^0$	$\gamma_{r\varphi} = \gamma_{r\varphi}^0, \quad \gamma_{\varphi z} = \gamma_{\varphi z}^0$
Components of the encounter tensor	$\omega_{r\varphi} = -\dfrac{1}{2}\dfrac{z}{r}(A\cos\varphi - B\sin\varphi) + \dfrac{1}{2}\dfrac{1}{r}(C\cos\varphi - D\sin\varphi)$ $\omega_{\varphi z} = -\dfrac{1}{2}(A\cos\varphi - B\sin\varphi)$ $\omega_{zr} = \omega_{rz}^0 + (A\sin\varphi + B\cos\varphi)$	$\omega_{r\varphi} = \omega_{r\varphi}^0 + \dfrac{1}{2}\dfrac{z}{r}(A\cos\varphi - B\sin\varphi) -$ $-\dfrac{1}{2}\dfrac{1}{r}(C\cos\varphi - D\sin\varphi)$ $\omega_{\varphi z} = \omega_{\varphi z}^0 - \dfrac{1}{2}(A\cos\varphi - B\sin\varphi)$ $\omega_{rz} = 0$
Stress tensor components	$\sigma_r = \sigma_z^0, \quad \sigma_\varphi = \sigma_\varphi^0, \quad \sigma_z = \sigma_z^0, \quad \tau_{rz} = \tau_{rz}^0$	$\tau_{r\varphi} = \tau_{r\varphi}^0, \quad \tau_{\varphi z} = \tau_{\varphi z}^0$

The components of the displacement vector and of the rotation and stress tensors of the deformation tensor as well as the reduced Lamé-equations are summarized in Table 2. (The terms $u_\varphi = cr\varphi$ and $u_z = a\varphi + b$ are neglected.)

The displacements $cr\varphi$ and $a\varphi$ yield the deformation demonstrated in Fig. 2, therefore, the analysis of these solids of revolution may be omitted.

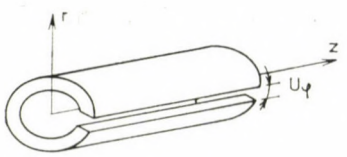

$U_\varphi = cr\varphi$
$\varepsilon_\varphi = c$
$\sigma_\varphi = (\lambda + 2G)\, cr$
$(\sigma_r = \sigma_z = \lambda\, cr)$
$\omega_{r\varphi} = -c\varphi$

a

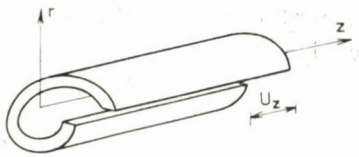

$U_z = a\varphi$
$\gamma_{\varphi z} = \frac{a}{2r}$
$\tau_{\varphi z} = G\frac{a}{r}$
$\omega_{\varphi z} = -\frac{a}{2r}$

b

Fig. 2 — Cylindric-symmetrical deformation states in dependence on φ
a. Limiting dislocation (1st variant); b. Torsional dislocation (Singular solution, $r \neq 0$)

Thus, it is proved that if a solid of revolution is in the state of cylindric-symmetrical or in evenly cylindric-symmetrical state of deformation and of stress deformation, also the field of displacement takes the same characteristics.

The displacement fields represented in Fig. 2 play an important role in the theory of dislocations.

In the displacement components the terms characterized by the constants A and B guarantee the rigid-solid-like rotation while the members of coefficients C and D characterize the rigid-solid-like translation.

5. Analysis of plane problems

5.1 *Inplane problem.* In consequence of the equivalence of Eqs (5) and (6) it is sufficient to analyse the following system of equations:

$$\frac{\partial}{\partial z}\frac{\partial u}{\partial x} = 0\,, \quad \frac{\partial}{\partial z}\frac{\partial v}{\partial y} = 0\,, \quad \frac{\partial}{\partial z}\frac{\partial w}{\partial z} = 0\,, \qquad (34, 35, 36)$$

$$\frac{\partial}{\partial z}\left(\frac{\partial u}{\partial y} + \frac{\partial v}{\partial x}\right) = 0\,, \quad \frac{\partial}{\partial z}\left(\frac{\partial v}{\partial z} + \frac{\partial w}{\partial y}\right) = 0\,, \quad \frac{\partial}{\partial z}\left(\frac{\partial w}{\partial x} + \frac{\partial u}{\partial z}\right) = 0. \quad (37,38,39)$$

Let us integrate Eqs (34 to 36):

$$u = u_0(x, y) + u_1(y, z), \tag{40}$$

$$v = v_0(x, y) + v_1(x, z), \tag{41}$$

$$w = w_0(x, y) + w_1(x, y)z. \tag{42}$$

Replacement of the results obtained in Eqs (37 to 39) yields the following relationships

$$\frac{\partial^2 u_1(y, z)}{\partial y\, \partial z} + \frac{\partial^2 v_1(x, z)}{\partial x\, \partial z} = 0, \tag{43}$$

$$\frac{\partial^2 v_1(x, z)}{\partial z^2} + \frac{\partial w_1(x, y)}{\partial y} = 0, \tag{44}$$

$$\frac{\partial^2 u_1(y, z)}{\partial z^2} + \frac{\partial w_1(y, x)}{\partial x} = 0. \tag{45}$$

From the expression (43) one obtains the following integrals for u_1 and v_1:

$$u_1(y, z) = y \cdot u(z) + f_u(y) + f_u(z), \tag{43'a}$$

$$v_1(x, z) = x \cdot v(z) + f_v(x) + f_v(z), \tag{43'b}$$

wherein $f_u(y)$ and $f_v(x)$ might be incorporated in the terms u_0 and v_0 without violating the principle of generality.

From the expressions (45, 46) follows that $u(z)$ and $v(z)$, are at most, the second-degree polynomials of z; $f_u(z)$ and $f_v(z)$ are, at most, second-degree functions of z, and $w_0(x, y)$ depends directly on its arguments.

Separation of the whole second-degree polynomial from the solutions u_0 and v_0 results in the following displacement components:

$$u = u_0(x, y) + a_{11}x^2 + a_{12}xy + a_{13}y^2 + 0{,}5\, c_3 z^2 + c_6 yz + c_1 z + c_u, \tag{46}$$

$$v = v_0(x, y) + a_{21}x^2 + a_{22}xy + a_{23}y^2 + 0{,}5\, c_4 z^2 - c_6 xz + c_2 z + c_v, \tag{47}$$

$$w = w_0(x, y) - (c_3 x + c_4 y + c_5) z - (c_1 x + c_2 y + c_w). \tag{48}$$

To the coefficients of the second-degree terms the following identities are valid (Lamé's equations):

$$(\lambda + G)(2a_{11} + a_{22}) + 2G(a_{11} + a_{13}) + \lambda c_3 = 0, \tag{49}$$

$$(\lambda + G)(a_{12} + 2a_{23}) + 2G(a_{21} + a_{23}) + \lambda c_4 = 0. \tag{50}$$

Table 3

	Inpalne problem	Symmetrical inplane problem	Plane deformation state	Plane stress state	General plane deformation state	General plane stress state
u	$u_0 + c_6yz + c_1z + c_u + a_{11}x^2 + a_{12}xy + a_{13}y^2 + 0{,}5\,c_3z^2$	$u_0 + c_1z + c_u + a_{11}x^2 + a_{12}xy + a_{13}y^2 + 0{,}5\,c_3z^2$	$u_0 + c_1z + c_u$	$u_0 + a_1x + c_1z + c_u + a_{11}x^2 + \left(\frac{\lambda+2G}{\lambda}c_4 - 2a_{23}\right)xy - \left(\frac{3\lambda+2G}{2\lambda}c_3 + a_{11}\right)y^2 + 0{,}5\,c_3z^2$	$u_0 - \frac{\partial w_0}{\partial x}z$	$u_0 - \frac{\partial w_0}{\partial x}z - \frac{\lambda}{3\lambda+2G}\nabla_0^2 u_0\frac{z^2}{2}$
v	$v_0 - c_6xz + c_2z + c_v + a_{21}z^2 + a_{22}xy + a_{23}y^2 + 0{,}5\,c_4z^2$	$v_0 + c_2z + c_v + a_{21}x^2 + a_{22}xy + a_{23}y^2 + 0{,}5\,c_4z^2$	$v_0 + c_2z + c_v$	$v_0 + \left(\frac{\lambda+2G}{\lambda}c_5 - a_1\right)y + c_2z + c_v - \left(\frac{3\lambda+2G}{2\lambda}c_4 + 2a_{23}\right)x^2 + \left(\frac{\lambda+2G}{\lambda}c_3 - 2a_{11}\right)xy + a_{23}y^2 + 0{,}5\,c_4z^2$	$v_0 - \frac{\partial w_0}{\partial y}z$	$v_0 - \frac{\partial w_0}{\partial y}z - \frac{\lambda}{3\lambda+2G}\nabla_0^2 v_0\frac{z^2}{2}$
w	$w_0 - (c_3x + c_4y + c_5)z - (c_1x + c_2y + c_w)$	$-(c_3x + c_4y + c_5)z - (c_1x + c_2y + c_w)$	$-(c_1x + c_2y + c_w)$	$-(c_3x + c_4y + c_5)z - (c_1x + c_2y + c_w)$	w_0	$w_0 - \frac{\lambda}{\lambda+2G}\left(\frac{\partial u_0}{\partial x} + \frac{\partial v_0}{\partial y}\right)z$
Reduced Lamé-equations	$(\lambda+G)\frac{\partial}{\partial x}\left(\frac{\partial u_0}{\partial x} + \frac{\partial v_0}{\partial y}\right) + G\left(\frac{\partial^2 u_0}{\partial x^2} + \frac{\partial^2 u_0}{\partial y^2}\right) = 0$ $(\lambda+G)\frac{\partial}{\partial y}\left(\frac{\partial u_0}{\partial x} + \frac{\partial v_0}{\partial y}\right) + G\left(\frac{\partial^2 v_0}{\partial x^2} + \frac{\partial^2 v_0}{\partial y^2}\right) = 0$			$\frac{\partial^2 u_0}{\partial x^2} + \frac{\partial^2 u_0}{\partial y^2} = 0$ $\frac{\partial^2 v_0}{\partial x^2} + \frac{\partial^2 v_0}{\partial y^2} = 0$ $\frac{\partial u_0}{\partial x} + \frac{\partial v_0}{\partial y} = 0$	$(\lambda+2G)\frac{\partial}{\partial x}\left(\frac{\partial u_0}{\partial x} + \frac{\partial v_0}{\partial y}\right) + G\left(\frac{\partial^2 u_0}{\partial x^2} + \frac{\partial^2 u_0}{\partial y^2}\right) = 0$ $(\lambda+2G)\frac{\partial}{\partial y}\left(\frac{\partial u_0}{\partial x} + \frac{\partial v_0}{\partial y}\right) + G\left(\frac{\partial^2 v_0}{\partial x^2} + \frac{\partial^2 v_0}{\partial y^2}\right) = 0$	$(3\lambda+2G)\frac{\partial}{\partial x}\left(\frac{\partial u_0}{\partial x} + \frac{\partial v_0}{\partial y}\right) + (\lambda+2G)\left(\frac{\partial^2 u_0}{\partial x^2} + \frac{\partial^2 u_0}{\partial y^2}\right) = 0$ $(3\lambda+2G)\frac{\partial}{\partial y}\left(\frac{\partial u_0}{\partial x} + \frac{\partial v_0}{\partial y}\right) + (\lambda+2G)\left(\frac{\partial^2 v_0}{\partial x^2} + \frac{\partial^2 v_0}{\partial y^2}\right) = 0$
	$\frac{\partial^2 w_0}{\partial x^2} + \frac{\partial^2 w_0}{\partial y^2} = 0$	—			$\frac{\partial^2 w_0}{\partial x^2} + \frac{\partial^2 w_0}{\partial y^2} = 0$	

The displacement components and reduced Lamé's equations are given in Table 3, while the components of the deformation, rotation and stress tensors are listed in Table 4.

5.2 *Symmetrical plane problem.* To the relationships analysed in paragraph 5.1 (34 to 39) the expressions

$$\frac{\partial v}{\partial z} + \frac{\partial w}{\partial y} = 0, \quad \frac{\partial w}{\partial x} + \frac{\partial u}{\partial z} = 0 \tag{51, 52}$$

should be attached. Since these expressions allow the previous ones to be valid, therefore, it is sufficient to examine what complementary conditions are prescribed by the expressions (51, 52).

Replacement of the displacement components (46, 47) in Eqs (51, 52) results in the following differential equation to w_0:

$$\frac{\partial w_0}{\partial y} - c_6 x = 0\,, \tag{53}$$

$$\frac{\partial w_0}{\partial x} + c_6 y = 0\,. \tag{54}$$

From integration of (53, 54) one finds that $c_6 = 0$ and w_0 is the first-degree polynomial of its arguments. Thus, the displacement components are as follows:

$$u = u_0(x, y) + a_{11} x^2 + a_{12} xy + a_{13} y^2 + 0{,}5\, c_3 z^2 + c_1 z + c_u \tag{55}$$

$$v = v_0(x, y) + a_{21} x^2 + a_{22} xy + a_{23} y^2 + 0{,}5\, c_4 z^2 + c_2 z + c_v\,, \tag{56}$$

$$w = -(c_3 x + c_4 y + c_5)\, z - (c_1 x + c_2 y + c_w)\,. \tag{57}$$

The displacement components and the reduced Lamé-equations are presented in Table 3, and the components of the fields characterizing the state are summarized in Table 4.

5.3 *Plane deformation state.* Beside the relationships (34 to 39) and (51, 52) analysed so far, also the equation

$$\frac{\partial w}{\partial z} = 0 \tag{58}$$

is to be taken into account. This equation also implies the conditions $c_3 = 0$, $c_4 = 0$ and $c_5 = 0$. Therefore, the second-order polynomial designated with a_{ij} should be re-incorporated into the terms u_0 and v_0. Therefrom the displacement components are:

$$u = u_0(x, y) + c_1 z + c_u\,, \tag{59}$$

$$v = v_0(x, y) + c_2 z + c_v\,, \tag{60}$$

$$w = -(c_1 x + c_2 y + c_w)\,. \tag{61}$$

Table 4

	Inplane problem	Symmetrical inplane problem
ε_x	$\varepsilon_x^0 + 2a_{11}x + a_{12}y$	$\varepsilon_x^0 + 2a_{11}x + a_{12}y$
ε_y	$\varepsilon_y^0 + a_{22}x + 2a_{23}y$	$\varepsilon_y^0 + a_{22}x + 2a_{23}y$
ε_z	$-(c_3x + c_4y + c_5)$	$-(c_3x + c_4y + c_5)$
γ_{xy}	$\gamma_{xy}^0 + \frac{1}{2}(a_{12} + 2a_{21})x + \frac{1}{2}(2a_{13} + a_{22})y$	$\gamma_{xy}^0 + \frac{1}{2}(a_{12} + 2a_{21})x + \frac{1}{2}(2a_{13} + a_{22})y$
γ_{yz}	$\frac{1}{2}\left(\frac{\partial w_0}{\partial y} - c_6x\right)$	0
γ_{zx}	$\frac{1}{2}\left(\frac{\partial w_0}{\partial x} + c_6y\right)$	0
ω_{xy}	$\omega_{xy}^0 + \frac{1}{2}(a_{12} - 2a_{21})x + \frac{1}{2}(2a_{13} - a_{22})y - c_6z$	$\omega_{xy}^0 + \frac{1}{2}(a_{12} - a_{21})x + \frac{1}{2}(2a_{13} - a_{22})y$
ω_{yz}	$-\frac{1}{2}\frac{\partial w_0}{\partial y} - \frac{1}{2}c_6x + \frac{1}{2}c_4z + \frac{1}{2}c_2$	$\frac{1}{2}c_4z + \frac{1}{2}c_2$
ω_{zx}	$\frac{1}{2}\frac{\partial w_0}{\partial x} - \frac{1}{2}c_6y - \frac{1}{2}c_3z - \frac{1}{2}c_1$	$-\frac{1}{2}c_3z - \frac{1}{2}c_1$
σ_x	$\sigma_x^0 - G(2a_{13} + a_{22})x - G(-a_{12} + 2a_{21} + 4a_{23})y - \lambda c_5$	$\sigma_x^0 - G(2a_{13} + a_{22})x - G(-a_{12} + 2a_{21} + 4a_{23})y - \lambda c_5$
σ_y	$\sigma_y^0 - G(4a_{11} + 2a_{13} - a_{22})x - G(a_{12} + 2a_{21})y - \lambda c_5$	$\sigma_y^0 - G(4a_{11} + 2a_{13} - a_{22})x - G(a_{12} + 2a_{21})y - \lambda c_5$
σ_z	$\sigma_z^0 - G\left(4\frac{\lambda+G}{\lambda}2a_{11} + \frac{\lambda+2G}{\lambda}2a_{13} + \frac{3\lambda+2G}{\lambda}a_{22}\right)x - G\left(\frac{3\lambda+2G}{\lambda}a_{12} + \frac{\lambda+2G}{\lambda}2a_{21} + 4\frac{\lambda+G}{\lambda}2a_{23}\right)y - (\lambda+2G)c_5$	$\sigma_z^0 - G\left(4\frac{\lambda+G}{\lambda}2a_{11} + \frac{\lambda+2G}{\lambda}2a_{13} + \frac{3\lambda+2G}{\lambda}a_{22}\right)x - G\left(\frac{3\lambda+2G}{\lambda}a_{12} + \frac{\lambda+2G}{\lambda}2a_{22} + 4\frac{\lambda+G}{\lambda}2a_{23}\right)y - (\lambda+2G)c_5$
τ_{xy}	$\tau_{xy}^0 + G(a_{12} + 2a_{21})x + G(2a_{13} + a_{22})y$	$\tau_{xy}^0 + G(a_{12} + 2a_{21})x + G(2a_{13} + a_{22})y$
τ_{yz}	$G\left(\frac{\partial w_0}{\partial y} - c_6x\right)$	0
τ_{zx}	$G\left(\frac{\partial w_0}{\partial x} + c_6y\right)$	0

The displacement components and the reduced Lamé-equations are summarized in Table 3 and those of the fields which characterize the state, in Table 5.

5.3 *Plane deformation state.* Beside the relationships (34 to 39) and (51, 52), also the relationship

$$\frac{\partial u}{\partial x} + \frac{\partial v}{\partial y} + \frac{\lambda + 2G}{\lambda} \frac{\partial w}{\partial z} = 0 \tag{62}$$

should be taken into account in characterizing the state. By replacing the expressions (55 to 57) into (62) one obtains the following differential relationships for u_0 and v_0:

$$\frac{\partial u_0}{\partial x} + \frac{\partial v_0}{\partial y} - \frac{\lambda + 2G}{\lambda} (c_3 x + c_4 y + c_5) = 0 \,. \tag{63}$$

By indicating the non-homogeneous solutions of this equation, one finds the following displacement components:

$$u = u_0(x, y) + a_{11} x^2 + \left(\frac{\lambda + 2G}{\lambda} c_4 - 2a_{23} \right) xy - \\ - \left(\frac{3\lambda + 2G}{2\lambda} c_3 + a_{11} \right) y^2 + 0{,}5\, c_3 z^2 + a_1 x + c_1 z + c_u \,, \tag{64}$$

$$v = v_0(x, y) - \left(\frac{3\lambda + 2G}{2\lambda} c_4 + a_{23} \right) x^2 + \left(\frac{\lambda + 2G}{\lambda} c_3 - 2a_{11} \right) xy + \\ + a_{23} y^2 + 0{,}5\, c_4 z^2 + \left(\frac{\lambda + 2G}{\lambda} c_5 - a_1 \right) y + c_2 z + c_v \,, \tag{65}$$

$$w = -(c_3 x + c_4 y + c_5) z - (c_1 x + c_2 y + c_w) \,. \tag{66}$$

But, in this case, Eq. (63) will be reduced to the equation $\partial u_0/\partial x + \partial v_0/\partial y = 0$. consequently, Lamé's equations will be separated with respect to u_0 and v_0.

The displacement components and the reduced Lamé-equations are shown in Table 3, and those of the fields characterizing the state, are presented in Table 5.

5.5 *General plane deformation state.* The state equations are as follows:

$$\frac{\partial w}{\partial z} = 0 \,, \tag{67}$$

$$\frac{\partial w}{\partial y} + \frac{\partial v}{\partial z} = 0 \,, \tag{68}$$

$$\frac{\partial w}{\partial x} + \frac{\partial u}{\partial z} = 0 \,. \tag{69}$$

Table 5

	Plane deformation state	Plane stress state
ε_x	ε_x^0	$\varepsilon_x^0 + 2a_{11}x + \left(\frac{\lambda+2G}{\lambda} c_4 - 2a_{23}\right) y + a_1$
ε_y	ε_y^0	$\varepsilon_y^0 + \left(\frac{\lambda+2G}{\lambda} c_3 - 2a_{11}\right) x + 2a_{23}y + \left(\frac{\lambda+2G}{\lambda} c_5 - a_1\right)$
ε_z	0	$-(c_3x + c_4y + c_5)$
γ_{xy}	γ_{xy}^0	$\gamma_{xy}^0 - \frac{1}{2}(2c_4 + 4a_{23})x - \frac{1}{2}(2c_3 + 4a_{11})y$
γ_{yz}	0	0
γ_{zx}	0	0
ω_{xy}	ω_{xy}^0	$\omega_{xy}^0 + \frac{1}{2} 4 \frac{\lambda+G}{\lambda} c_4x - \frac{1}{2} 4 \frac{\lambda+G}{\lambda} c_3y$
ω_{yz}	$\frac{1}{2} c_2$	$\frac{1}{2} c_4z + \frac{1}{2} c_2$
ω_z	$-\frac{1}{2} c_1$	$-\frac{1}{2} c_3z - \frac{1}{2} c_1$
σ_x	σ_x^0	$2G\varepsilon_x^0 + 2G(2a_{11} + c_3)x + 2G\left(2\frac{\lambda+G}{\lambda} c_4 - 2a_{23}\right) y + 2G(c_5 - a_1)$
σ_y	σ_y^0	$2G\varepsilon_y^0 + 2G\left(2\frac{\lambda+G}{\lambda} c_3 - 2a_{11}\right) x + 2G(2a_{23} + c_4)y + 2G\left(2\frac{\lambda+G}{\lambda} c_5 - a_1\right)$
σ_z	σ_z^0	0
τ_{xy}	τ_{xy}^0	$\tau_{xy}^0 - G(2c_1 + 4a_{23}) - G(2c_3 + 4a_{11})y$
τ_{yz}	0	0
τ_{zx}	0	0

First Eq. (67) should be integrated — $w_0 = w_0(x, y)$ — then, by making use of the result obtained, Eqs (68, 69) will be obtained. Thus, the displacement components are:

$$u = u_0(x, y) - \frac{\partial w_0}{\partial x} z \,, \tag{70}$$

$$v = v_0(x, y) - \frac{\partial w_0}{\partial y} z \,, \tag{71}$$

$$w = w_0(x, y) \,. \tag{72}$$

Table 6

	General plane deformation state	General plane stress state
ε_x	$\varepsilon_x^0 - \frac{\partial^2 w_0}{\partial x^2} z$	$\varepsilon_x^0 - \frac{\partial^2 w_0}{\partial x^2} z - \frac{\lambda}{3\lambda + 2G} \nabla_0^2 \varepsilon_x^0 \frac{z^2}{2}$
ε_y	$\varepsilon_y^0 - \frac{\partial^2 w_0}{\partial y^2} z$	$\varepsilon_y^0 - \frac{\partial^2 w_0}{\partial y^2} z - \frac{\lambda}{3\lambda + 2G} \nabla_0^2 \varepsilon_y^0 \frac{z^2}{2}$
ε_z	0	$-\frac{\lambda}{\lambda + 2G} (\varepsilon_x^0 + \varepsilon_y^0)$
γ_{xy}	$\gamma_{xy}^0 - \frac{\partial^2 w_0}{\partial x \partial y} z$	$\gamma_{xy}^0 - \frac{\partial^2 w_0}{\partial x \partial y} z - \frac{\lambda}{3\lambda + 2G} \nabla_0^2 \gamma_{xy}^0 \frac{z^2}{2}$
γ_{yz}	0	0
γ_{zx}	0	0
ω_{xy}	ω_{xy}^0	$\omega_{xy}^0 - \frac{\lambda}{3\lambda + 2G} \nabla_0^2 \omega_{xy} \frac{z^2}{2}$
ω_{yz}	$-\frac{\partial w_0}{\partial y}$	$-\frac{\partial w_0}{\partial y} + \frac{\lambda}{\lambda + 2G} \frac{\partial}{\partial y} (\varepsilon_x^0 + \varepsilon_y^0) z$
ω_{zx}	$\frac{\partial w_0}{\partial x}$	$\frac{\partial w_0}{\partial x} - \frac{\lambda}{\lambda + 2G} \frac{\partial}{\partial x} (\varepsilon_x^0 + \varepsilon_y^0) z$
σ_x	$\sigma_x^0 - 2G \frac{\partial^2 w_0}{\partial x^2} z$	$\sigma_x^0 - 2G \frac{\partial^2 w_0}{\partial x^2} z - \frac{2\lambda G}{3\lambda + 2G} \nabla_0^2 \varepsilon_x^0 \frac{z^2}{2} - \frac{\lambda^2}{\lambda + 2G} (\varepsilon_x^0 + \varepsilon_y^0)$
σ_y	$\sigma_y^0 - 2G \frac{\partial^2 w_0}{\partial y^2} z$	$\sigma_y^0 - 2G \frac{\partial^2 w_0}{\partial y^2} z - \frac{2\lambda G}{3\lambda + 2G} \nabla_0^2 \varepsilon_y^0 \frac{z^2}{2} - \frac{\lambda^2}{\lambda + 2G} (\varepsilon_x^0 + \varepsilon_y^0)$
σ_z	σ_z^0	0
τ_{xy}	$\tau_{xy}^0 - 2G \frac{\partial^2 w_0}{\partial x \partial y} z$	$\tau_{xy}^0 - 2G \frac{\partial^2 w_0}{\partial x \partial y} z - \frac{\lambda}{3\lambda + 2G} \nabla_0^2 \tau_{xy}^0 \frac{z^2}{2}$
τ_{yz}	0	0
τ_{zx}	0	0

The displacement components and the reduced Lamé-equations are presented in Table 3, while those of the fields characterizing the state are indicated in Table 6.

5.6 *General plane stress state.* The state equations are as follows:

$$\frac{\partial u}{\partial x} + \frac{\partial v}{\partial y} + \frac{\lambda + 2G}{\lambda} \frac{\partial w}{\partial z} = 0\,, \tag{73}$$

$$\frac{\partial w}{\partial y} + \frac{\partial v}{\partial z} = 0\,, \tag{68}$$

$$\frac{\partial w}{\partial x} + \frac{\partial u}{\partial z} = 0\,. \tag{69}$$

Eq. (73) should be solved, with the aid of Eqs (68, 69) for the displacement components:

$$\frac{\partial}{\partial z}\left(\frac{\partial^2 u}{\partial x^2} + \frac{\partial^2 u}{\partial y^2} - \frac{\lambda + 2G}{\lambda}\frac{\partial^2 u}{\partial z^2}\right) = 0\,, \tag{74}$$

$$\frac{\partial}{\partial z}\left(\frac{\partial^2 v}{\partial x^2} + \frac{\partial^2 v}{\partial y^2} - \frac{\lambda + 2G}{\lambda}\frac{\partial^2 v}{\partial z^2}\right) = 0\,, \tag{75}$$

$$\frac{\partial^2 w}{\partial x^2} + \frac{\partial^2 w}{\partial y^2} - \frac{\lambda + 2G}{\lambda}\frac{\partial^2 w}{\partial z^2}\Bigg) = 0\,, \tag{76}$$

and integrated (73) with respect to w

$$w = w_0(x, y) - \frac{\lambda}{\lambda + 2G}\int\left(\frac{\partial u}{\partial x} + \frac{\partial v}{\partial y}\right)dz\,. \tag{77}$$

Lamé's equations can be solved with the aid of Eqs (68, 69, 73) for u and v:

$$\frac{\partial^2 u}{\partial x^2} + \frac{\partial^2 u}{\partial y^2} + \frac{3\lambda + 2G}{\lambda}\frac{\partial^2 u}{\partial z^2} = 0\,, \tag{78}$$

$$\frac{\partial^2 v}{\partial x^2} + \frac{\partial^2 v}{\partial y^2} + \frac{3\lambda + 2G}{\lambda}\frac{\partial^2 v}{\partial z^2} = 0\,. \tag{79}$$

By integrating Eqs (74, 78) and (75, 79) u and v are determined:

$$u = Cu_2(x, y)\frac{z^2}{2} + u_1(x, y)\,z + u_0(x, y)\,, \tag{80}$$

$$v = Cv_2(x, y)\frac{z^2}{2} + v_1(x, y)\,z + v_0(x, y)\,. \tag{81}$$

This general integral has to satisfy the set of differential equations (74 to 79); the solution is:

$$u = u_0(x, y) - \frac{\partial w_0(x, y)}{\partial x}\,z - \frac{\lambda}{3\lambda + 2G}\,\nabla_0^2\,u_0(x, y)\,\frac{z^2}{2}\,, \tag{82}$$

$$v = v_0(x, y) - \frac{\partial w_0(x, y)}{\partial y}\,z - \frac{\lambda}{3\lambda + 2G}\,\nabla_0^2\,v_0(x, y)\,\frac{z^2}{2}\,, \tag{83}$$

$$w = w_0(x, y) - \frac{\lambda}{\lambda + 2G}\left(\frac{\partial u_0}{\partial x} + \frac{\partial v_0}{\partial y}\right)z\,. \tag{84}$$

The displacement components and the reduced Lamé equations are summarized in Table 3 while those of the fields, characterizing the state, are presented in Table 6.

6. Analysis of the results of plane problems

6.1 The results indicated in Table 3, at the first glance, verify the interconnection of the different states represented in Fig. 1.

The meanings of the members shown in the solution are:

— u_0, v_0 and w_0 — displacement components independent of z

— c_u, c_v and c_w — stiff-solid-like translation

— $c_1 z$, $c_2 z$ and a — $(c_1 x + c_2 y)$ — stiff-solid-like rotation round the axes X (c_2) and Y (c_1).

These and only these members enter in the solution of the plane deformation state. Therefore, in the following, this state will be called the representative of the first group. In this state all the state characteristics have subscripts "$_0$", excepting the stiff-solid-like rotation round the axis X, Y, i.e., they are independent of z.

The symmetrical plane problem is an enlarged state only in the case when taking into account the normal force **N** acting on the base plane of the normal **k**, the bending moments $\mathbf{M}_x$ and $\mathbf{M}_y$ and the shear force **Q** acting on the entire surface of the whole solid. These forces are independent of z and on the surface of an elementary cube may be represented by three normal stresses and one shear stress (Fig. 3).

The inplane problem is, beside the effect mentioned above, by a torsion about the axis Z an enlarged state in comparison to the representative.

In the paper, for the plane stress state a special field of displacement is obtained: determined by the coupled harmonic functions u_0 and v_0. In addition, also the state characterized by the displacement

$$u = a_{11} x^2 + \left(\frac{\lambda + 2G}{\lambda} c_4 - 2a_{23}\right) xy - \left(\frac{3\lambda + 2G}{\lambda} c_3 + a_{11}\right) y^2 + \\ + 0{,}5\, c_3 z^2 + a_1 x\,, \tag{85a}$$

$$v = -\left(\frac{3\lambda + 2G}{\lambda} c_4 + a_{23}\right) x^2 + \left(\frac{\lambda + 2G}{\lambda} c_3 - a_{11}\right) xy + \\ + a_{23} y^2 + 0{,}5\, c_4 z^2 + \left(\frac{\lambda + 2G}{\lambda} c_5 - a_1\right) y \tag{85b}$$

$$w = -(c_3 x + c_4 y + c_5) z \tag{85c}$$

yields a plane stress state. Since this state is only defined by five parameters,

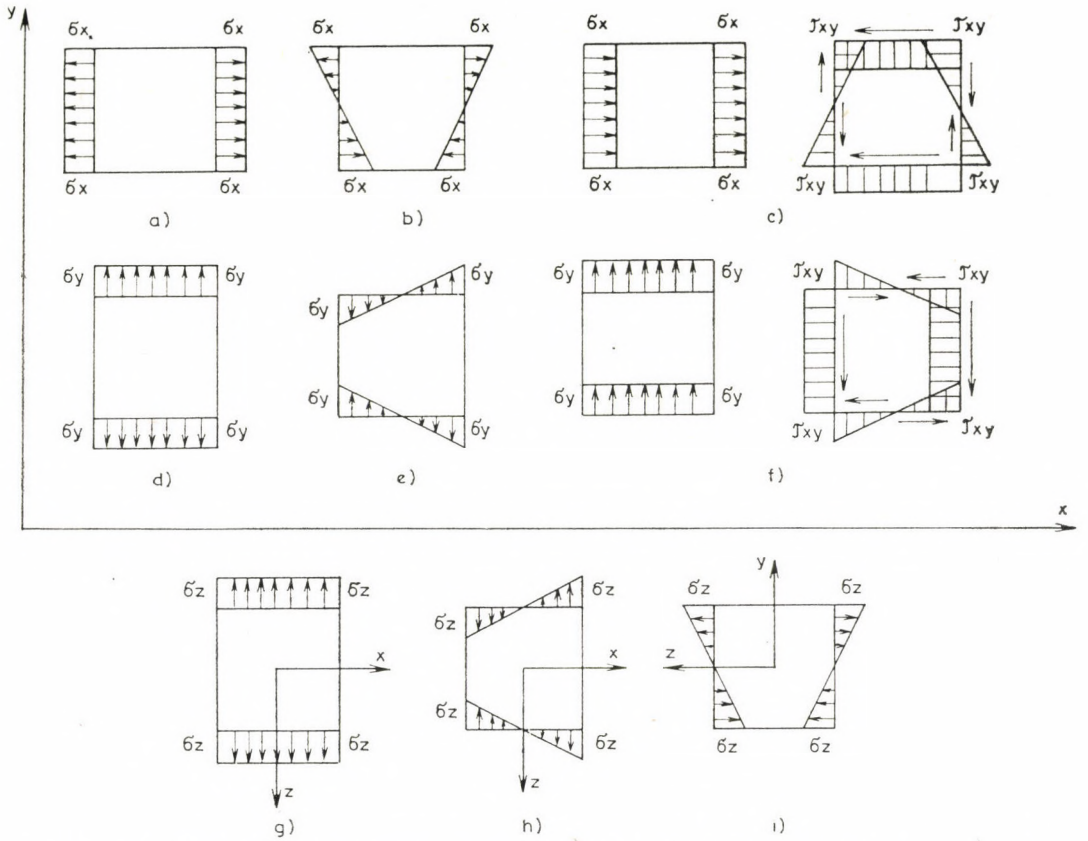

Fig. 3 — Resolution of the stress states compatible with the displacement $u = c_3 z^2/2$ and $v = c_4 z^2/2$ according to x and y; a) N_x — normal force; b) M_{xz} — flexural moment; c) $\delta - \tau$ equilibrium state in the x direction; d) N_y — normal force; e) M_{yz} — flexural moment; f) $\delta - \tau$ equilibrium state in the y direction; g) N_z — normal force; h) M_{zy} — flexural moment; i) M_{zx} — flexural moment

it cannot characterize the plane stress state. Thus, on the basis of the relationship $\sigma_z = 0$

$$\varepsilon_z^0 = -\frac{\lambda}{\lambda + 2G}\left(\frac{\partial u_0}{\partial x} + \frac{\partial v_0}{\partial y}\right), \tag{86}$$

i.e., the plane stress state is a specific case of the plane deformation state ($\sigma_z = 0$). In that case, by introducing the new moduli of elasticity $\lambda' = 2\lambda G/(\lambda + 2G)$ and $G' = G$, the plane stress state can be transformed unreservedly into the state of the plane deformation.

The generalized plane problems grouped into the second group differ from the representative in the lack of the member w_0 and in the fact that these solutions are not independent of z. The members w_0 and $\nabla_0^2 u_0$ and $\nabla_0^2 v_0$ are

harmonics, thus, they furnish solutions associated with deformation. Considering that the expression $\varepsilon_x^0 + \varepsilon_y^0$ is harmonic, by the formal integration $\int_{-z_0}^{+z_0} dz$ the operator members ∇_0^2 may be incorporated into the terms of "$_0$" subscript which are independent of z, therefore, the generalized stress state, disregarding the ratio of ε_z and σ_z, may be traced back to the generalized plane deformation state.

6.2 Comparison of the results on the subject obtained with those found in the literature. In the technical literature the distribution to the six types of problems and their special denominations are not to be found. It is KALISZKY [13] who applies division; he speaks about plane problem for the satisfaction of Eqs (5 to 10), and defines by the validity of the zero-conditions (3a and 4a) the states of plane deformation and plane stress. NOWACKI defines the plane problem as a plane stress state; author himself arrived at a result in close agreement with that of NOWACKI. LURJE and LOVE define the general plane stress states as the plane stress state; the finding of the author is in accordance with that, taking into account that $\lambda/(3\lambda + 2G) = 1/4(1 - \mu)$.

In the case of the plane stress state, taking as a base the definition presented here, author obtained a diverging result. In the paper, the analysed plane stress state is a special case of the plane deformation state $-\sigma_z = 0$. Then, by the transformation of the moduli of elasticity, the plane stress state itself may also be transformed into the state of plane deformation.

REFERENCES

1. АРУТЮНЯН Н. Х., АБРАМЯН Б. Л.: Кручение упругих тел. Физматгиз, Москва, 1963 г.
2. БЕЗУХОВ Н. И.: Основы теории упругости, пластичности и ползучести. Высшая школа, Москва, 1968 г.
3. БЕЗУХОВ Н. И., ЛУЖИН О. В.: Приложение методов теории упругости и пластичности к решению инженерных задач. Высшая школа, Москва, 1974 г.
4. CHOLNOKY, T.: Mechanics, Vol. 2, Strength of Materials. Tankönyvkiadó, Budapest 1971. (In Hungarian.).
5. CLOUGH, R. W.—RACHID, Y. R.: Finite Element Analysis of Axi-Symmetric Solids. Proc. ASCE, 91, EM 1, 1965.
6. ФИЛИН А. П.: Прикладная механика твердого деформируемого тела. Том I. Наука, Москва, 1975 г.
7. ФИЛИНЕНКО-БОРОДИЧ М. М.: Теория упругости. ГОСТЕХИЗДАТ, Москва, 1974 г.
8. FÖPPL, A.—FÖPPL, L.: Drang und Zwang, Band I. München, 1924.
9. HAJÓS, GY.: Introduction into the Geometry. Tankönyvkiadó, Budapest 1966. (In Hungarian).
10. Handbuch der Physik, Redigiert von R. Grammel. Band VI. Mechanik der elastischen Körper. GECKELER, J. W.: Statik der elastischen Körper. Springer, Berlin 1928.
11. Handbuch der Physik, Herausgegeben von S. Flügge. Band VI. Elastizität und Plastizität. SNEDDON, J. N.—BERRY, D. S.: The classical Theory of Elasticity. Springer-Verlag, Berlin 1958.
12. КАЛАНДИЯ А. И.: Математические методы двумерной упругости. Наука, Москва, 1973 г.
13. KALISZKY, S.: Theory of Plasticity. Akadémiai Kiadó, Budapest 1975. (In Hungarian).
14. КОЛОСОВ Г. В.: Применение комплексного переменного к теории упругости. ГОСТЕХИЗДАТ, Москва, 1935 г.

15. КОЛТУНОВ М. А., ВАСИЛЬЕВ Ю. Н., ЧЕРНЫХ В. А.: Упругость и прочность цилиндрических тел. Высшая школа, Москва, 1975 г.
16. ЛАМЕР, Г.: К расчету толстой цилиндрической оболочки при действии осесимметрической нагрузки. Acta Technika, 87/3—4, Budapest 1978.
17. ЛЕЙБЕНЗОН, Л. С.: Курс теории упругости. ГОСТЕХИЗДАТ, Москва, 1947 г.
18. LOVE, A. E.: A treatise on the mathematical theory of elasticity. Cambridge 1927.
19. ЛУРЬЕ, А. И.: Теория упругости. Наука, Москва, 1970 г.
20. Matematikai kislexikon (Concise Encyclopedia of Mathematics). Editor: Dr. M. FARKAS. Műszaki Könyvkiadó, Budapest 1972. (In Hungarian)
21. MÁRKUS, GY.: Theory and Calculation of Structures of Circular Symmetry. Műszaki Könyvkiadó, Budapest 1971. (In Hungarian)
22. МУСХЕЛИШВИЛИ, Н. И.: Некоторые основные задачи математической теории упругости. Наука, Москва, 1966 г.
23. NAGY, T.—SZILÁGYI, GY.: Analysis of the Behaviour of a General, Multilayer System under Loading, by Using the Finite Element Method. Report on research investigation, Part I. Budapest 1975. (In Hungarian)
24. НОВАЦКИЙ, В.: Теория упругости МИР, Москва, 1975 г.
25. ODEN, J. T.: Finite Elements of Nonlinear Continua. McGraw-Hill, New York 1972.
26. Прочность, устойчивость, колебания. Справочник в трех томах. Под общей редакции: Биргера И. А. и Пановко Я. Т. Машиностроение, Москва, 1968 г.
27. RACHID, Y. R.: Analysis of Axisymmetric Composite Structures by the Finite Element Method. Nucl. Eng. Design. 3. 1966.
28. SZILY, K. Jr., Dr.: Strength of Materials. Technika, Budapest 1921 (In Hungarian)
29. СКРИН, Э., РОЙ дж. Р.: Автоматическая система для кинематического анализа ASKA. В сборнике: Расчет упругих конструкций с использованием ЭВМ (пер. с англ.) СУДОСТРОЕНИЕ, Ленинград, 1974 г.
30. СОЛЯНИК-КРАССА, К. В.: Кручение валов переменного сечения. ГОСТЕХИЗДАТ, Москва, 1949 г.
31. Справочник по теории упругости. Под ред. Варвака П. М. и Рябова А. Ф. Будвельник, Киев, 1971 г.
32. ТИМОШЕНКО С. П.: Курс теории упругости (New edition of the work in two volumes, published in 1914—1916). Наукова думка, Киев, 1972 г.
33. TIMOSHENKO, S. P.: Theory of Elasticity. McGraw-Hill, New York 1934.
34. TIMOSHENKO, S. P.—GOODIER, J. N.: Theory of Elasticity. McGraw-Hill, New York 1970.
35. УФЛЯНД, Я. С.: Интегральные преобрезования в задачах теории упругости. Наука, Ленинград, 1968 г.
36. ВЛАСОВ, В. З.: Общая теория оболочек. ГОСТЕХИЗДАТ, Ленинград, 1949 г.
37. WILSON, E. L.: Structural Analysis of Axi-Symmetric Solids. J. AIAA 3. 1965.
38. ZIENKIEWICZ, O. C.: The Finite Element Method in Engineering Science. McGraw-Hill, London 1971.

Über die zylindersymmetrischen und ebenen Aufgaben — In der Abhandlung sind die zylindersymmetrischen und ebenen Aufgaben analysiert und systematisiert. Eine Übersicht über die Fachliteratur im Zusammenhang mit den Definitionen der Aufgaben wurde gewährt und auf die Abweichungen derselben hingewiesen. Zustände von neueren Typen wurden definiert, indem die abweichenden Definitionen als unterschiedliche Aufgaben betrachtet wurden, sowohl im Fall der Existenz der Zylindersymmetrie als auch im Zusammenhang mit den ebenene Aufgaben. Die einheitlichen Definitionen der neulich eingeführten Zustände, die diese letztere definierenden Gleichungen und die (für die Verschiebungskomponenten gültigen) Funktionklassen der Lösungen wurden angegeben. Es wurde nachgewiesen, daß die einheitlich definierten Zustände sich voneinander nur in gewissen Spannungskomponenten unterscheiden, und der ebene Spannungszustand nur in dieser Konzeption durch die Transformation des Elastizitätsmoduls auf den ebenen Verformungszustand zurückgeführt werden kann.

Acta Technica Academiae Scientiarum Hungaricae, Tomus 92 (3—4), pp. 291—299 (1891)

UPPER AND LOWER BOUNDS FOR THE TORSIONAL STIFFNESS OF A PRISMATIC BAR STRENGHTENED BY A THIN SHELL AT ITS EDGES

I. ECSEDI*

[Manuscript received 1980]

A prismatic bar of a simply continuous cross section made from elastic material, strengthened at its edge is treated. Verification of the upper and lower bounds for the torsional stiffness to be defined by making use of de Saint-Venant's theory is presented for the greater part by applying Schwarz inequality.

Symbols

x, y	orthogonal coordinates
$\mathbf{e}_x, \mathbf{e}_y, \mathbf{e}_z$	unit vectors
$\mathbf{R} = x\mathbf{e}_x + y\mathbf{e}_y$	position vector
$U = U(x, y)$	stress function
T	limited, simply continuous region in plane x, y
∂T	limiting curve of region T
G, Γ	moduli of shear elasticity
h	shell thickness
$\mathbf{n}$	normal unit vector of limiting curve ∂T
$\mathbf{e}$	tangent unit vector of limiting curve ∂T
s	arc coordinate defined at limiting curve ∂T
" . "	sign of the scalar product of two vectors
"×"	sign of the vectorial product of two vectors
$\mathbf{e}_z = \mathbf{e}_x \times \mathbf{e}_y$,	
$\nabla = \frac{\partial}{\partial x}\mathbf{e}_x + \frac{\partial}{\partial y}\mathbf{e}_y$	Hamiltonian differential operator
$\Delta = \nabla \cdot \nabla = \frac{\partial^2}{\partial x^2} + \frac{\partial^2}{\partial y^2}$	Laplace's differential operator
$\frac{\partial}{\partial n}$	sign of a derivative calculated in direction $\mathbf{n}$
$\frac{\partial}{\partial s}$	sign of a derivative calculated in direction $\mathbf{e}$
S	torsional stiffness

Introduction

It is commonly known that the torsional stiffness S to be determined on the basis of de Saint-Venant's theory for prismatic bar of simply continuous cross section, strengthened by a thin shell at its edge, (Fig. 1) may be calculated by using the formula

$$S = 2\int_T U \, dT \tag{1}$$

* Dr. I. Ecsedi, H-3531 Miskolc, Vászonfehérítő u. 24. Hungary

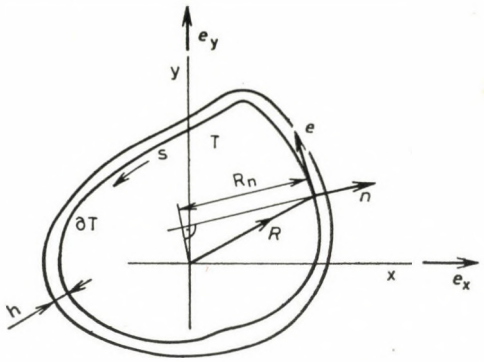

Fig. 1. Simply continuous cross section strengthened by a closed shell on its edges

The stress function $U = U(x, y)$ entering in formula (1) and being continuous in the closed region $T + \partial T$ satisfies the Poisson-type partial differential equation

$$\Delta U = -2G \qquad (x, y) \in T \tag{2}$$

in the region T, and the homogeneous boundary condition

$$U + \frac{\Gamma h}{G} \frac{\partial U}{\partial n} = 0 \qquad (x, y) \in \partial T \tag{3}$$

at the limiting curve ∂T of the region T [1].

In equations (1)—(3) the modulus of shear elasticity of the material of the homogeneous, isotropic, linearly elastic bar of cross section T is designated by G, and the modulus of shear elasticity of the material of homogeneous, isotropic, linearly elastic shell of thickness h is designated by Γ.

According to the formula (14) of paper [2] the torsional stiffness of the cross section may also be determined by making use of the relationship

$$S = \int_T \frac{(\nabla U)^2}{G} dT + \int \frac{U^2}{\Gamma h} ds. \tag{4}$$

2. The lower limit

Let us designate the torsional stiffness of a prismatic bar of elastic material not strengthened by a closed shell with S_0.

The value of S_0 may be calculated either from formula

$$S_0 = 2 \int_T U_0 \, dT, \tag{5}$$

or from that of

$$S_0 = \int_T \frac{(\nabla U_0)^2}{G}\, dT \tag{6}$$

in the case where the solution

$$U_0 = U_0(x, y)$$

of the boundary value problem defined by the equations

$$\Delta U_0 = -2G \qquad (x, y) \in T, \tag{7}$$

and

$$U_0 = 0 \qquad (x, y) \in \partial T \tag{8}$$

is known.

Theorem I

We have the inequality relation

$$S \geq S_0 + \frac{4 f^2}{\int \frac{ds}{\Gamma h}} \tag{9}$$

wherein f designates the cross-sectional area of the prismatic bar, i.e.,

$$f = \int_T dx\, dy\,. \tag{10}$$

Demonstration. According to formula (27) of paper [2] in case of any function of two variables $v = v(x, y)$, not being identically equal to zero, which is continuous in the closed region $T + \partial T$ and step-by-step derivable continuously in the region T, the inequality relation

$$S \geq \frac{\left(2\int_T v dT\right)^2}{\int_T \frac{(\nabla v)^2}{G}\, dT + \int_{\partial T} \frac{v^2}{\Gamma h}\, ds} \tag{11}$$

is valid.

We have

$$v = U_0(x, y) + C \tag{12}$$

wherein C is, for the moment, an optimal constant.

From the combination of formula (5), (6) with the inequality relation (11) and formula (12) one obtains the inequality

$$S \geq \frac{(S_0 + 2Cf)^2}{S_0 + C^2 \int_{\partial T} \frac{1}{\Gamma h}\, ds}\,. \tag{13}$$

The right-hand side of the inequality (13) is the function of parameter C.

It can easily be proved that the right-hand side of inequality (13) has an absolute maximum value at the location

$$C^* = \frac{2f}{\int_{\partial T} \frac{ds}{\Gamma h}} \tag{14}$$

and the value of this maximum is

$$\max_C \frac{(S_0 + 2Cf)^2}{S_0 + C^2 \int_{\partial T} \frac{ds}{\Gamma h}} = S_0 + \frac{4f^2}{\int_{\partial T} \frac{ds}{\Gamma h}} . \tag{15}$$

By deducing formula (15), essentially, the inequality relation (9) is proved.

3. An inequality relation

Theorem II

With any vector field

$$\boldsymbol{\varphi} = \boldsymbol{\varphi}(x, y) = \varphi_x(x, y)\, \mathbf{e}_x + \varphi_y(x, y)\, \mathbf{e}_y$$

being continuous in the closed region $T + \partial T$ and satisfying the partial differential equation

$$\nabla \boldsymbol{\varphi} = -2 (x, y) \in T \tag{16}$$

in region T the inequality relation

$$S \leq \int_T \frac{\boldsymbol{\varphi}^2}{G}\, dT + \int_T \frac{\Gamma h}{\mathbf{G}^2} (n \cdot \boldsymbol{\varphi})^2\, dS \tag{17}$$

is valid.

Demonstration

Be

$$\boldsymbol{\alpha} = \alpha_x(x, y)\, \mathbf{e}_x + \alpha_y(x, y)\, \mathbf{e}_y \quad \text{and} \quad \boldsymbol{\beta} = \beta_x(x, y)\, \mathbf{e}_x + \beta_y(x, y)\, \mathbf{e}_y$$

two such xy inplane vector fields, defined in region $T + \partial T$, for which the integrals

$$E(\boldsymbol{\alpha}, \boldsymbol{\beta}) = \int_T \frac{\boldsymbol{\alpha} \cdot \boldsymbol{\beta}}{G}\, dT + \int_{\partial T} \frac{\Gamma h}{G^2} (\mathbf{n} \cdot \boldsymbol{\varphi})\, (\mathbf{n} \cdot \boldsymbol{\beta})\, ds, \tag{18}$$

$$E(\boldsymbol{\alpha}, \boldsymbol{\beta}) = \int_T \frac{\boldsymbol{\alpha}^2}{G}\, dT + \int_{\partial T} \frac{\Gamma h}{G^2} (\mathbf{n} \cdot \boldsymbol{\alpha})^2\, ds\,, \tag{19}$$

$$E(\boldsymbol{\beta}, \boldsymbol{\beta}) = \int_T \frac{\boldsymbol{\beta}^2}{G}\, dT + \int_{\partial T} \frac{\Gamma h}{G^2} (\mathbf{n} \cdot \boldsymbol{\beta})^2\, ds \tag{20}$$

are actual and finite.

The above interpretations have the consequence that

$$E(\alpha, \alpha) \geq 0, \quad E(\beta, \beta) \geq 0\,, \tag{21), (22}$$

$$E(\alpha, \alpha)\ E(\beta, \beta) \geq \big(E(\alpha, \beta)\big)^2\,. \tag{23}$$

With a simple substitution it may be pointed out that

$$S = E(\nabla U, \nabla U). \tag{24}$$

From the Schwarz inequality, by chosing $\alpha = \nabla U$, $\beta = \varphi$ one obtains the inequality

$$SE(\varphi, \varphi) \geq \big(E(\nabla U, \varphi)\big)^2\,. \tag{25}$$

In the following the transformation of $E(\nabla U, \varphi)$ will be carried out:

$$\begin{aligned} E(\nabla U, \varphi) &= \int_T \frac{\nabla U \cdot \varphi}{G}\, dT + \int_{\partial T} \frac{\Gamma h}{G^2}\, \frac{\partial u}{\partial n}\, (\varphi \cdot \mathbf{n}) ds = \\ &= \int_T \nabla \cdot \left(\frac{U \cdot \varphi}{G}\right) dT - \int_T U \nabla \cdot \left(\frac{\varphi}{G}\right) dT + \\ &+ \int_{\partial T} \frac{\Gamma h}{G^2}\, \frac{\partial U}{\partial n}\, (\varphi \cdot \mathbf{u}) ds = 2 \int_T U\, dT + \\ &+ \int_{\partial T} \frac{\varphi \cdot \mathbf{n}}{G} \left(U + \frac{\Gamma h}{G}\, \frac{\partial U}{\partial n}\right) ds = 2 \int_T U\, dT = S\,. \end{aligned} \tag{26}$$

Combination of the inequality (25) and formula (26) yields the inequality relation to be demonstrated (17).

4. Upper limits

Theorem III

With any scalar function $A = A(x, y)$ continuously derivable in region $T + \partial T$ the inequality relation

$$S \leq \int_T G(\nabla A \times \mathbf{e}_z - \mathbf{R})^2\, dT + \int_{\partial T} \Gamma h \left(\frac{\partial A}{\partial s} - R_n\right)^2 dS \tag{27}$$

is valid, wherein

$$R_n = \mathbf{R} \cdot \mathbf{n},\ \mathbf{R} \in \partial T\,. \tag{28}$$

Demonstration

Be

$$\varphi = G[\nabla A \times \mathbf{e}_z - \mathbf{R}] \tag{29}$$

wherein $A = A(x, y)$ designates any arbitrary scalar function derivable in region $T + \partial T$.

It is easy to point out that the vector $\bar{\varphi} = \varphi(x, y) = \varphi_x, \mathbf{e}_x + \varphi_y \mathbf{e}_y$ of form (29) satisfies the partial differential equation (16).

Substitution of formula (29) into the inequality (17) results in the demonstration of Theorem III.

Theorem IV

With the function $A = A(x, y)$ derivable in the region $T + \partial T$, not being identically constant, but otherwise arbitrarily chosen, the inequality relation

$$S \leq I - \frac{\left(\int_T G(\nabla A \times \mathbf{e}_z) \cdot \mathbf{R}\, dT - \int_{\partial T} \Gamma h \frac{\partial A}{\partial s} R_n\, ds\right)^2}{\int_T G(\nabla A)^2\, dT + \int_{\partial T} \Gamma h \left(\frac{\partial A}{\partial s}\right)^2 ds} \tag{30}$$

is valid, wherein

$$I = \int_T GR^2\, dT + \int_{\partial T} \Gamma h R_n^2\, ds\,. \tag{31}$$

Demonstration

Let us apply the inequality function (27) to the function $A^* = \lambda A(x, y)$ of two variables, where λ is, for the moment, a real number, arbitrarily chosen.

By proceeding with the elementary calculation one obtains the following result:

$$\begin{aligned} S \leq \lambda^2 &\left(\int_T G(\nabla A)^2\, dT + \int_{\partial T} \Gamma h \left(\frac{\partial A}{\partial s}\right)^2 dS\right) + \\ &+ 2\lambda \left(\int_{\partial T} \Gamma h \frac{\partial A}{\partial s} R_n\, ds - \int_T G\,(\nabla A \times \mathbf{e}_z) \cdot \mathbf{R}\, dT\right) + \\ &+ \int_T GR^2\, dT + \int_{\partial T} \Gamma h R_n^2\, ds\,. \end{aligned} \tag{32}$$

Theorem V

Be $p = p(x, y)$ a function of two variables continuously derivable in the closed region $T + \partial T$ which, in the region T satisfies the partial differential equation

$$\Delta p = -2. \tag{33}$$

The inequality relation

$$S \leq G \int_T (\nabla p)^2\, dT + \int_{\partial T} \Gamma h \left(\frac{\partial p}{\partial n}\right)^2 dS \tag{34}$$

is valid.

Demonstration

Be in the formula (17)

$$\varphi = G \nabla p$$

The vector $\varphi = \varphi(x, y)$ of the above form, obviously, satisfies Eq. (16). Combination of formulae (35) and (17) the inequality relation, Q.E.D.

Theorem VI

The function $q = q(x, y)$ should satisfy the conditions

$$\Delta q = -2 \qquad (x, y) \in T\,, \tag{36}$$

$$\int_{\partial T} \frac{\partial q}{\partial n} \left(q + \frac{\Gamma h}{G} \frac{\partial q}{\partial n} \right) ds = 0\,. \tag{37}$$

We have the inequality relation

$$S \leq 2G \int_T q \, dT\,. \tag{38}$$

Demonstration

Be $p(x, y) = q(x, y)$. On the basis of the inequality relation (34) the following inequality can be written

$$S \leq G \int_T (\nabla q)^2 \, dT + \int_{\partial T} \Gamma h \left(\frac{\partial q}{\partial n} \right)^2 dS\,. \tag{39}$$

The right-hand side of inequality (39) may be transformed as follows:

$$G \int_T (\nabla q)^2 \, dT + \int_{\partial T} \Gamma h \left(\frac{\partial q}{\partial n} \right)^2 ds = G \int_T \nabla \cdot (q \nabla q) \, dT -$$

$$- G \int_T p \Delta q \, dT + \int_{\partial T} \Gamma h \left(\frac{\partial q}{\partial n} \right)^2 dS = 2G \int_T q \, dT +$$

$$+ G \int_{\partial T} \frac{\partial q}{\partial n} \left[q + \frac{\Gamma h}{G} \frac{\partial q}{\partial n} \right] ds = 2G \int_T q \, dT\,.$$

From this result and from inequality (39) the validity of Theorem VI follows.

5. Example to form limiting values

In Fig. 2 a square cross section is strengthened by a thin shell at its edges.

To make this easily understandable, in the numerical example the measurement units will not be given. We have

$$h = 0{,}1, \quad G = 10, \quad \Gamma = 100 .$$

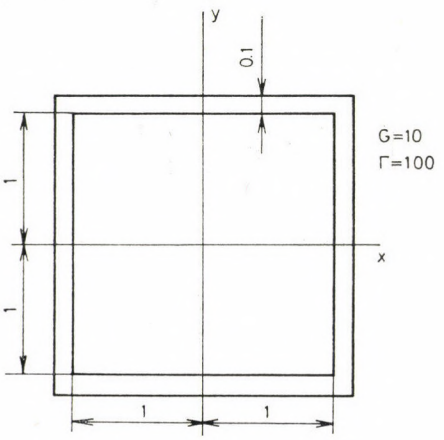

Fig. 2. Square cross section

5.1 From Formula (27), the substitution $A = 0$ yields

$$S \leq G \int_T R^2 \, dT + \Gamma h \int_{\partial T} R_n^2 \, ds = 106{,}6 .$$

5.2 In Formula (30) be $A = xy$.

Calculating with the above function, yields in the example in question:

$$S \leq 104{,}3 .$$

5.3 Let us apply Formula (34) to the function

$$p(x, y) = xy - \frac{x^2 + y^2}{2} .$$

An elementary calculation yields:

$$S \leq 104{,}8 .$$

5.4 In Formula (38) let us have

$$q = q(x, y) = c(x^2 - y^2) - \frac{x^2 + y^2}{2} .$$

The value of the constant c should be selected in such a way that the condition (37) should be valid. By applying elementary, although somewhat lengthy calculation one obtains:

$$c = 1{,}427\,.$$

Applying

$$q = q(x, y) = 1{,}427(x^2 - y^2) - \frac{x^2 + y^2}{2}$$

yields

$$S \leq 105{,}6\,.$$

5.5 From the known results ensues that the torsional stiffness of a solid square cross section not strengthened by a thin shell [3] is:

$$S_0 = 22{,}496\,.$$

On the other hand, in the problem in question:

$$\int_T \frac{ds}{\Gamma h} = 0{,}8, \quad f = 4\,.$$

Replacement of the results obtained in the foregoing into Formula (9) yields the lower limiting value

$$S \geq 102{,}5$$

for the torsional stiffness of the square cross section strengthened by a thin shell.

5.6 Combining the calculated upper bounds with the lower bound following from Formula (9) results in

$$102{,}5 \leq S \leq 104{,}3\,. \tag{40}$$

REFERENCES

1. Arutjunjan, N. H.—Abranjan, B. L.: Krutsenie uprugih tel. *Izd. Phys.-Math. Lit.* Moscow (1963), 394—447.
2. Ecsedi, I.: Contribution to the Problems of Torsion of Prismatic Bars Strengthened by Thin Layers. (In Hungarian) *MME Publications.* Series IV. *Natural Sciences* **23,** (1979), 165—174.
3. Timoshenko, S.—Goodier, J.: Theory of Elasticity. McGraw-Hill, 1951.

Schranken für die Torsionssteifheit eines am Rand durch eine dünne Schale befestigten prismatischen Stabes. — Die Abhandlung bezieht sich auf einen am Rand durch eine dünne Schale befestigten prismatischen elastischen Stab von einfach kontinuierlichem Querschnitt. Die Schranken der Torsionssteifheit, die durch die de Saint-Venantsche Theorie ermittelt werden, können größtenteils mit Hilfe der Schwarzschen Ungleichheit bestimmt werden.

Acta Technica Academiae Scientiarum Hungaricae, Tomus 92 (3–4), pp 301–321 (1981)

BRACKETING OF THE EIGENFREQUENCIES OF SPATIAL SKELETONS I.

GY. CZEGLÉDI*

[Manuscript received 2 april 1981]

This first part of the paper consisting of two parts states the problem, produces substituting structures for the bracketing of dynamic characteristics of space frame structures consisting of straight bars with length-wise varying characteristics, then the matrix equations describing the vibration of a single prismatic bar are established. For the analysis of vibrations of prismatic bar systems a theory applying dynamic stiffness and deformation matrices will be presented, relying on the continuum model.

1. Introduction

Certain structures in general mechanical engineering, vehicles or lightweight building systems can often be modelled as spatial skeletons. Their dynamic analysis invariably enhances natural frequency, or in the case of forced vibrations, the steady state amplitude distribution. This paper is a contribution to the determination of the quoted dynamic characteristics of spatial skeletons modelled as a continuum.

Because of its volume, the paper will be published in two parts. After having stated the problem and some theoretical preliminaries, two methods will be presented for the analysis of vibrations of structures consisting of prismatic bars. Also numerical features of the methods will be examined. Finally, the second method, considered as superior for practical applications, will be illustrated on two simple numerical examples.

2. Theory of bracketing the eigenfrequencies of spatial skeletons relying on a continuum model

Recently, among methods for the dynamic analysis of structures those giving lower and upper bounds for the wanted dynamic characteristics, such as natural frequency, are getting increasingly popularity, rather than other methods, advisably involving error assessment, where the trend of approxima-

* Gy. Czeglédi, Bartók Béla u. 3/d. H-1225 Budapest, Hungary

tion cannot often be defined in advance, the error assessment formulae are inaccurate or prohibitively intricate. Here it will be attempted to apply tools of the linear algebra to give a computerially surveyable and ready to use algorithm for the bracketing of natural frequencies of spatial skeletons. This aim is achieved by the following steps:

— To the structure consisting of bars with lengthwise varying characteristics, two systems of the same spatial arrangement, consisting of straight bars with lengthwise constant characteristics (later on called prismatic), with natural circular frequencies giving lower and upper bounds of the original structure, will be assigned.

— Matrix equations describing sine vibrations of circular frequency ω of the prismatic bar will be written.

— Frequency equation of the structure will be established.

Two methods will be presented for deriving — by uniform treatment — the frequency equation of the system. The first one may essentially be considered as a development of the exact displacement method, while the second achieves a result by writing a linear equation system for the integration constants, used in the theory of differential equations, by means of the boundary and fitting conditions.

2.1 *Derivation and features of substituting structures*

The spatial structure of straight bars with lengthwise varying characteristics — later on called "original structure" — is further divided by means of internal nodes (cross sections), and the obtained partial bars will be replaced by prismatic bars between the nodes. Aptly selecting characteristics of this substituting skeleton, its natural frequencies may be taken as the wanted lower or upper bounds of the original one. The selection specifications, however, can only be given when in the possession of the mathematical model of each bar. Rather than enumerating the existing or known to be missing characteristics of the bar model, it is simpler to define the model by appropriate equations such as:

$$\begin{aligned}
-\frac{\partial}{\partial x}\left(GI\,\frac{\partial\tilde{\varphi}}{\partial x}\right) &= -\Theta\,\frac{\partial^2\tilde{\varphi}}{\partial t^2}\,,\\
-\frac{\partial}{\partial x}\left(EA\,\frac{\partial\tilde{\xi}}{\partial x}\right) &= -\varrho A\,\frac{\partial^2\tilde{\xi}}{\partial t^2}\,,\\
\frac{\partial^2}{\partial x^2}\left(EI_\zeta\,\frac{\partial^2\tilde{\eta}}{\partial x^2}\right) &= -\varrho A\,\frac{\partial^2\tilde{\eta}}{\partial t^2}\,,\\
\frac{\partial^2}{\partial x^2}\left(EI_\eta\,\frac{\partial^2\tilde{\zeta}}{\partial x^2}\right) &= -\varrho A\,\frac{\partial^2\tilde{\zeta}}{\partial t^2}\,,
\end{aligned} \tag{1}$$

The above four equations describe the torsional and longitudinal vibrations of the bar, as well as its flexural vibrations in both principal planes, assumed to be simultaneous and independent of each other, where

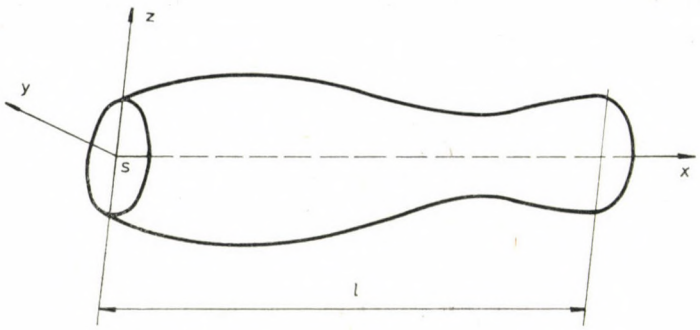

Fig. 1. Own system of coordinates of a bar

t — time;

x, y, z — coordinates in the right-hand Cartesian coordinate system (Fig. 1); if the bar is at rest, the origin coincides with the gravity centre of the end cross section, and the coordinate axes coincide with the centroidal principal axes of the cross section. (In the following, this system will be termed as its own system of coordinates.);

$\tilde{\varphi}(x, t)$ — angle of rotation of the cross section around axis x;

$\tilde{\xi}(x, t)$, $\tilde{\eta}(x, t)$, $\tilde{\zeta}(x, t)$ — are displacements of the cross section along x, y and z, respectively;

$G = G(x)$ — modulus of shear;

$GI = GI(x)$ — torsional stiffness;

$\theta = \theta(x)$ — specific moment of inertia of the bar about the torsion axis (referred to the axial dimension);

$E = E(x)$ — Young's modulus;

$EI_y = EI_y(x)$ and

$EI_z = EI_z(x)$ — bending stiffnesses of the bar referred to axes y and z, respectively;

$A = A(x)$ — area of cross section;

$\varrho = \varrho(x)$ — bar material density.

Positive direction of the vector assigned to $\tilde{\varphi}$ in compliance with the rule of turning right has to coincide with the x-axis, and the direction of the vectors ψ and $\tilde{\chi}$ (to be introduced later) assigned to the rotation of the bar cross

section about axes y or z have to coincide with the positive direction of axes y and z, respectively.

To obtain the lower limits for the natural frequencies, let us divide bar i in the range $0 \leq x_i \leq l_i$ to k_i parts (l_i being the length of bar i), and in the j-th closed partial interval let the substituting prismatic rod section be selected so as to have the equalities:

$$\begin{aligned}
(GI)_{ij}^{l} &= \min \left(GI_i(x_i)\right)_j, \\
(EA)_{ij}^{l} &= \min \left(E_i A_i(x_i)\right)_j, \\
(EI_z)_{ij}^{l} &= \min \left(EI_{z,i}(x_i)\right)_j, \\
(EI_y)_{ij}^{l} &= \min \left(EI_{y,i}(x_i)\right)_j, \\
\Theta_{ij}^{l} &= \max \left(\Theta_i(x_i)\right)_j, \qquad (i = 1, 2, \ldots, n) \\
(\varrho A)_{ij}^{l} &= \max \left(\varrho_i A_i(x_i)\right)_j, \qquad (j = 1, 2, \ldots, k_i)
\end{aligned} \tag{2}$$

min and max being minima and maxima of the functions in the j-th closed interval, superscript l referring to the lower bound.

Selecting characteristics of the partial bars of the substituting structure in conformity with equalities (2), then according to the theorem of comparisons (p. 7 in [2]) relying on Poincaré's minimax principle [1] natural circular frequencies of the system will yield lower bounds of the natural circular frequencies of the original system.

Upper bounds are obtained by selecting bar characteristics in the substituting system according to conditions (3):

$$\begin{aligned}
(GI)_{ij}^{u} &= \max \left(GI_i(x_i)\right)_j, \\
(EA)_{ij}^{u} &= \max \left(E_i A_i(x_i)\right)_j, \\
(EI_z)_{ij}^{u} &= \max \left(EI_{z,i}(x_i)\right)_j, \\
(EI_y)_{ij}^{u} &= \max \left(EI_{y,i}(x_i)\right)_j, \\
\Theta_{ij}^{u} &= \min \left(\Theta_i(x_i)\right)_j, \qquad (i = 1, 2, \ldots, n) \\
(\varrho A)_{ij}^{u} &= \min \left(\varrho_i A_i(x_i)\right)_j, \qquad (j = 1, 2, \ldots, k_i)
\end{aligned} \tag{3}$$

superscript u referring to upper bound.

With increasing the division number k_i lower bounds increase and upper bounds decrease. The improvement of accuracy is limited by the storage space needed for the applied computer, and by the demanded running time. For

practical structures where bar characteristics vary little lengthwise, relatively lower values of k_i will do.

For a structure made up of bars with lengthwise constant characteristics, the substitute above procedure is meaningless, natural circular frequencies are exactly calculated by procedures to be presented under *2.3* and *2.4*. Thus, in the following, the problem will be to determine natural circular frequencies of spatial structures consisting of prismatic bars.

2.2 Matrix equations of the vibration of a single prismatic bar

The selected bar model is defined by (1). If standing-wave, rather than general solutions are needed, then field equations describing displacements and rotations of any cross section of bar i of circular frequency ω vibrating at small amplitude (Fig. 2) can be deduced from Eqs (1):

$$\begin{aligned}
\tilde{\xi}_i &= (A_{1i} \sin \beta_{1i} x_i + A_{2i} \cos \beta_{1i} x_i) \sin \omega t\,,\\
\tilde{\eta}_i &= (A_{3i} \sin \beta_{3i} x_i + A_{4i} \cos \beta_{3i} x_i + A_{5i} \operatorname{sh} \beta_{3i} x_i + A_{6i} \operatorname{ch} \beta_{3i} x_i) \sin \omega t\,,\\
\zeta_i &= (A_{7i} \sin \beta_{2i} x_i + A_{8i} \cos \beta_{2i} x_i + A_{9i} \operatorname{sh} \beta_{2i} x_i + A_{10i} \operatorname{ch} \beta_{2i} x_i) \sin \omega t\,,\\
\tilde{\varphi}_i &= (A_{11i} \sin \beta_{4i} x_i + A_{12i} \cos \beta_{4i} x_i) \sin \omega t\,,\\
\tilde{\psi}_i &= (-A_{7i}\beta_{2i} \cos \beta_{2i} x_i + A_{8i}\beta_{2i} \sin \beta_{2i} x_i - A_{9i}\beta_{2i} \operatorname{ch} \beta_{2i} x_i -\\
&\quad - A_{10i}\beta_{2i} \operatorname{sh} \beta_{2i} x_i) \sin \omega t\,,\\
\tilde{\chi}_i &= (A_{3i}\beta_{3i} \cos \beta_{2i} x_i - A_{4i}\beta_{3i} \sin \beta_{3i} x_i + A_{5i}\beta_{3i} \operatorname{ch} \beta_{3i} x_i +\\
&\quad + A_{6i}\beta_{3i} \operatorname{sh} \beta_{3i} x_i) \sin \omega t\,,
\end{aligned} \tag{4}$$

where $A_{1i}, A_{2i}, \ldots, A_{12i}$ are momentarily unknown coefficients, and

$$\begin{aligned}
\beta_{1i} &= \sqrt[4]{\frac{\varrho_i}{E_i}}\,\omega\,, & \beta_{4i} &= \sqrt[4]{\frac{\Theta_i}{GI_i}}\,\omega\,,\\
\beta_{2i} &= \sqrt[4]{\frac{\varrho_i A_i}{EI_{yi}}\,\omega^2}\,, & \beta_{3i} &= \sqrt[4]{\frac{\varrho_i A_i}{EI_{zi}}\,\omega^2}\,,
\end{aligned} \tag{4a}$$

subscript i referring to the i-th bar in the structure.

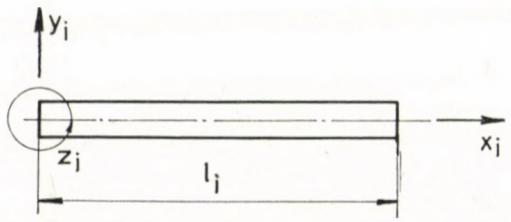

Fig. 2. Prismatic bar with its own system of coordinates

In the following, our equations will be written by using symbols of matrix calculus because of its conciseness and computerization advantages. Column matrices — with certain advantages — will be termed in short vectors, misunderstanding being excluded in this particular study.

Substituting values of displacement functions (4) at $x_i = 0$ and $x_i = l_i$ (bar ends) can be arranged into a displacement vector each:

$$\underline{\tilde{U}}_i = \begin{bmatrix} \tilde{u}_i \\ \tilde{v}_i \\ \tilde{w}_i \\ \tilde{\varphi}_i \\ \tilde{\vartheta}_i \\ \tilde{\chi}_i \end{bmatrix} = \underbrace{\begin{bmatrix} & 1 & & & & & & & & & \\ & & & 1 & & 1 & & & & & \\ & & & & & & & 1 & & 1 & \\ & & & & & & & & & & 1 \\ & & & & & & -\beta_{2i} & & -\beta_{2i} & & \\ & & \beta_{3i} & & \beta_{3i} & & & & & & \end{bmatrix}}_{\underline{U}_i} \begin{matrix} x_i = 0 \\ \\ \\ \\ \\ \\ \\ \\ \\ \\ \\ \\ \end{matrix} \begin{bmatrix} A_{1i} \\ A_{2i} \\ A_{3i} \\ A_{4i} \\ A_{5i} \\ A_{6i} \\ A_{7i} \\ A_{8i} \\ A_{9i} \\ A_{10i} \\ A_{11i} \\ A_{12i} \end{bmatrix} \sin \omega t \,, \quad \underline{a}_i$$

or

$$\underline{\tilde{V}}_i = \begin{bmatrix} \tilde{u}_i \\ \tilde{v}_i \\ \tilde{w}_i \\ \tilde{\varphi}_i \\ \tilde{\vartheta}_i \\ \tilde{\chi}_i \end{bmatrix} = \begin{bmatrix} \sin\beta_{1i} l_i & \cos\beta_{1i} l_i & & & & \\ & & \sin\beta_{3i} l_i & \cos\beta_{3i} l_i & \mathrm{sh}\,\beta_{3i} l_i & \mathrm{ch}\,\beta_{3i} l_i \\ & & & & & \\ & & & & & \\ & & & & & \\ & & \beta_{3i}\cos\beta_{3i} l_i & -\beta_{3i}\sin\beta_{3i} l_i & \beta_{3i}\,\mathrm{ch}\,\beta_{3i} l_i & \beta_{3i}\,\mathrm{sh}\,\beta_{3i} l_i \end{bmatrix} \begin{matrix} x_i = l_i \\ \\ \\ \\ \\ \\ \\ \\ \\ \\ \\ \\ \end{matrix}$$

$$\begin{bmatrix} & & & & & \\ & & & & & \\ \sin\beta_{2i} l_i & \cos\beta_{2i} l_i & \mathrm{sh}\,\beta_{2i} l_i & \mathrm{ch}\,\beta_{2i} l_i & & \\ & & & & \sin\beta_{4i} l_i & \cos\beta_{4i} l_i \\ -\beta_{2i}\cos\beta_{2i} l_i & \beta_{2i}\sin\beta_{2i} l_i & \beta_{2i}\,\mathrm{ch}\,\beta_{2i} l_i & \beta_{2i}\,\mathrm{sh}\,\beta_{2i} l_i & & \\ & & & & & \end{bmatrix} \underline{a}_i \cdot \sin\omega t \,,$$

$\underline{V}_i$

in short:

$$\tilde{u}_i = \mathbf{U}_i a_i \sin \omega t$$
$$\tilde{v}_i = \mathbf{V}_i a_i \sin \omega t . \tag{5}$$

(Empty matrix places being zeros.) Thus, $\tilde{u}_i$ and $\tilde{v}_i$ in (5) are displacement vectors referring to the displacements and rotations of left and right bar ends, respectively.

Field functions (4) permit to write the force and moment components of the pair of vectors at the bar cross section of coordinate x_i reduced from the side opposite the origin:

$$\begin{aligned}
\tilde{F}_i &= A_i E_i \beta_{1i} (A_{1i} \cos \beta_{1i} x_i - A_{2i} \sin \beta_{1i} x_i) \sin \omega t , \\
\tilde{G}_i &= -EI_{zi} \beta_{3i}^3 (-A_{3i} \cos \beta_{3i} x_i + A_{4i} \sin \beta_{3i} x_i + A_{5i} \operatorname{ch} \beta_{3i} x_i + \\
&\quad + A_{6i} \operatorname{sh} \beta_{3i} x_i) \sin \omega t , \\
\tilde{H}_i &= -EI_{yi} \beta_{2i}^3 (-A_{7i} \cos \beta_{2i} x_i + A_{8i} \sin \beta_{2i} x_i + A_{9i} \operatorname{ch} \beta_{2i} x_i + \\
&\quad + A_{10i} \operatorname{sh} \beta_{2i} x_i) \sin \omega t , \\
\tilde{M}_i &= GI_i \beta_{4i} (A_{11i} \cos \beta_{4i} x_i - A_{12i} \sin \beta_{4i} x_i) \sin \omega t , \\
\tilde{N}_i &= -EI_{yi} \beta_{2i}^2 (-A_{7i} \sin \beta_{2i} x_i - A_{8i} \cos \beta_{2i} x_i + A_{9i} \operatorname{sh} \beta_{2i} x_i + \\
&\quad + A_{10i} \operatorname{ch} \beta_{2i} x_i) \sin \omega t , \\
\tilde{K}_i &= EI_{zi} \beta_{3i}^2 (-A_{3i} \sin \beta_{3i} x_i - A_{4i} \cos \beta_{3i} x_i + A_{5i} \operatorname{sh} \beta_{3i} x_i + \\
&\quad + A_{6i} \operatorname{ch} \beta_{3i} x_i) \sin \omega t .
\end{aligned} \tag{6}$$

(6) yields external force effect components acting on the *bar ends* due to *surrounding* effects, to be united into a force effect vector each, similar to displacements:

$$\tilde{f}_i = \begin{bmatrix} \tilde{F}_i \\ \tilde{G}_i \\ \tilde{H}_i \\ \tilde{M}_i \\ \tilde{N}_i \\ \tilde{K}_i \end{bmatrix} = \begin{bmatrix} -A_i E_i \beta_{1i} & & & & & & & & & & \\ & -EJ_{zi}\beta_{3i}^3 & & EJ_{zi}\beta_{3i}^3 & & & & & & & \\ & & & & -EJ_{yi}\beta_{2i}^3 & & EJ_{yi}\beta_{2i}^3 & & & & \\ & & & & & & & & -GJ_i\beta_{4i} & & \\ & & & & & -EJ_{yi}\beta_{2i}^2 & & EJ_{yi}\beta_{2i}^2 & & & \\ & & EJ_{zi}\beta_{3i}^2 & & -EJ_{zi}\beta_{3i}^2 & & & & & & \end{bmatrix} \cdot \underline{a}_i \cdot \sin \omega t ,$$

$x_i = 0$

$\underline{F}_i$

or

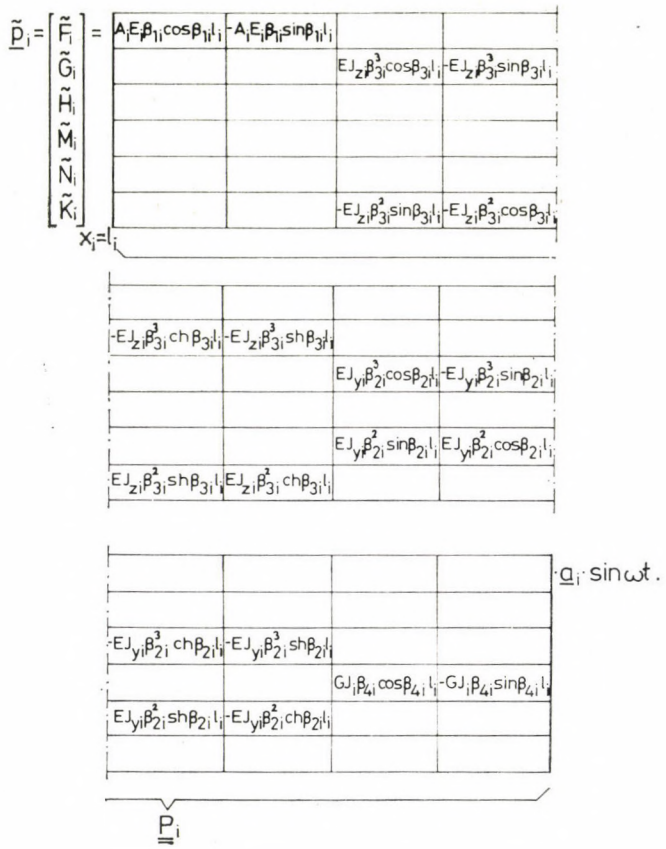

Again, written in a concise form:

$$f_i = \mathbf{F}_i a_i \sin \omega t ,$$
$$\tilde{p}_i = \mathbf{p}_i a_i \sin \omega t \tag{7}$$

where $\tilde{f}_i$ and $\tilde{p}_i$ are force effect vectors, comprising external forces and moments, acting on left and right bar ends, respectively. Of course, $\tilde{f}_i$ has been written by reckoning with the fact that the external force effect vector acting at $x_i = 0$ on the bar is -1 times that given by (6). Eqs (5) and (7) together are the parametric equation system of surrounding-induced external force effects on bar ends and bar end displacements. The parameter is vector a_i including unknown coefficients of field functions.

In the following, two algorithms will be presented for the calculation of the natural frequency of spatial skeletons made up of prismatic rods. The

first one is characterized by the elimination of parameter a_i from Eqs (5) and (7), while the second one keeps it exactly to establish the system frequency equation.

2.3 Analysis of the vibration of frameworks consisting of prismatic rods using dynamic stiffness and deformation matrices

Parts of the method to be presented are known in the literature as exact displacement or force methods and are similar to them. Accordingly, the relationships to be deduced and tabulated are strictly related to e.g. the Koloušek functions [3]. A detailed treatment is felt by the Author to be justified by the somewhat unusual start, the uniform treatment for bar systems, and by the consideration — in addition to bending and longitudinal vibrations in both principal planes — of torsional vibrations.

The essential of the method is to eliminate parameter a_i from Eqs (5) and (7), directly relating thereby to sinusoidal external force effects and the resulting sinusoidal bar end displacements.

2.3.1 Dynamic deformation matrix of a single bar and its characteristics

Let us comprise displacement and external force effect vectors into a hypermatrix each:

$$\tilde{s}_i = \begin{bmatrix} u_i \\ v_i \end{bmatrix} = \underbrace{\begin{bmatrix} \mathbf{U}_i \\ \mathbf{V}_i \end{bmatrix}}_{\mathbf{S}_i} a_i \sin \omega t\,,$$

$$\tilde{q}_i = \begin{bmatrix} f_i \\ p_i \end{bmatrix} = \underbrace{\begin{bmatrix} \mathbf{F}_i \\ \mathbf{P}_i \end{bmatrix}}_{\mathbf{Q}_i} a_i \sin \omega t\,; \tag{8}$$

or, in a concise form:

$$\tilde{s}_i = \mathbf{S}_i\, a_i \sin \omega t\,, \tag{9a}$$

$$\tilde{q}_i = \mathbf{Q}_i\, a_i \sin \omega t\,. \tag{9b}$$

$\mathbf{Q}_i$ is a quadratic matrix of order 12. It has an inverse for $\det(\mathbf{Q}_i) \neq 0$, in this case, expressing $a_i \sin \omega t$ from (9b) and substituting into (9a):

$$\tilde{s}_i = \mathbf{S}_i\, \mathbf{Q}_i^{-1} \tilde{q}_i\,,$$

or, using the notation $\mathbf{S}_i \cdot \mathbf{Q}_i^{-1} = \mathbf{R}_i$

$$\tilde{s}_i = \mathbf{R}_i\, q_i \tag{10}$$

where $\mathbf{R}_i$ is the dynamic deformation matrix. Thereby the wanted direct relationship between sinusoidal external force effect $\tilde{q}_i$ acting on ends of bar i, and bar end sine displacement $\tilde{s}_i$ is at hand. $\tilde{s}_i$ is the "response" on external force effects at bar ends — as poles of a part system.

Let us note that dynamic deformation matrix $\mathbf{R}_i$ is more expedient to establish from direct physical considerations — as usual in publications — than to start from the definition $\mathbf{R}_i = \mathbf{S}_i \mathbf{Q}_i^{-1}$ and establish it from matrices $\mathbf{S}_i$ and $\mathbf{Q}_i$.

Marking left-hand and right-hand bar ends with superscripts 1 and 2, resp., (poles 1 and 2 of a part system i), structure of matrix $\mathbf{R}_i$ will be presented by detailing relationship (10):

$$\begin{bmatrix} \tilde{\xi}_i^1 \\ \tilde{\eta}_i^1 \\ \tilde{\zeta}_i^1 \\ \tilde{\varphi}_i^1 \\ \tilde{\psi}_i^1 \\ \tilde{\chi}_i^1 \\ \tilde{\xi}_i^2 \\ \tilde{\eta}_i^2 \\ \tilde{\zeta}_i^2 \\ \tilde{\varphi}_i^2 \\ \tilde{\psi}_i^2 \\ \tilde{\chi}_i^2 \end{bmatrix} = \begin{bmatrix} r_{11} & & & & & & r_{17} & & & & & \\ & r_{22} & & & & r_{26} & & r_{28} & & & & r_{2,12} \\ & & r_{33} & & r_{35} & & & & r_{39} & & r_{3,11} & \\ & & & r_{44} & & & & & & r_{4,10} & & \\ & & r_{53} & & r_{55} & & & & r_{59} & & r_{5,11} & \\ & r_{62} & & & & r_{66} & & r_{68} & & & & r_{6,12} \\ r_{71} & & & & & & r_{77} & & & & & \\ & r_{82} & & & & r_{86} & & r_{88} & & & & r_{8,12} \\ & & r_{93} & & r_{95} & & & & r_{99} & & r_{9,11} & \\ & & & r_{10,4} & & & & & & r_{10,10} & & \\ & & r_{11,3} & & r_{11,5} & & & & r_{11,9} & & r_{11,11} & \\ & r_{12,2} & & & & r_{12,6} & & r_{12,8} & & & & r_{12,12} \end{bmatrix} \begin{bmatrix} \tilde{F}_i^1 \\ \tilde{G}_i^1 \\ \tilde{H}_i^1 \\ \tilde{M}_i^1 \\ \tilde{N}_i^1 \\ \tilde{K}_i^1 \\ \tilde{F}_i^2 \\ \tilde{G}_i^2 \\ \tilde{H}_i^2 \\ \tilde{M}_i^2 \\ \tilde{N}_i^2 \\ \tilde{K}_i^2 \end{bmatrix} \tag{10a}$$

(Empty places being zeros.)
Elements are detailed in Table 1 with the already used notations and

$$N_{2i} = 1 - \cos \beta_{2i} l_i \cdot \operatorname{ch} \beta_{2i} l_i ,$$

$$N_{3i} = 1 - \cos \beta_{3i} l_i \cdot \operatorname{ch} \beta_{3i} l_i .$$

The elements physically comprise steady-state sine displacement amplitudes due to unit excitation at the given place.

From the examination of the elements it is clear that partitioning matrix $\mathbf{R}_i$ into four matrices as seen in (10a) permits it to be written as

$$\mathbf{R}_i = \begin{bmatrix} \mathbf{D} & \mathbf{C}^T \\ \mathbf{C} & \mathbf{D}_1 \end{bmatrix} \tag{11}$$

Table 1

		r_{11}	r_{77}	$-\frac{1}{A_i E_i \beta_{1i}} \operatorname{ctg} \beta_{1i} l_i$
		r_{22}	r_{88}	$\frac{1}{EI_{zi}\beta_{3i}^3 N_{3i}} (\cos\beta_{3i} l_i \cdot \operatorname{sh}\beta_{3i} l_i - \sin\beta_{3i} l_i \cdot \operatorname{ch}\beta_{3i} l_i)$
		r_{33}	r_{99}	$\frac{1}{EI_{yi}\beta_{2i}^3 N_{2i}} (\cos\beta_{2i} l_i \cdot \operatorname{sh}\beta_{2i} l_i - \sin\beta_{2i} l_i \cdot \operatorname{ch}\beta_{2i} l_i)$
		r_{44}	$r_{10,10}$	$-\frac{1}{GI_i \cdot \beta_{4i}} \operatorname{ctg} \beta_{4i} l_i$
		r_{55}	$r_{11,11}$	$-\frac{1}{EI_{yi}\beta_{2i} N_{2i}} (\cos\beta_{2i} l_i \cdot \operatorname{sh}\beta_{2i} l_i + \sin\beta_{2i} l_i \cdot \operatorname{ch}\beta_{2i} l_i)$
		r_{66}	$r_{12,12}$	$-\frac{1}{EI_{zi}\beta_{3i} N_{3i}} (\cos\beta_{3i} l_i \cdot \operatorname{sh}\beta_{3i} l_i + \sin\beta_{3i} l_i \cdot \operatorname{ch}\beta_{3i} l_i)$
		r_{17}	r_{71}	$-\frac{1}{A_i E_i \beta_{1i}} \cdot \frac{1}{\sin\beta_{1i} l_i}$
r_{26}	r_{62}	$-r_{8,12}$	$-r_{12,8}$	$\frac{1}{EI_{zi}\beta_{3i}^3 N_{3i}} \sin\beta_{3i} l_i \cdot \operatorname{sh}\beta_{3i} l_i$
r_{35}	r_{53}	$-r_{9,11}$	$-r_{11,9}$	$-\frac{1}{EI_{yi}\beta_{2i}^2 N_{2i}} \sin\beta_{2i} l_i \cdot \operatorname{sh}\beta_{2i} l_i$
		r_{28}	r_{82}	$-\frac{1}{EI_{zi}\beta_{3i}^3 N_{3i}} (\sin\beta_{3i} l_i - \operatorname{sh}\beta_{3i} l_i)$
		r_{39}	r_{93}	$-\frac{1}{EI_{yi}\beta_{2i}^3 N_{2i}} (\sin\beta_{2i} l_i - \operatorname{sh}\beta_{2i} l_i)$
$r_{2,12}$	$r_{12,2}$	$-r_{68}$	$-r_{86}$	$-\frac{1}{EI_{zi}\beta_{3i}^3 N_{3i}} (\cos\beta_{3i} l_i - \operatorname{ch}\beta_{3i} l_i)$
$r_{3,11}$	$r_{11,3}$	$-r_{59}$	$-r_{95}$	$\frac{1}{EI_{yi}\beta_{2i}^2 N_{2i}} (\cos\beta_{2i} l_i - \operatorname{ch}\beta_{2i} l_i)$
		$r_{4,10}$	$r_{10,4}$	$-\frac{1}{GI_i \cdot \beta_{4i}} \cdot \frac{1}{\sin\beta_{4i} l_i}$
		$r_{5,11}$	$r_{11,5}$	$-\frac{1}{EI_{yi}\beta_{2i} N_{2i}} (\sin\beta_{2i} l_i + \operatorname{sh}\beta_{2i} l_i)$
		$r_{6,12}$	$r_{12,6}$	$-\frac{1}{EI_{zi}\beta_{3i} N_{3i}} (\sin\beta_{3i} l_i + \operatorname{sh}\beta_{3i} l_i)$

where $\mathbf{C}^T$ is the transpose of matrix $\mathbf{C}$; the symmetric matrix $\mathbf{D}_1$ differs from the equally symmetric matrix $\mathbf{D}$ by those non-zero elements of identical position, outside the main diagonal are -1 times the identical elements of $\mathbf{D}$. Accordingly, also $\mathbf{R}_i$ is obviously symmetric.

Matrix $\mathbf{R}_i$ has been established for a bar with two poles, and with six degrees of freedom for each pole. More complex systems may involve bars with a single pole, such as those in 1, 3 and 4 in Fig. 3. The dynamic deformation matrix $\mathbf{R}_i$ for such a *single-pole* bar is easy to derive from the *two-*

pole one. Substituting vectors $\tilde{s}_i$ and $\tilde{q}_i$ into the forms of (9) and $\mathbf{R}_i$ in the form in (11) into (10) and expanding yields:

$$\tilde{u}_i = \mathbf{D}\tilde{f}_i + \mathbf{C}^T\tilde{p}_i,$$
$$\tilde{v}_i = \mathbf{C}\tilde{f}_i + \mathbf{D}_1\tilde{p}_i. \tag{12}$$

Figure 3 also shows axes x_i of its own systems of coordinates assigned to the bars. For each single-pole bar, $\tilde{u}_i = 0$. Relationships (12) permit to directly relate $\tilde{u}_i$ and $\tilde{p}_i$:

$$\tilde{v}_i = (\mathbf{D}_1 - \mathbf{C}\mathbf{D}^{-1}\mathbf{C}^T)\tilde{p}_i.$$

Keeping the general formulation, applying notations $\tilde{s}_i \equiv \tilde{v}_i$ and $\tilde{q}_i \equiv \tilde{p}_i$ as well as $\mathbf{R}_i = \mathbf{D}_1 - \mathbf{C}\mathbf{D}^{-1}\mathbf{C}^T$

$$\tilde{s}_i = \mathbf{R}_i\tilde{q}_i$$

$\mathbf{R}_i$ being a *dynamic deformation matrix of the single-pole bar*. $\mathbf{R}_i$ exists if $\mathbf{D}$ is invertible.

According to this train of thought, and partitioning the dynamic deformation matrix written for a two-pole bar with six degrees of freedom for each pole, the dynamic deformation matrix of the bar can be written for any special case.

Another interesting characteristic of matrices $\mathbf{R}_i$ has still to be mentioned. For $\tilde{s}_i = 0$ — the case of a rigidly clamped bar at both ends — roots of equation

$$\det \mathbf{R}_i = 0$$

do not yield natural circular frequencies of the bar, since in this case, matrix $\mathbf{R}_i$ does not exist. Namely, deduction of elements of dynamic deformation matrix $\mathbf{R}_i$ had to involve stipulation $\tilde{s}_i \neq 0$, directly understandable from the consideration of the structure of matrix $\mathbf{Q}_i$ in $\mathbf{R}_i = \mathbf{S}_i\mathbf{Q}_i^{-1}$. For instance, for the longitudinal vibration of a bar clamped at both ends, $\sin\beta_{1i}l_i = 0$. Then matrix $\mathbf{Q}_i$ is singular, and has no inverse. Let us note that at the same time $\mathbf{S}_i$ is singular. If, according to the interpretation above, $\mathbf{R}_i$ is inexistent, speaking of its inverse would, of course, be meaningless. This statement will be used under *2.3.4.*

2.3.2 Dynamic stiffness matrix of a single bar and its characteristics

Provided it exists, the inverse relation of (10) can be written by means of (9a) and (9b):

$$q_i = \mathbf{R}_i^{-1}\tilde{s}_i, \tag{13}$$

where $\mathbf{R}_i^{-1} = \mathbf{Q}_i\mathbf{S}_i^{-1}$ is the dynamic stiffness matrix.

Dynamic stiffness matrix $\mathbf{R}_i^{-1}$ of a bar model with two poles, six degrees of freedom pole-wise, is of a structure similar to the dynamic matrix of deformation in (10a), with similar characteristics. Also $\mathbf{R}_i^{-1}$ is symmetric, the same holds as for partitioning in (11).

Its elements denoted by r'_{ij} have been compiled in Table 2. Their physical meaning is the amplitude of steady-state sine force effect producing unit sine displacement amplitude. [Also elements of matrix $\mathbf{R}_i^{-1}$ have been produced from direct mechanical considerations by means of the field functions (4) and (6) rather than using Eqs (9a) and (9b).]

Table 2

		r'_{11}	r'_{77}	$A_i E_i \beta_{1i} \operatorname{ctg} \beta_{1i} l_i$
		r'_{22}	r'_{88}	$EI_{zi}\beta_{3i}^3 \frac{1}{N_{3i}} (\cos\beta_{3i}l_i \operatorname{sh}\beta_{3i}l_i + \sin\beta_{3i}l_i \operatorname{ch}\beta_{3i}l_i)$
		r'_{33}	r'_{99}	$EI_{yi}\beta_{2i}^3 \frac{1}{N_{2i}} (\cos\beta_{2i}l_i \operatorname{sh}\beta_{2i}l_i + \sin\beta_{2i}l_i \operatorname{ch}\beta_{2i}l_i)$
		r'_{44}	$r'_{10,10}$	$GI_i \beta_{4i} \operatorname{ctg} \beta_{4i} l_i$
		r'_{55}	$r'_{11,11}$	$-EI_{yi}\beta_{2i} \frac{1}{N_{2i}} (\cos\beta_{2i}l_i \operatorname{sh}\beta_{2i}l_i - \sin\beta_{2i}l_i \operatorname{ch}\beta_{2i}l_i)$
		r'_{66}	$r'_{12,12}$	$-EI_{zi}\beta_{3i} \frac{1}{N_{3i}} (\cos\beta_{3i}l_i \operatorname{sh}\beta_{3i}l_i - \sin\beta_{3i}l_i \operatorname{ch}\beta_{3i}l_i)$
		r'_{17}	r'_{71}	$-A_i E_i \beta_{1i} \frac{1}{\sin\beta_{1i}l_i}$
r'_{26}	r'_{62}	$-r'_{8,12}$	$-r'_{12,8}$	$EI_{zi}\beta_{3i}^2 \frac{1}{N_{3i}} \sin\beta_{3i}l_i \operatorname{sh}\beta_{3i}l_i$
r'_{35}	r'_{53}	$-r'_{9,11}$	$-r'_{11,9}$	$-EI_{yi}\beta_{2i}^2 \frac{1}{N_{2i}} \sin\beta_{2i}l_i \operatorname{sh}\beta_{2i}l_i$
		r'_{28}	r'_{82}	$-EI_{zi}\beta_{3i}^3 \frac{1}{N_{3i}} (\sin\beta_{3i}l_i + \operatorname{sh}\beta_{3i}l_i)$
		r'_{39}	r'_{93}	$-EI_{yi}\beta_{2i}^3 \frac{1}{N_{2i}} (\sin\beta_{2i}l_i + \operatorname{sh}\beta_{2i}l_i)$
$r'_{2,12}$	$r'_{12,2}$	$-r'_{68}$	$-r'_{86}$	$-EI_{zi}\beta_{3i}^2 \frac{1}{N_{3i}} (\cos\beta_{3i}l_i - \operatorname{ch}\beta_{3i}l_i)$
$r'_{3,11}$	$r'_{11,3}$	$-r'_{59}$	$-r'_{95}$	$EI_{yi}\beta_{2i}^2 \frac{1}{N_{2i}} (\cos\beta_{2i}l_i - \operatorname{ch}\beta_{2i}l_i)$
		$r'_{4,10}$	$r'_{10,4}$	$-GI_i \beta_{4i} \frac{1}{\sin\beta_{4i}l_i}$
		$r'_{5,11}$	$r'_{11,5}$	$-EI_{yi}\beta_{2i} \frac{1}{N_{2i}} (\sin\beta_{2i}l_i - \operatorname{sh}\beta_{2i}l_i)$
		$r'_{6,12}$	$r'_{12,6}$	$-EI_{zi}\beta_{3i} \frac{1}{N_{3i}} (\sin\beta_{3i}l_i - \operatorname{sh}\beta_{3i}l_i)$

Dynamic stiffness matrix of a single-pole bar can be derived by simple partitioning from the two-pole one. Denoting 6×6 blocks of $\mathbf{R}_i^{-1}$ as $\mathbf{C}$, $\mathbf{D}$, $\mathbf{D}_1$ — as in (11) — expansion corresponding to (12) becomes:

$$\tilde{f}_i = \mathbf{D}\,\tilde{u}_i + \mathbf{C}^T\tilde{v}_i$$
$$\tilde{p}_i = \mathbf{C}\,\tilde{u}_i + \mathbf{D}_1\,\tilde{v}_i. \tag{14}$$

For $\tilde{u}_i = 0$:

$$\tilde{p}_i = \mathbf{D}_1\tilde{v}_i \tag{15}$$

or, according to the usual formulation, because of $\tilde{q}_i \equiv \tilde{p}_i$ and $\tilde{s}_i \equiv \tilde{v}_i$

$$\tilde{q}_i = \mathbf{R}_i^{-1}\tilde{s}_i \tag{16}$$

where $\mathbf{R}_i^{-1} = \mathbf{D}_1$ is the dynamic stiffness matrix of the single-pole bar.

Thus, for a bar clamped at one end, the other exempt from force effects, $\tilde{q}_i = 0$ hence:

$$\det(\mathbf{R}_i^{-1}) = \det(\mathbf{D}_1) = 0$$

is the bar frequency equation, its roots yield the known natural frequencies of longitudinal, transversal and torsional vibrations.

In cases meeting other constraints the dynamic stiffness matrix of a bar is easy to derive from the general one, along the same lines as that for the single-pole one.

The same anomaly as encountered for matrices $\mathbf{R}_i$ also occurs here, in analogous form. For a bar free at both ends $\tilde{q}_i = 0$, according to (13), the "frequency equation"

$$\det(\mathbf{R}_i^{-1}) = 0$$

is false, there being no $\mathbf{R}_i^{-1}$ in this case. Namely, mathematical derivation of the dynamic stiffness matrix $\mathbf{R}_i^{-1}$ involved the assumption $\tilde{q}_i \neq 0$. Matrices $\mathbf{Q}_i$ and $\mathbf{S}_i$ in the definition $\mathbf{R}_i^{-1} = \mathbf{Q}_i\mathbf{S}_i^{-1}$ are again singular. Correctness of this statement can be understood along the lines as for matrices $\mathbf{R}_i$.

Dynamic stiffness matrices of bar parts being available, let us now establish equations for the complete skeleton.

2.3.3 Equation of vibrations of the spatial skeleton

In possession of dynamic stiffness matrices of bars permits to establish the dynamic stiffness matrix of the complete framework and the vibration equation of the whole structure.

The following train of thought relevant to skeletons has been published in a more general form e.g. in [4] or [5], therefore, here it will only be outlined for the sake of completeness.

Bar equations were convenient to write in their own system of coordinates assigned to the bar, but equations for bars joined with ends are advisably established in a "common" coordinate system assigned to the structure, involving the imperative to transform the hitherto discussed force effect and displacement vectors into the common coordinate system. If unit vectors of their own system, x_i, y_i, z_i are e_{1i}, e_{2i}, e_{3i}, and those of the common system x, y, z are i, j, k, then the matrix transforming a tridimensional vector from its own to the common system is:

$$\mathbf{t}_i = \begin{bmatrix} i e_{1i} & i e_{2i} & i e_{3i} \\ j e_{1i} & j e_{2i} & j e_{3i} \\ k e_{1i} & k e_{2i} & k e_{3i} \end{bmatrix}.$$

Let us denote the displacement and force effect vectors for the bar i in the common coordinate system by s_i and q_i, respectively. Using diagonal hypermatrix $\mathbf{T}_i = \langle \mathbf{t}_i, \ldots, \mathbf{t}_i \rangle$ bar end displacements and external force effects in the common coordinate system are:

$$s_i = \mathbf{T}_i \tilde{s}_i$$

$$q_i = \mathbf{T}_i \tilde{q}_i . \tag{17}$$

The size of $\mathbf{T}_i$ depends on the degree of freedom of bar pole points: for a bar of a single pole with six degrees of freedom, it is 6×6, for a bar of two poles with six degrees of freedom each, it is 12×12.

$\mathbf{T}_i$ being an orthogonal matrix, its inverse equals its transposed:

$$\mathbf{T}_i^{-1} = \mathbf{T}_i^T .$$

Thus, the inverse relation between Eqs (17) is

$$\tilde{s}_i = \mathbf{T}_i^T s_i$$

and

$$\tilde{q}_i = \mathbf{T}_i^T q_i . \tag{18}$$

Writing (13) relating to external force effects and pole displacements in the common coordinate system using (18) yields

$$q_i = \mathbf{T}_i \mathbf{R}_i^{-1} \mathbf{T}_i^T s_i \tag{19}$$

referring to bar i.

The structure consists of n bars, a relationship similar to (19) can be written for each. For the ease of handling, let the n displacement and force effect vectors be comprised into a hypervector each:

$$s = \begin{bmatrix} s_1 \\ s_2 \\ \cdot \\ \cdot \\ \cdot \\ s_n \end{bmatrix}, \quad q = \begin{bmatrix} q_1 \\ q_2 \\ \cdot \\ \cdot \\ \cdot \\ q_n \end{bmatrix}.$$

Introducing a diagonal hypermatrix

$$\mathbf{R}^{-1} = \begin{bmatrix} \mathbf{T}_1 \mathbf{R}_1^{-1} \mathbf{T}_1^T & & & & \\ & \mathbf{T}_2 \mathbf{R}_2^{-1} \mathbf{T}_2^T & & & \\ & & \cdot & & \\ & & & \cdot & \\ & & & & \mathbf{T}_n \mathbf{R}_n^{-1} \mathbf{T}_n^T \end{bmatrix}$$

then n equations corresponding to (19) can be formally comprised into matrix equation

$$q = \mathbf{R}^{-1} s. \tag{20}$$

Bars join through poles. Pole jointing points will be called *nodes*. Let system nodes be denoted by mere capitals; pertaining displacement vectors declared in the common coordinate system are comprised in a single hypervector:

$$s_0 = \begin{bmatrix} s_A \\ s_B \\ \cdot \\ \cdot \\ \cdot \\ s_N \end{bmatrix}.$$

(The number of nodes N has nothing to do with n denoting the number of bars.)

Let *sine* force effect vectors acting on the nodes, to be considered as external for the whole system, be comprised in a single hypervector similarly to nodal displacement vectors:

$$q_0 = \begin{bmatrix} q_A \\ q_B \\ \cdot \\ \cdot \\ \cdot \\ q_N \end{bmatrix}.$$

For the sake of convenience, also vectors q_A, $q_B \ldots q_N$ have been written in the common coordinate system.

Jointing of bars requires the introduction of two other items. Let one be matrix **G**. It contains only ones and zeros, and expresses gapless fitting of bar poles to nodes. If **G** is declared as the matrix producing vector s from s_0 then:

$$G s_0 = s . \tag{21}$$

Matrix **G** may be called *kinematic coupling matrix*. (Publications often call it compatibility operator.)

A simple structure is seen in Fig. 3, as an illustration, also indicating axes x_i of its own system of coordinates of each bar. For this structure:

$$\mathbf{G} = \begin{bmatrix} \mathbf{E}_6 & \mathbf{O}_6 \\ \begin{bmatrix} \mathbf{E}_6 \\ \mathbf{O}_6 \end{bmatrix} & \begin{bmatrix} \mathbf{O}_6 \\ \mathbf{E}_6 \end{bmatrix} \\ \mathbf{O}_6 & \mathbf{E}_6 \\ \mathbf{O}_6 & \mathbf{E}_6 \end{bmatrix}$$

where **E** and **O** are unit and quadratic zero matrices, resp., subscript 6 refers to the order.

The other item mentioned is needed for writing nodal equilibrium equation of the nodes. Vector q comprises force effect vectors acting on each bar pole that are external from the aspect of bars but internal for the structure as a whole. Its -1-fold indicates force effects applied by the bars on the poles. Matrix **H** expresses the force effect of which bar is applied on which pole because of the connection. Considering the nodes as mass points of zero mass, nodal equilibrium equation becomes:

$$q_0 - \mathbf{H} q = 0 . \tag{22}$$

Writing the energy balance confirms that **H** is not independent of **G** but is exactly its transposed:

$$\mathbf{H} = \mathbf{G}^T . \tag{23}$$

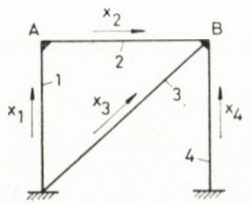

Fig. 3. Scheme of a simple framework

Replacing s into the right-hand side of (20) by (21) and substituting the term obtained for q into (22):

$$q_0 - \mathbf{H}\mathbf{R}^{-1}\mathbf{G}s_0 = 0\,.$$

Taking also (23) into consideration and applying notation

$$\mathbf{R}_0^{-1} = \mathbf{G}^T\mathbf{R}^{-1}\mathbf{G} \tag{24}$$

the equation for the sine vibration of the structure is

$$q_0 = \mathbf{R}_0^{-1}s_0\,, \tag{25}$$

where $\mathbf{R}_0^{-1}$ is the *dynamic stiffness matrix of the framework.*

(25) relates the nodal displacements and the external force effects acting on the nodes of the skeleton. In case of free vibrations $q_0 = 0$, producing from (25) the homogeneous linear equation system

$$\mathbf{R}_0^{-1}s_0 = 0$$

an equality to be met in two ways: either

$$s_0 = 0\,, \tag{26}$$

or

$$\det(\mathbf{R}_0^{-1}) = 0\,. \tag{27}$$

Equation (27) is the *frequency equation of the structure.* Reminding that, since matrices $\mathbf{G}$ and $\mathbf{G}^T$ are rectangular, the theorem for the determinant of the product of quadratic matrices cannot be applied, but the determinant of $\mathbf{R}_0^{-1}$ can only be computed after performing multiplications indicated in (24).

Dynamic stiffness matrix $\mathbf{R}_0^{-1}$ of the structure is of order $6N$ and it is a transcendent function of ω.

(25) also permits to determine the steady state response of the structure nodes. For an excitement effect of sine amplitude vector q_0, if circular frequency of the excitation is not equal to some natural circular frequency of the skeleton,

$$\det(\mathbf{R}_0^{-1}) \neq 0\,.$$

Now, nodal sine displacement vector is expressed by:

$$s_0 = \mathbf{R}_0 q_0\,, \tag{28}$$

where the *dynamic deformation matrix of the structure* is:

$$\mathbf{R}_0 = [\mathbf{G}^T\mathbf{R}^{-1}\mathbf{G}]^{-1}. \tag{29}$$

Let us note that inversion indicated in (29) cannot be formally performed because of the non-quadratic **G**, only after multiplying the factors with each other.

Determination of the steady-state vibration pattern of a forced vibration according to (28) has little advantageous from computer aspects. Solution of the inhomogeneous linear algebraic equation system (25) requires the selection of the numerically most stable method as far as possible.

2.3.4 Method of calculating eigenfrequencies, characteristic of the method

Relationship (27) is the structure frequency equation. The elements of the frequency determinant are transcendent fractional functions of the vibration of circular frequency ω. Roots of the determinant function are the natural circular frequencies of the vibration.

The formal properties of the function make the determination of the roots a computerially delicate problem. Besides steeply sloping sections, the function has several discontinuities (see e.g. p. 195 in [6]). Numerical analyses are mostly made by, so called, "shifting"; varying ω values by $\Delta\omega$ determinant values are computed, concluding from its variation trend on the occurrence of a root at the computed position. Zeros will be delimited by approximation relying on the interval-halving method. Convenient computer programming tricks permit the determination of roots of even multiplicity, and to avoid floating-point overflow around discontinuities. For *more than two* zeros in an interval $\Delta\omega$, *from computer causes*, it is not excluded that some root gets omitted in computation. This event is, however, rather unlikely for real structures, if $\Delta\omega$ is selected small enough (e.g. $\Delta\omega \leq 1$). This problem has been solved by WITTRICK and WILLIAMS [7]. Their procedure permits to check if no eigenfrequency was omitted below some fixed value of ω^* in computation, or even to make up for the omission.

Also a physical meaning of the discontinuities of the determinant function can be given. Be ω' one of the natural circular frequencies of a bar part assumed to have clamped ends. As quoted under *2.3.1*, for this circular frequency, the dynamic deformation matrix of the bar is not declared, has no inverse, not even the stiffness matrix. The stiffness matrix of the complete structure is composed of the stiffness matrices of the bars, thus, at ω' the stiffness matrix of the structure is not declared, the determinant function is singular. Mathematically, singularity may be of two kinds: removable and essential. Discontinuities of the determinant function belong to this latter type, while removable discontinuities do not come to light in numerical analyses, except by chance.

The above statements raise the question whether the set of natural circular frequencies computed from 0 to a given bound ω^* is safely complete, disregarding the omission of natural circular frequencies because of an exces-

sive interval $\Delta\omega$? Surely not. Let us assume, namely, the structure to have a natural circular frequency that is also the natural circular frequency of a bar part assumed to have clamped ends. Here the determinant function is singular. Singularity may be essential, thus, in computation, this natural circular frequency is omitted. This case has been represented by Fig. 3 on p. 264 of [8] — though starting from a discrete model. If singularity is removable, the bound is not necessarily zero (see — again for a discrete model — Fig. 2 on p. 262 in [8]). Thus, *principally*, completeness of the computed set of natural circular frequencies cannot be safeguarded.

A simple example will be evolved as a further illustration of our statement. Let us consider a prismatic bar of length L, both ends rigidly clamped. For the sake of simplicity, let us consider torsional vibrations alone. Let the bar be divided into lengths l_1 and l_2, considering the division point as a node. The dynamic stiffness matrix (for purely torsional vibration) of the resulting structure has a single element (omitting the otherwise simple deduction):

$$\mathbf{R}_0^{-1} = [\operatorname{cotg} \delta l_1 + \operatorname{cotg} \delta l_2]$$

where

$$\delta = \sqrt{\frac{\varrho}{G}}\,\omega\,.$$

Making use of identity of coth sums, the frequency equation corresponding to (27) becomes:

$$\frac{\sin \delta L}{\sin \delta l_1 \cdot \sin \delta l_2} = 0\,.$$

Roots of the function, that are meaningful with respect to vibration, are given by $\delta L = (1 + k)\pi$ ($k = 0, 1, 2, 3, \ldots$ etc.) but values $\delta l_1 = (1 + k)\pi$ and $\delta l_2 = (1 + k)\pi$ have to be excluded from the set.

For $l_1 = l_2 = L/2$, zeros are at $\delta L = (1 + 2k)\pi$ while for $\delta L = 2k\pi$ the function has a discontinuity. Thereby, every second natural circular frequency is omitted, namely they are natural circular frequencies also of bar parts of length $L/2$. Or, upon dividing $l_1 = L/4$ and $l_2 = 3L/4$ the zeros to be excluded are $\delta l_1 = \delta L/4 = (1 + k)\pi$ and $\delta l_2 = 3\delta L/4 = (1 + k)\pi$. The determinant function is discontinuous at every $3(1 + k)\pi/4$, these are zeros of the frequency function of the bar part of length $3L/4$ vibrating in torsion. Zeros of the frequency function of bar part of length $L/4$ are at $4(1 + k)\pi$. Thus, at 4π, 8π, 12π etc., numerator of the frequency equation has a single, and its denominator a double zero, thus, the function is boundless. These frequencies are omitted in the course of computation.

The discussed disadvantage results from the reduction of the degrees of freedom peculiar to the method under *2.3.3*. As was pointed out in [8], [9]

and [12] dynamic stiffness matrix in Eqs (27) is already a reduced stiffness matrix of the system, since the number of degrees of freedom explicited in the problem is finite, as against the infinite degrees of freedom of the continuum model, and equal to the sum of nodal degrees of freedom.

The Author feels it to be the greatest deficiency of the displacement method, no hint of which has been found in any publications except his own.

Let us note that even if Eqs (26) are met, vibration is possible, since the vibration nodes may coincide with the structural nodes, a special case of the phenomenon discussed in this item.

REFERENCES

1. Poincaré, H.: Sur les équations aux derivées partielles de la physique mathématique. *American J. Math.* **12** (1890).
2. Bazley, N.—Fox, D. W.: Methods for Lower Bounds to Frequencies of Continuous Elastic System. *Zeitschrift für angewandte Mathematik und Physik* **17** (1966), 1—37.
3. Kolousek, V.: Baudynamik der Durchlaufträger und Rahmen. Fachbuchverlag GmBH, Leipzig 1953.
4. Hübner, E.: Eigenschwingungszahlen zusammengesetzter Schwingungssysteme. *Ingenieur-Archiv* **29** (1960), 134—149.
5. Bosznay, Á.: Einzelne Probleme der Dynamik zusammengesetzter Systeme. *Periodica Polytechnica. Electrical Engineering* **17** (1973) 7—28.
6. Czeglédi, Gy.—Richlik, Gy.: Computation of Natural Circular Frequencies of Spatial Structures Made up of Prismatic Bars.* Proc. Ist Scientific Session of the Working Group of Departments of Engineering Mechanics. Hung. Ac. Sci. Budapest 1974, pp. 192—197.
7. Wittrick, W. M.—Williams, F. W.: A General Algorithm for Computing Natural Frequencies of Elastic Structures. *Quart. J. Mech. Appl. Math.* **24** (1971), 263—284.
8. Czeglédi, Gy.: Einige Bemerkungen zur Freiheitsgradreduktion von linear-elastischen mechanischen Modellen. *Periodica Polytechnica, Electrical Engineering* **19** (1975), 257—266.
9. Czeglédi, Gy.: Reduction of the Degree of Freedom and its Consequences in the Analysis of Linear-Elastic Structures.* *Műszaki Tudomány* **54** (1978), 115—124.
10. Cranch, E. T.—Adler, A. A.: Bending Vibration of Variable Section Beams. *J. Applied Mechanics* (1956), 103—108.
11. Weber, C.—Günther, W.: Torsionstheorie. F. Vieweg et Sohn. Braunschweig-Akademie Verlag. Berlin 1958.
12. Czeglédi, Gy.: Reduction of the Degrees of Freedom of Linear-Elastic Mechanical Models. *Periodica Polytechnica, Electrical Engineering* **23** (1981) 311—316.

* in Hungarian

Acta Technica Academiae Scientiarum Hungaricae, Tomus 92 (3—4), pp. 323—332 (1981)

BENDING STRESSES IN FOUR CORNERS SUPPORTED HYPAR SHELLS USING A VARIATIONAL SOLUTION

A. POCANSCHI—CS. KEGYES*

[Manuscript received 3 April, 1978]

The paper attempts to evaluate the bending state in a four corners supported shallow hypar shell by means of the Ritz method. Finally an illustrative example is given.

Symbols

x, y, z	— cartesian coordinate axis
n_x, n_y, n_{xy}	— normal and shear membrane stresses
N_x, N_y	— supporting beam axial forces
$w(x, y)$	— middle surface vertical displacement
m_x, m_y, m_{xy}	— shell bending and twisting moments
q_x, q_y	— vertical shear forces
P	— uniform load acting on the shell
g	— edge member line load
$2a$	— width of the shell
f	— rise of the shell
δ	— shell thickness
b, h	— width and height of the edge beam
E	— modulus of elasticity
K	— flexural stiffness of the shell
EI	— flexural stiffness of the edge beams
M_b^t	— torsional moment of the edge beams
D	— shell extensional stiffness
α, β, ν	— physical and geometrical constants of the structure
ξ, η	— dimensionless co-ordinates

The stress analysis of hyperbolic paraboloid shell structures bounded by straight generatrices is generally carried out according to the membrane theory, which proved its validity in most cases when the real shell boundary conditions were able to transmit the shell shear stresses to the supports. The assumption which the present analysis is based on, is the fact that, for usual uniform vertical loads, the solution furnished by the membrane theory is a particular solution of the general bending theory equations. As long as this particular solution satisfies the boundary conditions, the general integral of the homogeneous equation represents the secondary bending stresses. The analysis carried out in this paper attempts an investigation into the problem

* A. POCANSCHI, Dr. Eng., Lecturer in Civil Engineering, Department of Reinforced Concrete Structures, Polytechnic Institute, Cluj, Romania
Cs. KEGYES, Eng., Design Office, Tîrgu Mureş, Romania

of the bending stresses induced in four corners supported hyperbolic paraboloid shells using a strain energy method. The corner supports are able to withstand the horizontal thrust of the edge beams, e.g. the two lower supports are connected by a tie of infinite tensile stiffness.

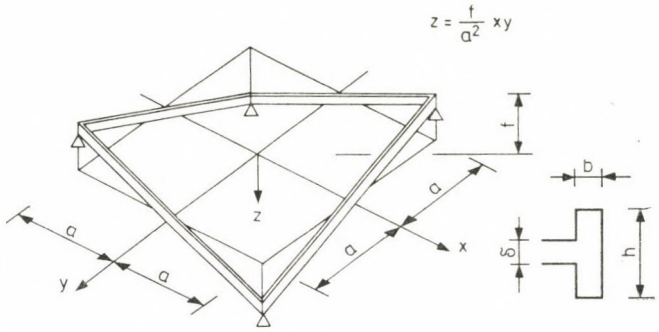

Fig. 1

1. Let us consider a square shallow hyperbolic paraboloid shell bounded by straight edge beams simply supported on the four corners, subjected to the uniform vertical load "p" per unit of the plan area (Fig. 1). The surface equation of the shell referred to the cartesian co-ordinate axes of Fig. 1 may be written as:

$$z = \frac{fxy}{a^2}. \tag{1}$$

According to the membrane theory, every point of the shell is subjected to the stresses:

$$n_x = n_y = 0, \quad n_{xy} = \frac{pa^2}{2f}. \tag{2}$$

At the shell edges, the shear stresses n_{xy} are transmitted to the supporting beams, subjecting them to the axial forces:

$$N_x = -\frac{pa^2}{2f}x \quad \text{and} \quad N_y = -\frac{pa^2}{2f}y. \tag{3}$$

2. The potential energy over the entire structure may be considered as the strain energy of the shell alone plus the strain energy of the beams parallel to the 0x and 0y axes:

$$V_t = U_i + U_{bx} + U_{by} \tag{4}$$

If $EI_x = EI_y$ denotes the flexural stiffness of the beams having the width "b", following the same way as in [4] one can write the strain energy of the structure of Fig. 1 as:

$$V_i = -\frac{K}{2}\int_{-a}^{a}\int_{-a}^{a}\left[\left(\frac{\partial^2 w}{\partial x^2}\right)^2 + 2\left(\frac{\partial^2 w}{\partial x\,\partial y}\right)^2 + \left(\frac{\partial^2 w}{\partial y^2}\right)^2\right]dx\,dy +$$

$$+ EI\left[\int_{-a}^{a}\left(\frac{\partial^2 w}{\partial x^2}\right)^2_{y=a} dx + \int_{-a}^{a}\left(\frac{\partial^2 w}{\partial y^2}\right)^2_{x=a} dy\right] -$$

$$- \nu\left[\int_{-a}^{a}\int_{-a}^{a}\left(\frac{\partial w}{\partial x}\right)\left(\frac{\partial w}{\partial y}\right)dx\,dy - \int_{-a}^{a}\left(\frac{\partial w}{\partial x}\right)^2_{y=a} x\,dx -\right.$$

$$\left. - \int_{-a}^{a}\left(\frac{\partial w}{\partial y}\right)^2_{x=a} y\,dy\right] + E_1\int_{-a}^{a}\int_{-a}^{a} w^2\,dx\,dy \tag{5}$$

where

$$\nu = \frac{pa^2}{2f}, \qquad E_1 = \frac{Ef^2\,\delta}{a^4}, \tag{6}$$

with Poisson's ratio taken equal to zero.

The potential energy due to the external loads, "g" denoting the edge beams loads, is given by the expression:

$$V_e = \int_{-a}^{a}\int_{-a}^{a} pw\,dx\,dy + \int_{-a}^{a} gw_{x=a}\,dy + \int_{-a}^{a} gw_{y=a}\,dx\,. \tag{7}$$

According to (5) and (7) the total energy of the structure becomes:

$$\Pi = V_i - V_e\,. \tag{8}$$

3. The boundary conditions to be satisfied by the displacement function w are:

$$\text{for}\begin{bmatrix} x = a \\ y = \pm a \end{bmatrix}, \quad w = 0\,, \tag{9}$$

$$\text{for}\begin{bmatrix} x = -a \\ y = \pm a \end{bmatrix}, \quad w = 0\,, \tag{10}$$

$$\text{for}\begin{bmatrix} x = 0 \\ y = 0 \end{bmatrix}, \quad \frac{\partial w}{\partial x} = \frac{\partial w}{\partial y} = 0\,, \tag{11}$$

$$\text{for}\begin{bmatrix} x = \pm a \\ y = \pm a \end{bmatrix}, \quad \begin{matrix} m_x = \partial M_b^t/\partial y \\ m_y = \partial M_b^t/\partial x\,. \end{matrix} \tag{12}$$

The expression of the displacement function w satisfying the conditions (9—12) may be chosen as a finite polynomial in ascending powers:

$$W = A\frac{x^2+y^2-2a^2}{2a^2} + B\frac{x^2y^2-a^4}{a^4} + C\frac{x^2y^4+x^4y^2-2a^6}{2a^6}. \quad (13)$$

The condition (12) cannot be fulfilled under its general form, for this reason it will be approximated as an equilibrium between the shell bending moment resultant and the edge beam torsional moment resultant

$$K\int_{-a}^{a}\left.\frac{\partial^2 w}{\partial x^2}\right|_{x=a} dy - GI_t\int_{-a}^{a}\left.\frac{\partial^3 w}{\partial x\,\partial y^2}\right|_{x=a} dy = 0, \quad (14)$$

which leads to the following relation among the polynomial coefficients:

$$A = \alpha B + \beta C \quad (15)$$

where

$$\alpha = 4\frac{GI_t}{Ka} - \frac{2}{3}, \quad \beta = 8\frac{GI_t}{Ka} - \frac{11}{5}. \quad (16)$$

With A given by (15) the deformation of the shell that satisfies the group of boundary conditions (9—12) is:

$$W = \frac{B}{2a^4}\left[2(x^2y^2-a^4) + \alpha a^2(x^2+y^2-2a^2)\right] + \\ + \frac{C}{2a^6}\left[(x^2y^4+x^4y^2-2a^6) + \beta a^4(x^2+y^2-2a^2)\right]. \quad (17)$$

4. Substituting expression (17) into (5) and (8), the total energy of the structure results in the form:

$$\Pi = \frac{K}{a^2}\left[B^2\lambda_1 + BC\lambda_2 + C^2\lambda_3\right] + \frac{4EI}{a^3}\left[B^2\lambda_4 + \right. \\ \left. + 2BC\lambda_5 + C^2\lambda_6\right] - 2pa^2\left[B\delta_1 + C\delta_2\right] - 2ga\left[B\delta_3 + C\delta_4\right]. \quad (18)$$

The parameters λ_i and δ_i from (18) are defined by the following expressions:

$$\lambda_1 = 10{,}311 + 5{,}33d + 4\alpha^2,$$
$$\lambda = 17{,}066 + 6{,}933\alpha + 5{,}333\beta + 8\alpha\beta,$$
$$\lambda_3 = 14{,}095 + 6{,}933\beta + 4\beta^2,$$
$$\lambda_4 = 4 + 4\alpha + \alpha^2,$$
$$\lambda_5 = 6 + 3\alpha + 2\beta + \alpha\beta,$$
$$\lambda_6 = 12{,}5 + 6\beta + \beta^2, \quad (19)$$

$$\delta_1 = 1{,}777 + 0{,}333\alpha\,,$$
$$\delta = 1{,}866 + 1{,}333\beta\,,$$
$$\delta_3 = 1{,}333 - 0{,}333\alpha\,,$$
$$\delta_4 = 1{,}466 + 0{,}666\beta\,.$$

5. Minimizing expression (18) with respect to parameters B and C results in two linear equations:

$$\frac{\partial \Pi}{\partial B} = 0\,, \quad \varphi_1 B + \varphi_2 C = \frac{pa^4}{K} T_1\,,$$
$$\frac{\partial \Pi}{\partial C} = 0\,, \quad \varphi_2 B + \varphi_3 C = \frac{pa^4}{K} T_2 \tag{20}$$

where:

$$\varphi_1 = 2\lambda_1 + \frac{8EI}{Ka}\lambda_4\,,$$
$$\varphi_2 = \lambda_2 + \frac{8EI}{Ka}\lambda_5\,,$$
$$\varphi_3 = 2\lambda_3 + \frac{8EI}{Ka}\lambda_6\,, \tag{21}$$
$$T_1 = 2\delta_1 + \frac{2g}{pa}\delta_3\,,$$
$$T_2 = 2\delta_2 + \frac{2g}{pa}\delta_4\,.$$

The solutions of equations (20) are:

$$B = \frac{pa^4}{K}\,\frac{\varphi_3 T_1 - \varphi_2 T_2}{\varphi_1\varphi_3 - \varphi_2^2} = \frac{pa^4}{K}\,\bar{B}\,,$$
$$C = \frac{pa^4}{K}\,\frac{\varphi_1 T_2 - \varphi_2 T_1}{\varphi_1\varphi_3 - \varphi_2^2} = \frac{pa^4}{K}\,\bar{C}\,. \tag{22}$$

6. Introducing the dimensionless co-ordinates

$$\xi = \frac{x}{a}\,, \qquad \eta = \frac{y}{a}\,,$$

the following expressions for displacement, bending and torsional moments and bending shear stress resultant are obtained:

$$w = \frac{pa^4}{K}\left\{\bar{B}\left[\xi^2\eta^2 - 1 + \frac{\alpha}{2}(\xi^2 + \eta^2 - 2)\right] + \right.$$
$$\left. + \frac{\bar{C}}{2}\left[\xi^2\eta^4 + \xi^4\eta^2 - 2 + \beta(\xi^2 + \eta^2 - 2)\right]\right., \tag{23}$$

$$m_x = -pa^2\left[\bar{B}(2\eta^2 + \alpha) + \bar{C}(\eta^2 + 6\xi^2\eta^2 + \beta)\right],$$
$$m_y = -pa^2\left[\bar{B}(2\xi^2 + \alpha) + \bar{C}(\xi^2 + 6\xi^2\eta^2 + \beta)\right], \tag{24}$$
$$m_{xy} = -pa^2\left[4\bar{B}\xi\eta + 4\bar{C}(\xi\eta^3 + \xi^3\eta)\right],$$

$$q_x = -pa\left[4\bar{B}\xi + 4\bar{C}(\xi^3 + 6\xi\eta^2)\right],$$
$$q_y = -pa\left[4\bar{B}\eta + 4\bar{C}(\eta^3 + 6\xi^2\eta)\right]. \tag{25}$$

7. *Numerical example.* For a hyperbolic paraboloid shell having following geometrical and loading characteristics

$$2a = 6\text{ m}, \quad f = 1\text{ m}, \quad \delta = 10\text{ cm}, \quad b = 25\text{ cm}, \quad h = 50\text{ cm},$$
$$E = 2{,}5 \cdot 10^5\ da\text{N/cm}^2,$$
$$G = 0{,}4\ \text{E}$$

uniform load on the shell $p = 500\ \text{daN/m}^2$
line load of the edge beams $g = 300\ \text{daN/m}$

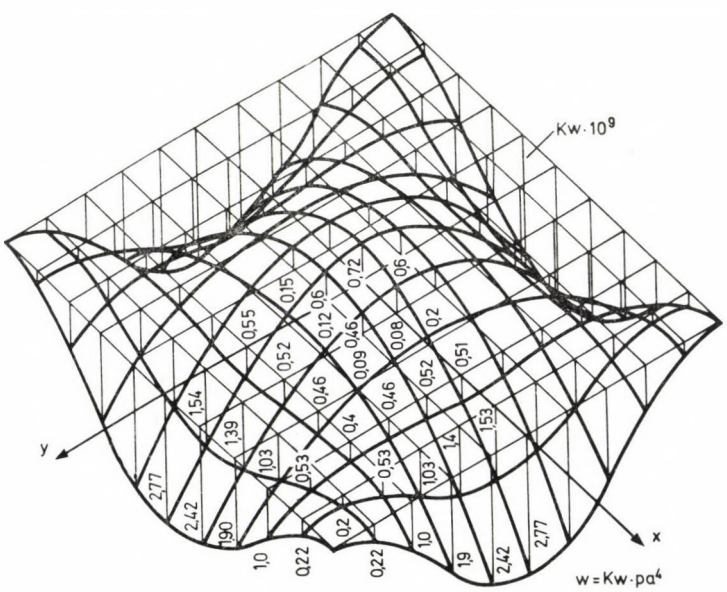

Fig. 2

the deformation, bending and torsional moments and the shear stress diagrams have been plotted in the figures 2, 3, 4, 5, 6, 7.

It is of interest to compare the values of the bending stresses calculated according to the relations (23) with the stresses given by the "pure membrane" theory. The normal membrane stress has the value:

$$\sigma_x = \pm \frac{2Nxy \sin 45^\circ \cos 45^\circ}{100\delta} = \pm \frac{pa^2 \sin^2 45^\circ}{100 f\delta} = \pm 2{,}18 \text{ daN/cm}^2.$$

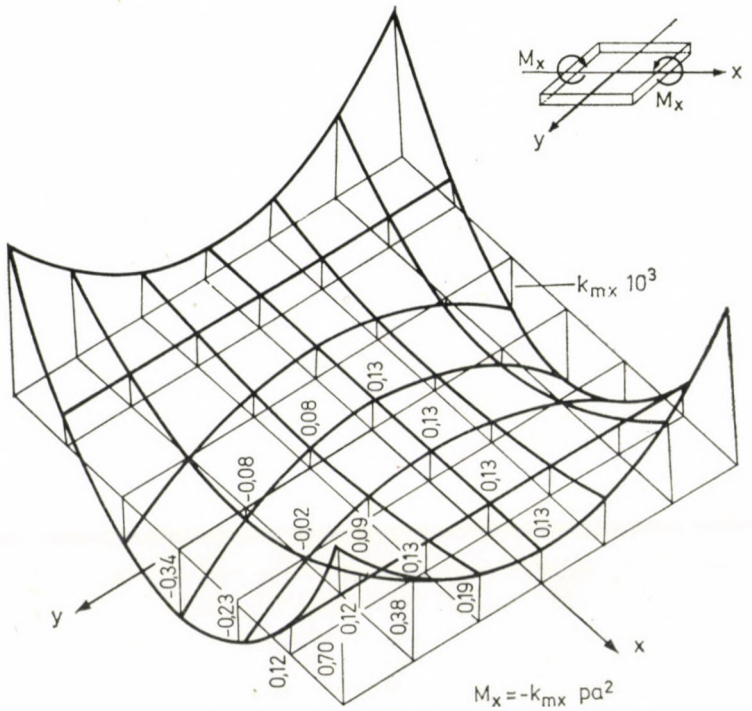

Fig. 3

The stress produced by the bending moment m_x has the values:

— at the low corner point:

$$\sigma_x = \frac{m_x}{W_x} = \frac{6 \cdot 0{,}7pa^2 \cdot 10^{-3}}{100} = 0{,}194 \text{ daN/cm}^2$$

that is about 9% of the membrane stress.

— in the origine point:

$$\sigma_x = \frac{6 \cdot 0{,}13 \cdot pa^2 \cdot 10^{-3}}{100} = 0{,}040 \text{ daN/cm}^2$$

that is about 1,8% of the membrane stress.

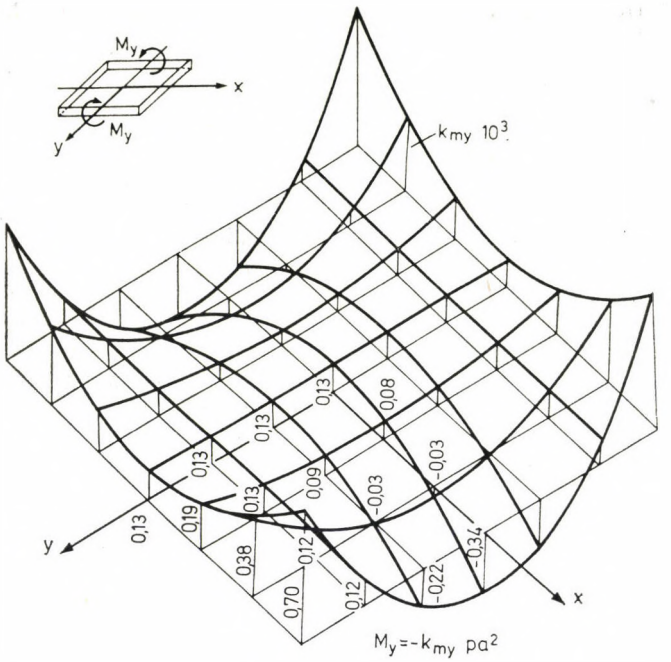
My
x
y
My
kmy 10³
0,13
0,13
0,13
0,08
0,13
0,09
0,03
-0,03
0,13
0,19
0,38
0,12
0,70
0,12
-0,22
-0,34
y
x
My=-kmy pa²

Fig. 4

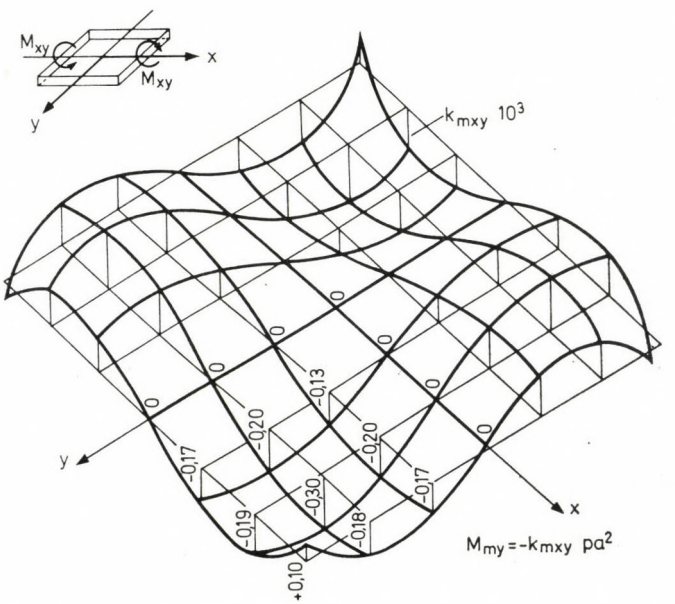
Mxy
x
Mxy
y
kmxy 10³
0
0
0
0
0
0
0
0
-0,13
-0,20
-0,20
-0,17
-0,17
-0,19
-0,30
-0,18
+0,10
y
x
Mmy=-kmxy pa²

Fig. 5

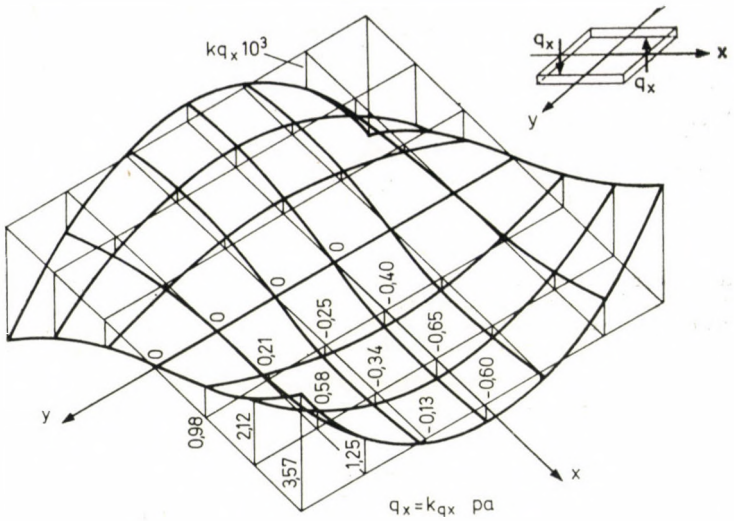
kq x 10³
qx
x
qx
y
0
0
0
0
0,21
-0,25
0
-0,40
0,58
-0,34
-0,65
0,98
2,12
-0,13
-0,60
3,57
1,25
y
x
qx = kqx pa

Fig. 6

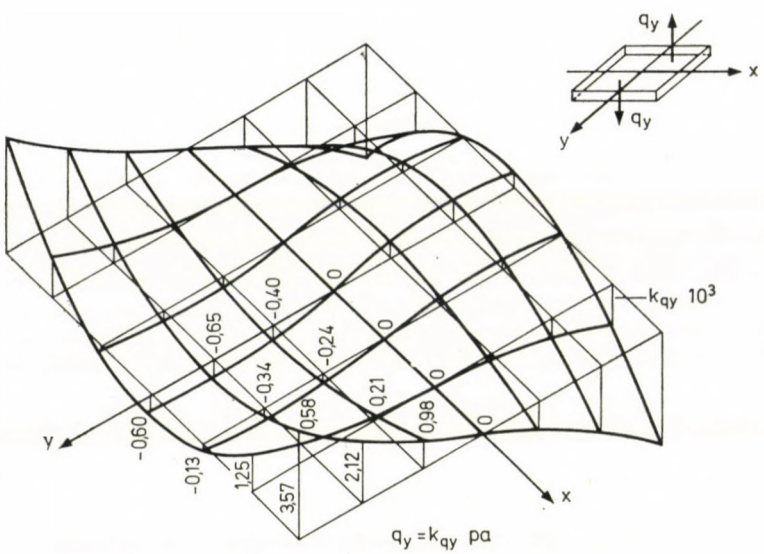
qy
x
y
qy
kqy 10³
-0,65
-0,40
0
-0,24
-0,34
0
0,58
0,21
0
0,98
-0,60
0
-0,13
1,25
3,57
2,12
y
x
qy = kqy pa

Fig. 7

REFERENCES

1. CROLL, C. A.—SCRIVENER, I.: Edge effects in hyperbolic paraboloid shells. *Journal of the Structural Division, Proc. ASCE* **95,** (1969).
2. BELEŞ, A.—SOARE, M.: Les paraboloides elliptiques et hyperboliques dans les constructions. Ed. Dunod, Paris.
3. BREBBIA, C. A.: On the calculation of shallow hyperbolic paraboloid shells. *Rev. Roum. Sci. Techn. Mech. Appliquée* **12,** (1967) No. 4.
4. DAYARATNAM, P.—GERSTLE, H. G.: Buckling of hyperbolic paraboloids. *World Conference on Shell Structures*, San Francisco 1962.

Ermittlung der Biegespannungen in auf vier Ecken abgestützten hyperbolischen Paraboloidschalen mit Hilfe einer Variationslösung. — Es wird die Ermittlung des Biegespannungszustands einer an vier Ecken abgestützten hyperbolischen Paraboloidschale mit Hilfe der Ritzschen Methode behandelt und ein Beispiel zur Anwendung der Theorie mitgeteilt.

Acta Technica Academiae Scientiarum Hungaricae, Tomus 92 (3—4), pp. 333—349 (1981)

APPLICATION OF THE BENEDICT, WEBB AND RUBIN EQUATION OF STATE TO THE EVALUATION OF THE VOLUMETRICAND THERMODYNAMIC PROPERTIES OF THE $CH_4—CO_2$ SYSTEM
PART II

Muhammad A. I. BUKHARI*

[Manuscript received March 14, 1978]

In part II of this paper the BWR equation is applied to the evaluation and plotting of the heat of mixing data and enthalpy-composition diagrams for the $CH_4—CO_2$ system over the whole composition range, for the temperature range from —120° to 30 °C and the pressure range from 10 to 80 atmospheres. Calculations cover the gaseous region, the liquid-vapour equilibrium region, the liquid region and the S-L-V equilibrium region.

Notation

A_0, B_0, C_0, a, b, c, α, ν = parameters of the BWR equation of state
BWR_{III} = BWR equation of state using the mixing rules and the pure component parameters of Bishnoi and Robinson
H = molal enthalpy
ΔH^M = molal heat of mixing
P = pressure
R = universal gas constant
T = temperature
V = molal volume
ΔV^M = molal volume of mixing
d = density
x = mole fraction
Δ = increment, a differential function
α_0 = coefficient of thermal expansion

Calculation of the volumetric and thermodynamic properties of the $CH_4—CO_2$ system using the BWR_{III}* equation of state

In the previous sections the development and the evolution of the BWR equation of state have been summarily and systematically outlined in full detail. Now that the super adaptability of this equation, in its new form, as a wide-reaching prediction technique, especially for low temperature applications, using the pure component parameters and the newly proposed mixing rules of BISHNOI and ROBINSON, being firmly resolved and established, we proceed to the application of this equation to the evaluation of the volumetric

* Present address: M. A. I. BUKHARI, P.O. Box 2408, Khartoum, Sudan

* The Benedict, Webb and Rubin equation of state using the pure component parameters of, and the mixing rules proposed by BISHNOI and ROBINSON.

and thermodynamic properties of the CH_4-CO_2 system over the whole composition range, for temperatures from 30 °C to as low as −120 °C and pressures from 10 and up to 80 atmospheres. Calculations cover:

a) The gaseous region, where two homogeneous gas-phases are mixed.

b) The saturated liquid-vapour equilibrium region and its surroundings where liquid CO_2 mixes with gaseous CH_4 to form a gas-phase, a saturated mixture or a liquid-phase.

c) The liquid region, where two homogeneous pure liquid components are mixed, isothermally and isobarically.

d) The vapour-phase and the liquid-phase in the solid-liquid-vapour equilibrium region.

For pressures below 50 atmospheres, dry ice starts to separate from the system at temperatures close to and below the triple-point temperature of CO_2, −56,6 °C. Therefore, for the isobars 40, 30, 20 and 10 atmospheres, the BWR_{III} main computer programme is used for calculating the densities, isothermal enthalpy departures and heats of mixing data for a limiting low temperature of −56,6 °C. This helps to observe the effect of CH_4 on the melting point of CO_2 in the CH_4-CO_2 system.

Densities are calculated using Equation (1):

$$P = RTd + \left(B_0 RT - A_0 - \frac{C_0}{T^2}\right) d^2 + (bRT - a)\, d^3 + \\ + a\alpha d^6 + \frac{cd^3 (1 + \nu d^2) \exp(-\nu d^2)}{T^2} \tag{1}$$

and isothermal enthalpy departures are henceforth evaluated using Eq. (2)

$$(H - H^\circ) = \left(B_0 RT - 2A_0 - \frac{4C_0}{T^2}\right) \cdot d + (2b\, RT - 3a) \cdot \frac{d^2}{2} + \\ + 6a\alpha \cdot \frac{d^5}{5} + \frac{cd^2}{T^2}\left[3 \cdot \frac{1 - \exp(-\nu d^2)}{\nu d^2} - \right. \\ \left. - \frac{\exp(-\nu d^2)}{2} + \nu\, d^2_{\exp}(-\nu d^2)\right]. \tag{2}$$

From these, heats of mixing are calculated from the relationship:

$$\Delta H^M = (H - H^\circ) - x(H - H^\circ)_1 - (1 - x)(H - H^\circ)_2 \tag{3}$$

since in the ideal gas state there is no change in enthalpy on mixing.

Mixture enthalpies are calculated from the relation:

$$H = (H - H^\circ) + xH_1^\circ + (1 - x)\, H_2^\circ \tag{4}$$

where H_1° is the hypothetical ideal gas enthalpy of pure component 1 at a reference pressure of 1 atmosphere.

Mixture enthalpies could also have been calculated as follows:

$$H = \Delta H^M + xH_1 + (1 - x)H_2 \tag{5}$$

where H_1 is the enthalpy of pure component 1.

Heat of mixing curves

a) *Liquid mixtures*

Calculated heats of mixing values for liquid CH_4—CO_2 mixtures at 50, 60, 70 and 80 atmospheres are plotted in Figures 11 through 14.

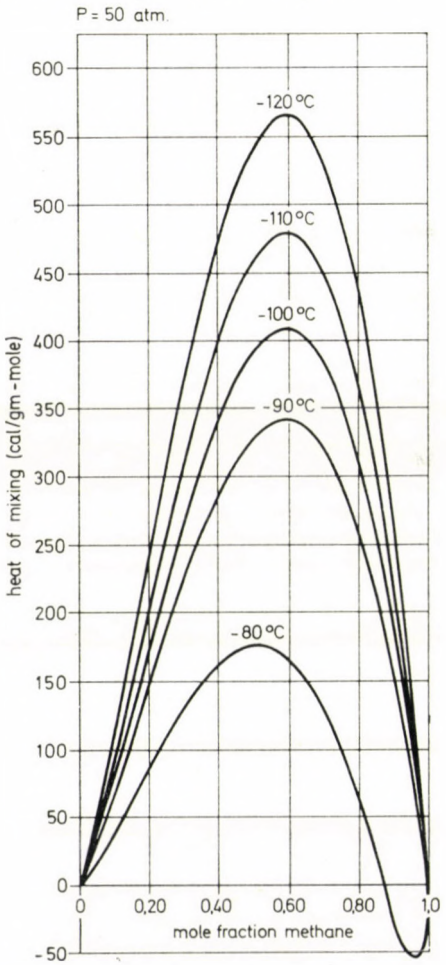

Fig. 11. Liquid-phase heats of mixing in the CH_4—CO_2 system estimated by the BWR_{II} equation of state

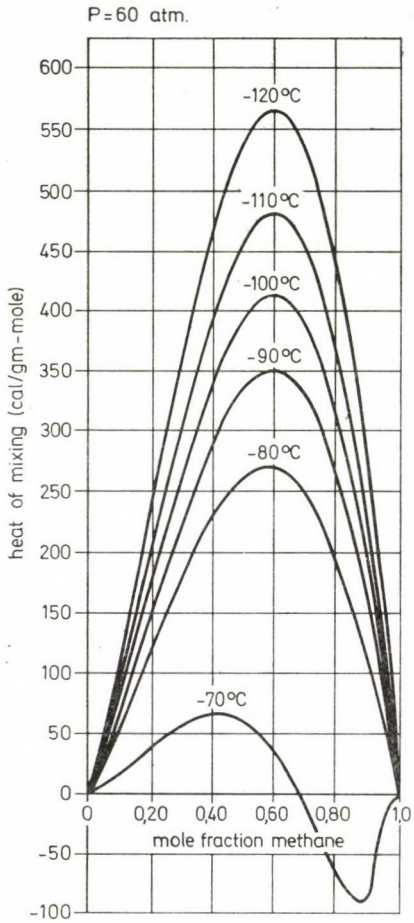

Fig. 12

At lower temperatures, the curves have regular shapes, with upward concavity indicating endothermic mixing, and show maximum values at $x \cong 0{,}60$. As the temperature is raised more and more toward the critical temperature of the mixture, where liquid CO_2 mixes with gaseous CH_4 to form a liquid mixture, the heats of mixing decrease, and the shapes of the curves become increasingly irregular toward solutions rich in the more volatile CH_4. Here, the dissolution process is accompanied by changes in enthalpy and entropy, just as occurs when two pure liquids are mixed. However, the dissolution process for gaseous CH_4 is accompanied by a large decrease in volume, since the partial volume of CH_4 in the liquid mixture is much smaller than its volume in the pure gas-phase. This large decrease in volume causes the

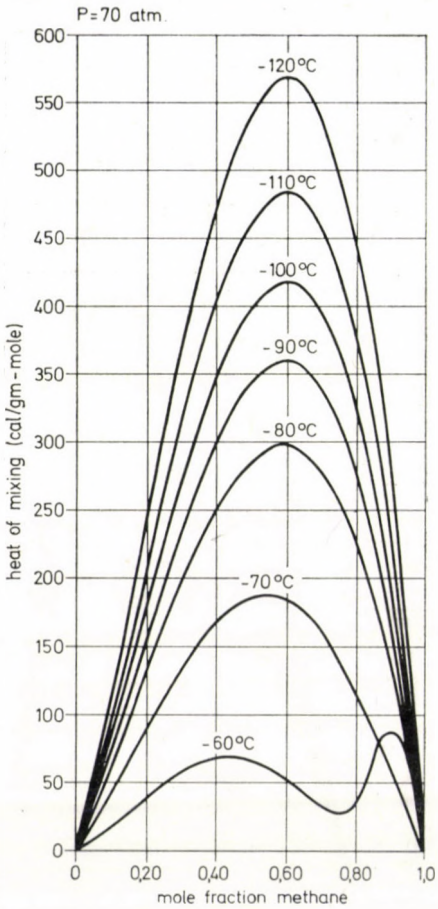

Fig. 13

volume change, ΔV^M, to become increasingly negative and increasingly unsymmetrical in x, and the enthalpy of mixing to decrease and frequently to reverse sign.

b) *Solid-liquid locus*

BWR_{III} is also applied to calculate the heats of mixing of saturated liquid solutions of CO_2 in CH_4 in the S-L-V equilibrium region. For temperatures close to and below the critical temperature of CH_4 (191,1 °K), BWR_{III} is directly applied to predict the densities and isothermal enthalpy departures of the mixture. However, for temperatures equal to or greater than 180 °K CH_4 it is assumed to behave as a hypothetical supercritical liquid with volumes estimated from Eq. (6), [14]

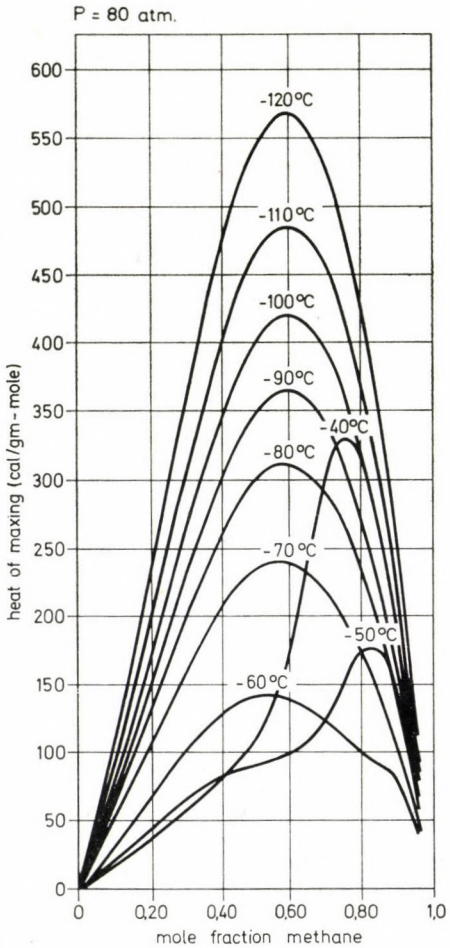

Fig. 14

$$V = V_0 \exp \alpha_0 (T - 180)] \; T \geq 180 \; ^\circ\mathrm{K} \tag{6}$$

where: $V_0 = 57{,}0288$ (cm^3/gm-mole) is a constant and corresponds to the volume of liquid CH_4 at 180 °K;
$\alpha_0 = 1{,}25063 \times 10^{-2} \; ^\circ\mathrm{K}^{-1}$, is the coefficient of thermal expansion of CH_4 at 180 °K.

Figure 15 is a plot of the excess enthalpies of mixing along the liquidus locus.

Enthalpy-composition diagrams

Figures 16 through 22 are the enthalpy-composition diagrams for the $CH_4 - CO_2$ system at pressures 10, 20, 30, 40, 50, 60 and 70 atmospheres. The bulk of the gaseous mixture enthalpies are based on the experimental

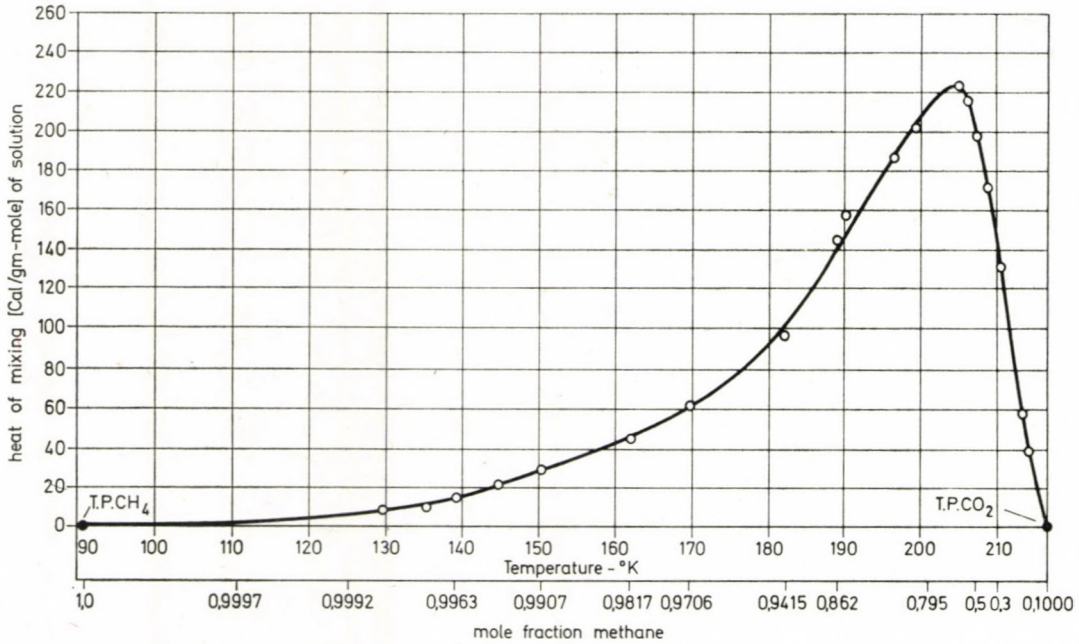

Fig. 15. **Heat of mixing for the saturated liquid solution of carbondioxide in methane in the three-phase region**

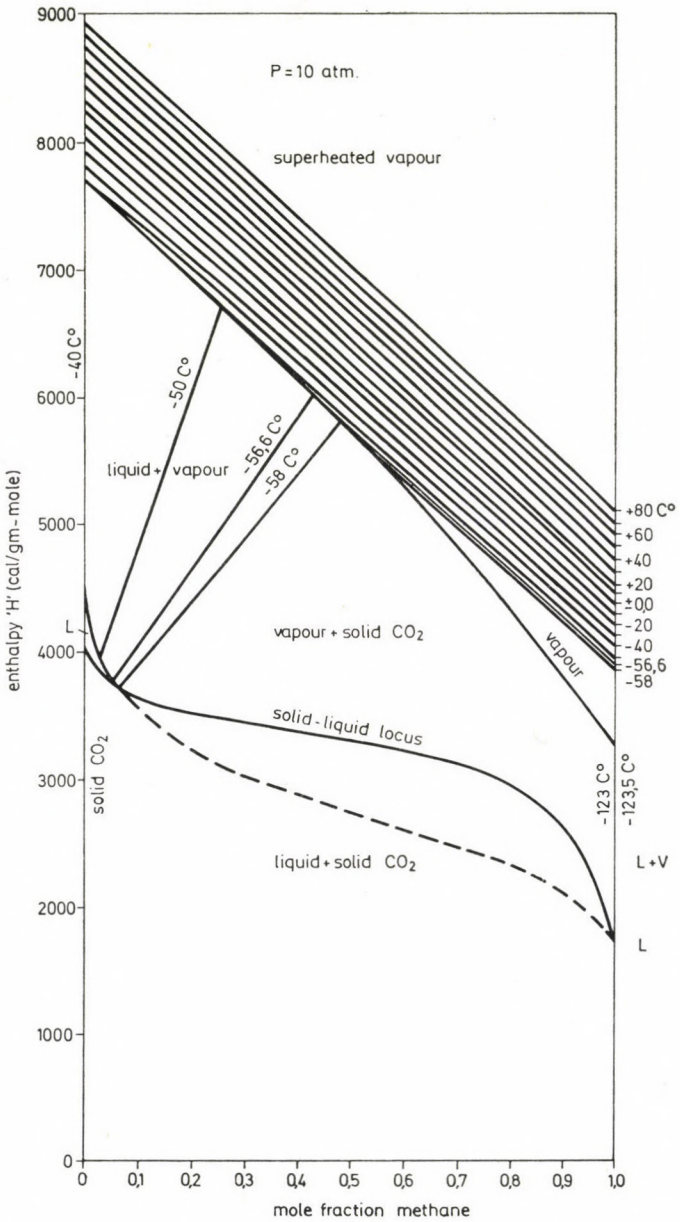

Fig. 16. Enthalpy-composition diagram for the methane-carbondioxide system at 10 atm.

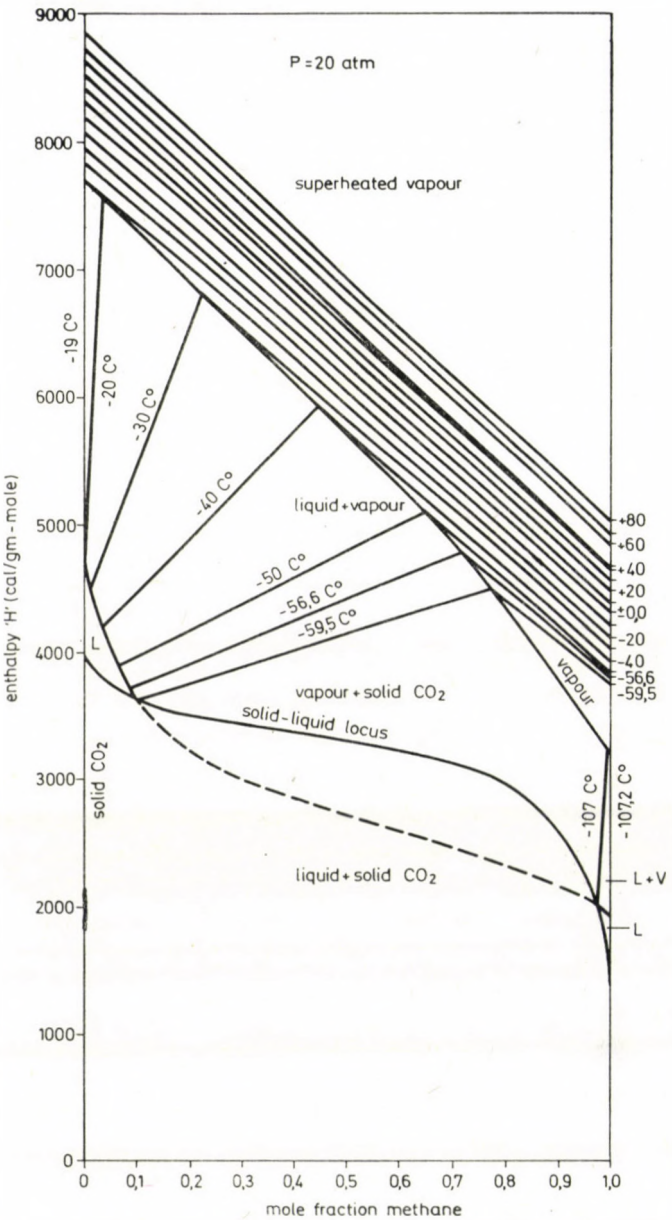

Fig. 17. **Enthalpy-composition diagram for the methane-carbondioxide system at 20 atm.**

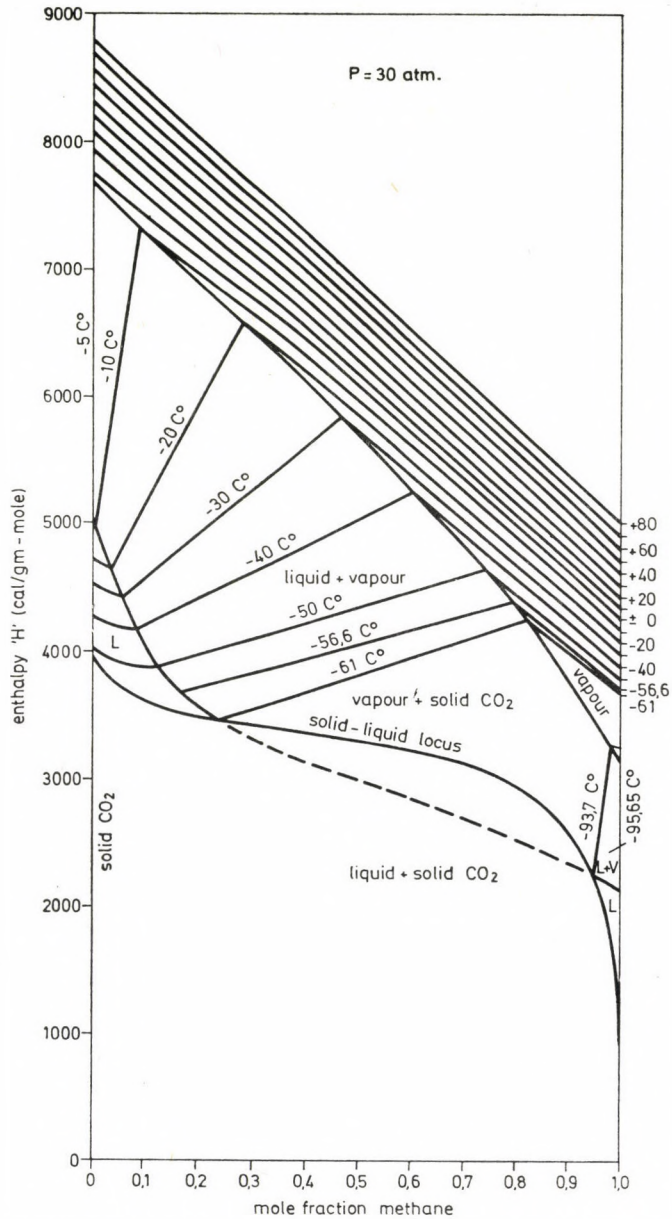

Fig. 18. Enthalpy-composition diagram for the methane-carbondioxide system at 30 atm.

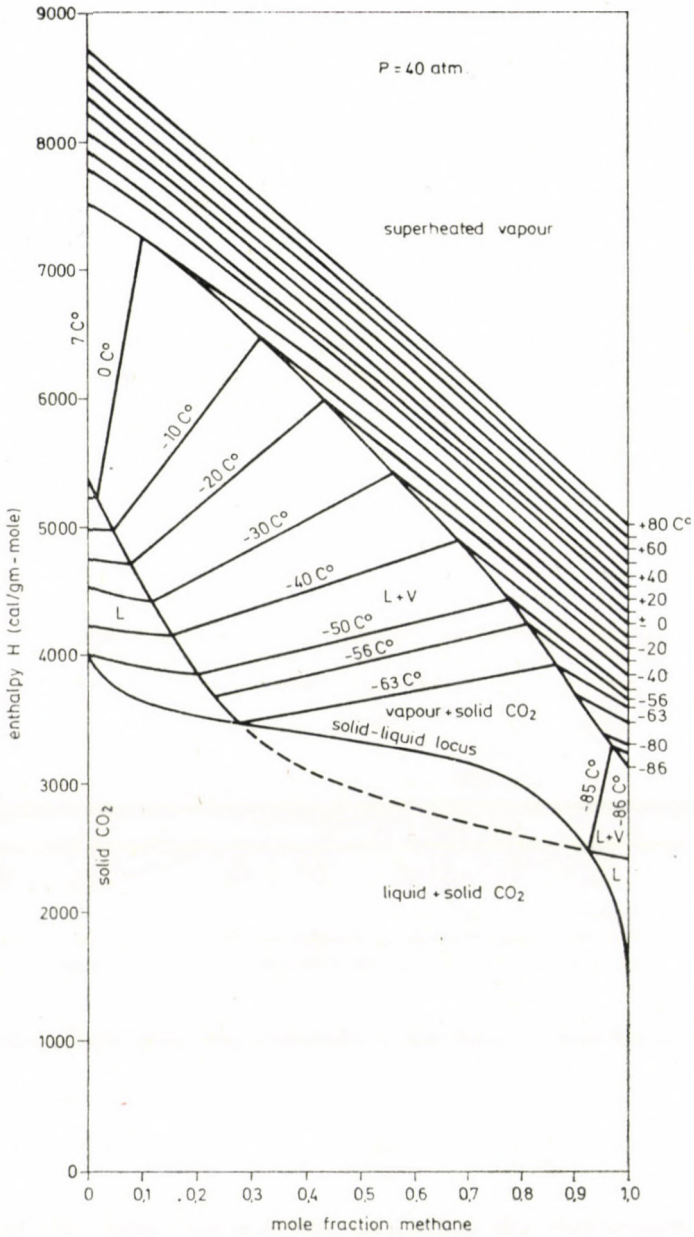

Fig. 19. Enthalpy-composition diagram for the methane-carbondioxide system at 40 atm.

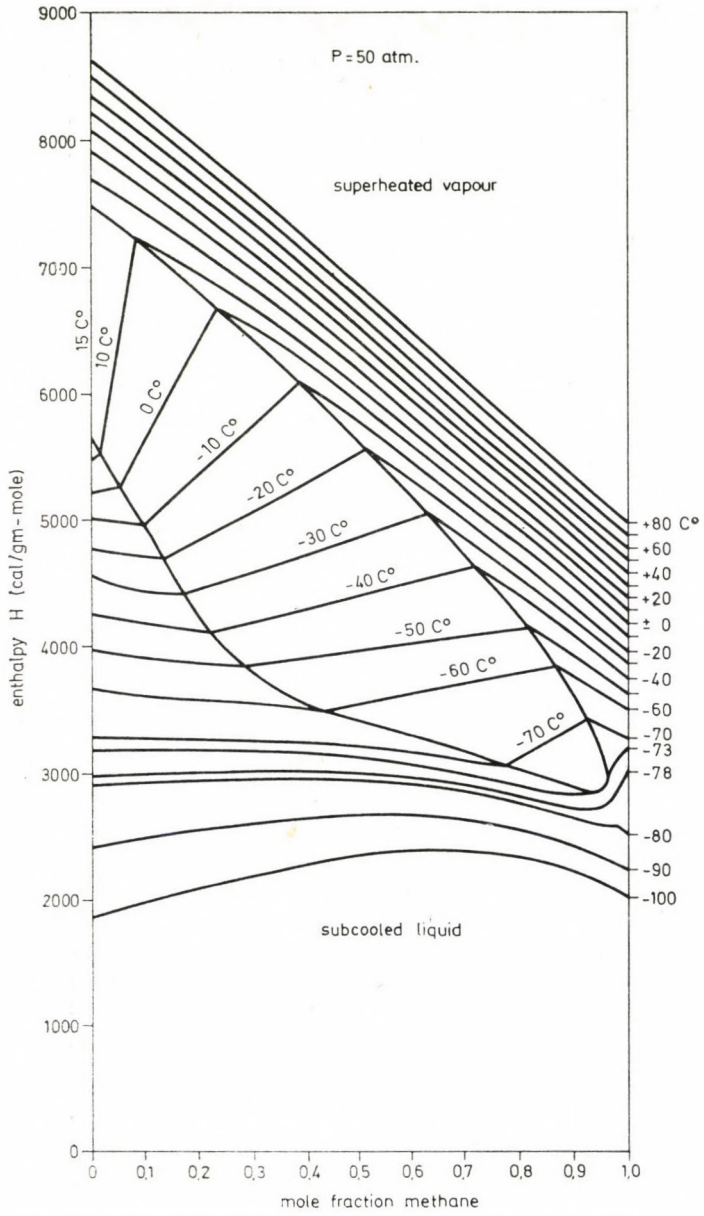

Fig. 20. **Enthalpy-composition diagram for the methane-carbondioxide system at 50 atm.**

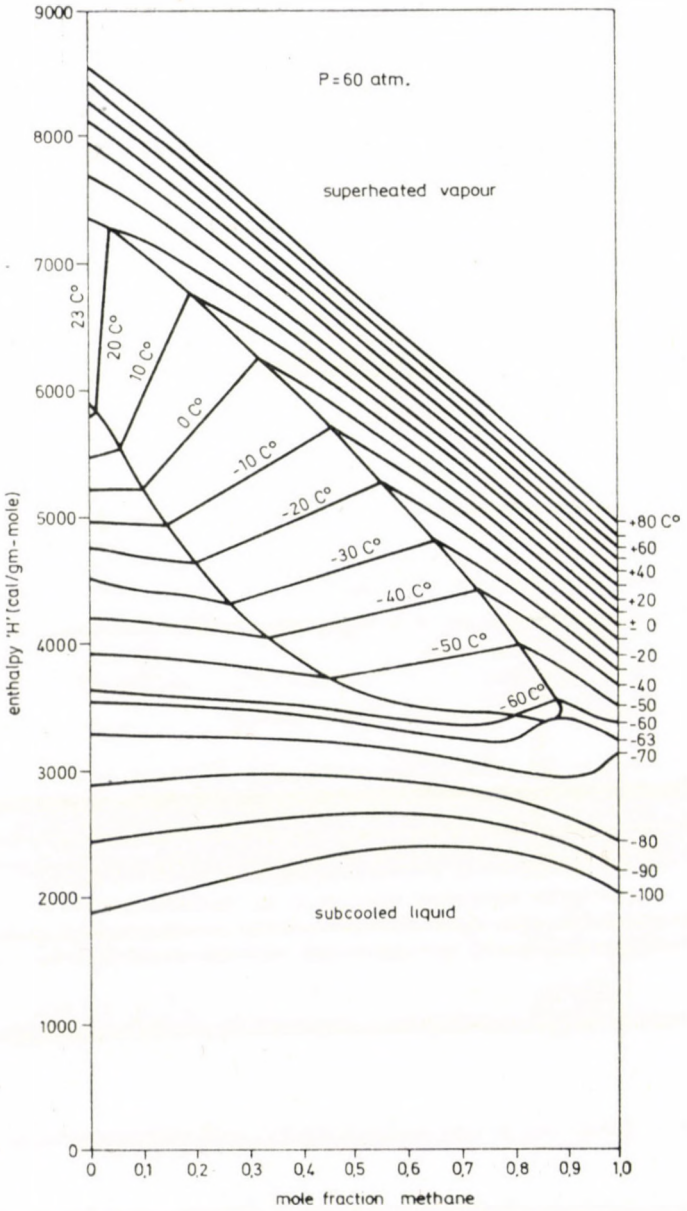

Fig. 21. Enthalpy-composition diagram for the methane-carbondioxide system at 60 atm.

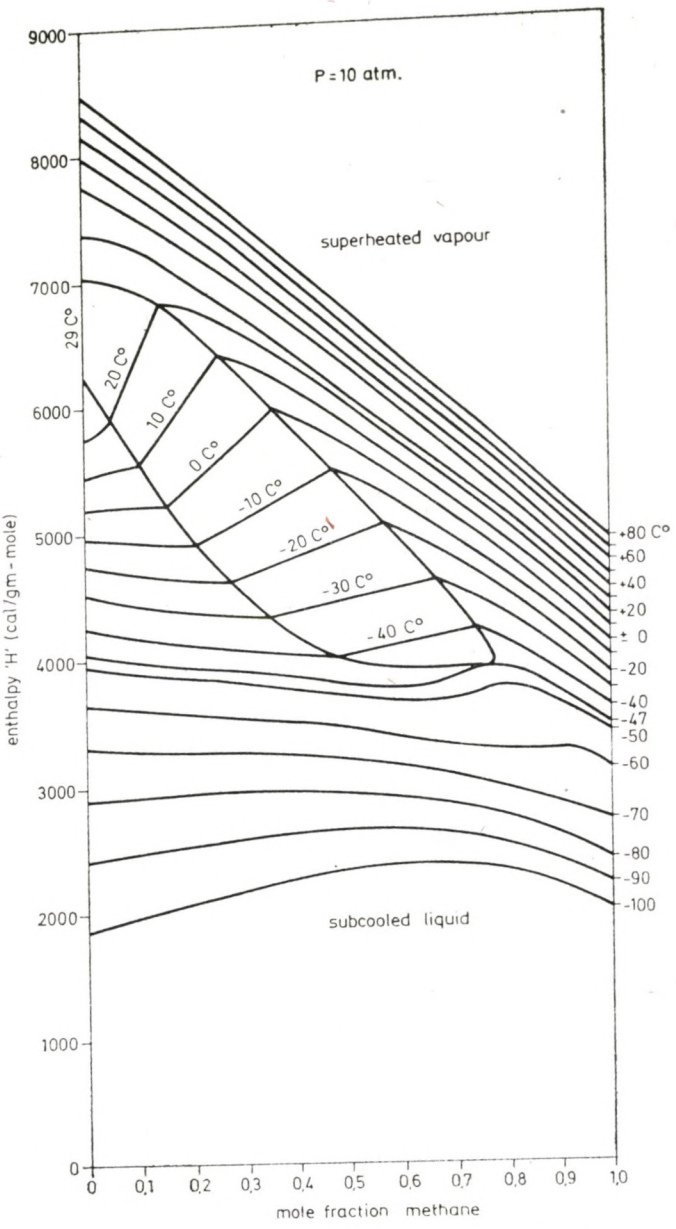

Fig. 22. Enthalpy-composition diagram for the methane-corbondioxide system at 70 atm.

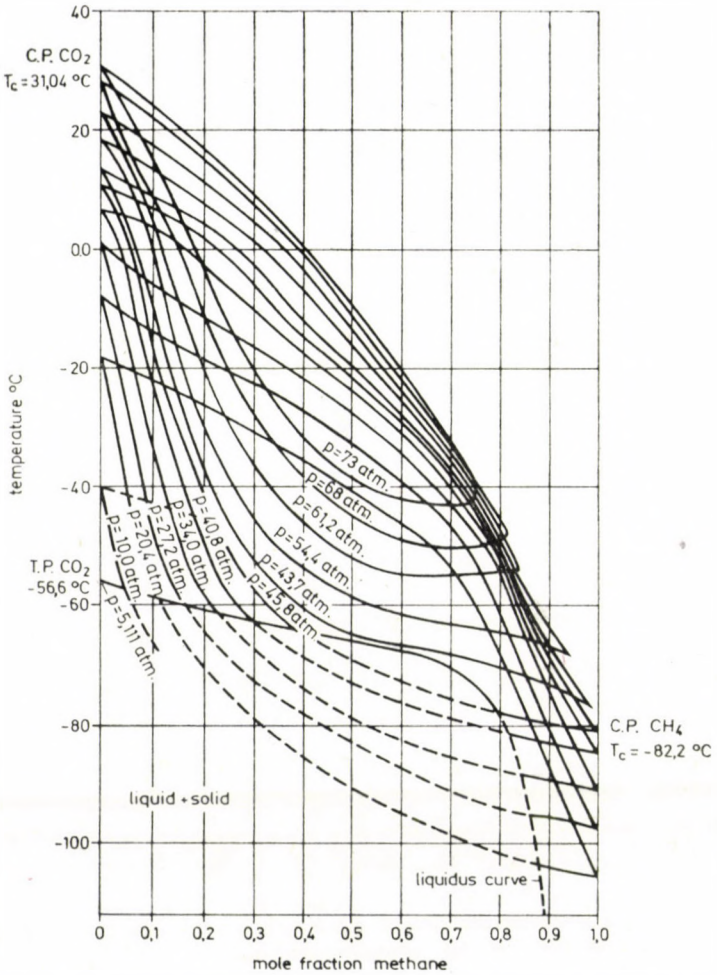

Fig. 23. Temperature-composition diagramme for methane-carbondioxide system (DONELLY & KATZ)

gas-phase excess enthalpy measurements of LEE and MATHER [11]. The remaining isothermal enthalpy curves are plotted from the data calculated by the BWR_{III} equation of state. The liquidus curve for the 10, 20, 30 and 40 atmosphere isobars is also drawn. The bubble point (saturated liquid) and the dew point (saturated vapour) curves are drawn with boiling points and dew points interpolated from Figs 23 and 24 based on the liquid-vapour equilibrium data of KAMINISHI et al. [12] and DONNELLY and KATZ [13]. Marked consistency is to be observed in these diagrams between the vapour-liquid, vapour-liquid-solid and the enthalpy data, both measured and calculated.

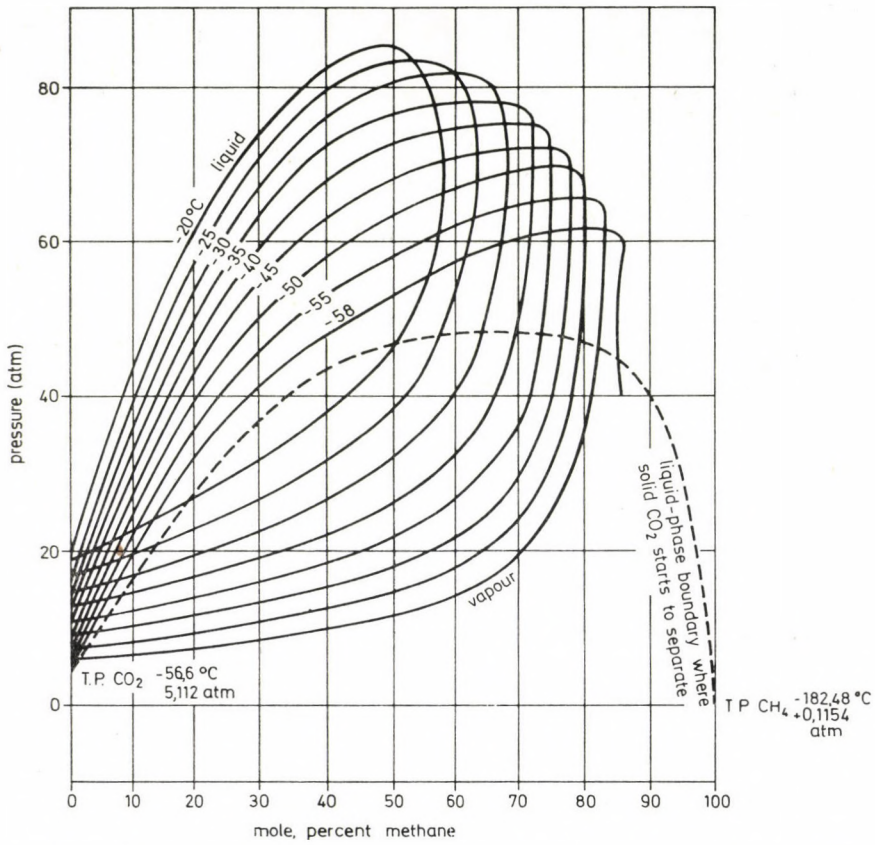

Fig. 24, Pressure-composition diagramme for the methane-carbondioxide system (Based on data of DONELLY & KATZ)

REFERENCES

1. BUKHARI, M. A. I.—BENEDICT, M.—WEBB, G. B. and RUBIN, L. C.: Equation, Part I.
2. BENEDICT, M.—WEBB, G. B.—RUBIN, L. C.: *J. Chem. Phys.* **8** (4), (1940), 334.
3. BENEDICT, M.—WEBB, G. B.—RUBIN, L. C.: *J. Chem. Phys.* **10**, (1942), 747.
4. BENEDICT, M.—WEBB, G. B.—RUBIN, L. C.: *Chem. Eng. Progress.* **47** (9), (1951), 449.
5. BENEDICT, M.—WEBB, G. B.—RUBIN, L. C.: *Chem. Eng. Progress.* **47** (11), (1951), 571.
6. BENEDICT, M.—WEBB, G. B.—RUBIN, L. C.: *Chem. Eng. Progress.* **47** (12), (1951), 609.
7. BISHNOI, P. R.—ROBINSON, D. B.: *Can. J. Chem. Eng.* **49**, (1971), 642.
8. BISHNOI, P. R.—ROBINSON, D. B.: *Can. J. Chem. Eng.* **50**, (1972), 101.
9. BISHNOI, P. R.—ROBINSON, D. B.: *Can. J. Chem. Eng.* **50**, (1972), 506.
10. ARAI, Y.—KAMINISHI, G.—SAITO, S.: *J. Chem. Eng. Japan* **4** (2), (1971), 113.
11. LEE, J. I.—MATHER, A. E.: *Can. J. Chem. Eng.* **50, 95,** February (1972).
12. KAMINISHI, G. I.—ARAI, Y.—MAEDA, S.: *J. Chem. Eng. Japan* **1** (2), (1968), 109.
13. DONELLY, G. H.—KATZ, D. L.: *Ind. Eng. Chem.* **46** (3), (1954), 511.
14. BUKHARI, M. A. I.: Enthalpy-Composition Diagrams for the Methane-Carbondioxide System and Correlations of Volumetric and Thermodynamic Properties. A Candidate of Science Dissertation, Technical University of Budapest, Department of Energetics, 1974.

Anwendung der Zustandsgleichung zur Ermittlung der volumetrischen und thermodynamischen Kennwerte des CH_4—CO_2 Systems. II. Teil. — Im ersten und zweiten Teil der Abhandlung wurden die BWR Zustandsgleichung, die revidierten Komponentenparameter und die durch die Anwendung der neuen Mischungsregel gerechneten P-V-T-X Angaben mit besonderer Rücksicht auf die hohen Druck- und niedrigen Temperaturwerte, wo die binäre Wechselwirkung eine immer größere Rolle spielt, behandelt. Die Endresultate der Rechnungen, d. h., die Diagramme der Mischungswärmen, sowie dieselben der Enthalpiezusammensetzung im Druckbereich von 10 bis 80 at und im Temperaturbereich von —120 bis +30 °C werden präsentiert. Die Rechnungen umfassen das Gasbereich, das L-V Gleichgewichtsbereich, das L-bereich und das S-L-V Gleichgewichtsbereich.

Acta Technica Academiae Scientiarum Hungaricae, Tomus 92 (3—4), pp. 351—370 (1982)

THE EFFECT OF WATER JET LANCING ON MEMBRANE-WALL TUBES LIFE

Z. PAMMER*

[Manuscript received 21 January 1981]

Ash and slag deposits on furnace tubes of coal-fired power station boilers are, in most cases, removed by high-speed cold water jet, also called water lancing. Due to sudden temperature changes in the membrane wall this technology causes severe thermal shock which, after to a certain number of repeated applications, may result in the rupture of the membrane wall. Frequency of the use of water-lance is a matter of economy. If they are rarely used, the large amount of slag deposits on steam generating surfaces would unfavourably modify the temperature conditions of heat transferring boiler surfaces and would thereby reduce boiler efficiency and the life of superheater surfaces. If it is frequently used, they would shorten the life of membrane wall which is also functioning as an evaporation surface. Determination of the stresses caused by water lancing is fundamentally important with regard to the frequency of optimal watering and a technology for longer wall-life are to be elaborated. To reach this goal, the finite-element programme system developed earlier has been applied.

Symbols

P	pressure	MPa
r	radius	m
t	time	s
x, y, z	Cartesian coordinates	m
A_x, A_z	cross-sections perpendicular to x and z axis, respectively	m^2
E	modulus of elasticity	MPa
N	number of cycles	—
T	temperature	K
σ_r, σ_t	stress components in a polar coordinate system	MPa
$\sigma_x, \sigma_y, \sigma_z$	stress components in Cartesian coordinates	MPa
σ_E	equivalent stresses according to MOHR	MPa
σ_a	stress amplitude	MPa
β	linear thermal expansion coefficient	1/K
μ	Poisson's ratio	—
ε_z	strain in direction of z axis	—
α	heat transfer coefficient	W/m^2 K
T_s	saturation temperature of the steam-water mixture	K
q	heat flux	W/m^2

1. Introduction

The steam generating surface of an up-to-date gas-tight steam boiler is the so-called membrane-wall type where gas-tightness is provided by "fins" welded between the evaporator tubes (Fig. 1). In case of pulverized coal

* PAMMER Z., Kazinczy u. 9, H-1191 Budapest, Hungary

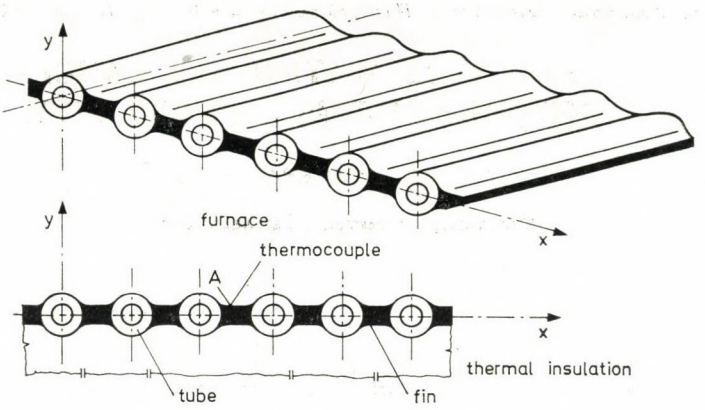

Fig. 1. A membrane wall configuration

firing, and depending on the coal type and firing method, slag of different thickness and compactness would be formed on the membrane wall surface. Because of the bad heat conductivity of the slag layers heat transmission from the furnace would be reduced, temperature conditions of the membrane wall would be altered, resulting in an uneconomical steam production.

One of the methods most widely used for the removal of slag is the so-called water lancing, carried out with a cold water jet. The essence of this technology is that the high-speed water jet from the water lance (penetrating into the furnace), has a mechanically cleaning effect and, on reaching the glowing slag, will abruptly cool down the latter. Thermal stresses thus arising will break the whole slag layer to pieces and would thus help to remove it. The drawback of the method is that, the water jet reaching the membrane wall surface (already cleaned), would cause considerable thermal stresses, leading to a rupture of the tubes after frequent repetitions.

2. Operating conditions of membrane wall

The heat transmission in the combustion chamber takes place by radiation. The heat flux depends largely on the firing method and on wall slagging. The wall has a thermal insulation on the outside surface. Radiated heat quantity is received by the steam-water mixture (flowing in the tubes) at a high heat transfer coefficient being characteristic of boiling (under adequate flow conditions [1, 2]). Wall temperature would then remain near to saturation temperature. Water blowing being started, a water jet bundle from water lance cleans the surface, while passing along a spiral line around the lance axis. A simple water blower is able to clean the inside wall surface within

a 3.0—3.8 m radius circle. During a blowing cycle the blower-head will advance 350 mm inside the furnace, by making 11 or 28 turns (type Dukla or Bergemann respectively). From the Dukla blower-head water flows through 2 nozzles, from the Bergemann head through 1 nozzle, of 8 mm diameter in each case. Recommended water pressure: 1—1.5 MPa; temperature: about 10—20 °C.

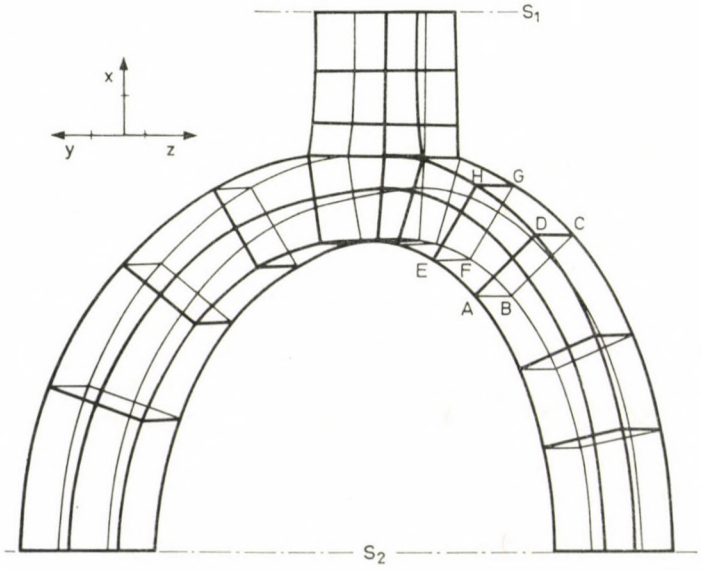

Fig. 2. Membrane wall finite element model

Under the effect of strong cooling a process of transient temperature change would take place. This is well illustrated by measurements made in the Tusimice-2 Power Station [3]. In Fig. 2 the thermo-couple can be seen, installed at point marked "A", on the furnace side of the front surface of the membrane-wall fin. (Figure 5 shows the temperature variation vs. time.) Water jet bundle, while going around, and reaching wall surface near to the thermo-couple, resulted in a thermal shock of more than 100 °C. During a cleaning cycle this transient process would be repeated several times (11 or 28 times) with a cycle time equal to the number of rotations of the water sprayer.

2.1 *Recent studies for determining stresses*

Research on membrane wall structures can be divided into 3 groups:
- observations, experiments made in laboratories and plants,
- investigations of effects on membrane wall during operations, using temperature measurements,

— distribution of temperatures and stresses in membrane wall, determined for given temperature and mechanical boundary conditions.

Tests carried out by K. H. Bieber and W. Hermann [7] belong to the first two groups. The experimental device constructed for this purpose was exposed, similar to normal operating conditions. Water jet bundle came periodically in contact with various parts of the wall.

The number of cycles leading to the rupture of the tubes was between 12×10^3 and 140×10^3, in function of the angle between the water jet bundle and tube axis, of flow conditions and of tube surface fouling. In each case damages arose in the tube crown-fin zone.

Tests by J. Misek [3] in the Tusimice-2 Power Station (mentioned before) concern the second group. He used water blowers, types Bergmann and Dukla, and measured temperature changes at different distances from the lances axis. There were significant differences in temperature drop amplitudes both in the function of location and in the course of successive cycles resulting from the circular motion of lance during a single water spraying period.

The calculation method by J. Voborsky [6] concerns the third group. For determining the arising stress he used the formula:

$$\sigma = \frac{E\beta\Delta T}{1-\mu} AB$$

where:

E	MPa	modulus of elasticity
β	1/K	linear thermal expansion coefficient
μ		Poisson's ratio
ΔT	K	amplitude of thermal shock during cycle
A		dimensionless constant determined in function of Fourier's number produced by the fin wall thickness, by means of a diagram [10]
B		dimensionless "weld factor"

Constant value of B was established by Voborsky with $B = 3.0$ under reference to [7]. Following this calculation and by using Langer's fatigue relationship he obtained $13.,5 \times 10^3$ as a marginal cycle number for fatigue.

This calculation has a certain advantage in its simplicity. Its physical conception could be accepted if value of "weld factor" B could be determined in function of temperature boundary conditions, geometrical design, etc. However, the present information, either from research results or operating conditions, is insufficient.

Bijlaard et al. used a refined model [11] for determining stresses arising in a steady-state condition (without lancing). They determined the temperature distribution by using the finite difference method and, for calculating the stress distribution. The membrane wall was separated into two parts. They tried to find solutions in analytic forms and used assumptions on continuity between tubes and fins. Bijlaard's method was questioned by Pasquantonio and Macchi [12] because it did not provide for continuity of

stresses between tubes and fins, and conditions of equilibrium were not satisfied. To make calculation more accurate, they used the finite element method for determining both stationary temperature and stress distribution. BRANDES and MARTIN [13] also used the finite element method for analysing the steady-state condition of the membrane wall structure. Stresses on tubes was studied by them for the case of internal pressure and for weight load distributed along the longitudinal sections of fins. The latter case of load had to be considered because the wall construction consisted of tubes with horizontal axes. Apart from the analysis of the components tubes and fins the entire membrane wall was modelled as an orthotropic plane wall, and included in the analysis were the stresses caused by unequal warming-up and supports.

WILHELM et al. [8] measured temperatures on front surfaces on the furnace side of tubes and fins, under effect of water lancing applied in a 60 MW boiler with the membrane wall of the Midwestern Power Station, and considered these time-temperature histories as a checking parameter of the calculation model. They obtained 48 000 as an estimated number of cycles for fatigue from the calculated stress amplitudes, in accordance with the ASME Boiler and Pressure Vessel Code (§ VIII).

In the light of these experimental and operating experiences the reliability of membrane-wall boilers (either existing ones like those at DHV or "7 November" or under planning like those at Bicske) would call for the developing of an up-to-date testing method. This has been made possible by the finite element programme system (elaborated by VEIKI) suitable for two-dimensional and axi-symmetric transient heat conductivity and elasticity problems [14, 15].

3. The finite-element model

In the light of the above operating and experimental experiences the distribution of temperatures and stresses and their variations with time are influenced by the following factors.

3.1 *Factors influencing the process of temperature changes*

- Distribution of heat flux density in a furnace. Tests made with the view factor described in [12] confirmed that the temperature field shows little sensitivity to the investigated heat flux distribution.
- Velocity profile, temperature of the water jet; angles between the water jet axis, the wall plane normal and the axes of tubes respectively; effects of geometric ratios of tube fin and of slagging size on water jet deflection; thermal properties of solid layer deposits on surface. These factors are taken into account by an equivalent heat

transfer coefficient with a varying distribution along the surface; size of this coefficient can be determined from the temperature measurement points mentioned in the previous paragraph. In cases of extreme watering angle or slagging, additional intermediate measuring points may be needed.

— Temperature, heat transfer coefficient of medium flowing inside the tube. Both in steady-state condition and during watering process high heat transfer may be assumed because of the presence of a two-phase medium. For determining the heat transfer coefficient a number of measurement results and relationships obtained from experiments can be seen [2], which show highly different values in dependence on measurement conditions. Order of magnitude of the heat transfer coefficient is 10^4 W/m^{2}K.

— The membrane wall can be considered as being practically perfectly heat-insulated from the external side. If required, special examinations can be made for determining temperature conditions arising around supports.

— Thermal characteristics of materials. Thermal conductivity, density, specific heat of wall may vary in function of location; their dependence on temperature can be considered by an iteration procedure. In view of the possible ranges of temperature and steel types no major error will be made, even if average values related to temperature intervals are taken into consideration, as experienced during our earlier examinations [2].

3.2 *Factors influencing distribution of stresses*

Effects caused by stresses in the membrane wall can be reasonably divided into two main groups as was done by BRANDES and MARTIN [13]. Accordingly, examination should be carried out on two levels, in accordance with the properties of construction.

I. Stresses arising because of suspensions, supports, net weight and thermal expansion of the wall. In this case the membrane wall consisting of a series of tubes and fins can be modelled as an orthotropic plane wall.

II. Local stresses arising in a single tube-fin component, is caused in the tube crown and fin by unequal distribution of temperatures and by internal pressure.

For calculating stresses mentioned in case II. a piece of tube crown—fin (Fig. 2) cut out from a membrane wall (Fig. 1) will be examined in the following. Conditions of connection to the surrounding membrane wall will be considered as geometric and mechanical load boundary conditions contained in a finite-element model shown in Figure 2.

3.2.1 Geometric conditions

a) Planes perpendicular to axis x: planes S_1 and S_2 shown in Figure 2 will remain median planes, even during deformation.

b) Planes perpendicular to axis z will remain parallel during deformation; i.e. strain along axis z would change only in function of time:

$$\varepsilon_z = \varepsilon_{z0}(t) .$$

3.2.2 Boundary loads

Distribution of boundary loads along the surfaces can be written in a general form as divided into a "force" and a "moment" parts.

a) In planes perpendicular to axis x:

$$\sigma_{xS_1}(y, z, t) = \sigma_{xF}(t) + \sigma_{xM}(y, z, t)$$

where

$$\sigma_{xF}(t) = \frac{1}{A_x} \int_{A_x} \sigma_{xS_1}(y, z, t)\, dy\, dz .$$

A_x — unit cross section of z length, cut out from membrane wall by plane S_1.

b) In planes perpendicular to axis z:

$$\sigma_{zS}(x, y, t) = \sigma_{zF}(t) + \sigma_{zM}(y, x, t)$$

where

$$\sigma_{zF}(t) = \frac{1}{A_z} \int_{A_z} \sigma_{zS}(x, y, t)\, dx\, dy$$

A_z — tube-fin cross section cut out by planes perpendicular to axis z.

The integrals written in paragraphs *a)* and *b)* can be determined from the following relationships:

$$\sigma_{xF}(t) = \sigma_{xH} + \sigma_{xT}(t) ,$$

$$\sigma_{zF}(t) = \sigma_{zP} + \sigma_{zW} + \sigma_{zT}(t)$$

where each load component can be interpreted as follows:

I. σ_{xH}: additional stress in direction x resulting from external support of membrane wall;
II. σ_{zP}: stress in direction of tube axis, resulting from internal pressure;
III. σ_{zW}: additional stress resulting from weight load (membrane design has been assumed to have vertical tube axes).

In the following the additional loads σ_{xH} and σ_{zW}, which can be determined as based on the knowledge of location and the given construction, will

be neglected. The boundary load in direction of tube axis, resulting from internal pressure, can be determined from the equilibrium:

$$\sigma_{zP} = p \frac{A_{z0}}{A_z}$$

where A_{z0} is the area of circle calculated with the inner tube diameter.

IV. $\sigma_{xT}(t)$; $\sigma_{zT}(t)$. During water lancing the wall section cooled by water jet would contract. The surrounding wall, having a steady temperature, wants to restrain this contraction. This mutual effect will be considered with these boundary loads acting in directions x and z, respectively.

WILHELM et al. [8] determined boundary stresses described in the preceding paragraph IV from a condition that they considered to be in the neighbourhood of a wall section touched by water jet to have infinite rigidity; the fin edge was fixed to the steady-state thermal growth.

Let us test the correctness of this assumption by a model giving more appropriate boundary conditions. Let the wall, except for the section touched by water jet, be considered as having a constant temperature. In order to simplify the deduction let us assume that temperature distribution has a circular symmetry, and reaches a maximum value at a location where $r = 0$ (Fig. 3).

Orthotropy of membrane wall will be abandoned, and a plane wall of constant thickness will be examined. The condition for equilibrium in this

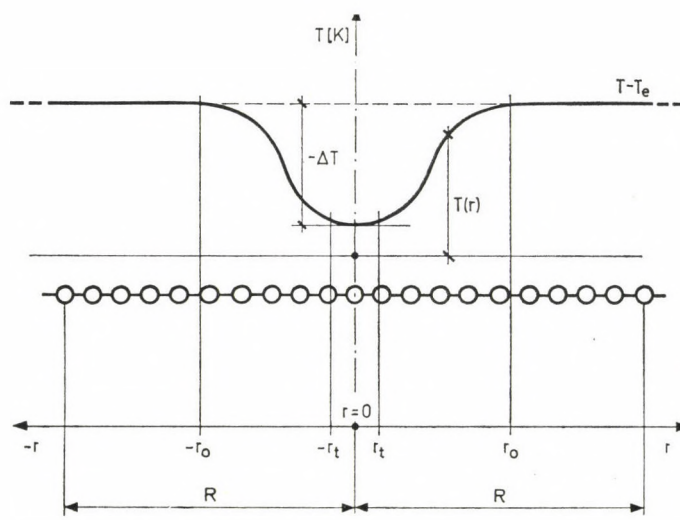

Fig. **3.** Temperature distribution above membrane wall

case (condition of plane stress) is given by the differential equation

$$r\frac{d\sigma_r}{dr} + (\sigma_r - \sigma_t) = 0$$

where
σ_r, σ_t is the radial and tangential stress component, respectively. A general solution can be written in the forms:

$$\sigma_r(r) = -E\beta\frac{1}{r^2}\int_0^r T(r)\, r\, dr + C$$

$$\sigma_t(r) = E\beta\left(\frac{1}{r^2}\int_0^r T(r)\, r\, dr - T\right) + C$$

where C is a constant dependent on boundary condition.

Let us approximate temperature distribution, in the neighbourhood of symmetry axis $r = 0$, by its tangent within a range of $|r| < r_t$.

In the following the stresses will be examined, which would arise in wall section $|r| < r_t$ if it is considered to be surrounded by an extensive wall area of radius R, or if the edge of radius r_t has been fixed.

I. In case of a plane wall with a free edge dimensioned with $R \gg r_t$ maximum stress values will be obtained at the point $r = 0$:

$$\sigma_r = \sigma_t = -E\beta\frac{\Delta T}{2}\,.$$

II. By assuming a clamped edge with radius r_t that means an infinite rigid enclosure of temperature, T_e we obtain:

$$\sigma_r^* = \sigma_t^* = -E\beta\frac{\Delta T}{1-\mu}$$

where, by using symbols of Figure 3, the temperature difference of ΔT will be:

$$\Delta T = T(r = 0) - T_e\,,$$

Ratio of stresses obtained in the previous cases:

$$b = \frac{\sigma_r}{\sigma_r^*} = \frac{\sigma_t}{\sigma_t^*} = \frac{1-\mu}{2}\,,$$

if

$$\mu = 0{,}3 \Rightarrow b = 0{,}35\,.$$

In a fixed condition as assumed by WILHELM et al. [8], related to a model where reality is better approximated. Boundary load resulting from

differential thermal expansion will be obtained with a value of nearly three times as high.

Results obtained from the approximating model will be used as follows for determining boundary load $\sigma_{xT}(t)$, $\sigma_{zT}(t)$:

I. In direction of coordinate axis x:

Planes S_1, S_2 are fixed in direction x, the boundary load $\sigma_{xT}(t)$ will be determined from the modified temperature distribution:

$$T^*(x, y, t) = T(x, y, t) - T_e$$

T_e is an average temperature characteristic of the surrounding wall section with constant temperature whose value will be determined from the following condition:

$$\sigma^*_{xT}\,(t < t_e) = 0$$

where $t < t_e$ indicates steady-state condition prior to operation of the water blower. Actual boundary load will be given by the following relationship:

$$\sigma_{xT}(t) = \frac{1 - \mu}{2}\,\sigma^*_{xT}(t)\,.$$

II. In direction z, since cross-sectional dimensions have not changed along this axis, we obtain:

$$\sigma_{zT}(t) = -E\beta\,\frac{1}{A_z}\int_{A_z}\frac{T^*(x, y, t)}{2}\,dx\,dy\,.$$

The strain value of $\varepsilon_z(x, y, t) = \varepsilon_{z0}(t)$, which was written in item 3.2.1 b, have to be determined from the following expression:

$$\sigma_{zF}(t) = p\,\frac{A_{z0}}{A_z} + \sigma_{zT}(t)\,.$$

4. Calculation results

Pressure of the steam-water mixture flowing inside the tube was $p =$ $= 18$ MPa according to data in [3]. The equivalent stress distribution is indicated along a few longitudinal sections in Figure 4.

As shown by these results, the stress distribution caused by internal pressure is hardly influenced by fins. In Figure 4 a comparison is made between the analytic solution for thick-walled tubes and the finite element results obtained in S_2 sections of Figure 2, which show a good agreement.

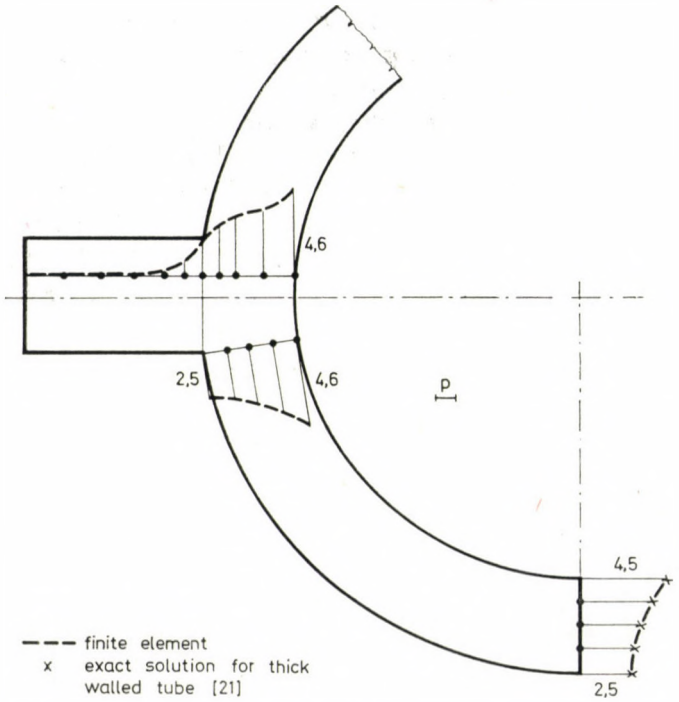

Fig. 4. Distribution of equivalent stress according to MOHR, caused by internal pressure p, related to value of internal pressure

4.1 *Temperature distribution during water blowing process*

For calculating transient temperature distribution we used the measurement results in Figure 5. This shows time-temperature variation measured by thermo-couple during watering process. This result was used for determining the external boundary condition of the computation model. Heat transfer coefficient on the inner side was considered constant during water lancing: $11{,}5 \cdot 10^3$ W/m^{2}K.

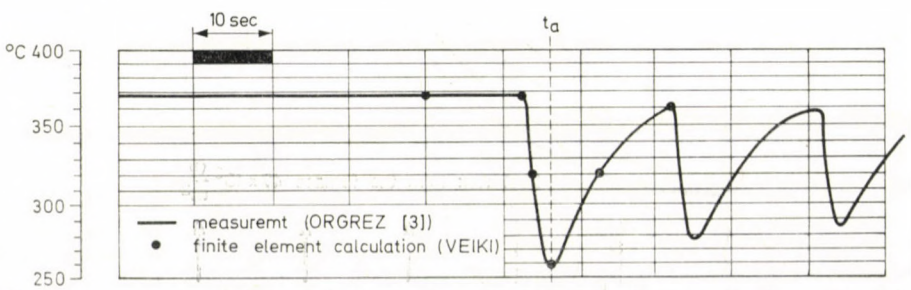

Fig. 5. Temperature variation with time under the influence of water lancing, at point A (Fig. 1)

The heat flux furnace was 47×10^3 W/m^2 in a steady-state condition. When water jet bundle, travelling around, reached the neighbourhood of measuring point, it caused a high temperature change in the wall (in Figure 10 the descending part of the curve ending at time *ta*). Water temperature was 20 °C, and the heat transfer coefficient of water-blowing 1725 W/m^{2}K. When the water jet had left the point of thermocouple location, a warming-up period followed (in Figure 5 a rising curve section after time *ta*) under the effect of heat radiation in the furnace and of internal heat transfer. Heat input in the tube was reduced by the heat required for evaporating water flowing down from the upper wall sections and, for this reason, the heat flux in this period was taken with a value of $29{,}4 \times 10^3$ W/m^2. Characteristics for tube materials 15MO3:

thermal conductivity:	41,13	W/m K
density:	7850	kg/m^3
specific heat:	0,6	KJ/kg K

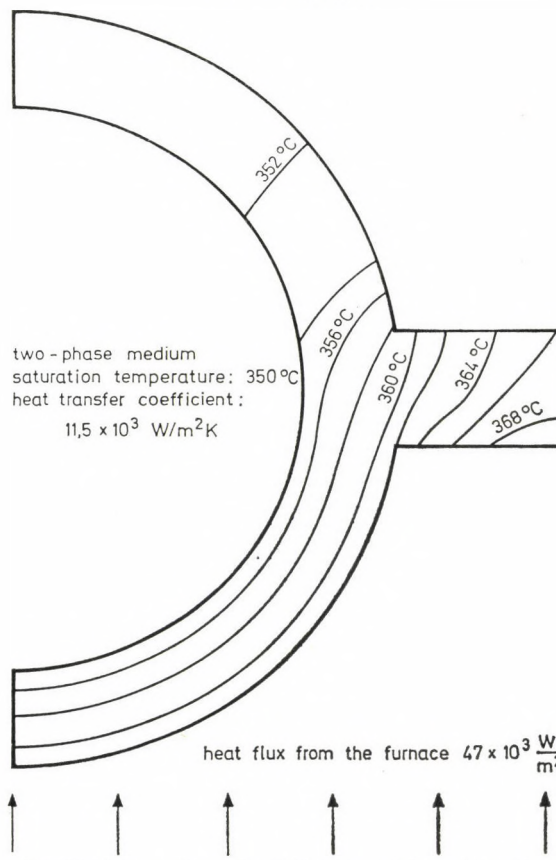

Fig. 6. Temperature distribution under the influence of heat flux from furnace, in steady-state condition

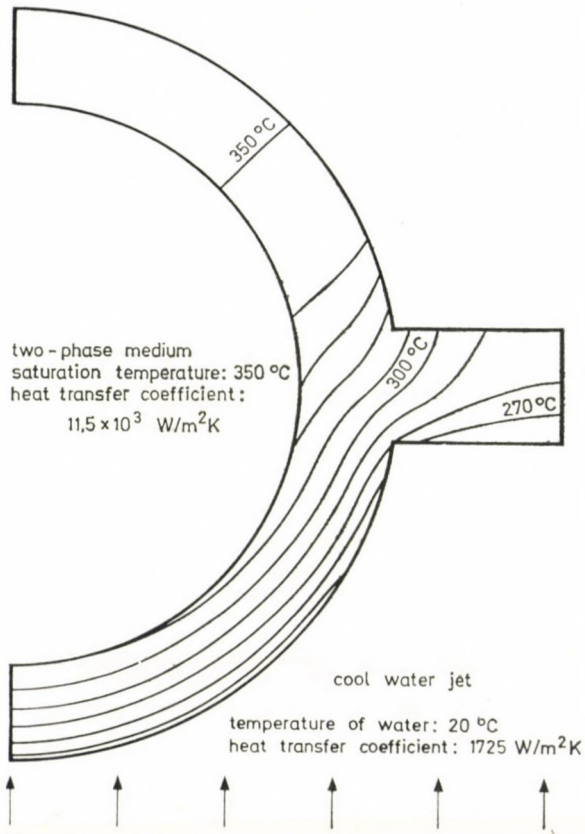

Fig. 7. Temperature distribution under influence of water lancing at a time marked t_a in Figure 5. Isotherms follow each other every 10 °C

The finite element mesh in the time-space range were determined in accordance with criteria established earlier for element dimensions [15]. This finite element mesh is applied to the calculation of stresses, as well.

Figures 6 and 7 contain isotherms of temperature; Fig. 6 shows operating condition prior to water blowing, while in Fig. 7 the effect of water lancing is indicated.

4.2 *Distribution of stresses under the influence of internal pressure and temperature differences*

Equivalent stresses were determined by using the calculation result of the transient temperature distribution described in section 4.2 and by applying boundary conditions discussed in section 3.2. In Figure 8 deformations of membrane-wall elements are shown; related to the condition of a constant temperature field T_e mentioned in section 3.2 (thin solid line).

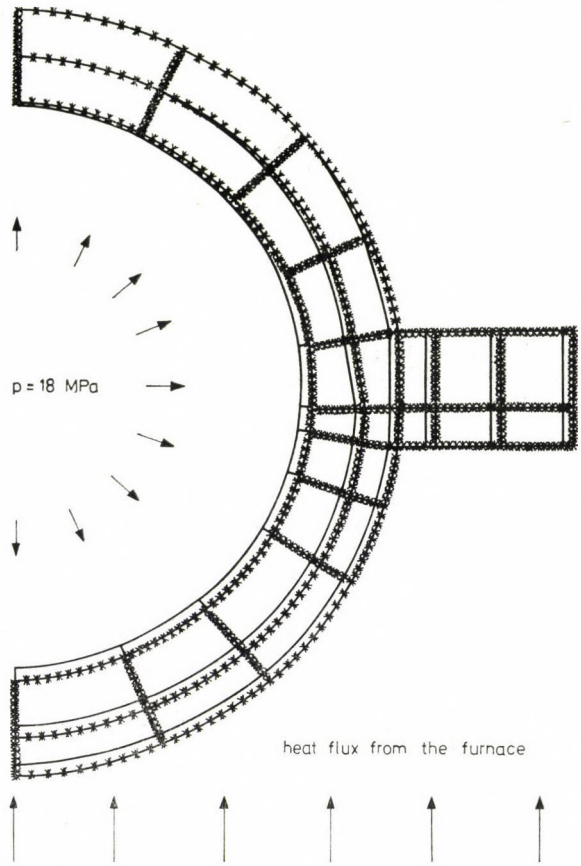

Fig. 8. Membrane-wall element deformed under the effects of internal pressure and heat flux from the furnace. Steady-state condition

Figure 9 contains the results of calculations made for determining boundary load in plane S_1 (shown in Figure 2) by preventing the parallel displacements of planes S_1 and S_2. Figure 10 shows the deformation obtained by applying boundary load, previously determined and modified, according to section 3.2.

In Figs 11 and 12 the distribution of stresses is illustrated. The type of distribution in a steady-state condition is decisively determined by stresses from internal pressure. During water lancing, due to the change of thermal conditions, there is a strong increase in stress on the furnace side, along the tube periphery and on the front surface of fin. Stress increase arising on surfaces on the furnace side is the smallest at the corner-point where tube and fin meets: 203 MPa. In respect of steady-state condition, PASQUANTONIO [12] also found a definite minimum for the stress distribution on the surface at this

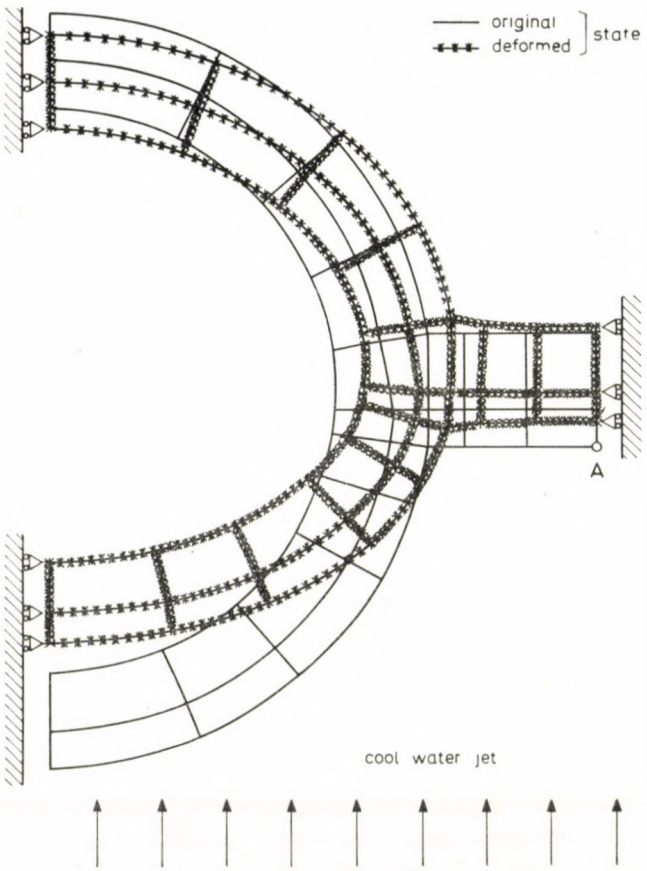

Fig. 9. Membrane-wall element deformed under the effect of water jet lancing. Displacement boundary conditions to calculate the boundary load distribution on the fin edge S_1 (Fig. 2)

point (in accordance with HMH theory). On the other hand, the experiments by BIEBER and HERRMANN [7] led to identify the majority of cracks just at this point. This contradiction is a strong indication that the theories (widely applied at present) *by* MOHR *or* HUBERT—MISES—HENCKY *for condition of equivalent stress do not give reliable information on damages in cases of multi-axial fatigue stresses.* Considering deformations in the neighbourhood of corner-point, together with the stress components, this is the case of a three-axle tensile stress.

In accordance with the theories both of MOHR and HMH the triaxial stress state is less dangerous, the smaller are the differences between the principal stress values. Thus, in case of "hydrostatic" tension or compression (when principal stresses are equal) even infinitely high stresses are not dangerous.

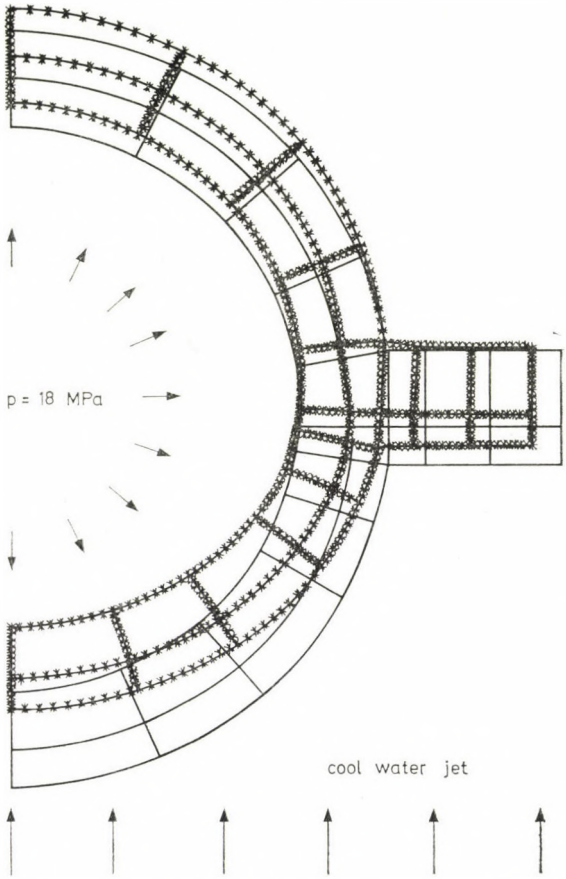

Fig. 10. Membrane-wall element deformed under effects of internal pressure and water lancing at a time marked t_a in Figure 5

The function of stress components has to be evaluated in a different way as was discussed from the viewpoint of fracture mechanics. In the course of manufacturing and operation cracks and discontinuities would arise, which start from the surface (e.g. at the corner-point mentioned a weld is located). WILLIAMS [17] has demonstrated that a crack tends toward a state of multi-axial hydrostatic tension. According to the HMH theory the dangerous character of a multi-axial stress condition is proportional to the size of deformation work. Tests made by WILLIAMS concerning fracture mechanics showed that cracks would start in the direction at the minimum of deformation work.

4.3 *Expected life of membrane wall*

Using stress distributions in Figs 11 and 12 we can determine the equivalent stress amplitude which will reach its maximum on the front surface (facing furnace) of tube. Maximum alternating stress amplitude:

$$\sigma_a = \frac{1}{2}(\sigma_{E\,max} - \sigma_{E\,min}) = \frac{1}{2}(294 - 33{,}5) = 130{,}3 \text{ MPa}\,.$$

Since diagrams of fatigue usually concern a medium stress of $\sigma_m = 0$, the equivalent stress amplitude σ_{a0} will be, on the basis of (23):

$$\sigma_{a0} = \sigma_a \frac{(2\sigma_B)^2}{(2\sigma_B)^2 - (2K_{0,2} - 2\sigma_a)^2}\,.$$

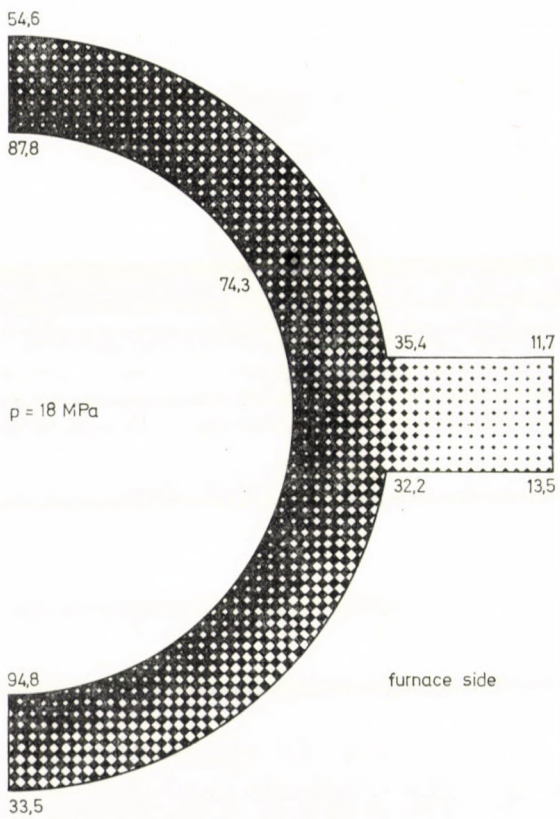

Fig. 11. Equivalent stress in MPa, under effects of internal pressure p and heat flux from furnace, according to MOHR. Steady-state condition

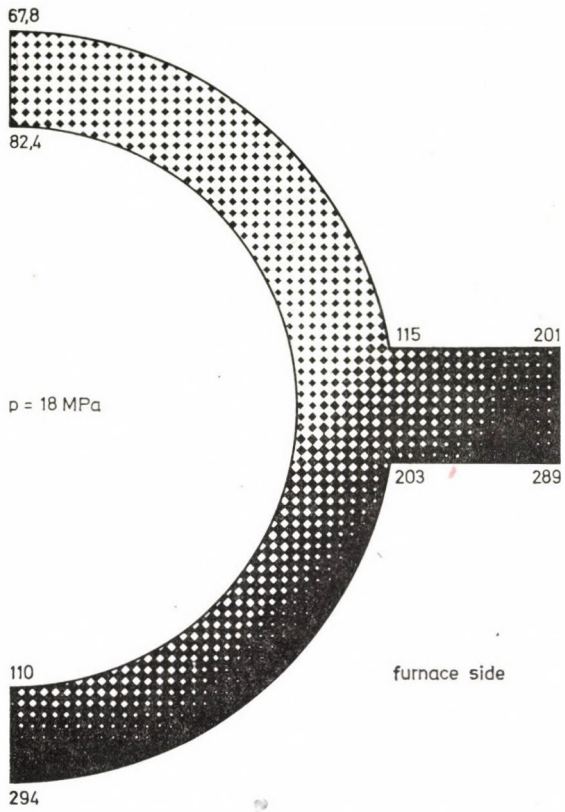

Fig. 12. Equivalent stress (according to MOHR) in MPa, under effects of internal pressure p and water lancing, at time marked t_a in Figure 5

According to standard MSZ 4747-63 the material characteristics of steel Mo 45.47 (equivalent with steel 15 Mo3), at temperature of 350 °C, are the following:

tensile strength	σ_B	= 350	MPa (VOBORSKY [6])
elasticity modulus	E	= $1{,}8\times10^5$	MPa
yield-point	$K_{0.2}$	= 190	MPa
linear thermal expansion factor	β	= $13{,}2\times10^{-6}$	1/K

Taking into account the above material characteristics:

$$\sigma_{a0} = 133 \text{ MPa} .$$

The temperature correction factor required for using diagram in accordance with ASME Boiler and Pressure Vessel Code (Sect. III) is

$$C = \frac{207}{E} = \frac{207\times10^3}{180\times10^3} = 1{,}15 ,$$

and so the permissible number of cycles from ASME fatigue curves for carbon steels:

$$N = 60 \times 10^3 .$$

A similar result is obtained by LANGER's [6] analytic relationship as well:

$$N = \left[\frac{0{,}174 \times E}{2\sigma_a - 0{,}35 \times \sigma_B} \right]^2 = 52 \times 10^3 .$$

Thermal fatigue tests by WELLINGER and KUSSMAUL [20] have shown that the probability interval of marginal cycle number for fatigue is applicable to the material 15 Mo3 at temperatures of 20 °C and 475 °C by performing a small-scale extrapolation, to consider plastic deformation:

$$20 \times 10^3 < N < 60 \times 10^3 .$$

Considering the temperature diagram of measuring point No. 9 [3] there are 13 cycles during a single water blowing operation. By assuming a single water lancing per day the *expected life of tube is* 12 *years*. Data from fatigue tests can be converted with a fairly high error percentage into normal operating conditions. These diagrams are not allowable for the effects resulting from heat-treatment, surface smoothness, quality of welding, stress corrosion, crack etc. for individual cases in manufacturing and operation. Thus, because of cracks arising from possible manufacturing defects, an occasional rupture of boiler tubes prior to the period specified should also be reckoned with.

5. Conclusions

The process of temperature changes is influenced by a number of factors which can be determined with difficulty. Therefore, in each case when the effect of water lancing is examined during operation, the temperatures measured by thermo-couples located on the front surfaces of tube and fin should be used as matching parameters of the calculation procedure.

According to calculations the greatest stress would be present in the crown of tubes front surface facing the furnace. From the value of equivalent stress amplitude obtained at this point, and from fatigue diagram applicable to the given material, the cycle number for fatigue resulting from water spraying can be determined. However, at tube-fin intersection (in the neighbourhood of welds) the presence of cracks caused by possible defects during manufacturing can be anticipated, and these cracks need to be considered differently in respect of useful life.

REFERENCES

1. SZABOLCS, G.: Investigation of the Flow in Parallel Boiler Water Tubes. *Acta Techn. Hung.* **81** (1975) 135—153.
2. PAMMER, Z.: Investigation of Thermal Stresses in Furnace Tube Wall under Operating Conditions. Diploma thesis. Budapest Technical University, 1976. (In Hungarian)
3. MISEK, J.: Overovani ucinnosti ostrikovacu. Dilci. ORGREZ 1976.
4. KUBICA, J.—ROSKO, Z.: Zkusenosti s ostrikovaci spalovaci komory kotlu v elektárne Tusimice-II. *Vizkumny Ustav Energeticky.* (1977).
5. PETZL, M.: Experimentalni overeni vlivu provozu ostrikovacu na zivotnost materiálu vyparniku kotle. *Vyzkumni Ustav Energeticky* (1978).
6. VOBORSKY, J.: Odhad zivotnosti membranové steny ohniste pri nasazení vodnich ostrikovacu. *Vizkumny Ustav Energeticky* (1976).
7. BIEBER, K. H.—HERRMANN, W.: Versuchsergebnisse und Betriebserfahrungen über den Einsatz von Wasserrussbläsern auf verschweißten Rohrwänden. *VGB Kraftwerkstechnik* **54** (1974), 699—707.
8. WILHELM, B. W.—SIMON, J. J.—NELSON, J. E.: The Effect of Water Jet Lancing on Furnace Wall Tubes. *Proc. Amer. Power Conf.* **37,** V. Chicago III. (1975), 410—420.
9. BORBÉNYI, I.—ERDEI, J.: Developed Technology of High-Temperature Strain-Gauges Fixing. Report. VEIKI, Budapest 1979. (In Hungarian)
10. Design Guide for LMFBR Sodium Piping. US Atomic Energy Commmission. Alabama, California 1971.
11. BIJLAARD, P. P. et al.: Thermal Stress Analysis of Nonuniformly Heated Cylindrical Shell and its Application to a Steam Generator Membrane Wall. *J. Engn. Power* Jan. (1968), 73—81.
12. DI PASQUANTONIO, F.—MACCHI, A.: Temperatures and Stresses in a Boiler Membrane Wall Tube. *Nuclear Eng. and Design* **31** (1974), 280—293.
13. BRANDES, H.—MARTIN, H.: Spannungen in Membranwänden durch Wärmebeanspruchung und mechanische Belastung. *VGB Kraftwerkstechnik* **55** Heft 1, Jan. (1975).
14. PAMMER, Z.: Finite Element Method for Stress Analysis. *Report. VEIKI,* Budapest 1978. (In Hungarian)
15. PAMMER, Z.: A Mesh Refinement Method for Transient Heat Conduction Problems Solved by Finite Elements. *Int. J. for Num. Meth. in Engn.* **15** (1980), 495—505.
16. GOLDENBLAT, I. I.: Stress Analysis in Engineering. Technical Press. Budapest 1969. (In Hungarian)
17. WILLIAMS, M. L.: On the Stress Distribution at the Base of a Stationary Crack. *Journal of Applied Mechanics.* March (1957).
18. ASME Boiler and Pressure Vessel Code. (sect. III, sect. VIII) 1974.
19. FREUDENTHAL, A. M. et al.: High Temperature Structures and Materials. Pergamon Press 1964.
20. WELLINGER, K.—KUSSMAUL, K.: Festigkeitsverhalten von Stählen bei wechselnder überelastischer Beanspruchung. *Mitteilungen der VGB* Heft **92** (1964).
21. GERSE, K.—MÓRICZ, I.—PAMMER, Z.: Stress Analysis of Boilers. Text-book press, Budapest 1979. (In Hungarian)
22. HAYMAN, J. R.—NELSON, J. E.: Water Lance Effectively Controls Slag. *Electrical World.* Dec. **15** (1973).

Auswirkung des Wasserstrahllancierens auf die Lebensdauer der Feuerrohre des Feuerbüchsenmembrans. — Eine der am meistens verbreiteten Entfernungsmethoden der Schlakkenablagerungen von den Feuerbüchsenrohren von kohlgeheizten Kraftwerkkesseln ist das mit großer Wassergeschwindigkeit durchgeführte sog. Kaltwasserstrahllancieren. Zur Ermittlung der in der Zeit veränderlichen Größe der Wärmespannungsbeanspruchung wurde das Programmsystem der Elementenmethode VEIKI angewandt. Das Modell der Elementenmethode, sowie die Rechnungs- und Messungsergebnisse werden für die Fälle von ständigen und transienten Betriebszuständen vorgeführt.

Acta Technica Academiae Scientiarum Hungaricae, Tomus 92 (3—4), pp. 371—382 (1981)

BRACKETING OF THE EIGENFREQUENCIES OF SPATIAL SKELETONS II.

GY. CZEGLÉDI*

[Manuscript received: 2 April. 1981]

This paper is the second part of a study, the first part of which has been published in this review. Another method will be presented for the analysis of vibrations of prismatic bar skeletons modelled as continua, relying on the basic system of differential equations and eliminating drawbacks proper to the previous method. In the last chapter, the practical application is illustrated on two simple numerical examples. Numbering of chapters, figures, formulas and tables is continued from the previous part rather than to start again.

2.4. Vibration analysis of prismatic bar skeletons using the basic system of differential equations

Mathematical fundamentals of the method presented in this chapter arise from the scope of the theory of differential equations. Its essential is to write boundary conditions for each bar of the skeleton yielding sufficient equations to determine the integration constants of the field functions.

In the following, parametric equation systems (5) and (7) for the external bar end force effects and bar end displacements will be reconsidered. The essential of this method is exactly not to eliminate equation parameters but to use them as unknown coefficients of the field functions, thereby the amplitude distribution of bars in the skeleton are directly available. Nodal displacement amplitudes are given by the field function.

2.4.1 Equation system comprising displacements and force effects of the skeleton components

Bar end displacement and force effect vectors in Eqs (5) and (7) have been conveniently written in the own system of coordinates, but bar jointing equations will also here be written in the common coordinate system. Displacement and force effect vectors in (5) and (7) will be transformed into the common coordinate system by means of transformation matrix $\mathbf{T}_i$:

* Gy. Czeglédi, Bartók Béla út 3/d, H-1225 Budapest, Hungary

$$
\begin{aligned}
u_i &= \mathbf{T}_i \tilde{u}_i = \mathbf{T}_i \mathbf{U}_i a_i \sin \omega t \,, \\
v_i &= \mathbf{T}_i \tilde{v}_i = \mathbf{T}_i \mathbf{V}_i a_i \sin \omega t \,, \\
f_i &= \mathbf{T}_i \tilde{f}_i = \mathbf{T}_i \mathbf{F}_i a_i \sin \omega t \,, \\
p_i &= \mathbf{T}_i \tilde{p}_i = \mathbf{T}_i \mathbf{P}_i a_i \sin \omega t \,,
\end{aligned} \tag{30}
$$

where — applying $\mathbf{t}_i$ from item *2.3.3*:

$$\mathbf{T}_i = \langle t_i, \; t_i \rangle \,.$$

Four equations in (30) refer to the i-th bar of the system. The equations above can be established for each of the n bars in the skeleton, formally comprised in the matrix equation:

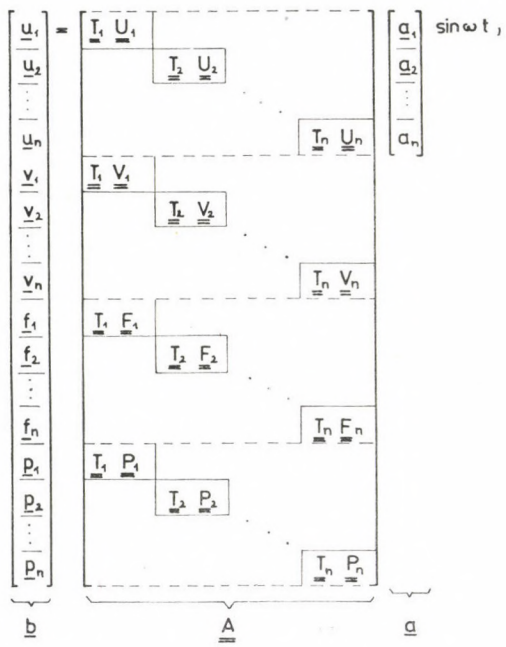

(31a)

or, in concise form:

$$b = \mathbf{A} a \sin \omega t \,. \tag{31b}$$

Thus Eq. (31b) contains bar end displacements and bar end force effects considered as external from the aspect of the n disjointed bars of the skeleton.

2.4.2 Equation for the skeleton vibrations

Matrices b and $\mathbf{A}$ defined in (31a) being available, now the disjointed skeleton bars will be recoupled to establish the equation for the vibration of the complete skeleton.

The way how separate bars are coupled to a structure is advisably expressed by a coupling matrix $\mathbf{K}$.

Matrix $\mathbf{K}$ comprises features of the boundary conditions of the structure, and of nodal joints of the bars, as well as nodal equilibria. Thus, it is more informative than are kinematic coupling matrix $\mathbf{G}$ under *2.3.3* and its transposed $\mathbf{G}^T$, since it comprises even the boundary conditions. Its establishment will be illustrated on the plane framework of four bars safely coupled at their ends against displacement and rotation, seen in Fig. 3.

Characteristics of the indicated boundary and fitting structures are expressed by

$$\begin{aligned} u_1 &= O, & v_2 &= v_3, \\ u_3 &= O, & v_2 &= v_4, \\ v_1 &= u_2, & u_4 &= O, \end{aligned} \tag{32a}$$

and nodal equilibria by

$$\begin{aligned} p_1 + f_2 &= q_A, \\ p_2 + p_3 + p_4 &= q_B, \end{aligned} \tag{32b}$$

where q_A and q_B are amplitude vectors of the sine external force effects acting at nodes A and B, respectively. Also (32a) and (32b) can be written in matrix form:

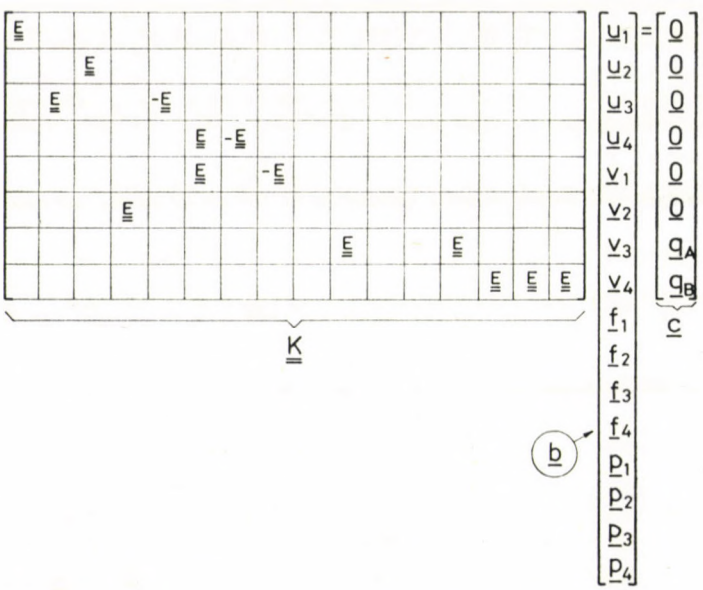

or, in concise form:

$$\mathbf{K}b = c, \tag{33}$$

K being the mentioned coupling matrix. **E** in **K** are unit matrices of order six, the zeros are quadratic zero matrices of order six.

Obviously, this is only a possible form of **K**; there being others differing only formally rather than by purport. [For instance, $v_2 = v_4$ may be replaced by $v_3 = v_4$ in (32a), and so on.] Thus, the column hypermatrix in the right-hand side of (33) contains zeros and external nodal sine force effects. Denoting the amplitude of c by c_0, and substituting the term for b in (31b) changes (33) into:

$$\mathbf{K}\mathbf{A}a \sin \omega t = c_0 \sin \omega t .$$

Assumption of a motion permits to simplify by $\sin \omega t$, thereby the sine vibrations of the skeleton is expressed by the linear inhomogeneous equation system

$$\mathbf{K}\mathbf{A}a = c_0 . \tag{34}$$

Within the method under 2.3, Eq. (34) had (25) as counterpart equations differing by both form and purport. In the actual case vector a comprising integration constants is the unknown quantity of the matrix equation, the same function being accomplished in (25) by vector s_0 comprising nodal displacement amplitudes. Of course, both equations are a kind of mathematical image of the same phyical phenomenon — skeleton vibrations.

In case of free vibrations $c_0 = 0$ Eq. (34) will be homogeneous. Vector a comprising unknown coefficients of field functions cannot be zero in case of vibration, imposing to meet condition

$$\det (\mathbf{K}\,\mathbf{A}) = 0 \tag{35}$$

equation of the skeleton frequency. Quadratic matrix **KA** is of order $12n$.

In forced vibration, steady-state response of nodes of the system can also be determined by this method. If the circular frequency of the forced system does not coincide with some circular eigenfrequency of the structure, coefficient matrix $\mathbf{K} \cdot \mathbf{A}$ of the linear inhomogeneous algebraic equation system (34) will be other than singular, thus, it has a solution. The resulting vector a comprises coefficients of field functions of each bar, permitting, in turn, to determine bar end — hence nodal — displacements.

2.4.3 Computation of eigenfrequencies, features of the method

Determinant function (35) is already a continuous function of ω, elements of **A** being other than fractions. Determination of a sufficient number of roots is computerially much easier than according to the method under 2.3 in spite of the higher order number of the frequency determinant. It is in-

herent in the method that the set of circular eigenfrequencies principially cannot be deficient.

Also here, roots may be found by means of "shifting" as described under *2.3.4*, taking care to assume $\Delta\omega$ small enough.

The procedure is readily algorithmized, and suits the computation method for frequency bounds described at the beginning of chapter 2. The computer may select itself — or even increase — the division number k_i quoted under 2.1 and produce the frequency equation. The degree of accuracy is only limited by the storage capacity of the computer. Numerical utility of the method will be illustrated on simple numerical examples in Chapter 3.

3. Practical application, numerical examples

Two methods have been presented in Chapter 2 for the vibration analysis of skeletons consisting of prismatic bars. Features of the algorithms have been discussed under 2.3 and 2.4. Confrontation of both advantages and inconvenients of both methods leads to the conclusion that both numerically and principially, the method under 2.4, relying on the basic system of differential equations, is the more expedient. Although computer program packages have been made for both methods, and numerical examples have been solved by both, here only computation results obtained by the program made for the numerically superior algorithm will be presented.

Two numerical examples will be presented below. The first one is illustrating the bracketing of eigenfrequencies, while the second one will refer to the eigenfrequencies of a spatial structure made of prismatic bars.

3.1 Bar of variable cross section, one end clamped

For the computation of the frequency bounds, purposefully a problem has been selected that could be exactly solved analytically. For instance, CRANCH and ADLER [10] have already determined the circular eigenfrequencies of a bar of rectangular cross section exponentially varying lengthwise, one end clamped, the other end free. The model in Fig. 4 has been used for numerical analysis.

Circular eigenfrequencies of the bar performing bending vibration around axis z are obtained from frequency equation (Eq. (31), p. 106 in [10]):

$$a + a\cos\frac{1}{b}\operatorname{ch}\frac{1}{c} + 3\sin\frac{1}{b}\operatorname{sh}\frac{1}{c} + \\ + c\sin\frac{1}{b}\operatorname{ch}\frac{1}{c} + b\cos\frac{1}{c}\operatorname{sh}\frac{1}{c} = 0\,, \tag{36}$$

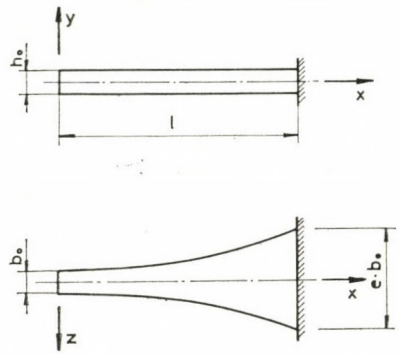

Fig. 4. Bar of exponentially varying cross section, one end clamped. (Model data: $E = 2{,}148 \cdot 10^{11}$ Pa; $G = 8{,}142 \cdot 10^{10}$ Pa, $\varrho = 7800$ kg m^{-3}, $l = 1$ m, $h_0 = 2 \cdot 10^{-2}$ m, $b_0 = 3 \cdot 10^{-2}$ m)

with simplified notations

$$a = \sqrt{\gamma^2 - 1}, \quad b = 2\sqrt{\gamma - 1}, \quad c = 2\sqrt{\gamma + 1},$$

and

$$\gamma = 2l\omega \sqrt{\frac{\varrho A_0}{E I_{z0}}}.$$

With data in Fig. 4:

$$A_0 = h_0 \cdot b_0,$$

$$I_{z0} = \frac{b_0 \cdot h_0^3}{12},$$

First three roots of Eq. (36):

$$\gamma = 18{,}9366261693, \qquad 96{,}8072531389, \qquad 255{,}457961136$$

With numerical data of the example, first three circular eigenfrequencies of the bending vibration around axis z:

$$\omega = 144{,}8294039, \qquad 740{,}3925409, \qquad 1953{,}770640 \ [s^{-1}].$$

To obtain lower and upper bounds for the circular eigenfrequencies, the bar of variable cross section has been divided by nodes into k parts — as seen under 2.1 — the parts between nodes being replaced by prismatic bar parts, with characteristics selected according to relationships (2) and (3). Magnitude I involved in the torsional rigidity **GI** of the rectangular cross section has been calculated according to Eq. 9,4 p. 71 in [11] from

$$I = \frac{16}{3} b^3 \left\{ a - b \left[0{,}6302488761 - \frac{192}{\pi^5} \sum_{i=1}^{\infty} \frac{1 - th\left(\frac{2i-1}{2b} \cdot \pi \cdot a \right)}{(2i-1)^5} \right] \right\},$$

where a and b are half side lengths of the cross section. This formula is valid if $a \geq b$.

Computer program outputs have been compiled in Tables 3 and 4 including the first five circular eigenfrequencies up to two decimals, together with the division number k. All computed circular eigenfrequencies are simple roots of the frequency equation. Figures 5 to 9 are more illustrative in showing the outputs.

Table 3

Lower bounds of circular eigenfrequencies [s^{-1}]

	$k=1$	$k=2$	$k=3$	$k=4$	$k=5$	$k=6$	$k=8$	$k=10$
1	65,24	104,22	118,30	125,27	129,37	132,07	135,38	137,34
2	97,86	241,75	309,89	346,89	369,75	385,19	404,63	416,33
3	408,86	533,02	603,99	639,49	660,63	674,55	691,68	701,77
4	613,28	987,54	1303,93	1466,46	1566,11	1633,33	1717,83	1768,57
5	1134,62	1476,40	1597,83	1689,51	1743,93	1780,20	1825,16	1851,77

Table 4

Upper bounds of circular eigenfrequencies [s^{-1}]

	$k=1$	$k=2$	$k=3$	$k=4$	$k=5$	$k=6$	$k=8$	$k=10$
1	177,34	171,83	165,10	160,85	158,02	156,02	153,41	151,78
2	723,10	657,14	603,58	571,92	551,61	537,58	519,56	508,52
3	1111,38	878,80	842,93	821,12	806,90	796,89	783,78	775,58
4	3111,91	2434,17	2229,96	2169,38	2130,04	2103,06	2068,17	2046,52
5	4531,59	2684,41	2539,71	2417,78	2336,37	2279,50	2205,74	2160,14

From the tables and the diagrams it is obvious that the computed circular eigenfrequencies 1, 3 and 5 are circular eigenfrequencies 1, 2 and 3 of the bending vibration around the z-axis; circular eigenfrequencies 2 and 4 may be identical to circular eigenfrequencies 1 and 2 of the bending vibration around the y-axis. Figures 5, 7 and 9 clearly illustrate bracketing of circular eigenfrequencies computed by CRANCH and ADLER.

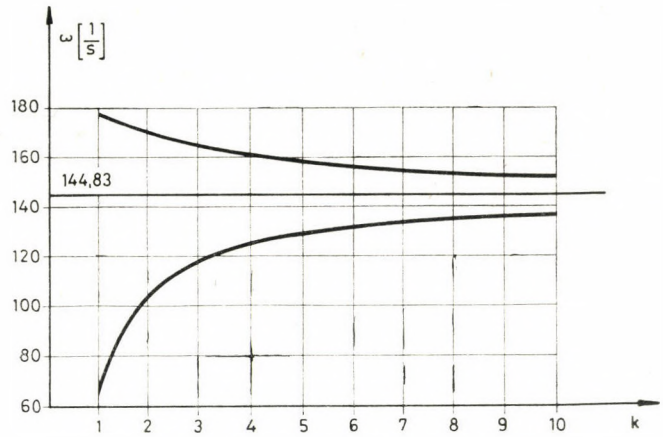

Fig. 5. First circular eigenfrequency

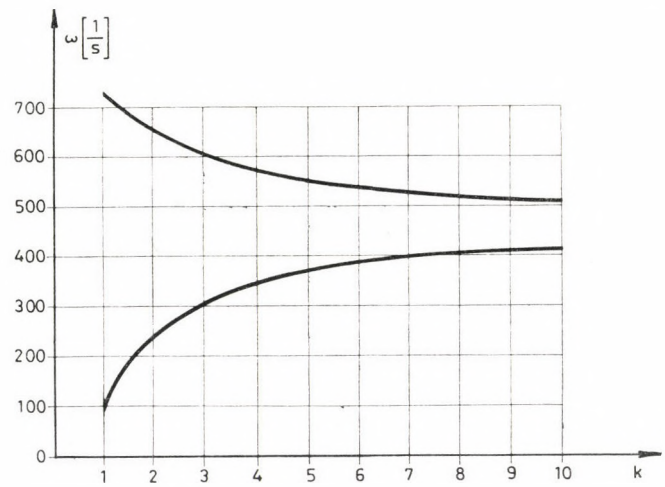

Fig. 6. Second circular eigenfrequency

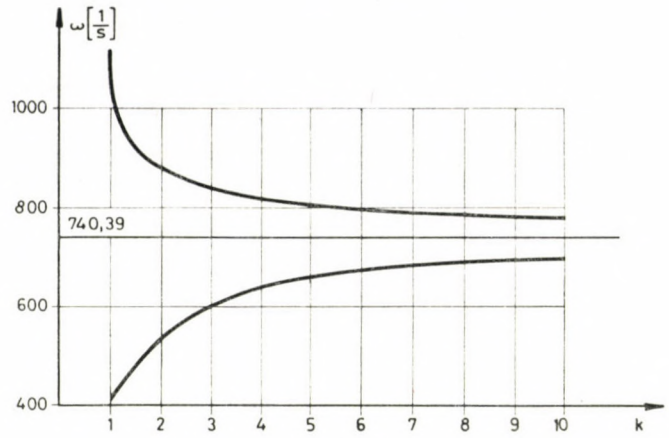

Fig. 7. Third circular eigenfrequency

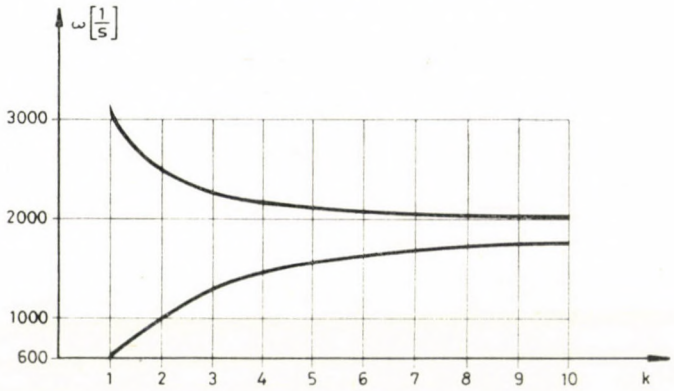

Fig. 8. Fourth circular eigenfrequency

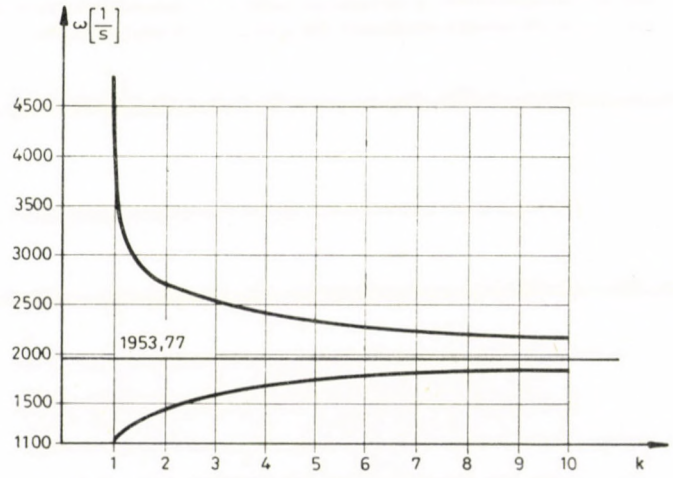

Fig. 9. Fifth circular eigenfrequency

3.2 Spatial skeleton composed of prismatic bars

Scheme of the spatial skeleton considered is seen in Fig. 10. Advantages due to peculiarities of the builtup (e.g. the regular geometrical configuration) are not utilized by the computer program, hence these are not to the detriment of general validity. Also the selected own systems of coordinates of the bars have been indicated. The bar ends are rigidly connected to each other permitting no relative displacement or rotation.

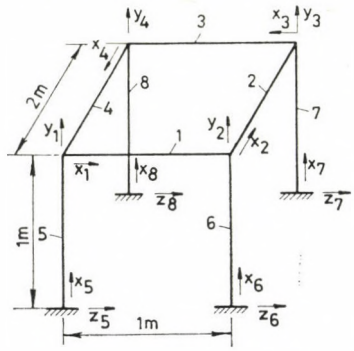

Fig. 10. Spatial skeleton composed of prismatic bars. (Model data: $E = 2{,}148 \cdot 10^{11}$ Pa, $G = 8{,}142 \cdot 10^{10}$ Pa, $\varrho = 7800$ kg m^{-3})

Identical cross sectional dimensions of frame bars 1, 2, 3 and 4, and identical cross section dimensions of columns are seen in Figs 11 and 12, respectively.

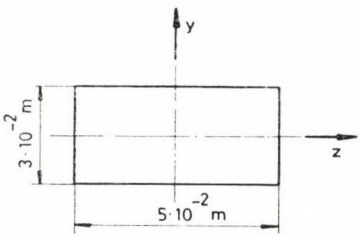

Fig. 11. Cross section of frame bars

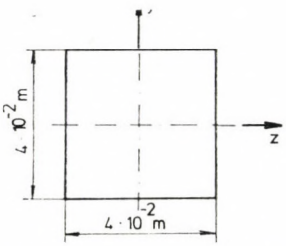

Fig. 12. Cross section of columns

The first eight computed circular eigenfrequencies, all of them being simple, have been tabulated in Table 5. Remark that also the vibration figure belonging to a circular eigenfrequency ω_i can be determined from (34), applying the assumption $c_0 = 0$ corresponding to free vibration. Solving the obtained linear homogeneous equation system for vector a comprising field function coefficients, and substituting a into (5) yields bar end — hence nodal — displacements. This computation is — of course — possible for both presented examples.

Table 5

Circular eigenfrequencies of the structure

	ω (s^{-1})		ω (s^{-1})
1	110,48	5	217,16
2	120,45	6	235,50
3	157,40	7	283,13
4	210,47	8	456,30

REFERENCES

1. Poincaré, H.: Sur les équations aux dervées partielles de la physique mathématique. *American J. Math.* **12** (1890).
2. Bazley, N.—Fox, D. W.: Methods for Lower Bounds to Frequencies of Continuous Elastic System. *Zeitschrift für angewandte Mathematik und Physik* **17** (1966), 1—37.
3. Kolousek, V.: Baudynamik der Durchlaufträger und Rahmen. Fachbuchverlag, GMBH, Leipzig 1953.
4. Hübner, E.: Eigenschwingungszahlen zusammengesetzter Schwingungssysteme. *Ingenieur-Archiv* **29** (1960), 134—149.
5. Bosznay, Á.: Einzelne Probleme der Dynamik zusammengesetzter Systeme. *Periodica Polytechnica, Electrical Engineering* **17** (1973), 7—28.
6. Czeglédi, Gy.—Richlik, Gy.: Computation of Natural Circular Frequencies of Spatial Structures Made up of Prismatic Bars.* *Proc. Ist Scientific Session of the Working Group of Departments of Engineering Mechanics.* Hung. Ac. Sci. Budapest 1974, pp. 192—197.
7. Wittrick, W. M.—Williams, F. W.: A General Algorithm for Computing Natural Frequencies of Elastic Structures. *Quart. J. Mech. Appl. Math.* **24** (1971), 263—284.
8. Czeglédi, Gy.: Einige Bemerkungen zur Freiheitsgradreduktion von linear-elastischen mechanischen Modellen. *Periodica Polytechnica, Electrical Engineering* **19** (1975), 257—266.
9. Czeglédi, Gy.: Reduction of the Degree of Freedom and its Consequences in the Analysis of Linear-Elastic Structures.* *Műszaki Tudomány* **54** (1978), 115—124.
10. Cranch, E. T.—Adler, A. A.: Bending Vibration of Variable Section Beams. *J. Applied Mechanics* (1956), 103—108.
11. Weber, C.—Günther, W.: Torsionstheorie. F. Vieweg et Sohn. Braunschweig-Akademie Verlag, Berlin 1958.
12. Czeglédi, Gy.: Reduction of the Degrees of Freedom of Linear-Elastic Mechanical Models. *Periodica Polytechnica, Electrical Engineering* **23** (1981), 311—316.

*In Hungarian

Einschließung der Eigenfrequenzen von räumlichen Stabwerken, II. — Dieser Aufsatz ist die Fortsetzung des ersten Teils, der in derselben Zeitschrift erschien. Für die Untersuchung der Schwingungen von Stabwerken aus prismatischen Stäben modelliert als Kontinua wird jetzt eine andere Methode vorgestellt, die auf dem Grundsystem der Differenzialgleichungen beruht und die beim vorigen Verfahren erwähnten Nachteile beseitigt. Das letzte Kapitel stellt zwei einfache Zahlenbeispiele für die praktische Anwendung vor. Die Numerierung der einzelnen Kapiteln, Abbildungen, Gleichungen und Tafeln beginnt in diesem Teil nicht vom Anfang an sondern sie ist die Fortsetzung der im ersten Teil angewendeten Numerierung.

Acta Technica Academiae Scientiarum Hungaricae, Tomus 92 (3—4), pp. 383—392 (1981)

DEVELOPMENT OF AN EXPERIMENTAL APPARATUS FOR THE MEASUREMENT OF THE THERMODYNAMIC PROPERTIES OF CO_2-CONTAMINATED NATURAL GASES

PART I

M. A. I. BUKHARI*
G. VERES**

[Manuscript received 14 March 1978]

The increasing demand for energy has necessitated extensive investigations to find ways and means of utilizing the huge reserves of largely CO_2-contaminated CH_4 gas, previously considered uneconomical. Two kinds of equipment have been specifically devised and tested for the purpose of measuring the thermodynamic properties of $CH_4—CO_2$ mixtures at desired P-T-X ranges. One of these is suitable for concomitantly determining the integral isobaric heats of condensation, together with vapour-liquid equilibria. The other is intended for simultaneous measurement of heat capacities at constant pressure and the mixing heats of liquid mixtures.

Introduction

The huge reserves of natural gas available in various parts of Hungary, and those highly contaminated with carbon dioxide, have for long been considered as uneconomical sources of energy. However, the increasing demand for natural gas in recent times has necessitated the embarkation on extensive efforts for finding ways and means to economically and successfully utilize these huge sources of natural wealth, both in domestic utilities and public services. The high pressure conditions under which these gases exist provide an inherent potential energy that reduces to a minimum the amount of work required by any technique that may be applied in a separation process, etc. The Department of Energetics of the Technical University of Budapest has been preoccupied in recent years with the task of investigating and reporting on such ways and means whereby these carbon dioxide contaminated natural gases may be economically and appropriately separated in a manner that warrants useful utilizations. Owing to the fact that the bulk of these natural gas well effluents are mixtures of methane and carbon dioxide, with only traces of other hydrocarbon gases such as ethane and propane, attention has been focussed primarily on a $CH_4—CO_2$ system in carrying out the major objectives of this scheme.

* M. A. I. BUKHARI, P.O. Box 2408 Khartoum, Sudan
** G. VERES, Bogár u. 29/d, H-1022 Budapest, Hungary

Handicapped by the unavailability of published experimental thermodynamic data for this system, an initial trial approach for tackling this problem was attempted earlier by the construction, using theoretical means, of enthalpy-composition diagrams for the CH_4-CO_2 system in its liquid-vapour equilibrium region. On the basis of data thus obtained a gas separating model apparatus was constructed and tested. Comparisons between measured values using the model set-up and those corresponding, predicted from the theoretically constructed enthalpy-composition diagrams, have revealed disparities sizable enough for tolerable engineering accuracy [1].

Thus, initial results obtained during the first phase of this work have necessitated the embarkation on more serious efforts to determine, as accurately as possible, both experimentally and theoretically, the required thermodynamic data of the methane-carbondioxide system. A direct experimental determination in a single, one go, series of experiments of a wide scope of thermodynamic properties for a system such as the CH_4-CO_2 system, if not impossible is, by all means, inconceivable from the point of view of required costs, human efforts and time.

The purpose of this report is to present the experimental procedures already adopted in the Department's laboratory, the progress achieved so far in this stage of their development, and the limitations and short-comings revealed by the results of initial test runs.

Experimental measurements

Previous experimental measurements, as has already been portrayed [1] have been made in this laboratory of the Department of Energetics using a simple model gas separating apparatus, a flow diagram which is shown in Figure 1. The gaseous mixture contained in a cylinder G at about 70 atmospheres and 20 °C is passed through a dehydrater T into a cooler H where it is cooled by means of carbon dioxide from its initial supercritical state into a partially condensed state where it separates into a vapour-phase rich in CH_4 and a liquid-phase of poorer quality. This process is illustrated in the diagram of Figure 2. Point 3 represents the liquid-phase in equilibrium with the vapour-phase, point 4, a sample of which is collected in the bleeder E_1. The liquid-phase in the separator SZ_1 flows through valve F where it is throttled to a pressure of about 20 atmospheres and further separates into a liquid-phase, state point 6, and a vapour-phase state point 7.

The experimental trials described here involve the determination of two kinds of calorimetric data using two sets of equipment, specifically designed and constructed for this purpose. Because of considerable discrepancy, in engineering terms, between the values measured using the above model, and those corresponding, predicted using the theoretically constructed enthalpy-

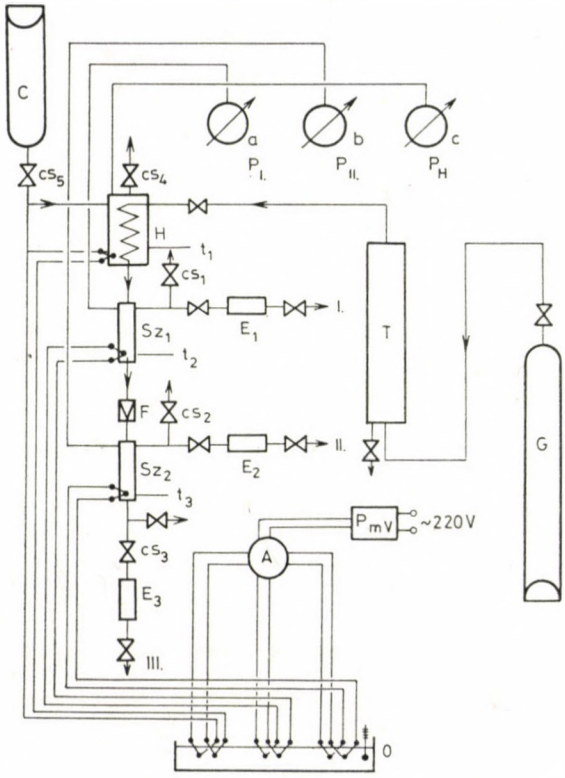
C
a
b
c
P_I
P_{II}
P_H
cs_5
cs_4
H
t_1
cs_1
I.
E_1
Sz_1
t_2
F
cs_2
II.
E_2
T
G
Sz_2
t_3
P_{mV}
~220V
A
cs_3
E_3
III.
0

Fig. 1

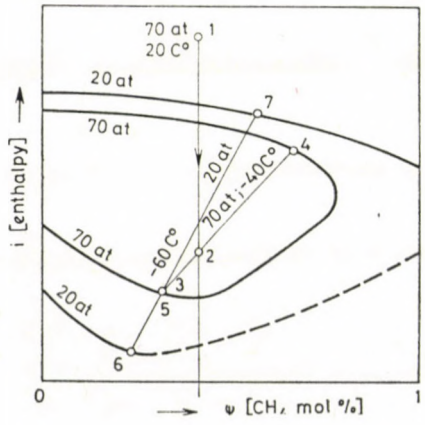
70 at
20 C°
1
20 at
7
70 at
20 at
4
70 at; -40C°
-60 C°
70 at
2
3
5
20 at
6
i [enthalpy]
0
1
ψ [CH, mol %]

Fig. 2

composition diagrams, it has been deemed necessary to devise a special equipment set up for the determination of the saturated phase enthalpy differences, at least over a P-T-X range that is essential for this purpose. Consequently, one set of these experiments is for the determination of the integral, isobaric heats of condensation of largely CH_4-CO_2 vapour mixtures over possible pressure, temperature and composition ranges. In each of the experimental determinations related to the measurements of integral, isobaric, heats of condensation, it has been found necessary to make calculations involving the heat capacity at constant pressure of the liquid solutions. For this purpose, another set of equipment is used for the measurement of heat capacity data of liquid CH_4-CO_2 mixtures. In the first case, heat capacity data is needed for measuring the flow rates calorimetrically in the heat of condensation apparatus, and also to correct the heat balance for the enthalpy of the condensate from its subcooled temperature to the bubble-point temperature, whenever it turns out to be necessary. In the second case the heat capacity data is necessary for the determination of heat of mixing values from the temperature change of each mixture and for the correction of the heat of mixing to the isotherm suitable for all mixtures of the system.

Previous work in the literature

a) Excess enthalpies and heat capacities

Many calorimetric determinations of the enthalpy of mixing liquids (usually at normal pressure) have been made, but only a few workers have studied the excess enthalpies H^E of gaseous mixtures. Pioneering work has been done by BEENAKKER and co-workers [2, 3] who have announced that the Kamerlingh Onnes Laboratory has started work on direct measurement of H^E using a flow calorimeter and have presented a few preliminary results. They have determined H^E at one composition around 50 mole % for the system N_2-H_2, $Ar-H_2$, $Ar-N_2$. CH_4-H_2 and CH_4-Ar, as a function of pressure up to about 20 atm. KLEIN, BENNETT and DODGE (1971) [4] have made extensive measurements in the system CH_4-N_2 and HEIMADI, KATZ and POWERS (1971) [5] have obtained some data in the system N_2-CO_2. ZEMLIN (1972) [6] has shown that knowing the Joule—Thomson effect (adiabatic throttling) of the mixture and its pure components, it is possible to calculate the heat of mixing and has compared calculated values with measured ones for the binary systems CH_4-CO_2, $C_2H_6-CH_4$, CO_2-N_2 and $C_2H_6-N_2$. To date, the only available, extensive excess enthalpy data of CH_4-CO_2 gaseous mixtures are those of LEE and MATHER (1972) [7] who have recently reported their results for this system at temperatures between 10 °C and 80 °C, at pressures up to 100 atmospheres.

BISHNOI and ROBINSON (1971) [8] have used the heat exchanger method for determining the ratio of the heat capacity at a pressure, to obtain data on two binary mixtures of CH_4 and CO_2 containing 14,49 and 42,30 mole % CH_4. The data obtained are in the pressure range up to 2250 psi and the temperature range from ambient to 150 °C.

b) Heats of condensation

Industrial design calculations, such as in separation processes, and theoretical comprehension of solutions and phase equilibrium require information on the heat of vaporization (or condensation) of mixtures. Before its practical and theoretical importance can be realized, however, several properties of the heat of vaporization of mixtures, which do not exist with pure components, should be borne in mind. There are three distinct types of latent heats of mixtures: one at constant pressure and temperature, a second at constant pressure and composition, and a third at constant temperature and composition. These three are known as differential, integral isobaric, and integral isothermal, respectively.

To cope with the difficulties of determining experimental heat of vaporization data for binary systems, TALLMADGE et al. (1959) [9] and several investigators have resorted to modifications of the flow type of calorimeter already conceived by DANA [10] in 1925 for liquid air studies. BLOOM, CLUMP and KOECKERT (1961) [11] have used a complex assembly suitable for simultaneous determination of vapour-liquid equilibrium and latent heat of vaporization. All those investigators have depended on others to provide heats of mixing, heat capacities of mixtures, and in some cases, the phase-equilibrium data. SHAH and DONNELLY (1967) [12] have recently presented a fundamentally original adaptation of the OTHMER (1948) [13] type of liquid-vapour equilibrium still (the first equilibrium yet which functioned satisfactorily) to measure the integral isobaric heat of condensation of a vapour mixture at a pressure of one atmosphere.

Experimental apparatus

Heat capacity and heat of mixing

The experimental equipment devised to determine the heats of condensation and heats of mixing data requires knowledge of the amount of enthalpy equivalent to the temperature change permitted during experimentation. Although many investigators have for simplicity's sake used either weight or molar average heat capacity data for binary mixtures, such cor-

rections are known to be imprecise; the factors which contribute to the excess enthalpy of mixing in non-ideal systems are, without doubt, contributors to the excess heat capacities for such systems. To maintain the type of accuracy desired, it has been found necessary to determine experimentally the heat capacity data for several mixtures at different pressures and temperature in the liquid-phase where pure CH_4 which is a gas above its critical temperature is dissolved in liquid CO_2 below its critical temperature to form a liquid mixture. It is not known to the author whether any such measurements, at all, have been performed.

Figure 3 shows a flow diagram of the apparatus. The individual gases, stored in standard gas cylinders a_1 and a_2 flow independently through high pressure regulators, *c*, into the cooling bath. Constant flow is maintained

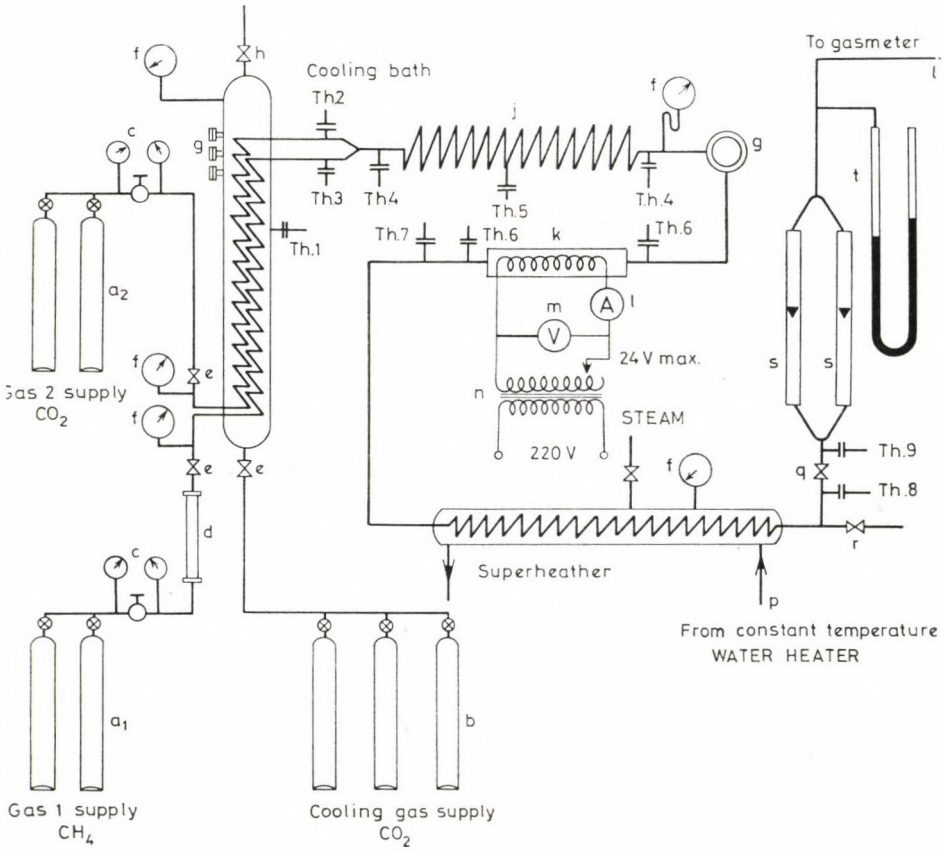

Fig. 3

by establishing a constant pressure drop across flow control valves, *e*, through the setting up of the high pressure regulating valves. The two gases flow separately, in two concentric coils, through a CO_2-cooled constant temperature bath, the temperature of which is manually controlled by evaporating CO_2 gas from saturated liquid-vapour phases in the bath at a set pressure through the adjustments of flow control valve *e* and flow metering valve *h*. Next, the two fluids, CO_2 now liquified, at the same pressure and almost uniform temperature contact each other prior to entering an approximately five metre long mixing coil where they mix. The pressure is essentially constant upon mixing regardless of any volume changes, though the temperature generally tends to drop slightly upon mixing, indicating endothermic interaction.

The two fluids are believed to be thoroughly mixed by passing through the long spiral tube. The liquid mixture then passes through a liquid sight glass to a heater intended for heat capacity measurements. The sight glass serves to insure the existence of a homogeneous liquid-phase with no vapour bubbles. The electric power input to the heater is determined by measuring the voltage drop across and the current into a 20 Watt, 24 Volt electric resistance heating element. The liquid mixture exiting from the heater passes through an evaporator-superheater, heated by means of a hot water thermostat, before being throttled to approximately atmospheric pressure by means of throttling valve *q*. The gaseous mixture then passes through a pair of rotameters *S* connected in parallel for flow indication purposes and then through a low pressure gasmeter *u* for accurate flow rate determination. An H_g manometer *t* is used to measure the pressure of the gas entering the gasmeter. The composition of the gaseous mixture is determined by flow through an Uras 2 methane gas detector calibrated from zero to 30 mole % CH_4. Samples of the flowing gas are directed into the gas analyzer through sampling valve *r*.

Temperatures are measured at various locations by means of Nickel, Chrome-Nickel thermocouples.

Th_1, Th_2 and Th_3, respectively, measure the temperatures of the cooling bath, CO_2 liquid and CH_4 gas. Th_4 and Th_6 are differential thermocouples, that measure the temperature change due to mixing in the mixing coil, and the temperature rise across the electric heater. Th_5 measures the average temperature of the mixing coil. Th_7 and Th_8 the temperatures before and after the superheater. Th_9 measures the temperature of the gas entering the gasmeter. Thermocouple voltages are recorded by a Kent voltage amplifier. All pressure gauges, of the bourdon tube type have been calibrated against a dead-weight tester. All relevant parts of the system are thermally insulated to reduce heat leakage to a minimum.

Measurements and calibration

The experimental determination of heat capacities and heats of mixing in flow calorimeters has been found by several investigators to be a simple and a satisfactory one. The basic design principle adopted here is to determine the change in temperature of the two fluids from their initially identical temperatures when they are brought together and rapidly homogenized in a well insulated mixing coil. Such data can then be converted to heat of mixing data for the particular mixture composition from the simultaneously measured heat capacity at constant pressure for the same mixture, and the known heat capacities of the pure components. This simultaneous measurement of the two interrelated thermodynamic properties on the same apparatus provides a more precise check on internal consistency. Trial runs have indicated that there is no need for mechanical stirring, no vapour spaces, and the pressure is essentially constant upon mixing, regardless of any volume changes on mixing. However, and to begin with, one major disadvantage in this apparatus is that, in the rush of work, not enough attention was paid to the construction of proper flow calorimeters, as originally planned, for the heat of mixing and heat capacity measurements, to minimize external heat effects, including radiation from surrounding objects. Initial attempts for obtaining heat capacity data have not provided the type of accuracy desired to complement the accuracy of the heat of condensation and the heat of mixing data. Considerable time and efforts have been consumed in testing, adjusting and calibrating the simple equipment used in this work before it could have been possible to demonstrate the adequacy of the system to obtain fairly satisfactory results. The apparatus has been calibrated using pure CO_2, the error thus established and adjusted for the mixtures. Because of the limited range of P-T-X values in the liquid region over which measurements can be performed using this apparatus at this stage of progress, the objective of having these experiments run is limited to evaluation purposes.

The gases used are approximately 99,9% pure CO_2, and the natural gas:

CH_4	85,0%
C_2H_6	03,3
C_3H_8	01,8
CO_2	03,6
N_2	04,6

Procedure

Before starting a run, the cold temperature bath is set at a predetermined temperature by allowing CO_2 liquid to evaporate at a manually controlled saturation pressure indicated by pressure gauge *f*. The superheater is also set at a temperature of 80 °C by setting the hot water thermostat. Because

the pressure regulator used is suitable for a maximum gauge pressure of about 40 atmospheres, various CH_4-CO_2 liquid mixtures have been tested at only one isobar — 40 atmospheres absolute. The valves on the cooling CO_2 supply cylinders and the CO_2 gas flow control valves are opened. The gas pressure is set at 40 atmospheres by regulator *c* and an approximate flow rate, indicated by the rotameters, is established by adjusting the flow control valve and the throttling valve *q*. Flow of CO_2 is allowed to continue until the sight glass *g* indicates complete liquifaction of the CO_2 gas, with no vapour bubbles. Then the same process is repeated with the CH_4 gas supply. A sample of the gaseous mixture is flown through the Uras methane gas detector and the flow rate of the two gases is metered, thereby setting the mole fraction of the liquid mixture. In the majority of runs, the flow rate indicated by the rotameters, has been about 3000 litres per hour. This was established as the minimum desirable one in order to overcome the effect of spurious heat transfer. At lower rates the errors in the values of C_p are higher. Input power to the heat exchanger is simultaneously secured. At least about one hour, or more, is required to obtain fairly steady operating conditions indicated by constant composition, constant flow rate in the rotameters, and fairly stable thermocouple voltages. The addition of heat is conveniently and accurately controlled in the evaporator-superheater thermostatically, and also in the heat capacity heat exchanger where the electric energy, converted to heat can easily be measured. However, manual control of heat removal in the cold bath is much more difficult and the thermocouples particularly 1, 2 and 3, are very sensitive to any adjustments and register zigzaging paths, whose average values are used. When all instrument readings indicate fairly steady state conditions, readings are taken every 2 or 3 minutes and averaged over a period of 4 to 6 minutes. The prime measurements taken are temperature, pressure, gas composition, voltage and amperage of the heater, volume of gas flowing, its temperature and time interval, manometer reading and barometric pressure.

REFERENCES

1. Heller, L.—Erdődy, I.: Nagy szénsavtartalmú földgázak szétválasztásának elméleti és kísérleti vizsgálata (A Theoretical and Experimental Investigation for the Separation of Natural Gases Highly Contaminated with CO_2). Technical University of Budapest, Department of Energetics, 1969.
2. Beenakker, J. J.—Cormans, M. J.: Progress in International Research on Thermodynamic and Transport Properties. Pp. 3—7. *Am. Soc. Mech. Eng.*, New York 1962.
3. Beenakker, J. J.—van Einsbergen, M. B.—Knoester, M.—Taconis, K. W.—Zandberger, P.: Advances in Thermophysical Properties at Extreme Temperatures and Pressures. P. **114**, *Am. Soc. Mech. Eng.*, New York 1965.
4. Klein, R. R.—Benett, C. O.—Dodge, B. F.: Experimental Heats of Mixing for Gaseous Nitrogen and Methane. *AI. Ch. E. J.* **17** (1971), 958.
5. Heimadi, R. V.—Katz, D. L.—Powers, J. E.: Experimental Determination of the Enthalpy of Mixing of $N_2 + CO_2$ Under Pressure. *J. Chem. Thermodynamics* **3** (1971), 483—496.

6. HERMANN, Z.: Der Zusammenhang zwischen dem Integralen Joule—Thomson Effect von Gasgemischen und Mischungswärme ihre theoretische Bestimmung. *Chemie Ing. Techn.* **44,** Nr. 9, Gol (1972).
7. LEE, J. I.—MATHER, A. E.: The Excess Enthalpy of Gaseous Mixtures of Carbon Dioxide with Methane. *Can. J. Chem. Eng.* **50** (1972), 95.
8. BISHNOI, P. R.—ROBINSON, D. B.: Experimental Heat Capacities of Carbon Dioxide-Methane Mixtures at Elevated Pressures. *Can. J. Chem. Eng.* **49** (1971), 657.
9. TALMADGE, J. A.—SCHROEDER, D. W.—EDMISTER, W. C.—CANJAR, L. N.: Integral Isobaric Heat of Vaporization of Methane Benzin Mixtures. *Chem. Eng. Prog. Symp.* Ser. No. **10, 50,** (1954), 137.
10. DANA, L. I.: *Proc. Am. Acad. Arts Sci.* **60** (1925), 241.
11. BLOOM, C. H.—CLUMP, C. W.—KOECKERT, A. H.: *Ind. Eng. Chem.* **53,** (1961), 829.
12. SHAH, V.—DONELLY, H. G.: Complete Experimental Data for the Iso-Propanol-Toluene Enthalpy-Composition Diagram. *Chem. Eng. Prog. Symp.* Series 81, **63,** (1967), 105.
13. OTHMER, D. F.: *Ind. Eng. Chem. Anal.* Ed. **20,** (1948), 763.

Entwicklung einer Versuchsvorrichtung zur Messung der thermodynamischen Kennwerte des durch CO_2 verunreinigten Erdgases. I. Teil. — Der zunehmende Energiebedarf erfordert die Benutzung der eher für unwirtschaftlich abgeschätzten, mit CO_2 verunreinigten Erdgasvorräte. Zur technischen Berechnung der Erdgas vorbereitenden Einrichtungen sind zuverlässige thermodynamische Angaben erforderlich im gewünschten P-T-x Bereich des als ein Modell vorteilig brauchbaren CH_4—CO_2 Systems. In der vorhandenen Abhandlung werden jene Versuchsvorrichtungen vorgeführt, die zur gleichzeitigen Messung der integral-isobaren Kondensationswärme, der Gleichgewichtswerte der Dampf-Flüßigkeit sowie der Mischungswärme der in der Flüßigkeitsphase befindlichen Mischung und der Isobarwärmekapazität geeignet sind.

Acta Technica Academiae Scientiarum Hungaricae, Tomus 92 (3—4), pp. 393—404 (1981)

APPLICATION OF TREFFTZ—FICHERA'S METHOD FOR IMPROVABLE BRACKETING OF THE NATURAL ANGULAR EIGENFREQUENCIES OF A BEAM SUBJECT TO BENDING VIBRATION

GY. RICHLIK,* GY. TÓTH**

[Manuscript received January 31, 1979]

The numerical experiments suggest that in case of beams subject to some kind of oscillation it is not necessarily reasonable to apply to improvable bracketing of the angular eigenfrequency the method in general use for the functional analysis due to the laboursome numerical calculation work. The purpose of the paper is to justify the efficiency of the Trefftz—Fichera's method in connection with the calculation of the improvable lower limits of the angular eigenfrequencies associated with flexural oscillation. The upper limits needed for the delimitation might be determined by the Poincaré—Rayleigh—Ritz's method. To the application of the Trefftz—Fichera's method the invertation of the differential operator of variable coefficient, originally entering in the calculations, is needed. The paper carries out the invertation by making use of the theory of distribution and, at the same time, summarizes the respective elements of the general theory.

1. Introduction

The improvable bracketing of eigenfrequencies of the elastic continuous structures may be carried out in several ways. A common characteristic of several procedures is that with the aid of Poincaré—Rayleigh—Ritz's method upper bounds for the eigenfrequencies are calculated and, with their knowledge, lower bounds are defined by the application of the different methods of the functional analysis. Namely, WEINSTEIN as well as BAZLEY and FOX present procedures for the determination of the lower bounds with the aid of the so-called intermediate operators [1], [2], while BOSZNAY does that with the aid of Fichera's method of the orthogonal invariants [3], [4]. The development of the method of intermediate operators by BOSZNAY permits the improvable bracketing of the angular eigenfrequencies of space frame structures of variable characteristics [5]. (This method does not use Poincaré—Rayleigh—Ritz's procedure.)

On the basis of their numerical experiments, authors found that the direct application of these general methods to the case of a single beam subject to bending vibration is not advantageous, because the determination of both the lower and upper bounds needs comparatively a great deal of numerical work.

* Gy. Richlik 1073. Budapest, Akácfa u. 59.
** Gy. Tóth 1016. Budapest, Gellérthegy u. 20—22.

For this reason, authors set themselves the task of investigating the numerical efficiency of Trefftz—Fichera's procedure for the calculation of the lower bounds associated with this very same problem. They assumed, for example, that upper bounds obtained by Poincaré—Rayleigh—Ritz's method, having sufficient accuracy, are available in sufficiently great number.

The solution of the problem requires the invertation of a differential-operator; to the methodological realization of this operation authors applied the distribution theory. The method used immediately establishes the so-called kernel function and does not require the knowledge of Green's function (and its properties). Therefore, authors inserted, on account of preparation, the relevant elements of the distribution theory. The way of treatment is limited to the interval [0, 1] which, however, may be extended to an arbitrary, finite interval $[a, b]$ with the aid of the transformation

$$x = a + (b - 1)\xi, \quad x \in [a, b] \wedge \xi \in [0, 1] .$$

2. Trefftz—Fichera's method

Let $\mathcal{K}^{-1}$ be a real, symmetrical, positive semidefinite, completely continuous integral operator defined at the interval [0, 1] according to the relationship

$$\mathcal{K}^{-1} v \doteq \int_0^1 K(x, t)\, v(t)\, dt \tag{1}$$

by the kernel $K(x, t) = K(t, x)$. If the eigenvalues of $\mathcal{K}^{-1}$ (which cannot be negative) are denoted with μ_i and their corresponding eigenfunctions with v_i, then, by virtue of [6]

$$K(x, t) = \sum_{i=1}^{\infty} \mu_i\, v_i(x)\, v_i(t). \tag{2}$$

[These eigenvalues μ_i, in case of their interpretability by the theory of vibration, are, according to the formulae (28), the inverse squares of the angular eigenfrequency.]

Let us assume that the eigenfunctions constitute an orthonormal system, i.e.,

$$\int_0^1 v_i(x)\, v_j(x)\, dx = \begin{cases} 0, & \text{if} \quad i \neq j \\ 1, & \text{if} \quad i = \mathrm{j} \end{cases} \tag{3}$$

and assume also further that the lower bounds

$$\mu_1' \geq \mu_2' \geq \ldots \geq \mu_k' \tag{4}$$

coordinated to the first $\mu_1, \mu_2, \ldots, \mu_k$ k members of the eigenvalues are known. If now $n \leq k$, so, by making use of (2) and (3)

$$\int_0^1 K(x, x)\, dx = \sum_{i=1}^{\infty} \mu_i = \sum_{i=1}^{n-1} \mu_i + \mu_n + \sum_{i=n+1}^{\infty} \mu_i \geq \sum_{i=1}^{n-1} \mu_i + \mu_n + \sum_{i=n+1}^{k} \mu_i .$$

Making use of (4) yields

$$\int_0^1 K(x, x)\, dx \geq \sum_{i=1}^{k} \mu_i' + \mu_n - \mu_n' ,$$

i.e.,

$$\mu_n \leq \mu_n' + \int_0^1 K(x, x)\, dx - \sum_{i=1}^{k} \mu_i' . \tag{5}$$

(It is worth mentioning that (5) is a specific case of the so-called Fichera's formula [3].)

Thus, with knowledge of the lower bounds (4) and the kernel $K(x, t)$ upper bounds may be given to the first k eigenvalues of μ_i of the integral operator $\mathfrak{K}^{-1}$ with the aid of inequality (5). (In case of formulating the inequality to the squares of the angular eigenfrequencies, the lower and upper designations exchange their roles.)

In applying the procedure described above, it is assumed that the kernel $K(x, t)$ is known in an explicit form. (It should be noted that in cases where the kernel function cannot be established in an explicit form, there the method of intermediate Green's functions might be applied [6], [7].) In the following the problem is treated of how the kernel function of the inverse of the ordinary linear differential operator may be produced. On this occasion some concepts from the subject matter of the distributions to be utilized in the following should, by way of preliminary, be mentioned.

3. Principles of the distribution theory

Let us designate with $\mathfrak{D}$ the space of the so-called test functions and be t an independent real variable. Those $\Phi \in \mathfrak{D}$-functions are called test functions which are real valued and which can be derived as many times as needed and outside the interval $[0, 1]$ are equal to zero. Distributions are called those continuous linear functionals [8] interpreted at $\mathfrak{D}$ whose space will be denoted with $\mathfrak{D}'$.

The locally integrable function $f(t)$ interpretes at $\mathfrak{D}$ the regular distribution f with the integral

$$\langle f, \Phi \rangle = \langle f(t), \Phi(t) \rangle \doteq \int_{-\infty}^{\infty} f(t)\, \Phi(t)\, dt, \qquad \Phi(t) \in \mathfrak{D} \tag{6}$$

[$f(t)$ may locally be integrated in the case where, according to LEBESGUE they can be integrated at all finite intervals.] The non-regular distribution is called singular. A singular distribution is, for example, the distribution δ, whose interpretation is as follows:

$$\langle \delta, \Phi \rangle \doteq \Phi(0), \quad \Phi \in \mathcal{D} \wedge \delta \in \mathcal{D}'. \tag{7}$$

In the following the symbol $f(t)$ will be used whether $f \in \mathcal{D}'$ is regular or singular distribution, wherein t denotes the independent variable of the test functions. The symbol f has only been selected for the sake of convenience; in the case of a singular distribution it does not designate a function in the usual sense. For example, in the case of the δ functional the symbol $\delta(t)$ will be used. The meaning of the expression

$$\int_{-\infty}^{\infty} \delta(t)\, \Phi(t)\, dt = \Phi(0)\,, \quad \Phi(t) \in \mathcal{D}$$

established with that functional, is given by the right-hand side of the relationship. The symbol $f(t)$ denoting the singular distribution is often called symbolic function by the pertinent professional literature [8].

The equality between the distributions $f, g \in \mathcal{D}'$ is defined as follows

$$\langle f, \Phi \rangle \doteq \langle g, \Phi \rangle, \quad \Phi(t) \in \mathcal{D},$$

their addition by the expression

$$\langle f + g, \Phi \rangle \doteq \langle f, \Phi \rangle + \langle g, \Phi \rangle\,, \quad \Phi(t) \in \mathcal{D}$$

and the multiplication of the distribution $f \in \mathcal{D}'$ with the real number λ is defined by the equality

$$\langle \lambda f, \Phi \rangle \doteq \langle f, \lambda \Phi \rangle, \quad \Phi(t) \in \mathcal{D}\,. \tag{8}$$

The operation of the so-called translation is interpreted by the relationship

$$\langle f(t - \tau), \Phi(t) \rangle \doteq \langle f(t), \Phi(t + \tau) \rangle, \quad \Phi(t) \in \mathcal{D}$$

wherein $f(t)$ is a symbolic function corresponding to the distribution $f \in \mathcal{D}'$; τ is a given real number.

In case of the distribution δ, the introduction of the designation

$$\delta_\tau \doteq \delta(t - \tau)$$

yields

$$\langle \delta_\tau, \Phi \rangle = \langle \delta(t), \Phi(t + \tau) \rangle = \Phi(\tau)\,. \tag{9}$$

Be $\psi(t)$ a function which may be derived as many times as needed, then in case of $f \in \mathcal{D}'$

$$\langle \psi f, \Phi \rangle \doteq \langle f, \psi \Phi \rangle , \quad \Phi(t) \in \mathcal{D} . \tag{10}$$

It may be proved that in case of $\psi(t)$ of the above properties and of an arbitrary $\Phi(t) \in \mathcal{D}$ $\psi(t)\,\Phi(t) \in \mathcal{D}$ [8].

The derivation for the distribution $f \in \mathcal{D}'$ is interpreted by the rule

$$\langle f', \Phi \rangle \doteq \langle f, -\Phi' \rangle , \quad \Phi(t) \in \mathcal{D} \tag{11}$$

which, in case of a regular f ensues from the derivation rule of the ordinary multiplication. By the function

$$h(t) = \begin{cases} 0, & \text{if} \quad t < 0 \\ 1, & \text{if} \quad t > 0 \end{cases}$$

the Heaviside's distribution h is interpreted with the aid of which, by introducing the notation

$$h_\tau \doteq h(t - \tau)$$

on the basis of (7), (8) and (10), in case of an arbitrary $\Phi(t) \in \mathcal{D}$ the expression

$$\begin{aligned} \langle h'_\tau, \Phi \rangle = - \langle h_\tau, \Phi' \rangle = - \int_{-\infty}^{\infty} h(t)\,\Phi'(t + \tau)\,dt = \\ = - \int_0^{\infty} \Phi'(t + \tau)\,dt = \Phi(\tau) = \langle \delta_\tau, \Phi \rangle \end{aligned} \tag{12}$$

is obtained.

Let $\Phi(t) \in \mathcal{D}$ and $\psi(t)$ be a function which may be derived sufficiently many times. Then, in consequence of what has been said above, we have

$$\langle \delta_\tau, \psi\Phi \rangle = \psi(\tau)\,\Phi(\tau) = \psi(\tau)\,\langle \delta_\tau, \Phi \rangle = \langle \delta_\tau, \psi(\tau)\,\Phi \rangle$$

i.e., by making use of the relation using also (10),

$$\langle \psi\delta_\tau, \Phi \rangle = \langle \psi(\tau)\delta_\tau, \Phi \rangle$$

and the definition of the equality concerning the distributions

$$\Psi(t)\,\delta(t - \tau) = \Psi(\tau)\,\delta(t - \tau) \tag{13}$$

is obtained.

Be $g \in \mathcal{D}'$ a given distribution and its primitive function (taken in a symbolic sense) is required. This, by agreement, means the solution of the equation

$$\langle g, \Phi \rangle \doteq \langle f', \Phi \rangle , \quad \Phi(t) \in \mathcal{D}$$

for f; $f \in \mathcal{D}'$ being the primitive function required. It may be proved that the primitive functions differ only in additive constant from each other [9]. However, it may also be proved that from the relationship

$$\langle f', \Phi \rangle \doteq \langle \delta_\tau, \Phi \rangle = \langle h'_\tau, \Phi \rangle$$

holding true in case of an arbitrary $\Phi(t) \in \mathcal{D}$ for the primitive function of δ_τ

$$f(t) = h(t - \tau) + \text{const.} \tag{14}$$

is obtained and the primitive function of h_τ is given from the equality

$$\langle f', \Phi \rangle \doteq \langle h_\tau, \Phi \rangle$$

by the formula

$$f(t) = (t - \tau)\, h(t - \tau) + \text{const.} \tag{15}$$

Finally, the relationship

$$\int_0^x h(t - \tau)\ \psi(t)\ dt = h(t - \tau) \int_\tau^x \psi(t)\, dt \tag{16}$$

immediately recognizable from the definition of the function $h(t)$ which will be utilized later is mentioned wherein $\psi(t)$ is an arbitrary continuous function and t, τ, $x \in [0, 1]$.

4. Inverse operators and the δ-function

Be the ordinary, linear differential operator $\mathcal{K}^{-1}$ interpreted in the space of the functions $v(x)$, $x \in [0, 1]$. The functions $v(x)$, in correspondence with $\mathcal{K}$ are many times derivable functions satisfying certain boundary conditions. $\mathcal{K}^{-1}$ should designate the inverse of $\mathcal{K}$ in such a way as $\mathcal{K}\mathcal{K}^{-1} = \mathcal{K}^{-1}\mathcal{K} = \mathcal{E}$ and $\mathcal{E}v = v$[10].

Let us assume that $\mathcal{K}^{-1}$ is an integral operator, with the kernel $K(x, t)$ according to the relationship

$$\mathcal{K}^{-1} v = \int_0^1 K(x, t)\, v(t)\, dt \tag{17}$$

formally may be written as

$$v(x) = \int_0^1 \mathcal{K}\, K(x, t)\, v(t)\, dt\,, \tag{18}$$

because $\mathcal{K}$ means derivation with respect to x.

Since the functions $v(x)$ satisfy the conditions prescribed for the test functions, so by using (9) and (18)

$$\mathcal{K}\, K(x, t) = \delta(x - t)\,. \tag{19}$$

is obtained.

Thus, in summarizing, the kernel function $K(x, t)$ may be determined from (19) by carrying out the designated integrals by $\mathcal{K}^{-1}$ in the relationship

$$K(x, t) = \mathcal{K}^{-1}\, \delta(x - t) \tag{20}$$

and by considering all that have been said in the preceding chapter. The constants entering by the integrations may be defined by the boundary conditions established for the functions $v(x)$.

To investigate this problem more closely, consider the boundary problem

$$\mathcal{K}v = f, \quad \mathcal{S}v = 0 \tag{21}$$

where f is an arbitrary function of $x \in [0, 1]$, $\mathcal{S}$ is the linear operator designating the boundary conditions prescribed to the functions $v = v(x)$. From (21)

$$\mathcal{S}v = \mathcal{S}\mathcal{K}^{-1} f = 0$$

that is:

$$\int_0^1 \mathcal{S}\, K(x, t) f(t)\, dt = 0$$

and from this equation, due to arbitrary function $f(t)$ it follows:

$$\mathcal{S}\, K(x, t) = 0\,. \tag{22}$$

Therefore, the kernel $K(x, t)$, as a function of x, has to satisfy the constraints prescribed to all the $v(x)$.

5. Solution to the dynamic problem

Instead of describing the equation of motion of the problem mentioned in the introduction, and the detailed presentation of the physical quantities entering in the equation of motion (which may be found on pp. 37 and 38 of [4]) it is convenient to select the operator equation

$$(\mathcal{A} - \alpha^2\, \mathcal{B})\, v = 0 \tag{23}$$

of the problem to begin with, where

$$\mathcal{A}v \doteq \frac{d^2}{dx^2}\left(p\frac{d^2v}{dx^2}\right), \tag{24}$$

$$\mathcal{B}v \doteq qv. \tag{25}$$

The notations used in Eqs (23), (24) and (25) are

α — angular eigenfrequency
$v = v(x)$ — amplitude distribution function
$p = p(x)$, $q = q(x)$ — positive, sufficiently many times derivable functions involving geometric and material characteristics of beam which, within interval [0, 1] are nowhere equal to zero
x — independent variable along beam axis

Considering, that $x \in [0, 1]$, the set of boundary conditions associated with Eq. (23) is

$$\begin{aligned} v(0) &= 0, \qquad v'(0) = 0, \\ v''(1) &= 0, \qquad v'''(1) = 0. \end{aligned} \tag{26}$$

(Here and in the following with the comma the derivation with respect to x is designated.)

The operators $\mathcal{A}$ and $\mathcal{B}$ defined in Eqs (24) and (25) are linear, positive, symmetric, and $\mathcal{A}$ is, at the same time, also a self-adjoint differential operator. As a result, the eigenvalue problem defined by Eqs (23) and (26) innumerable, has infinitely many isolated positive eigenvalues, which cannot be accumulated in the finite [5]. The eigenvalues may be ordered according to their magnitudes and taking conveniently many times the multiples:

$$\alpha_1^2 \leq \alpha_2^2 \leq \ldots \leq \alpha_\nu^2 \leq \ldots . \tag{27}$$

Then, introducing the notation

$$\mathcal{K}^{-1} \doteq \mathcal{A}^{-1}\mathcal{B}, \qquad \mu \doteq \frac{1}{\alpha^2}. \tag{28}$$

Eq. (23) takes the form

$$\mathcal{K}^{-1}v = \mu v \tag{29}$$

wherein $\mathcal{K}^{-1}$ is an operator interpreted with the kernel $K(x, t)$ according to (1). From (27), using the substitution (28), yields

$$\mu_1 \geq \mu_2 \geq \ldots \geq \mu_\nu \geq \ldots . \tag{30}$$

Our task is to calculate upper bounds for the series of eigenvalues (30) with

the aid of Trefftz—Fichera's method, if we assume that we have k quantity of

$$\mu_1' \geq \mu_2' \geq \ldots \leq \mu_k'$$

lower bounds defined in the way reported in [4].

First, the kernel $K(x, t)$ should be established by using Eq. (19). Consideration of the interpretation of the operators, as well as Eq. (13) yields the equation

$$\frac{d^2}{dx^2}\left[p(x)\frac{d^2 K(x,t)}{dx^2}\right] = q(t)\,\delta(x-t)\,.$$

By making use of Eq. (14)

$$\frac{d}{dx}\left[p(x)\frac{d^2 K(x,t)}{dx^2}\right] = q(t)\,h(x-t) + \beta_1(t), \tag{31}$$

is obtained, then performing the integration again

$$\frac{d^2 K(x,t)}{dx^2} = q(t)\,h(x-t)\frac{x-t}{p(x)} + \beta_1(t)\frac{x}{p(x)} + \beta_2(t)\frac{1}{p(x)} \tag{32}$$

will be received.

Carrying out further two integrations of Eq. (32) one obtains

$$\begin{aligned} K(x,t) = {} & q(t)\,h(x-t)\int_t^x\int_t^u \frac{s-t}{p(s)}\,ds\,du + \\ & + \beta_1(t)\int_0^x\int_0^u \frac{s}{p(s)}\,ds\,du + \beta_2(t)\int_0^x\int_0^u \frac{1}{p(s)}\,ds\,du + \\ & + \beta_3(t)\,x + \beta_4(t)\,. \end{aligned} \tag{33}$$

wherein $\beta_1(t), \ldots, \beta_4(t)$ are arbitrary functions which may be determined by making use of (26) according to (21) and (22). Thus, from $K'''(1, t) = K''(1, t) = 0$, taking into account Eqs (31) and (32) and considering that $h(1 - t) = 1$, we have

$$\beta_1(t) = -q(t)\,, \quad \beta_2(t) = tq(t)\,. \tag{34}$$

From $K'(0, t) = K(0, t) = 0$ and on the basis of Eqs (33) and (34), knowing that $h(-t) = 0$,

$$\beta_3(t) = \beta_4(t) = 0 \tag{35}$$

may be obtained. Substituting (34) and (35) into Eq. (33) yields

$$K(x,t) = q(t)\,h(x-t)\int_t^x\int_t^u \frac{s-t}{p(s)}\,ds\,du + q(t)\int_0^x\int_0^u \frac{t-s}{p(s)}\,ds\,du\,. \tag{36}$$

By introducing the functions

$$\chi(x) = \int_0^x \frac{ds}{p(s)}, \quad \psi(x) = \int_0^x \frac{sds}{p(s)}.$$

$$\eta(x) = \int_0^x \chi(s)\, ds, \; \zeta(x) = \int_0^x \psi(s)\, ds,$$

Eq. (36) may be written in the form

$$K(x,t) = \begin{cases} q(t)\left[t\eta(x) - \zeta(x)\right], & x < t \\ q(t)\left[xt\,\chi(t) - x\psi(t) + t\psi(t) - \right. \\ \qquad \left. - t^2\chi(t) + t\eta(t) - \zeta(t)\right]. & x > t \end{cases} \tag{37}$$

By continuing the investigation of the case $x > t$, the expression in the square brackets, by adding and at the same time subtracting $x\eta(t) - \zeta(t)$ may be written in the form

$$x\eta(t) - \zeta(t) + (x - t)\,\xi(t)$$

wherein

$$\xi(t) = t\chi(t) - \psi(t) - \eta(t). \tag{38}$$

Derivation of Eq. (38) with respect to t yields

$$\frac{d\xi}{dt} = \chi(t) + \frac{t}{p(t)} - \frac{t}{p(t)} - \chi(t) = 0,$$

wherefrom $\xi(t) = \text{const.}$ follows for any $t \in [0, 1]$. The value of the constant is, due to $\xi(0) = 0$, equal to zero, wherefore (37), after introduction of the symmetrical function

$$G(x,t) = \begin{cases} t\eta(x) - \zeta(x), & x < t \\ x\eta(t) - \zeta(t), & x > t \end{cases} \tag{39}$$

becomes the following simple expression:

$$K(x,t) = q(t)\, G(x,t) \tag{40}$$

(It should be noted that $G(x, t)$, in case of the boundary conditions (26), is a Green's function associated with the operator $\mathcal{A}$ [11], [12], [15].)

From Eq. (29), by making use of Eq. (40), follows

$$\int_0^1 q(t)\, G(x,t)\, v(t)dt = \mu v(x).$$

Multiplication of the above equation with $\sqrt{q(x)}$ and substitution of $w(x) = \sqrt{q(x)}\, v(x)$ [13], [14], yields

$$\int_0^1 \sqrt{q(x)\, q(t)}\, G(x, t)\, w(t)\, dt = \mu\, w(x)\,. \tag{41}$$

By the transformation carried out in this way the eigenvalue μ are not changed, in turn, the new kernel

$$K^*(x, t) = \sqrt{q(x)\, q(t)}\, G(x, t)$$

is symmetrical whereby Trefftz—Fichera's method can be applied, i.e., in consequence of the equality

$$K^*(x, x) = K(x, x)$$

(5) may immediately be utilized.

6. Numerical example

To illustrate the practicability, be the diameter of 1 m long beam of circular cross section

$$d(x) = ax + b$$

wherein $a = -10^2$, $b = 4 \cdot 10^{-2}$ m. Then,

$$p(x) = \frac{\pi E\,(ax + b)^4}{64}\,,$$

$$q(x) = \frac{\pi \varrho\,(ax + b)^2}{4}\,.$$

Herein, E = const., elasticity modulus, and ϱ = const., density.

Considering these values as parameters, Table 1 shows the result of the calculations related to the first five angular eigenfrequencies.

Table 1

	$i = 1$	$i = 2$	$i = 3$	$i = 4$	$i = 5$
$\alpha_{fi}^2 \frac{\varrho}{E}$	$1{,}0284 \cdot 10^{-3}$	$4{,}327 \cdot 10^{-2}$	$3{,}062 \cdot 10^{-1}$	1,143	3,217
$\alpha_{ai}^2 \frac{\varrho}{E}$	$1{,}0283 \cdot 10^{-3}$	$4{,}311 \cdot 10^{-2}$	$2{,}986 \cdot 10^{-1}$	1,045	2,545

In the first line of the Table the upper bounds calculated according to the Poincaré—Rayleigh—Ritz's method; in the second line, the lower bounds calculated with Trefftz—Fiechera's method are to be found. The numerical calculation work required for the determination of the upper bounds has been carried out with the use of the computer type SZTAKI C.D.C. of the Hungarian Academy of Sciences. For the definition of the lower bounds the use of a hand calculator proved to be sufficient.

REFERENCES

1. WEINSTEIN, A.: Bounds for Eigenvalues and the Method of Intermediate Problems Partial Differential Equations and Continuum Mechanics. Editor R. E. Langer, Madison. The University of Wisconsin Press 1961, pp. 39—53.
2. BAZLEY, N. W.—FOX, D. W.: Truncations in the Method of Intermediate Problems for Lower Bounds to Eigenvalues. *Journal of Research of the National Bureau of Standards.* B. Mathematics and Mathematical Physics **65** B (1961), 105—111.
3. BOSZNAY, Á.: Lectures on the Université de Liège, 1976 Nov. Old and New Methods for Improvable Bracketing of Eigenfrequencies of Structures
4. KOVÁCS, M.—RICHLIK, GY.—TAKÁCS, F.—TÓTH, GY.: Improvable Bracketing of the Angular Eigenfrequencies of a Beam of Straight Axis having Characteristics Variable at its Length, Submitted to Bending Vibration. *Műszaki Tudomány* **54** (1978),
5. BOSZNAY, Á.: Improvable Bracketing of the Eigenfrequencies of a Space Frame Structure Modelled as Continuum. Doctor's dissertation, 1974.
6. WEINBERGER, H. F.: Variational Methods for Eigenvalue Approximation. Society for Industrial and Applied Mathematics. J. W. Arrowsmith Ltd., Bristol 3, England 1974, 115—121.
7. WEINSTEIN, A.—STENGER, W.: Methods of Intermediate Problems for Eigenvalues. *Mathematics in Science and Engineering* **89**, (1972), 118—122.
8. ZEMANIAN, A. H.: Distribution Theory and Transform Analysis International Series in Pure and Applied Mathematics. McGraw-Hill Book Company, 1965, pp. 1—79.
9. SCHWARTZ, L.: Théorie des distributions, vol. I. Actualités Scientifiques et Industrielles. Hermann & Cie, Paris 1957, 1959.
10. ROACH, G. F.: Green's Functions: Introductory Theory with Applications. Van Nostrand Reinhold Company, London 1970, pp. 142—164.
11. COLLATZ, L.: Eigenwertaufgaben mit technischen Anwendungen. Akademische Verlagsgesellschaft Geest u. Portig K.-G. Leipzig 1949, S. 60—81.
12. KANWAL, R. P.: Linear Integral Equations. Theory and Technique. Academic Press New York and London 1971, pp. 61—93.
13. FRANK, PH.—MISES, R.: Differential and Integral Equations of Mechanics and Physics. Vol. 1. Műszaki Könyvkiadó, Budapest 1966, pp. 620—636.
14. PENNY, J. E.—REED, I. R.: An Integral Equation Approach to the Fundamental Frequency of Vibrating Beams. *Journal of Sound and Vibration* **19** (4), (1971), 393—400.
15. SCHMEIDLER, W.: Integralgleichungen mit Anwendungen in Physik u. Technik I. Akademische Verlagsgesellschaft Geest u. Portig K.-G., Leipzig 1950, S. 328—348.

Anwendung der Trefftz—Ficheraschen Methode zur korrigierbaren Eingrenzung der Eigenkreisfrequenzen des Biegeschwingungen durchführenden Stabes. — Die numerischen Versuche zeigen, daß im Fall der einerlei Schwingung durchführenden Stäbe zur korrigierbaren Eingrenzung der Eigenkreisfrequenzen die Anwendung der allgemein geltenden Methoden der Funktionalanalysis nicht unbedingt zweckmäßig ist. Das Ziel der Abhandlung ist die Wirksamkeit des Trefftz—Ficheraschen Verfahrens im Zusammenhang mit der Berechnung der korrigierbaren unteren Grenzen der zur Biegeschwingungen gehörigen Eigenkreisfrequenzen zu beweisen. Die zur Eingrenzung benötigten oberen Grenzen können mit Hilfe der Poincaré—Rayleigh—Ritzschen Methode ermittelt werden. Zur Anwendung der Trefftz—Ficheraschen Methode ist die Invertierung des ursprünglich vorgekommenden Differentialoperators von veränderlichem Koeffizient nötig. Die Invertierung wird mit Hilfe der Distributionstheorie durchgeführt und die betreffenden Elemente der allgemeinen Theorie werden zusammengefaßt.

Acta Technica Academiae Scientiarum Hungaricae, Tomus 92 (3–4), pp. 405–418 (1981)

DEVELOPMENT OF AN EXPERIMENTAL APPARATUS FOR THE MEASUREMENT OF THE THERMODYNAMIC PROPERTIES OF CO_2-CONTAMINATED NATURAL GASES

PART II

M. A. I. BUKHARI* – G. VERES**

[Manuscript received: 14 March 1978]

The increasing demand for energy has necessitated extensive investigations to find ways and means of utilizing the huge reserves of largely CO_2-contaminated CH_4 gas, previously considered uneconomical. Two kinds of equipment have been specifically devised and tested for the purpose of measuring the thermodynamic properties of CH_4-CO_2 mixtures at desired P-T-X ranges. One of these is suitable for concomitantly determining the integral isobaric heats of condensation, together with vapour-liquid equilibria. The other is intended for simultaneous measurement of heat capacities at constant pressure and the mixing heats of liquid mixtures.

Experimental apparatus

Integral isobaric heat of condensation

Method adopted

A circulation method, based on a common principle shown schematically on Figure 4, is used for the measurement of integral isobaric heats of condensation. This method is the most widely used in vapour-liquid equilibrium measurements and is chosen here for its simplicity and convenience to use in the region of low, medium and also high pressures, with the proper construction. The vapours evolved from the boiling mixture in the boiler, where a quantity of heat Q_{in} is being steadily added, passes through the upper conduit into the condenser where it is completely condensed by the removal of a quantity of heat Q_{out} and returned to the boiling vessel. When steady state conditions, corresponding to phase equilibrium, are established the compositions in both vessels do not change with time, i.e.:

$$\frac{dx}{dt} = \frac{dy}{dt} = 0. \tag{1}$$

* M. A. I. Bukhari, P.O. Box 2408 Khartoum, Sudan
** G. Veres, Bogár u. 29/d H-1022 Budapest, Hungary

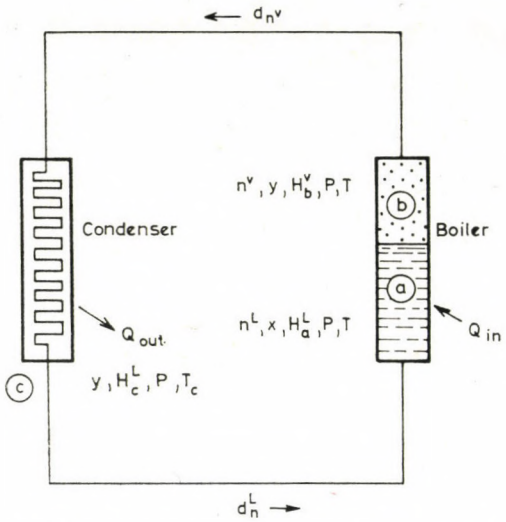

Fig. 4. Schematic diagram of the circulating stills

The vapour, condensing in the condenser, is continuously in equilibrium with the boiling liquid, with no superheating or partial condensation. If the distillation occurs with finite velocity, then during the time interval dt, dn^v moles of vapour mixture pass from the boiler to the condenser, and in the same period dn^L moles of liquid condensate return in the reflux from the condenser to the boiler. Since the total number of moles n, or hold-up, of both liquid and vapour phases in the boiler is constant, then

$$n = n^L + n^V = \text{constant}\,, \tag{2}$$

and

$$\frac{dn}{dt} = \frac{dn^L}{dt} + \frac{dn^V}{dt} = 0\,.$$

Therefore

$$\frac{dn^L}{dt} = -\frac{dn^V}{dt}\,. \tag{3}$$

If the vapour evolved above the liquid mixture of composition x, has the composition y_b, then the amount of volatile constituent transferred from the boiler to the condenser is

$$dn_1^V = y_b\, dn^V, \tag{4}$$

and the amount of this constituent returned from the condenser to the boiler is

$$dn_1^L = y_c\, dn^L. \tag{5}$$

If Eq. (1) is to be satisfied, as well as the condition for hold-up, then a mass balance on the volatile component requires that

$$y_c \, dn^L = -y_b \, dn^V \tag{6}$$

which, when combined with Eq. (3), gives

$$(y_c - y_b) \frac{dn^L}{dt} = 0 \, . \tag{7}$$

Since for a finite velocity of distillation

$$\frac{dn^L}{dt} \neq 0 \, .$$

Eq. (7) can be fulfilled only if

$$y_c = y_b = y \tag{8}$$

(steady state, or phase equilibrium).

This means that, under steady state conditions, the composition of the liquid in the condenser is identical with that of the evolved vapours.

Figure 5 illustrates the processes, that occur in Figure 4 in an enthalpy-composition diagram. Here, the condensate rich in the more volatile con-

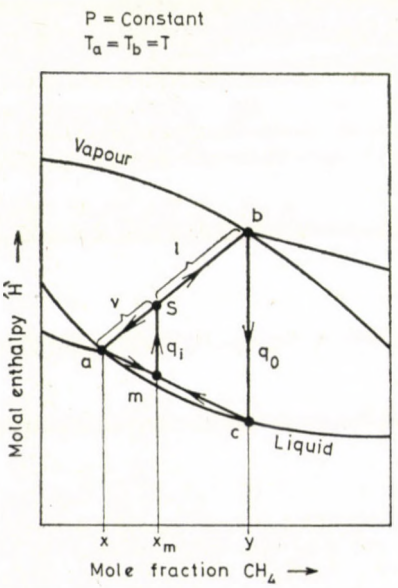

Fig. 5. Illustration of the processes of Fig. 4 in an enthalpy-composition diagram

stituent returning from the condenser mixes with the liquid in the boiler causing the composition of the liquid mixture to rise to x_m, where x_m is the total amount of the volatile component per mole of hold-up in the boiler

$$1 = \frac{n^L}{n} + \frac{n^V}{n} = l + v, \tag{9}$$

where l is the quantity of the liquid-phase per mole of hold-up in the boiler, and v is the corresponding quantity of the vapour-phase. From the above equation, the total amount of the volatile component x_m per mole of hold-up in the boiler is

$$x_m = xl + yv\,. \tag{10}$$

From Eqs (9) and (10)

$$l = \frac{y - x_m}{y - x}\,, \tag{11}$$

and

$$v = \frac{x_m - x}{y - x}\,. \tag{12}$$

The addition, at a certain rate, of a quantity of heat q_i per mole of saturated liquid mixture in the boiler causes an enthalpy rise of the mixture by the amount q_i from the mixture state point m to the partially saturated point S where a quantity l of the liquid-phase is in equilibrium with a quantity v of the vapour-phase. The vapour generated in the boiler (point b) passes to the condenser, where it is caused to condense to the state point c, and the cycle is repeated.

The heat added to the system in the boiler is

$$Q_{in} = (H^S - H_m)\,n\,, \tag{13}$$

and the heat added per mole of hold-up in the boiler

$$q_i = \frac{Q_{in}}{n} = H^S - H_m\,. \tag{14}$$

From the diagram

$$H^S = H_a^L + (H_b^L - H_a^L) \cdot \frac{x_m - x}{y - x} = H_a^L + (H_b^V - H_a^L)v\,,$$

$$H_m = H_a^L - (H_a^L - H_c^L)\frac{x_m - x}{y - x} = H_a^L - (H_a^L - H_c^L)\,v.$$

Therefore,

$$q_i = H^S - H_m = (H_b^V - H_c^L)\, v\,. \tag{15}$$

The heat removed by the condenser per mole of vapour condensed, or the integral isobaric heat of condensation is

$$q_0 = \frac{Q_{\text{out}}}{dn} = H_b^V - H_c^L\,. \tag{16}$$

In the steady state condition, when heat gain from or heat loss to the surroundings is absent, the heat balance requires that

$$Q_{\text{in}} = Q_{\text{out}}\,, \tag{17}$$

or

$$q_i = q_0\, v\,. \tag{18}$$

Description

An adaptation of the circulating equilibrium stills shown in Figure 4 is used for the simultaneous measurement of integral isobaric heats of condensation of CH_4-CO_2 mixtures and their phase equilibrium. Figure 6 represents the flow diagram for this assembly which consists primarily of a boiler and three identical condensers in which the vapours generated are condensed. The system is designed for operating pressures up to 70 atmospheres and for test mixtures of up to 30 mole % CH_4. Design data for the major components of this system are included in a report entitled "Experimental Apparatus for Measurement of H-x Diagrams of the CO_2-CH_4 System" [1] issued by the Department of Energetics.

The boiler is suitable for pressures up to 70 atm. and boiling temperatures down to −15 °C and is heated by means of a 1200 Watt electric resistance heater. A level — gauge indicates the existence of liquid and vapour phases, and the liquid level in the boiler. The condensers are suitable for temperatures as low as −50 °C, and are cooled by the evaporation of Refrigerant 12 circulated by means of a water-cooled, semi-hermetic compressor-condensing unit, Model MAV-10 of rated capacity of 9000 K.cal/hr at −15/+40 °C and 2500 K.cal/hr at −30 °C. Compressor capacity is manually controlled by means of a manual expansion valve and a hot gas by-pass. A liquid preheater, fitted with a 1200 Watt electric resistance heater, is used to overcome liquid subcooling produced in the condensers. Power to this heater is maintained constant and controlled by a variable transformer, and is measured by a voltmeter and an ammeter. The preheater is slightly pitched to allow any vapours that may be formed to flow into the boiler in order to avoid vapour back-flow or flow stoppage.

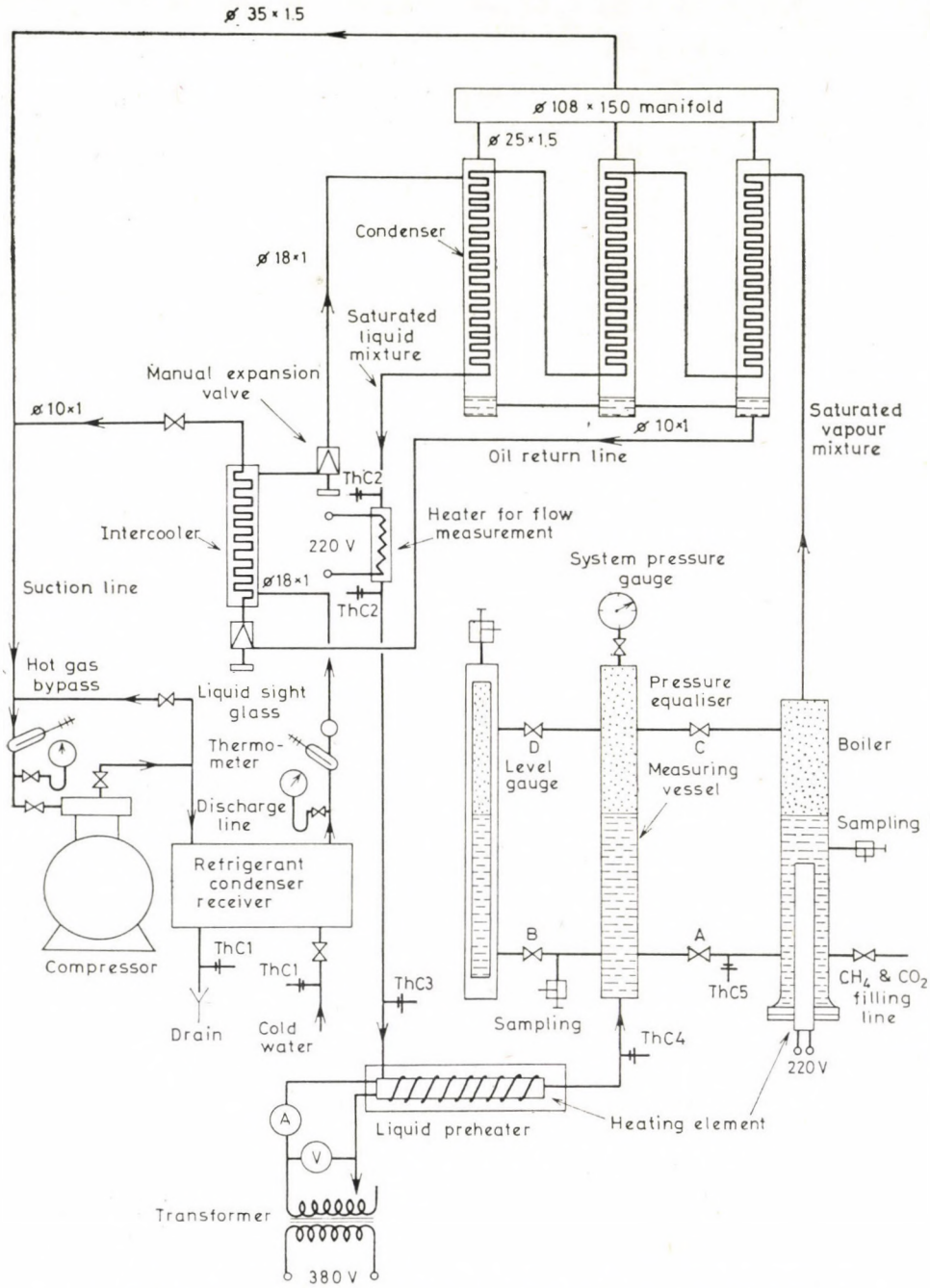

Fig. 6. **Flow diagram for the integral heat of condensation measuring apparatus**

Circulation of the vapour-phase is thermally induced, and this requires minimization of conduction heat losses and maintenance of unidirectional flow without too large a pressure drop by using the shortest possible pipe loop and adequate pipe inside diameter. Because of the lack, at the time, of a suitable means for measuring such minute flows under high pressure conditions, a special flow rate measuring vessel, connected to the boiler as seen, has been devised for this purpose. Its operation requires disruption of the liquid circulation to the boiler by closing valve *A*, leaving valves *B*, *C* and *D* open. The liquid level in the boiler now starts to drop due to continued evaporation and no reflux, and the liquid condensate will back-up in the measuring vessel and in the liquid level-gauge which is calibrated to measure the condensate volume rate of flow, by measuring the volume of liquid flowing over a short time interval. However, in order to avoid inaccuracies introduced by disturbing the system equilibrium and steady-state conditions, another solution resorted to is to measure the flow rate calorimetrically by measuring the temperature rise across a specially installed condensate heater, as shown, immersed in a bath of glycol. Heat is electrically supplied to this heater by means of a 200 Watt resistance element.

Ni, Cr-Ni thermocouples are used to measure temperature differentials across condenser cooling water and the glycol bath, condensate temperature before and after the preheater and the boiler temperature. Special sampling probes, as shown, are installed for measuring the compositions of the liquid in the boiler, the vapour and the condensed liquid. A calibrated pressure gauge measures the system pressure. The boiler, the condensers and the measuring vessel are thermally insulated with polystyrene slabs. The piping and other parts of the system are covered with asbestos wrappings.

Operation

To operate the equipment, air is first thoroughly evacuated from the system by means of a vacuum pump connected to the filling line. Pure CO_2 is then charged into the system at room temperature until liquid is formed in the equilibrium boiler, its presence being shown by the liquid-level indicator, at a pressure of about 60 atmospheres. The saturated phases are then superheated by supplying power to the boiler heater up to a temperature of slightly above the critical point temperature of pure CO_2, 31 °C. Methane gas is then charged into the system by repeatedly opening and closing the valve in the filling line and checking the composition of the mixture until the desired mixture is approximately formed. Then, the compressor is set into operation. The superheated gaseous mixture cools down with its pressure and tempera-

ture decreasing, and after sufficient time for heat transfer, the mixture partially condenses and splits into a liquid and a vapour phase.

Circulations is induced thermally by boiler heating and condenser cooling and the process continues until equilibrium is attained. Heat input to the boiler, in initial trials, was maintained constant by an electrically powered 1200 Watt heating element. The heater for flow measurement has two heating elements, 100 Watts each. The desired system equilibrium pressure, at various temperatures, is adjusted by manually controlling the compressor capacity through adjustment of the manual expansion valve, and also the hot gas bypass valve when necessary. The liquid preheater is used to remove the subcooling of the liquid condensate produced in the refrigerant evaporators by heating the reflux to approximately the corresponding boiling point temperature as indicated by system liquid-vapour equilibrium curves. Equilibrium conditions are indicated by constant thermocouple voltage readings, constant system pressure and constant liquid level in the boiler.

When the steady state is reached, which is generally between 2 and 3 hours, a run is begun for a duration of 10 to 20 minutes during which time the phases are sampled. The phases are sampled by letting a sample of each phase, taken from the probe by a tube, flow steadily through a Hartmann and Braun Uras 2 infrared gas analyzer calibrated up to 30 mole % CH_4. Analysis of both phases is carried out in the vapour state, and in sampling the liquid-phase a copper tube coil through which steam flows is placed around the probe head to vaporize the flowing sample and to prevent dry-ice formation at the capillary opening owing to throttling. Gauge pressure and thermocouple readings are recorded, and conditions are then changed for additional runs on the same liquid.

Results and comments

The experimental results reported herein do not constitute more than initial results in the process of testing, adjusting and calibrating the simple equipment used in this preliminary study, as necessitated by the importance of redesigning and retesting of the various components of the equipment or accessories before it can be possible to demonstrate and firmly establish the adequacy of the equipment to obtain fairly reliable experimental results.

Heat capacity

The heat capacity heat exchanger was calibrated by the measurement of the heat capacities of pure liquid CO_2 for pressures of 30, 40 and 50 atmospheres and temperatures between -10 and -25 °C. Four determinations

Table 1

Summarized pure component CO_2 heat capacity values

Pressure	P atm.	30	40	40	50
Average temp.	T °C	−10,5	−14,5	−25	−19
Gas pressure	P_g atm.	1,054	1,06	1,053	1,050
Gas temp.	T_g °C	19,5	31	19	14,8
Volume of gas flowing	$\Delta\dot{V}_g$ m³	3,286	3,395	0,272	0,245
Time interval	Δt min.	60	60	5,0	5
Rate of molal flow	$\dot{n}$ mol/hr	144,09	144,16	142,56	130,12
Temp. rise	ΔT °C	4,6	5,0	2,4	2,8
Heat input	$\dot{Q}$ cal/hr	14 955	15 274	6 880	7 095
C_p cal/gmol−°K	This work	22,638	21,29	20,11	19,47
	Din [2]	23,150	21,87	20,64	21,04
	% Dev.	2,203%	2,67%	2,58%	7,45%

have been made and the results are summarized in Table 1, compared with literature data [2]. At three measurements the % deviation from literature value is less than 3%, but at the 50 atm isobar the recorded deviation is 7,45%. The fact that all the values measured are smaller than those of Din [2] indicate considerable heat gain from the surroundings, in particular radiation.

In the table $\dot{n}$ the rate of flow of the gas is, in moles per hour, calculated assuming the gas to be ideal at approximately atmospheric pressure

$$\dot{n} = \frac{P_g \dot{V}_g}{RT_g} \times 10^3$$

where $\dot{V}_g$ is the rate of gas flow in m³/hr, and

$$R = 0{,}08207 \text{ atm–lit/gmol– °K}$$

is the universal gas constant.

$$\dot{Q} = V \cdot I \cdot 860 \text{ cal/hr}$$

is the rate of heat input into the heater, from which heat capacities are calculated using the relationship

$$C_p = \frac{\dot{Q}}{\dot{n}\Delta T}$$

where ΔT is the temperature rise across the heater, V the voltage in volts and I the current in amperes.

Afterwards, heat capacity measurements were taken for 8 liquid mixtures at an absolute pressure of 40 atmospheres and an average temperature of −21 °C, Table 2. The use of the commercial type of gas regulators, though

Table 2

Summarized CH_4—CO_2 liquid mixtures heat capacity data

Pressure P atm		40	40	40	40	40	40	40	40
Average temp. T °C		−21	−21	−21	−21	−21	−21	−21	−21
Composition x mol % CH_4		1,2	2,7	3,0	5,0	5,7	6,5	10,0	12
Volumetric gas flow rate $\dot{V}$ m³/hr		1,831	1,961	1,986	2,610	2,880	2,920	3,360	3,258
Molal flow rate $\dot{n}$ mol/hr		77,05	82,53	83,61	113,54	125,29	127,25	146,5	142,05
Heat input $\dot{Q}$ cal/hr		13 846	13 846	13 846	13 846	13 846	13 846	13 846	13 846
Temp. rise ΔT °C		8,7	8,3	8,26	6,4	6,0	5,7	5,0	5,0
C_p	measured	20,655	20,214	20,05	19,054	18,420	19,22	18,98	19,49
$\frac{\text{cal}}{\text{gmol—°K}}$	BWR [3]	21,34	21,20	21,13	20,90	20,85	20,75	20,36	20,17
	% Dev.	3,21	4,65	5,09	8,83	11,66	7,40	6,80	3,37

it has proved to be fairly satisfactory in assuring a steady flow process with pure CO_2, has turned problematic when measurements are run, using the two gases. Control of the compositions, which often fluctuated, has been a difficult task, and has required vigilant metering of the regulator settings. Metering the flow rate and composition control are the most critical of all measurements, since their accuracy is the limiting factor in the entire set of measurements. The values measured are listed with those calculated with the BENEDICT, WEBB and RUBIN equation of state [3], with % deviations presented. An average % deviation of 7,27% is shown over the entire range of compositions. Here, deviations are also all positive indicating, among other things, that heat gain from the surroundings plays a considerable role.

Error analysis

The accuracy of the values of C_p depend directly upon errors in the determination of volumes of gas flowing through the gasmeter, time interval, voltage and amperage to the heater and the determination of the null point

on the thermopile. Heat leakage is also a possible source of error which is almost impossible to estimate and can only be minimized by the design of a proper calorimeter. Temperature, pressure and composition are involved only in the fixing of the state at which C_p is obtained. The extent to which these latter affect C_p depends on their magnitude. A summary of possible maximum error analysis is given in Table 3.

Table 3

Sources of uncertainty in the heat capacity results

Item	Max. % error
Mass flow	2,00
Power input	0,20
Composition	2,00
Temperature	0,50
Pressure	0,20
Heat leakage	5,00
Total	9,90

Heat of mixing

The heat of mixing coil, conceived as a means of producing, in a short time, abundant data of a degree of accuracy sufficient for heat of mixing measurements, has been shown to be incapable of producing the kind of accuracy contemplated. The basic idea is to determine the change in temperature due to interaction when the two fluids are brought together and homogenized in a well-insulated mixing coil. However, initial runs with pure CO_2 and with mixtures have shown that spurious heat transfer to this 5 metre long coil is too excessive to allow accurate determinations of the small heat of mixing values in the range of measurements. This necessitates a return to the original idea and redesigning, as much as possible, a proper flow calorimeter in which the mixing fluids are rapidly homogenized in composition as well as temperature, and well insulated against conduction, as well as radiation, heat gains.

Heats of condensation

Table 4 presents the results of initial trial runs for the heat of condensation of a CH_4—CO_2 mixtures at various pressures and temperature settings. The experimental data obtained are not possible to interpret without heat

Table 4

Summarized heat of condensation data measurement

Test pressure	P atm.	50	50	50	60	70	70
Boiler temp.	T_b °C	8,3	5,0	9,0	17,6	21	14
Liquid composition x CH_4	mol %	2,7	3,0	2,7	0,07	3,3	3,0
Vapour composition y CH_4	mol %	9,8	12,5	10,0	7,0	15,9	16,5
Heat input to heater	$\dot{Q}_h$ K.cal/hr	172,00	172,00	86,00	172,00	172,00	172,00
Heat input to preheater	$\dot{Q}_{p.h.}$ K.cal/hr	745,62	580,50	0,00	828,20	835,92	1032,00
Heat input to boiler	$\dot{Q}_b$ K.cal/hr	1032,00	1032,00	1032,00	1032,00	1032,00	1032,00
Temp. rise across heater	ΔT °C	9,6	10,5	6,5	7,1	5,0	4,3
Heat cap. of condensate	C_p · cal/gmol—°K	22,22	22,21	22,21	21,88	29,46	24,69
Molal flow rate	$\dot{n}$ K · mol/hr	0,807	0,732	0,596	1,107	1,179	1,387
ΔH^{COND}	measured	2415	2439	1877	1835	1731	1612
$\frac{cal}{mol}$	$H - x$ Diagram (3)	2200	2200	2200	1870	1420	1640

capacity data for the various mixtures. The heat capacity data, necessary for flow rate determinations, is calculated from Table (3—16) [3]. Molal flow rates are calculated as follows:

$$\dot{n} = \frac{\dot{Q}_H}{C_p \Delta T} \tag{19}$$

where $\dot{Q}_H$ is the heat input into the glycol bath, and ΔT is the temperature rise across it. The heat of condensation is the net heat input into the system, divided by the flow rate:

$$\Delta H^{COND} = \frac{\dot{Q}_{in}}{\dot{n}} . \tag{20}$$

Alongside the measured values are listed values of ΔH^{COND} obtained from the constructed enthalpy-composition diagrams [3]. Qualitative agreement between the two sets of data is encouraging, though these initial runs have

indicated several shortcomings which have to be dealt with before further runs can be performed. The experimental determination of the heats of condensation concomitantly with the liquid-vapour equilibrium of the coexisting phases provide a check on the internal consistency of the data obtained. The measured compositions of the coexisting liquid and vapour phases do not agree exactly with literature liquid-vapour equilibrium data, particularly those of the liquid-phase. Because the boiling itself is not sufficient to ensure by mixing of the boiling liquid with returning cold condensate, concentration and temperature gradients can arise in the boiler. The liquid in equilibrium with vapour mixes with part of the returning condensate during the withdrawal of the sample. This error can be diminished by the use of a large amount of solution, indicated by the liquid level, in the boiler. Equilibrium temperatures also do not correspond exactly to literature values and this may be attributed partly to the presence of impurities in the methane gas. Other sources of error to be beware of are premature boiling produced by the preheater, and excessive condensate subcooling not compensated for by the preheater and not corrected in the calculations, leakage in the system and inadequate pipe insulation.

Conclusion

Because of the difficulties cited above, the disparities between measured values and literature ones, and those calculated on the other hand, are comprehensible. Consequently, further efforts still continue to rectify these various defficiencies, in the process of adjusting, recalibrating and testing the various components of the experimental apparatus in this laboratory, in order to reduce to a minimum every defect and to establish its reliability for precise experimental data measurement. Further endeavours are forecoming to extend the range over which further measurements can be performed, and to explore and develop new areas of investigation.

REFERENCES

1. Heller, L.—Erdődy, I.—Balikó, S.—Mika, Gy.: Kísérleti berendezés CO_2—CH_4 elegy i-ξ diagramjának kimérésére. Technical University of Budapest, Department of Energetics, Budapest 1971.
2. Din, F.: Thermodynamic Functions of Gases. Vol. 1 (1956), Vol. 3 (1961). Butterworth Scientific Publications, London.
3. Bukhari, M. A. I.: Enthalpy-Composition Diagrams for the Methane-Carbon Dioxide System and Correlations of Volumetric and Thermodynamic Properties. A Candidate of Science Dissertation, Technical University of Budapest, Department of Energetics, Budapest 1974.

Entwicklung einer Versuchsvorrichtung zur Messung der thermodynamischen Kennwerte des durch CO_2 verunreinigten Erdgases. II. Teil. — Der zunehmende Energiebedarf erfordert die Benutzung der eher für unwirtschaftlich abgeschätzten, mit CO_2 verunreinigten Erdgasvorräte. Zur technischen Berechnung der Erdgas vorbereitenden Einrichtungen sind zuverlässige thermodynamische Angaben erforderlich im gewünschten P-T-x Bereich des als ein Modell vorteilig brauchbaren $CH_4—CO_2$ Systems. In der vorhandenen Abhandlung werden jene Versuchsvorrichtungen vorgeführt, die zur gleichzeitigen Messung der integralisobaren Kondensationswärme, der Gleichgewichtswerte der Dampf-Flüßigkeit sowie der Mischungswärme der in der Flüßigkeitsphase befindlichen Mischung und der Isobarwärmekapazität geeignet sind.

INDEX

PRINTED IN HUNGARY
Akadémiai Nyomda, Budapest

The *Acta Technica* publish papers on technical subjects in English, French, German and Russian.

The *Acta Technica* appear in parts of varying size, making up one volume.

Manuscripts should be addressed to

Acta Technica
H-1051 Budapest
Münnich Ferenc u. 7.
Hungary

Correspondence with the editors and publishers should be sent to the same address.

Orders may be placed with "Kultura" Foreign Trading Company (H-1389 Budapest 62, P.O.B. 149. Account No. 218-10990) or its representatives abroad.

Les *Acta Technica* paraissent en français, allemand, anglais et russe et publient des travaux du domaine des sciences techniques.

Les *Acta Technica* sont publiés sous forme de fascicules qui seront réunis en volumes.

On est prié d'envoyer les manuscrits destinés à la rédaction à l'adresse suivante:

Acta Technica
H-1051 Budapest
Münnich Ferenc u. 7.
Hongrie

Toute correspondance doit être envoyée à cette même adresse.

On peut s'abonner à l'Entreprise du Commerce Extérieur «Kultura» (H-1389 Budapest 62, P.O.B. 149. Compte courant No. 218-10990) ou chez représentants à l'étranger.

«*Acta Technica*» публикуют трактаты из области технических наук на русском-немецком, английском и французском языках.

«*Acta Technica*» выходят отдельными выпусками разного объема. Несколько выпусков составляют один том.

Предназначенные для публикации рукописи следует направлять по адресу:

Acta Technica
H-1051 Budapest
Münnich Ferenc u. 7.
Венгрия

По этому же адресу направлять всякую корреспонденцию для редакции и администрации.

Заказы принимает предприятие по внешней торговле «Kultura» (H-1389 Budapest 62, P.O.B. 149. Текущий счет № 218-10990) или его заграничные представительства и уполномоченные.

Periodicals of the Hungarian Academy of Sciences are obtainable at the following addresses:

AUSTRALIA
C.B.D. LIBRARY AND SUBSCRIPTION SERVICE
Box 4886, G.P.O., *Sydney N.S.W. 2001*
COSMOS BOOKSHOP, 145 Ackland Street
St. Kilda (Melbourne), Victoria 3182

AUSTRIA
GLOBUS, Höchstädtplatz 3, *1206 Wien XX*

BELGIUM
OFFICE INTERNATIONAL DE LIBRAIRIE
30 Avenue Marnix, *1050 Bruxelles*
LIBRAIRIE DU MONDE ENTIER
162 rue du Midi, *1000 Bruxelles*

BULGARIA
HEMUS, Bulvar Ruszki 6, *Sofia*

CANADA
PANNONIA BOOKS, P.O. Box 1017
Postal Station "B", *Toronto, Ontario M5T 2T8*

CHINA
CNPICOR, Periodical Department, P.O. Box 50
Peking

CZECHOSLOVAKIA
MAD'ARSKÁ KULTURA, Národní třida 22
115 66 Praha
PNS DOVOZ TISKU, Vinohradská 46, *Praha 2*
PNS DOVOZ TLAČE, *Bratislava 2*

DENMARK
EJNAR MUNKSGAARD, Norregade 6
1165 Copenhagen K

FEDERAL REPUBLIC OF GERMANY
KUNST UND WISSEN ERICH BIEBER
Postfach 46, *7000 Stuttgart 1*

FINLAND
AKATEEMINEN KIRJAKAUPPA, P.O. Box 128
SF-00101 Helsinki 10

FRANCE
DAWSON-FRANCE S. A., B. P. 40, *91121 Palaiseau*
EUROPÉRIODIQUES S. A., 31 Avenue de Versailles, *78170 La Celle St. Cloud*
OFFICE INTERNATIONAL DE DOCUMENTATION ET LIBRAIRIE, 48 rue Gay-Lussac
75240 Paris Cedex 05

GERMAN DEMOCRATIC REPUBLIC
HAUS DER UNGARISCHEN KULTUR
Karl Liebknecht-Straße 9, *DDR-102 Berlin*
DEUTSCHE POST ZEITUNGSVERTRIEBSAMT
Sraße der Pariser Kommüne 3–4, *DDR-104 Berlin*

GREAT BRITAIN
BLACKWELL'S PERIODICALS DIVISION
Hythe Bridge Street, *Oxford OX1 2ET*
BUMPUS, HALDANE AND MAXWELL LTD.
Cowper Works, *Olney, Bucks MK46 4BN*
COLLET'S HOLDINGS LTD., Denington Estate
Wellingborough, Northants NN8 2QT
WM. DAWSON AND SONS LTD., Cannon House
Folkstone, Kent CT19 5EE
H. K. LEWIS AND CO., 136 Gower Street
London WC1E 6BS

GREECE
KOSTARAKIS BROTHERS INTERNATIONAL BOOKSELLERS, 2 Hippokratous Street, *Athens-143*

HOLLAND
MEULENHOFF-BRUNA B.V., Beulingstraat 2,
Amsterdam
MARTINUS NIJHOFF B.V.
Lange Voorhout 9–11, *Den Haag*
SWETS SUBSCRIPTION SERVICE
347b Heereweg, *Lisse*

INDIA
ALLIED PUBLISHING PRIVATE LTD., 13/14 Asaf Ali Road, *New Delhi 110001*
150 B-6 Mount Road, *Madras 600002*
INTERNATIONAL BOOK HOUSE PVT. LTD.
Madame Cama Road, *Bombay 400039*
THE STATE TRADING CORPORATION OF INDIA LTD., Books Import Division, Chandralok 36 Janpath, *New Delhi 110001*

ITALY
INTERSCIENTIA, Via Mazzé 28, *10149 Torino*
LIBRERIA COMMISSIONARIA SANSONI, Via Lamarmora 45, *50121 Firenze*
SANTO VANASIA, Via M. Macchi 58
20124 Milano
D. E. A., Via Lima 28, *00198 Roma*

JAPAN
KINOKUNIYA BOOK-STORE CO. LTD.
17-7 Shinjuku 3 chome, Shinjuku-ku, *Tokyo 160-91*
MARUZEN COMPANY LTD., Book Department, P.O. Box 5050 Tokyo International, *Tokyo 100-31*
NAUKA LTD. IMPORT DEPARTMENT
2-30-19 Minami Ikebukuro, Toshima-ku, *Tokyo 171*

KOREA
CHULPANMUL, *Phenjan*

NORWAY
TANUM-TIDSKRIFT-SENTRALEN A.S., Karl Johansgatan 41–43, *1000 Oslo*

POLAND
WĘGIERSKI INSTYTUT KULTURY, Marszałkowska 80, *00-517 Warszawa*
CKP I W, ul. Towarowa 28, *00-958 Warszawa*

ROUMANIA
D. E. P., *Bucureşti*
ILEXIM, Calea Grivitei 64–66, *Bucureşti*

SOVIET UNION
SOJUZPECHAT — IMPORT, *Moscow*
and the post offices in each town
MEZHDUNARODNAYA KNIGA, *Moscow G-200*

SPAIN
DIAZ DE SANTOS, Lagasca 95, *Madrid 6*

SWEDEN
ALMQVIST AND WIKSELL, Gamla Brogatan 26
101 20 Stockholm
GUMPERTS UNIVERSITETSBOKHANDEL AB
Box 346, *401 25 Göteborg 1*

SWITZERLAND
KARGER LIBRI AG, Petersgraben 31, *4011 Basel*

USA
EBSCO SUBSCRIPTION SERVICES
P.O. Box 1943, *Birmingham, Alabama 35201*
F. W. FAXON COMPANY, INC.
15 Southwest Park, *Westwood Mass. 02090*
THE MOORE-COTTRELL SUBSCRIPTION AGENCIES, *North Cohocton, N. Y. 14868*
READ-MORE PUBLICATIONS, INC.
140 Cedar Street, *New York, N. Y. 10006*
STECHERT-MACMILLAN, INC.
7250 Westfield Avenue, *Pennsauken N. J. 08110*

YUGOSLAVIA
JUGOSLOVENSKA KNJIGA, Terazije 27, *Beograd*
FORUM, Vojvode Mišića 1, *21000 Novi Sad*

HU ISSN 0001—7035

Index: 26.025